The College of Engineering
University of Wisconsin-Madison

SECOND WISCONSIN SYMPOSIUM ON HELIUM-3 AND FUSION POWER: PROCEEDINGS OF A SYMPOSIUM HELD IN MADISON, WISCONSIN, 19–21 JULY 1993

WCSAR-TR-AR3-9307-3

Technical Report

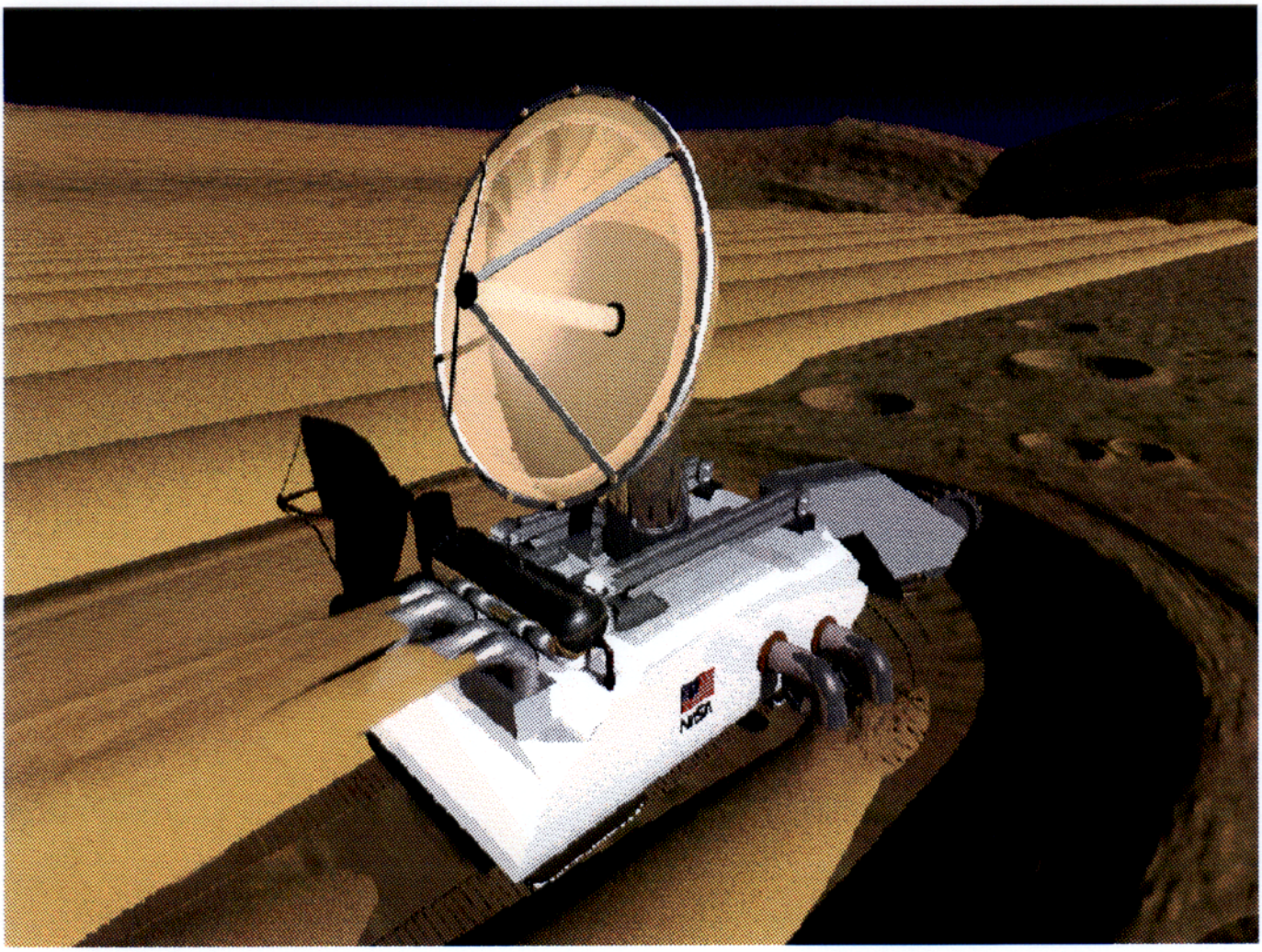


**Wisconsin Center for
Space Automation and Robotics**

•

**A NASA supported Center for
the Commercial Development of Space**

Second Wisconsin Symposium on Helium-3 and Fusion Power



Proceedings of a Symposium held in
Madison, Wisconsin
19–21 July 1993

WCSAR

Wisconsin Center for
Space Automation and Robotics

SECOND WISCONSIN SYMPOSIUM ON HELIUM-3 AND FUSION POWER

Proceedings of a Symposium held in Madison, Wisconsin, 19–21 July 1993

WCSAR-TR-AR3-9307-3

John F. Santarius, compiler

Wisconsin Center for Space Automation and Robotics
University of Wisconsin
1500 Johnson Drive
Madison WI 53706

July 1993

CONTENTS

Preface i

Organizing Committees vi

Keynote Speech 1

Political Implications of D/He-3 Fusion 3
Harrison H. Schmitt

1) ^{3}He and Space Development 7
W.D. Carrier III, Chair

1-1 History of Research on ^{3}He Fusion 9
G.L. Kulcinski

1-2 NASA Perspective on Lunar Helium-3 Mining 25
Raymond Whitten

1-3 Concepts for Industry Involvement in Lunar Development 27
Michael B. Duke

1-4 Deutsches Aerospace-ERNO Perspective on He-3 and Power from Space 35
J. Sved and K. Fuchs

1-5 U.S. Army Perspectives on Lunar Resource Recovery and Utilization 41
Edward B. Kiker

2) Lunar ^{3}He Resources
E. Rice, Chair

2-1 Evidence of Helium-3 on the Moon: Model Assumptions and Abundances 49
Lawrence A. Taylor

2-2 Further Evaluation of the Helium Resources of Mare Tranquillitatis 57
Eugene N. Cameron

2-3 Remote Sensing of ASTROFUEL™ 65
K.R. Harris, H.Y. Khater and G.L. Kulcinski

2-4 By-products of Lunar Helium-3 Mining 75
Larry A. Haskin

3) **D-^{3}He Fusion and Energy Policy** **81**
J.M. Dawson, Chair

3-1 Utility Perspective on Clean Nuclear Energy 83
D. Louis Peoples

3-2 My Perspective on D-^{3}He Fusion 95
David H. Crandall

3-3 Industrial Perspectives on Helium-3 and Fusion Power 101
Stephen O. Dean

4) **Advanced D-^{3}He Fusion Reactor Concepts and Applications-I** **105**
V.I. Pistunovich, Chair

4-1 About the Concept of Utmost Clean and Beneficial D-^{3}He Reactor 107
I.N. Golovin, V.V. Arsenin, A.Yu. Kujanov,
V.I. Khvesjuk, D.V. Semenov, N.V. Schabrov

4-2 Characteristics of D-^{3}He Fueled FRC Reactor: ARTEMIS-L 115
Hiromu Momota and Yukihiro Tomita

4-3 D-^{3}He Mirror Reactors 121
D.D. Ryutov

4-4 Non-Energy Applications for Fusion 127
John M. Dawson

4-5 Magnetic Fusion Propulsion: Opening the Solar-System Frontier 137
John F. Santarius

5) **Lunar Mining and Non-Lunar ^{3}He Resources** **145**
L.A. Haskin, Chair

5-1 The Lunar Environment and He-3 Mining 147
W.D. Carrier, III

5-2 Coaxing He3 from Lunar Regolith; Processes and Challenges 149
Igor N. Sviatoslavsky

5-3 Cost of ^{3}He from the Moon 159
Howard E. Thompson

5-4 Potential ^{3}He Resources for D-^{3}He Fusion Development 173
William R. Wilkes

5-5 Non-Lunar ^{3}He Resources 179
Layton J. Wittenberg

6) **D-^{3}He Near-Term and Commercial Tokamak Reactor Design** **193**
P. Komarek, Chair

6-1 Near-Term Experiments on D-He^3 Burning 195
B. Coppi

6-2 Potential for D-^{3}He Experiments in ITER 205
G.A. Emmert

6-3 ARIES-III: D/He-3, Second Stability, Tokamak 211
R.W. Conn

6-4 D-^{3}He, Second Stability Tokamak Reactor Study 213
V.I. Pistunovich and S.G. Bespoludennov

6-5 Overview of Apollo Studies and Economic Assessment of Several Proposed Variations 221
Laila A. El-Guebaly and Charles W. Maynard

7) **Non-Maxwellian D-^{3}He Fusion Reactor Concepts** **233**
D.D. Ryutov, Chair

7-1 Physics Issues for Large Orbit Fusion Schemes 235
Nicholas A. Krall

7-2 Inertial-Electrostatic Fusion from D to ^{3}He: A Practical Strategy for Fusion Development 241
Robert W. Bussard and Lorin W. Jameson

7-3 Overview of IEC at Illinois 249
G.H. Miley

7-4 Self Colliders for D-He^3 Fusion 257
Norman Rostoker

8) **Advanced D-^{3}He Fusion Reactor Concepts and Applications-II** **265**
H. Momota, Chair

8-1 Next Step in FRC Development 267
Alan L. Hoffman and John T. Slough

8-2 Direct Energy Conversion System for D-^{3}He Fusion 273
Y. Tomita, L.Y. Shu, and H. Momota

8-3 Overview of the Mirror Fusion Propulsion System (MFPS): An Optimized Open Magnetic Field Configuration Using D-^{3}He 279
Scott A. Carpenter and Marc E. Deveny

8-4 Prospects for Novel Thermonuclear and Non-Thermonuclear Fusion 285
L.J. Perkins

9) D-^{3}He Tokamak Reactor Design-I 287
R.W. Conn, Chair

9-1 Synchrotron Radiation from High-Temperature Plasmas 289
Winfried Kernbichler

9-2 Assessment of First Wall Lifetime in D-^{3}He and D-T Reactors with Impact on Reactor Availability 299
M.E. Sawan and I.N. Sviatoslavsky

9-3 Engineering Design of ARIES-III 309
D.K. Sze, C. Wong, E. Cheng, M.E. Sawan, I.N. Sviatoslavsky, J.P. Blanchard, L.A. El-Guebaly, H.Y. Khater, E.A. Mogahed, P. Gierszewski, R. Hollies, and the ARIES Team

10) D-^{3}He Tokamak Reactor Design-II 319
S.O. Dean, Chair

10-1 Parametric Analysis of the ARIES-III D-^{3}He Tokamak Reactor 321
C.G. Bathke, K.A. Werley, R.L. Miller, R.A. Krakowski, J.F. Santarius, and the ARIES Team

10-2 The Physics of Apollo: A D-^{3}He, First Stability, Tokamak Reactor 329
G.A. Emmert, J.F. Santarius, and J.P. Castro

10-3 Safety Characteristics of D-^{3}He Fusion Reactors 337
Hesham Y. Khater

10-4 Safety Analysis of the ARIES-III D-^{3}He Tokamak Reactor Design 349
J. Stephen Herring and Thomas J. Dolan

Appendix: Post-Conference Contributed Paper 357

Implications of the Results from the CTX Experiment Towards the Development of a D-^{3}He Dipole Fusion Reactor 359
Michael E. Mauel and Harry P. Warren

Preface

The Second Wisconsin Symposium on Helium-3 and Fusion Power was held on July 19–21, 1993 in Madison, Wisconsin. In the seven years since the value of the lunar ^{3}He resource to fusion power was recognized, the number of related publications has burgeoned, as shown in Fig. 1. The purpose of the Symposium was to bring together researchers in both the fusion and space communities to present the latest results of research on D-^{3}He fusion and on the acquisition of ^{3}He fuel. The Wisconsin Center for Space Automation and Robotics and the Fusion Technology Institute at the University of Wisconsin sponsored the meeting. All papers were given as oral presentations in plenary sessions, divided into seven categories:

- D-^{3}He Fusion Physics
- D-^{3}He Fusion Technology
- D-^{3}He Next Step Experiments
- D-^{3}He Reactor Design
- D-^{3}He Reactor Safety and Environment
- Lunar ^{3}He Resources
- Non-Lunar ^{3}He Resources
- Policy Considerations

The international participation in the Symposium, shown in Fig. 2, included industry, government laboratory, and university representatives. A broad mix of high-quality papers, split into various topics as shown in Fig. 3, was presented. The Symposium photo and identification guide are Figs. 4 and 5.

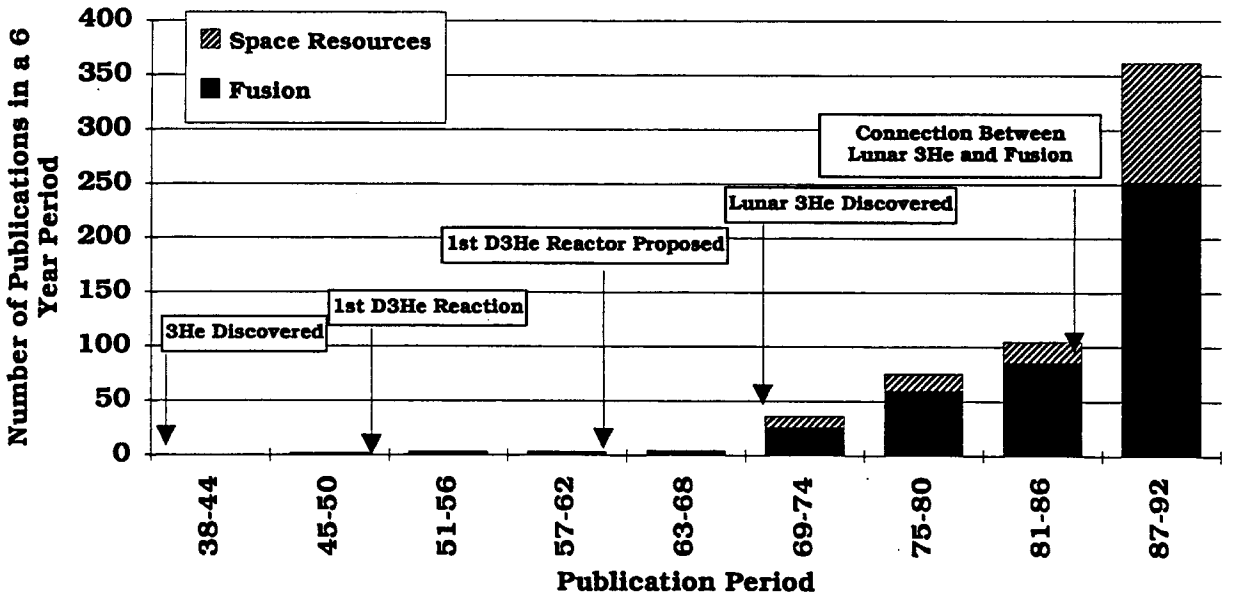


Figure 1: *Publications pertaining to ^{3}He fusion and space ^{3}He resources have risen dramatically in the past decade.*

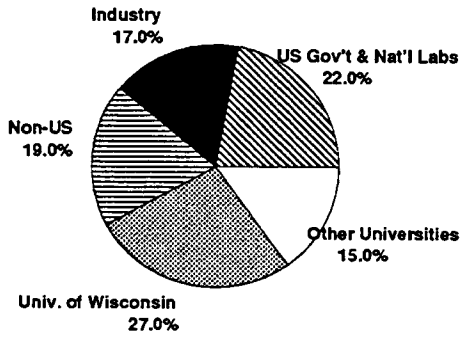


Figure 2: *Participation in the Second Wisconsin Symposium on Helium-3 and Fusion Power.*

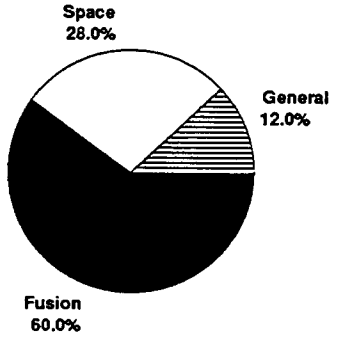


Figure 3: *Distribution of paper topics at the Second Wisconsin Symposium on Helium-3 and Fusion Power.*

It was our pleasure to be the General Chairperson and the Technical Program Chairperson for the Symposium. We are grateful for a great deal of excellent assistance. The Technical Program Committee included W. David Carrier III (Bromwell and Carrier), George H. Miley (University of Illinois), Richard F. Post (Lawrence Livermore National Laboratory), and Igor N. Sviatoslavsky (University of Wisconsin). Joyce Wessley and Linda Kraft ably coordinated local arrangements. Dennis Bruggink and Elaine DuCharme smoothly handled Symposium publications and correspondence. We heartily thank them all for a job well done.

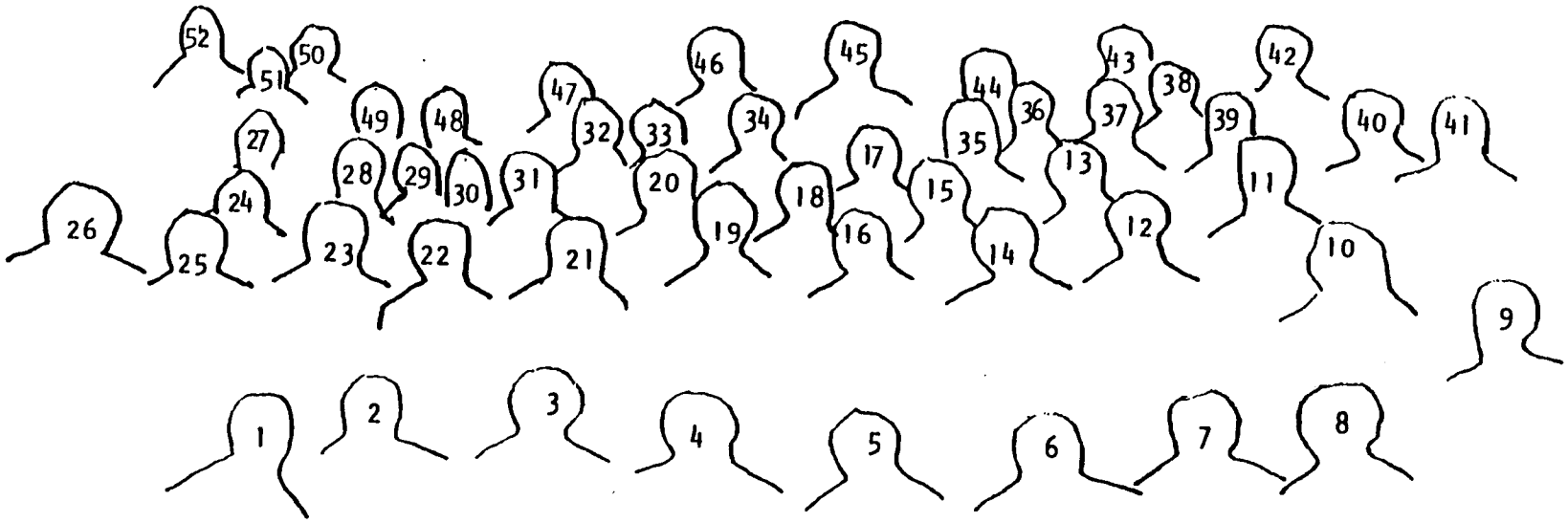
The papers speak for themselves but there is, perhaps, time for one final thought: We believe that the chief success of the Second Wisconsin Symposium on Helium-3 and Fusion Power is that it demonstrated to the space community that many fusion options exist for burning D-^{3}He fuel and to the fusion community that the lunar ^{3}He resource is substantial and its acquisition is feasible. We salute the 'can do' attitude of the participants in the Symposium and their technical communities.

G.L. Kulcinski
General Chairperson
Director, Fusion Technology Institute
University of Wisconsin

J.F. Santarius
Technical Program Chairperson
Fusion Technology Institute
University of Wisconsin



Figure 4: *Photo of attendees at the Second Wisconsin Symposium on Helium-3 and Fusion Power.*



Attendees

2nd Wisconsin Conference on He3 and Fusion Power, 19–21 July 1993, Madison WI

1 Dave Carrier
2 Scott Carpenter
3 Ed Kiker
4 Dmitri Ryutov
5 Bruno Coppi
6 Harrison Schmitt
7 John Sved
8 Charles Morgan
9 Hesham Khater
10 Kazue Kimura
11 Yukihiro Tomita
12 Kim Harris
13 Dai–Kai Sze
14 Hiromu Momota
15 Bill Wilkes
16 Steve Dean
17 Elsayed Mogahed
18 Chuck Bathke
19 Steve Herring
20 Larry Taylor
21 Mrs. Taylor
22 John Dawson
23 Mike Duke
24 Layton Wittenberg
25 John Perkins
26 Jerry Kulcinski
27 Igor Golovin
28 Andy Franklin
29 Diane Krall
30 Laila El–Guebaly
31 John Santarius
32 Mohamed Sawan
33 Steve Kratz
34 Gil Emmert
35 Igor Sviatoslavsky
36 Alan Hoffman
37 Winfried Kernbichler
38 Harvey Bloomfield
39 R.W. Bussard
40 Howard Thompson
41 Dave Crandall
42 Joel Crabb
43 Lou Wainwright
44 George Miley
45 Scott White
46 Vladimir Pistunovich
47 Bill Dove
48 Nick Krall
49 Edward Whitehurst
50 Lou Peoples
51 Mrs. Komarek
52 Peter Komarek

Figure 5: *Guide to photo of attendees at the Second Wisconsin Symposium on Helium-3 and Fusion Power.*

Technical Program Committee

W. D. Carrier III
(Bromwell & Carrier)

G. H. Miley
(University of Illinois)

R. F. Post
(Lawrence Livermore National Laboratory)

J. F. Santarius (UW)

I. N. Sviatoslavsky (UW)

Local Arrangements

J. Wessley (UW)
L. M. Kraft (UW)

Publications

D. Bruggink (UW)
E. DuCharme (UW)

Keynote Speech **1**

Political Implications of D/He-3 Fusion 3
Harrison H. Schmitt

POLITICAL IMPLICATIONS OF D/HE-3 FUSION

Harrison H. Schmitt
Consultant, University of Wisconsin
P.O. Box 14338, Albuquerque, NM, 87191

Introduction

The overall political backdrop against which new challenges in energy will be addressed during the 1990s and early decades of the Third Millennium appears to be coalescing into three major themes: Empowerment of People, Stewardship of Earth, and, indeed, Settlement of Space.

Political debate concerning Empowerment has been part of history for thousands of years, and knowing the human spirit, probably long before. Today and into the future, Empowerment of People involves finding an acceptable societal balance between individual freedom and individual responsibility. Energy, in combination with vastly improved education, must provide the foundation for economic growth and quality of life without which dreams of worldwide Empowerment will have no basis in reality. In contrast to our focus on energy here, education constitutes possibly the most critical single issue within the theme of Empowerment. Without education, a people will lose most of the empowering force of affordable and environmentally benign energy sources.

Political concerns about Stewardship began to appear early in this century but sprang full blown into public consciousness only after World War II. Exploding populations, nuclear concerns, and the Apollo views of Earth thrust environmental issues on to the world political stage. Continued poverty and unrest throughout the Third and Fourth Worlds and in newly independent nations makes it clear that Stewardship for the future embodies not only protection of Earth but improvement of the human condition. Without an alternative to the burning of fossil fuels and rain forests, how do you persuade hungry billions to stop such burning?

Energy, thus, makes up the most significant technical component of the theme of Stewardship of Earth. The basic justification for a sense of urgency with respect to energy lies in the provision of abundant and environmentally acceptable energy resources, or put more bluntly, finding a worldwide alternative to fossil fuels. This search increasingly will become a global imperative.

Strong scientific evidence now exists that the ever increasing and largely indiscriminate use of fossil fuels has contributed significantly to the modern rise in carbon dioxide in the atmosphere. Scientific evidence does not yet prove that this rise will accelerate global warming over that expected for a natural interglacial warming period. Although the ultimate response of the Earth and its climate to increasing atmospheric and thermal pollution remains unclear, prudence clearly demands that we find acceptable alternatives to fossil fuels as quickly as technically and economically feasible. If nothing else, the value of fossil chemicals to the feeding of more billions of people on Earth will soon overwhelm their value as sources of electrical power.

Finally, as access to space near Earth became relatively routine in the 1960s, the theme of Settlement of Space moved from the pages of science fiction to the speculations of futurists and the reports of strategic planners. With former President Bush's Apollo 11 Anniversary speech of July 20, 1989, Settlement moved beyond speculations and reports into national policy considerations. Unfortunately, little has happened since, except for NASA Administrator Daniel Goldin's recent intriguing remarks, recognizing the potential value of lunar He-3. European and Russian space activities have seen further retrenchment. Japanese investments appear to have plateaued. Nonetheless, Settlement of Space has reached a position of political visibility not unlike that reached by Stewardship during the 1950s.

Technopolitical Environment

In the Third Millennium, the D/He-3 fusion cycle using lunar He-3 (Wittenberg et al, 1986, and Kulcinski and Schmitt, 1990), and possibly the He-3/He-3 cycle later (Kulcinski, 1993), promises not only a global alternative to fossil fuels and deforestation, one that could empower all the people of Earth to vastly improve their lives, but something else as well. It will empower developed nations to do something about Stewardship and Settlement. On the darker side of global politics, however, the domination of either He-3 fusion technology or He-3 supply by any nation or small group of nations could seriously compromise worldwide freedom, the primary aim of Empowerment.

Other technically, economically, and environmentally acceptable alternatives to fossil fuels besides He-3 will find future niches depending on local circumstances. Conservation, solar energy, nuclear fission energy, and nuclear fusion energy represent reasonable possibilities to consider relative to

current applications of fossil fuel for the generation of electrical power. Reasonable global substitutes for gasoline and oil as portable fuels appear less obvious, although once excess quantities of electrical power exist, hydrogen fuels can be produce by the electrolysis of water.

Solar energy has many potentially helpful contributions to make, particularly in regions with significant year round insolation. The production of hydrogen from water using biotechnology and solar energy has become one of the more exciting possibilities. However, broad scale substitution of solar energy sources for fossil fuels, such as solar power beaming from space (Glaser, 1989, and Criswell, 1989) brings its own direct and indirect environmental and political problems and does not appear to be the ultimate solution. Nonetheless, solar energy used in space or imported from space has some interesting possibilities and should be evaluated against He-3 on a net technological, economic, environmental, and political basis, always, of course, comparing apples to apples.

Nuclear fission lies politically crippled at the present time and even if revived, presents waste disposal, plant decommissioning, and political challenges as yet without obviously acceptable solutions. Dismantling Fort St. Varain, abandonment of Shoreham, stalemate at WHIP, and pseudoscience at Yucca Mountain, and the dangers of out-moded nuclear technology in former Eastern Block nations represent just the most recent manifestations of these problems.

In the case of D/He-3, however, electrical power can be created from nonradioactive fuels by direct conversion in inherently safe reactors. Nuclear fission and tritium fusion, on the other hand, bring with them fuel radioactivity, thermal conversion inefficiencies, loss of cooling questions, and long lived radioactive wastes. In addition, nonHe-3 systems require frequent refurbishment or replacement of thermal conversion systems, fuel loads, and, in the case of D/T and D/D reactors, replacement and disposal of neutron degraded walls. Thus, the advantages of He-3 cycles also would contribute to a relatively rapid progression from system development to plant commercialization.

Development

As a consequence of our space experience with Apollo and terrestrial experience with large scale mining and refining, it seems likely that the establishment of commercial and profitable mining operations on the moon could be completed by about 2015 (Kulcinski et al, 1989). What has been done in the past from a much less vigorous technology base supports this estimate. This time-frame matches the Wisconsin team's estimates of the time required to develop and build the first commercial D/He-3 reactor on Earth.

Simultaneous development of commercial fusion plants and lunar mining systems clearly would be necessary. Unless the fusion community can be convinced that, upon completion of fusion plant development, He-3 supplies will be available for commercial use and unless the space community can be convinced that commercial fusion plants will exist to buy He-3, there will not be commitment by either. Therefore, for anything to happen, there must be a believable national, international, or private sector commitment to both fusion development and a permanent lunar base.

A near-term policy and budgetary commitment to He-3 fusion and lunar mining appears consistent with an initial commercial He-3 delivery and use date of about 2015. Such a commitment implies start-up costs in the range of 40 billion dollars for a full lunar support base (roughly half the current dollar cost of the full Apollo Program of nine lunar missions), 15 billion for the mining infrastructure (5 billion for R&D and 10 billion for implacement on the moon), and 10 billion for research and development leading to a prototype commercial fusion reactor.

Management

United States' independent management of a full scale He-3 based enterprise would follow traditional NASA lines, although we can hope that the stream-lined, can-do approach of the Apollo Program could be recaptured. In fact, a new agency combining the appropriate parts of NASA and the Departments of Energy and Defense with a major influx of young enthusiasts might be advantageous given the current constraints in these fields in existing agencies.

Under favorable circumstances, one also can imagine the formation of a private consortium to undertake the overall management of a He-3 based enterprise. The costs suggested previously probably could be significantly lower under this scenario. On the other hand, sufficient investment capital for such an enterprise could only be attracted if the return on investment could compete with other potential uses of capital. For private capital to be committed to an enterprise in which the major return on investment (ROI) would be 15-20 years away, competitive and rising ROI "plateaus" spaced 3-5 years apart would be required prior to significant sales of power plants and lunar helium-3, the "big ROI in the sky." Such interim ROI plateaus might include government contracts for lunar

resource data, fusion rockets, and lunar base utility support and technology spin-off or "dual-use" profits.

A number of key scientific, engineering, manufacturing, and political assumptions would be part of investor's considerations of the potential business opportunity presented by helium-3 fusion. These key assumptions include that an alternative to fossil fuels for the generation of electrical power will be required early in the 21st Century, that He-3 fusion is a scientifically sound concept, that He-3 fusion power systems are commercially feasible with no prohibative global competitors, that He-3 fusion power is politically and environmentally defensible, that lunar He-3 resources can be extracted at commercially competitive costs, that permanently occupied settlements on the moon are techically and physiologically feasible, and that Space Station Freedom will be constructed and operational within the next 10 years.

We of the Wisconsin group currently are formulating a draft comprehensive Business Plan that may serve as a means of evaluating the validity of these assumptions and the financial viability of a largely private initiative in He-3 fusion.

If circumstances dictated that a He-3 based enterprise should be international in scope, participant based international organizations appear to have the best chance for success. An International Lunar Enterprise might be based on the INTERLUNE concept (Joyner and Schmitt, 1984, and Schmitt, 1992). INTERLUNE would be responsible for developing both the terrestrial technology base for He-3 fusion power and the infrastructure for extracting He-3 and other materials from the lunar soils.

The charter of INTERLUNE would create relationships between nations, users, and investors modeled in part after the commercially successful INTELSAT (Alper and Pelton, 1984) and INMARSAT Agreements, but structured to recognize the special legal, technical, and financial considerations inherent in a commercial, human based activity in space (Bilder et al, 1989). For example, as envisioned by provisions of the 1967 Outer Space Treaty, organizational mechanisms for the cooperative use of lunar resources and the sharing of the economic and environmental benefits derived from those resources ought to be included within the INTERLUNE Charter.

Initiation and then implementation of a new international concept or organization never will be simple, even in the face of as great economic and environmental incentives as presented by lunar supported He-3 fusion. INTERLUNE would be no exception. However, establishment of such an organization probably would be possible (see Kearney, 1989) if there exists both an unequivocal commitment to the development of He-3 fusion power and a sincere willingness to search for a fair and beneficial means of international participation in such an endeavor.

The initial forum for discussions of an INTERLUNE Charter could well be between the international participants in the Space Station Freedom and MIR and ITER. Indeed, in addition to a scientifically credible investigation of human space adaptation and a technically credible development of space facilities of indefinite life, evaluation of an INTERLUNE-type management system including both Freedom and MIR would be an additional strong justification of both space station efforts. MIRFREEDOM might be an appropriate name for this experimental management organization.

Although not ratified by nations with major space activities, the existence of the Moon Agreement of 1979 as a negotiated addition to the space law environment nevertheless may be viewed by most governments as the starting point for initiating new international agreements related to lunar resources. The development of an INTERLUNE Charter along the lines discussed here, and its ratification in the context of a conformable and coordinated ratification of the Moon Agreement, particularly with regard to Article 11, would satisfy most past objections raised against that treaty.

Current Political Environment

In the United States, no clear signs exist as to the receptivity of the current Administration and the Congress to a "space energy alternative to fossil fuels" and to United States, private, or international management of such an alternative.

On the plus side, concerns about the environment played a central role in the 1992 election campaign, particularly on the part of the Vice President, and past surveys have indicated a strong positive tie in the public's mind between environment and space. Also, a space initiative of this magnitude would go a long way to reducing the impact of defense cut-backs and to bringing Russia, Europe, China, Japan, and others into a cooperative venture of unprecedented magnitude and benefits in peacetime, eliminating the possibility that one or more players might "go it alone." The initiative also might be a means to maintain an ITER (1988) program vunerable to budget axes and charges of environmental problems.

On the minus side, the new Administration and the majority in the Congress

have committed themselves to a vast array of new social spending programs that will continue to squeeze the so-called discretionary portion of the federal budget. Further, the Department of Energy and influential members of the Congress appear fully committed to the current D/T research program possibly to the exclusion of federal funding of advanced fuels cycles like He-3. Attempts to salvage the Space Station Freedom continue to distract NASA. There may be a short sighted political reluctance as well to agree to major roles for either the private sector or international partners.

On balance, however, and in spite of the negatives, it would appear that proponents of a space energy alternative have a reasonably favorable over-all climate in which to make their case one more time.

Conclusion

Lunar He-3 and fusion power offer the possibility of doing more than just monitoring the deterioration of the Earth's environment, the focus of current global change research. Power plants fueled by He-3 from the moon could supply the environmentally acceptable energy human civilization will require in succeeding centuries. No other foreseeable option yet exists for us to maintain and expand freedom and the quality of life on Earth as we enter the Third Millennium and as we move civilization towards the stars.

References

Alper, J. and Pelton, J.N., editors (1984) "The INTELSAT Global Satellite System", AIAA Press, New York.

Bilder, R.B., Cameron, E.N., Kulcinski, G. L., and Schmitt, H.H. (1989) Legal Regimes for the mining of Helium-3 from the Moon. WCSAR-TR-AR3-8901-1, University Wisconsin, Madison, WI.

Criswell, D.R. (1989) Lunar power system. In J.J. Kearney, chairman, Report of NASA Lunar Energy Enterprise Case Study Task Force. NASA Technical Memorandum 101652, 84-96.

Fusion Power Associates (1991) ITER Progress, in Executive Newsletter, August 1991.

Glaser, P.E. (1989) The solar power satellite (SPS)-Progress so far. In J.J. Kearney, chairman, Report of NASA Lunar Energy Enterprise Case Study Task Force. NASA Technical Memorandum 101652, 68-83.

ITER (1993) International Thermonuclear Experimental Reactor. U.S. Project Office, Oak Ridge National Laboratory, DOE/ER-ITER-0004,

Joyner, C.C., and Schmitt, H.H. (1984) Extraterrestrial Law and Lunar Bases: General Legal Principles and a Particular Regime Proposal (INTERLUNE), in Lunar Bases and Space Activities of the 21st Century, W.W. Mendell, editor. LPI, Houston.

Kearney, J.J., chairman (1989) Report of NASA Lunar Energy Enterprise Case Study Task Force. NASA Technical Memorandum 101652.

Kulcinski, G.L., Thompson, H., and Ott, S. (1989) Analysis of the Financial Factors Governing the Profitability of lunar Helium-3. In J.J. Kearney, chairman, Report of NASA Lunar Energy Enterprise Case Study Task Force. NASA Technical Memorandum 101652, 40-55.

Kulcinski, G.L., and Schmitt, H.H. (1990) Fusion Power from Lunar Resources. Proceedings of the 41st Congress of the International Astronautical Federation, IAA-90-606.

Schmitt, H.H. (1992) INTERLUNE concept for Helium-3 Fusion Development. In W.Z. Sadeh, S. Sture, and R.J. Miller, editors, Engineering, Construction, and Operations in Space III (SPACE '92), American Society of Civil Engineers, 1, 804-814.

Wittenberg, L.J., Santarius, J.F., and Kulcinski, G.L. (1986) Lunar source of He-3 for commercial Fusion Power. Fusion Technology, 10, 167.

1) ^{3}He and Space Development 7

W.D. Carrier III, Chair

1-1 History of Research on ^{3}He Fusion 9
G.L. Kulcinski

1-2 NASA Perspective on Lunar Helium-3 Mining 25
Raymond Whitten

1-3 Concepts for Industry Involvement in Lunar Development 27
Michael B. Duke

1-4 Deutsches Aerospace-ERNO Perspective on He-3 and Power from Space 35
J. Sved and K. Fuchs

1-5 U.S. Army Perspectives on Lunar Resource Recovery and Utilization 41
Edward B. Kiker

History of Research on ^{3}He Fusion

G. L. Kulcinski
University of Wisconsin
1500 Johnson Drive
Madison, WI 53706

ABSTRACT

Discovered in 1939, ^{3}He now plays an important role in the quest for safe, clean, and abundant fusion energy. It was recognized, in the early days of fusion research, that the D^{3}He reaction could be important in providing a low neutron emitting plasma. However, a general lack of terrestrial resources kept fusion researchers from devoting much time to developing a commercial power source based on this fuel. The discovery, by Apollo astronauts in 1969, of ^{3}He on the Moon went essentially unnoticed by the fusion community until 1986 when the connection between ^{3}He and lunar resources was made. Since 1986, the ^{3}He resource base has been estimated at ≈1 million tonnes, enough to power the earth for a 1000 years or more. There has been a tremendous increase in research since 1986 on various ways to utilize ^{3}He in fusion power reactors. A brief chronology is presented along with recent ideas on how ^{3}He fusion may impact the future world energy picture.

1. INTRODUCTION

Scientists have been looking for safe, clean, economical, and abundant sources of energy throughout the 20th century. At first, the search centered on the fossil fuels; oil, coal, and natural gas. However, events in the middle of the 20th century opened an entirely new arena in which to conduct this search, namely, the discovery of how to release nuclear energy. Initially, the effort concentrated on controlling the fission process. However, the release of nuclear energy by thermonuclear fusion was not far behind and today, we are spending more of our federal R&D dollars on finding a way to control fusion energy than in finding new ways to control the release of fission energy [1].

The search for a fusion reactor has been one of the most difficult projects that the scientific community has ever undertaken. Early efforts have concentrated on magnetic confinement of DT plasmas (see reaction below)

$$^2D_1 + {}^3T_1 \rightarrow {}^1n_0 + {}^4He_2 \qquad Q = 17.6\ MeV$$

within the tokamak configuration (invented by I.M. Tamm and Andrei Sahkarov) [2]. A smaller, but equally determined group of scientists have pursued the burning of DT fuel in targets compressed to ignition by external beams of lasers or ions [3]. Thus far , over 6 billion dollars (not corrected for inflation) has been spent in the US on the magnetic confinement fusion (MCF) approach in the US alone and another 2 billion dollars invested in DT inertial confinement fusion (ICF) [4]. Cumulative investment outside the US is estimated to be 2 to 3 times the level in the US. It is hoped that break-even (energy out = energy in) will be obtained in DT tokamaks in 1994-5 [5], and that ignition in a tokamak will achieved by approximately the year 2005 [6]. The ICF community hopes to obtain ignition in DT targets by approximately the year 2000 [7]. After these milestones have been reached, the real work of constructing a power producing plant will

begin. Such a power plant will have to withstand intense bombardment with 14 MeV neutrons as well as safely and reliably breed copious amounts of tritium for re injection into the plasma.

When some scientists and engineers realized the magnitude of the problem faced with handling the intense neutron fluxes of a DT device, they looked for other fusion fuel cycles that might work in MCF or ICF configurations. Considering the energetics and reaction rates of the over 64 known fusion reactions [8], two other reactions appeared promising; DD and D-^{3}He.

$^2D_1 + {}^2D_1 \rightarrow {}^3T_1 + {}^1H_1$	Q = 3.3 MeV (50%)
$^2D_1 + {}^2D_1 \rightarrow {}^3He_2 + {}^1n_o$	Q = 4.4 MeV (50%)
$^2D_1 + {}^3He_2 \rightarrow {}^4He_2 + {}^1H_1$	Q = 15.4 MeV

The DD cycle removes the need to breed tritium, but it actually generates more neutrons per unit of energy released than does DT so it does not solve the problem presented by neutron damage and neutron activation [9]. The D-^{3}He reaction does not need to breed tritium and the fundamental reaction does not release neutrons. However, depending on which confinement approach taken (i.e., colliding ions, Tandem Mirrors, Tokamaks, etc.), the side DD reactions can amount to as little as 1% of the reaction energy being released in neutrons [10]. As we shall see later, the main problem faced by the D-^{3}He cycle is the lack of terrestrial sources of ^{3}He and the somewhat more stringent plasma physics requirements on reaching ignition in a tokamak reactor.

It is within this framework that we can now assess the history of ^{3}He fusion research. The remainder of this paper will specifically address the events that have shaped work in this field to the present time and, at the end, some observations will be made on where future investigations may lead us.

2. EARLY WORK

Little did Dr. Louie Alvarez and Dr. Robert Cornog realize the energy implications of what they had discovered in 1939. (See Fig. 1 for a chronology of this and other events) In an effort to find out if tritium was a stable isotope, they separated ^{3}He [11]. After the discovery of ^{3}He, the next step was to locate resources of the isotope. In the post-W.W.II era, most efforts concentrated on the atmosphere where, in 1946, it was found at an abundance of 5 ppm (by weight) [12].

The first D-^{3}He fusion reaction was produced in 1949 [13] and it confirmed the good news that the reaction products were a proton and a helium-4 atom. This introduced the world to the possibility that it could have a nuclear energy source with little induced radioactivity.

It then took a little more than 20 years after its discovery, actually 1961, before the first kg of ^{3}He was collected in one place [14]. This ^{3}He came from the decay of tritium which was being produced for thermonuclear weapons in the US.

3. THE FIRST D-^{3}HE REACTORS ARE PROPOSED

The first documented practical application of the D-^{3}He reaction was proposed by Englert in 1962 [15] and it had to do with fusion propulsion (see Fig. 2). The great advantage of D-^{3}He

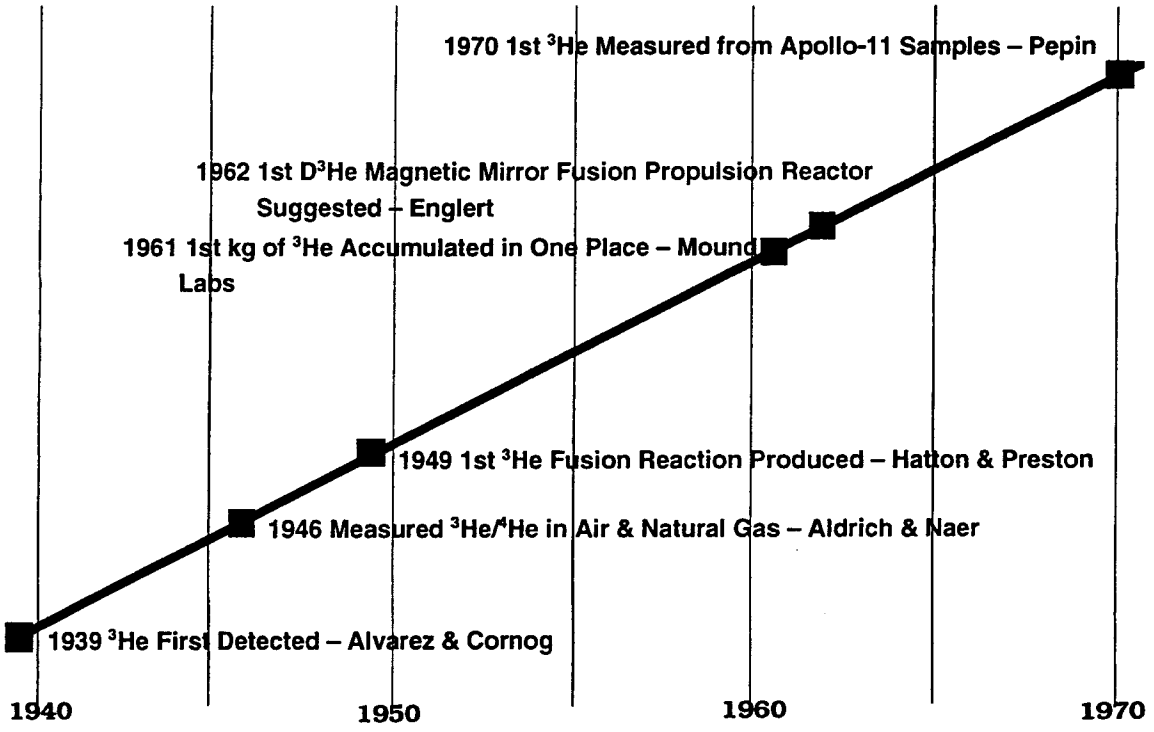


Fig. 1. Chronology of important ^{3}He milestones.

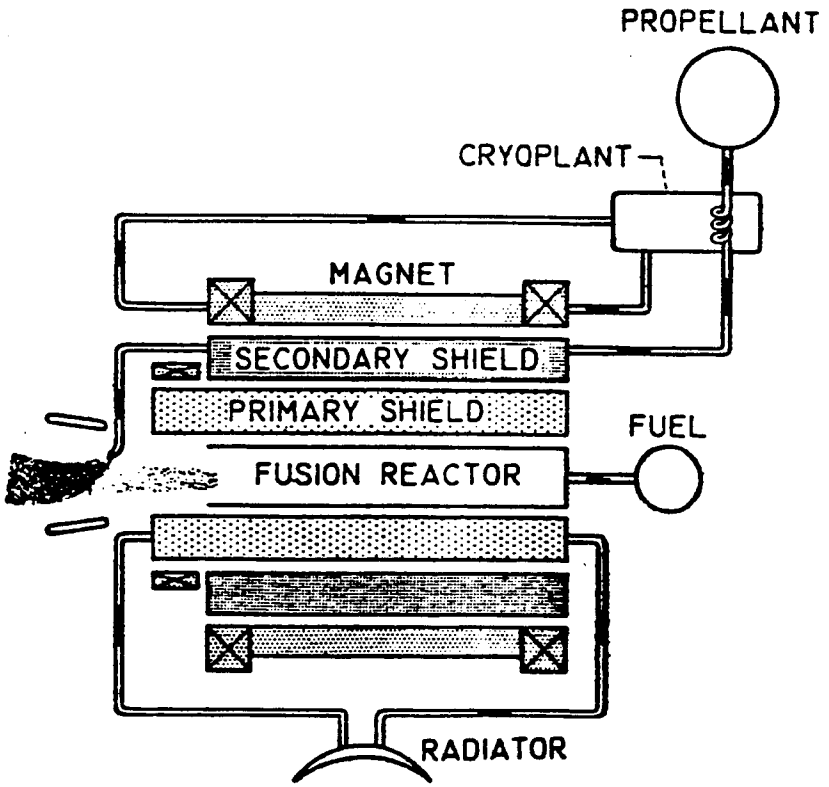


Fig. 2. The earliest known D-^{3}He fusion reactor was designed by Englert for propulsion [15].

in this application is the fact that essentially all of the reaction products are charged particles which can be used to provide thrust at high specific impulse (exhaust velocities) for fusion rockets. There was no indication of where the ^{3}He resources would come from to power the rockets. Aside from groups at NASA-Lewis and Aero-Jet General, there was little further activity in the 1960's in the fusion area.

A major non fusion event took place in 1969 with the first landing on the Moon of Apollo-11. In 1970, the lunar material collected on that mission was analyzed by Professor Pepin at the University of Minnesota [16] and others [17]. It was shown that if the samples were heated, most of the solar wind implanted volatile gases could be evolved. Specifically, it was found that when heated to 700 or 800°C, the lunar regolith released most of the ^{3}He that was contained in the solar wind (see Fig. 3). Unfortunately, this important event completely escaped the fusion community.

The first D-^{3}He terrestrial electrical power plant design was performed by Werner et al., in 1971[18] (Fig. 4). They investigated the use of a simple mirror and postulated the use of direct conversion to make electricity without going through the traditional Rankine cycle. A different form of fusion device, the Migma, using D-^{3}He bred from DD reactions was proposed by Maglich in 1973[19]. This was the first non thermalized, electrostatic confinement approach to a fusion reactor and the Migma concept also relied on the direct conversion of ion kinetic energy to electricity. There was very little further activity in ^{3}He applications until 1977 when Professor Miley, of the University of Illinois, proposed the first terrestrial toroidal D-^{3}He fusion electric power plants [20]. These reactors derived their ^{3}He from DD reactions and the decay of tritium. The problem with this approach was that it took several DT or DD fusion power plants to produce the ^{3}He needed to power one similar sized D-^{3}He power plant.

The Daedalus project [21], funded by the British Interplanetary Society in 1978, was the first group to propose the use of ^{3}He from space for fusion reactors. They proposed to collect it from the atmosphere of Jupiter and Saturn and use it for propulsion. They also considered using lasers to power the reactor.

The group at Illinois got back into the act in 1979 by proposing the first D-^{3}He field reversed mirror (FRM) [22] and, in 1983, the first terrestrial D-^{3}He fueled laser electric power plant [23]. Again, the ^{3}He came from the DD breeding cycle.

During the period from 1985-8 (Fig. 5), scientists and engineers at Wisconsin designed an orbiting D-^{3}He tandem mirror electric power plant for SDI applications [24] (see Fig. 6). In this case, the ^{3}He source was from the US stockpile that results from the decaying tritium in thermonuclear weapons. It was at this point that the group at Wisconsin decided to look for a larger ^{3}He source for civilian applications.

4. THE CONNECTION BETWEEN FUSION AND SPACE IS MADE

In late 1985, scientists at Wisconsin, in particular Dr. Layton Wittenberg and Dr. John Santarius, recognized the solar wind as a source of ^{3}He for fusion and postulated that it should still be entrapped on the surface of the Moon. After some research it was discovered that not only was the hypothesis right, but that ^{3}He from the Moon had actually been brought to the Earth in 1969, almost 20 years earlier. The results were published in the journal Fusion Technology in May 1986 [25] and showed that on the order of 1,000,000 tonnes of ^{3}He is still available from

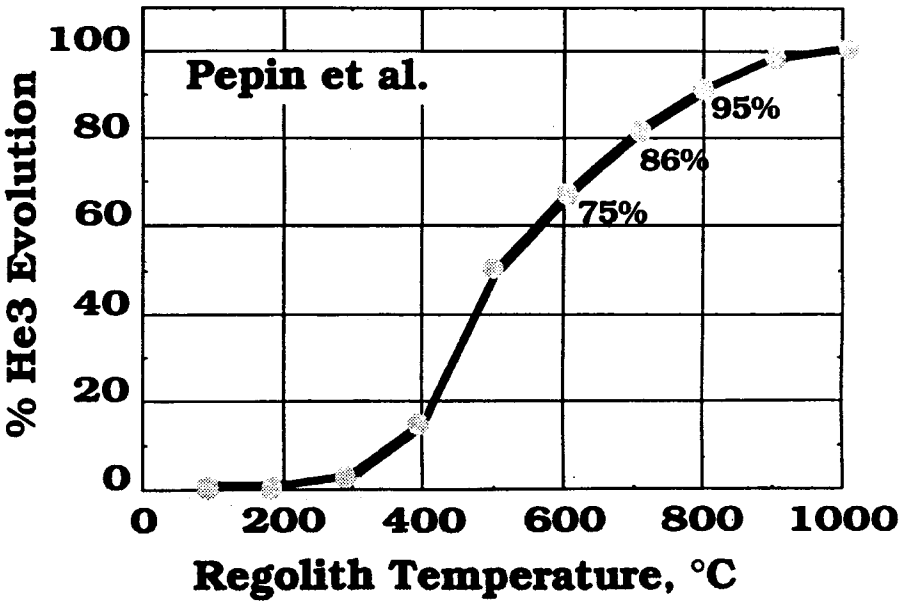


Fig. 3. Helium-3 evolution from lunar regolith.

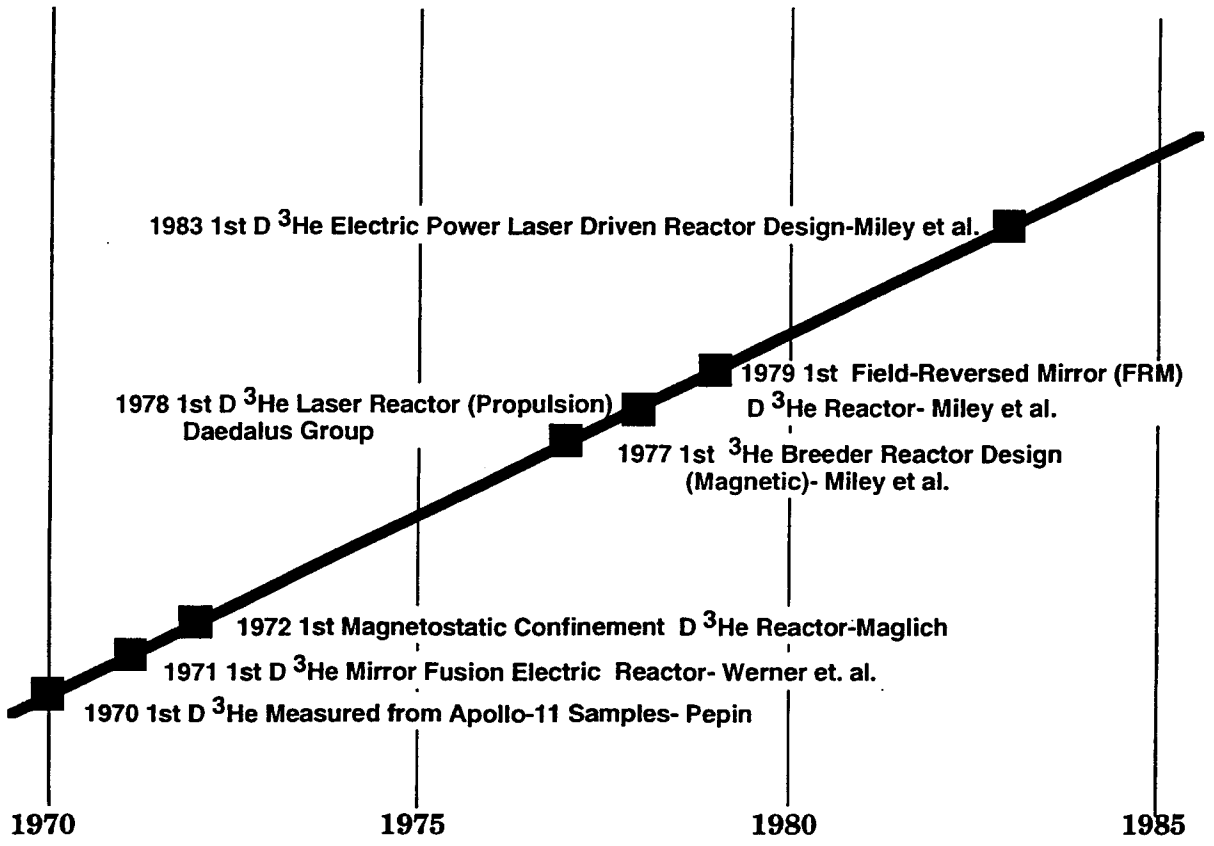


Fig. 4. Chronology of important ^3He milestones.

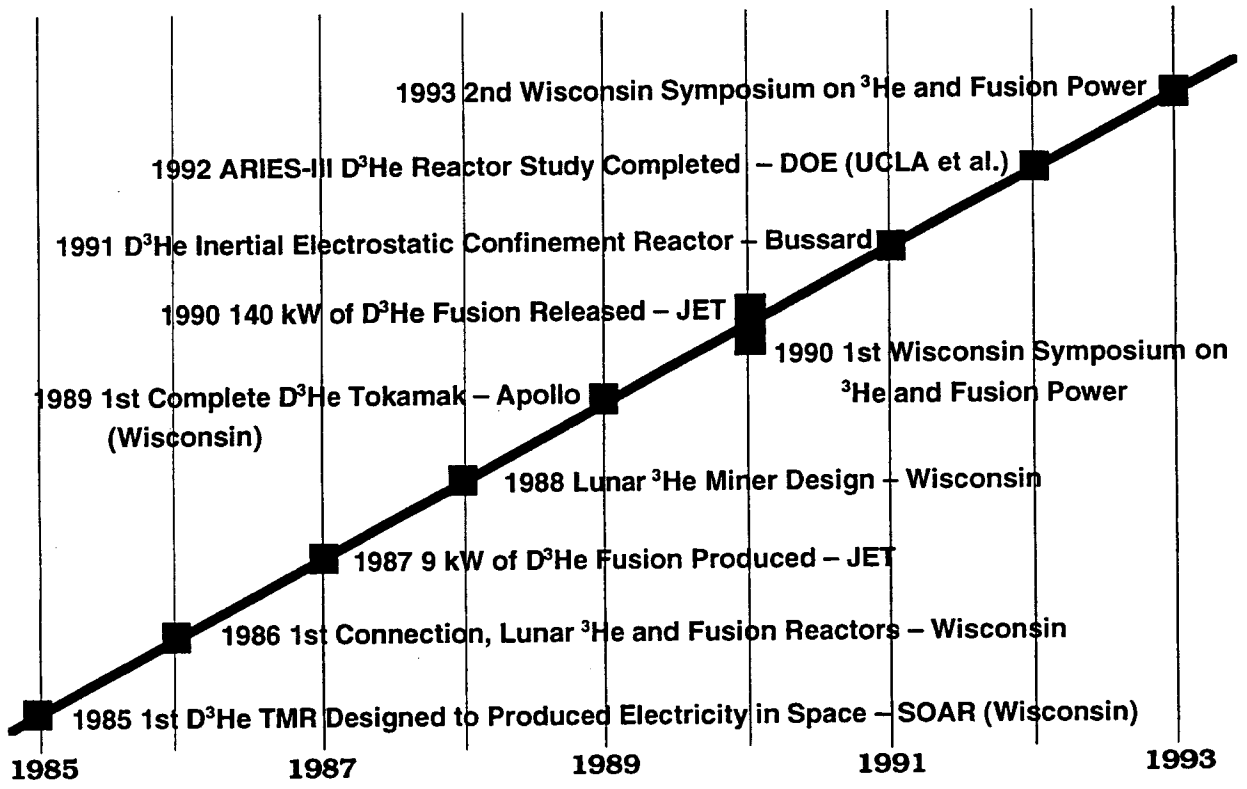


Fig. 5. Chronology of important ^{3}He milestones.

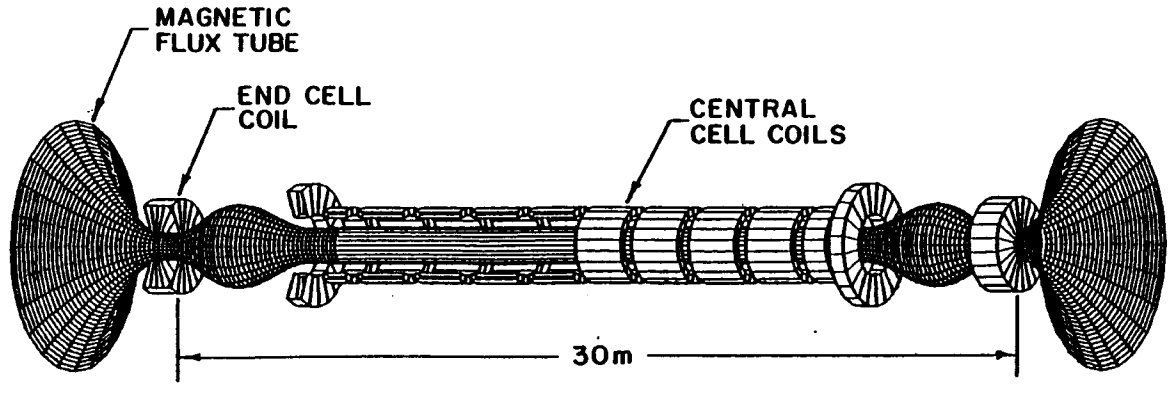


Fig. 6. The SOAR (Space Orbiting Advanced Reactor) concept utilized 3He from tritium decay to make electricity in space [24].

the Moon's surface. After "rediscovering" the earlier work by Pepin et al. [16], we then went on to propose using Lunar ^3He for terrestrial D-^3He fusion electric power plants.

Shortly thereafter, in 1987, experiments performed in the Joint European Torus (JET) in Culham, England, released 9 kW of thermonuclear power from the D-^3He reaction [26]. This was about 50% of the world's record fusion power released by the DD reaction up to that point and the results followed the theory developed for the DD and DT plasmas at that time.

Work at Wisconsin continued in the 80's and a Lunar Volatiles Miner (Fig. 7) was designed by 1988 to extract not only ^3He, but the H_2, water, N_2, and many other C containing molecules that would be evolved by heating the regolith [27]. These elements and compounds are valuable for life support, chemical rocket fuel, and other applications in space [28-30]. The legal [31], international[32] and environmental [33] aspects of lunar ^3He mining have also been explored since that time.

5. D-^{3}HE ELECTRIC POWER REACTORS SHOW PROMISE

After it was shown that a large source of ^3He was available, scientists and engineers began to get more serious about a D-^3He reactor. Even though it was felt that the tokamak was not the best magnetic configuration to release thermonuclear energy from the D-^3He reaction, it was felt that because of the world emphasis on the tokamak from a physics standpoint, one should try to make that fuel cycle work in that configuration.

The Apollo study [34-37] was the first industry supported D-^3He Tokamak study and the key parameters of the various Apollo designs are shown in Table 1 [37]. The conclusions derived from the Apollo series were that even though the plasma *physics* requirements associated

	Harder	Similar	Easier
Physics			
Fueling			
Heating			
Current Drive			
First Wall Heat Flux			
Materials			
High Efficiency Operation			
Safety			
Environmental Impact			
Licensing			
Decommissioning			

Fig. 7. While the plasma physics of D-^3He tokamaks is more challenging than in DT tokamaks, the technology, safety and factors that affect cost are more favorable in D-^3He systems.

Table 1. Key Parameters for Apollo Series of D-^{3}He Tokamak Power Reactors [31].

Design Year of Study	Apollo-L 1988	Apollo-L2 1989	Apollo-L3 1991	Apollo-L4 1993
Energy conversion	synchrotron	synchrotron	mixed	mixed
Net power (MWe)	1200	1200	1000	1000
Shield type-thickness (cm)	SS/H_2O-57	SS/H_2O-59	SS/OC-65	SS/H_2O-57
Direct conversion efficiency	80%	80%	80%	80%
Thermal conversion efficiency	---	---	44%	35%
Net system efficiency	42%	41%	43%	37%
Fusion power (MW)	2872	2807	2144	2437
Synchrotron power (MW)	1626	1663	1027	1082
Bremsstrahlung power (MW)	959	790	652	756
Transport power (MW)	192	267	456	485
Neutron power (MW)	118	138	147	171
Injected power (MW)	23	40	138	57
Average G (MW/m^2)	0.1	0.1	0.1	0.1
Average first wall heat flux (W/cm^2)	91	67	84	98
Major radius (m)	8.0	7.1	7.9	8.06
Aspect ratio	4	2.5	3.15	3.12
Peak coil/on-axis field (T)	20/13	20/10	19/10.9	19/11.2
Plasma current (MA)	47	80	53	55
Beta	6.3%	9.3%	6.7%	6.7%
Troyon coefficient	3.5%	3.25%	3.5%	3.5%
H-mode coefficient	2	2.5	4	4
Density/temperature profile exponent	1/1.5	0.75/0.75	0.95/0.55	0.95/0.55
$n_e \tau_E$ (10^{20} m^{-3}s)	80	41	29	31
$\tau_P^{ash}/\tau_E^{bulk}$	1	0.55	1	1
Energy confinement time (s)	38	24	16	16
Average ion/elec. temperature (keV)	69/55	71/56	57/51	57/51
Average ion/elec. density (10^{20} m^{-3})	1.3/2.1	1.1/1.7	1.3/1.9	1.4/1.95

with the D-^{3}He fuel cycle were indeed harder than those for the DT cycle, the much reduced *technology* requirements more than offset those difficulties (see Fig. 7). The technological advantages arise mainly from the greatly reduced level of neutron emission and the fact that much more of the energy released in the D-^{3}He reaction can be converted directly to electricity via rectennas (synchrotron radiation) The data in Fig. 8, shows how different the form of energy release is in the more popular fuel cycles.

In 1990, the scientists at JET increased the power output from the D-^{3}He reaction by a factor of 16 to 140 kW, a new world's record(in 1990) for thermonuclear energy released in a controlled manner up to that time [38].

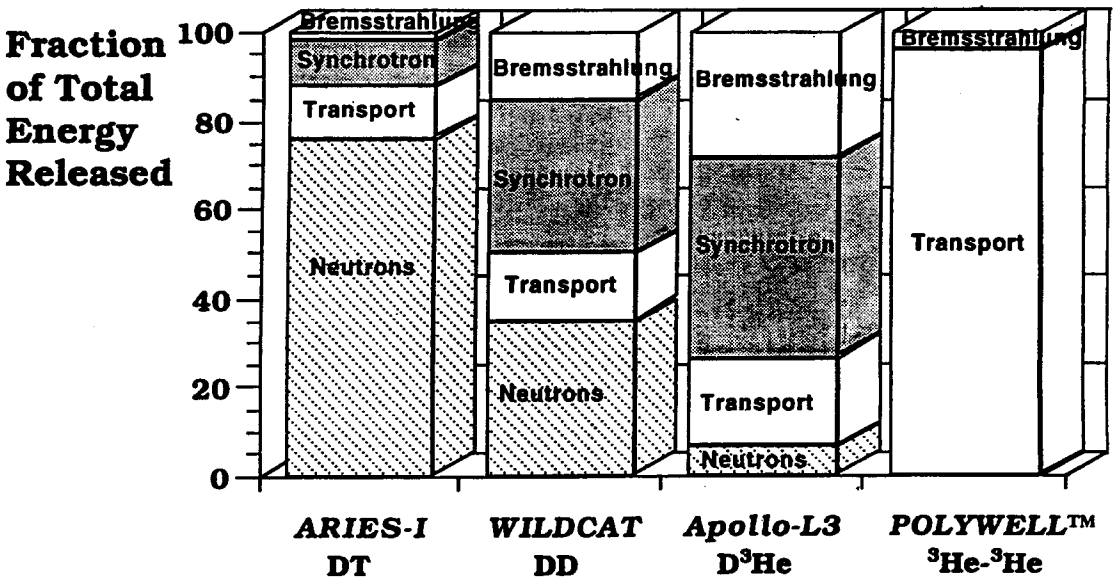


Fig. 8. The form of energy release is quite different in DT, DD, D-^{3}He and ^{3}He-^{3}He fuel cycles.

During the early 1990's several International Symposia were conducted on the promise and problems associated with the D-^{3}He cycle. The 1st Wisconsin Symposium on D-^{3}He fusion was held in 1990 [39] and a D-^{3}He workshop was also held in Moscow in 1991 [40]. These were followed by a second workshop in Russia [41] in 1991 and the 2nd International Wisconsin Symposium on ^{3}He and Fusion Power held in Madison, Wisconsin, 1993 [42].

A new approach to the production of electricity by the fusion of advanced fuels was proposed by Bussard in 1989 [43]. The concept, that he worked on is known generally as Inertial Electrostatic Fusion (IEF), which involves the electrostatic confinement of ions in a spherically convergent geometry. This concept was improved by the application of weak (1-2 T) magnetic fields to confine the electrons while maintaining the electrostatic confinement of ions. Bussard calls the latest modification to IEF, the Polywell™, and in 1991, published the first reactor design using these concepts [44]. The Polywell™ concept is also the first one that makes the ^{3}He-^{3}He reaction feasible.

$$^3\text{He} + {}^3\text{He} \rightarrow {}^1\text{H} + {}^1\text{H} + {}^4\text{He} \qquad Q = 12.9 \text{ MeV}$$

This fuel cycle would completely eliminate residual radioactivity (there are no side reactions that produce neutrons or radioactive isotopes) and essentially all the reaction energy is available for direct conversion to electricity (see Fig. 8).

The Polywell™ concept is also backed up by an experimental facility at Directed Technologies Inc. (see Figure 9). This experiment was started in 1990 and did demonstrate the production of a virtual cathode which provides the electrostatic potential for the ion confinement. A considerable effort on the theory of the Polywell™ operation has been developed by Krall et al., since 1990 [45].

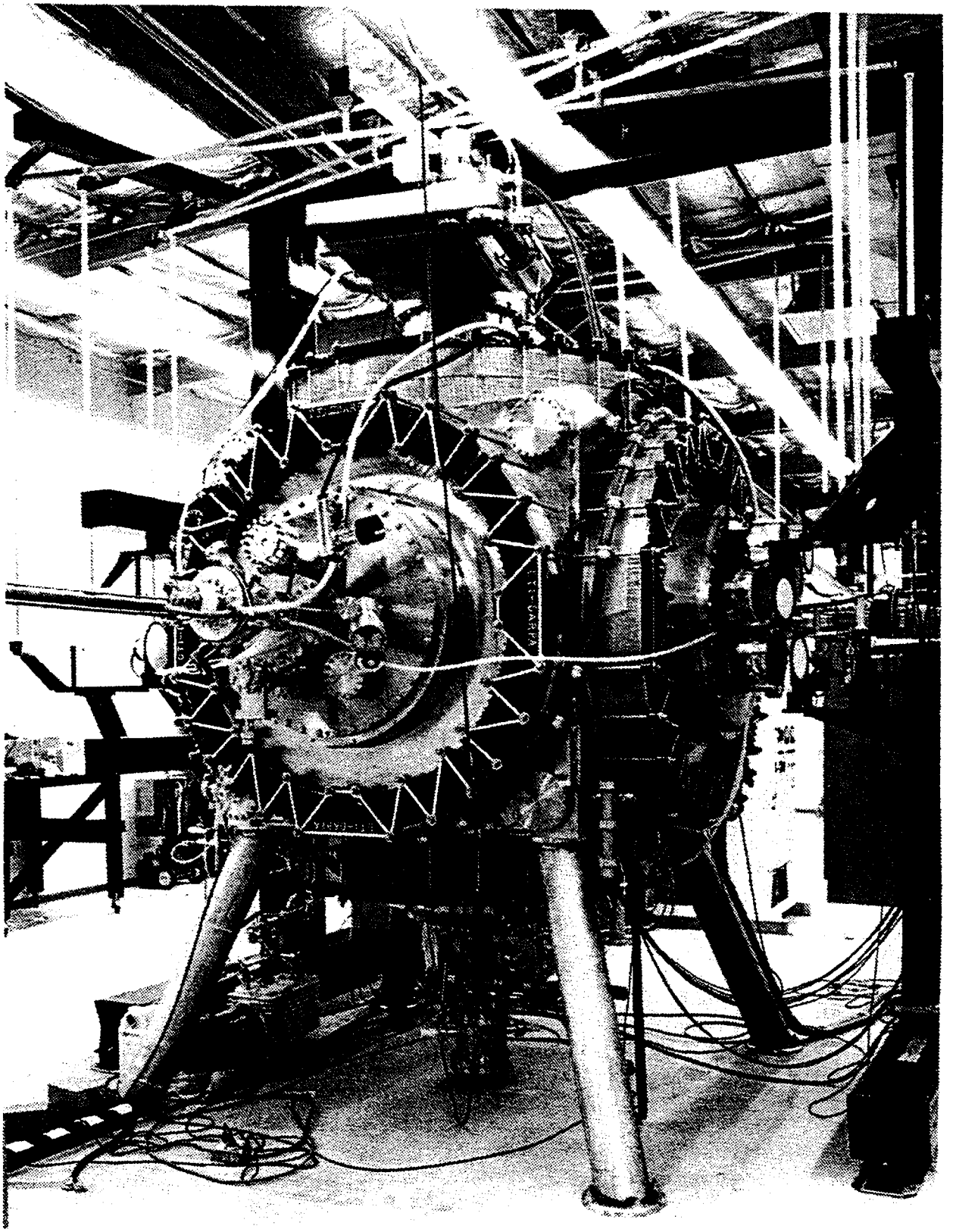


Fig. 9. The Polywell™ experiment at the Directed Technologies, Inc. laboratory was designed to test the D-^{3}He fuel cycle.

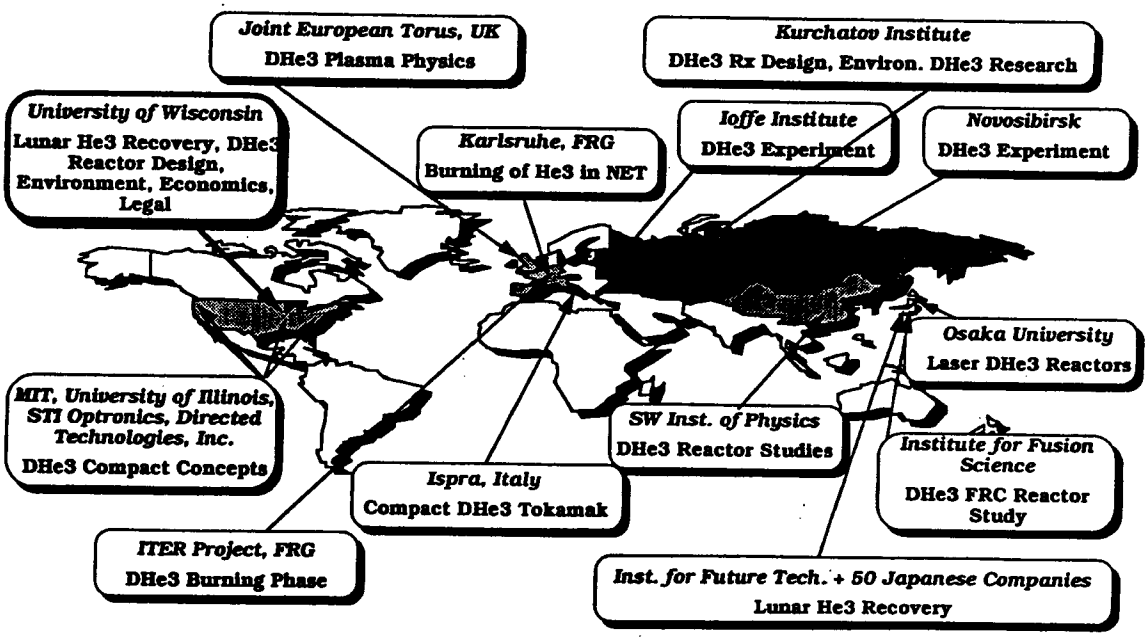


Fig. 10. Worldwide effort in Helium-3 fusion and lunar recovery research.

The increased interest in advanced fuels was shown by the completion of the US DOE study of a second stability tokamak called ARIES-III (remember, all the Apollo reactors were first stability tokamaks). The conclusion of the ARIES study was that the cost of electricity (COE) is comparable to DT tokamaks, at least to the accuracy that we can cost tokamak now. In comparing the first stability Apollo series with the second stability ARIES-III design, it is apparent that if the D-^{3}He cycle is to be used in a tokamak, then the first stability represents a more attractive operating regime[37, 46].

6. WORLDWIDE PROGRAM IN ^{3}HE FUSION IS EXPANDING

There are now programs in 8 countries (U.S., Japan, Russia, Austria, Germany, England, China, and Australia) spanning both the fusion and space resource aspects of ^{3}He use (see Fig. 10). Interest in terrestrial based ^{3}He resources has also been investigated[47,48]. The increased interest is perhaps best shown by reporting the publications that have appeared since the discovery of ^{3}He nearly 55 years ago. Figure 11 shows that the number of open literature publications and reports that have dealt with the fusion and space resource aspects of ^{3}He is now over 600. Since 1962, over 440 publications have been reported on ^{3}He fusion and over 160 publications on the ^{3}He resource question. There were relatively few publications until the early 1970's after which there was an average of one publication every 1-2 months. However, after the "rediscovery" of ^{3}He in 1986, the publication rate jumped up considerably to the point that in 1992, there was an average of more than one new publication a week. The increase in ^{3}He resource papers was particularly dramatic, jumping a factor of over 350% in the 6 year period 1987-1992 compared to the previous 6 years.

7. CONCLUSIONS

The potential benefit to society of ^{3}He has only now begun to be realized some 50 years after its initial discovery and some 40 years after it was shown to be capable of releasing energy

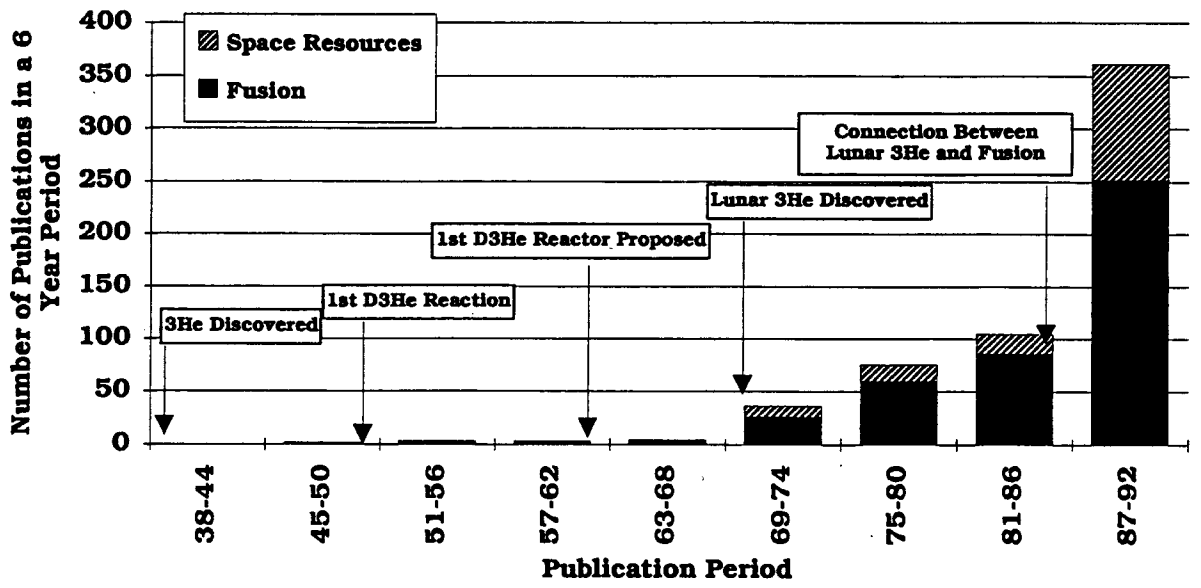


Fig. 11. Publications pertaining to ^{3}He fusion and lunar ^{3}He resources have risen dramatically in the past decade.

in a fusion reaction. Throughout the history of ^{3}He fusion research, the lack of a large, readily available source of fuel has hampered the work in this field. The "rediscovery" in 1986 of data generated in 1970 from the Apollo-11 lunar samples has solved the resource problem and currently many groups around the world are working diligently to reap the benefits that a world economy based on ^{3}He fusion might present. Future work in this area will reveal whether these benefits can be achieved and if we can develop a source of clean, safe and abundant fuel for the generations that follow.

ACKNOWLEDGMENTS

The author wishes to thank Messieurs Joel Crabb, Scott White, Lou Wainwright, and Steve Kratz for their assistance in the background research for this article. This work was supported by NASA and the Grainger Foundation.

REFERENCES

[1] J.R. Long, "House Budgets for Modest Growth in 1994 Federal R&D Programs," *Chem. & Engr. News*, p. 17, August 2, 1993.

[2] I.E. Tamm and A.D. Sahkarov, "*Plasma Physics and the Problem of Controlled Thermonuclear Reactions*," (M.A. Leontovich, ed.), Vol. 1, pp. 1-47. Pergamon, Oxford (1961).

[3] See review in "Nuclear Fusion by Inertial Confinement," (G. Velearde, Y. Ronen, and J. Martinez-Val, eds), CRC Press Inc., Boca Raton, FL. (1993).

[4] Summary of annual funding levels from 1951 to present from official AEC/ERDA/DOE budget reports.

[5] J.G. Cordey, R.J. Goldston, and R.R. Parker, "Progress Toward a Tokamak Fusion Reactor," *Physics Today*, p. 22 (Jan. 1992).

[6] R.W. Conn, V.A. Chuyanov, N. Inoue, and D.R. Sweetman, "The International Thermonuclear Experimental Reactor," *Sci. Am.*, 266 (April 1992).

[7] "Laboratory Microfusion Capability Study-Phase II Report," U.S. Dept. Energy Report DOE/DP-0017 (May 1993).

[8] K. Fowler et al., *Annual Review of Astronomy and Astrophysics,* Annual Reviews Inc., Palo Alto, CA. Vol. 13, p. 69 (1975).

[9] H.A. Attaya, M.E. Sawan, and G.L. Kulcinski, "Waste Disposal of Candidate Structural Materials in Fusion Reactors Utilizing Different Fuel Cycles," *Fusion Technology,* **22**, 115 (1992).

[10] G.L. Kulcinski, et al., "The Commercial Potential of D-3 Fusion Reactors," *12th IEEE Symp. Fusion Engineering*, Monterey, CA, IEEE Cat. No. 87CH2507-2, Vol. 1, p. 772, (1987).

[11] L.W. Alvarez and R. Cornog, "^{3}He in Helium," *Physical Review*, **56**, 379 (1939).

[12] L.T. Aldrich and A.O. Nier, "The Occurrence of ^{3}He in Atmospheric and Well Helium", *Physical Review*, **70**, 983 (1946).

[13] J. Hatton and G. Preston, "Long Range Protons from the ^{3}He(d,p)α Reaction," *Nature*, **164,** 143 (1949).

[14] Personal Communication, W. Wilkes.

[15] G.W. Englert, "Towards Thermonuclear Rocket Propulsion", *New Scientist*, **16**, 16 (1962).

[16] R.O. Pepin et al., "Isotopic Composition of Rare Gases in Lunar Samples," *Science*, **167**, 550 (1970).

[17] "Preliminary Examination of Lunar Samples from Apollo-11," *Science*, **165**, 1211 (1969).

[18] R.W. Werner et al., "Engineering and Economic Aspects of Mirror Machine Reactors With Direct Conversion," Plasma Physics and Controlled Thermonuclear Fusion Research, IAEA, Vienna, 329 (1971).

[19] B Maglich, "The Migma Principle of Controlled Fusion," *Nucl. Instr. and Methods*, **111**, 213 (1973).

[20] G.H. Miley et al., "Concepts for D-^{3}He Satellite Reactors," *7th IEEE Symp. on Engr. Prob. Fusion Res.*, Knoxville, TN, 1172 (1977).

[21] R.C. Parkinson, "Project Daedalus: Propellant Acquisition Techniques," *J. Brit. Interplanetary Soc., Supplement*, 583 (1978).

[22] G.H. Miley, et al., "SAFFIRE-A D-^{3}He Pilot Unit for Advanced Fuel Development," Elec. Power Res. Inst. Report ER-645-1 (1979).

[23] G.H. Miley, et al., "An ICF Reactor Concept Using ^{3}He-AFLINT Targets," *Nuclear Technology/Fusion*, **4**, 889 (1983).

[24] J.F. Santarius, et al., "SOAR-Space Orbiting Advanced Fusion Power Reactor," *Space Nuclear Power Systems*, Vol. 6, Orbit Publ., 167 (1988).

[25] L.J. Wittenberg, J. F. Santarius, and G. L. Kulcinski, "Lunar Source of ^{3}He for Commercial Fusion Power," *Fusion Technology*, **10**, 167 (1986).

[26] J. Jacquinot et al., *Proceedings of the 7th Intn. Conf. on Appl. of Radiofrequency Power to Plasmas*," Kissimmee, FL, May 4-6, 1987.

[27] I.N. Sviatoslavsky, "Mobile ^{3}He Mining and Extraction Systems and Their Benefits Toward Lunar Base Self-Sufficiency," Space 88, Albuquerque, NM (1988).

[28] G.L. Kulcinski, E.N. Cameron, J.F. Santarius, I.N. Sviatoslavsky, L.J. Wittenberg, and H.H. Schmitt, "Fusion Energy from the Moon for the 21st Century," *Second Conference on Lunar Bases and Space Activities of the 21st Century*, Houston, 1988, NASA Conference Publication 3166, 459 (1992).

[29] R.J. Bula, L.J. Wittenberg, T.W. Tibbets, and G.L. Kulcinski, "Potential of Derived Lunar Volatiles For Life Support," *Second Conference on Lunar Bases and Space Activities of the 21st Century*, Houston, 1988, NASA Conference Publication 3166, 547 (1992).

[30] G.L. Kulcinski and H.H. Schmitt, "Fusion Power from Lunar Resources," *Fusion Technology*, **21**, No. 4, 2221 (1992).

[31] R.B. Bilder, E.N. Cameron, G.L. Kulcinski, and H.H. Schmitt, "Legal Regimes for the Mining of ^{3}He from the Moon," University of Wisconsin Report WCSAR-TR-AR3-8901-1 (1989).

[32] H.H. Schmitt, "INTERLUNE Concept for Helium-3 Fusion Development" SPACE '92, *Proc. of Third International Conference on Engineering, Construction, and Operations in Space*, (W. Z. Sadeh, S. Sture, and R. J. Miller, eds), ASCE, 804 (1992).

[33] G.L. Kulcinski, E.N. Cameron, W.B. Carrier III, H. H. Schmitt, "Environmental Aspects of Lunar ^{3}He Mining," SPACE '92, *Proc. of Third International Conference on Engineering, Construction, and Operations in Space*, (W.Z. Sadeh, S. Sture, and R.J. Miller, eds.) ASCE, 606 (1992).

[34] G.L. Kulcinski, et al., "Apollo-An Advanced Fuel Fusion Power Reactor for the 21st Century," *Fusion Technology*, **15**, 1233 (1989).

[35] G.A. Emmert, et al., "Apollo-L2, An Advanced Fuel Tokamak Reactor Utilizing Direct Conversion," *Proc. of 13th IEEE Symp. on Fusion Engr.*, Knoxville, TN, IEEE Cat. No. 89CH2820-9, 1043 (1990).

[36] G.L. Kulcinski, et al., "Apollo-L3, An Advanced fuel fusion power Reactor Utilizing Direct and Thermal Energy conversion," *Fusion Technology*, **19**, 791 (1991).

[37] L. El Guebaly and C.W. Maynard, "Overview of Apollo Studies and Economic Assessment of Several Proposed Variations," this conference (1993).

[38] D.A. Boyd, et al., "D-^{3}He Fusion Reaction Rate Measurements During Fast Wave Heating Experiments in JET," *Nuclear Fusion*, **29**, 593 (1989).

[39] *First Wisconsin Symposium on D-^{3}He Fusion*, University of Wisconsin Fusion Technology Institute Report UWFDM-843 (1990).

[40] *Proceedings on Low Radioactivity Thermonuclear Fusion Based on D-^{3}He*, Internal Kurchatov Nuclear Laboratory Report, Moscow, USSR (April, 1991).

[41] *Proceedings of the Workshop on D-^{3}He Based Reactor Studies*, Kurchatov Atomic Energy Inst., Moscow, USSR, Sept. 25 to Oct. 2, 1991, University of Wisconsin Fusion Technology Institute Report UWFDM-916 (1993).

[42] *Second Wisconsin Conference on ^{3}He and Fusion Power*, Madison WI, July 19-21, 1993. University of Wisconsin Report, WCSAR-9307-3 (1993).

[43] R.W. Bussard, "Method and Apparatus for Controlling Charged Particles," U.S. Patent 4,826,646, Granted May 2, 1989.

[44] R.W. Bussard, "Some Physics Considerations of Magnetic Inertial-Electrostatic Confinement: A New Concept for Spherically Coverging-flow Fusion," *Fusion Technology*, **19**, 273 (1991).

[45] N. Krall, this conference.

[46] G.A. Emmert, this conference.

[47] L.J. Wittenberg, E.N. Cameron, G.L. Kulcinski, S.H. Ott, I.N. Sviatoslavsky, and H.E. Thompson, "A Review of Helium-3 Resources and Acquisition for Use as Fusion Fuel," *Fusion Technology*, **21**, No. 4, 2230 (1992).

[48] L.J. Wittenberg, "Non-Lunar ^{3}He Resources," this conference.

NASA Perspective on Lunar Helium-3 Mining

Raymond P. Whitten
NASA Headquarters
Commercial Infrastructure Division
Mail Code: CI
Washington, DC 20546

(Due to circumstances beyond his control Dr. Whitten was unable to attend this conference. Below is a copy of his prepared remarks on ^{3}He.)

. . . More germane to today, the Fusion Technology Institute offers a unique resource to the Nation's viability into the 21st century. During the 2nd Symposium on ^{3}He and Fusion Power, you will hear much about the science and vision relating to ^{3}He and fusion power. In this regard, the following thoughts are offered as a perspective on ^{3}He.

- Assuming a commercial need for ^{3}He on Earth, the U.S. industry in partnership with NASA could deliver it within the time frame of 2015-2020 (probably faster than we can build fusion reactors). Before that time, it is reported that there is enough ^{3}He in Dayton, Ohio (>100 kg) to supply research reactors for the next 20 years.

- Assuming a commercial need for ^{3}He on Earth, the U.S. industry and NASA will need a focused effort on space science and lunar exploration to lay the ground work for future industrial activity.

- There is no doubt that a large resource (~1 million tonnes) of ^{3}He exists on the Moon.

- Is this an incentive for U.S. industry to build the infrastructure to stockpile ^{3}He to avoid any interruption in the future fuel supply?

- If the U.S. needs ^{3}He, . . . it is technically feasible to get it!

- It is not a scientific problem, like the development of fusion, but it is an engineering problem like Apollo.

- Some preliminary financial analyses show that the procurement of ^{3}He could be a tremendous opportunity for U.S. business to be in the forefront of a $100 billion/year market.

CHALLENGE

- Given ^{3}He may be a major fuel in the 21st century, we cannot afford, strategically, to lose the race (Persian Gulf of the 21st century).

BENEFITS

- The use of ^3He can go a long way toward solving our environmental problems in the 21st century.
- Its use could justify all of our early investments in the Space Program.

FOR THE FUTURISTS

- This is an area where you can have a major impact on the economic, social, and environment future of the U.S. and the world (most students in the audience will be alive in the year 2050).

Concepts for Industry Involvement in Lunar Development

Michael B. Duke
NASA Johnson Space Center
Houston, Texas 77058

ABSTRACT

A strategy for government-industry sharing of investment in lunar development is defined by which early industry investment in lunar development is encouraged. The key elements of the strategy include near-term shared "dual-use" technology development, jointly sponsored space flight demonstrations, a government decision to build an outpost on the Moon, and the demonstration of profitable commercial enterprises such as Helium-3 mining. A mechanism for bringing industry, government and academia together to plan these activities from the beginning is recommended.

BACKGROUND

The concept that the Moon is strategically important to Earth in an economic sense has been discussed since the 1960's, when the prospect of the Apollo program's lunar exploration was imminent and knowledge of the lunar surface was nil. Between 1969 and 1972 six Apollo missions explored local areas on the Moon, discovering a bleak and water-free, rocky surface changed only by occasional crater-forming impacts from large meteoroids, an unending rain of micrometeoroids that melt and stir the uppermost surface materials, and charged particles from the sun that cause radiation damage in surfaces and imbed themselves in the particles of lunar soil. We learned a great deal scientifically about the Moon, its history and its relationship to the origin and history of the Earth. However, dreams of concentrations of metal, or even ice or water, vanished. Yet, ideas for utilizing lunar materials in space and on Earth could not be restrained. O'Neill's [1] concept of space settlements was a means for construction of solar power satellites in space using lunar materials. In 1977, a workshop on utilization of lunar and asteroidal resources was sponsored by NASA (Arnold and Duke [2]). A General Dynamics report on the construction of solar power satellites utilizing lunar materials was completed (Bock [3]). Waldron and Criswell [4] were meanwhile developing their alternative concept for a lunar-based space power collection and beaming system. In 1986, the recognition of the large reservoir of Helium-3 in the lunar regolith (Wittenberg, et al [5]), implanted as charged particles from the solar wind, added to the potential prospects for large scale use of lunar resources for economic benefits on Earth.

However, with this potential utilization of lunar materials under discussion, the U.S. lunar exploration program died as the attention of the scientific community turned to Mars and the outer planets. Attempts to get funds for even modest lunar orbiter missions, capable of mapping global distributions of key indicator elements, failed. The U.S. has not conducted a lunar exploration mission in over 20 years, and none are on NASA's books. The plethora of reports of learned Committees and Commissions have gone for naught with respect to lunar exploration. The speech by President George Bush on July 20, 1989, initiating the now-

expired Space Exploration Initiative's mandate to "Go back to the Moon, this time to stay," did not contribute to the cause of lunar exploration and in some people's view even prolonged the hiatus in lunar exploration.

The U.S. space program currently is undergoing considerable turmoil, due to imminent reductions in space expenditures, an attempt to focus expenditures on new technology that can benefit the U.S. economy or international competitiveness, and an unwillingness to start megaprojects due to their political unpopularity. One of the manifestations of this restructuring is an emphasis on small space missions that can utilize new technologies, in part developed in Department of Defense programs. The one lunar exploration mission that is now being developed in the U.S. is the "Clementine" mission, which is a test of sensor and system capabilities sponsored by the Ballistic Missile Defense Organization. It will obtain a global data set that promises some new, but not very high resolution, lunar information. This clearly is a tactical mission, not a strategic one.

In searching anew for its long term rationale in space exploration, NASA is developing themes and "strategic business units" by which it might organize its future work. Although this strategic planning activity is immature, it has begun to focus on the question of whether NASA's true goal involving human activities in space should be exploration in its broadest sense, or the economic development of space. With the existing focus in the United States on economics and return on investment, it appears that economic development could become a key NASA objective, which could result in expanded attempts to create new industries in low Earth orbit or expand human presence to the Moon as part of a plan to utilize lunar resources (in the broadest sense, including using its location, real estate, and energy sources). This would imply that a new look be taken at the opportunities for returning profit from lunar enterprises that would be attractive to private investment.

CONCEPT

The barriers to commercial development of the Moon are several. They include: (1) absence of any demonstrated government interest in the Moon, which limits the opportunities to have the government as a customer; (2) the long time frames associated with building the infrastructure that would allow lunar development and profits to flow back to investors; (3) the high cost of space transportation that make any mission, however small, a multi-tens-of-million dollars project; (4) uncertainties in international law regarding the ownership of lunar resources. Something is needed to build the proper bridges between current capabilities and resources and the future, grander visions of lunar commercial enterprises. In the case of using lunar resources as the basis for a new, non-polluting and essentially unlimited source of energy for the Earth, such strategies may be available.

As part of the new technological strategy embarked upon by the U.S., the concept of "dual-use" technologies has been emphasized. Dual-use technologies are those which are necessary for space exploration, but can also have applications in the domestic or international economy in the near future. An example might be the development of fuel cells that could power lunar outposts or electric automobiles on Earth. The Advanced Research Project Agency (DOD) and NASA are initiating Technology Reinvestment Programs in which such

dual uses are sought. Typically, the government may be willing to invest 50% of the cost of technology development if industry puts up 50%. Rights to the technology would remain with industry.

Within the space program, technologies for planetary surface activities are likely to spawn many near-term applications on Earth. This will occur because the planetary surface technologies will be required for doing things that people normally have to do on Earth, such as providing safe and comfortable living quarters in environmentally extreme conditions; operating complex and potentially dangerous equipment automatically; developing more reliable inventing power systems for surface transportation; new manufacturing techniques for rapid and versatile production; or developing new technologies for terrestrial mining and material processing. All these and more are inherent in the requirements for lunar surface activities. Thus, it appears that the dual-use concept is applicable to lunar technology development. Further, it may be that this is the type of leverage that can be provided to attract industry into a longer term commitment to lunar development. Glaser [6] has

In a general way, Fig. 1 shows conceptually the manner in which stepwise investments could be staged to allow industry continuing returns on their technology investments while promoting their long-term interests in profits from lunar industrialization described a similar

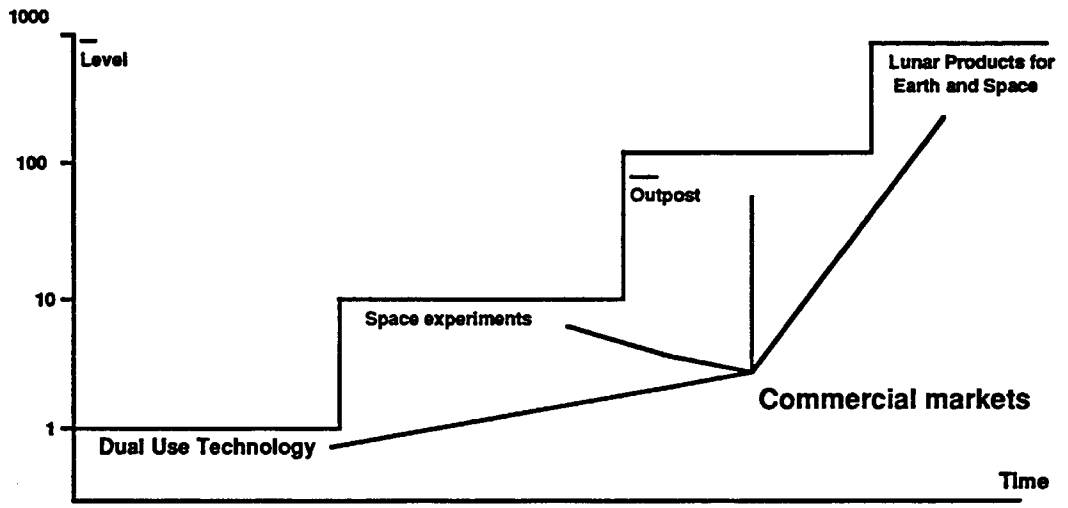


Fig. 1 "Stairstep approach to developing commercial involvement in Lunar Development"

scenario with respect to the growth of power-beaming and solar power satellites. In relationship to the development of lunar Helium 3, the scenario might work as follows:

Step 1. Dual use technology development.

A joint industry-government program would focus on the development of the extractive and surface support technologies that would ultimately be necessary on the lunar surface to support Helium-3 mining and extraction. This could include new technologies to extract very low concentrations of gases from lunar regolith, automated miners, solar reflectors-concentrators, life-support systems to support human crews, and a wide range of automation and robotics tools and applications. Industry would focus on the near-term applications and would provide human and monetary resources and marketing skills; government would provide space technology expertise, technology development funding and perhaps in-house resources. These development projects would typically be conducted as laboratory investigations and field demonstrations on Earth. Industry would expect to recover its own investment over time from sales of new technological products, either hardware or software. The government would benefit through reduction of risks associated with future space programs and from stimulation of new markets for technology.

Step 2. Space experiments

Some of the technologies developed in step 1 will need to be tested in space as the next level of their application. Space programs — U.S., European, Japanese, or Russian, may be the customers for these technologies; alternatively, industry may gain enough confidence in the eventual payback to support demonstrations in the space or lunar environment. Possibilities include expeeriments in the U.S. or Russian space stations, or automated missions to lunar orbit or the lunar surface. These could include the development of industry-proprietary information on the distribution of Helium-3 on the lunar surface, the demonstration of excavation and volatile extraction capabilities by landing experiments on the Moon, or a verification of energy or life support system technology in the lunar environment. In these programs, industry might sponsor the experiments, while government provided the transportation system, perhaps again with a 50/50 split of expenditure. Part of the return to commercial investors would be the expertise and technological leadership that would return profits at the next step.

Step 3. Lunar outpost

A key step in the lunar development process is likely to be a government commitment to the establishment of a lunar outpost. This would be undertaken when the confluence of reasons to resume human lunar exploration — science, education, exploration, commercial interest, national pride, etc. — resulted in a concensus needed for a government program to begin. It is not impossible that economic interest alone could drive such a program, but economic gain is likely to be only a part of the rationale for the outpost. If industry could convince itself of a favorable return from an industry-sponsored lunar outpost, they would need no government sponsorship. On the other hand, there are such clear reasons that the government should support lunar development aside from economic gain. Thus, it is likely to happen earlier as a government program than as a private one. In that case, the participating industry would find the government to be a customer for some of its technology (volatile extraction, lunar propellants, energy systems, life support systems, exploration data, etc.). The potential to extract Helium-3 would be demonstrated as part of the lunar outpost program;

however, industry would have to support costs of the experimental verification of the processes and systems that they would use in the production phase. The government would be able to show reduced costs for its activities because of industry involvement, while at the same time contributing to the development of lunar infrastructure (particularly the transportation system) that would provide leverage for subsequent steps. The development of lower-cost access to space can also be a significant factor in enabling commercial return.

Step 4. Lunar products for Earth and Space

After the initial government-sponsored lunar outpost program, the development of commercial industry would be up to industry itself. It is expected that all of the R&D needed to confirm the potential for Helium-3 extraction would be done as part of the previous step, either through the government investment in infrastructure or as commercial investment in technology development.

RECOMMENDATIONS

This scenario is painted in broad terms only. If it is a realistic scenario, it speaks to a need for an early government-industry dialog, which would focus on key questions, such as:

(1) What are the research projects with real dual-use potential in the near-term? How should they be undertaken? What commitments are needed from industry and government? What cost-sharing agreements can be reached? What is the proposed and beneficial role of universities, Centers for Commercial Development of Space, Space Engineering Research Centers and related organizations? Who are the proper industry participants?

(2) How can commercial funding of flight experiments be expedited? What industry and government commitments make sense? How should industry and government work together in this arena?

(3) How should intellectual rights to the discoveries made in the program be apportioned? How should industry's proprietary investments be protected to encourage commercial investment? How should technology licenses to industry be managed? How can the public interest in new discoveries and technologies be protected?

(4) What international agreements must be made to enable industry to effectively invest in this area? Must international agreements come first, or will some level of investment be possible in their absence?

(5) What must be done to promote the evolution of commercial involvement in lunar development? Is the dual-use technology approach sufficient? Are other government subsidies or agreements to buy data or products required? What is the government's commitment to a lunar outpost based on other national priorities and needs? From industry's point of view, what opportunities are there to reduce the risk associated for long term investments?

(6) What are the technological show-stoppers in Helium-3 fusion that require near-term research and development attention? What is the market that will drive the rate of investment and the time of return? What needs to be done to provide the optimum pathway to investors while protecting the interests of the public investors in lunar development.

These proposals are not new. In 1989, NASA sponsored the Lunar Energy Enterprise Case Study [7]. That report recommended that:

> "industry, the financial community, and academia be given a primary role in planning the overall [lunar energy] program. This could be accomplished through the establishment of a high-level private sector advisory committee."

Further, they recommended that:

> "a Workshop be held in accordance with its [the Task Force's] conclusion that national policy on extraterrestrial energy supply concepts must be developed. The purpose of the Workshop would be to expose the issue of long-term energy supply options to high-level decision makers, provide understanding about the issue, and seek policy direction and commitment. To be successful, the participants must include high-level representatives of the Administration, appropriate government agencies such as DOE, EPA and NASA, the energy, environment and space leadership of the Congress, electric utilities, the space and energy supply industries, and the financial communities. The Task Force recommends that the suggested private sector advisory committee's participation in the planning aspects would be essential."

A mechanism is needed now to initiate this required dialog. The environment is not conducive to big projects, however beneficial they may be in the long term. However, it may be possible to gain support for a study group or Center for Lunar Development as a part of the Centers for Commercial Development of Space Program (CCDS). The initial objective of this Center would not be to develop a funded research program at the level undertaken by current CCDS Program Centers, but to focus on the development of the data base and industry involvement in the discussions that could lead to a firm relationship between the various partners.

Although this is a long term process, it needs to begin now, for several reasons. First, the world's energy problems are long term, but can attain critical dimensions suddenly (for example, a disruption of world oil or gas supplies). Second, there is a need for direction in the space program — vital future opportunities can be cut off with little opportunity to regain them if poor decisions are made in the near term. If the commercialization of the Moon is a valid possibility, supported by a clear vision of economic return, substantial guidance would be given to the nation's space program. Third, world energy problems are inherently international in nature. Any U. S. efforts aimed at developing the commercial potential of space should be done with a sensitivity to the interests of the international community. At a time of increased international participation in space exploration associated with the space station program, this would be an excellent time to incorporate the interests and needs of the entire world as the project concepts are developed.

REFERENCES

[1] G. K. O'Neill, "Space Colonies and Energy Supplies to the Earth," Science, 190, 943. (1975)

[2] J. R. Arnold, and Duke, M. B., "Summer Workshop on Near-Earth Resources," NASA CP-2031, NASA, Washington, D. C. (1977)

[3] E. H. Bock, "Lunar Resources Uses for Space Construction," Final report for contract NAS9-15560. General Dynamics Convair Division, Advanced Space Programs, San Diego, California. (1979)

[4] R. D. Waldron and Criswell, D. R., "Concept of the Lunar Power System," Space Solar Power Review, 5, 53. (1985)

[5] L. J. Wittenberg, Santarius, J. F., and Kulcinski, G.L., "Lunar Source of He-3 for Commercial Fusion Power," Fusion Technology 10, 167. (1986)

[6] P. Glaser, in Enterprise Case Study Task Force, "Report of NASA Lunar Energy Enterprise Case Study Task Force," NASA Technical Memorandum 101652, NASA, Washington, D.C. (1989)

[7] Enterprise Case Study Task Force, "Report of NASA Lunar Energy Enterprise Case Study Task Force," NASA Technical Memorandum 101652, NASA, Washington, D.C. (1989)

Deutsches Aerospace-ERNO Perspective on He-3 and Power from Space

J. Sved and K. Fuchs
DASA-ERNO Raumfahrttechnik GmbH
Hunefeldstrasse 1-5
2800 Bremen 1
Germany

ABSTRACT

Extraterrestrial power generation and delivery to Earth has been a long term application of space technology that ERNO Raumfahrttechnik GmbH has investigated since 1985 through the Global Solar Energy Concept (GSEK) project. As the name indicates, consideration of Helium 3 and fusion power was excluded. The raising of awareness of the Helium 3 option has to overcome an established corporate vision of the space business future. The Helium 3 fusion power option has had advocacy from within the company and stimulus from customers such as the European Space Agency. It has now attained inclusion in corporate "working group" discussion papers but in the frame of long term projects such as planetary terra forming. Informed scepticism is the next barrier which the Helium 3 advocates must overcome. Internal research funds will be allocated to support investigations which will either increase corporate interest to a level similar to that which sustains the current GSEK effort or continue at a very low level of enthusiast interest. This paper elaborates the arguments and types of answers that may be needed to advance corporate awareness of the business potential of lunar Helium 3 mining industry and support infrastructure.

1 INTRODUCTION

Within the Deutsches Aerospace companies the potential of extraterrestrial energy sources for electrical power generation on Earth has been investigated for many years under the title of the Global Solar Energy Concept (GSEK). This effort was started in the past decade before there was any awareness of the realization by Kulcinski et al. that the abundance of Helium 3 in the lunar regolith may enable a commercial clean fusion power industry [1]. The possibility of two distinct sources of business for a space infrastructure company interested in developing a space power industry seems very appealing. However, the reality is that an established vision of a future space business scenario has become entrenched. The Helium 3 option is not widely regarded as a near term option at present because of the perception that demand for it will not arise until clean fusion power is ready for commercial development in some 50 years from now.

This paper will review the progress of a more positive assessment of Helium 3 made during the past few years within DASA and the possible next steps. The advocacy effort relies on the progress made by the Helium 3 fusion power community. The next steps required of this community by the space industry are suggested in order to stimulate some planning of the

advocacy effort. A mutual benefit synergy is foreseen where the industrial space community is able to support the Helium 3 fusion community.

2 GSEK

The research for GSEK is financed by the German Ministry for Research and Technology (BMFT). Several institutes and companies are engaged in research of technologies and infrastructure support systems.

The GSEK concept envisages an initial, affordable start through the establishment of solar radiation collection stations in desert regions such as the Sahara. This energy would be used to electrolyze water to yield hydrogen. Bulk shipment of the liquefied hydrogen to Europe would establish a demand for this form of energy as a fuel [2].

Space based Solar Power Satellites would be built over several decades. A key technology that is being developed is the Free Electron Laser. This form of energy transmission is regarded as a necessary element to reduce the system cost. Today the break through is awaited and the research continues in various laboratories.

On the space infrastructure side, it is apparent that a lifting capacity that greatly exceeds the total annual traffic of launchers operating today is mandatory. DASA-ERNO has conceived and detailed an ADvanced European LaunchER (ADLER) that could deliver 40 to 60 tons to Low Earth Orbit. The tanks of the Single Stage To Orbit ADLER rocket would be consumed as part of the SPS structure, while the propulsion module would return ballistically to Earth. The partially reusable ADLER would cost approximately $10 million per launch when 600 are launched per year. After assembly and check-out of each SPS in LEO, an electric ion rocket would gradually boost the SPS to geostationary orbit. The rate of traffic for this scenario is truly immense if the ADLER launcher is used to its optimal capacity. In addition to the SPS units, an infrastructure of assembly support facilities is necessary even if a pure robotic assembly sequence can be devised.

3 HELIUM 3 BASED INFRASTRUCTURE

Preliminary investigation of appropriate economic cis-lunar transport infrastructures has been stimulated in the context of a European Space Agency funded study with the short name of SYSTEMSI [3]. A scenario was set where, in the year 2050, the supply of lunar Helium 3 would satisfy a demand from terrestrial power stations amounting to 25 % of total world demand for electricity. This target served to assess the likely demand based on current projections for total power demand growth and the likely market penetration of a clean fusion power industry. The reference traffic growth curve is shown in figure 1.

The power demand and fusion power station construction rates were adopted from reference [4]. The estimates of Helium 3 mining and processing plant specifics were established from the estimates in several references. The tonnage of facilities needed on the Moon was then

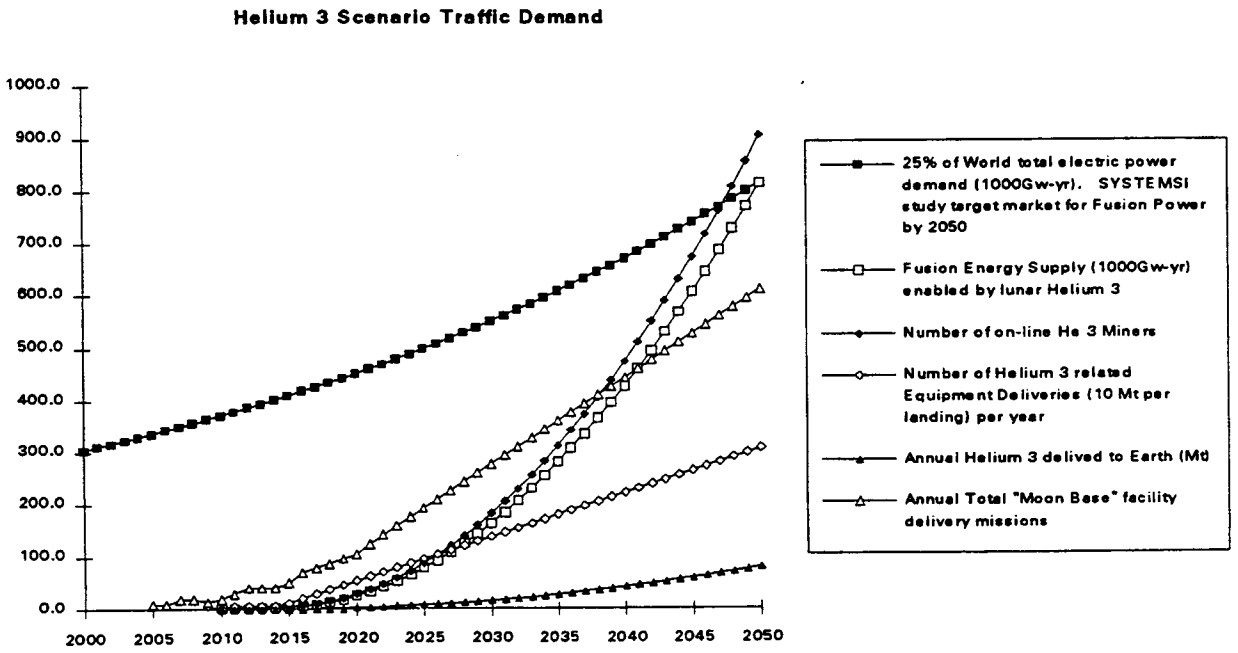


Fig. 1 Helium 3 cis-lunar traffic demand projection

estimated for direct support of the ^{3}He operations. The additional infrastructure for Lunar operations was set equal to the direct ^{3}He mining and refining facility tonnage.

The resulting traffic demand curve was based on a capability to deliver 10 metric tons of cargo per mission. The actual transportation system capability would most certainly evolve over the period of 40 years. The early lunar transport system that was set by scenario constraints imposed by ESA would most likely deliver less than 10 tons perhaps as many as 12 times per year. A medium term cis-lunar transport system would need to deliver more than 1000 tons per year.

At present, in Europe, the type of space infrastructures that are being considered are based on Future Space Transport Systems with missions only concerned with delivery to and return from Low Earth Orbit. The requirements on a cis-lunar transport system that is able to be scaled up for support of Helium 3 mining are not being seriously considered because the potential of Helium 3 is not accepted or because advocates of rather incompatible transport infrastructure concepts have a more prominent position to promote their views. There are many similarities to the Helium 3 versus Tritium rivalries.

4 STRATEGIC PLANNING

DASA-ERNO has commissioned working groups to look forward and postulate future scenario options. In 1987 the selected "Group of Six" published their scenarios for the

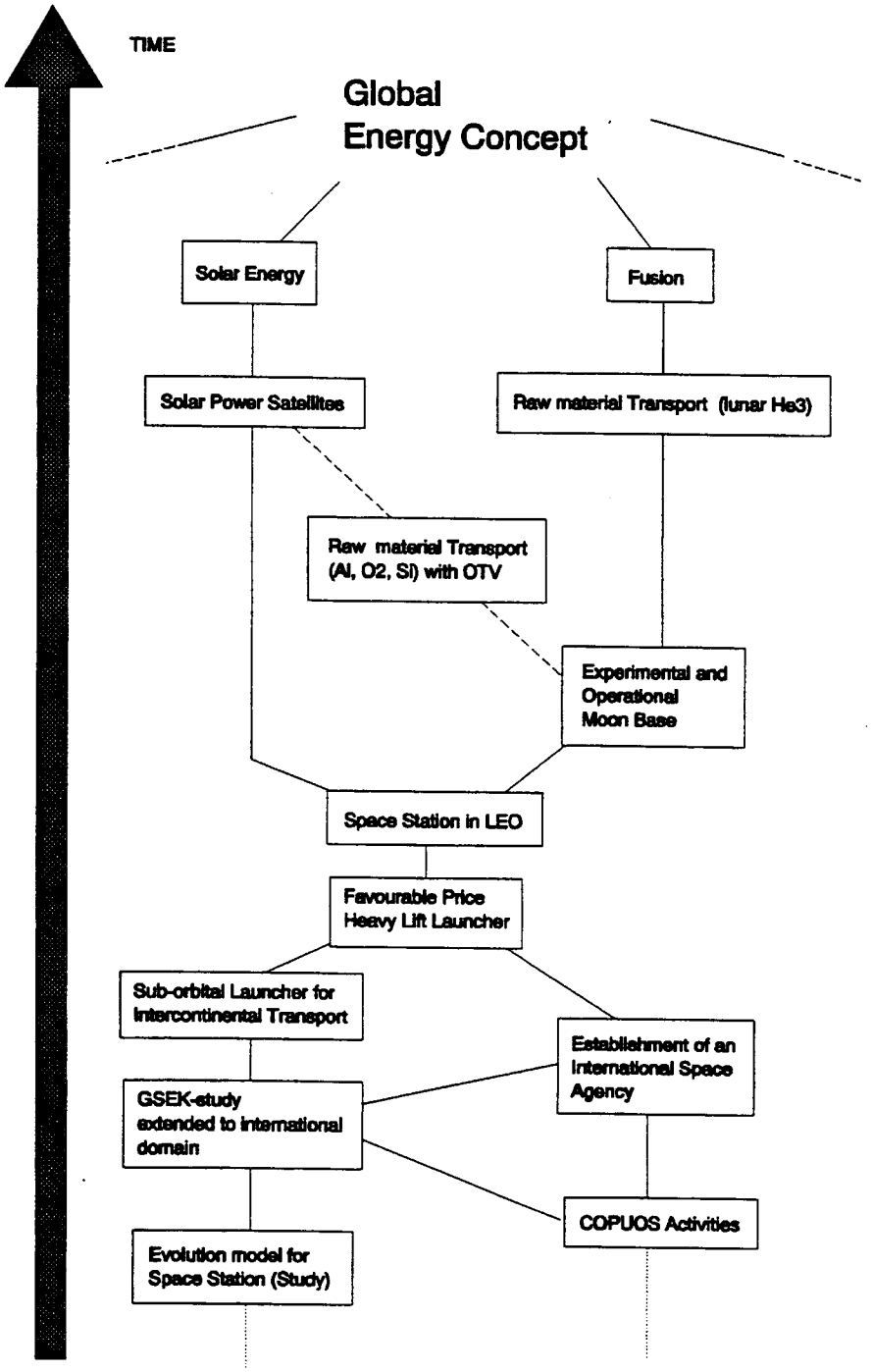


Fig. 2 Paths to global energy supply from space.

utilization of space [5]. Helium 3 was mentioned as a long term option with lunar fusion power stations beaming energy to Earth via lasers. The availability of published investigations of ^{3}He at that time was virtually nil.

The Space industry is in a period of major upheaval due to the cancellation, indefinite postponement, major down-sizing of some leading projects due to escalating costs and a tough economic climate. The 1991 European Space Ministers conference triggered a review of long term space objectives.

DASA-ERNO again commissioned a "Perspective" working group in 1992. It addressed the prospects for a World Space Organization which would take charge of major projects such as energy from space. Alternative organization structures with other than the current Space Agency led hierarchy were investigated [6]. The Helium 3 option was given a more positive assessment. In a chart of evolutionary paths it was placed at the same level as the SPS option. This is shown in figure 2. The background information for this more positive assessment was the body of information collected by Sved [7]. An appropriate transport infrastructure and the steps required to achieve it were also indicated and included as an optional path. However, sceptical judgments based on the expectation that commercial fusion power remains 50 years in the future, as indicated in most reports on fusion power, persist.

The "Perspective" group advocated DASA internal funding to research three scenarios deemed most promising:

- Ozone restoration by means of laser beams from orbital stations proposed by N.P.O. Energia
- Global Telepresence for medical monitoring as an application of personal communications technology.
- Extraterrestrial resources and alternative energy which includes ^{3}He.

No selection has been made so far and further investigation of these options will be necessary.

More recently a new coordination initiative for DASA space transportation systems development has been established. The proposed applications that may be foreseen for space transportation in the period 2010 to 2020 are being collected for assessment. This company funded activity provides another opportunity to review the potential of lunar ^{3}He and the most cost effective cis-lunar transportation architecture. Attention is also given to the immediate future steps towards such a major industrial goal.

5 THE WAY FORWARD

With the establishment of a new advance projects and studies department for utilization missions and operations, in-house R&D funding is being sought to continue the investigations into ^{3}He. Team partners are being sought in order to acquire study contracts from various organizations such as the European Commission and national government agencies.

The interest of a company such as Deutsches Aerospace extends beyond the space transport and infrastructure issues. The parent company, Daimler Benz, has a wider industrial perspective where the Earth based and Moon based functions must be facilitated. As with the GSEK investigations, a comprehensive infrastructure and market strategy assessment is necessary.

The most obvious impediment to an acceleration of Daimler Benz (or similar industrial companies) interest is the availability of information to enable a broad based assessment of the potential for D + ^{3}He fusion power. The potential of a break through design and demonstration of a more affordable reactor design is tantalizing. But the information is too scarce. The symposium at which this paper is presented is a timely opportunity to improve the above described situation.

The collection of information and its refinement into digestible reports for Chief Executive Offices is not likely to be successful without the addition of external influences such as interest from potential or actual customers seeking a comprehensive assessment of ^{3}He fusion power as an economic business sector of the energy industry.

REFERENCES

[1] L.J. Wittenberg, J.F. Santarius and G.L. Kulcinski "Clean Thermonuclear Power from the Moon," Symposium '86 - The First Lunar Development symposium, S86-42, Sept 1986.

[2] Global Solar Energy Concept - Technology, Operability and Programmatics, J. Spies, IAF-93-R.2.432

[3] Cis-lunar Transport Infrastructure Analysis for SYSTEMSI study, ERNO TN-OT122-11-92, Iss 1 Rev. C, J. Sved, Oct. 1992

Paper to be published in proceedings of ASCE Space 94, Engineering Construction and Operations in Space (TBC)

[4] Fusion Power from Lunar Resources, G.L Kulcinski and H.H Schmitt, IAF-90-??

[5] Raumfahrt - Option fuer die Zukunft, Part 1 Nutzung Szenarien Strategie, U. Becker, Dr. H.P. Richarz, J. Spies, W. Koenig, W. Schmidt, Bremen/Munich 12.5.1987, 1988 EPNO Raumfahrttechnik GmbH

[6] Die Notwendigkeit einer globalen Raumfahrt (The necessity for global astronautics), Dr. F. Pohlemann, DASA-ERNO, 25-8-1992

[7] A Vision of a Space Market, J. Sved, Feb 1992.

U.S. Army Perspectives on Lunar Resource Recovery and Utilization

Edward B. Kiker
21824 Edwards Drive
Easton, KS 66020

ABSTRACT

The U.S. Army Corps of Engineers is involved with space access, development and utilization by virtue of its traditional roles in exploration, Federal property and infrastructure maintenance, and contracting agent for Federal construction. Within these roles the Corps has been the construction contracting agent for other branches of the government for facilities involving launch, maintenance, and monitoring of spacecraft. The Corps was involved with topographic map preparation supporting missions to the Moon and Mars. The Corps has also been active in working with NASA in developing planning documents for fielding of large space structures and Lunar base design and construction. At this time it appears that helium-3 as a fuel for fusion energy may become the primary commercial and national incentive for returning to the Moon and establishing permanent facilities. The promise of fusion involves national security, health care, and Earth environmental improvement concerns. Lunar mineral resources will be required for construction materials for both Lunar bases and large orbital structures, and the Corps is concerned as it maintains large laboratories and databases for construction engineering technology. Lastly, the Corps will be involved with preparation of Environmental Impact Statements supporting Lunar surface activities.

1. INTRODUCTION

1.1. Representation

The views expressed in this paper are entirely those of the author, and do not represent the official position of the U.S. Government, the U.S. Army, or the U.S. Army Corps of Engineers.

1.2. Why the Moon

There is no question whether or not we will return to the Moon to stay. We will return to stay, and we will mine the Moon for resources to be used on the Lunar surface, in space, and on the Earth. The only questions are what incentive will finally induce us to commit the considerable national resources which that return requires, and when will we attain a national popular appreciation and demand for that incentive? This popular demand is necessary before the return can happen, and it must come from the working, voting public. The most likely incentives are

three:

- a small scientific research and exploration station
- a search for cleaner energy due to environmental pollution
- a search for cheaper energy due to rising energy costs.

The first, a small scientific research and exploration station, is perceived by the public to be a cultural extravagance, nice to have if it can be afforded, but not necessary to vital national interests. Even such a station, however, would find it economically advisable to do some resource utilization to partially support itself with oxygen and some construction materials. This modest start would begin to build an experience base for Lunar resource use. This incentive for its own sake is not likely in the foreseeable future.

The second, a search for cleaner energy due to environmental pollution on the Earth, is highly likely in the next thirty years. The popular awareness is already very widespread that electric vehicles must soon begin large-scale displacement of hydrocarbon internal combustion vehicles, that industries which use fossil fuels and nuclear fission to produce heat must convert to electricity, and that industries which use fossil fuels and nuclear fission to produce electricity must convert to another energy source. There is some public perception that hydrogen combustion engines are a viable alternative, but that has foundered on the fact that electricity is needed to produce the hydrogen. Thus, we know we will need more electricity than we now use, and we are no longer willing to utilize the traditional sources at the traditional rates.

The third incentive, a search for cheaper energy due to rising energy costs, is also fairly likely, but not in the near-term, and even then it will not be the cost of producing the energy from fossil fuels and nuclear fission. Production costs can be held down because coal is still plentiful, if not of the best quality. Natural gas is also available. The cost increases come from the public insistence that plant emissions be scrubbed, always an expensive task, and from the growing public demand that pollution-producing industries be made to pay for the health care costs resulting from their pollution. Both of these costs will be passed on to the consumer. These two costs are directly related to the search for cleaner energy. We have also already seen governmental desires to both raise revenue and reduce energy use by imposing energy use taxes.

The transition which the government and the public at large have not yet completed is the transition from dissatisfaction with the energy sources we have to the search for the sources we need. That transition has begun in a small way, with increased

government and private investment in alternative Earth-based energy sources such as solar, wind, geothermal, tide, and ocean temperature gradients. Experience in the availability, reliability and costs of those sources, however, is bringing home the realization that they will never produce more than a small fraction of the need and even that fraction will be expensive. The resulting frustration is just now beginning to turn some public attention towards what are still popularly considered far-fetched solutions: fusion energy, and solar power stations in orbit or on the Lunar surface beaming their energy to the Earth by microwave. Articles on these solutions are becoming more and more frequent in the popular press. The general public is not yet at all aware that both of these possible solutions require Lunar resource utilization, the first for the helium-three fuel, the second for construction materials. Only when that awareness grows and becomes conventional knowledge will the return to the Moon become a certainty in order to pursue one or both of these solutions. Of these two solutions fusion energy based upon helium-three requires far less infrastructure than solar power stations either in orbit or on the Moon, and is therefore our best technology investment.

2. ARMY INVOLVEMENT IN LUNAR ACTIVITIES

2.1. Army Corps of Engineers

All that said, where does the U.S. Army fit into the picture? Because of the great initial expense of insurance, transport to the Moon and subsequent construction, the entire cost is not likely to be borne by private enterprise. The U.S. Government will have to play its traditional role of providing much of the exploration, mapping, and infrastructure of transportation and Lunar surface structures as we move into this next frontier. It is hoped that many other countries will participate in this endeavor as partners. Exploration and mapping for the government are traditional roles for the U.S. Army Corps of Engineers (USACE), often in cooperation with the U.S. Geological Survey. Construction contracts for the building of space transportation launch and landing facilities and of Lunar surface structures must be arranged, and the construction contracting agent for the U.S. Government is the Army Corps of Engineers. Construction contracting is a mission of the Civil Works arm of the Corps, and is performed in support of other branches of the government. The Corps does not operate most of the facilities it builds. Rather, it accepts requirements and funding from the customer, for example NASA, "builds to suit" by letting and monitoring construction contracts, and turns the finished facility over to the customer for occupancy and operation.

The key point here is that the Lunar and space transportation infrastructures will not be designed and built just by soldiers or government civilian employees, but also by private sector civilian construction firms under contract to the Corps. The workers will be architects, heavy equipment operators, pipefitters, electricians, chemists, cooks, administrators, engineers, mathematicians, doctors, and all the other skills needed to design and build a small industrial town. Those who must actually go to the Moon will all be given the specialized training they will need to operate successfully in the unique Lunar environment. A very close analogy to Corps-contracted Lunar construction is construction already accomplished on the North Slope and in the Interior of Alaska. The Moon is just a little more remote than the usual jobsite.

The USACE has put considerable effort into Lunar research since the beginning of the Apollo program, creating organizational structures and data bases specifically tailored for space exploration. There are four major organizations within the Corps which have been or will be heavily involved with a return to the Moon. These are the Topographic Engineering Center (TEC) at Fort Belvoir, Virginia, the Construction Engineering Research Laboratory (CERL) at Champaign, Illinois, the Cold Regions Research and Engineering Laboratory (CRREL) at Hanover, New Hampshire, and the Waterways Experiment Station (WES) at Vicksburg, Mississippi. All of these offices maintain relations with similar organizations in other countries, and these international relations can be expected to extend to Lunar research and operations.

TEC, as its name implies, is a topographic mapping center. It is highly involved with remote sensing systems such as imagery development and analysis, laser rangefinding, and position/navigation systems. It turns the data thus obtained into map products, and is constantly researching ways to automate and refine these products. Many of the systems which TEC has developed for Earth sensing are equally applicable to Lunar and other planetary surfaces. In cooperation with the U.S. Geological Survey and NASA, TEC provided many of the map products for the Apollo program.

CERL is the Army lead agency for research and development of large space structures. It researches and tests construction material behaviors. In the period 1990-1992 CERL produced a number of studies looking at in-space and Lunar construction. For example, one such document was the Large Space Structures Fielding Plan (USACERL Technical Report M-91/14, January 1991), and another was Operations Analysis for Lunar Surface Construction: Results of Two Office of Exploration Case Studies (USACERL Technical Report M-91/21, August 1991).

CRREL researches construction methods in cold regions, such as the Interior of Alaska where it maintains a large facility. CRREL looks into such areas as construction on and in permafrost, soil moisture studies, ice radar studies, and modifications required for construction equipment to keep it operational in the cold. CRREL works extensively with civil educational and research institutions, such as the University of Alaska, and with foreign nations in cold regions such as Russia and China.

WES deals with construction research where groundwater and surface water are concerned, and may in the future be involved with creating construction materials such as cement block or sintered block from Lunar regolith. It will conduct research into rock and soil mechanics, and perform terrain surface modeling.

2.2. Surface Activities

Because of the harsh temperature, vacuum, meteorite and radiation environment of the Moon, it will be necessary to accomplish many surface construction, industrial and maintenance activities robotically or telerobotically with human operators safe in shielded structures. Developments in robotics and telerobotics are therefore of great interest. Communications systems of all kinds are of interest as well, for imagery, data transmission, position/navigation, and command and control of surface or orbital activities.

Surface activities which will require detailed Lunar environmental knowledge and/or in-situ resource utilization (ISRU) are site selection/mapping, site survey/subsurface analysis (including searching for lava tubes), lander unloading/loading, road building, landing pad preparation, mining/excavation/trenching, surface transportation, surface emplacement of equipment, electrical and fluid connections, regolith shielding, lander servicing, power plant deployment, modular habitat construction, ISRU operations, ISRU-derived product storage, and ISRU-derived habitat construction.

2.3. Environmental Impact Statement

All of these activities must be well enough anticipated to allow their incorporation into the Environmental Impact Statement (EIS) which must precede the return to the Moon. It is worth noting here that the EIS for the return to the Moon will be international in scope because of the legal status of the Moon, and because of the likely international character of the first Lunar base. As an EIS must be prepared by the organization doing the work, the Army Corps of Engineers will likely be in charge of the U.S. portion of it. An EIS must consider all environmental and socioeconomic impacts of the project it represents, both positive and negative, not only on the

construction site but also in the communities which may be affected by it. It must consider trade-off analyses, and mitigation of negative impacts. In the case of Lunar mining for helium-three, therefore, it must consider the impacts of cleaner, cheaper energy on a global scale, as well as the jobs created in particular communities. An EIS effort is also required to hold public participation input/information meetings, and these meetings may be a key element in generating public attention and support. It may well be that an early EIS effort would do far more to make the return to the Moon happen than any other endeavor at all.

2.4. Spin-off Technologies

Partially related to the EIS is the topic of terrestrial applications of research results developed for the Lunar effort. Things which go into space go faster, get hotter and colder, are subjected to greater and more rapidly changing stresses, and must be more self-maintaining than most any other creations. Space research therefore translates into improved bearings, seals, fuels, computers, coatings, plastics, metals, ceramics, and recycling systems, all of which have applications to terrestrial uses. This has been true in the past, and will continue to be true in the future.

3. CONCLUSION

In closing, the Army Corps of Engineers is prepared to build for the U.S. Government anywhere, anytime. When the country decides to return to the Moon, it will find the Corps organized and ready to implement that decision. The research facilities are in place, the data base has been building for thirty years. We know without doubt that the mission is coming - and look forward to it with great anticipation.

END

2) Lunar ^{3}He Resources 47
E. Rice, Chair

2-1 Evidence of Helium-3 on the Moon: Model Assumptions and Abundances 49
Lawrence A. Taylor

2-2 Further Evaluation of the Helium Resources of Mare Tranquillitatis 57
Eugene N. Cameron

2-3 Remote Sensing of ASTROFUEL™ 65
K.R. Harris, H.Y. Khater and G.L. Kulcinski

2-4 By-products of Lunar Helium-3 Mining 75
Larry A. Haskin

Evidence of Helium-3 on the Moon: Model Assumptions and Abundances

. **Lawrence A. Taylor**

Director, Planetary Geosciences Institute
Department of Geological Sciences
University of Tennessee
Knoxville, TN 37996

1. ABSTRACTS

Solar-wind particles are present in the outer few 100 Å of each soil particle of the Moon. Of particular interest, are the volatiles hydrogen (40-100 ppm) and helium (5-45ppm). The potential use of D-3He fusion for energy generation requires a ready supply of 3He, and there is a distinct paucity of this on Earth. However, compared to the Earth, the Moon is a virtual "oasis with springs of solar-wind helium." Conservative estimates of the helium contents of the regolith are 3 ppb (5.4 mg/m^3) of ^{3}He for the highland areas and 6 ppb (10.8 mg/m^3) for the maria. **At 50% recovery rate, this would require the mining of about 600 mare football fields (= 3.1 km^2 ≅ 1.1 mi^2) per year, to a depth of 3m, to supply sufficient ^{3}He for a 500 MW fusion D-^{3}He plant.**

2. INTRODUCTION

The Sun expels portions of its outer layers into space in a steady stream of particles which constitutes the "solar wind". The flux of solar wind decreases as the square of the distance from the Sun. The Earth's magnetic field and atmosphere practically deflects the solar wind such that the Earth receives little. However, the lack of a magnetic field and shielding atmosphere on the Moon permits solar-wind particles to impinge upon the lunar regolith and to become implanted into the outer few 100 Å's of the various soil fragments. With the effective "gardening" of the lunar soil by meteorite and micro-meteorite impacts, soil grains are turned over, rolled around, and mixed together, such that all surfaces of soil particles are "coated" with implanted solar-wind particles.

Solar wind consists of about 90% protons (hydrogen nuclei), 7% alpha particles (helium), and lesser amounts of most other elements present in the Sun. And these low-energy solar particles are present in lunar soil. For example, hydrogen, helium, and carbon are particularly abundant (50-100; 3-50; 100-150 ppm, resp.; Taylor, [1]). The possibilities of using these and other lunar resources for the establishment of a lunar base have been discussed and promoted by numerous publications (e.g., Taylor [2]; Taylor and Carrier [3], Wittenberg et al. [4]). It is the goal of this paper to discuss and evaluate the several factors which must be considered for an estimation of the ^{3}He content of lunar soil.

3. HELIUM ON THE MOON

It was Wittenberg et al. **[4]** who first pointed out to the fusion community that the lunar soil contains relatively large quantities of ^{3}He, compared to Earth. And it has been the Fusion Technology Institute at the University of Wisconsin, under the direction of Dr. Gerry Kulcinski, that has championed the cause for fusion of this ^{3}He **[5]**. In fact, ^{3}He may be the only true economic "ore" on the Moon. At $40,000 to $60,000 per kilo for transporting materials from Earth to the Moon, it is not cost effective to go to the Moon even for pure Au, at today's price of <$10,000/kilo. But the paucity of readily available ^{3}He on Earth makes the Moon appear attractive as a source of this reactant.

The outer portions of the Moon are covered by broken, crushed rock matter called regolith. The finer fraction (<1 cm) of this material is termed soil **[1, 2]**. It is on the surfaces of the rock, mineral, and glass fragments that the solar-wind particles have been implanted, including the subject of this paper -- ^{3}He. The distribution of this helium is relatively uniform over large areas of the lunar surface, but does vary systematically. High-Ti mare basalt regions, such as at the Apollo 17 locale, appear to be the best areas for He mining with ~10-20 ppb ^{3}He, versus only about 2-4 ppb in the Highlands **[2, 6]**. It should be remembered that although the mare soils contain appreciably greater amounts of helium, the mare only constitute some 16% by area of the Moon, and the major portions of these areas are on the central portion of the Moon's frontside.

3.1. Factors Affecting Helium Abundances in the Soil

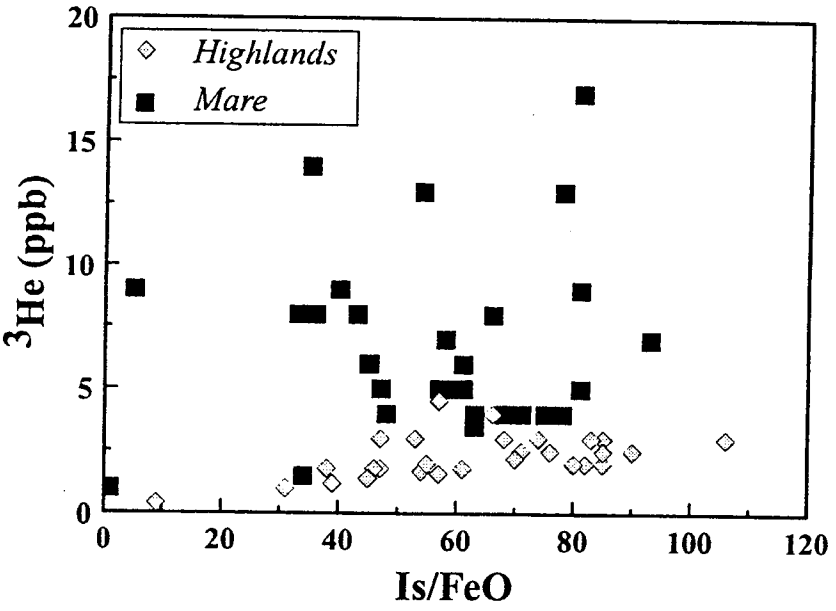
There are several factors which must be taken into consideration in evaluating the abundances of helium within the lunar soil. The primary ones that we have hard data for concern ***exposure age, mineralogy***, and ***grain size*** **[2]**. The effects of the Earth's magnetic field and the incidence angle (latitude effect) will be discussed below.

3.1.1. Exposure Age

Exposure age is effectively the amount of time that a soil fragment has been at the surface of the Moon, being gardened by the micro-meteorite impacts. In general, the longer the exposure age of a soil, the more intense have been the soil forming processes of comminution and agglutination. Comminution is the simple disaggregation or breaking of rocks and minerals into smaller pieces, a process which tends to decrease the average grain size. Agglutination, on the other hand, is the welding of lithic and mineral fragments together by the glass produced by the quenching of micro-meteorite-produced impact melt, a process which tends to increase the average grain size. It is these fragile, aggregates of rocks, minerals, and glass - the agglutinates - which are the key to the maturation process of the soil.

The soil already contains large amounts of solar-wind-implanted hydrogen and carbon, when it is partially melted by small impacts. These elements impose an extreme reducing environment, several orders of magnitude below the iron-wustite stability curve, which forces much of the Fe^{2+} in the silicate melt to Fe^{o}, causing saturation and precipitation of billions of "tiny" Fe^{o} spheres. The Ferro-Magnetic Resonance (FMR)

signal for this "single -domain"(40-200 Å) elemental Fe is divided by the total FeO content of the soil to give I_s/FeO, a par-ameter which in-creases as soil ma-turity (= exposure) increases[1,2]. There is a rough correla-tion between I_s/FeO and ^{3}He [2, 6, 8], as shown in Figure 1, particularly for high-land soils. Notice that the correlation for the mare soils is not as good.



.**FIGURE 1.** I_s/FeO (maturity) versus ^{3}He for lunar soils.

3.1.2. Mineralogy

Ilmenite ($FeTiO_3$) and other oxide mineral phases such as spinel common to the basaltic soils in Maria, have trapping efficiencies (= retention) for solar-wind particles up to 10 times greater than those of the silicate minerals, such as olivine, pyroxene, and plagioclase. There-fore, there is a rough correlation between the TiO_2 content of a soil (asthis largely reflects the ilmenite content) and ^{3}He, as shown in Figure 2 [2]. In fact, the lack of correlation seen in Figure 1 between I_s/FeO and ^{3}He for high-Ti basaltic soils (mare), such as with the Apollo 17 sam-ples, is explained as a function of ilmeni-te content of a soil, which has effectively overwhelmed the effects of maturity. Even though a high-Ti mare soil may be relatively immature, its ilmenite can contain considerable He.

As shown by Figures 1 and 2, the He contents of the soils are a strong function of both I_s/FeO and TiO_2. Figure 3 combines these two factors and demonstrates an excellent correlation between ^{3}He and [(I_s/FeO) x TiO_2], a similar plot to that used by Jordan [8]. It should be noted once again that these data are by no means comprehensive for the mare, the highlands, or the overall Moon. They are representative of a limited number of samples from only a few small locales on the lunar surface. However, as discussed below, the ^{3}He estimates made below are conservative because of additional factors.

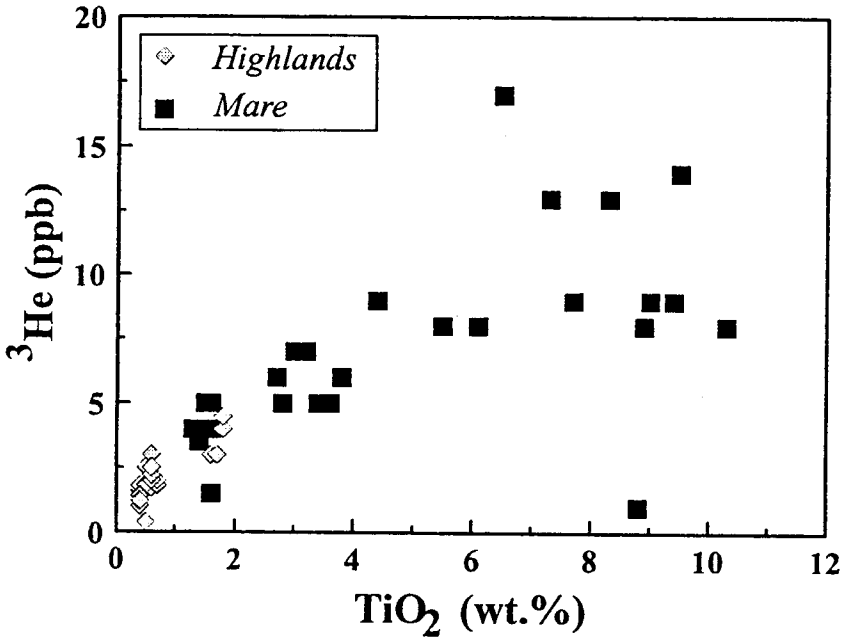


FIGURE 2. TiO_2 versus ^{3}He for lunar soils.

3.1.3. Grain Size

Solar-wind particles are implanted in only the outer few 100 Å of each soil grain. It is, therefore, the surface area of the grains which is of importance in considerations of the abundance of He. Inasmuch as the surface area/vol. increases with a decrease in grain size of a soil, it is no surprise that solar-wind contents of lunar soils are a function of grain size. Typically about 50% of a soil by weight is <50 μm in size [9]; however, this fine-sized fraction contains considerably greater total surface area than the >50 μm portion. Consequently, ***the <50 μm portion of lunar soils typically contain about 80% of the*** He_T [10]. Fully 90% of the He is present in the <100 μm size fraction.

At first glance, it might seem to be more practical to mine only the <50 μm of the soil for ^{3}He. However, the speciation of ^{4}He versus ^{3}He, that is the ^{4}He/^{3}He ratio, varies from 1200 to 3800 (mean about 3000) on the Moon and is strongly in favor of ^{4}He in the fine fractions, whereas the coarser sizes (i.e., >50 μm) contain less He_T, yet higher ^{3}He speciation and contents [2]. Therefore, there may be little to be gained by sizing the soil to <50 μm (no easy task,) and treating this portion for its ^{3}He content. However, it will be necessary initially to roughly size the regolith to remove the larger rock fragments (e.g., >1 cm); therefore, an additional sizing to <100 μm or so, may not be that much more difficult. But this sizing may have deleterious effects.

It has been noted by several investigators (e.g., Li and Wittenberg [11]) that there is a considerable loss (up to 50%) of the loosely-held solar-wind He during simple sieving in the laboratory. This may affect the efficiency of the He recovery process. Of course, if the sizing is done in an enclosed environment, the released He, and other gases can be captured. This should be taken into consideration during design of the He-recovery process.

Processing of the lunar soil to recover the solar-wind gases should not be difficult. It has been determined by several studies that the solar-wind gases are easily released from their sites on the outer surfaces of the soil particles by simple heating [12]. By 700 °C, over 80% of the H_2 and He_T have been evolved off the grains. In fact, a mining machine, patterned upon a continuous-feed bucket dredge used on Earth for Au mining, has been designed for mining of lunarsoil for volatiles [13].

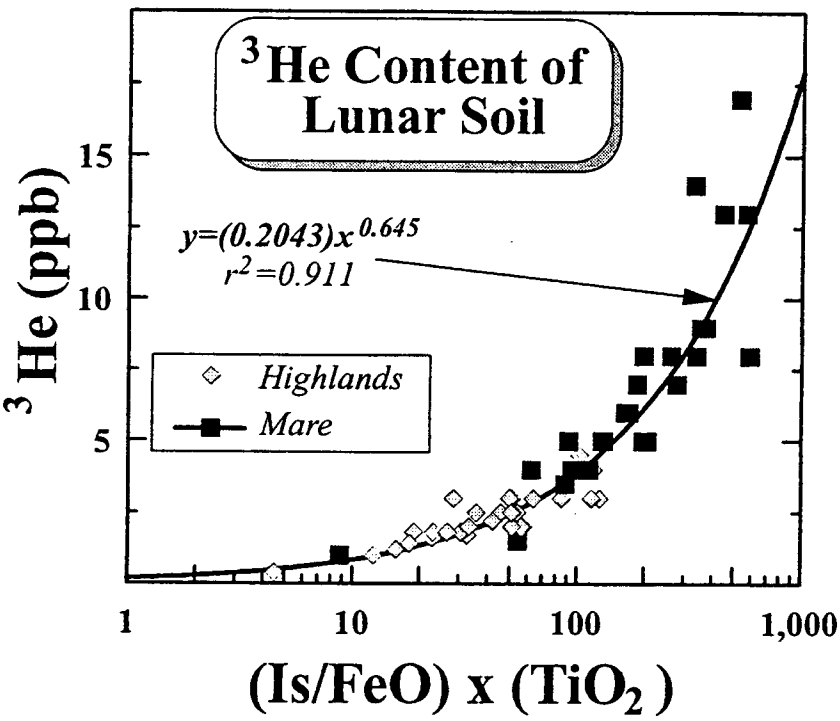


FIGURE 3. [I_S/FeO x TiO_2] versus ^{3}He for lunar soils.

TABLE 1. Factoids for Consideration of He Abundances of Lunar Regolith.

Physical Properties

- **Regolith Depths are 3-6 m in maria and 10-20 m in the highlands;**
- **Average Density of the upper regolith ≃ 1.8 gm/cm^3;**
- **One m^3 of regolith ~ 1.8 tonnes;**
- **Radius of the Moon = 1738 km; Surface Area ~ 3.8 x 10^{13} m^2;**
- **Maria constitute 16%, the Highlands about 84% of the Moon's surface.**

Chemical Properties

- **Most He measurements were taken on the <250 μm size fraction;**
- **The > 1mm fraction of the upper regolith is only 5-15%;**
- **He contents are constant with depth in the regolith to 3 m;**
- **Maria have ^{3}He contents which average ≃ 6 ppb (10.8 mg ^{3}He/m^3);**
- **Highlands have ^{3}He contents which average ≃ 3 ppb (5.4 mg ^{3}He/m^3);**
- **Moon-Wide ^{3}He content of regolith ≅ 3.5 ppb (6.3 mg ^{3}He/m^3).**

3.2 Variations in Helium with Depth in the Regolith

Based upon profiles into the lunar regolith as revealed by the numerous cores taken during the Apollo and Luna missions, the deepest being 2.8m, the maturity of the soils, as revealed by I_S/FeO, does not vary in any systematic manner with depth. That is, the fluctuations are random. *The lunar regolith does not vary in maturity with depth down to 3m* **[1]**, and because Is/FeO is indicative of solar-wind content of the soil, it is probable that He_T does not vary with depth at least down to about 3m. **[1]**. Therefore, it is a safe assumption that ***the He_T and ^3He contents of the upper several meters of the regolith are constant.*** What these contents are at greater depths is unknown and various other scenarios have been evaluated **[14].**

4. HELIUM CONTENTS OF THE LUNAR SOIL

It must be emphasized that ***the estimates for ^3He given below are conservative*** in that lunar soils may contain substantially more solar-wind volatiles than have been sampled by the Apollo missions. In part this may be due to *longitudinal variations* in exposure to solar-wind particle flux. The Moon is shielded from solar wind by the Earth's magnetotail for 6-8 days/month **[14]**. At this time, the soils on the far-side and on near-side limbs continue to receive the full flux, while the central regions of the lunar near-side are effectively shielded. Over time, the center of the near-side should have received only 25-50% as much solar wind as the far-side and the limbs. This may have a positive consequence for absolute He abundances since all our estimates have been made on data from the Apollo regions which are in this shadow area and should contain reduced amounts of solar-wind particles.

The effects of solar-wind flux versus latitude may also be significant **[15]** such that regions near the poles of the Moon receive considerably less flux. It is mainly those latitudes above about 60° that are affected, and then not significantly. Realistically, these regions are not under consideration for mining since the temperatures there reach below -200 °C during the night It is obvious that further lunar exploration will be necessary to determine the actual effects which the longitudinal and latitudinal variations in flux conditions have had upon the solar-wind contents of lunar soils.

4.1. Factoids about the Lunar Regolith

There are several data, as well as assumptions, to be incorporated into any estimate of the He contents of lunar regolith. I have termed these "factoids" [read - data resembling facts], since they are based upon fact but include the generalization and assumption that they are applicable over large areas of the Moon. Table 1 compiles many of these data and factoids, along with other salient facts. Many of these data are from Taylor **[2]** or the *Lunar Sourcebook* (Cambridge Univ. Press, 1991).

It must be stated that in making the estimates of ^3He contents in lunar soil, no consideration was given to the actual recovery process that might be employed. This includes the possible losses which can occur upon sizing. The efficiencies of various aspects of the helium recovery process have been addressed by several studies (e.g., **[4, 11, 13]**.

TABLE 2. Conservative Estimates of ^{3}He in Lunar Regolith

- **One Mare Football Field (~50m x 100m) to a Depth of 3 meters = 162 g ^{3}He;**
- **One Highlands Football Field to a Depth of 3 meters = 81 g ^{3}He;**
- ***Entire Surface of the Moon to a Depth of 3 meters ≅ 715,000 tonnes of ^{3}He.***
- **500 MW Fusion D-^{3}*He plant ≅ 300 Mare Football Fields / year ≅ 1.5 km^2/yr.***

4.2 Absolute Helium-3 Abundances

Based upon facts and factoids, in addition at certain assumptions listed in Tables 1 and 2, ***the entire surface of the Moon to a depth of 3 m contains at least 715,000 tonnes of ^{3}He.*** As explained above, this is a conservative estimate and the real value may be considerably higher, particularly when variations in flux as a function of longitude are considered.

In order to operate a **500 MW fusion D-^{3}He plant**, it would take about **50 kg ^{3}He/yr. [11]**. As shown in Table 2, the quantity of ^{3}He in an area about the size of a football field to a depth of 3m is 162 g for a mare and 54 g for a highlands region. It would be necessary to mine about **300 mare football fields per year to obtain 50 kg ^{3}He**. This may sound like a huge amount, but it represents only **1.5 km^2, some 150 hectares, ≅370 acres.**

This assumes 100% efficiency in recovery and that 100% of the available regolith at the surface can be mined, thereby neglecting crater morphologies and large boulders. For example, the heating of the lunar soil to temperatures of 700 ^{o}C will only recover about 80% of the available He. Even if the ***overall efficiency of recovery is 50%***, the areas and volumes are only increased by a factor of 2 - to some **3.1 km^2, a little over one square mile.** In the highlands, these values would be about double. And if a high-Ti mare region is mined, like that of Mare Tranquillitatis where the ^{3}He contents are about 15-20 mg ^{3}He/m^3, these volumes and areas would be effectively cut in half.

Kulcinski et al. **[5]** have estimated that the ***entire electrical consumption of the U.S. for 1987 was equivalent to the energy from D-^{3}He fusion of 25 tonnes of ^{3}He.*** At a recovery efficiency of 50%, ***this 25 tonnes of ^{3}He represents mining, to a depth of 3m, a total area of about 550 mi^2 (1500 km^2) of a mare.*** Several studies of the engineering aspects of such large scale mining have been performed, and indeed, such an operation is entirely feasible **[e.g., 11, 13]**.

5. SUMMARY

The ^{3}He resources of the regolith of the Moon are vast, by terrestrial standards. Conservative estimates of the helium contents of the regolith are 3 ppb (5.4 mg/m^3) of ^{3}He for the highland areas and 6 ppb (10.8 mg/m^3) for the maria. *At 50% recovery rate, this would require the mining of about 600 mare football fields per year, an area of 3.1 km^2, to a depth of 3m, to supply sufficient ^{3}He for a 500 MW fusion D-^{3}He plant.*

6. REFERENCES

[1] L.A. Taylor, "Resources for a Lunar Base: Rocks, Minerals, and Soil of the Moon," In *The Second Conference on Lunar Bases and Space Activities of the 21st Century*. NASA Conf. Publ. 3166, vol. 2, 361-377 (1992).

[2] L.A. Taylor, "Hydrogen, Helium, and other Solar-Wind Components in Lunar Soil: Abundances and Predictions," *Engr., Constr., & Oper. in Space II*, ASCE Publ., *Proc. of Space '90*, 68-78 (1990).

[3] L.A. Taylor and W.D. Carrier, III, "Production of Oxygen on the Moon: Which Processes are Best and Why," AIAA Journal, vol. 30, no. 12, 2858-2863 (1992).

[4] L.J. Wittenberg, J.F. Santarius, and G.L. Kulcinski, "Lunar Source of ^{3}He for Fusion Power," *Fusion Technol. 10*, 167-178 (1987).

[5] G.L. Kulcinski, E.N. Cameron, J.F. Santarius, I.N. Sviatoslavsky, L.J. Wittenberg, and H.H. Schmitt, "Fusion Energy from the Moon for the Twenty-First Century," In *The Second Conference on Lunar Bases and Space Activities of the 21st Century, NASA Conf. Publ. 3166*, Vol. 2, 459-474 (1992).

[6] E.N. Cameron, "Helium Mining on the Moon: Site Selection and Evaluation," In *The Second Conference on Lunar Bases and Space Activities of the 21st Century, NASA Conf. Publ. 3166*, Vol. 1, 189-197 (1992).

[7] R.V. Morris, "Surface Exposure Indices of Lunar Rocks: A Comparative FMR Study," *Proc. Lunar Sci. Conf. 7th*, 315-335 (1976).

[8] Jordan, J.L., "Prediction of the HE Distribution at the Lunar Surface," *U of AZ/NASA SERC, Space Min. & Manuf.*, VII-38-50 (1989).

[9] D.S. McKay et al., "The Lunar Regolith," In *Lunar Sourcebook*, Heiken, Vaniman, and French [Eds.], Cambridge Univ. Press, New York, 285-356 (1991).

[10] P. Eberhardt et al., "Trapped Solar Wind Noble Gases, Exposure Age, and K/Ar-age in Apollo 11 Lunar Fine Material," Proc. Apollo 11 Lunar Sci. Conf., 1037-1070 (1970).

[11] Y.T. Li and L.J. Wittenberg, "Lunar Surface Mining fpr Automated Acquisition of Helium-3: Methods, Processes, and Equipment," In *The Second Conference on Lunar Bases and Space Activities of the 21st Century, NASA Conf. Publ. 3166*, Vol. 2, 609-617 (1992).

[12] J.L. Carter, "Lunar Regolith Fines: A Source of Hydrogen," In *Lunar Bases and Space Activities of the 21 Century*, LPI Publ., 571-581 (1985).

[13] I.N. Sviatoslavsky, "Mobile ^{3}He Mining System and its Benefits Toward Lunar Base Self-Sufficiency," U Wisc. Rept. *WCSAR-TR-AR3-8808 (1988).*

[14] S.H. Fegley and T.D. Swindle, "^{3}He and Other Lunar Volatiles," *Resources of Near-Earth Space*, U of AZ Press, in press (1993).

[15] M. Neugebauer, C.W. Snyder, D.R. Clay, and B.E. Goldstein, "Effects of the Magnetic Field of the Earth upon the Solar-Wind Flux of the Moon," *Planet Space Sci. 20*, 1577-1591 (1972).

[16] T.D. Swindle, "Abundance of ^{3}He and Other Solar-Wind-Derived Volatiles in Lunar Soil," *U of AZ/NASA SERC, Annual Progress Rept. APR-91/F*, III-35-41 (1991).

Further Evaluation of the Helium Resources of Mare Tranquillitatis

Eugene N. Cameron
Wisconsin Center for Space Automation and Robotics
University of Wisconsin-Madison
1500 Johnson Drive
Madison WI 53706

ABSTRACT

Study of the availability of Helium-3 from the Moon is currently focused on Mare Tranquillitatis, owing to its vast extent, its accessibility, and the presence of large areas of high-TiO_2 regolith that should be enriched in helium. The He-3 content of minable regolith has been estimated at 7,041 tonnes, but this only is a preliminary estimate based on sampling at the Apollo 11 site, reflectance mapping, and study of high-resolution photographs of the Apollo 11 and Ranger VIII sites. The true He potential of the Mare must be determined by systematic exploration. Reflectance data must be calibrated against samples representing the range of reflectance characteristics, and current spectral reflectance maps must be revised accordingly. Areas of high-TiO_2 regolith physically minable in terms of surface characteristics shown by high-resolution photographs should then be scanned by robotic vehicles equipped with ground-penetrating radar, to determine variations in depth of regolith and distribution of blocks too large to be handled by the mining system. Areas ultimately classified as minable should then be systematically sampled for variations in He content. Finally, mining and processing methods should be tested by pilot operations on the Moon.

Reflectance data currently available indicate that first exploration of Mare Tranquillitatis should be directed to the western part of the mare. An area centering on 9 N. 20 E. is recommended from work done to date.

1. INTRODUCTION

Since 1986 I have been studying the occurrence, distribution, and availability of helium from the regoliths of the Moon. There are two major groups of regoliths - highland regoliths and mare regoliths. Highland regoliths contain more than half, perhaps two-thirds of the helium present on the Moon, but at least for the next hundred years they can be ruled out as sources of helium, for two reasons. One, they contain less than 15 wppm helium. Two, the highlands are mostly so rugged that large-scale mining will be impossible except at enormous cost.

This leaves the regoliths of the maria. The high-TiO_2 regoliths of certain maria contain 20 to as much as 45 wppm He, and large portions of such maria are physically favorable to mass mining. For three reasons the most promising mare is Mare Tranquillitatis, which appears in Figure 1 as the large dark area northeast of the center. One, the mare is huge, roughly 300,00 sq. km. in area. Two, it is easily accessible from Earth. Three, large areas of the mare are covered by regolith that is high in TiO_2 and should be relatively high in helium. Ultimately my investigation therefore focused on Tranquillitatis.

As shown in Table 1, I have estimated the He-3 content of Mare Tranquillitatis at 7,041 metric tonnes in minable regolith containing 20 wppm or more He (8 wppb He-3). However,

Table 1. Minable Regolith and Helium Content of Mare Tranquillitatis

Regolith Category	Area in km^2	Average He Content wppm	Regolith Minable tonnes	He tonnes	^3He tonnes
A	84,000	38	252×10^9	9.58×10^6	2,726
B	195,000	25	598×10^9	14.96×10^6	4,315
Totals	279,000		850×10^9	24.54×10^6	7,041

Basis: (1) 50% minability, (2) regolith thickness 3m, (3) He (total)/He-3 = 2600.
From Cameron [1]

this is only a preliminary estimate based mainly on sampling at the Apollo 11 site, reflectance mapping, and study of high-resolution photographs of the Apollo 11 and Ranger VIII areas. The firm estimate of He-3 potential that will be required for planning mining operations and for economic evaluation must next be acquired by systematic exploration of the mare, and this is the subject of my paper.

2. PURPOSE OF EXPLORATION

Exploration of Mare Tranquillitatis should be designed to obtain the following information:

(1) The distribution of high-TiO_2 regolith in Tranquillitatis.

(2) The location and extent, within areas of high-TiO_2 regolith, of portions that are physically minable.

(3) Variations in depth of regolith in physically minable areas, and the distribution of buried ejecta blocks.

(4) Lateral and vertical variations in He-3 content of minable regolith.

(5) The effectiveness of procedures and equipment for mining and processing regolith for He-3 and other volatiles.

The distribution of high-TiO_2 regolith (TiO_2 content 6% or more) in Tranquillitatis is important because analysis of regolith samples from the Apollo and Luna missions has indicated a positive correlation between TiO_2 contents of regoliths and their He contents [2]. Regoliths low in TiO_2 are low in He. Given sufficiently long exposure to the solar wind, regoliths high in TiO_2 content are relatively high in He contents. There are problems in using this relationship, as I will indicate later, but at present the TiO_2 contents of regoliths are the best guide we have to the areal distribution of regolith that should be relatively enriched in helium.

For my estimate of the helium content of Tranquillitatis [1], the distribution of high-TiO_2 regolith was obtained from an enlargement of the portion of Fig. 1 that covers the mare, calibrated against the spectral ratio map by T. V. Johnson and others [4]. The result is shown in Fig. 2. Note that large areas of high-TiO_2 regolith appear both in the western and eastern parts of

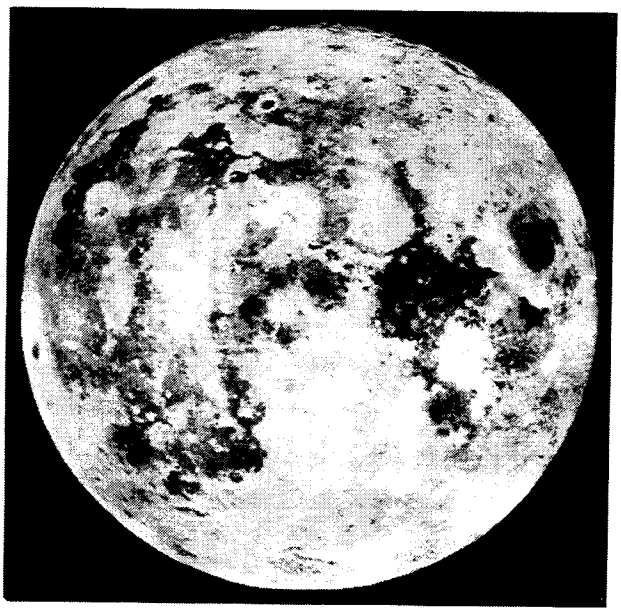


Fig. 1. Color difference photograph of the near side of the Moon by E.A. Whitaker [3]. Mare Tranquillitatis is the large dark area east of the center. Darkest areas will be highest in TiO_2.

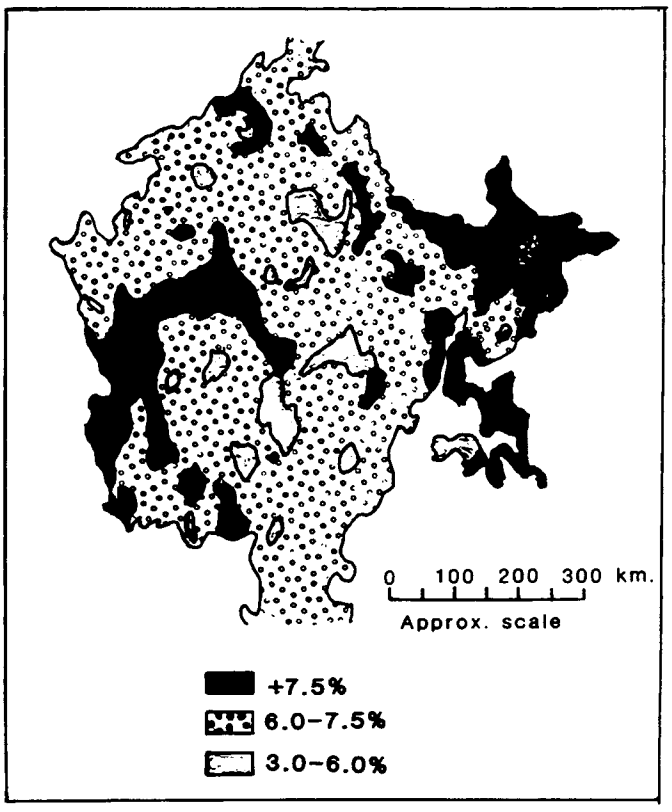


Fig. 2. Inferred TiO_2 content of Mare Tranquillitatis. From Cameron [1].

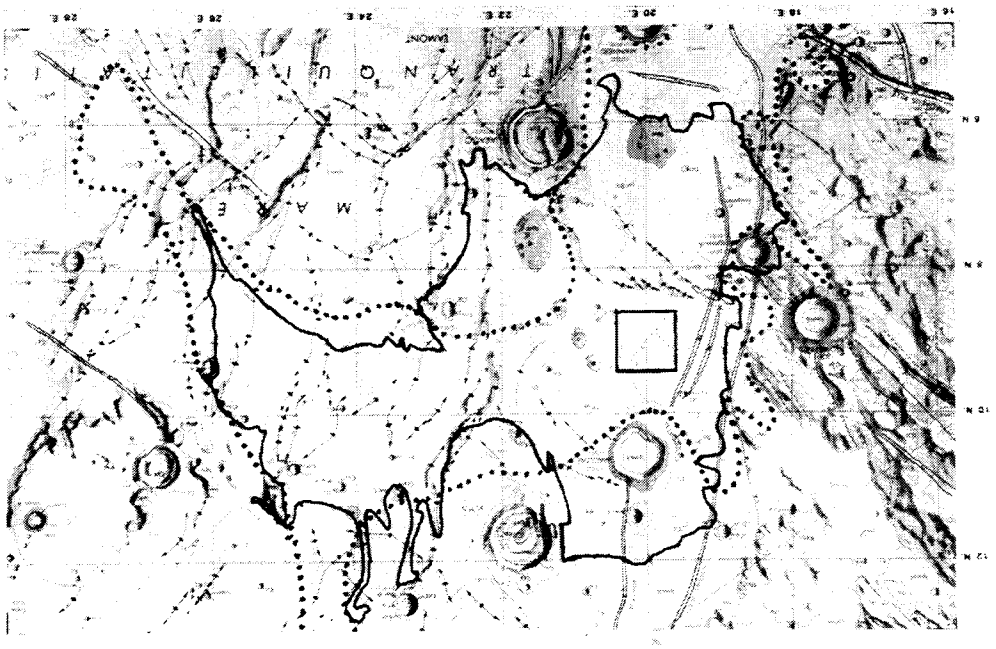


Fig. 3. Part of Julius Caesar quadrangle. Solid heavy black line is boundary of region of TiO_2 abundances ≥7 wt.%, from Johnson and others [5]. Heavy dotted line is boundary of region with TiO_2 ≥7.5%, from Fig. 2. Black rectangle is exploration target area.

the mare. In the meantime, J. R. Johnson and others [5] have published a TiO_2 abundance map based on 0.40/0.56 μm ratio images classified into 9 units ranging from <3% to >10% TiO_2. On part of the geologic map of the Julius Caesar quadrangle showing the western part of the mare (Fig. 3), these authors plotted the boundary of high-TiO_2 regolith (7% or more TiO_2) as the heavy solid line. On this map, as a heavy dotted line, I have plotted the boundary of +7.5% TiO_2 regolith from Fig. 2. For this western part of the mare agreement is reasonably good. However, the Whitaker photograph indicates large areas of high-TiO_2 regolith also in the eastern half of the mare, whereas the abundance map of the entire mare by Johnson and others shows only small areas

At present, attempting to reconcile discrepancies between reflectance ratio maps is not a profitable undertaking, for several reasons. First, further calibration of the Charette curve relating He contents to TiO_2 contents is needed. Second, error in spectral ratio maps is ±2 wt.% TiO_2 for TiO_2 contents above 3 wt.%. Third, the Charette relation holds only for mature regoliths, those that have had long exposure at the surface. At present we cannot map variations in maturity. Fourth, there is the problem of resolution. The resolution of the Whitaker photograph is only about 3 km. The resolution (pixel size) of the reflectance map on which Fig. 3 is based is 1.2 km. This is a substantial improvement, but high-resolution photographs of the Apollo 11 and Ranger VIII sites show that within any 1.2 km square area there are variations in albedo, and any reflectance ratio measurement for such an area will be an average of a range of values. These problems can only be resolved by surface investigations that include calibration of reflectance ratios against regolith samples representing the full range of TiO_2 contents and maturity. This work should be undertaken as soon as possible in the exploration of Tranquillitatis.

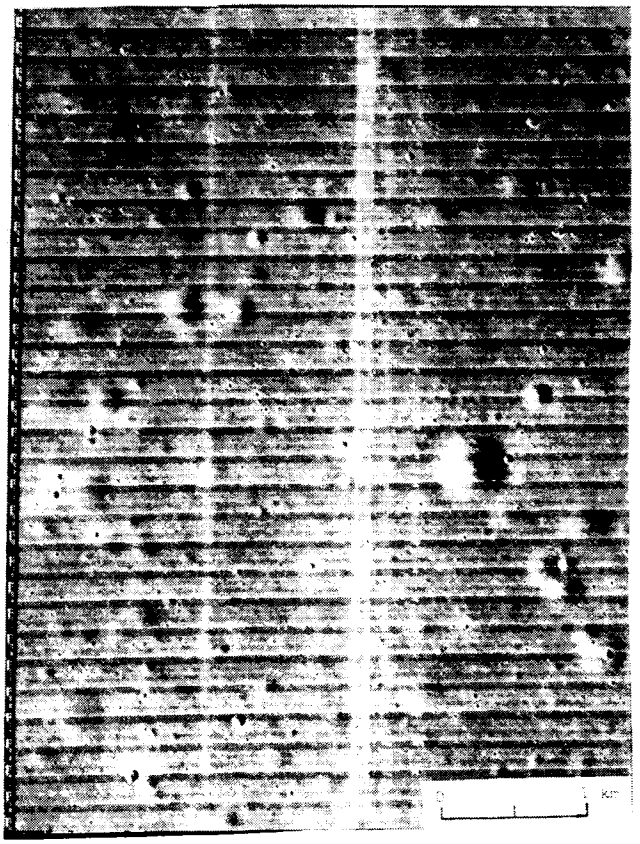


Fig. 4. Lunar Orbiter print II-84 H_3, reduced from original size of 40 × 90 cm. From Cameron [1].

3. DELINEATION OF PHYSICALLY MINABLE AREAS OF HIGH-TiO_2 REGOLITH

As a first target of exploration, I have selected (Fig. 3) an area 25 km square, centered at 20° E. 9° N. This area is relatively free of large craters and other major obstacles to mining, and reflectance mapping indicates that the area is mostly covered by high-TiO_2 regolith. The first step in delineation of physically minable areas of the regolith should be high-resolution photography of the target area from a lunar orbiter. Study of high-resolution photographs of the Apollo 11 and Ranger VIII areas indicates that by far the most abundant obstacles to mining are craters and their ejecta haloes that contain blocks too large to be handled by a bucket excavator, but from place to place on the mare there is much variation in their number, distribution, distinctness, diameter, and depth. Figure 4 is a reduced high-resolution photograph of an area near the Apollo 11 landing site. The largest crater is about 490 m in diameter. A plot of craters and their inferred ejecta halos (Fig. 5) indicates that at least 50% of this area will be physically minable, if the minimum economic mining unit is 300 m square, and the mining system is capable to rejecting ejecta blocks <40 cm in diameter. In marked contrast is Fig. 6, which shows part of the heavily cratered belt that crosses the Ranger VIII area. Besides the largest craters shown, 600-1000 m in diameter, there are numerous others 100 to more than 300 m in diameter. Most of this area will be unminable by large excavating machines.

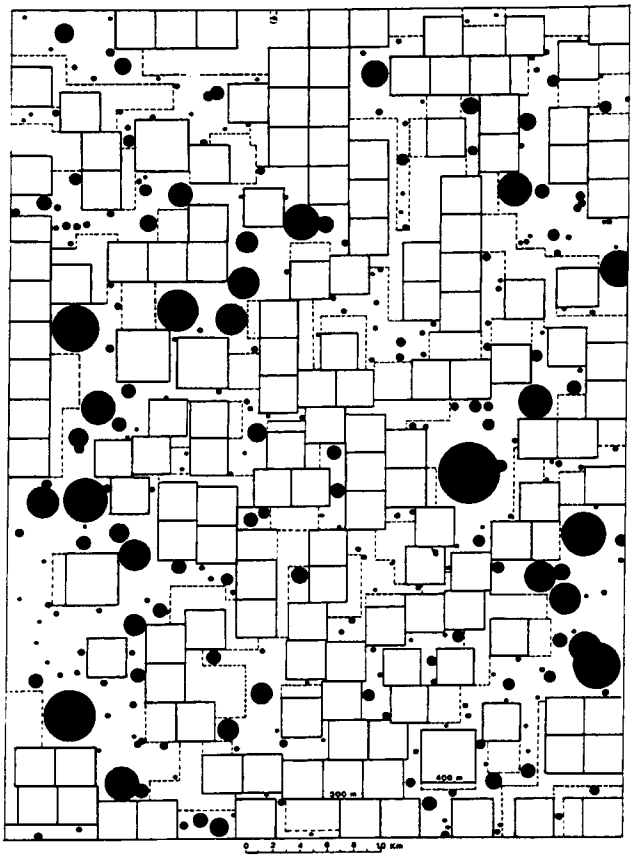


Fig. 5. Craters 23.4 m or more in diameter, with their inferred ejecta halos, plotted on an overlay of Fig. 4. Unit mining blocks are 300 m square; possible extensions are shown by dashed lines. From Cameron [1].

The 2 m resolution limit of available photographs sets a limit on their usefulness in delineating minable areas. Higher resolution photography would alleviate this problem. The other limitation, of course, is that they do not indicate distribution of blocks in older, buried ejecta haloes, nor do they furnish positive information on variations in depth of regolith. Nonetheless it is clear that high-resolution photography can serve an important function in exploration of the mare regolith, making it possible to eliminate much ground that is physically not amenable to mining.

4. VARIATIONS IN REGOLITH DEPTH: DISTRIBUTION OF BURIED EJECTA

For determining depth of regolith and distribution of buried ejecta blocks, ground-penetrating radar scanning from a mobile vehicle should be done. Radar scanning would give continuous depth profiles along the lines of traverse. Blocks of rock would give bumps on the bedrock profile.

5. VERTICAL AND LATERAL VARIATIONS IN HE-3 CONTENT OF REGOLITH

The work outlined above should permit a firm estimate of tonnage of minable regolith in the portions of the mare investigated. However, grade in terms of contents of He-3 and other

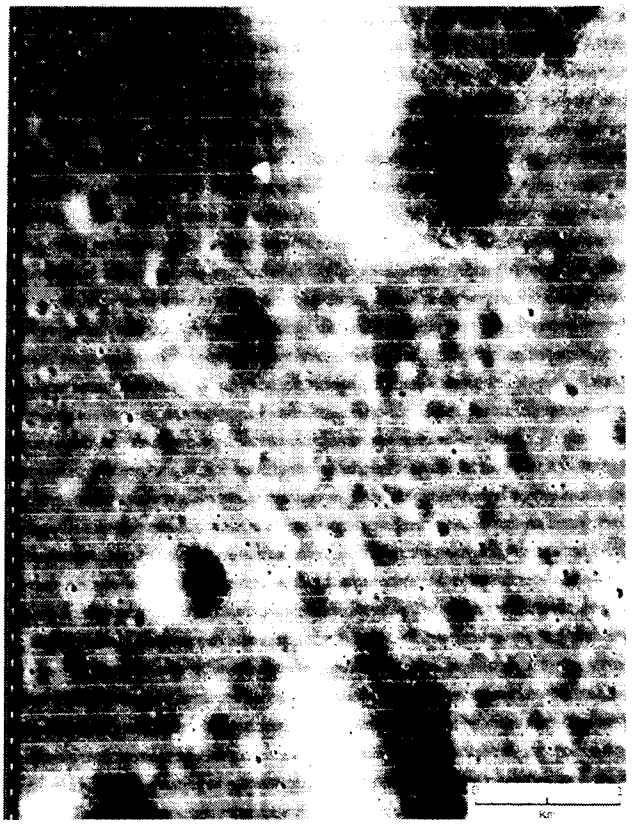


Fig. 6. Lunar Orbiter print II-71H_2, reduced from original size of 40 × 90 cm. From Cameron [1].

gases can be determined only by sampling to whatever depth of mining is planned. If sampling is done by drilling the pattern of drillholes will in general be that used in terrestrial exploration of deposits that are so poorly exposed and internally unpredictable as to offer no guides to drillhole location. In such cases, drillholes on a grid pattern or equally spaced along parallel lines are generally used. Statistical analysis is used to evaluate the results in terms of overall grade. Spacing of drillholes is ultimately dictated by the nature and scale of variation in grade as indicated during the earlier stages of exploration.

The depth of drillholes will be dictated by the depth of regolith to be excavated with the mining system ultimately selected. A choice will have to be made between onsite analysis of drill cores and transporting cores to a central analytical laboratory at the lunar base. The latter would seem to offer advantages in uniform handling of core and recovery of gases.

6. PERCENTAGES OF GASES RECOVERABLE FROM LUNAR REGOLITH

In most mining operations the amounts of valuable constituents recovered per unit of material mined and processes are less than the amounts originally present, and mining for He-3 and other volatiles on the Moon will certainly be no exception. There is some concern that portions of the volatiles will be lost during excavation and other physical handling. There will be losses during heat treatment of regolith to release the volatiles and in the processes for recovery

of the different volatiles. No final evaluation of the potential of the regolith as a source of He-3 can be made until probable losses can be estimated with reasonable precision. Neither mining nor processing operations can be satisfactorily evaluated on the basis of experiments on Earth. It will thus be necessary to establish pilot-scale operations on the Moon. Mining systems can then be tested against regolith material under the severe conditions of the lunar environment. Processing methods can be tested with large bulk samples, again under actual lunar conditions.

The above scheme of exploration is framed with reference to the selected initial target area. However, if the total potential of the mare is to be appraised, exploration must be extended to other portions of the mare. It is especially important that exploration of selected portions of the eastern part of the mare be investigated, to explain and resolve the discrepancies between various reflectance surveys. The magnitude of the estimate of the total potential of the mare will be markedly affected by the results. The magnitude of the estimate will also be affected by the cutoff grade that is finally established after economic evaluation; the cutoff grade of 8 ppb He-3 used in making the current estimate is certainly subject to revision.

Summing up, we have at present enough information to indicate that Mare Tranquillitatis has a high potential as a source of He-3. We must now proceed along the same course of action that is involved in the evaluation of a major mineral deposit on Eartn.

REFERENCES

[1] E.N. Cameron, WCSAR-TR-AR3-9207-1, 1-67 (1992).

[2] E.N. Cameron, *2nd Conf. on Lunar Bases and Space Activities of the 21st Century*, NASA Conf. Publ. 3166, Vol. 1, 169 (1992).

[3] E.A. Whitaker, *The Nature of the Moon*, IAU Symposium, 79 (1965).

[4] T.V. Johnson, R.S. Saunders, D.L. Matson, and J.L. Mosher, *Proc. 8th Lunar Sci. Conf.*, Vol. 1, 1029 (1977).

[5] J.R. Johnson, S.M. Larson, and R.B. Singer, *J. Geophys. Res.*, **96(E3)** 18861 (1991).

REMOTE SENSING OF ASTROFUEL™

K. R. Harris, H. Y. Khater and G. L. Kulcinski
Wisconsin Center for Space Automation and Robotics
University of Wisconsin - Madison
1500 Johnson Drive
Madison WI 53706

ABSTRACT

A direct, high-resolution measurement from lunar orbit of the location of high concentrations of ^3He in the lunar regolith is needed for the initiation of cost-effective mining operations on the moon. Gamma-ray spectroscopy has been successfully used to map the abundances and distributions of certain elements present in planetary regoliths. Helium-3 is unique among these elements since the gamma-rays produced in the $^3He(n, \gamma)^4He$ reaction are 20.6 MeV or above. Thus, detection of the gamma-ray flux from ^3He should be free of interference from the gamma-rays of any other neutron capture reaction. Since ^3He is present in the relatively small concentration of about 10 - 30 parts per billion by weight, the gamma-ray flux resulting from the $^3He(n, \gamma)^4He$ reaction using galactic cosmic-ray (GCR)-induced neutrons will be extremely small. We propose to map the 20.6 MeV gamma-ray from ^3He during very large solar proton flares (VLSPF) to take advantage of the increased flux of solar cosmic-ray (SCR)-induced neutrons. The neutron production spectrum in the lunar regolith has been calculated from GOES-7 satellite observations of the October 1989 VLSPF using the BRYNTRN charged-particle transport code. This spectrum is used as input for the ONEDANT neutron/gamma-ray transport code. The production of SCR-induced neutrons during a VLSPF is thus calculated to be several orders of magnitude greater than the production expected for GCR-induced neutrons. The production of 20.6 MeV gamma-rays is also calculated to be several orders of magnitude greater during a VLSPF. This method of mapping the 20.6 MeV gamma ray from the $^3He(n, \gamma)^4He$ reaction would also provide increased sensitivity for mapping other elements in the lunar regolith, and may allow the detection of previously unmapped elements in the lunar regolith as well as trace elements in the Earth's upper atmosphere.

1.0 INTRODUCTION

A map of the spatial distribution of ^3He in the lunar regolith is needed to locate the first cost-effective mining operations on the moon. While the concentration of titanium has been shown to be a good guide to helium distribution, the amount of solar-wind deposited helium also depends upon the maturity of the regolith. Thus, a direct method of detecting ^3He from lunar orbit is desired. One such method involves the production and detection of prompt gamma-rays from the neutron capture reaction involving the $^3He(n, \gamma)^4He$ reaction. Due to the complicated nature of the problem, we will only discuss the production of these prompt gamma-rays in the current paper. The detection of these gamma-rays will be discussed in a future publication.

2.0 PRODUCTION OF PROMPT GAMMA-RAYS FROM ^{3}HE IN THE LUNAR REGOLITH

2.1 Helium-3 - Neutron Capture Reaction

This detection scheme depends on the neutron capture reaction, $^3He(n, \gamma)^4He$. The flux of prompt gamma-rays yielded by this reaction depends on three quantities: the flux of neutrons present. $\phi_n(E)$; the neutron capture cross section of ^3He, $\sigma_{n,\gamma}(E)$; and the concentration of ^3He atoms in the regolith, $N_{^3He}$ (1).

$$\frac{\text{Gamma-rays}}{\text{cm}^2\text{-s}} = \sum \phi_n(E)\sigma_{n,\gamma}(E)N_{^3He} \qquad (1)$$

The quantities in Equation (1) are quite small: ϕ_n = 10 - 20 neutrons/cm^2-s for galactic cosmic-ray (GCR) induced thermal neutrons [1], $\sigma_{n,\gamma}$ = 0.03 mb at thermal energies [2] and $N_{^3He}$ = 10^{16} atoms of ^3He per cm^3 in the lunar regolith. Since all of these values are relatively small, we are essentially "looking for a needle in a haystack." Fortunately, it is a different colored needle. The Q-value of this reaction is 20.6 MeV [2]. The only other neutron capture reactions capable of producing gamma-rays in this energy range are isotopes of the other low-Z elements which are more diffuse than ^3He in the lunar regolith. There should be very little competition from gamma-rays produced by other (n, γ) reactions at energies greater than about 20 MeV. The cross sections for the $^3He(n, \gamma)^4He$ reaction as well as two other possible neutron reactions involving ^3He and a neutron are shown in Figure 1. These data show that the probability of a prompt gamma-ray being produced is extremely small. Thus, the number of prompt gamma-rays available for remote detection is dependent only upon the flux of neutrons in the lunar regolith over a few attenuation lengths for the gamma-rays in the lunar regolith. The attenuation length of 20.6 MeV gamma-rays in the lunar regolith is 30.2 cm.

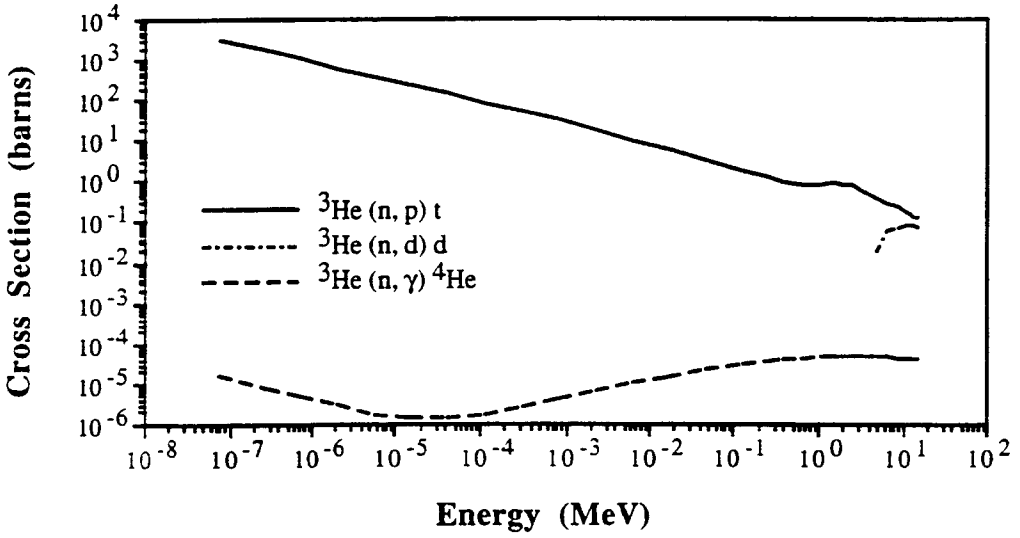


Figure 1. Possible ^3He - neutron interaction cross sections (National Nuclear Data Center, BROND-2 data base).

2.2 Possible Sources of Neutrons in the Lunar Regolith

The flux of prompt gamma-rays from ^3He in the lunar regolith is directly dependent on the number of neutrons available for capture. We have examined several possible sources of neutrons in the lunar regolith to determine if any might provide enough neutrons to make ^3He detectable. These sources include natural radioactivity from primordial and cosmogenic radioactive species, the solar wind, galactic cosmic-rays, solar flares and neutrons produced from neutral particle beams. Most of the neutrons in the regolith are the products of (p, n) reactions between incident protons and higher-Z nuclei with energies above about 30 MeV/amu and the major constituents of the regolith such as SiO_2.

The flux of neutrons in the regolith due to natural radioactivity and solar wind particles is negligible (<< 1 neutron/cm^2-s) while GCR's induce approximately 10-20 neutrons/cm^2-s [2]. Using this flux in Equation (1) results in a prompt gamma-ray flux of about $1.1x10^{-3}$ gamma-rays/m^2-hr. This flux is far too small to make remote detection feasible. Thus, very large solar proton flares (VLSPF's) were considered due to the large numbers of particles incident on the lunar surface during such events. A neutral particle beam (NPB) was also considered as a possible means of artificially inducing neutrons in the lunar regolith. Calculation of the neutron flux induced by a VLSPF and a NPB are discussed below.

3.0 Neutron Source Characteristics

3.1 Very Large Solar Proton Flares (VLSPF's)

The ideal means of remotely detecting ^3He from lunar orbit would use naturally present neutrons reacting with the ^3He as discussed above. Since the GCR-induced flux of neutrons is thought to be too small to make detection feasible, another naturally present source was sought. Solar flares present a danger to astronauts living and working on the moon due to the large doses of proton-induced radiation. If the peak neutron flux created by flare protons -- via (p, n) reactions -- is large enough to overcome the background continuum, then a satellite could be placed in lunar orbit to wait for a large solar proton event.

Very large solar proton flares are relatively short and unpredictable. Only six VLSPF's have been recorded in the last three decades; three of these events occurred in 1989 alone. These events are predictable only in the sense that they tend to occur during the period leading to the maximum of the sun's 11-year sunspot cycle. These cycles vary greatly in amount of activity, and VLSPF's have also been known to occur after the maximum in the solar cycle. Very large solar proton flares are generally characterized by three bursts of high proton fluxes (Figure 3). These peaks vary greatly in duration, which is generally on the order of one day. The short duration of the peak flux would limit the surface coverage attainable by an orbiting detector.

The spectral properties of these flares are also highly unpredictable (Figure 4). The October 1989 solar flare was taken to be a typical VLSPF. The peak proton flux of this flare was about 10^5 protons/cm^2-s about 30 hours into the flare [3]. The omnidirectional integral fluence of protons with energies above 30 MeV contained in this event was $4.24x10^9$ protons/cm^2 [5]. The flare of Feburary 1956 generated a proton spectrum much harder than any of the other VLSPF's on record and lasted for only about 2 hours [3]. Since this flare was

expected to generate more neutrons than any of the other VLSPF's, it was included in the current study as an upper limit to the neutron spectrum that could be produced.

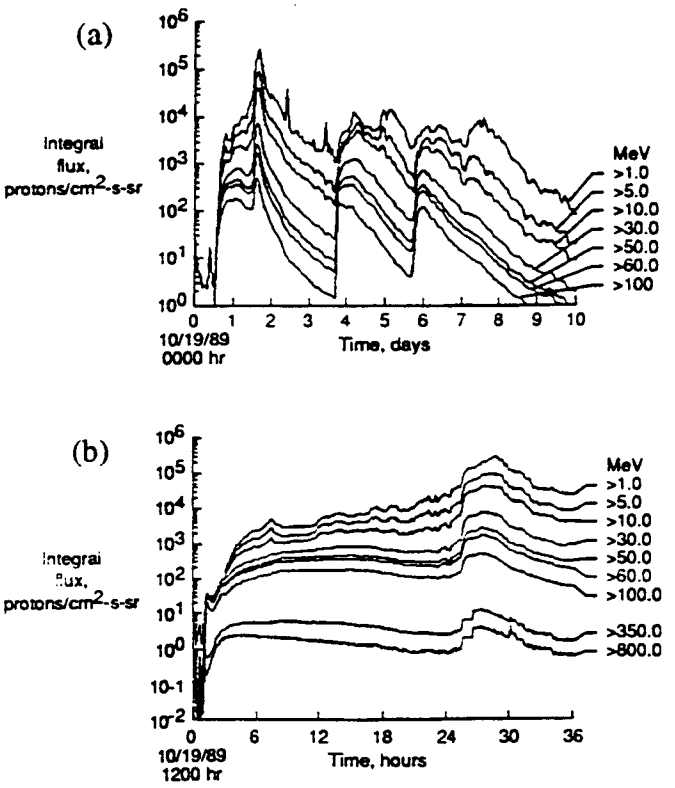


Figure 2. October 1989 VLSPF: (a) GOES-7 hourly average integral flux history and (b) GOES-7 five minute average integral flux history (GOES-7 data from NOAA Space Environment Laboratory) [3].

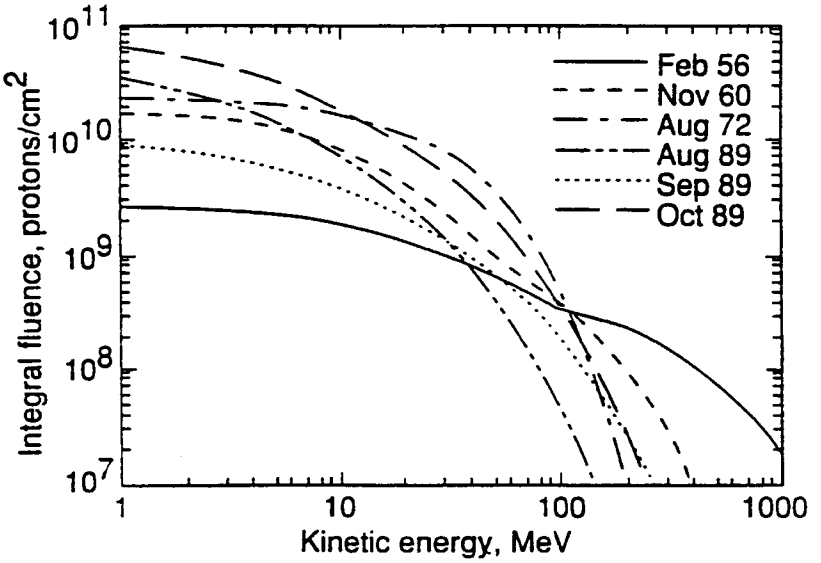


Figure 3. Integral fluence energy specta for six very large solar proton flares [4].

3.2 Characteristics of A Neutral Particle Beam

A neutral particle beam (NPB) device was considered as an artificial means of introducing protons or higher-Z particles into the lunar regolith for the purpose of inducing high neutron fluxes, and in turn, high fluxes of 20.6 MeV gamma-rays from the neutron capture reaction of these neutrons with ^{3}He. Neutral particle beam devices have been developed for use in space for the interrogation of nuclear warheads, and many of their properties remain classified. We have considered a 100 MeV, 30 mA beam of protons and assumed an beam area of 10 cm^2 in the calculations and results described below. The advantages of using a NPB for the remote detection of ^{3}He are the control of the device energies and beam direction. Instead of waiting for an unpredictable event on the Sun, the neutrons could be induced at any time. By rastering the beam over the lunar surface and detecting the resulting gamma-rays from a separate satellite, high-resolution maps of lunar ^{3}He could be obtained.

4.0 PARTICLE INTERACTION AND TRANSPORT CALCULATIONS

The objective of this research is to calculate the flux of prompt gamma-rays coming from ^{3}He in the lunar regolith during a VLSPF or due to a NPB. A computational procedure that could model the production of neutrons via the interaction of incident protons with the regolith, transport the neutrons, model the (n, γ) reaction with ^{3}He and finally transport the resulting gamma-rays to the lunar surface was needed. Since a single computational model was unavailable, BRYNTRN was used to perform the charged particle interactions and generate the neutrons within the regolith ONEDANT was used to transport the resulting neutrons and generate the prompt gamma-ray flux (Figure 4). These codes are summarized in the following.

4.1 Charge Particle Interactions and Neutron Production: BRYNTRN

In order to utilize the neutron fluxes generated by the protons incident on the Moon during a solar flare, a numerical model capable of performing the interaction calculations is needed. Preferrably, this model would include a data base of VLSPF events. The NASA-Langley Research Center has been heavily involved in developing numerical tools for the transport of baryons through shield materials based on a straight ahead approximation of the time-independent Boltzmann equation [6]. The BRYNTRN code is self-contained, computationally efficient and requires only a fraction of the computer resources needed by a typical Monte Carlo code. The code also contains an input data base consisting of GOES solar flare data from the National Oceanic and Atmospheric Administration (NOAA). In the current study, BRYNTRN is also used to calculate the neutron flux induced in the lunar regolith by the February 1956 and October 1989 VLSPF's and by a 100 MeV, 3 mA/cm^2 neutral proton beam.

4.2 Neutron and Gamma-Ray Transport: ONEDANT

Once a neutron production spectrum has been calculated for a particular event using BRYNTRN, the neutrons must be transported through the lunar regolith, the local gamma-ray yield calculated and the gamma-rays transported to the surface of the regolith. The neutron and gamma-ray transport calculations are performed using the one-dimensional discrete ordinates neutral-particle transport code ONEDANT together with the Los Alamos National Laboratory

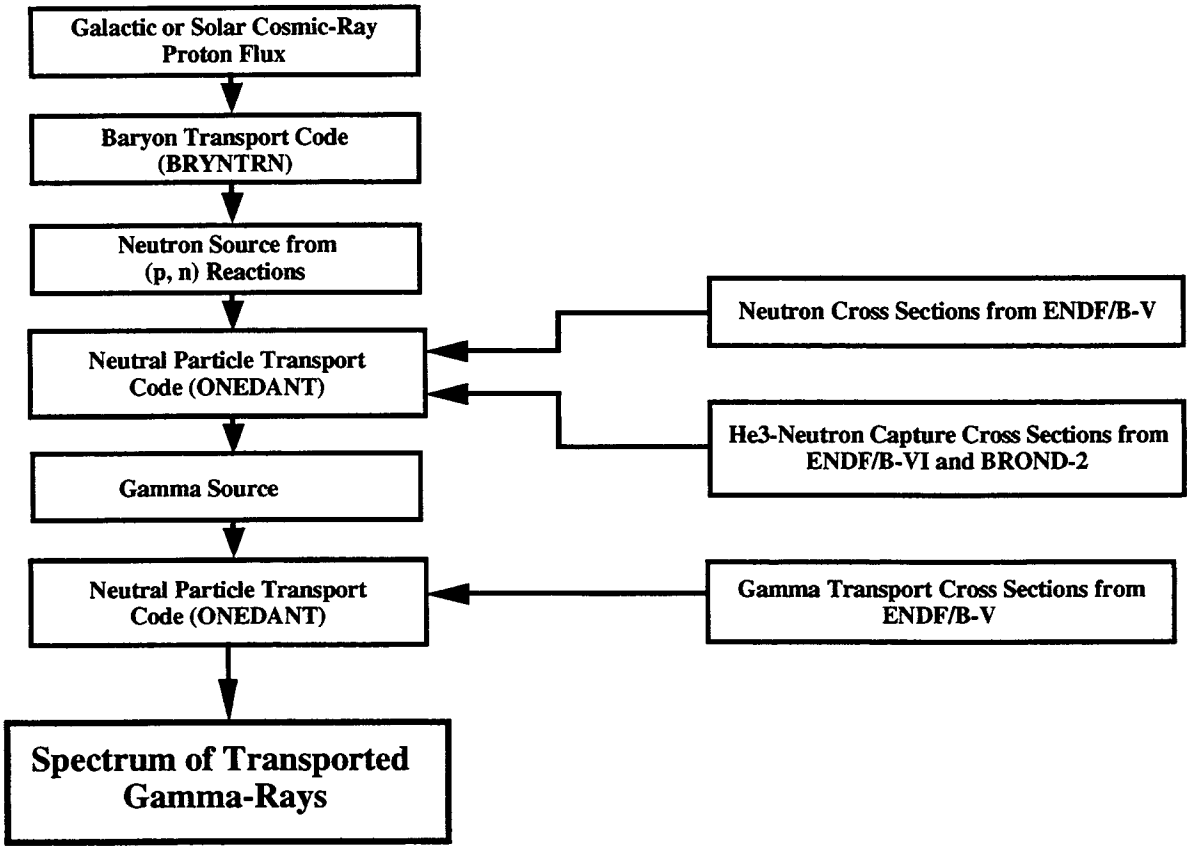


Figure 4. Flow chart of the computational method used in calculating the gamma-ray flux from ^{3}He due to an incident proton flux.

(LANL) MATXS5 cross section data library processed from the ENDF/B-V evaluated files. The standard LANL 30 neutron, 12 gamma-ray energy group structure are used and the calculations are performed using the P_3-S_8 approximation. Since cross section data does not exist for neutrons above 20 MeV, all neutrons with higher energies were included in the highest energy group available. This approximation will result in an underestimation of the gamma-ray flux since approximately 20% of the VLSPF-induced neutrons have energies higher than 20 MeV.

The gamma-ray flux was calculated for the top three meters of the lunar regolith using the neutron flux at 6.7 cm. This gamma-ray flux for VLSPF's can then be multiplied by the area of a detector in orbit around the moon to yield the number of counts per second that could be detected from a theoretical semi-infinte plane. Since the NPB is essentially a point source, the flux generated at the lunar surface must be divided by $4\pi r^2$ (where r is the detector's orbital distance from the lunar surface) before it is multiplied by the detector area.

5.0 RESULTS

5.1 Neutrons Induced in the Lunar Regolith by Various Proton Sources

The total GCR-induced neutron production rate used was 16±5 neutrons/cm^2-s [7]. The neutron flux was calculated using BRYNTRN for each of the cases described above. This

flux was then used as input for ONEDANT. At a depth of 6.7 cm (10 g/cm^2), the total neutron flux for the October 1989 flare was determined to be 2485 neutrons/cm^2-s. Figure 5 shows that the neutron flux as a function of depth below 10 MeV for the October 1989 flare is several orders of magnitude greater than the thermal neutron flux induced by galactic cosmic rays calculated by Lingenfelter, et. al., 1972 [7]. The local neutron flux induced by the NPB was calculated to be approximately 10^{16} neutrons/cm^2-s at a depth of 6.7 cm for a 100 MeV, 3 mA/cm^2 proton beam.

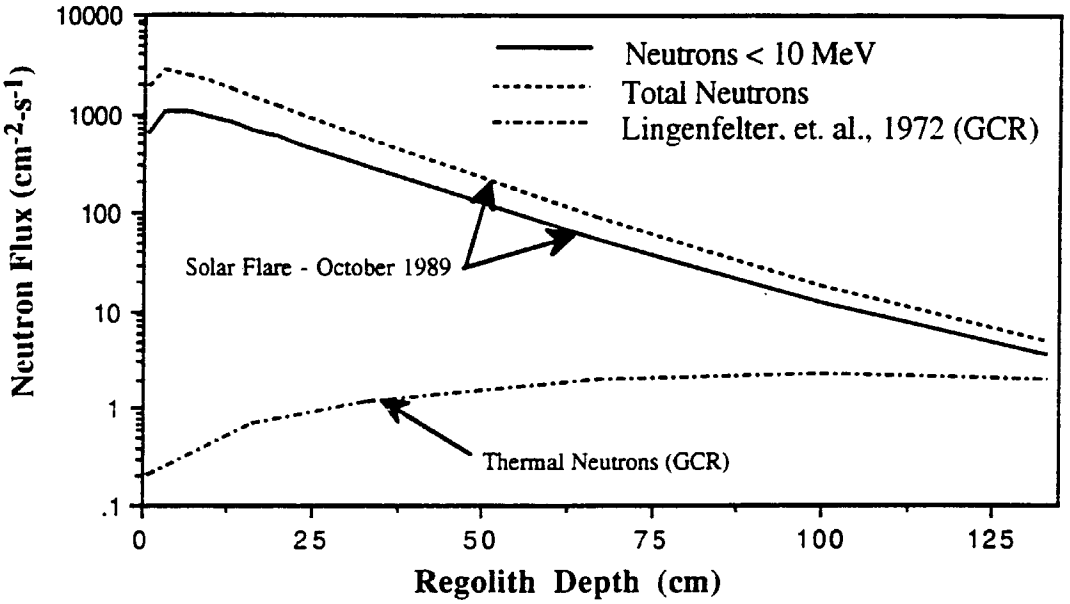


Figure 5. Neutron flux as a function of depth for the October 1989 VLSPF as calculated using BRYNTRN. The thermal neutron flux is that calculated by Lingenfelter, et. al. (1972) [7].

5.2 Gamma-ray Fluxes from ^{3}He Resulting from Various Proton Sources

The GCR-induced gamma-ray flux was calculated using 16 neutrons/cm^2-s to be 4.2x10^{-3} gamma-rays/m^2-hr. The gamma-ray fluxes from ^{3}He were obtained by using the neutron fluxes calculated by BRYNTRN for the two VLSPF's and the NPB as input for ONEDANT. The VLSPF's of October 1989 and February 1956 yielded values of 0.85 and 8.8 gamma-rays/m^2-hr, respectively. The NPB yielded a flux of 5.5x10^9 gamma-rays/m^2-hr at the lunar surface. The increased gamma-ray flux due to VLSPF's and NPB's is seen to be significant compared to the background levels provided by GCR-induced reactions (Figure 6).

6.0 CONCLUSIONS

Very large solar flares can increase the ^{3}He(n, γ)^{4}He reaction rate by a factor of approximately 3000 over the background rate generated by galactic cosmic-rays interacting with the lunar regolith via (p,n) reactions. This increased reaction rate will enhance the detectability of ^{3}He from low lunar orbit. A 100 MeV, 3 mA/cm^2 neutral particle beams have been shown to increase the local ^{3}He(n, γ)^{4}He reaction rate by a factor of approximately 10^{12} over the background rate due to incident GCR particles. The potential exists for high-

resolution measurements of the spatial distribution of ^{3}He from lunar orbit using VLSPF's or optimized NPB's.

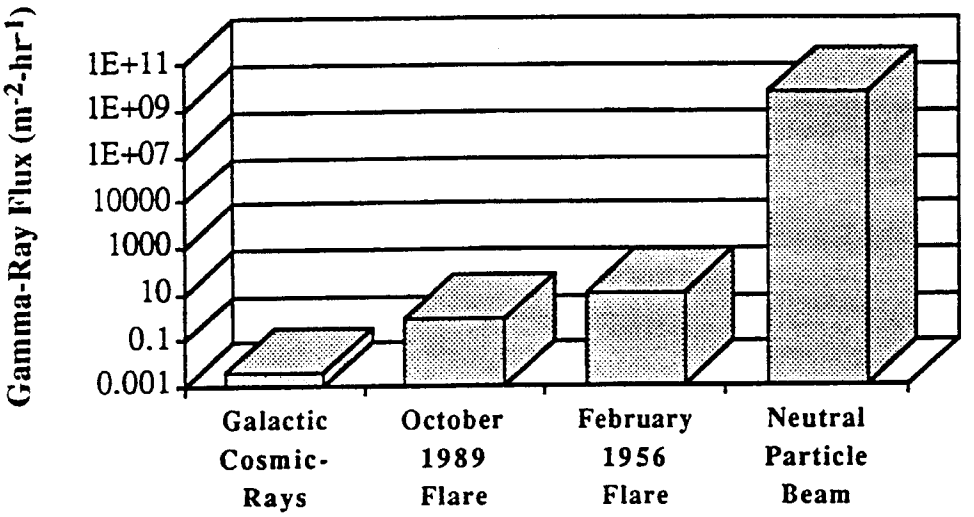


Figure 6. The 20.6 MeV gamma-ray flux from lunar ^{3}He calculated from various neutron sources. Note that the gamma-ray source from the NPB is a point source at the lunar surface.

7.0 ACKNOWLEDGEMENTS

The authors would like to thank Dr. John Nealy at the NASA-Langley Research Center for providing access to the baryon transport code BRYNTRN and support in modifying the code for the present purpose. Thanks also go to Dr. Layton Wittenberg and Dr. Eugene Cameron of the Wisconsin Center for Space Automation and Robotics for many fruitful discussions concerning the search for ^{3}He.

REFERENCES

[1] G. H. Heiken, D. T. Vaniman and B. M. French, eds.,1991: *Lunar Sourcebook: A User's Guide to the Moon*, Cambridge University Press, Cambridge.

[2] National Nuclear Data Center, (1993): ENDF/B-VI Data Base.

[3] L. C. Simonsen, J. E. Nealy, H. H. Sauer and L. W. Townsend, 1991: "Solar Flare Protection for Manned Lunar Missions: Analysis of the October 1989 Proton Flare Event," SAE Paper No. 911351, 21st International Conference on Environmental Systems, San Fransisco, CA, 1991.

[4] J. E. Nealy, S. A. Striepe and L. C. Simonsen, 1992: "MIRACAL: A Mission Radiation Calculation Program for Analysis of Lunar and Interplanetary Missions," NASA TP-3211, p. 5.

[5] H. H. Sauer, private communication, NOAA Space Environment Laboratory, February 12, 1993.

[6] J. W. Wilson, L. W. Townsend, J. N. Nealy, S. Y. Chun, B. S. Hong, W. W. Buck, S. L. Lamkin, B. D. Ganapol, F. Khan and F. A. Cucinotta, 1989: "BRYNTRN: A Baryon Transport Model," NASA TP-2887.

[7] R. E. Lingenfelter, E. H. Canfield and V. E. Hampel (1972): "The Lunar Neutron Flux Revisited," *Earth and Planetary Science Letters*, 16, pp. 355-369.

By-products of Lunar Helium-3 Mining

Larry A. Haskin
Dept. of Earth and Planetary Sciences and
McDonnell Center for the Space Sciences
Washington University
One Brookings Drive
St. Louis, MO 63130

ABSTRACT

The general nature of the lunar surface and the principal materials available there are known well enough to permit general planning to use common lunar materials as resources and to permit sensible, initial development of equipment for mining and manufacturing on the Moon's surface. An actual venture to extract ^{3}He should be preceded by further, quantitative study of the release of solar-wind-implanted gases and their reaction products during vacuum pyrolysis, and by proof of the ore body. Such a venture will produce other gases as by-products and will surely be accompanied by other uses of lunar materials.

1. INTRODUCTION AND OVERVIEW

Mining of ^{3}He on the Moon could yield large quantities of other noble gases and of hydrogen, carbon, and nitrogen, plus gravel and rock sieved from the lunar soil. The solar wind has implanted these chemical elements into grains of lunar "soil," which consists of pulverized rock and glass produced by meteoroid impacts onto the lunar surface. We know enough about lunar soils and their solar-wind-implanted gases that we may confidently rely on the presence of those gases for purposes of planning. Gases released from soils along with ^{3}He will be valuable, and should be conserved for use in space, not wasted into the lunar atmosphere, from which they will escape into space. We must acquire a better understanding of gaseous extraction by vacuum pyrolysis before designing equipment for catching, separating, and storing gases driven off from lunar soils. Once a specific project is under development, detailed proof of the quality of the proposed ore body would be desirable, if not essential, both to assure concentrations of solar-wind gases and to assure mineability (freedom from excess craters and boulders, adequate soil depth, etc.). One probable by-product of ^{3}He mining that should be collected will be gravel, a scarce commodity on the Moon.

The ubiquitous, easily collected lunar soils are likely to be the chief feedstocks for all early lunar resource extraction. Their principal chemical constituents are oxygen, silicon, aluminum, iron, magnesium, calcium, and sodium, present almost entirely as oxides or as silicates and alumino-silicates. The infrastructure put in place for lunar ^{3}He mining would permit or attract other lunar industries, to use the accompanying gases, and to the soils for thermal and radiation shielding and as a source of metals and ceramic products. Owing to the Moon's special conditions (e.g., long days and nights; no atmosphere for light scattering, heat transfer, or oxidation; extreme temperatures; hard vacuum; no existing industrial

infrastructure; unfamiliar feedstocks and lack of specialized ores), terrestrial technologies cannot be easily transferred to the Moon, and new, appropriate technologies must be developed. For economy and reliability, these must have few and simple steps be robust, and be accomodating of some variability in feedstock composition.

The purpose of this short article is to call attention to the literature on the use of lunar materials. Reference [1], the *Lunar Sourcebook*, is a comprehensive but readable summary of lunar conditions and materials, written by a group of lunar researchers and intended to provide a coherent understanding of the Moon's surface and its materials. Two books by S. R. Taylor summarize much of the geoscience of the Moon [2,3]. Much of the basic science done on the Moon or on lunar materials has been published in the *Proceedings of the Apollo 11 Lunar Science Conference*, the *Proceedings of the Lunar Science Conferences* (vol.s 2-8), and the *Proceedings of the Lunar and Planetary Science Conferences* (vols. 9-22). Proceedings of these conferences were discontinued after the 1991 (22nd) conference in favor of publishing in regular journals. Both during the time frame of the Lunar Science Conferences and the Lunar and Planetary Science Conferences and since discontinuation of the proceedings of those conferences, articles on lunar science have appeared in geoscientific journals, particularly the following ones: *Geochimica et Cosmochimica Acta*, *Earth and Planetary Science Letters*, *Journal of Geophysical Research*, *Geophysical Research Letters*, *Reviews of Geophysics and Space Physics*, *Meteoritics*, and *The Moon*.

Discussions of the resources of the Moon and how they might be used appear in the proceedings of the conferences *Space 88*, *Space 90*, and *Space 92* [4-6]. Other discussions are contained in the proceedings of the conferences on *Lunar Bases and Space Activities of the 21st Century* [7,8]. References [9,10] report the extensive results of NASA-sponsored summer studies on space resources, with some emphasis on lunar materials. References [11,12] are an extensive, particularly informative overview of possible uses of the Moon. The proceedings of the *Princeton Conferences on Space Manufacturing*, published by the AIAA, are an important source of information on materials and operations in space. Further results on studies of space resources are available as the annual reports of the University of Arizona-NASA Space Engineering Research Center for Utilization of Local Planetary Resources. A book on near-Earth space resources is in press [13]. Extensive bibliographies of articles on possible uses of lunar materials are found in references [14-16].

Because byproducts of ^{3}He mining are the emphasis of this article, references [17-49] are included as representative of the state of our knowledge of other gases. Reference [16] is a similar bibliography, divided according to topic (Beneficiation, Concrete, Glass and Ceramics, etc.). The reader is referred to the *Lunar Sourcebook* for a general introduction, before reading these more specialized articles.

Reference [50] is a readable and reasonable introduction to lunar conditions as might be experienced in a lunar company town. References [51,52] describe this investigator's views on guidelines for early lunar technologies and ideas on early, most common products for use in space and obtainable from lunar soils may be.

REFERENCES

[1] G. Heiken, D. Vaniman, and B. French, eds., *Lunar Sourcebook*, Cambridge (1991).

[2] S. R. Taylor, *Lunar Science, A Post-Apollo View*, Pergamon (1975).

[3] S. R. Taylor, *Planetary Science: A Lunar Perspective*, Pergamon (1982).

[4] S. W. Johnson and J. P. Wetzel, *Engineering, Construction, and Operations in Space I*, Amer. Soc. Civil Eng., New York (1988).

[5] S. W. Johnson and J. P. Wetzel, *Engineering, Construction, and Operations in Space II*, Amer. Soc. Civil Eng., New York (1990).

[6] W. Z. Sadeh, S. Sture, and R. J. Miller, eds., *Engineering, Construction, and Operations in Space III*, Amer. Soc. Civil Eng., New York (1992).

[7] W. W. Mendell, ed., *Proceedings of the Conference on Lunar Bases and Space Activities of the 21st Century*, Lunar and Planetary Institute, Houston (1985).

[8] W. W. Mendell, ed., *Proceedings of the 2nd Conference on Lunar Bases and Space Activities of the 21st Century*, NASA Special Conf. Public. 3166 (1992).

[9] M. J. Duke and J. R. Arnold (eds), *Summer Workshop on Near Earth Resources*, NASA CP-2031 (1977).

[10] M. F. McKay, D. S. McKay, and M. B. Duke, eds., *Space Resources*, NASA SP-509 (1992).

11] D. R. Criswell, *Extraterrestrial Materials Processing and Construction*, Final Report, NASA CR-158870, Washington (1978).

[12] D. R. Criswell, *Extraterrestrial Materials Processing and Construction*, Final Report, NASA CR-167756, Washington (1980).

[13] J. Lewis, ed., *Resources of Near-Earth Space*, Univ. Ariz. Press (in press).

[14] P. A. Puzzo, *Bibliography of Topics in Space Industrialization*, Cal. Space Ref. No. 82-01, University of California-San Diego, La Jolla (1982).

[15] J. C. Seltzer, *A Lunar Base Bibliography*, Planetary Materials Branch Publ. 79, JAS 22873, NASA Johnson Space Center, Houston (1988).

[16] L. A. Haskin and R. O. Colson, "Resource Availablilty at Taurus-Littrow" (abstract) *Workshop on Geology of the Apollo 17 Landing Site*, LPI Tech. Rept. 92-09, Lunar and Planetary Institute, Houston pp. 9-14 (1992).

[17] J. R. Arnold, "Ice in the Lunar Polar Regions," *J. Geophys. Res.* **84**, 5659 (1979).

[18] J. R. Arnold, "Water on the Moon," *Lunar Science* VII, Special Session Abstracts, Lunar and Planetary Institute, Houston pp. 61-65 (1976).

[19] D. D. Bogard, "Effects of Soil Maturation on Grain-Size Dependence of Trapped Solar Gases," *Proc. Lunar Sci. Conf.* **8**, 3705-3718 (1977).

[20] R. Bustin and E. K. Gibson, Jr., "Availability of Hydrogen for Lunar Base Activities," *The Second Conference on Lunar Bases and Space Activities of the 21st Century*, NASA Conf, Publ. 3166 pp. 437-445 (1992).

[21] R. Bustin, R. K Kotra., E. K. Gibson, G. A Nace., and D. S. McKay, "Hydrogen Abundances in Lunar Soils," *Lunar and Planetary Science XV*, Lunar and Planetary Institute, Houston pp. 112-113 (1984).

[22] J. L. Carter, "Lunar Regolith Fines: A Source of Hydrogen," *Lunar Bases and Space Activities of the 21st Century*, Lunar and Planetary Institute, Houston pp. 571-581 (1985).

[23] S. Chang, K. Lennon, and E.K. Gibson, Jr., "Abundances of C, N, H, He, and S in Apollo 17 Soils from Stations 3 and 4: Implications for Solar Wind Exposure Ages and Regolith Evolution," *Proc. Lunar Sci. Conf.* **5**, 1785-1800 (1974).

[24] B. L. Cooper, "Experimental Microwave Processing of Lunar Regolith Simulant for The Recovery of Volatiles," *Engineering, Construction, and Operations in Space II*, Amer. Soc. Civil Eng., New York pp. 168-176 (1990).

[25] B. L. Cooper, "Sources and Subsurface Reservoirs of Lunar Volatiles," *Proc. Lunar Planet. Sci. Conf.* **20**, 259-269 (1989).

[26] T. M. Crabb and M. K. Jacobs, Synergism of He-3 Acquisition with Lunar Base Evolution," *The Second Conference on Lunar Bases and Space Activities of the 21st Century*, Lunar and Planetary Institute, Houston pp. 475-482(1992).

[27] D. J. DesMarais, J. M. Hayes, and W. G. Meinschein, "The Distribution in Lunar Soil of Carbon Released by Pyrolysis," *Proc. Lunar Sci. Conf.* **4**, 1543-1558 (1972).

[28] H. N. Friedlander, "An Analysis of Alternate Hydrogen Sources for Lunar Manufacture," *Lunar Bases and Space Activities of the 21st Century*, Lunar and Planetary Institute, Houston pp. 611-618 (1985).

[29] E. K. Gibson, R. Bustin, and P. Mannion, "Hydrogen Abundances in Apollo 16 and 17 Deep Drill Core and 79001/79002 Core Samples," *Lunar and Planetary Science XXI*, Lunar and Planetary Institute, Houston pp. 387-388 (1988).

[30] E. K. Gibson, Jr. and G. W. Moore, "Inorganic Gas Release and Thermal Analysis Study of Apollo 14 and 15 Soils," *Proc. Lunar Sci. Conf.* **3**, 2029-2040 (1972).

[31] P. Gorenstein, L. Golub, and P. Bjorkholm, "Radon Emission from the Moon, Spatial and Temporal Variability," *The Moon* **9**, 129-140 (1973).

[32] L. A. Haskin, "Water and Cheese from the Lunar Desert: Abundances and Accessibility of H, C, and N on the Moon," *The Second Conference on Lunar Bases and Space Activities of the 21st Century*, NASA Conf, Publ. 3166 pp. 393-396 (1992).

[33] L. A. Haskin and P. Warren, "Lunar Chemistry," in *Lunar Sourcebook*, G. Heiken, D. Vaniman, and B. French, eds. Cambridge pp. 357-474 (1991).

[34] B. R. Hawke, C. R. Coombs, and B. Clark, "Pyroclastic Deposits: An Ideal Lunar Resource," *Lunar and Planetary Science XX*, Lunar and Planetary Institute, Houston pp. 389-390 (1989).

[35] B. R. Hawke, C. R. Coombs, and B. Clark, "Ilmenite-Rich Pyroclastic Deposits: An Ideal Lunar Resource," *Proc. Lunar Planet. Sci. Conf.* **20**, 249-258 (1990).

[36] G. L. Kulcinski, E. N. Cameron, W. D.Carrier, III, and H. H. Schmitt, "Environmental Aspects of Lunar Helium-3 Mining," *Engineering, Construction, and Operations in Space III*, Amer. Soc. Civil Eng., New York pp. 606-616 (1992).

[37] G. L. Kulcinski and H. H. Schmitt, "The Moon: An Abundant Source of Safe Fusion Fuel for the 21st Century," *11th Int. Sci. Forum on Fueling the 21st Century*, Moscow (1987).

[38] Y. T. Li and L. J. Wittenberg, "Lunar Surface Mining for Automated Acquisition of Helium-3: Methods, Processes, Equipment," *The Second Conference on Lunar Bases and Space Activities of the 21st Century*, NASA Conf, Publ. 3166 pp. 609-617 (1992).

[39] H. H. Schmitt, G. L. Kulcinski, I. N. Sviatoslavsky, and W. D. Carrier, III, "Spiral Mining For Lunar Volatiles," *Engineering, Construction, and Operations in Space III*, Amer. Soc. Civil Eng., New York pp. 1162-1170 (1992).

[40] B. R. Simoneit, P. C.Christiansen, and A. L. Burlingame, "Volatile Element Chemistry of Selected Lunar, Meteoritic, and Terrestrial Samples," *Proc. Lunar Sci. Conf.* **4**, 1635-1650 (1973).

[41] I. N. Sviatoslavsky and M. K. Jacobs, "Mobile ^{3}He Mining System and Its Benefits toward Lunar Self-Sufficiency," *Engineering, Construction, and Operations in Space I*, Amer. Soc. Civil Eng., New York pp. 310 (1990).

[42] I. N. Sviatoslavsky, "Lunar He-3 Mining: Improvements on the Design of the UW Mark II Lunar Miner," *Engineering, Construction, and Operations in Space III*, Amer. Soc. Civil Eng., New York pp. 1080-1091 (1992).

[43] L. A. Taylor, Hydrogen, "Helium, and Other Solar-Wind Components in Lunar Soil: Abundances and Predictions," *Engineering, Construction, and Operations in Space II*, Amer. Soc. Civil Eng., New York pp. 68-77 (1990).

[44] D. S. Tucker, D. T. Vaniman, J. L. Anderson, F. W. Clinard, Jr., R. C. Feber, Jr., H. M. Frost, T. T. Meek, and T. C. Wallace, "Hydrogen Recovery from Extraterrestrial Materials Using Microwave Energy," *Lunar Bases and Space Activities of the 21st Century*, Lunar and Planetary Institute, Houston pp. 583-590 (1985).

[45] K. Watson, B. C. Murray, and H. Brown, "On the Possible Presence of Ice on the Moon," *J. Geophys. Res.* **66**, 1598 (1961).

[46] W. R. Wilkes and L. J. Wittenberg, "Isotopic Separation of ^{3}He/^{4}He from Solar-Wind Gases Evolved from the Lunar Regolit,h" *Engineering, Construction, and Operations in Space III*, Amer. Soc. Civil Eng., New York pp. 547-554 (1992).

[47] L. J. Wittenberg, "In-Situ Release of Solar Wind Gases from Lunar Soil," *Engineering, Construction, and Operations in Space III*, Amer. Soc. Civil Eng., New York pp. 537-546 (1992).

[48] L. J. Wittenberg, "A Review of Helium-3 Resources and Acquisition for Use as Fusion Fuel," *Fusion Technol.*, (1992) (in press).

[49] L. J. Wittenberg, J. F. Santarius, and G. L. Kulcinski, "Lunar Source of ^{3}He For Commercial Fusion Power," *Fusion. Technol.* **10**, 167-178 (1986).

[50] B. Bova, *Welcome to Moonbase*, Ballantine, NewYork (1987).

[51] L. A. Haskin, "A Spartan Scenario for Use of Lunar Materials," *Lunar Bases and Space Activities of the 21st Century*, Lunar and Planetary Institute, Houston pp. 435-443 (1985).

[52] L. A. Haskin and R. O. Colson, "Lunar Resources: Toward Living off the Lunar Land," *Proc. 1st Ann. Invit. Sympos., UA/NASA Space Eng. Res. Ctr. for Util. Local Planet. Res.*, T. Triffet, ed. pp. I12-I19 (1990).

3) D-^{3}He Fusion and Energy Policy 81
J.M. Dawson, Chair

3-1 Utility Perspective on Clean Nuclear Energy 83
D. Louis Peoples

3-2 My Perspective on D-^{3}He Fusion 95
David H. Crandall

3-3 Industrial Perspectives on Helium-3 and Fusion Power 101
Stephen O. Dean

Utility Perspective on Clean Nuclear Energy
A Presentation Prepared Especially For
The Second Wisconsin Symposium on ^{3}He and Fusion Power

D. Louis Peoples
Executive Vice President
Madison Gas and Electric Company
Post Office Box 1231
Madison, Wisconsin 53701-1231

1. OVERVIEW

1.1 Perspective

A utility perspective on clean nuclear energy must be long term. New base load capacity requirements will evolve in the later half of the 90's decade and will be increasing in the first decade of the twenty-first century.

I begin from the viewpoint of an experienced utility executive with the background in nuclear operations, engineering, construction, licensing, and start-up. The tremendous technological development of the twentieth century provides a basis for the belief that there are significant benefits to be gained from innovation at the ever expanding edge of human imagination (e.g. fusion power).

1.2 Highlights

This utility perspective on clean nuclear energy will address the following topics:

a. Factors impacting development of electric energy generation technologies in the 90's;

b. Criteria for the selection of new electric generation technologies;

c. Implications for the development of clean nuclear energy/fusion power; and

d. Conclusions and recommendations to assist in the development of clean nuclear energy as a competitive technology for the twenty-first century.

2. FACTORS IMPACTING DEVELOPMENT OF ELECTRIC ENERGY GENERATION TECHNOLOGIES IN THE '90's

2.1 National Energy Strategy/National Energy Policy Act of 1992

The development of clean nuclear energy will be driven, in part, by the National Energy Strategy of 1991/1992 and the National Energy Policy Act of 1992. The National Energy Strategy of 1991/1992 provides for:

a. "A road map to a more secure and cleaner energy future...

b. Achieving greater energy security (especially reducing our dependence on foreign oil by utilizing a sustainable and balanced approach);

c. Increasing energy and economic efficiency;

d. Securing future energy supplies;

e. Enhancing environmental quality; and

f. Fortifying foundations (fundamental science and engineering research; technology transfer; education; investing in human resources)."

Clean nuclear energy, both fission and fusion, can help the United States (U.S.) to achieve all of these goals.

The implementation of the 1991/1992 National Energy Strategy was begun in ernest with the National Energy Policy Act of 1992. Key points related to electric power generation include:

a. The creation of electric wholesale generators (EWG's);

b. Wholesale transmission access;

c. Transmission pricing;

d. Voluntary reduction of greenhouse gases;

e. Energy efficiency standards; and

f. Restructuring of federal energy research development and demonstration programs.

The last item, restructuring of federal energy research development and demonstration programs, should be of special interest to all developers of advanced and long-term energy supply alternatives. According to Richard D. Grundy, Senior Professional Staff (Republican) for the Committee on Energy and Natural Resources, United States Senate, "The Act restructures federal research and development programs to establish commercial applications as a principal objective for federal energy research development and demonstration programs. In the future, any demonstration programs supported by the Department of Energy (DOE) must determine the technical and commercial feasibility of new energy technologies. As a commercialization incentive, the Act extends the provisions of the 1990 Amendments to Stevenson Wydler Technology Innovation Act of 1980 regarding the protection of intellectual property and other sensitive information to any DOE research development and demonstration (RD&D) activities." In short, proposed RD&D programs must include near-term benefits if they are to be funded.

2.2 Deregulation/Competition

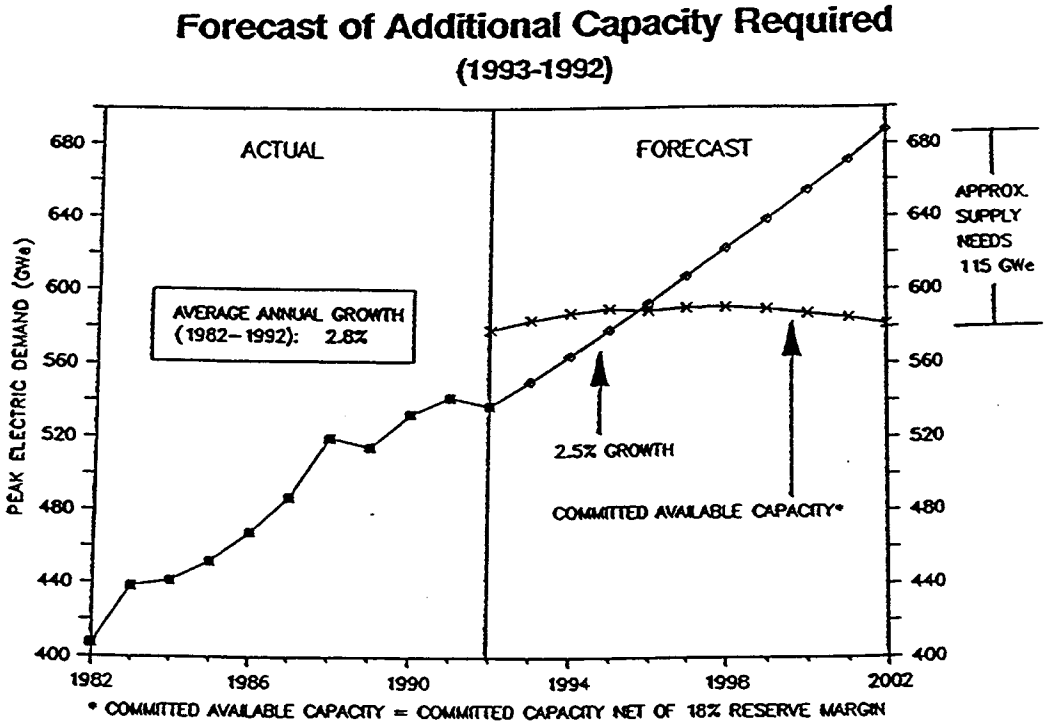
The entire regulated U.S. energy industry is currently undergoing a metamorphosis. The electric power industry is in the process of devolution, that is, splitting into generating companies, transmission companies, and distribution companies. Segmented competition, with its anticipated benefits (principally lower costs), is replacing the highly regulated and vertically integrated electric utility industry. Independent power producers (IPP's) have already been established, vis-a-vis the development of co-generation sponsored by the Public Utility Regulatory Policy Act of 1978. Consolidation by merger and acquisition will be one aspect to the competitive response by managers of companies in the electric power industry.

The prospective purchasers of new generation will therefore include utilities as competitors plus IPP's. Utilities and IPP's will establish EWG's in accordance with the National Energy Policy Act of 1992. In 1990 and 1991, IPP's brought into commercial operation more than 50 percent of all new U.S. electrical generation.

In some cases, utilities themselves are participants in, or wholly own, independent power companies. It is also conceivable that foreign companies may aggressively enter the large and growing U.S. market. Developers of electric generating technologies must, therefore, sell to a whole new set of players (owners) who will be aggressively competing with a marketplace mentality.

2.3 Need for New Generation

The good news is that there is a relatively strong growth in U.S. electric energy demand, even taking into account current and projected demand-side management (DSM) efforts. For the past two decades, the consumption of electricity in the U.S. has grown at a rate slightly exceeding the growth in gross domestic product (GDP). Looking out ten years, a moderate forecast suggests the need for approximately 115 gigawatts new additional generating capacity beyond the already committed available capacity. In order to meet the increased demands anticipated in the first decade of the twenty-first century, nearly 200 gigawatts of new orders must be placed by the year 2002.



Reference: Bechtel Power Corporation, 1993

However, none of the forecasts to-date fully anticipate the probable retirement of many of the 649 U.S. coal plants aggregating over 70,000 megawatts which will be more than 40 years old by the year 2003. In addition, fission reactors, which currently provide 21 percent of all U.S. electricity consumed in a year, may be retired and decommissioned in large numbers beginning about 2015, unless life extension is determined to be a technically viable and economic alternative. The following charts show in some detail the forecasts of additional capacity required and new generation requirements determined on a regional basis as defined by the North American Electric Reliability Council.

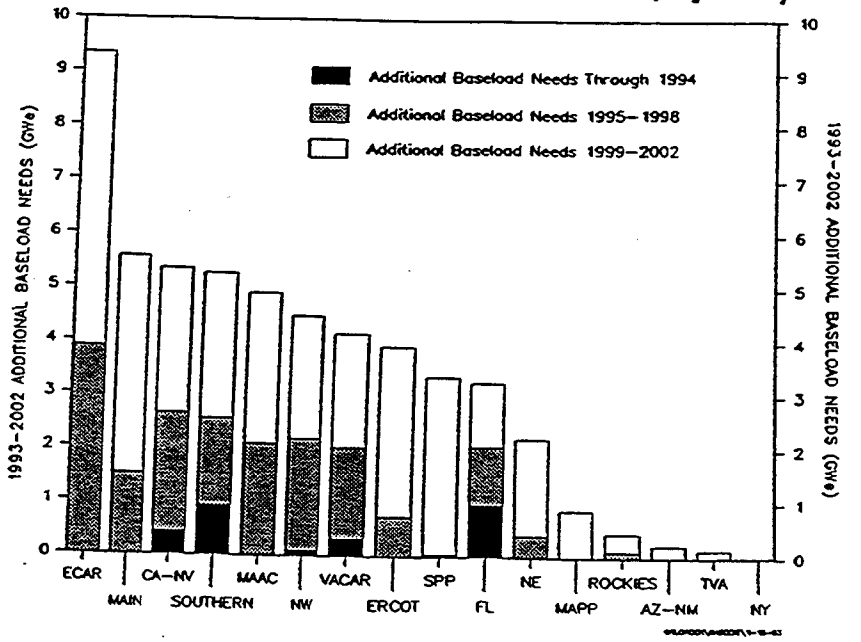
North American Electric Reliability Council



Reference: North American American Reliability Council, 1993

Magnitude and Timing of Regional Baseload Needs

(Cumulative Additions, Above Committed, by 2002)



Reference: Bechtel Power Corporation, 1993

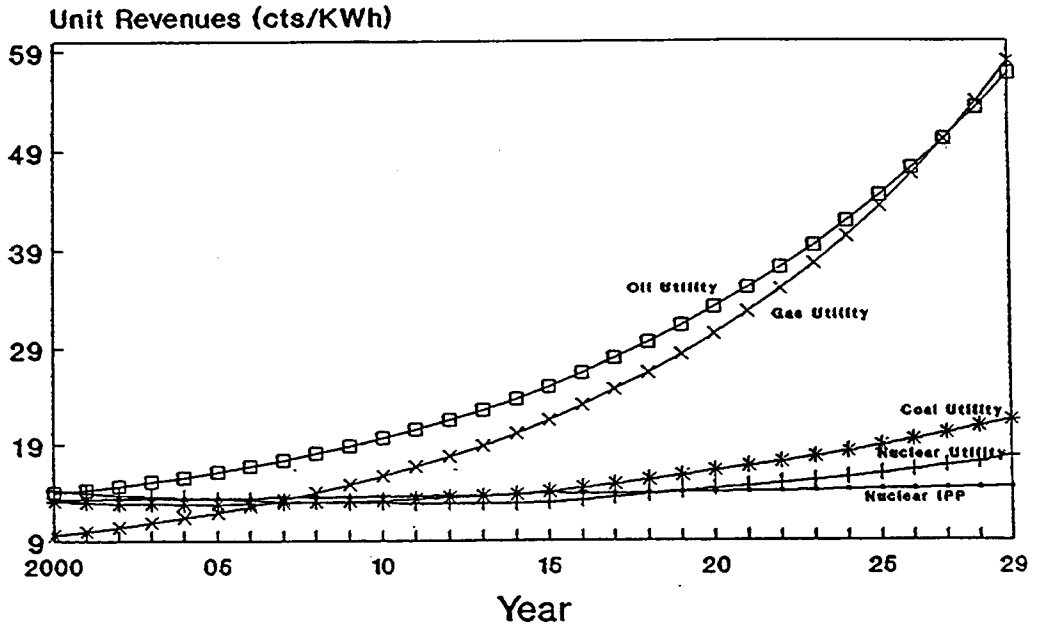
3. CRITERIA FOR THE SELECTION OF NEW ELECTRIC GENERATION TECHNOLOGIES

3.1 Economics

In the competitive world of the future, electric generation technologies must first meet the economic tests of both power plant owners and customers/ratepayers. The minimization of front-end capital costs is important to the owner to reduce investment risk and capital carrying charges.

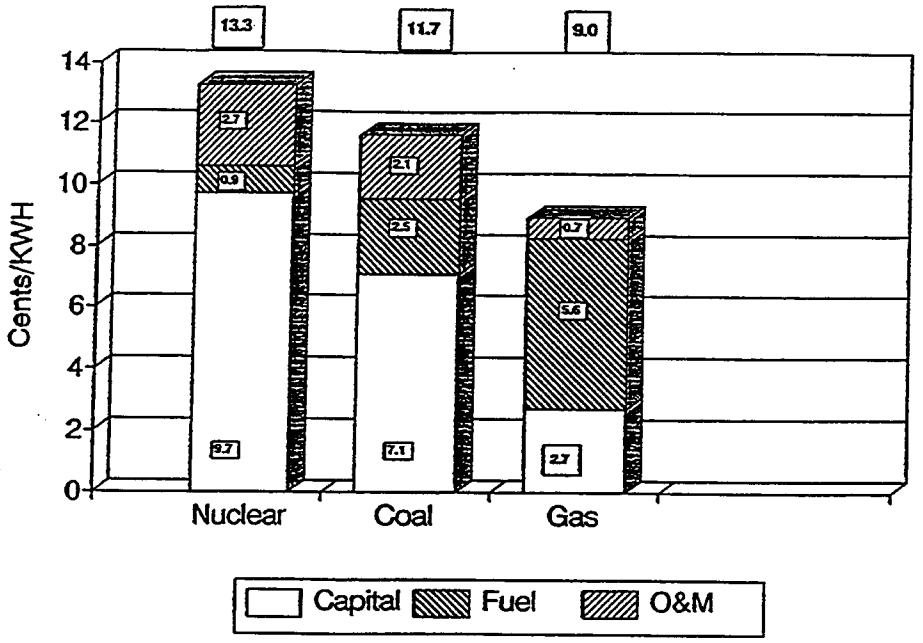
The cost of production, i.e., fuel plus operations expenses, should be both economically competitive and to the extent possible, predictable. It is important to note that the increases in fission reactor operation and maintenance (O&M) expenses during the 1980's caused concern with both the level and the uncertainty of such expenses. However, for the past two years, average U.S. nuclear power plant O&M costs per kilowatt hour have actually dropped as a result of aggressive cost management by facility operators.

The following charts illustrate economic comparisons between advanced light water reactor nuclear (ALWR), coal, oil and natural gas technologies. Annual unit revenues are driven by fuel cost over the life of the plant. On a first year total electric energy cost comparison, advanced LWR nuclear is not an attractive option, primarily because of high front-end capital costs. However, on a levelized revenue requirements basis, nuclear is cost competitive with coal, oil, and natural gas.



Reference: Bechtel Power Corporation, 1990

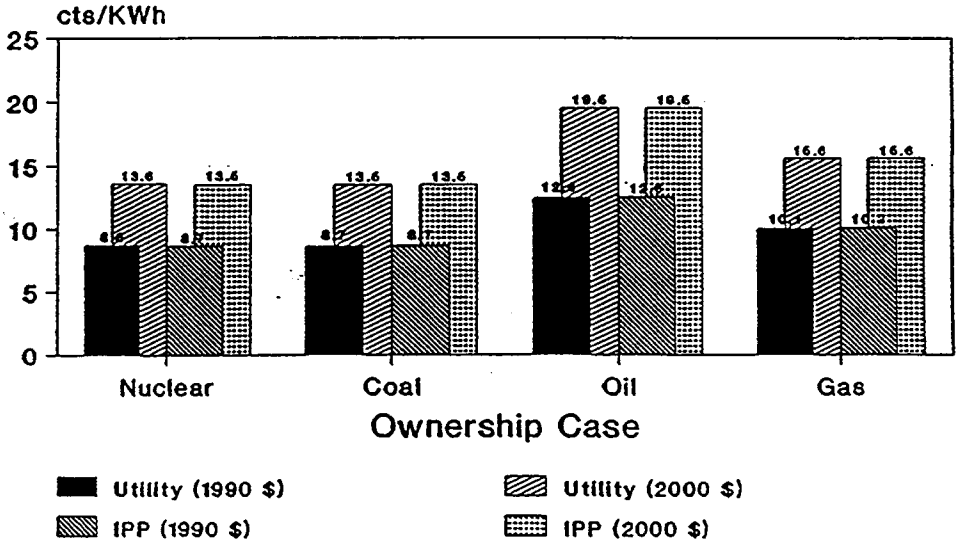
FIRST YEAR TOTAL ELECTRIC ENERGY COST COMPONENTS



(Cents/KWH in Year 2000 $)

Reference: Bechtel Power Corporation, 1990

Levelized unit revenues



Reference: Bechtel Power Corporation, 1990

New generating capacity must also be sized to meet system growth needs, i.e., in the range of 300 to 800 megawatts. The practical difficulties encountered in co-ownership have encouraged many utility executives to acquire generation on an independent basis. The reluctance of regulators to include in ratebase generating capacity beyond that immediately "used and useful" forces utilities to consider smaller increments of capacity addition, albeit less economical in the long run for customers.

Of course, any generating technology to be selected must be considered reliable, must be capable of being sited within a reasonable geographic proximity to the load demand and must have access to transmission. Nuclear units will also be judged with regard to the potential costs and uncertainty of decommissioning activities.

Overall, the prospective purchasers/owners of new generation technology in the future will balance the economic issues to obtain rewards which fully justify the risks taken.

3.2 Environmentally Acceptable to the Public

Of course, any new electric energy generation technology, including clean nuclear, must be safe from both a technical and public perception viewpoint. In addition, both low-level and high-level radioactive waste disposal must be resolved in a manner acceptable to both the government and the public.

The U.S. and international concerns for both clean air and the control of gases contributing to global warming will promote the consideration of renewable technologies and nuclear energy. Already, some environmental groups are touting nuclear fuel as a "green technology" because no carbon dioxide is emitted in the power production process. Newly defined "environmental externalities" are required to be quantified by some state public utility commissions (e.g. New York, Massachusetts, and California) so that competing technologies may be rank ordered economically. These externalities vary widely but may add 25 percent to the cost of coal and 14 percent of the cost of natural gas electric generation. The nuclear "externalities" of low- and high-level radioactive waste disposal and decommissioning are already included in the cost of nuclear power. Thus, the application of such environmental externalities should benefit clean nuclear energy.

3.3 Diverse and Secure Fuel Supply

The significant investment in long asset life electric generation technologies forces utility executives to take a long-term view of the asset mix to be acquired. Appropriate technologies are selected for base, intermediate, and peaking load operating requirements. Also, the widely varying and sometimes quickly changing costs of various fuels (oil, coal, natural gas, uranium) suggests that utilities not "put all of their eggs in any one basket," but rather hedge bets by utilizing technologies that consume different fuels. The very existence of a diverse fuel consumption capability may assist a utility in its negotiations to competitively acquire fuels. Also, the potential interruption of fuel transportation, (e.g. natural disaster such as flood or frozen rivers; or labor strikes) suggests the need for both diverse and secure fuel supplies, including significant inventory at the power plant site. Clean nuclear energy offers a particular advantage of low-cost fuel with an on-site storage inventory capability of one year or more at very low cost.

4. IMPLICATIONS FOR THE DEVELOPMENT OF CLEAN NUCLEAR ENERGY/FUSION POWER

Clean nuclear energy must provide economic benefits to match the risks seen by investors and customers. New nuclear technologies must demonstrate persuasive economics. In addition, the disposal of nuclear waste must be technically, politically, and publicly resolved.

To gain funding support, the long-term development of new advanced nuclear technology such as fusion must satisfy alternative national goals such as training scientists and engineers and the encouragement of international cooperation, or must yield near-term spin-off technologies of value within our society. In either case, it can be expected that some private sharing of funding with the government will be necessary. To spur achievement in research and development in this long-term development program, a national prize may be in order.

5. CONCLUSIONS

Requirements for over 200 gigawatts new electric generating capacity in the United States during the first decade of the twenty-first century will provide the opportunity for clean nuclear power to compete as one of the technologies to be selected by developers of generating capacity.

The deregulated electric generation business of the future will select technology winners based on objective competitive performance. The new owners of generating companies will be independent power producers/electric wholesale generators, competing utilities and, perhaps, foreign companies. Generation will be sized to meet system growth requirements, probably in the 300- to 800-megawatt capacity range.

Clean nuclear technologies must meet the tests of economic and environmental acceptability with sufficiently clear advantage to overcome the current capital market aversion to the perceived risk of nuclear power. The current national and international concerns for clean air and management of gases that contribute to global warming may enable clean nuclear power to fill a role as a "green" technology.

The long-term development of clean nuclear energy will require industry and research institutions to cooperate in innovative ways. Government support is likely to be reduced in dollar amount and may be sporadic. Co-funding and the development of near-term wins/spin-offs will be required to assure program continuity and ultimate success. Clean nuclear energy is a challenge that can only be met by the application of some of the finest academic minds in science and engineering working together cooperatively with industry.

REFERENCES

[1] "Electricity Supply and Demand 1993-2002, Summary of Electric Utility Supply and Demand Projections," North American Electric Reliability Council (1993).

[2] "Starpower, The U.S. and The International Quest for Fusion Energy," Office of Technology Assessment Congress of the United States (October 1987).

[3] "National Energy Strategy," Department of Energy, First Edition (1991/1992).

[4] "Outlook for U.S. Electric Markets and Nuclear Power," Bechtel Power Corporation (February and June 1993).

[5] "Environmental Policy and Governance; Economic Implications and Energy Systems Impacts," The Aspen Institute Energy Policy Forum (August 1992).

[6] Robert A. Hefner III, "An Econergenic Policy for 21st Century America," The Hefner Foundation (1992).

[7] John Shlaes, "Technology Cooperative and the Developing Countries," Global Climate Coalition (July 1993).

[8] Richard D. Grundy, "Energy Policy Act of 1992: A Change in Perspective," Committee on Energy and Natural Resources United States Senate, Senior Professional Staff (Republican) (July 1993).

[9] Thomas E. White, "Policy Initiatives Required to Maintain U.S. Industry Competitiveness in International Electrical Power Markets," Presentation to the 1993 Policy Issue Forum Energy, Environment and the Economy, The Aspen Institute (July 1993).

[10] "Energy for Tomorrow's World," World Energy Council (1993).

[11] "Nuclear Power - A Current Risk Assessment: Moody's Special Comment," Moody's Investors Service (April 1993).

MY PERSPECTIVE ON D-3HE FUSION

David H. Crandall
Advanced Physics and Technology Division
Office of Fusion Energy, Department of Energy

ABSTRACT

The fusion reaction of deuterium with helium-3 has been recognized for more than 20 years as a possible basis for fusion energy. Relative to the reaction of deuterium with tritium, the advantages of non-radioactive fuel and fewer product neutrons are accepted. However, the advantages have been balanced by other factors: higher collision energy or temperature required, scarcity of helium-3, issues of conversion of the fast charged fusion products to heat or electricity. As a consequence it has been common to conclude that helium-3 fusion could be an advanced follow-on to tritium fusion.

That view could change because of better knowledge of helium-3 availability and keener understanding of how to employ the helium-3 fuel cycle. We now know of helium-3 from deep geologic sources and on the surface of the moon. This takes away the simple rule that "there is no helium-3", but questions surrounding costs of recovery will be important. The issue of physical means of harnessing the reaction of deuterium with helium-3 is more subtle. The leading confinement schemes, tokamaks and inertial, may not be able to effectively use helium-3. Then the "follow-on" notion is not quite valid. What may be most important is alternate confinement approaches specifically for helium-3.

INTRODUCTION

The issue of availability of helium-3 has changed over the past few years. Breeding, mining the moon, and collection from deep geologic sources are all now plausible. All of these sources have economic and environmental baggage that would have to be carefully weighed before embarking on a fusion energy development program. There have been helpful studies on these sources, but my perception is that there are large uncertainties in the cost of helium-3. The view is no longer that "there is no helium-3", only that we are uncertain of its cost. This cost question should not preclude exploration of methods of using helium-3. Thus, for fusion, the principle question is not can you obtain the helium-3 but how do you use it.

The attractive features of helium-3 fusion are well known to this audience: nonradioactive fuel, few neutrons to activate and damage structural materials, potential for direct conversion of fast charged particles to electricity. Few neutrons is usually taken as the principle advantage; I will discuss it briefly. Any system relying on nuclear reactions will have radiation hazards deriving

from some mixture of fast particles, gamma rays, and neutrons and, secondary reactions will change the mix of these. For fusion systems based on reactions of deuterium with helium-3, a few per cent of the energy is likely to be carried by neutrons, enough to activate the system structure. Figure 1 [1] shows anticipated activation for several materials from a tritium-based plasma reactor and a comparable helium-3-based one. The difference in radioactivity is much greater for the different materials than for the different fuel. The advantage for helium-3 may lie more with reduced radiation damage than with radioactivity. In any case, materials development and radiation damage testing are likely to be needed for any fusion reactor concept and are needed to better quantify the advantage for helium-3 over tritium.

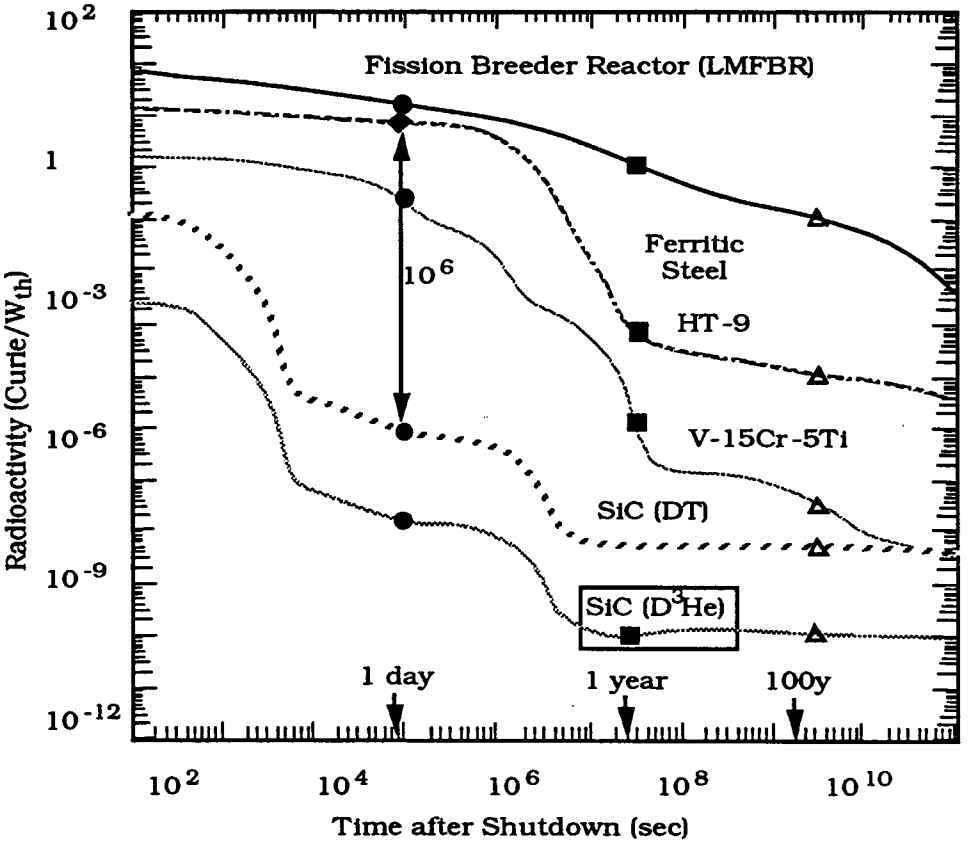


Figure 1: Radioactivity levels in fusion reactors showing reduction of one million by choice of materials and one hundred by choice of helium -3 fuel.

The fundamental nuclear reaction determines the underlying advantages and disadvantages for deuterium helium-3 fusion. The fact that the nuclear charge is two rather than one signals the fact that greater collision velocity (temperature) is needed to overcome the Coulomb repulsion and cause the reaction. The reactivity for Maxwellian distributions of fuel particles [2], shown in Fig. 2 and familiar to all in this audience, is the most fundamental evidence.

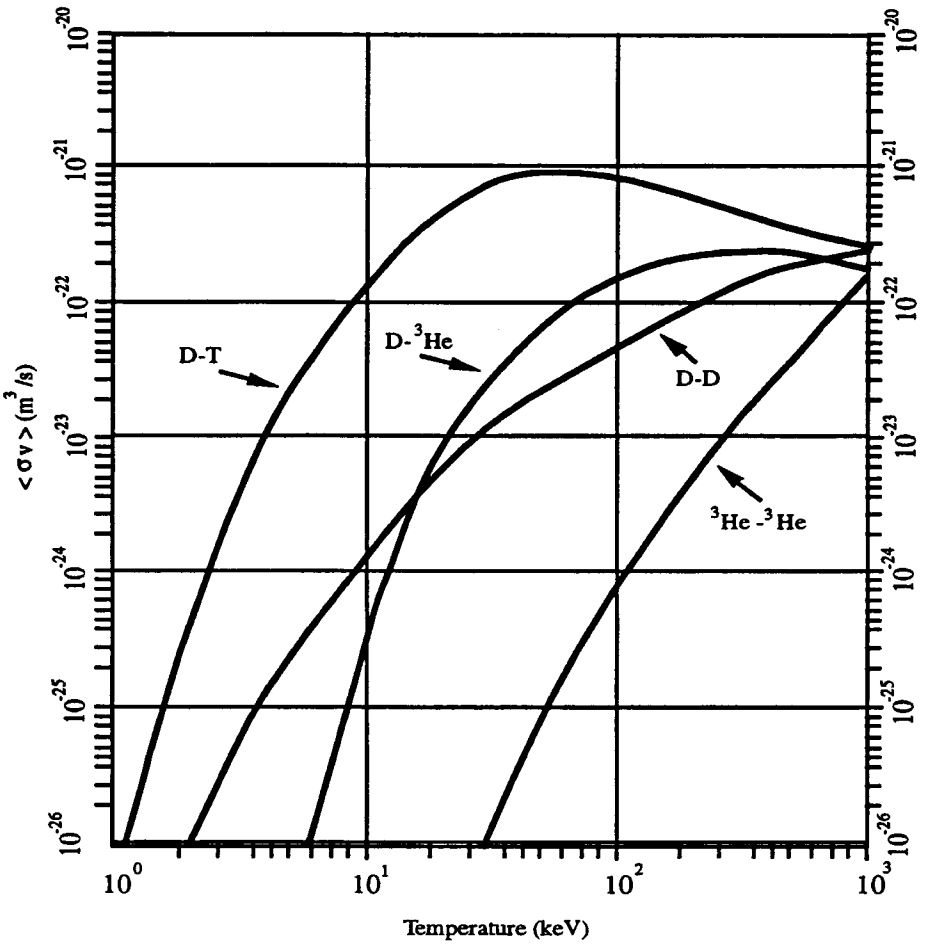


Figure 2: Reaction rates of candidate fusion fuels

Many observers of fusion are instantly persuaded by this reactivity that deuterium - tritium fusion is appropriately emphasized. Scientists are always willing to look further. For helium-3, the nature of the products of the reaction (proton and helium-4) both suggests different energy extraction approaches and relieves some of the problems. These features have been well recognized, but some scientists dismiss helium-3 fusion and others claim it should be the leading approach. Why so great a difference?

SCIENTIFIC CREDIBILITY OF CONFINEMENT CONCEPTS

Scientists who have experienced the significant difficulty of devising the confinement schemes for deuterium - tritium fusion find it hard to imagine solving what is supposed to be a harder problem. The advocates for deuterium - helium-3 tend to use conceptual or theoretical extrapolations that most fusion researchers discount as unrealistic or simplistic. Since the tokamak is the established magnetic confinement concept, it is natural to examine its potential to use helium-3. Such studies have been carried out [3,4] and some will be

discussed at this meeting; I will not attempt an in depth discussion here. My perception is that the standard or conventional tokamak is not well suited to helium-3. Confinement of the fast charged particles requires too high a plasma current, the higher fields and associated system stresses are undesirable, and synchrotron radiation presents problems that don't yet have credible solutions. I think that many scientists will judge that helium-3 fusion in conventional tokamaks is unrealistic. In any case, a program, beyond what is in progress world-wide, is not needed to advance the tokamak for helium-3 potential use.

What about confinement approaches specifically for helium-3. An examination of one reactor concept can illustrate this issue. I choose the "ARTEMIS" concept of Momota, et. al. [5] that uses the field reversed configuration and direct conversion of fast reactor products. This reactor concept, shown in Fig. 3 and Table 1, has desirable features unique to helium-3.

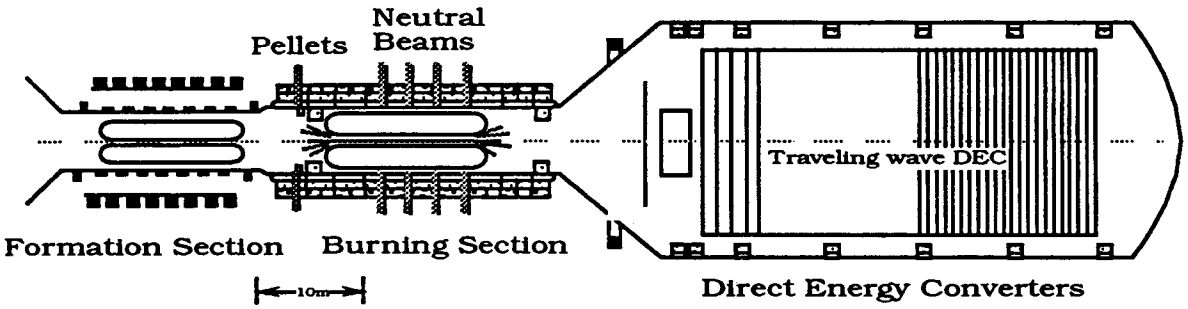


Figure 3: The D-^{3}He field reversed configuration reactor "ATREMIS" composed of formation chamber, burning chamber, and direct energy converters.

Fusion Power:	1.6 GW
Carried by 14.7 MeV Protons--368 MW; Neutrons--77 MW; Thermal Ions--770 MW; Radiation--357 MW; Other Fusion Products--43 MW	
Plasma Volume:	67.0 m^3
Radius--1.12 m; Length--17.0 m	
Number Density of Electron:	$6.6*10^{20}/m^3$
Deuterium--$2.9*10^{20}/m^3$; Helium-3--$1.4*10^{20}/m^3$; Others--$0.6*10^{20}/m^3$	
Fueling:	$7.8*10^{21}$/sec
Pellet Injection--$7.77*10^{21}$/sec; Neutral Beam Injection--$3.1*10^{19}$/sec	
Plasma Temperature	87.5 KeV
Current Drive	1 MeV * 5 A (NBI)
Energy Confinement Time:	2.09 sec
Particle Confinement Time:	4.18 sec
External Magnetic Field	6.7 T
Beta Value:	0.90

Table 1: Plasma parameters of a steady burning D-^{3}He FRC

A number of positive features apply to this reactor concept. The required plasma, in the field reversed configuration, can be formed and translated. The configuration is more stable than theory predicted. The configuration is naturally high beta, meaning that the magnetic field is low and the synchrotron radiation losses associated with particle motion in the magnetic field should not be limiting. After fusion reactions of deuterium with helium-3, a significant fraction of the fast (18.3 MeV shared) charged particles (proton and helium-4) should escape along the field. These particles can carry out the fusion energy and that energy in charged particles might be efficiently and directly converted to electricity. Altogether this concept is attractive, especially over the standard tokamak, for fusion based on helium-3.

However, skeptics see a very different set of features. Instabilities may destroy the configuration at the higher temperatures and larger size. If that disaster does not occur, the instabilities may simply reduce confinement. If all instability issues are solved, how can the burning configuration be sustained and repeated - is this a steady-state reactor concept? These are detailed technical questions that few scientist accept as having definitive answers. To some extent these uncertainties focus on a single parameter in the reactor features of Table 1 - the confinement times. The confinement time given for the "ARTEMIS" are assumed as reasonable and needed values, but skeptics have no reason to accept that they will be obtained.

In 1990, when the Department elected to discontinue major efforts on alternates to the tokamak, the decision on the study of this concept was the most difficult. The Large S Experiment (LSX is a $15M device) was just beginning and needed several million dollars per year for several years to address stability and confinement time issues. A larger next step might be needed to establish the scientific credibility of this confinement concept. We elected to stop the experiments but went to some trouble to preserve the equipment. In June of 1992, the Fusion Energy Advisory Committee (FEAC) recommended that "DOE consider the benefits of operating the LSX field-reversed configuration facility in order to determine the validity of its physics principles." We have established a smaller program intended to benefit both tokamak and field reversed configuration concepts through use of the LSX equipment.

The decision on the LSX program provides an important test of how fusion funding decisions will be made in the present constrained budget environment. If definitive answers can be obtained through small experiments (a few million dollars total) combined with theoretical understanding, it may be seen as appropriate to conduct the research. If definitive answers can only be obtained by building full scale experiments, the development path is not obviously superior to that for the tokamak.

In June of 1992 FEAC also suggested "that a small but formal and highly visible periodic competition be established to foster new concepts and ideas that if

verified would make a significant improvement in the attractiveness of fusion reactors." In December 1992, the Department issued a notice of program interest in small scale tests of new ideas for fusion. Three projects were selected at a total cost of just over $1M/yr. Two of these will explore concepts that might be useful for helium-3. The principal issue is to find confinement solutions that avoid instabilities in a manner that is scientifically extendable to reactor use. If the basic configurations can be established, then reactor concepts can be based on them.

CONCLUSION

I see the establishment of a confinement concept that could use helium-3 as the central issue. Without this, mining the moon or the deep oceans is hardly justifiable. Ever stronger statements about the desirability of helium-3 ring hollow without this. For helium-3 fusion, there is skepticism about all of the ideas that are plausible confinement concepts. The required work is research in the face of such skepticism. So, the research must be designed to scientifically address the issues causing skepticism at a reasonable cost. What will be credible and what cost is fundable? These are judgement calls influenced by many factors that change. I have given my best estimates of what can be accepted in today's environment. You are welcome to push the boundaries of that environment.

REFERENCES

[1] J.P. Holdren, et al., "Report of the Senior Committee on Environmental, Safety, and Economic Aspects of Magnetic Fusion Energy, UCRL-53766, Lawrence Livermore National Laboratory, Sept. 1989.

[2] J. R. McNally, Jr., et al., "Fusion Reactivity Graphs and Tables for Charged Particle Reactions, ORNL/TM-6914, Oak Ridge National Laboratory, Aug. 1979.

[3] B. Coppi and L.E. Sugiyama, "Questions in Advanced Fuel Fusion", Report PTP-88/6, Massachusetts Institute of Technology, June 1988.

[4] F. Najmabadi, et al., "The ARIES-III D-3He Tokamak Reactor Study" (The collection of papers from 14th IEEE Symposium on Fusion Engineering), UCLA-PPG-1386, University of California at Los Angeles, Dec. 1991.

[5] H. Momoto, et al., "Conceptual Design of D-3He FRC Reactor 'ARTEMIS'", NIFS-101, National Institute for Fusion Science, Nagoya Japan, July, 1991.

Industrial Perspectives on Helium-3 and Fusion Power

Stephen O. Dean
Fusion Power Associates
2 Professional Drive, Suite 249
Gaithersburg, MD 20879

ABSTRACT

Industrial interest in helium-3 for fusion power depends in part on the perception that industry has of the proponents. Industrial interest will be highest if the perception is that the proponents are innovators and if they believe that substantial commercial benefits can be obtained on a commercially relevant time scale. Strategies for achieving the goal of helium-3 fusion reactors is discussed.

1. INTRODUCTION

The possibility of using helium-3 as a fusion fuel cycle has been known from the very early days of fusion research. However, it has always been viewed by most fusion researchers as an "advanced" fuel cycle, which is to acknowledge that it is more difficult to achieve than the favored deuterium-tritium fuel cycle.

In addition, the use of helium-3 has the disadvantage that helium-3 does not occur in significant quantities on earth. Until the relatively recent discovery that there were significant quantities of helium-3 on the moon, and analyses suggesting that it may be economically recoverable, helium-3 was not considered seriously for use as a basic fuel cycle for fusion. Even now, the prospect of mining the moon for helium-3 seems like an unlikely prospect to many people.

The well-known advantages of the helium-3 cycle, which reduces markedly the number and energy of fusion neutrons, thus easing the perceived materials problems of future fusion reactors, and the possibility it offers of direct energy conversion of the charged fusion reaction products, thus increasing plant efficiency, have caused a continuing interest among a minority of scientists working in the fusion field.

2. PERCEPTIONS OF HELIUM-3 PROPONENTS

Proponents of helium-3 as a base fuel for fusion reactors face the problem of being a minority among the mainline fusion researchers who advocate the development of fusion reactors based on the deuterium-tritium fuel cycle. In evaluating the ambitions of helium-3 proponents, industry (and others) must judge the credibility of these proponents. The degree of interest in evaluating the helium-3 fuel cycle will depend in part on industry's perception of helium-3 proponents as being either (1) crazy, (2) radical or fringe minorities, (3) innovators aiming at near-term payoffs, (4) mainline conservative thinkers, or (5) impractical visionaries.

If helium-3 proponents are perceived to be near the extremes of this spectrum, there will be very little industrial interest.

Of course, industry is not monolithic; my comments apply primarily to the larger, more established companies. Small businesses devoted to high risk technical ventures are quite common in the U.S. In general, however, industrial interest will be highest if helium-3 proponents are perceived as innovators, with realistic commercial timetables in mind.

3. DEVELOPMENT STRATEGIES

In presenting their concepts, it is important for helium-3 proponents to carefully consider both their strategic and tactical plans.

On the strategic planning issue, is it their goal that the helium-3 fuel cycle be used in the first generation of fusion reactors, or as a second generation improvement over the deuterium-tritium fusion reactor? The answer to this question has many tactical ramifications on the detailed balance among many existing research and development programs, e.g., in materials testing, plasma physics and some supporting technologies.

A strategic plan that aims at second generation success does not appeal to most helium-3 proponents because it attaches no urgency or priority to their work, yet it is the present day reality in which they live. In the ever-present tight budget situation that fusion finds itself in, it is also true that there is no money at all to fund proponents for second generation technologies; all the money and more is needed for the deuterium-tritium systems.

To advocate a development path which is optimized to allow helium-3 to be the fuel cycle in first generation fusion reactors is viewed by most mainline fusion scientists as technically irresponsible. It also, of course, is extremely threatening to their existing programs and ambitions.

If forced to chose between these two strategic plans today, most industries would back the deuterium-tritium fuel cycle for first generation fusion reactors. This is in part because their experience is that it is important to get some early demonstration of a successful product and then to engage in product improvement. It also reflects their assessment of present day realities and near-term prospects for significant government-funded business. However, industry, in general, is sympathetic to urging the government to spend some fraction of its budget on advanced concepts and is more optimistic that this could result in breakthroughs than are the mainline program scientists and managers.

4. IS THERE A MIDDLE GROUND?

If the idea of planning for second generation success does not appeal to helium-3 proponents, and if displacing the deuterium-tritium fuel cycle is not currently realistic, is

there some middle ground strategy that helium-3 proponents could explore? Here is one for consideration.

First, helium-3 proponents could advocate maintaining the near-term focus of the program on proving out the viability of the deuterium-tritium fuel cycle. Second, they could ask DOE program managers to initiate an intense near-term program to prove out physics approaches for helium-3 fusion reactor concepts. In order to pay for the latter, DOE would have to slow something else down e.g., some part of the program that is specific to the deuterium-tritium program but is not critical to near-term progress. An example of such a program is materials testing using 14 MeV neutrons.

Helium-3 proponents cannot expect an open-ended commitment for such a strategy; hence it would be necessary to suggest a decision point a few years (perhaps 5-6 years) hence, at which time a choice would be made whether to proceed toward deuterium-tritium reactors as first generation, or switch the program goal to helium-3 as first generation.

If helium-3 proponents are serious about urging that helium-3 be considered as a possible first generation technology, I would recommend that they involve industry on the front end of the planning and development process. Failure to do that is one of the major shortcomings of the current mainline program.

4) Advanced D-^{3}He Fusion Reactor Concepts and Applications-I 105
V.I. Pistunovich, Chair

4-1 About the Concept of Utmost Clean and Beneficial D-^{3}He Reactor 107
I.N. Golovin, V.V. Arsenin, A.Yu. Kujanov,
V.I. Khvesjuk, D.V. Semenov, N.V. Schabrov

4-2 Characteristics of D-^{3}He Fueled FRC Reactor: ARTEMIS-L 115
Hiromu Momota and Yukihiro Tomita

4-3 D-^{3}He Mirror Reactors 121
D.D. Ryutov

4-4 Non-Energy Applications for Fusion 127
John M. Dawson

4-5 Magnetic Fusion Propulsion: Opening the Solar-System Frontier 137
John F. Santarius

ABOUT THE CONCEPT OF UTMOST CLEAN AND BENEFICIAL D3He REACTOR

I.N.GOLOVIN, V.V.ARSENIN, A.Yu.KUJANOV
Nuclear Fusion Institute, Russian Research Center - Kurchatov Institute
123182 Moscow, Russia, fax: 095.943.0073

and

V.I.KHVESJUK, D.V.SEMENOV, N.V.SCHABROV
Power Engineering Institute,
Moscow State Technical University
P.O. Box 38, 107005 Moscow, Russia

1. Introduction

Can the fusion of light atomic nucleus become in the future a clean power source, which don't accumulate like fission high radioactive vasts on the Earth threatening by death for all living on Earth? Hopes for this exists. The fission reactors are inavoidable gigantic radioactive, but fusion has no need in neutrons and the radioactivity of fusion reactors is defined by materials used for their construction. The materials can be prepared beforehand till they are not radioactive to not accept high radioactivity during the reactor work.

Let us try to understand what follow from our knowledges and what we must learn to answer the question: can the nuclear fusion become an industrial power source enough environmentally safe and not too expensive that fusion reactor research development would be justified in spite of rising expences for their continuation?

2. Materials for Nuclear Fusion Reactors

Among DT and D3He fusion reactions the second produce in reactor conditions 30 times less neutrons than the first if their powers are equal. That define the qualitative advantage of the D3He reaction over the DT. In most designes

of D3He reactors the neutron power flux density on the first wall is less or equal 0,1MW/m^2. Therefore during 60 full power years (this time of life is accepted for the fission reactors which will be build in the 21-st century) in the first wall materials will arise approximately only 60 dpa and the material will not be heavely radiation damaged.

If the reactor first wall gamma-radioactivity would decrease up to hands on level (25 microSv/h) during less than 100 years after shutdown the fusion power production will not significant destroy the environment. For vanadium-chromium alloys this cooling time is 15 years [1]. But receiving up to 6MW*y/m^2 neutron irradiation such alloys will swell unacceptable. For the external parts of the radiation shield, for the vacuum wall, for the cases of superconducting coils the cryostate wall and other parts which are placed outside the radiation shield these binar alloys can be used with success. But for the first wall and for the internal parts of radiation shield only the triple alloys VmCrnTi can be used. Titanium activation calculation results differ one from the other by some orders of magnitude in the time interval from 1 to 100 years after shutdown [2]. In the worst case the gamma contact dose of Ti exceed the hands on level 200 times after 100 years cooling. Therefore the Ti concentration in alloys must be as small as possible. For instance the V10Cr5Ti alloy can with necessary caution be handled after 50 years cooling when its gamma contact dose may be 20 times higher than the hands on level. To receive sure information it is necessary to know more precisely the radioactivity and the cross sections of H3, Ar39, Ar42 and Ca45 creation by neutron impact.

Geological world resources of vanadium are small - only 60 million tons. Therefore the recycling of vanadium is absolutely necessary if we want to produce a significant part of power by fusion in the world. The use of vanadium alloys in DT reactors with its replacements of the first wall and the internal part of shield every 5 years by cooling time 100 years would 20 times rise the vanadium consumption and significantly diminish the total power production by fusion in the world.

3. Necessary Purity of Alloys

To ensure short cooling times of vanadium alloys it is necessary that their components contain no more impurities than it is shown in the Table 1. For Cr and Ti in the VmCrnTi alloy the figures can be 1/m and 1/n times bigger. Materials used in present engineering are sometimes of higher purity but in small amounts. In our case are necessary thousands tons of such super pure alloys for one reactor. Such big amount of super pure materials are not produced till now. The atomic industry has a new technology for elements and isotopes separation in big quantities. That is the centrifugal separation. Present experience in uranium isotope separation and in purification of some other elements shows that vanadium, chromium and titanium production in thousand tons and with purity indicated in the Table 1 is a realistic task. But an experimental checking is nevertheless necessary, especially of chemical processes involved in the receiving of gaseous compounds and in metallurgy - melting, forging, rolling etc - during which the alloys must not be contaminated.

Molecular Physics Institute of RRC - Kurchatov Institute has already experience in chromium cleaning by the centrifugal cascades and has received gaseous vanadium fluoride suitable for centrifugal purification. Titanium was till now not cleaned by centrifuges. Bochvar Institute of Nonorganic Materias has big experience in technologies of atomic metal industry and is able to develop the metallurgy of extra-pure vanadium alloys for fusion reactors. But during the present economical crysis in Russia this work can be performed only by financial support from abroad.

4. Possible Versions of Fusion D3He Reactors

In the ESECOM report [3] is comprehensive studied the environmental impact, economy and safety only for closed fusion systems - different versions of tokamaks and even a reversed field pinch reactor in spite of its small plasma parameters received in experiments. But the tandem mirrors are lost out of sight, though its plasma confinement and temperature are much higher. Progress in GAMMA-10 experiments in which the confinement time appoach to one

second by density up to $2*10^{18} m^{-3}$ [4] encourage us to study the reactor regimes of tandem mirrors.

A beta limitation study in the central cell of axisymmetrical tandem mirror by ballooning mode of MHD flute instability in the case of perfectly rigid anchors on both ends shows, that beta values higher than 80% on the axis can be received for parabolic radial plasma pressure profile [5]. A detailed study of plasma kinetics and power balance in the central cell of a tandem [6] show that for a D3He reactor the Q value can exceed 100 if ash pumping is used (look the Fig. 1 and 2). A principle of selective ion radial removal in axisymmetrical magnetic field is developed [7].

In all tokamak reactor studies both in the first and in the second stability regions (APOLLO, ARIES-III, the work [8]) the average beta is less or equal 24%, what is significally lower than it can be in the tandems. Therefore the fusion power density in plasma of tokamaks is much lower than in tandems, the required confinement time is longer and the plasma volume is much bigger. Now we can not exclude that the tandems can be developed up to the reactors. No unsurmountable difficulties are discovered till now. Some additional preferences of tandems over closed systems (tokamaks, stellarators, RFP) can be mentioned: no heat overloaded divertor, clear scheme of direct converter and some others.

The FRC's look attractive and they are the third version of magnetic fusion reactor which must be within our eyeshot.

5. About the Amount of Vanadium for Fusion Reactors.

Vanadium alloys are necessary for all parts of reactors including the cryostate wall where the neutron flux density is five-six order of magnitude lower than on the first wall. For the external parts the purity must be lower for cheaping the used materials.

Much vanadium is to spend for the radiation shields. In tokamaks the inboard shields differ from the outboard shield. For example in ARIES-III the thickness of these shields are 650 and 835 mm.

For lowering the radioactivity we propose in all

shields to use only vanadium alloys and water, excluding lithium, copper, iron, tungsten. The shield thickness will rise in this case. That is very infavourable for tokamaks inboard shield, but it does not matter for the tandems and FRC's.

To compare the amount of vanadium necessary for tokamaks and tandems let us use the ESECOM study of V-D3He/TOK reactor [3]. The total shield mass of this tokamak is 12 000 tons and the average density of the shield is 4,6 ton/m^3. For an axisymmetric tandem we can not exclude that the plasma radius would be as small as 1 m, because its magnetic field has no island structure inavoidable in tokamaks and rising its plasma thermal conductivity across the magnetic field. With 1 m radius the same fusion power 3300 MW(th) as in V-D3He/TOK can be received with the central cell length 100 m, and the shield mass would be 6400 tons if we take the shield thickness as of the outboard shield and the length of the anchor and barrier cells of tandem of 20 meter on each end. If it would be necessary to rise the plasma radius up to 2 meters then we have to shorten the central cell length for the same fusion power. With the length 35 m we reduce the shield mass up to 5600 tons.

On both ends of the tandem we can imagine Momota's [9] direct converters.They can be made of vanadium-chromium alloys because the neutron flux density in its region is many times lower than on the first wall of the central cell.

6. Helium-3 Production on the Earth

Helium-3 production through beta-decay of tritium can not provide fueling of industrial fusion by two reasons: it is too expensive and don't remove high radioactive vasts accumulation on the earth globe, because tritium is produced on fission reactors.

The DD satelites must also be excluded as high radioactive ones.

Aneutronic reaction p(6Li,4He)3He has attracted attention. If we inject protons with energy 300-400 keV in a lithium plasma target then $\langle\sigma v\rangle$ of this reaction is close to $\langle\sigma v\rangle$ in a D3He reactor and therefore the physical sizes of such a 3He breeder must be approximately the same as of a

D3He reactor. We want to gain net power from the system reactor + breeder. For this power balance the lithium plasma confinement time must be 10-20 second. That is hard to achieve. Moreover we want that this industry would be low radioactive. But in the interactions between p,D,6Li,7Li are eight reactions which produce neutrons. Therefore it is necessary to reduce at least tenfold the content of deuterium in natural hydrogen and 7Li in the industrial produced lithium for the hydrogen bombs.

These results follow from rough estimates. For valuable comparison of the economy of earth 3He production with the cost of lunar 3He is necessary to perform a strong plasma physics study of the p-6Li breeder.

7. Conclusion

From the mentioned consideration it follow that from the the point of view of super pure and therfore expensive material economy it can not be excluded that the tandems are more beneficial than the tokamaks. Other tandems advantages are many times mentioned in different scientific articles.

We can nothing prove because the experimental results for tandems are too incomplete. We want only to attract the attention to the danger that we can lose decades on our way to the industrial fusion reactors if we ignore investigations of qualitatively distinct alternatives and spend all our brain capacity and financial support only for tokamaks.

Today ITER is the chief in our work, but the alternatives must also be developed.

The question rised in the beginning of this article has no comprehensive answer today. The D3He fusion will have significant advantage against DT if D3He reactor radiation hazard potential would be many order of magnitude lower and the cost not much (less than twice) higher. To be shure that this is possible one must know the precise cross sections of neutron interactions borning long living radioactive nuclides. This study is comparatively cheap. Significantly more expensive is the development of plasma physics. It is now incomplete. We can not insist that the quasimaxwellian plasma approach is better than the use of nonmaxwellian particles ensembles with the extreme case - the colliding

beams. The trend to small reactors is justified, but no one proposal in this area is now supported by convincing theoretical considerations and experiments.

The need in environmental safe power sources for the 21-st century call us to continue the nuclear fusion program with rising efforts.

References

1. D. L. Smith, *Vanadium Alloy Development Program. Argonne National Laboratory Fusion Power Program.* Presented to Fusion Energy Advisory Commitee. Dallas, Texas, January, 1993.
2. E. T. Cheng et al. *International Fusion Activation Calculation Comparison Study.* TST Research. TSIR-12, 1991.
3. J. P. Holdren et al. *Report of the Senior Committee on Environmental, Safety and Economic Aspects of Magnetic Fusion Energy.* UCRL-53766, 1989.
4. T. Tamano et al. *Overview of Experimental Results on the GAMMA-10.* Proc. Internat. Conf. "Open Systems - 93". Novosibirsk, June 14-18, 1993, Rep. N 1.1. In press.
5. V. V. Arsenin, I. N. Golovin, A. Yu. Kujanov. *Beta Limit in Axisymmetric Tandem Mirrors.* Sent to Fusion Technology for publication.
6. D. V. Semionov, V. I. Khvesjuk, D. L. Poletaev. *Power Plasma Analysis in Central Cell of Tandem Mirror Reactor.* Proc. Internat. Conf. "Open Systems - 93". Novosibirsk, June 14-18, 1993. Rep. N 1.15. In press.
7. N. V. Shabrov. *Selective Ions Pumping from an Axisymmetric Tandem Mirror Reactor.* Proc. Internat. Conf. "Open Systems - 93". Novosibirsk, June 14-18, 1993. Rep. N 1.16. In press.
8. S. G. Bespoludennov, V. I.Khripunov, V.I.Pistunovich, G. A. Emmert, J. E. Santarius, G. I. Kulcinski. *D3He Tokamak Reactor.* UWFDM-908, Sept. 1992. Presented at the 14th Internat. Conf. on Plasma Physics and C.N.Fusion, Wurzburg, Germany, 30 Sept -7 Oct, 1992.
9. H. Momota et al. *Conceptual Design of the D3He Reactor ARTEMIS.* Fusion Technology Vol 21 (1992) 2307.

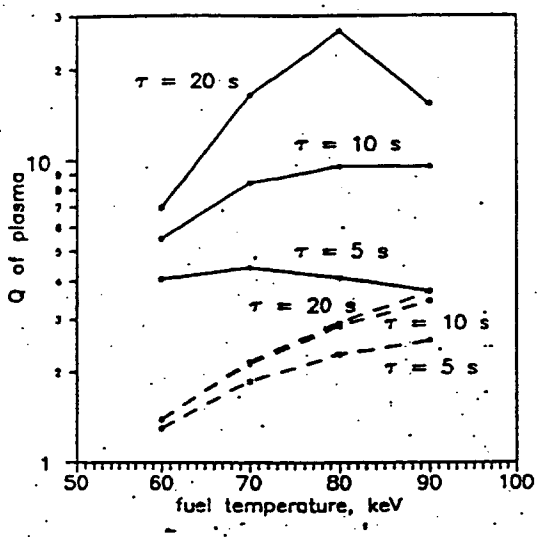


Fig. 1
B=5T; $\Delta\varphi/T=4$; $\beta=0,7$.
Pumping region 400-550 keV for all ions.
τ - time of radial transport
— — — without pumping
——— with ash pumping

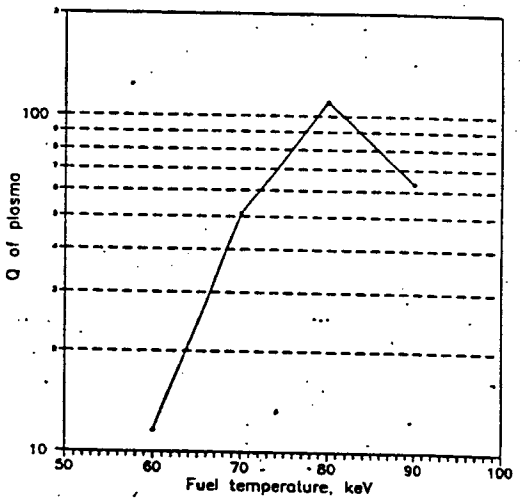


Fig. 2
B=5T; $\Delta\varphi/T=4$; $\beta=0,7$.
Pumping regions: 400-550 KeV for α-particles; 200-275 keV for protons and tritons.
Radial transport time 20 s.

Table 1

Cooling times	50 years	100 years
Ta	$1*10^{-4}$	$3*10^{-4}$
Nb	$1*10^{-8}$	$3*10^{-8}$
Mn	NL	NL
Ni	$1*10^{-7}$	$4*10^{-5}$
Mo	$3*10^{-6}$	$1*10^{-5}$
Fe	$3*10^{-5}$	$2*10^{-2}$
Al	$2*10^{-5}$	$1*10^{-4}$
W	$2*10^{-4}$	$1*10^{-3}$
Si	$3*10^{-3}$	$1*10^{-3}$

NL - Not Limited

Maximum concentrations by weight of element in vanadium alloys reaching all together hands on level in indicated cooling times.

Characteristics of D-^{3}He Fueled FRC Reactor: ARTEMIS-L

Hiromu Momota and Yukihiro Tomita
National Institute for Fusion Science,
Nagoya 464-01, Japan

ABSTRACT

Attractive characteristics of D-^{3}He fueled fusion reactor concept "ARTEMIS-L" are described. A complete and consistent scenario of developing to and sustaining a burning plasma is proposed by utilizing favorable characteristics of a field-reversed configuration (FRC). Although a development of 1MeV neutral beam sources and verification of a direct energy converter system are important issues for developing the fusion plant, all the engineering bases for this reactor are conventional. A compact and high-β FRC plasma with a temperature of ~ 83.5 keV allows us to constitute an economical electric power plant. The life of the structural materials is sound during full reactor life (30 years) and the safety of the reactor is inherent to D-^{3}He fueled fusion. The amount of the disposed materials is small and intruder dose of these materials are so small that a surface disposal can be environmentally acceptable.

1. INTRODUCTION

After the discovery of minable helium-3 on the Lunar surface [1], researches on D-^{3}He fueled fusion have been stimulated appreciably. In this fuel cycles, major fusion power is carried by charged particles and only a few percent is carried by neutrons. Charged particles are introduced to highly efficient direct energy converters. The plant efficiency of the reactor with D-^{3}He fuels, therefore, can be very high. Damages and radioactivities of structural materials due to the neutrons reduce appreciably. One finds, consequently, a possibility of constituting an economic, safe, and environmentally sound power plant with this D-^{3}He fueled fusion.

A design study of a D-^{3}He fueled commercial fusion reactor ARTEMIS [2] was carried out as a US-Japan collaboration research. The purpose of this design study was to clarify critical issues for a D-^{3}He fueled reactor, and plasma parameters were optimized so as to give the maximum plant efficiency. By applying a field-reversed configuration (FRC) as a plasma container, a very high plant efficiency of 60.2 % was obtained. The averaged neutron load on the first wall was 0.423 MW/m^2 and further reduction of the neutrons was recommended. An effectiveness of "Venetian-blind" direct energy converter was unclear.

ARTEMIS-L is a modified version of ARTEMIS: modified so as to reduce the neutron yields of a reactor as low as possible. A reasonable cusp-type direct energy converter system is applied. Further, a care for "unwanted links to weapons" has been paid.

2. REQUIREMENTS FOR D-^{3}He FUSION AND AN FRC

The neutron yields of a 1 GWe fusion reactor is obtained in terms of operating plasma temperature, concentration of fuels,and ash confinement. In a case of low operation temperature or

high deuterium concentration, comparatively dominant D–D tritium reacts with deuterium to yield 14 MeV neutrons. On the other hand, in a case of very high temperature or high helium-3 concentration, fusion power decreases due to large radiation losses. As is demonstrated in Fig.1, the fusion power carried by neutrons takes its minimum value as the operation temperature is 83.5 keV and helium-3 density is 1.35 times the deuterium density. Note that the assumption that one reinjects whole fusion tritium that is extracted out of the plasma chamber has been introduced and therefore the ash confinement gives no effect on the above values.

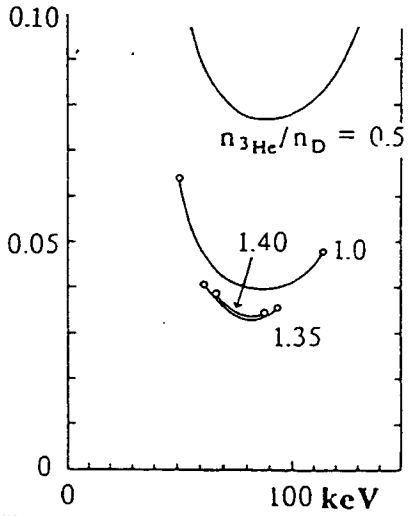


Fig.1. Neutron yields in 1 GWe reactor

Confinement parameters $\langle n_e \rangle \tau_E$ needed to sustain a plasma in a steady burning state is $3.5 \times 10^{21} s/m^3$. The required confinement parameter is one order larger than that for D–T fusion.

A high plasma beta-value defined by the ratio of the averaged plasma pressure and the external magnetic pressure reduces synchrotron radiation loss of the plasma and gives larger amount of the fusion power carried by charged particles. Thus the consequence of the high-beta plasma is a high plant efficiency by using highly efficient direct energy converters.

Once one obtain a needed high beta plasma, accessibility of high power direct energy converters are also needed to complete a high efficient plant. This requirement seems hard to meet with closed magnetic confinement systems such as a tokamak since its plasma is surrounded closely by toroidal magnetic coils.

Among various configuration for plasma confinements so far discussed, a field reversed configuration (FRC) appears to meet those requirements. Because no toroidal magnetic field is applied, beta-values of FRC plasmas [3] observed in experiments are much larger than 50 % and stable if their averaged gyroradius calculated is comparable to the plasma radius. Energy confinement time τ_E of a plasmas are fairly good [4] and can be expressed empirically as

$$\tau_E(\mathrm{sec}) = 3.0 \times 10^{-5} (r_S/\sqrt{\rho_0})^{2.7} \; T \; (\mathrm{keV}) \qquad (1)$$

where r_S and ρ_0 stand for respectively the separatrix radius and the averaged Larmor radius of ions. Plasma is surrounded by open lines of force which allow us to install a high power direct energy converters in a free space. Kinetic effects attributed large ion gyration orbit seem to stabilize MHD modes in an FRC. Further, a directed flow of energetic protons due to the preferential trapping of fusion protons produces a bootstrap current needed to keep a plasma in a steady equilibrium.

3. FORMATION OF BURNING PLASMA

The method to obtain a burning plasma succeeds to that applied in ARTEMIS study [2]. An initial FRC plasma is produced at the formation chamber with the fast reversed theta-pinch method. For the purpose of obtaining the configuration reliably, an axial symmetry of the chamber is kept as possible. The FRC plasma is then translated to the adjacent burning chamber and heated up to a burning state by means of 1 MeV neutral deuterium beam injections of 100 A, magnetic compression, and injections of D-^{3}He fuel pellets. Injection of fuels is achieved by "Pac-man" method: a fuel pellet made of liquid helium-3 in a ice deuterium vessel is dropped into the plasma chamber. FRC plasma moves towards the pellet with a very high sound speed to involve pellet deeply inside the plasma volume before it evaporates. The FRC plasma is heated up to an ignition state during 50 seconds.

A set of principal plasma parameters of 1 MWe fusion reactor is tabulated in Table 1. The plasma volume is still as small as 200 m^3. The separatrix radius which is needed to obtain required energy confinement given by Eq.(1) is 1.68 m. An extremely high beta-value of an FRC equilibrium is achieved by the edge fueling [5]. Plasma current needed to keep plasma in an equilibrium is performed basically by the bootstrap current with a seed current due to a preferential trapping of fusion protons.

Table.1 Principal Plasma Parameters of ARTEMIS-L

	[ARTEMIS-L]	[ARTEMIS-H]
Electron Density (n_e)	5.1× 10^{20} m^{-3}	6.8× 10^{20} m^{-3}
Density Ratio between ^{3}He and D	1.35	0.5
Averaged Plasma Temperature (T)	83.5 keV	85.0 keV
External Magnetic Field (B_{ext})	5.36 T	6.44 T
Averaged β-value	98 %	95 %
Plasma Radius (r_s)	1.68 m	1.14 m
× Plasma Length (l_s)	× 22.2 m	× 17.4 m
Plasma Current (I_p)	189 MA	168 MA
Energy Confinement Time (τ_E)	6.9 s	2.8 s
Fusion Power (P_f)	1757 MW	1650 MW
Neutron Fraction (P_n/P_f)	0.032	0.046

Corresponding parameters for the high-efficiency ARTEMIS version (:ARTEMIS-H) is also tabulated for a comparison. Since the effective charge number is larger and radiation losses are large in a low-neutron version, a larger confinement parameter is required. The plasma volume for the case of low-neutron version is accordingly larger than that for high-efficiency version.

4. D-^{3}He/FRC FUSION REACTOR: ARTEMIS-L

On the bases of these considerations, a conceptual design of a D-^{3}He fueled FRC reactor: ARTEMIS-L has been performed, whose cross-sectional drawing is exhibited in Fig.2. The reactor consists of a formation section, burning section, and a pair of direct energy converter systems each of which composed of a cusp type direct energy converter for leaked fuel plasma component and a travelling wave direct energy converter for direct lost 14.7 MeV fusion protons.

Principles and details of the converter will be presented separately in the symposium. The total length of the reactor is 160 meters and its weight is less than 4,900 tons.

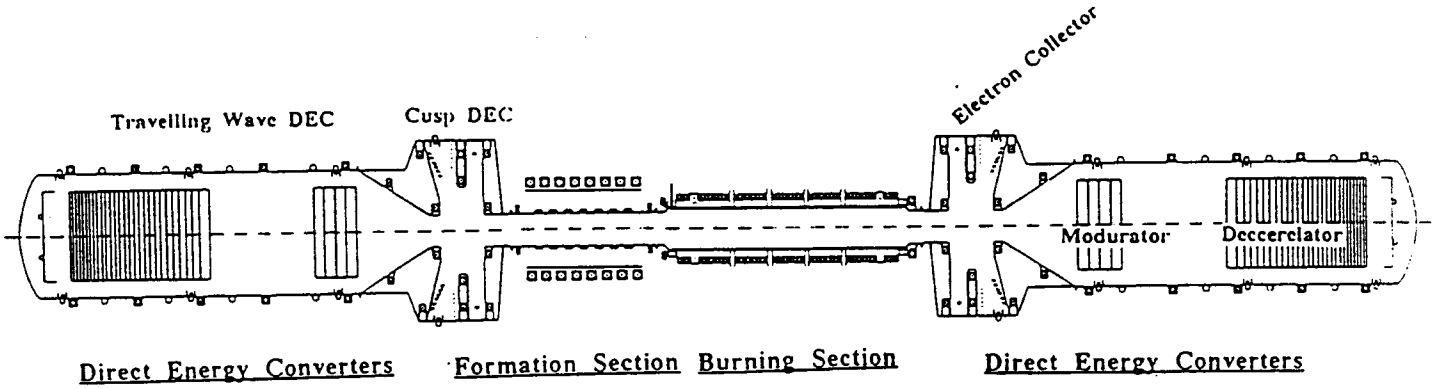


Fig.2. Cross-sectional drawing of ARTEMIS-L

The power flow diagram of ARTEMIS is exhibited in Fig.3. Approximately 1/3 of the fusion power is carried by radiation, 1/3 by leaked thermal particles, and another 1/3 by 14.7 MeV fusion protons; each of which is introduced respectively to heat converters-turbine generators with an efficiency 33 %, cusp type direct energy converters with an efficiency 65 %, and travelling wave direct energy converters with an efficiency 76 %. Fusion power carried by neutrons is only 3.2 %.

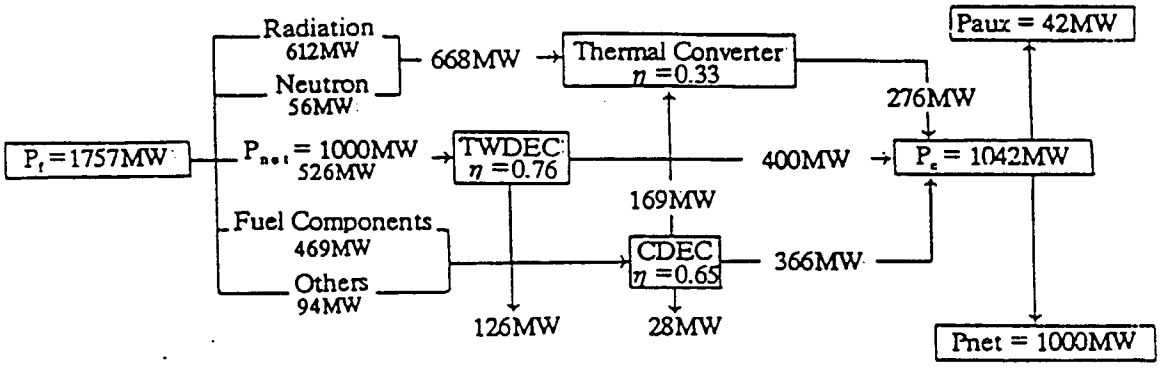


Fig.3. The power flow diagram of ARTEMIS-L

For the purpose of avoiding problems of unwanted links to weapons, exhausted fusion tritium is reinjected into the burning plasma. Consumed helium-3 for 1 GWe fusion reactor is 63.7 kg/yr provided that the duty factor is 0.75.

Engineering characteristics of ARTEMIS-L reactor are tabulated in the Table 2. By utilizing high-efficiency direct energy converters for D-^{3}He fueled fusion reactor, the plant efficiency defined by the ratio between the fusion power and output electric power is as high as 56.9 %. The maximum magnetic field of 6.3 T on the coils is low enough to apply present technology. Neutron load on the first wall is 0.18 MW/m^2, which enable us to keep the first wall be sound during the full reactor life.

Table 2. Engineering characteristics of ARTEMIS-L

Fusion Power	1,757 MW
Output Electric Power	1,000 MWe
Power to Heat Converters	668 MW
Power to TWDECs	526 MW
Power to Cusp DECs	563 MW
Total Weight	4,900 tons
Total Length	160 m
Maximum Magnetic Field	6.3 T
Radius of the First Wall	2.28 m
Heat Load on the First Wall	2.0 MW/m^2
Neutron Load on the First Wall	0.18 MW/m^2

5. ATTRACTIVE CHARACTERISTICS OF D-^{3}He/FRC REACTOR:ARTEMIS-L

Detailed studies on the reactor components are needed to clarify their attractive characteristics precisely. Nevertheless, the cost of electricity from ARTEMIS-L can be estimated roughly after ESECOM [6] studies. The estimated direct cost of the reactor is 1,030 M$ and the total capital cost is 1,800 M$. Since the average neutron wall load is 0.18 MW/m^2 or equivalently their approximate fluence is 60 dpm after 30 years operation, Tenelon as the first wall material seems sound during 30 years. As is show in the Table 3, the resultant cost of electricity (COE) is 30.5 mill/kW·h. The helium-3 cost is assumed to be 0.2 M$/kg. This assumption affects,

Table 3. The estimated cost of electricity

Net Electric Rating (P_E)	1,000,000 kW
Total Direct Cost for Construction	1,030,000,000 $
Total Capital Cost (C_T)	1,800,000,000 $
Annual Capital Cost ($Ca = C_T \times 0.0844$)	151,000,000 $
Operation and Maintenance Cost (C_{om})	36,000,000 $
Fuel Cost (C_f)	13,000,000 $

$$COE = [Ca + C_{om} + C_f]/[P_E \times 8760 \times 0.75] = 0.0304\ \$/kW{\cdot}h$$

a fixed-charge rate of 0.0844, the interest during 6 years construction of 8.56 %/yr, and a capacity factor of 75 % are assumed. Costs are in constant 1986 Dollars.

however, a little the cost of electricity. An expensive cost of helium-3 by a factor 5 still gives a cheep COE as 38.4 mill/kW.h.

The safety and environmental effects from ARTEMIS-L are also to be studied in details. Nevertheless, one is able to infer the following approximate results from interpolations of previous

studies including "ESECOM" studies: Since neutron yield in ARTEMIS-L fusion reactor is as small as 4×10^{19} n/s (10^{19} n/s is 14 MeV D-T neutrons and 3×10^{19} n/s is 2.45 MeV D-D neutrons) and only several grams of tritium is contained in a plant. In a normal operation, the public surface exposure is less than 4 mSv which value is much smaller than the allowable maximum of 0.25 Sv, and the occupational whole body exposure can be less than 1.4 mSv which value is also much smaller than the allowable maximum of 2.0 Sv.

Since no breeding blanket is installed and neutron yield is very few in a D-^{3}He fusion reactor, no nuclear heating of structural materials is appreciable even for a case of a loss of coolant accident or a loss of flow accident and the plant appears inherently safe.

The total volume of disposed radioactive wastes after 30 years operation is 460 m^3, whose intruder dose is 0.0024 mSv and much smaller than the allowable limit of 5 mSv.

6. CONCLUSIONS

1: A complete scenario to obtain and sustain a burning plasma is available. Nevertheless, studies on plasma equilibrium, stability, and transports in an FRC are needed to develop ARTEMIS-L commercial fusion reactor.
2: Engineering bases applied in D-^{3}He fueled ARTEMIS-L design are conventional. Developments of high power - high energy neutral beam injectors and a high efficiency direct energy converter system are needed.
3: The cost of electricity (COE) from ARTEMIS-L reactor is cheaper than that from present power plant. The cost of helium-3 changes little the COE.
4: Inherently safe and environmentally sound characteristics of ARTEMIS-L is intrinsic to D-^{3}He Fusion.
5: Experimental data base available to evaluate the scenario is very poor. Extensive studies on FRCs and experimental verification of the scenario (the Proof of Principle Experiment) are argent.

REFERENCES

[1] L.J.Wittenberg, J.F.Santarius, and G.L.Kurcinski, "*Lunar Source of ^{3}He for Commercial Fusion Power*", *Fusion Technology* **10**, 167 (1986)

[2] H.Momota, A.Ishida, Y.Kohzaki, G.H.Miley, S.Ohi, M.Ohnishi, K.Sato, L.C.Steihauer, Y.Tomita, and M.Tuszewski, "*Conceptual Design of the D-^{3}He Reactor ARTEMIS*", *Fusion Technology* **21**, 2307 (1992)

[3] A.L.Hoffman and J.T.Slough, "*Field Reversed Configuration Lifetime Scaling Based on Measurements from the Large s Experiment*", *Nuclear Fusion* **33**, 27 (1993)

[4] M.Tuszewski, "*Field Reversed Configurations*", *Nuclear Fusion* **28**, 2033 (1988)

[5] Y.Tomita and H.Momota, "*Steady Equilibrium of a Cylindrically Symmetric Plasma Sustained by Fueling*", *KAKUYUGO KENKYU* **67**, 801 (1993)

[6] J.P.Holdren, D.H.Berwald, R.J.Budnitz, J.G.Crocker, J.G.Delene, R.D.Endicott, M.S.Kazimi, R.A.Krakowski, B.G.Logan, and K.R.Schultz, "*Report of the Senior Committee on Environmental, Safety", and Economic Aspects of Magnetic Fusion Energy*, **UCRL--53766** (1989)

D-^{3}He Mirror Reactors

D.D. Ryutov
Budker Institute of Nuclear Physics
Novosibirsk, Russia 630090

ABSTRACT

After a brief survey of the present status of mirror research (in conjunction with its possible role in the D^{3}He reactor development), we consider one particular version of D^{3}He mirror reactor whose distinctive feature is a strong difference in the temperatures and densities of the deuterons and electrons, on the one side, and fast helium ions, on the other: $T_{e,D}/W_{He}<<1$, $n_{e,D}/n_{He}>>1$. Such a version of the mirror reactor provides a high power density of the fusion reactions (~20 MW/m^3) and a very low neutron production rate (neutron power ~ 10^{-4}-10^{-5} of the fusion power), at the expense of a relatively low Q value (Q~0,4). Though the last figure is rather discouraging, the fact that all the energy in the system is circulating in the form of charged and neutral particle fluxes (the bremsstrahlung losses being negligible), the system may have some chances as an energy producing device, as soon as the highly efficient direct energy converters are developed.

1.INTRODUCTION

The mirror systems attract much attention as a possible candidate for developing the economically viable D^{3}He mirror reactor (see, e.g., [1,2] and references therein). This fact can be easily explained by a number of important merits of the mirrors, in particular: i) experimentally proven capability to operate at high betas exceeding 50%; ii) intrinsic stationarity and absence of the catastrophic events of the major disruption type; iii) the presence of the "natural divertors" in the form of the end tanks (which allow to accomodate large plasma absorbing surfaces). These advantages, strongly supporting the positions of mirrors as DT fusion systems, may become of a decisive importance when considering the D^{3}He reactors. More detailed assessments of the prospects of mirror systems in the context of both DT and D^{3}He reactor applications, can be found in Refs. [3,4].

Despite some narrowing of the mirror research that followed the US decision to terminate the LLNL mirror program, there still exist rather large scale mirror devices in Russia and Japan; a continuous progress is being made both in the sense of a better understanding of the plasma behavior and improvement of the plasma parameters. In particular, some mirror facilities routinely operate at high electron temperature, exceeding a few hundred eV. There have been theoretically discovered and experimentally verified several techniques that allow to maintain plasma stability in the framework of the fully axisymmetric mirror configurations. There have been

found regimes with two component plasma (with the sloshing ion population) which demonstrate a remarkable microstability. Some further details with regard to the recent progress in mirror research can be found in the surveys [3,4] and in the Proceedings of the Conference on the Open Confinement Systems for Fusion (Novosibirsk, 1993, to be published).

These developments may have a considerable effect on the future designs of D^3He mirror reactor. Of special importance is the possibility to exploit fully axisymmetric magnetic configurations. This would certainly improve the characteristics of the mirror reactors of a "Ra" type [1], with approximately equal temperatures of all the plasma components. The chances of a more exotic two-component system, which is the subject of the present paper, would also increase.

2. TWO-COMPONENT SCHEME

The main attraction of the D^3He fuel consists in a low neutron yield, as compared to the traditional DT schemes. A few years ago, it was pointed out [2] that a very deep further reduction of the neutron yield could be achieved by using a so called two-component version of the reactor. The words "two-component" refer here to the plasma composition: the plasma should consist of a relatively dense and cold deuterons and electrons, plus a small admixture of very hot (~ 1MeV) ^3He ions. The density of the latter is determined by the balance between two processes: i)the NB trapping and ii)the subsequent slowing down of thus formed fast ions. As soon as ^3He ions are slowed down to the plasma temperature, they should be removed from the system (for more details see Sec.3). A detailed analysis of this scheme can be found in Ref.[2]. Here we present a brief summary.

Because of the exponentially strong temperature dependence of the DD reaction rate, the neutron yield at a low deuterium temperature will be significantly (by the orders of magnitude) reduced with respect to the usually considered case of the equal temperatures, $T_D \sim T_{He} \sim$(70-100) keV. At the same time, owing to the high energy of ^3He ions, the D^3He reaction rate will remain high.

At low temperature of electrons and deuterons, one can considerably raise the deuterium density n_D over that of the fast ^3He ions, without producing any noticeable effect on the total plasma pressure; the high n_D means, in turn, high volume density of the fusion power P_{fus} (as the latter scales as $n_D n_{He}$).

Low temperature of the bulk plasma provides also favourable conditions for its radial confinement: at low T, the parameter a/ρ_i (where a is the plasma radius) is large, thus eliminating the possibility for the most hazardous drift-type instabilities to develop (see [5]). The population of the hot sloshing ions is immersed into the cold and dense plasma. As was mentioned in the Introduction, such a system demonstrates a remarkable microstability (see, e.g.,[6]).

The analysis carried out in paper [2], was based on the assumption of the negligibly small transverse particle losses - an assumption that agrees with the present understanding of the physics of the axisymmetric mirror devices. As was shown in [2], in such a situation, the energy balance equations for various plasma species predetermine the approximate equality of T_D and T_e: $T_D \sim T_e$. This fact, in turn, imposes a severe constraint on the achievable level of plasma Q. Indeed, in order to reduce the drag losses of fast ions on the electrons, one should increase T_e. But, at T_D

~T_e this would mean a corresponding increase of T_D and of the neutron yield - the consequence that makes the whole system less attractive than the conventional scheme, with equal temperatures of all components.

As a compromise, the reactor with T_e= 20 keV was proposed in Ref.[2]. In this case, the neutron power could be kept at the level of approximately 10^{-3} of the fusion power and, at the same time, the Q value would be equal to 0.2. Though quite small, this value left some chances for the system under consideration, provided very efficient direct energy converters would be developed.

In the next section we consider a possibility of improving the performance of the two-component reactor by selective enhancement of the cross-field deuterium transport.

3.IMPROVED TWO-COMPONENT SCHEME

Possible improvement of the two-component scheme is based on the observation that the energy exchange between electrons and deuterons at T_e> 30-40 keV is a relatively slow process, weakly affecting the energy balance of either of the two species: the approximate equality of T_e and T_D was caused not by the energy exchange between these two species but by the peculiarities of the axial power losses in the mirror devices.

This means that, by introducing an additional transport mechanism that would selectively cool the deuterons, we wouldn't deteriorate the energy balance for the electrons and, on the contrary, we could raise their temperature (by reducing their axial losses). Accordingly, we would be able to increase Q and, simultaneously, reduce the neutron yield.

For selective cooling of the deuterons, a version of the drift pumping technique [7] could be used. By applying a localized time-varying non-axisymmetric perturbations of the magnetic field, with the frequency exceeding the bounce frequency of the thermal deuterons, we could bring them into the regime of a so-called "stochastic diffusion" [8] characterized by a generally large transport coefficients. The loss rate is controlled by the amplitude of the perturbations.

In order to avoid any increase of the radial losses of the electrons and fast ^{3}He ions, the perturbation frequency should be chosen below the bounce frequency of these two species. Since the deuterium bounce frequency is much lower than the other two, such a possibility does indeed exist. If necessary, one can totally eliminate the effect of the non-axisymmetric perturbations on the fast ^{3}He ions, by placing the perturbing windings outside the turning points of these ions (note that the fast ^{3}He ions have well defined turning points: their scattering occurs slower than their energy loss). A detailed numerical analysis of this pumping scheme will be published elsewhere.

As the bounce frequency of the slowed down and thermalized ^{3}He and ^{4}He ions is comparable with that of the deuterons, the thermalized helium particles will also be removed from the system by stochastic diffusion.

In order to maintain the overall power balance in the system, we would have to recover a considerable fraction of the deuterium energy transported to the plasma periphery. This could be done by reducing the axial lifetime of the plasma in the outer regions of the plasma column. The energy of the particles escaping along the magnetic field lines could then be recovered by the direct energy converters. The

deuterium particle balance at the plasma periphery could be maintained by the pellett injection to this region.

Under conditions described, the energy balance in the plasma core is established in the following way: the fast ^{3}He ions transfer their energy to deuterons and electrons; then, the deuterons loose their energy predominantly by the cross-field transport, while the electron losses occur mostly along the field lines. There exist also bremsstrahlung losses (usually small) and energy exchange between electrons and deuterons. Accordingly, the energy balance equations for deuterons and electrons of the plasma core can be presented in the form:

$$P_{He}^{(D)} - P_{\perp}^{(D)} - P_{\parallel}^{(D)} + P_{eD} = 0 \tag{1}$$

$$P_{He}^{(e)} - P_{\perp}^{(e)} - P_{\parallel}^{(e)} - P_{eD} - P_{rad} = 0 \tag{2}$$

The first term in (1) and (2) represents the power (per unit plasma volume) transferred from the fast ^{3}He ions to deuterons and electrons, respectively; the last term describes the energy exchange between electrons and deuterons (small). The other terms are self-descriptive. For the sake of completeness, we have retained in (1) and (2) also small terms ($P_{\parallel}^{(D)}$, P_{eD}, $P_{\perp}^{(e)}$ and P_{rad}) which do not affect the further analysis. Plasma heating by the fusion products is neglected for the reason of a small Q value.

In the energy balance of the fast helium ions, we neglect their direct losses to the mirrors: as has been already mentioned, their scattering occurs much slower than their energy losses. In such a case,

$$P_{inj} = P_{He}^{(D)} + P_{He}^{(e)} \tag{3}$$

where P_{inj} is the power injected into the unit plasma volume. The following formulas are valid:

$$P_{He}^{(D)} = 9.2 \cdot 10^{-26} \gamma_D \propto n_D^2 \, W_{inj}^{-1/2} \tag{4}$$

$$P_{He}^{(e)} = 1.9 \cdot 10^{-28} \, \gamma_e \propto (1 + 2 \propto) n_D^2 \, W_{inj} \, T_e^{-3/2} \tag{5}$$

where P_{He} is measured in MW/m^3, n_D in cm^{-3}, W_{inj} and T_e in keV; γ_D and γ_e are dimensionless parameters of the order of unity which depend on the details of the energy distribution (see below). The parameter α is determined as follows: $\alpha = n_{He}/n_D$.

When the electron temperature is high, $T_e > (1/50)W_{inj}$, the energy distribution function f(W) of the fast ^{3}He ions is controlled by their collisions with D ions. In this case

$$f(W) = \text{const} \cdot \sqrt{W} \tag{6}$$

(we use the definition $dn_{He} \backsim f(W)\, dW$). For this distribution, $\gamma_D = \gamma_e = 1$.

The Q of the system ($Q = P_{fus}/P_{inj}$), according to (3)-(5), can be presented in the form:

$$Q = \frac{3.2 \cdot 10^{13} \; < \sigma_{fus} v >}{\gamma_D W_{inj}^{-1/2} + 2 \cdot 10^{-3} \, \gamma_e (1 + 2 \propto) W_{inj} T_e^{-3/2}} \tag{7}$$

where $<\sigma_{fus} v>$ is expressed in cm^{4}s^{-1}, while T_e and W_{inj} in keV.

At a given injection energy, by a proper adjustment of the transverse energy transport (by deuterons) and axial energy transport (by electrons), one can establish the desired values of T_D and T_e, the most important parameters of the system. As a base variant of the improved two-component scheme, we consider the following one: T_D=5 keV, T_e= 45 keV, W_{inj}= 1 MeV. The further increase of T_e, according to (7), gives only a relatively insignificant gain in Q; a further decrease of T_D would impose too strong constraints on the selective transport system.

For the given values of α, T_D, T_e, and W_{inj}, the plasma density is determined from the pressure balance condition

$$\beta \frac{B^2}{8\pi} = n_D \left[T_D + (1+2\alpha) T_e + \frac{3}{5} \alpha \sin^2 \Theta_{inj} W_{inj} \right] \tag{8}$$

where θ_{inj} is the injection angle of the fast helium ions. When calculating the pressure of these particles, we have taken into account relation (6). At given values of β and B, the fusion power density, if considered as a function of α, has a broad maximum around the point

$$\alpha = \frac{T_e + T_D}{2T_e + \frac{3}{5} \sin^2 \Theta_{inj} W_{inj}} \tag{9}$$

(Cf.[2]). This maximum is:

$$P_{fus} = \frac{\beta^2}{4} \left(\frac{B^2}{8\pi} \right)^2 \frac{E < \sigma_{fus} v >}{(T_D + T_e)(2T_e + \frac{3}{5} \sin^2 \Theta_{inj} W_{inj})} \tag{10}$$

where E is the energy released in one reaction event. Possible reactor parameters, corresponding to B=5T, β=0.6, are: W_{inj}= 1 MeV; θ_{inj}= 60°; T_D=5 keV; T_e= 45 keV; α=0.3; P_{fus}= 12 MW/m^3; P_{rad}= 0.4 MW/m^3; Q=0.4.

At T_D=5 keV, the neutron and tritium production in the side DD reactions is very small: for the example given above, P_n is approximately $3\ 10^4$ times less than P_{fus}, with approximately 40% of P_n carried by DT neutrons. As was pointed out in [2], the further reduction of the neutron yield is possible, by cutting off the exponential tail of the deuterium distribution function at W_D exceeding a few T_D. In our case this could lead to an additional reduction by a factor of 10.

4.CONCLUSION

We have shown that the mirror physics opens the possibility of developing a D^{3}He reactor with unique characteristics in the sense of an extremely low radioactivity ($P_n \sim 10^{-5} P_{fus}$) and a high power density (P_{fus} ~20 MW/m^3). The drawback of this system is a low Q value (~0.4). However, as all the energy is circulating in the system in the form of the charged particles flows (the bremsstrahlung losses are very small), some chances remain that development of highly efficient direct energy converters will allow to obtain a net energy production with such a system.

5.ACKNOWLEDGEMENTS

The author is grateful to the Fusion Technology Institute (University of Wisconsin, Madison) for its hospitality during the Symposium; the support of the Laboratory of Plasma Studies (Cornell University) in the course of preparation of this paper is also gratefully acknowledged.

REFERENCES

[1] J.F.Santarius, H.M.Attaya, M.L.Corradini, L.A. El-Guebaly, G.A. Emmert et al., "Ra: A High Efficiency, D-^{3}He, Tandem Mirror Fusion Reactor", UWFDM-741 (1987).

[2] B.A. Knyazev, D.D. Ryutov, "Low Radioactive Open-Ended Fusion Reactor with D^{3}He Fuel", *"Tritium and Advanced Fuels in Fusion Reactors", Proc. Intern. School of Plasma Physics "Piero Caldirola"*, p.693, Editrice Compositori, 1990.

[3] D.D.Ryutov, "Review of Mirror Fusion", *Proceedings of the 1989 International Conference on Plasma Physics (Invited Papers)* , Indian Academy of Science, Bangalore, p.391 (1991).

[4] N.Hershkovitz, S.Miyoshi, D.D.Ryutov, "Mirror Devices", *Nuclear Fusion*, 30, 1761 (1990).

[5] A.B.Mikhailovski. *"Theory of Plasma Instabilities"*, v.2, Consultants Bureau, New York (1974).

[6] P.A. Bagryanskij, A.A. Ivanov, V.V. Klesov et al. *"Experiments on Neutral Beam Injection in a Gasdynamic Trap", "Plasma Physics and Controlled Nuclear Fusion Research" (Proc. XII IAEA Conference, Nice, 1988)*, IAEA, Vienna, v.2, p.483 (1989)

[7] D.E. Baldwin in: *"Mirror Based and Field Reversed Approaches to Magnetic Fusion", Proc. of the 1983 Varenna School of Plasma Physics*, Monotypia Franchi, v.1, p.109 (1984)

[8] D. D. Ryutov, G.V. Stupakov. "Transport Processes in Non-Axisymmetric Open Traps". *Reviews of Plasma Physics*, Consultants Bureau, New York, v. 13, p. 93 (1988).

Non-Energy Applications for Fusion: Presented at Second Wisconsin Symposium on ^{3}He and Fusion Power

John M. Dawson
University of California, Los Angeles
Physics Department, 1-130 Knudsen Hall
405 Hilgard Avenue
Los Angeles, CA 90024-1547

ABSTRACT

Non-Energy Applications of Fusion Reactors are considered. The direct use of the 14.7 MeV protons from the D-^{3}He reaction for the production of positron emitting isotopes for medical, industrial, and scientific uses is explored in some detail. Inside a working D-^{3}He reactor the 14.7 MeV proton flux is of the order of 10^{22} - 10^{23}cm^2/sec. The conversion of fertile nuclei to useful nuclei can be very prolific. Since the value of such isotopes can be very large (~ \$$10^{12}$/gm), it is possible to have an economical reactor for a machine that just breaks even or may even be below break even in energy terms. Existing research devices can produce interesting quantities of isotopes for experimental and demonstration purposes. A major problem will be the development of a demand for the large quantities of positron emitters that could be produced. If such a source of isotopes exists, as with many new developments, the demand will probably follow.

1. INTRODUCTION

Fusion reactions represent a new form of fire which produces its energy in unique forms which can find special applications besides power production. When used these ways, the criteria for an economic fusion reactor can be radically altered and one need not achieve ignition, and possibly need not get energy break even, to have an economic device. Such possibilities have been explored very little. Given the substantial technological developments in fusion reactor research, it is worthwhile to explore some of the possibilities.

Probably the application that has been given the most attention is the fusion breeder for fuel for fission reactors (also the fusion fission hybrid reactor) (Moir [1]). Here one makes use of the 14 MeV neutrons produced by the D-T reaction to produce extra neutrons through n-2n and n-3n reactions and uses the excess neutrons to breed ^{239}Pu or ^{233}U. For the ^{233}U option there is the interesting possibility of mixing it with normal U to produce enriched U fuel. The mixture could not be easily diverted to weapons because this would require isotopic separation to produce weapons grade material; this is unlike Pu which can be separated chemically.

unique to this type of reactor. These energetic protons can be used in a number of different ways. One application is to produce proton rich nuclei. Such proton rich isotopes often emit positrons which have many scientific, medical, and industrial applications. The value of these isotopes is so large that one would not need an ignited plasma in order for it to pay for itself. A Wet Wood Burning reactor (Dawson et al. [2]) almost certainly would suffice; it might not even require a Q of one to be practical. Many new applications for such isotopes almost certainly would be found if they could be produced abundantly and relatively cheaply.

The most efficient way to produce proton rich isotopes is through the use of the p-n reactions. Table I shows some possibilities. These are exchange reactions where a proton knocks out and replaces a neutron. They have relatively large cross sections (~ 200 milli-barns) over a wide range of energies. Figure 1 shows an example of a p-n cross section (Sajjad et al. [3]). Protons of 14.7 MeV energy are sufficiently energetic to penetrate the Coulomb barrier of all atoms so that this application can be applied to the whole periodic table.

Table 1. Some p-n Reactions

	$D + {}^3He \rightarrow {}^4He + p$	(14.7 Mev)	
(1)	$p + {}^{11}B \rightarrow {}^{11}C + n$ ${}^{11}C \rightarrow {}^{11}B + {}^+e$	(E_T = 2.76 MeV) ($\tau_{1/2}$ = 20 min.)	
(2)	$p + {}^{13}C \rightarrow {}^{13}N + n$ ${}^{13}N \rightarrow {}^{13}C + {}^+e$	(E_T = 3 MeV) ($\tau_{1/2}$ = 10 min.)	
(3)	$p + {}^{15}N \rightarrow {}^{15}O + n$ ${}^{13}N \rightarrow {}^{13}C + {}^+e$	(E_T = 3.53 MeV) ($\tau_{1/2}$= 2.03 min.)	$\sigma \sim 200$ mb
(4)	$p + {}^{17}O \rightarrow {}^{17}F + n$ ${}^{17}F \rightarrow {}^{17}O + {}^+e$	(E_T = 3.55 MeV) ($\tau_{1/2}$ = 66 sec.)	
(5)	$p + {}^{18}O \rightarrow {}^{18}F + n$ ${}^{18}F \rightarrow {}^{18}O + {}^+e$	(E_T = 2.45 MeV) ($\tau_{1/2}$ = 1.87 hr.)	
(6)	$p + {}^{19}F \rightarrow {}^{19}Ne + n$ ${}^{19}Ne \rightarrow {}^{19}F + {}^+e$	(E_T = 4.03 MeV) ($\tau_{1/2}$ =18 sec.)	
(7)	$p + {}^{21}Ne \rightarrow {}^{21}Na + n$ ${}^{21}Na \rightarrow {}^{21}Ne + {}^+e$	(E_T = 3.52 MeV) ($\tau_{1/2}$ = 23 sec.)	
(8)	$p + {}^{22}Ne \rightarrow {}^{22}Na + n$ ${}^{22}Na \rightarrow {}^{22}Ne + {}^+e$	(E_T = 2.84 MeV) ($\tau_{1/2}$ =2.58 yr.)	
(9)	$p + {}^{26}Mg \rightarrow {}^{26}Al + n$ ${}^{26}Al \rightarrow {}^{26}Mg + {}^+e$	(E_T = 5.01 MeV) ($\tau_{1/2}$ = 6.5 sec.)	

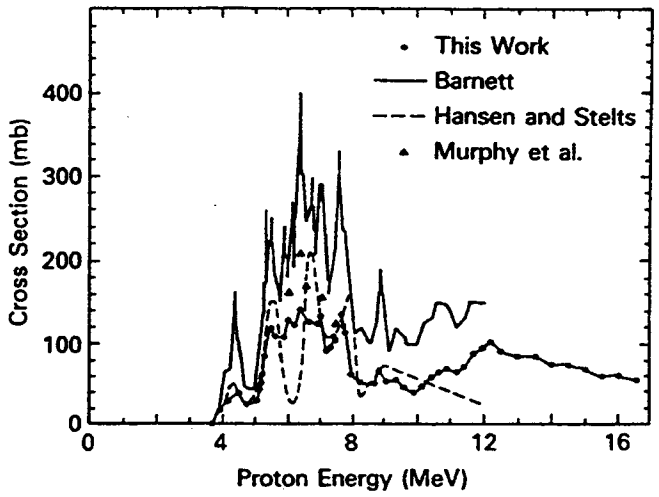


Fig. 1. Measurements for the cross section for the $^{15}N(p,n)^{15}O$ reactions.

Another potential application for the 14.7 MeV protons is for nuclear waste disposal by the transmutation of long lived fission products. These are neutron rich nuclei and replacing a neutron in their nucleus with a proton can convert them to stable nuclei. The 14.7 MeV proton flux inside an operating D-^{3}He reactor is very high, of the order of 10^{22} - 10^{23} protons per cm^2 per sec. At this flux level and with cross sections of the order of 0.2 barns, the burn out time for such nuclei inside the reactor is roughly 50 - 500 sec. or 1 - 8 min.

For example, ^{90}Sr can under go a p-n transition to ^{90}Y which undergoes a β decay to ^{90}Zr (which is stable) in 64.2 hours. A second example would be the transformation of ^{137}Cs to stable ^{137}Ba through p-n reactions.

The effectiveness of a D-^{3}He reactor for burning fission waste can be estimated. In an operating fusion reactor we probably do not want to increase the effective Z of the fuel mixture (Dawson [4]) by more than a factor of 2. If we assume that there are no other impurities and that the fuel is a 50 - 50 mixture of D and ^{3}He, then its Z effective is 1.67. Suppose that we are trying to burn up ^{90}Sr, Z = 38. Doubling the effective Z to 3.33 allows us to incorporate a Sr density equal to 3.8 x 10^{-3} times the deuteron or ^{3}He density. Taking their densities as 10^{14} per cm^3, gives a Sr density of 3.8 x 10^{11} per cm^3. With a burn-out rate of 10^{-2} per sec. (using an internal proton flux of 5 x 10^{22}), we are burning up ^{90}Sr at a rate of 3.8 x 10^9 nuclei per cm^3 per sec. If we assume that the reacting plasma has a volume of 10^9 cm^3, then we are destroying ^{90}Sr at a rate of 3.8 x 10^{18} atoms per sec. In one year we would destroy 1.15 x 10^{26} atoms of ^{90}Sr or about 17.5 Kg. This would process 3.5 x 10^7 Curies per year. A 3 GW thermal PWR produces 13.5 Kg/yr (Bowman et al. [5]) of ^{90}Sr. Thus, the above calculation indicates that a large D-^{3}He reactor could burn up a significant

amount of the radioactive fission ash of a large reactor. The calculation is of course rough but a more detailed evaluation seems warranted.

2. POSSIBLE APPLICATIONS OF POSITRON EMITTERS

I will now give some examples of present uses of positron emitters as well as some potential applications.

2.1. PET Scans

2.1.A. Medical Applications

One of the major application for proton rich isotopes is in medicine for positron emission tomography (PET scans). Tracer elements are incorporated into special compounds which are selective in the parts of the body they go to (brain, heart, liver, kidneys, tumors, etc.) The proton rich nuclei emit positrons which annihilate with electrons with the emission of two photons, each of 0.5 MeV energy and propagating in opposite directions. By coincidence detection of these two photons a line that passes through the source region can be constructed. With the detection of many such pairs of photons, a computer can construct a picture of the source region. From such images information like where tumors are located, where oxygen is being used, or many other details about the functioning or malfunctioning of the body can be obtained.

At present the source of isotopes for medical PET scans comes from cyclotrons which typically produce 100 micro amps of 10 MeV protons. The cost of such cyclotrons is in the range of \$1 - 10M. Typically 10^{-3} of the protons produce a positron-emitting atom. A typical PET scan requires 10 milli-Curies or about 4×10^{12} atoms of ^{18}F. A 100 micro-amp cyclotron will produce this amount in about 10 sec. Several times this amount must be produced to allow for decay during extraction and chemical processing. The value of one dose is in the range of a few hundred dollars.

The cyclotrons for producing medical PET scan images are located at the hospitals where the scans are made because of the relatively short half lives of the useful isotopes (~ 110 min for ^{18}F) and the relatively low production rates of these machines. Thus, many hospitals must maintain and operate these relatively expensive facilities.

To produce positron emitters in a D-^{3}He reactor, fertile target atoms would be included as part of the plasma; generally the density of fertile atoms will be kept at a few times 10^{-3} of the D or ^{3}He density. Although the fractional density of fertile nuclei is small, a similar fraction (10^{-3}) of the 14.7 MeV protons in a D-^{3}He fusion reactor produce positron emitters. This is because the stopping power of the protons in the hot plasma is much less than that of cold matter (for a 50 KeV temperature plasma it is ~ 3×10^{-2} of that for cold gas; and the ratio of electrons to fertile nuclei is about 30 times greater in the fusion

reactor); the chance of a proton undergoing a p-n reaction on a fertile nuclei is nearly the same as for the cold target (Dawson [6]).

A D-^{3}He reactor producing 20 MW produces about 1 amp of 14.7 MeV protons. In some sense, such a reactor is equivalent to 10^4 cyclotrons. Of course, such a reactor will be in only one location whereas the cyclotrons would be widely distributed. A central factory could not replace the cyclotrons in all aspects; however, a central plant has advantages of its own. It certainly could be run by many fewer people than are required for 10^4 cyclotrons.

It would be possible to ship positron emitters by air to all parts of the U.S. from a centralized facility for isotopes that have half lives of more than an hour. For example, it should be possible to ship, in a few hours, ^{18}F with an 1.83 hour half life by air from a central facility to places where PET scans are carried out; not too much of the activity will be lost. The short half life of most positron emitters means that problems related to accidents are not so serious. For ^{18}F the activity will decay by a factor of 1.3×10^{-8} in two days. If the containers are made crashproof and there was an accident, after a few days their radioactivity would have decayed to negligible values. Having a central facility seems feasible for many PET scan applications. Many hospitals that make PET scans could do away with the expensive operation of a cyclotron facility.

Having a central facility would allow the building of associated centralized laboratories that could be used in scientific and industrial research. The facility could be operated much as synchrotron radiation sources are today.

Although the above arguments are rather glib, they do show the potential economics for such a facility to reduce the cost of producing and using positron emitters.

2.1.B. Possible Industrial Applications of PET Scans

There are also many potential industrial applications of PET scans; I will mention one or two and give a number of potential examples.

Rolls Royce has employed fluorocarbon oils using ^{18}F to make PET scans of an operating engine (Perkins [7]; Int. J. Res. [8]) by synchronizing the detectors with the engine cycles, the lubrication process throughout a cycle can be followed in detail. Similar tests could be done on the lubrication in all types of engines and bearings. One could also use ^{11}C oils if one believes they behave differently. One might also investigate fuel and air mixing in engines using hydrocarbons containing ^{18}F and ^{11}C.

Another such application that could be useful would employ the gas CF_4 (using ^{18}F). This gas could be put in pipes. It would penetrate into the smallest cracks. If the CF_4 were then pumped out and a PET scan were made of the

pipe, the cracks would show up. Other industrial components where cracks are a serious problem could be similarly tested. For example, one could also put turbines or turbine blades in a chamber containing CF_4. Again the CF_4 would penetrate into cracks. After removal from such a chamber and PET scanned, the cracks would be revealed.

Another possible application of ^{18}F is in the analysis of computer chip manufacturing. Often in chip manufacture, compounds containing F are used. By using ^{18}F compounds, we would have tagged F and we could monitor the reactions taking place and possibly even the steps of the reaction process inside the chamber. The progress and efficiency of the etching process might also be measured and improved (Coburn [9]).

For plasma materials processing (National Research Council [10]) many possibilities exist for using positron emitters as diagnostic tools. For carbonizing or nitriding surfaces ^{11}C and ^{13}N could be used in the processes; these have half lives of 20 and 10 minutes respectively. For the diagnosis of plasma production of diamond films ^{11}C could prove valuable. For applications like these, a central PET scanning facility could have great advantages.

2.1.C. Applications in Fusion Research

An interesting possible application of D-^{3}He produced positron emitters is for diagnosing the plasma behavior in fusion reactors (Dawson et al. [12]). To a large degree positrons provide us with tagged electrons. We can determine the positron density from their rate of annihilation (through PET scan imaging) and the electron density. We can determine where they are, how they move, and thus get some direct measure of electron transport.

For this purpose we would seed the D-^{3}He plasma with an atom that produces a short lived positron emitter. A good candidate is ^{19}Ne produced from ^{19}F; it has a half life of 17s. For plasma confinements of 1s, 6% of the ^{19}Ne would decay before escaping the plasma. If the plasma is producing 3 x 10^{17} protons per sec (100 Kw D-^{3}He power) and 10^{-3} of these produce ^{19}Ne with 6% of these decaying, then we are producing 2 x 10^{13} positrons per sec. in the plasma. Assuming that their confinement time is also 1s and that the volume of the plasma is 10^8 cm^3, the density of positrons would be 2 x 10^5 per cm^3.

The rate of positron annihilation by free electrons for nonrelativistic energies is (Baltenkov et al. [11])

$$R = \pi r_0^2 c n_e \qquad (1)$$

where r_0 is the classical radius of the electron ($r_0 = e^2/mc^2$). Numerically the rate works out to be

$$R = 6.9 \times 10^{-15} n_e \, . \qquad (2)$$

This rate is slow enough so that the emitted positrons (emitted in the MeV range) will thermalize with the plasma electrons through the emission of synchrotron radiation and Coulomb collisions with the electrons. If the plasma confinement time is a Lawson time ($n_e\tau = 10^{14}$ sec/cm^3), then roughly half the positrons will be annihilated in the plasma. If we know the positron production rate, by measuring the positron density through their annihilation rate we will get a direct measurement of their confinement time. This should be very similar to the electron confinement time which is very hard to measure any other way (of course effects of the plasma potential would have to be taken into account). By measuring annihilation at the wall one could find where the positrons are escaping. By using biased positron collectors and a knowledge of the electron temperature one could determine something about the plasma potential.

It should be possible to measure the positron density using standard positron annihilation tomography. Since conditions along field lines are quite uniform, we are mainly interested in crossectional images. Crossectional images from a 50 cm. long section could be obtained which should give good statistics and time and space resolution (cm. space resolution, milesec time resolution).

It should also be possible to measure the electron temperature from positron annihilation. Because of the motion of the center of mass of the annihilating electron and positron, the two photons that are emitted will not be propagating in exactly opposite directions. The difference in angle from 180 is proportional to $\Delta\Theta^2 = (v_T/c)^2$; for a 10 KeV temperature this is ~ 10°.

Another application to fusion research would be to follow in detail where impurities are escaping. If ^{11}C (half life of 20 m) were produced from ^{11}B, then it would be easy to measure where it was deposited on the wall after a shot. It should also be easy to determine how it travels through the gas handling system.

Other applications of positron producing isotopes can be thought of in fusion research but these examples give some idea of the possibilities; many of them could be tried out in a modest way on todays machines.

2.2. Other Scientific and Industrial Uses of Positrons

There are also many potential applications of positron sources in science and industry (chemistry, solid state physics, material science, positron microscopic, etc.)

One interesting possibility would be the production of positron sources. An ideal isotope for this is ^{22}Na produced from ^{22}Ne. ^{22}Na has a half life of 2.58 years which is long enough to incorporate into application sources but not so long that it will present a long-term radiation problem. A positron emitting

anode could be made from such a source; micro amp. sources of this type could easily be made. Such sources could have many applications. Some possibilities are:

(a) A positron source can make a unique gamma ray or hard X-ray source for X-raying objects.

(b) Positrons have proved to be a powerful tool for analyzing chemical compounds and for investigations in the solid state (Green et al. [13]; Brandt et al. [14]).

(c) It has been proposed that a positron microscope would have advantages over an electron microscope because it is possible to cool the positrons transverse energy to kT, whereas the electrons energy spread is given by their Fermi distribution.

(d) A positron source would make a unique tool for studying the earths magnetosphere and its dynamics. A positron beam will follow magnetic field lines and its detection is straight forward. Thus, it should be possible to trace the earths field lines and where they go. One should also be able to learn something about the dynamics of field lines and perhaps even detect reconnection events.

One should be able to measure how positrons are accelerated and scattered by turbulence in the magnetosphere; thus our understanding of these processes could be checked much more completely. Along this line one should also be able to follow what happens to positrons when they pass through the earths bow shock, see how they are energized, etc.

For these applications one would not employ PET scans but one would use the unique signature of positron annihilation for their detection.

ACKNOWLEDGEMENT

This work was supported by DOE Contract DE-FG03-86ER53225.

REFERENCES

1. R.W. Moir, "The Fusion-Fission Fuel Factory" *Fusion*, Volume 1, Part B, p. 411, ed. E. Teller, Academic Press, New York (1981).

2. J.M. Dawson, H.P. Furth, and F.H. Tenney, "Production of Thermonuclear Power by Non-Maxwellian Ions in a Closed Magnetic Field Configuration," *Phys. Rev. Lett.*, **26**, 1156 (1971).

3. M. Sajjad, R.M. Lambrecht, and A.P. Wolf, "Cyclotron Isotopes and Radiopharmaceuticals," *Radiochim. Acta*, **36**, 159 (1984).

4. J.M. Dawson, "Advanced Fusion Reactors," *Fusion*, Volume 1, Part B, pg. 465, ed. E. Teller, Academic Press, New York (1981).

5. C.D. Bowman, P.W. Lisowski, and E. D. Arthur, "Spallation-Based Science and Technology and Associated Nuclear Data Requirements," *Proceedings of the International Symposium on Advanced Nuclear Energy Research--Near-Future Chemistry in Nuclear Energy Field*, Mito City, Japan, January 22-26, 1990.

6 J.M. Dawson, "Non-Energy Applications for Fusion," *Fusion Technology*, **22**, 98 (1992).

7. J. Perkins, Lawrence Livermore National Laboratory, Private Communication (1985).

8. *Int. J. Res., Devel. Quality Assur.*, **28**, 33 (March 1986).

9. J.W. Coburn and H.F. Winters, "Ion- and Electron-Assisted Gas-Surface Chemistry -- An Important Effect in Plasma Etching," *J. Appl. Phys.*, **50**, 3189 (1979).

10. "Plasma Processing of Materials: Scientific Opportunities and Technological Challenges", *Panel on Plasma Processing of Materials, Plasma Science Committee, Board on Physics and Astronomy, Comission on Physical Sciences, Mathematics, and Applications, National Research Council*, National Academy Press, Washington, D.C. (1991).

11. A.S. Baltenkov and V.B. Gilerson, "Measurement of the Temperature of a Dense Plasma by Means of a Positron Annihilation," *Sov. J. Plasma Phys.*, **10**, 632 (1984).

12. J.M. Dawson and P.L. Pritchett, "Positron Production by Fusion Devices and Potential Applications," *Bull. A. P. S.*, **31**, 870, Abs. JG6, (1986).

13. J. Green and J. Lee, *Positronium Chemistry*, Academic Press, New York (1964).

14. *Proc. Positron Solid-State Physics,* International School of Physics, "Enrico Fermi", Course LXXXIII, Varenna, Italy, 1981; ed. by W. Brandt and A. Dupasquiter, North-Holland Publishing Co., Amsterdam (1981).

Magnetic Fusion Propulsion: Opening the Solar-System Frontier

John F. Santarius
University of Wisconsin–Madison
1500 Johnson Drive
Madison, WI 53706

ABSTRACT

The exploration and development of the Solar System require propulsion capabilities that only D-^{3}He magnetic fusion power appears able to deliver. Both conceptual design studies and generic arguments indicate that space propulsion systems based on D-^{3}He magnetic fusion reactors can provide performance dramatically beyond that of chemical, fission, and D-T fusion rockets for long-range missions. D-^{3}He fusion's capabilities include flexibility, a specific power of 1–10 $kW_{thrust}/kg_{reactor}$, and exhaust velocities up to ~0.2 c (c ≡ speed of light). Such capabilities, for example, allow two-month missions to Mars with the same payload as nine-month chemical missions or allow greatly increased payloads for longer durations. More distant missions, such as to the gas giant planetary systems, show D-^{3}He fusion to even better advantage. The mass estimates for D-^{3}He fusion propulsion systems can be made with some confidence, because the masses of the key components—shields, magnets, radiators, and refrigerators—can be calculated with good accuracy. The main uncertainties lie in the systems for input power and power conversion, but these corrections should only be tens of percent. Besides propulsion, fusion energy can provide power and materials processing capabilities. Three typical applications will be transporting humans and supplies to settlements, accessing the vast resources on asteroids and moons, and enabling scientific outposts analogous to antarctic bases. Thus, developing D-^{3}He magnetic fusion would open the Solar System to humankind.

1 INTRODUCTION

Every frontier motivates *exploration*, and space is no exception. The *development* of a frontier, however, inevitably awaits a *why*, usually an economic or political incentive. Yet a *why* alone is not sufficient for the development of a frontier—a *how* is also necessary. For space beyond Earth orbit, a major economic motivation may be the lunar resource of the isotope helium-3 (^{3}He) for use in terrestrial fusion power plants [1]. Eventually, humans will be tapping the even larger ^{3}He resources of the gas-giant planets, accessing the multitude of resources in the asteroids, and settling Mars and other Solar-System bodies. Thus, the *why* of space development exists, but the question of the *how* remains.

The outer Solar System has long been known to be beyond the capabilities of chemical rockets [2], and even very advanced systems such as gas-core fission or nuclear-electric propulsion greatly lose efficiency and attractiveness for destinations beyond Mars. The present situation parallels in many ways that of the American West in the year 1803, when Thomas

Jefferson is reported to have predicted that it would take 800 years to settle fully the newly acquired Louisiana Purchase [3]. Yet, in only 1907, Oklahoma achieved statehood—the last part of the Louisiana Purchase to do so. Why was Jefferson so far off in his prediction? He did not foresee the development of a new technology—the railway. Ironically, 1803 was the year in which the first public freight railway operated [4]. Solar System exploration and development require an analogous technology breakthrough. The thesis of this paper is that fusion power can be that enabling technology.

2 RATIONALE FOR ADVANCED SPACE PROPULSION SYSTEMS

Efficient long-range propulsion requires both a high specific power (ratio of the thrust power to the mass of the power and thruster systems) and a high exhaust velocity. This can be seen from the simplest form of the *rocket equation*, which is derived from momentum conservation for a rocket and its exhaust, assuming an impulsive thrust:

$$\frac{M_{final}}{M_{initial}} = \exp\left(\frac{-\Delta v}{v_{exhaust}}\right) \tag{1}$$

where M_{final} is the mass with which the rocket arrives at its destination, $M_{initial}$ is the initial rocket mass including propellant, $\Delta v \equiv \sqrt{2\Delta E/M}$ indicates the velocity increment for a mission requiring energy ΔE, and $v_{exhaust}$ is the exhaust velocity. Chemical rockets are limited to exhaust velocities of ~5,000 m/s, and a minimum-energy 9-month trajectory between the orbits of Earth and Mars requires a Δv of about 6,000 m/s. Thus, for either a significantly faster (higher energy) or larger-payload-fraction mission, a higher exhaust velocity is required. Nuclear thermal (NERVA) rockets can approximately double the chemical exhaust velocity, but this gains only an incremental capability. Nuclear electric rockets can reach high exhaust velocity, but at low specific power levels, so their acceleration is very low and trip times are long. Only fusion systems appear capable of achieving both the exhaust velocities and specific powers necessary for efficient Solar System development. The operating regimes for various propulsion systems are indicated in Fig. 1.

Rocket trajectory analysis and optimization is, of course, much more complicated than discussed above, especially including gravity and long thrust times. Nevertheless, the essential rationale for advanced propulsion remains qualitatively similar to that based on Eq. 1. Section 3 examines the reasons why fusion propulsion systems can be expected to operate in the interesting parameter regime at the center of Fig. 1, and Sec. 4 discusses the mission implications of achieving those capabilities.

3 CAPABILITIES OF FUSION PROPULSION

The high exhaust velocity for fusion derives from the high temperature of the plasma used to generate the fusion reactions. The fusion core plasma temperature of ~100 keV (~10^9 K) for a reactor fueled with deuterium (D) and helium-3 (^{3}He) actually gives an exhaust velocity too high for most Solar-System applications. If this plasma is directly

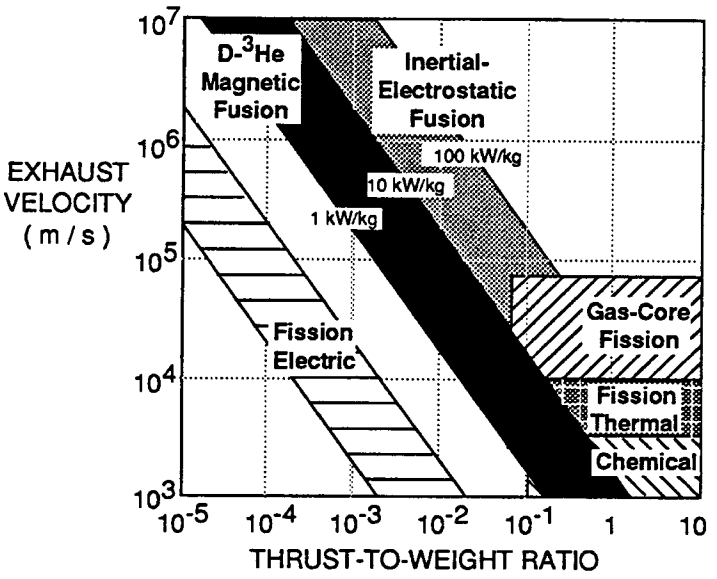


Fig. 1. Thrust-to-weight ratio and exhaust-velocity regimes for various space propulsion options.

exhausted, it must be diluted with other material, hydrogen for example, in order to reduce the plasma temperature and exhaust velocity while increasing thrust.

A high specific power, which allows useful thrust-to-weight ratios at relevant exhaust velocities, has been calculated in several fairly detailed recent conceptual design studies. Some of these are listed in Table I, as are two whose specific power was not calculated. These studies support the assertion that fusion will provide at least an order of magnitude higher specific power than typically predicted for the eventual performance of nuclear-electric propulsion systems. Note that the specific power goal for the SP-100 fission-electric space power plant is 0.03 kW/kg, even without a thruster system.

The magnetic fusion configurations required for space applications are generally at an early stage of development with regard to physics. Nevertheless, the total mass of the systems can be predicted with fair accuracy, because the masses of the key engineering components are well characterized. These components are the magnets, radiation shields, radiators, and helium refrigerators (for the superconducting magnets). A simple, generic fusion rocket model has been developed [5] and will be summarized in order to help give a qualitative understanding of the good performance calculated by the more detailed studies.

The generic model assumes cylindrical geometry, a LiH shield with 10% Al structure, magnet masses either current-density or virial-theorem limited, and the default parameter assumptions listed in Table II for mid-term (year 2020) and long-term (year 2050) cases. Both D-T and D-^{3}He fuels are treated, and optimization is done over the plasma density, plasma temperature, and shield thickness. The main results are shown in Fig. 2.

Table I. Some Recent Conceptual Designs Studies of Magnetic Fusion Reactors for Space Propulsion.

First Author	Year	Configuration	Specific Power (kW/kg)
Borowski [7]	1987	Spherical Torus	5.75
Borowski [7]	1987	Spheromak	10.5
Santarius [8]	1988	Tandem Mirror	1.2
Chapman [9]	1989	Field-Reversed Configuration	–
Haloulakis [10]	1989	Colliding Spheromaks	–
Bussard [11]	1990	Riggatron Tokamak	3.9
Teller [12]	1992	Dipole	1.0
Deveny [13]	1992	Tandem Mirror	4.3
Bussard [14]	1993	Inertial-Electrostatic	$\gg$10

Table II. Default Parameter Assumptions for the Generic Fusion Rocket Model.

Parameter	Mid-Term (2020) Cases	Long-Term (2050) Cases
β (P_{plasma}/P_{Bfield})	0.6	0.9
Surface heat flux limit, MW/m^2	5	10
Neutron wall load limit, MW/m^2	20	20
Magnet average current density, MA/m^2	50	250
He-refrigerator mass per heat pumped, kg/kW	1000	1000
Radiator: power rejected per unit mass, kW/kg	5	5
Transport power-to-thrust efficiency	0.8	0.8

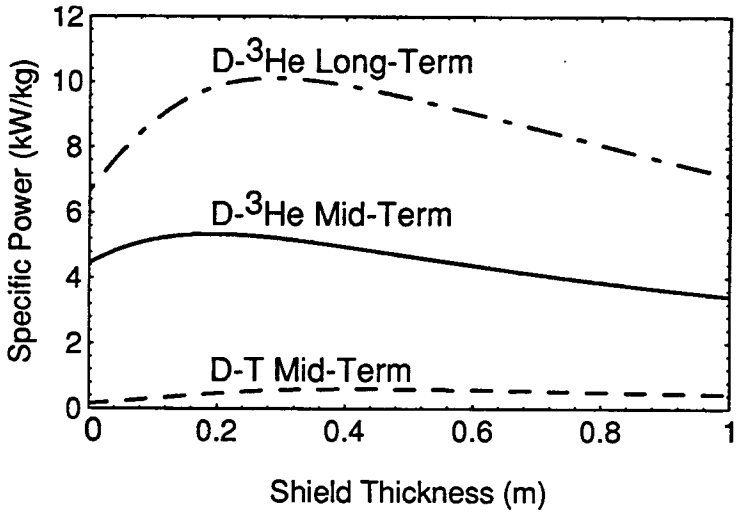


Fig. 2. Variation of specific power with shield thickness for D-T and D-^{3}He generic fusion rocket cases.

Both the detailed studies and the generic model find that D-^{3}He is the fuel of choice for space propulsion with magnetic fusion, as had been realized even in some of the earliest space fusion studies [6]. The reasons that D-^{3}He outperforms D-T, despite a lower fusion power density in the plasma, are the leverage gained by the high charged-particle fraction, which facilitates direct thrust, increases useful power and reduces radiator mass, and by the low neutron power, which reduces radiation shielding mass. Furthermore, the D-^{3}He fuel cycle does not require the very complicated tritium-breeding blanket and related systems necessary for D-T fuel. A fusion reactor burning D-^{3}He fuel also has the great political advantage over fission that no radioactive materials are present at launch and only low-level radioactivity is generated during operation.

4 MISSION IMPLICATIONS OF FUSION PROPULSION

The benefits of high exhaust velocity, even at low thrust levels, have been analyzed in detail [2]. For the present purpose of gaining a qualitative understanding of how magnetic fusion propulsion would enable Solar-System development, it suffices to look at two key missions in the approximation of transfer between circular orbits centered on the Sun. These missions are Earth–Mars and Earth–Jupiter. Fusion rockets at specific powers of 1 kW/kg and 10 kW/kg will be compared to chemical rockets.

Two typical applications will be considered: human transport and cargo transport. For humans, the key consideration is fast travel to avoid the harmful effects of low gravity, so the performance will be normalized by assuming the same payload fraction for each system. In the present context, 'payload' is defined as all of the mass delivered except the power and thrust systems (parameterized by specific power); that is, the rocket structure is part of

the 'payload.' Figure 3 shows that Earth-Mars travel times (one-way) can be reduced from the 260 days for a minimum-energy chemical-rocket trajectory to 53–80 days for a fusion rocket, while Earth–Jupiter travel can be reduced from 1000 days to 150–240 days [15]. On the other hand, for cargo transport, now comparing to chemical-rocket minimum-energy-trajectory transport times, Fig. 4 shows that Earth-Mars payload fractions can be increased from 33% to 83–91% and Earth-Jupiter payload fractions can be increased from 7% to 60–90% [15].

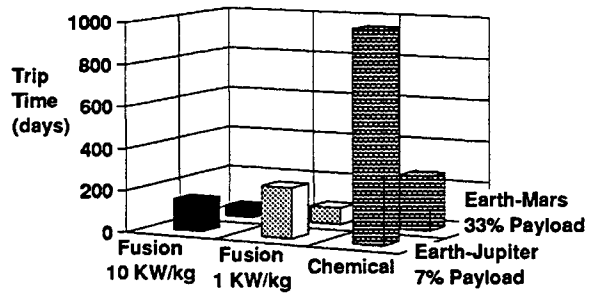


Fig. 3. One-way trip times for Earth-Mars and Earth-Jupiter travel, assuming chemical-rocket payload fractions.

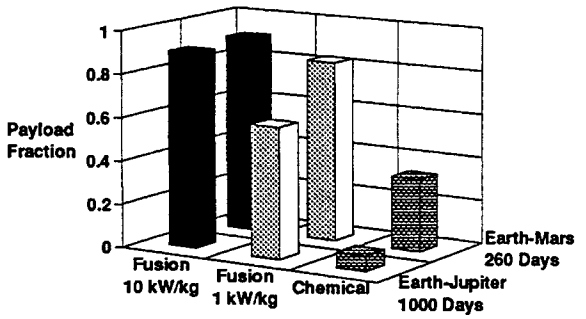


Fig. 4. Payload fractions for Earth-Mars and Earth-Jupiter travel, assuming chemical-rocket trip times.

This paper has focused on propulsion, but it is important to recognize that the fusion system which arrives at a destination has other applications. In particular, linear magnetic fusion systems could be converted with only a small mass penalty from producing thrust to producing electricity [16]. This would be accomplished by the installation of an electrostatic direct energy converter in the form of a spider-web conductor configuration. Another application for the system would be as a 'fusion torch' for processing materials [17]. Thus, a magnetic fusion system could provide efficient propulsion, power, and materials processing for many applications throughout the Solar System. Such magnetic fusion systems would enable

- human settlements on Mars and other rocky bodies or in space,
- scientific outposts near the gas-giant planets (analogous to antarctic bases), and
- access to the vast resources of the asteroids.

5 CONCLUSIONS

Detailed design studies calculate very attractive exhaust velocities (up to 10^7 m/s) and specific powers (1–10 kW/kg) for magnetic fusion propulsion systems, and a simple generic model has been used to understand this performance qualitatively. These performance levels would enable fast human transport or high-payload-fraction cargo transport throughout the Solar System. On this basis, I confidently predict that, as the train did in opening the American West, D-^{3}He magnetic fusion will open the Solar-System frontier.

ACKNOWLEDGMENTS

Useful discussions with Stuart Brandes and with colleagues in the UW Fusion Technology Institute are gratefully acknowledged. This research was supported by NASA and by the Grainger Foundation.

REFERENCES

[1] L.J. Wittenberg, J.F. Santarius, and G.L. Kulcinski, "Lunar Source of ^{3}He for Commercial Fusion Power," *Fusion Technology* **10**, 167 (1986).

[2] E. Stuhlinger, *Ion Propulsion for Space Flight* (McGraw-Hill, New York, 1964).

[3] W. Ley, *Satellites, Rockets and Outer Space* (Signet, New York, 1958).

[4] P. Hastings, *Railroads: An International History* (Praeger Publishers, New York, 1972).

[5] J.F. Santarius and B.G. Logan, "Generic Magnetic Fusion Rocket Model," *29th Joint Propulsion Conference*, paper AIAA-93-2029 (1993).

[6] G.W. Englert, "Towards Thermonuclear Rocket Propulsion," *New Scientist*, **16**:16, 307 (1962).

[7] S.K. Borowski, "A Comparison of Fusion/Antiproton Propulsion Systems for Interplanetary Travel," *23rd Joint Propulsion Conference*, paper AIAA-87-1814 (1987).

[8] J.F. Santarius, "Lunar ^{3}He, Fusion Propulsion, and Space Development," in *Second Conference on Lunar Bases and Space Activities of the 21st Century* (Houston, Texas, April 5–7, 1988) (NASA Conf. Pub. 3166, Vol. 1, p. 75, 1992).

[9] R. Chapman, G.H. Miley, and W. Kernbichler, "Fusion Space Propulsion with a Field Reversed Configuration," *Fusion Technology*, **15**, 1154 (1989).

[10] V.E. Haloulakos and R.F. Bourque, "Fusion Propulsion Systems," *25th Joint Propulsion Conf.*, paper AIAA 89-2629 (1989).

[11] R.W. Bussard, "Fusion as Electric Propulsion," *J. Propulsion and Power* **6**, 567 (1990).

[12] E. Teller, A.J. Glass, T.K. Fowler, A. Hasegawa, and J.F. Santarius, "Space Propulsion by Fusion in a Magnetic Dipole," *Fusion Technology* **22**, 82 (1992).

[13] M. Deveny, S. Carpenter, T. O'Connell, and N. Schulze, "Mirror Fusion Propulsion System: A Performance Comparison with Alternate Propulsion Systems for the Manned Mars Mission," *29th Joint Propulsion Conference*, paper AIAA-93-2094 (1993).

[14] R.W. Bussard and L.W. Jameson, "The QED Engine Spectrum: Fusion-Electric Propulsion for Air-Breathing to Interstellar Flight," *29th Joint Propulsion Conference*, paper AIAA-93-2006 (1993).

[15] J.F. Santarius, "Magnetic Fusion for Space Propulsion," *Fusion Technology* **21**, 1794 (1992).

[16] J.F. Santarius, G.L. Kulcinski, L.A. El-Guebaly, G.A. Emmert, H. Khater et al., "Critical Issues for SOAR: The Space Orbiting Advanced Fusion Power Reactor," *Space Nuclear Power Systems 1988*, p. 161 (Orbit, Malabar, Florida, 1989).

[17] B.J. Eastlund and W.C. Gough, "The Fusion Torch—Unique Applications of Ultra-High Temperature Plasmas," *British Nuclear Energy Soc. Nucl. Fusion Reactor Conf.*, p. 410, Culham Laboratory, England (1969).

5) Lunar Mining and Non-Lunar ^{3}He Resources 145
L.A. Haskin, Chair

5-1 The Lunar Environment and He-3 Mining 147
W.D. Carrier, III

5-2 Coaxing He3 from Lunar Regolith; Processes and Challenges 149
Igor N. Sviatoslavsky

5-3 Cost of ^{3}He from the Moon 159
Howard E. Thompson

5-4 Potential ^{3}He Resources for D-^{3}He Fusion Development 173
William R. Wilkes

5-5 Non-Lunar ^{3}He Resources 179
Layton J. Wittenberg

The Lunar Environment and He-3 Mining

W. David Carrier, III
Bromwell & Carrier, Inc.
P.O. Box 5467
Lakeland, FL 33807-5467

ABSTRACT

The primary environmental factors that must be considered for human operations on the lunar surface are: (1) Low gravity: 1/6-th that of Earth; (2) Hard vacuum: less than 10^{-8} torr; (3) Fourteen Earth-days of sunlight and fourteen days of darkness; (4) Thermal extremes at the surface: typically -170°C to 110°C; (5) Thermal near-constancy below 1 m: about -20°C (due to the insulating properties of granular soil in vacuum); (6) Cosmic radiation and solar flares: humans cannot be exposed on the surface for long periods; and (7) Dust: the lunar soil is very fine and, because of electrostatic charge, adheres to spacesuits, metal fittings, optical lenses, etc. Housekeeping is a major headache.

However, there are definite advantages from a mining point of view: except for solar flares, the "weather" on the Moon is precisely predictable and there is no wind, rain, snow, or ice. Furthermore, there is no overburden to be stripped: the ore is the surficial lunar soil and is directly accessible.

The top few centimetres of lunar soil are loose and fluffy, but the density increases very rapidly with depth. Just to 5 to 10 cm below the surface, the soil density is much greater than can be accounted for by the weight of the overlying soil; denser, in fact, than could be achieved with heavy compaction equipment on Earth. This phenomenon is due to meteorite impacts, which stir and loosen the surface, and at the same time, shake and densify the underlying soil. As a result, the lunar soil is quite strong and is capable of supporting virtually any conceivable structure.

Trafficability on the lunar surface is well-understood: The energy consumed by the rolling resistance of the soil is small compared to other energy losses, most notably inertia. The cruising speed of a lunar roving vehicle is limited by surface roughness and terrain to about 6 to 7 km/hr. Slope-climbing of a wheeled-vehicle is limited to 23° without grousers; and to about 30° with grousers.

Excavation on the lunar surface, whether for mining or habitat installation, will require mechanical equipment. Vertical faces in the lunar soil can be excavated to a depth of 2 to 3 m. Once excavated, the lunar soil cannot be re-compacted to its original *in situ* density and, consequently, it will occupy about 15% more volume.

NO PAPER RECEIVED

Coaxing He3 from Lunar Regolith; Processes and Challenges

Igor N. Sviatoslavsky
Fusion Technology Institute
University of Wisconsin-Madison
1500 Johnson Drive
Madison WI 53706

ABSTRACT

The identification of large quantities of He3 on the moon in 1985 has rekindled the prospects for near aneutronic fusion and all the benefits which accrue from it. Although the total amount of He3 on the moon is enormous, it exists in the lunar regolith in a very dilute form. It has been shown that the samples of lunar regolith brought back by the Apollo astronauts and the Russian LUNA robots, give up most of their trapped solar wind products upon heating them to 700°C. The major challenge in extracting He3 from lunar regolith is the large amount of material that must be processed. There are many other challenges such as the most suitable source of process energy and the means of delivering it, the problem of working in the vacuum of space as well as the separation of the solar wind products. This paper will describe the UW Mark II lunar miner and the processes that are needed in order to end up with pure liquid He3, ready to be shipped to earth for use in D-He3 fusion reactors.

1. INTRODUCTION

The concept of aneutronic fusion reactors has been and will continue to be the ultimate dream of fusion reactor designers. The fact that the tokamak may not be the most suitable device for burning D-He3 plasmas should not detract from this vision. For those of us who have struggled for many years to design DT fusion reactors in which the first wall and blankets have to be periodically replaced, the concept of a permanent non-breeding shield which is a reactor lifetime component is a breath of fresh air.

If the concept of D-He3 fusion is ever to be realized, however, it means the return of man to the moon and the invoking of a rather large mining operation. There simply is not enough easily accessible He3 on earth to even contemplate starting such a power economy [1]. Obtaining He3 on the lunar surface requires a fairly sophisticated operation involving lunar robots with multifunctional capabilities. Because He3 is found in the lunar regolith in a very dilute form (10 ppb), a large amount of material has to be processed in order to obtain a small amount of He3. The biggest challenge is, therefore, to design a machine which will process a high volumetric throughput of lunar regolith with the least amount of handling. Thus the concept of digging up the regolith and transporting it to a central processing station is simply not practical. More in line with what is needed is similar to a farm combine, which harnesses the grain while leaving behind the stalks. The concept of the Mark II miner was thus born from these considerations. This machine excavates the regolith to a depth of 3 m, beneficiates it to the desired size, heats it and cools it to release the solar wind products, and finally returns the regolith back to the lunar surface while collecting and storing the solar wind products. The total distance which the regolith travels within the miner is ~10 m, and the effect on the lunar landscape is a slight fluffing up and rippling of the surface. The miner can cover one square kilometer per year, operating only during the lunar day and can obtain ~33 kg of He3 in the

process. At the same time, huge quantities of He4, H_2, N_2, CO, CO_2 and CH_4 are obtained, which are essential materials for supporting a lunar colony on the moon. This paper will describe the operation of the Mark II lunar miner and will outline the processes needed for separating the He3 from the remaining solar wind products.

2. DESCRIPTION OF THE MARK II MINER

Figure 1 is a CAD (Computer Aided Design) rendition of the miner as presently envisaged operating on the lunar landscape. The most prominent feature of the miner is the large 12 m diameter solar collector which is mounted on a tower capable of 360° rotation about a vertical axis and the ability to tilt the collector about a horizontal axis going through the support gimbal. Energy is beamed to the collector from a large 110 m diameter solar dish mounted at some distance on the lunar landscape. Approximately 70 cm of the outer perimeter of the 12 m dish is devoted to photovoltaic cells capable of generating 200 kW of electric power. The solar energy is beamed into the miner and is distributed onto surfaces immersed in liquid sodium. Heat pipes are used to transfer the energy to the regolith.

At the front of the miner a bucket wheel excavator executes a 150° arc as it cuts into the regolith in front of it. The trench which is opened up is 3 m deep and 11 m wide. The regolith is dumped onto a conveyer belt which drops it into the miner onto a set of progressively smaller sieves. All of the fraction which does not pass the sieves is immediately returned to the trench. This can be seen coming out of the first return pipe of which there is one on each side of the miner. The remaining fraction which is reduced to particles smaller than 250 μm now must be transferred from the lunar vacuum to the miner operating pressure. This is accomplished by two power screws or augers. Once inside the miner proper, the regolith is injected into a flowing stream of gas moving at a predetermined velocity. Particles smaller than 100 μm are fluidized and carried upwards in the gas stream. Those that are larger fall down into the bottom of the fluidizing cylinder and are ejected from both sides of the miner into the trench. They can be seen coming out of the second pipe forming a mound on either side of the miner.

The regolith which makes it through the fluidized bed goes through a cyclone separator which centrifugally separates the particles from the gas. The gas goes back to a fan where it is pumped back into the fluidizer cylinder. The regolith, which now consists of particles smaller than 100 μm is dumped into hoppers which surround a heat exchanger consisting of heat pipes. There are three parts to this heat exchanger, a preheater, a supplemental heater and a recouperator. Some heat pipes shuttle energy from the bottom of the heat exchanger to the top. Thus, energy which is recovered from the hot exiting regolith is transferred to the top of the heat exchanger for preheating the cool incoming regolith. The supplemental heater which is nested between the preheater and recouperator sections of the heat exchanger only supplies the energy which is not recovered by the recouperator, ~15% of the total. This is done by using the collected solar energy for boiling sodium in a boiler connected to a series of heat pipes. The processed regolith, which is only a 100° hotter than its ambient temperature on the lunar surface, now goes to a differentially pumped ejection chamber from which it is ejected through a reciprocating nozzles out the back of the miner. By reciprocating the ejection nozzles, the trench is filled up relatively uniformly, minimizing the effect on the lunar landscape.

As the regolith percolates through the maze of heat pipes which are on a triangular pitch, it is preheated to 600°C, then heated to 700°C in the main heater and finally, cooled to 100°C in the recouperator. The residence time of a particle in the heater is 20 s. During this time, which

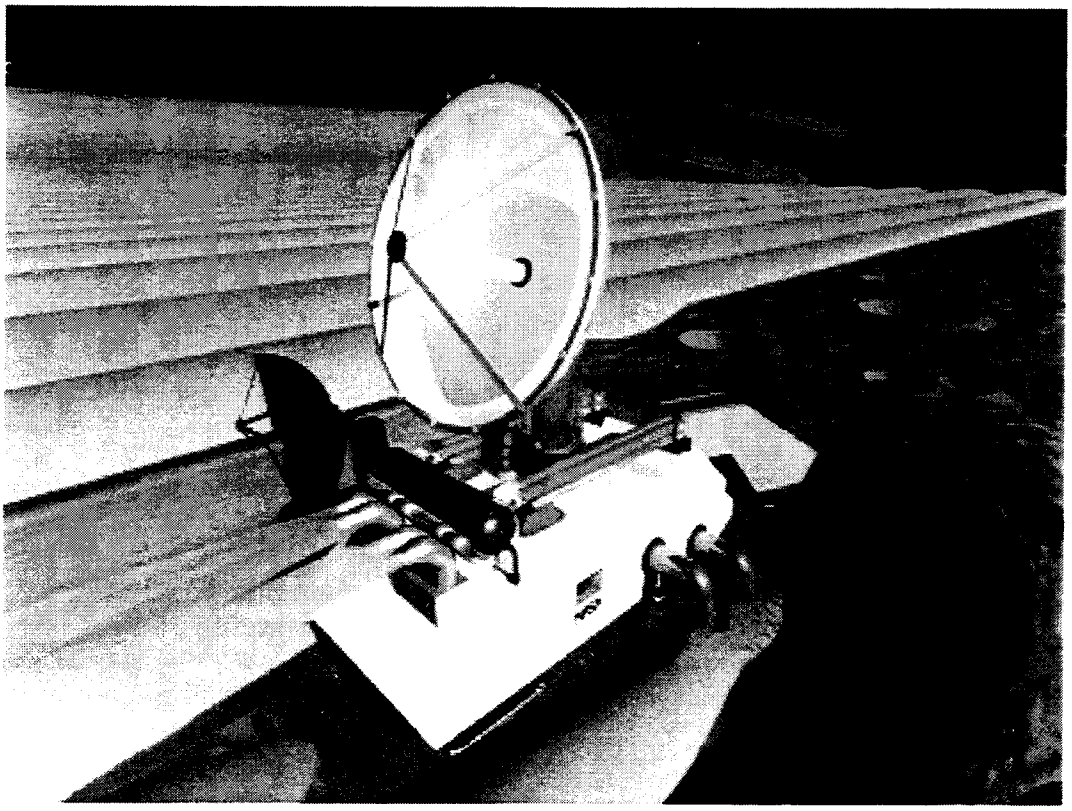


Fig. 1. Picture of the Mark II miner.

is very long compared to the diffusion time of gas from the particles, the solar wind products emerge from the regolith and are pumped into high pressure cylinders. One such cylinder is shown on the back of the miner. As the cylinder reaches 20 MPa, it is disconnected and, with the use of manipulators shown on either side of the miner, it is removed and placed on the side of the trench. An empty cylinder is picked up and connected and the miner proceeds forward. Table 1 gives the pertinent parameters of the miner.

3. LUNAR VACUUM/MINER ATMOSPHERE INTERFACE

One of the several challenges of lunar He3 mining is the issue of dealing with the vacuum of space. Inserting the regolith from lunar vacuum into the miner interior which is at one atmosphere and back out again without the loss of solar wind products is not an easy task. A batch process using several valve operated systems was considered and rejected [2]. The system which has been adopted is a power screw or auger. It is estimated that 3 units of 0.8 m diameter each rotating at 35 rpm will be needed to transfer ~340 m^3/h of lunar fines into the interior of the miner. These screws which are 1.5 m long will be two staged, such that the volume separating the stages can be evacuated by a vacuum pump to an intermediate pressure on the order of 380 torr. As long as the velocity of the regolith in the power screws exceeds the diffusion rate of gases through the regolith columns, there will be no losses of solar wind products. The estimated

Table 1. Pertinent Miner Parameters

Annual collection rate of He-3 (kg)	33
Mining hours per year	3942
Excavating rate (tonnes/hr)	1258
Depth of excavation (m)	3
Forward speed of miner (m/hr)	23
Area excavated per year (km^2/y)	1.0
Processing rate (tonnes/hr)	556
Lunar process energy (MW)	12.3
Heat recovery (%)	85
Estimated operating electric power (kW)	200

diffusion rate of H_2 gas through 38% void fraction regolith is ~60 cm/s while the velocity of the regolith in the conveyer is 140 cm/s.

Similar power screws will be used at points where regolith must be returned to the lunar surface, such as after beneficiation and at the final ejection after heating. Staged units will be used again but the intermediate chamber will be evacuated to ~1 torr. The loss of solar wind products is estimated to be <0.1%. The total power requirement for all the power screws is ~10 kW.

4. BENEFICIATION

Some 80% of all the solar wind products are concentrated in particles smaller than 100 μm. Two methods of beneficiation have been considered; electrostatic separation and fluidized beds. Considering the large volumetric throughput that is needed, the fluidized bed is more suitable than an electrostatic separator and for this reason has been selected for the Mark II miner.

Fluidized beds are routinely used in the chemical industry for transporting, drying and separating many kinds of materials. The minimum fluidization velocity, defined as the point at which the particles begin to separate from each other, depends on the particle size, particle and fluidizing medium densities, particle shape factor, fluidizing medium viscosity and acceleration due to gravity. For He gas at one atmosphere and 300 K, and particles of 100 μm, the minimum fluidization velocity is 5.4×10^{-3} m/s. The terminal velocity is what determines the gas volumetric throughput and is the point at which the particles begin to rise upwards. For these conditions the terminal velocity is 0.5 m/s. Using this velocity in a fluidizing chamber of 1.5 m diameter and 3 m high, the pressure drop if 5 kPa and the pumping power ~3.5 kW [3,4].

The power screws deliver the regolith approximately midway of the miner height and would be appropriately located for injection into the fluidized bed. As the particles caught in the gas stream move upwards, they are deflected to the periphery of the cylinder by a cone on the top of the cylinder. Here the cylinder converts to a cyclone separator where the centrifugal force separates the particles from the gas. At this elevation the particles enter the chutes leading to the heater.

5. HEATER

Another major challenge of He3 mining on the lunar surface in the supply of process energy. For example, assuming a 10 ppb concentration, in order to obtain one gram of He3, 150 tonnes of lunar regolith must be excavated and 66 tonnes of lunar fines must be processed requiring 37 GJ of heating energy. One obvious conclusion that comes out of this set of circumstances is that energy must be recycled if He3 acquisition is to proceed at a reasonable rate. Figure 1 shows solar energy being beamed into the miner through the tower supporting the solar collector. This section will describe how this energy is used to heat the regolith fines.

Figure 2 is a side view of the heater which is 5.4 m wide, 2 m deep and 3 m high, and consists entirely of heat pipes with no moving parts. In the vertical direction, the heat pipes are divided into three primary zones, the preheater, the supplemental heater and the recouperator. The regolith flows by gravity through the left and right enclosures which contain the straight parts of the heat pipes, while the U shape is the isothermal part of the heat pipes. Each enclosure is 1 m long and 2 m wide, accommodating 188 heat pipes per row. Figure 2 also shows a temperature profile of the regolith as it flows through the heat exchanger. It enters the heat exchanger at 300 K and exits at 400 K. The heat pipes in the low temperature end of the recouperator transfer heat to the low temperature end of the preheater. As the regolith works its way through the 3 m high maze of heat pipes it progressively encounters higher temperatures until it exits the supplemental heater at 700°C and then it begins to cool down in the recouperator. We feel that staged heat pipes operating with water, mercury, potassium and sodium can be used to provide the temperature progression which is needed for this design.

Figure 3 shows two views of the supplemental heater with an enlargement showing details of the heat pipes in the boiler section. Solar energy enters through a flange which is sealed to the oven housing, and is distributed onto surfaces immersed in liquid sodium in the boiler. In this way, the oven enclosure is sealed from the lunar vacuum. As the sodium evaporates it flows into the heat pipes where it condenses and flows back to the boiler through the wicks. To determine the heat transfer coefficients it was necessary to obtain an effective thermal conductivity for the regolith. The bulk of the released gas in the oven is He and H_2 both of which have very high conductivities down to pressures of a few torr. We have used the Deissler Boegli method for determining the k_{eff} which is given as a function of the ratio of conductivity of the solid to that of the gas. The conductivity and the specific heat of ilmenite as a function of temperature was taken from the 1980 Handbook of Lunar Materials [5]. Having calculated the Reynolds and Prandtl numbers we use the Dietus Boelter formulation to obtain the Nusselt number and the heat transfer coefficients. Using a pressure of 0.1 MPa of He + H_2 gas we obtain heat transfer coefficients ranging from 1180 W/m^2K at 300 K to 1470 W/m^2K at 750 K. We have benchmarked these values against experimental work performed at the UW in 1980-1982 [6] and have found remarkable agreement.

In calculating the heat transfer areas needed we assume 1.5 cm diameter heat pipes spaced on a triangular pitch at 1.7 cm between centers. The effective vertical velocity of the regolith through the heat exchanger is 15 cm/s. We have used a temperature difference of 50°C between the regolith and the heat pipes. This means that the temperature of the regolith will be 400 K when it is replaced on the lunar surface, giving an energy recovery of 85% in the recouperator. At this regolith velocity erosion should not be a problem and since heat pipes operate essentially isothermally, liquid metal corrosion will not exist. Assuming the preheater and recouperator are

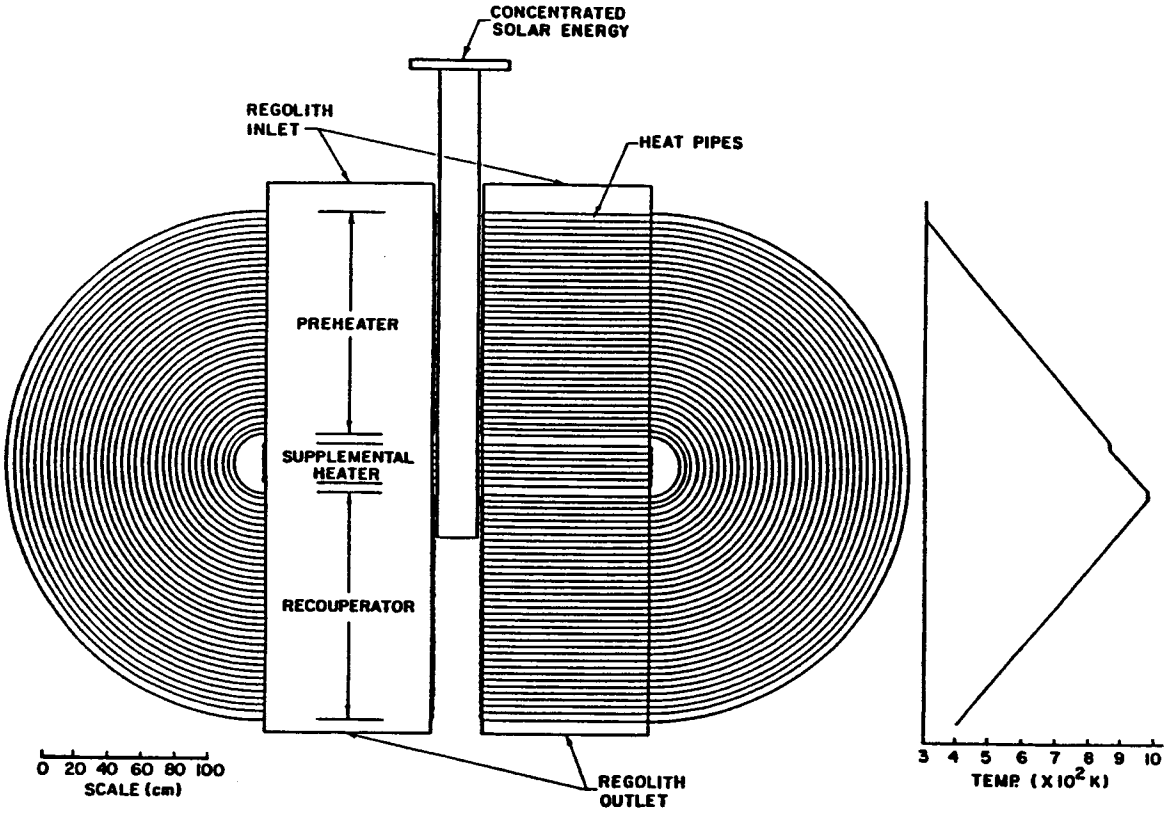


Fig. 2. Side view of the lunar miner heater.

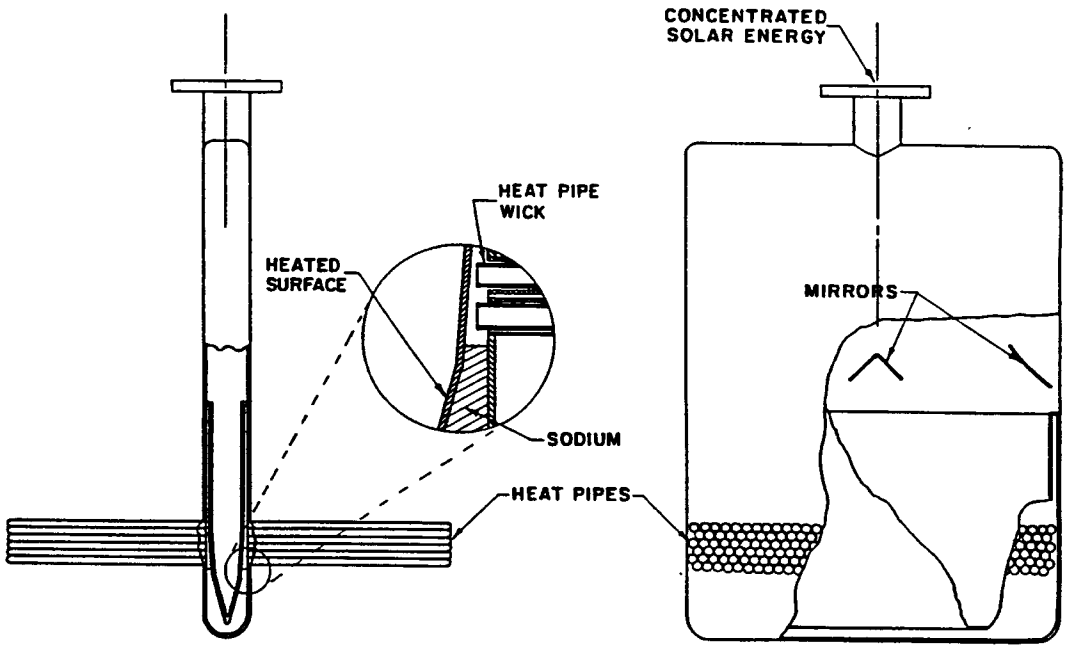


Fig. 3. Several views of the supplemental heater

Table 2. Parameters of the Heater

	Preheater	Supplemental Heater	Recouperator
Regolith inlet temp. (K)	300	873	973
Regolith outlet temp. (K)	873	973	400
Mass flow rate (kg/s)	154.4	154.4	154.4
Actual regolith velocity (m/s)	0.20	0.20	0.20
Heat transfer area (m^2)	1012	187	1012
Depth of zone (m)	1.36	0.255	1.36
Regolith residence time (s)	9.1	1.7	9.1

made of stainless steel, and the supplemental heater from a molybdenum alloy, and using a heat pipe wall thickness of 0.25 mm, the total mass of the heater will be ~9 tonnes. Table 2 gives the parameters of the heater.

A heater which recovers 85% of the process energy means that only 5.6 GJ of solar energy will be needed to obtain one gram of He3. The limiting parameter for the He3 acquisition rate now falls on the rate of excavation instead of the rate of energy supply.

6. SOLAR WIND PRODUCTS COLLECTION

As the solar wind products are released from the regolith fines, they are collected in pressure vessels mounted on the miner. A three stage compressor with intercooling is used to maintain the pressure in the miner at 0.1 MPa while delivering the gases to the pressure vessel which is pumped up to 20 MPa. The power requirement of the compressor is 50 kW.

When a cylinder is full, it is disconnected from the supply line and removed from the miner by means of two robotic arms shown in Fig. 1. The cylinders are deposited on the mined side of the trench where service vehicles pick them up and take them to a central processing unit. A new cylinder is picked up on the unmined side of the trench, connected to the supply line and the operation can then proceed.

7. REGOLITH EJECTION

After going through the heater, the regolith fines are conveyed through the vacuum barrier by means of staged power screws where the intermediate stage is pumped out to ~1.0 torr. At this pressure the solar wind product losses are very low, <0.1%. The final step which the regolith undergoes is ejection from the miner back onto the lunar surface. This is accomplished by means of rotating paddles which fling the regolith through reciprocating nozzles located on the back of the miner.

8. ESTIMATED POWER BUDGET FOR THE MARK II MINER

The largest amount of power is required for the bucket wheel excavator and here, the lion's share is needed to overcome the shear strength of the lunar regolith. At a depth of 3 m, the normal stress of the soil is 8.8 kPa, and for an 80% relative density, the cohesion is 1.4 kPa at a

Table 3. Power Budget for the Mark II Miner

Locomotion	10
Excavation	75
Regolith transport	5
Power screws	10
Fluidized bed	4
Compressor	50
Vacuum pumps	2
Ejection mechanism	5
	161

friction angle of 48° [7]. This gives a shear stress at 3 m depth of 11 kPa. Using this value and a lift of 3 m, to excavate 21 tonnes/min (or 3.5 tonnes/min on the moon), the estimated power is 75 kW. The next largest requirement is that of the compressor at 50 kW. Table 3 gives the estimated power requirement for the remaining systems. The total requirement is ~161 kW, which is 190 kW assuming 85% motor efficiency.

9. SEPARATION OF SOLAR WIND PRODUCTS

The pressure cylinders which contain the solar wind products are equipped with palladium membranes which act as windows for H_2 but do not allow other gases to diffuse through. It is assumed that most of the H_2 will have diffused to one side of the cylinder by the time the gases are prepared for separation. The solar wind gases will be cooled from 300 K down to 40 K in a radiator which radiates to outer space during the lunar night. The radiator will consist of tubes attached to the back side of plates with some fins for surface enhancement. The gases will be continuously circulated through the radiator, and as each species begins to condense, it will drain out into a vessel and will be stored in liquid form.

Figure 4 is a plot of the radiator area time product in m^2h as a function of temperature, needed to cool the He, and condense the remaining volatiles for obtaining 1.0 kg of He3. The mass of the radiator is not included since it can be shielded from the sun and kept cold during the lunar day. The vertical lines on the graph represent condensation temperatures of the species. Nitrogen is the last to condense at ~78 K at this pressure. We selected 40 K as the temperature at which the He is fed into a cryogenerator for further cooling and liquefying.

It can be seen that a radiator area time product of 3.2×10^5 m^2h is needed to obtain a kg of He3. If this is done during one lunar night, this implies an area of ~950 m^2 or 31.0 m × 31.0 m. The radiator can be made of aluminum to minimize the mass and has an earth weight of ~6 tonnes. We estimate the compressor power for circulating the gases at ~0.5 kW.

10. SEPARATION OF He ISOTOPES

The remaining stream of He4 and He3 at 40 K is now fed into a cryogenerator for further cooling and liquefaction. Assuming this process takes place during the lunar day using solar energy to power the cryogenerator, an estimate of the power requirement was made for separating one kg of He3. Table 4 gives the estimated work and power requirements assuming 17% of Carnot efficiency for all three stages of cooling and liquefaction. The time allocated for

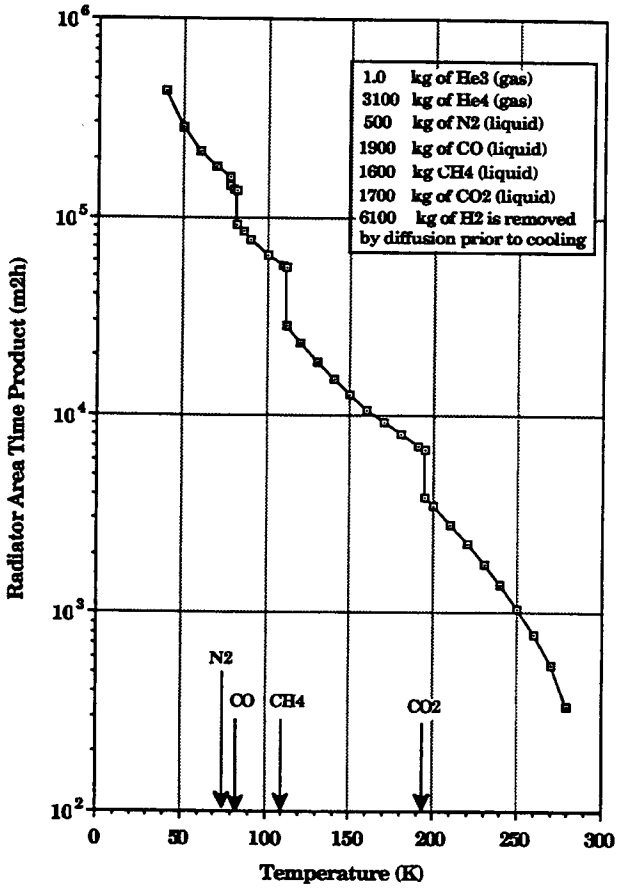


Fig. 4. Radiator area time product as a function of temperature.

Table 4. Cryogenerator Parameters

	Cooling 40 K - 4.4 K	Liquefying 4.4 K - 4.2 K	Subcooling 4.2 K - 1.6 K
Ideal work (J/kg-He4)	1.66×10^5	2.27×10^4	4.68×10^3
Actual work (J/kg-He4)	9.78×10^5	1.33×10^5	2.75×10^4
Actual work (J/kg-He3)	3.03×10^9	4.12×10^8	8.53×10^7
Room temp. work (J/kg-He3)	1.21×10^{11}	1.24×10^{11}	8.53×10^{10}
Number of days allotted	5.14	5.25	3.61
Power requirement (kW)	273	273	273

each process is determined by making the needed power the same for each process assuming the processes are carried on in series. In real life there will be a lot of overlap between these processes and the actual power requirement will be somewhat lower than the estimated 273 kW. Furthermore, modern cryogenerators have been achieving Carnot efficiencies of 40-45% in units with capacities of >1 kW of refrigeration at 4.2 K [8].

Once the He is cooled to 1.6 K, a superleak separator is used to enrich the He3/He4 ratio from 4×10^{-4} to ~10^{-2}. Cryogenic distillation is then employed for a separation of >99% of He3 [9]. The nearly pure liquid He3 is then shipped to earth for use in D-He3 reactors.

11. CONCLUSIONS

Coaxing the He3 atoms from lunar regolith will require overcoming many challenges, of which only the most obvious have been mentioned in this paper. It appears that the limiting aspect for the acquisition process is the rate at which regolith can be excavated. A multipurpose mobile mining machine which handles the regolith as little as possible is found to be most suitable for this operation. Energy recycling is essential if a reasonable acquisition rate is to be achieved. A mobile miner can cover one square kilometer of lunar surfaces to a depth of 3 m in one year, operating during the lunar days, while harvesting 33 kg of He3. Such a miner needs ~200 kW of electric power to operate and will be controlled telerobotically. Many issues still need further investigation not the least of which is the problem of tribology and dealing with the lunar dust.

REFERENCES

[1] L.J. Wittenberg, "Non-Lunar He-3 Resources," these proceedings.

[2] I.N. Sviatoslavsky, "The Challenge of Mining He-3 on the Lunar Surface: How All the Parts Fit Together," *Engineering Construction and Operations in SPACE IV*, Albuquerque, NM, Feb. 26-March 3, 1994, to be published.

[3] N.P. Cheremisinoff and P.N. Cheremisinoff, *Hydrodynamics of Gas-Solids Fluidization*, Gulf Publishing Co., Houston, TX (1984).

[4] I.N. Sviatoslavsky, "Lunar He3 Mining: Improvements on the Design of the UW Mark II Lunar Miner," SPACE'92, *Proceedings of the Third International Conference on Engineering, Construction and Operation in Space*, Denver, CO, June 1992.

[5] "Handbook of Lunar Materials," NASA Reference Publication 1057, Feb. 1980.

[6] R.E. Nietert, "Heat Transfer Characteristics of Flowing and Stationary Particle Bed Type Fusion Reactor Blankets," Ph.D. Thesis, UW Madison, WI (1982).

[7] "Lunar Sourcebook," Edited by Grant Heiken, David Vaniman and Bevan M. French, Cambridge University Press, Sept. 1990.

[8] T.R. Strobridge, "Cryogenic Refrigerators - An Updated Survey," NBS Technical Note 655, U.S. Government Printing Office, Washington, DC (1974).

[9] W.R. Wilkes and L.J. Wittenberg, "Isotopic Separation of He3/He4, From Solar Wind Gases Evolved From Lunar Regolith," SPACE'92, *Proceedings of the Third International Conference on Engineering, Construction and Operation in Space*, Denver, CO, June 1992.

[8] T.R. Strobridge, "Cryogenic Refrigerators - An Updated Survey," NBS Technical Note 655, U.S. Government Printing Office, Washington, DC (1974).

Cost of ^{3}He from the Moon

Howard E. Thompson
School of Business
University of Wisconsin-Madison
Madison WI 53706

ABSTRACT

The purpose of this report is to estimate the cost of ^{3}He from the Moon. Any estimate of this cost must be based on assumptions regarding the scale of ^{3}He use on earth and therefore the scale of the lunar mining operations, whether or not manned lunar scientific bases are present on the Moon, and whether or not volatiles extracted from the lunar regolith can be "sold" to the lunar colony. The calculations will be made assuming a "Lunar Mining Company" exists which holds the US monopoly on mining ^{3}He on the Moon and which sells ^{3}He to terrestrial electric utilities and provides volatiles to the lunar scientific bases. The cost effectiveness of ^{3}He fusion plants in competing with coal and fission plants will determine both the extent to which the lunar company can earn its cost of capital and the price of ^{3}He to terrestrial utilities.

1. INTRODUCTION

In order to assess the feasibility of using ^{3}He from the Moon in a D-^{3}He fuel cycle it is helpful to assume the existence of a lunar mining company (LMCo) which holds a monopoly on lunar mining. It alone mines, transports and markets ^{3}He for the United States. It is useful to segregate the costs of obtaining the lunar fuel into the following categories: i) mining equipment, labor, and habitat costs; ii) launch costs; iii) profits; and iv) taxes. Estimates of the impact of each of these cost categories on the cost per gram of ^{3}He will be developed. The profits and taxes components of the price of ^{3}He will depend on the costs of capital which, in turn, will depend on the risks of operating a lunar mining company as perceived by the financial markets. The cost of capital is the investor required rate of return that the LMCo would have to earn, after taxes, on its investment in order to engage in mining, transportation, and marketing ^{3}He. Since it depends on the investors' perceptions of the risks and returns on the project, it cannot be readily measured in the abstract. In addition to estimating the price of ^{3}He, since fusion using ^{3}He must compete with coal and fission, the costs of generating electricity using these three alternative approaches must be compared. This means it is not only the price of ^{3}He as a fuel that is important but the costs to build, maintain and operate fusion, coal and fission plants as well. An estimate of the cost per kwh of electricity using fusion, coal and fission will also be compared.

An added cost of supplying ^{3}He, which is not included in the categories described, is the *additional* flow of Space R&D expenditures that are necessary to develop lunar mining technology and capability. These expenditures are sizable but uncertain. They are also "up-front" outlays made many years before initiation of mining operations. Thus they add considerable risk that must be borne by someone. If the LMCo must pay for the *additional* Space R&D costs associated with the development of ^{3}He mining and its investors must absorb the risk, the price of ^{3}He must necessarily be higher than if the LMCo did not have to bear these costs and risks. An alternative to having LMCo investors financing the R&D activity would be for the government to take over R&D efforts thus spreading the risk over

all members of society. This alternative would not only make lunar mining activities by private enterprise feasible, it could also provide substantial cost savings for future Moon and Mars scientific bases. If, in return for the R&D financing, some or all of the volatile by-products of mining ^{3}He could be made available to the Government's Moon and Mars bases, some launch costs necessary to bring consumables for these bases could be avoided. This paper also analyses the cost-benefit trade-off of government financed R&D in return for later launch cost avoidance in obtaining consumables for Moon and Mars bases.

It is assumed that the first lunar mining of ^{3}He will take place in 2015 when the first commercial D-^{3}He fusion power plant could be available. The scale of Lunar mining that is necessary to supply ^{3}He fuel would be initially quite small consisting of the production of a single miner. The scale of mining activity by the middle of the 21st century is assumed to be on the order of 64 tonnes of ^{3}He per year.

Section 2 develops the cost of ^{3}He assuming that all R&D costs are covered by the government in return for future delivery of all volatile by-products of producing ^{3}He. Section 3 estimates the cost of electricity using coal, fusion, and fission plants based on the cost development of section 2. Section 4 analyzes the costs of R&D and benefits of by-product production to scientific bases on the Moon and Mars. Section 5 is a summary of the paper. The appendix contains the formulas used in the calculations. All costs quoted in the remainder of the paper are in 1993 dollars.

2. COSTS

2.1. Costs of the Labor, Mining Equipment and Habitat

The current designs for the miner [Sviatoslavsky and Jacobs, 1988] are for a system that scoops up lunar soil to the depth of 60 cm in front of the robotic unit. Only particles less than 100 microns in diameter are retained with the rest immediately returned to the surface. These retained particles are heated to 700°C on the miner. The gases (^{3}He, ^{4}He, H_2, H_2O, N_2, and C compounds) are collected and the spent lunar soil is dropped off the back of the miner. The miner and associated equipment used to separate ^{3}He would have an earth mass of approximately 50 tonnes [Kulcinski, Sviatoslavsky, et. al.,1989, Sviatoslavsky and Jacobs, 1988]. It could mine 33 kg of ^{3}He per year and would have a life of 20 years.

It is assumed that the personnel required to operate the miner roboticly will be three persons per miner (assuming three shifts per day). Consumables and living habitat would be 820 kg per person per year [Bula et. al.,1990].

It is also assumed that each miner and associated equipment would cost \$200/kg to fabricate and have a purchase price on earth of \$10,000,000. The uniform annual cost component of the miner can then be divided into three components: the depreciation; the net return or profit after taxes on the investment in the miner; and the income taxes arising from the gross return on investment. The depreciation charge on the miner, using straight line depreciation over a 20 year life, is \$15.15/g of ^{3}He produced. The net profit after taxes and

the income taxes are dependent on the cost of capital. These costs are shown in Table 1 for three values of the cost of capital. To estimate the labor cost it is assumed that each human will receive salary and fringe benefits of $500,000 per year. Thus the costs of labor to keep one miner running three shifts a day will be $1,500,000 per year. This translates into $45.45/g of ^{3}He produced by the miner. These are also shown in Table 1. The cost of habitat and consumables per person, exclusive of launch costs, would be insignificant and can be dropped from further consideration.

Table 1. Labor and Mining Equipment Components of Cost of ^{3}He

($/gram of ^{3}He)

Cost of Capital	15 %	20 %	25 %
Miner Depreciation	$ 15.15	$ 15.15	$ 15.15
Net Profit: Miner Investment	$ 33.26	$ 47.08	$ 61.49
Income Taxes: Miner Investment	$ 18.71	$ 26.48	$ 34.59
Labor Cost	$ 45.45	$ 45.45	$ 45.45

Note in Table 1 that the cost of capital has a significant impact on the net profit and income tax components of mining equipment costs. These costs nearly double as the cost of capital increases from 15% to 25%. The profit and tax components are significant amounts resulting from the fact that the return is earned gradually over a twenty year period but the capital expenditure for the miner is made at the beginning of the period. Depreciation and labor costs are not affected by the cost of capital.

2.2. Launch Costs

The launch costs are the most significant costs. The cost to launch a miner in the 2015 time frame, in 1993 dollars, is assumed to be $1000/kg [Koelle, 1993]. Each miner is assumed to have a mass of 50 tonnes giving a launch cost of $50,000,000/miner. The launch cost of a single miner can then be thought of as an initial cost subject to amortization over the miner's 20 year life. Table 2 shows the launch costs for both the miner and the habitat and consumables. It assumes that the miner will operate 20 years and will be fully utilized each year and that the habitat and consumables will be replenished each year. The launch costs can also be separated into amortization, profit and income taxes in a manner similar to the treatment of the cost of the miner itself.

2.3. Total Costs of Producing ^{3}He

The required profit and taxes make up a considerable component of costs of ^{3}He. The amortization, profit and tax components of miner and miner launch costs from Tables 1 and 2 are combined in Table 3, which also includes the labor, habitat and consumables launch costs. From Tables 1 and 2 it is clear that the launch costs are the most important element in the cost of mining lunar ^{3}He. However Table 3 shows that the main elements of

the launch costs are profit and income taxes.

Table 2. Launch Components of Cost of ^{3}He

($/gram of ^{3}He)

Cost of Capital	15 %	20 %	25 %
Amortization: Miner Launch Investment	$ 75.76	$ 75.76	$ 75.76
Net Profit: Miner Launch Investment	$166.31	$235.39	$307.45
Income Taxes: Miner Launch Investment	$ 93.55	$132.41	$172.94
Habitat & Consumables Launch Costs	$ 74.55	$ 74.55	$ 74.55

The profit depends on the cost of capital which is treated as a required rate of return on the "up-front" miner and miner launch costs. The profit is obtained by subtracting labor costs, habitat launch costs, depreciation of the miner, amortization of miner launch costs and income taxes from the revenues obtained by selling the ^{3}He at a price which yields the specified cost of capital. The income taxes are calculated assuming all capital is provided by common stock in the LMCo and an income tax rate of 36%.

Table 3. Component Costs and Total Cost of ^{3}He (Excluding R&D Costs)

($/gram of ^{3}He)

Cost of Capital	15 %	20 %	25 %
Amortization	$ 91(17.4%)	$ 91(13.9%)	$ 91(11.5%)
Net Profit	$200(38.2%)	$282(43.3%)	$369(46.9%)
Income Taxes	$112(21.4%)	$159(24.4%)	$208(26.4%)
Habitat & Consumables Launch	$ 75(14.3%)	$ 75(11.4%)	$ 75(9.5%)
Labor Cost	$ 45(8.7%)	$ 45(7.0%)	$ 45(5.7%)
Total Cost	$523(100%)	$652(100%)	$788(100%)

Table 3 indicates that the profit and taxes components range from 59.6% to 73.3% of the total costs of supplying ^{3}He. Adding the amortization of the miner and the miner launch costs raises the total portion of the cost associated with the miner to between 77.0% and 84.8%. They are the main cost components. These costs depend on the risks which investors perceive the LMCo to face and on the tax policies of the Federal government. They are also dependent on the investments made for the miner and its launch costs. Labor and habitat launch costs make up only approximately 20% of the total cost. If R&D costs

were to be included the total cost of ^{3}He would be increased substantially.

3. COMPETITION WITH COAL AND FISSION

Utilities making the choice of power plant type will compare the costs of coal, fission and fusion plants. Table 4 shows estimates of the costs of these alternative methods of producing power.

Table 4. Plant, Fuel and O&M Costs for Coal, Fusion, and Fission

Type of Plant	Plant Cost	Fuel Cost	O & M Costs
Coal	\$1,715/kwe[b]	17.4 mills/kwh[a]	4.45 mills/kwh[a]
Fusion (D-^{3}He)	\$3,000/kwe[d]	3.32 mills/kwh[e]	5.00 mills/kwh[f]
		4.34 mills/kwh	
		5.41 mills/kwh	
Fission	\$2,650/kwe[c]	6.95 mills/kwh[a]	15.60 mills/kwh[a]

[a]Average of 1990 and 1991 data from [Department of Energy, 1993, p92]
[b]Average of 1990 and 1991 data from [Department of Energy, 1993, p36]
[c]From summaries in [Department of Energy, 1986]
[d]The plant cost from the "Apollo" study [Kulcinski, et. al., 1989] was \$2,035. An additional amount for indirect costs was added to get \$3,000. Indirect costs are included in the coal and fission plant costs.
[e]The next three lines are determined from the fuel costs in Table 3 for cost of capital of 15%, 20%, and 25% respectively. The estimates use an efficiency factor of .7 and an assumption that 1kg of ^{3}He will provide 19MW-years of heat.
[f]See the "Apollo" study of note d.

The data in Table 4 can be converted to costs per kwh. This is done in Table 5 where it is assumed that all plants have a 40 year economic life and the yearly amortization of the plant cost, required profit and taxes are incorporated into a 10% amortization rate.

These data suggest that D-^{3}He plants will be competitive with coal plants because of low ^{3}He fuel costs. Their advantage over fission plants arises primarily because of the lower operation and maintenance costs and an assumed capacity factor of 0.8 for fusion and 0.7 for fission.

4. FINANCING OF R&D AND BENEFIT FOR SCIENTIFIC BASES

The cost comparisons so far have excluded both the *additional* Space R&D necessary

to develop the lunar mining capability and the potential benefits from production of volatile by-products of the lunar mining operations. Without including R&D costs the calculations in Table 5 suggest that lunar ^{3}He may be a competitive fuel for the generation of electricity in the 21st century. However, R&D expenditures will be necessary to allow ^{3}He to meet the promise shown in Table 5. In this section the costs of R&D as well as the value of the by-products which ^{3}He mining produces will be analyzed. The impact of R&D alone will be analyzed first after which the benefits of the volatiles will be considered.

Table 5. Cost to Produce Electricity Using Coal, Fusion and Fission (Excluding R&D Costs and Sales of Volatiles)

(Mills/kwh)

Cost Category	Coal	Fusion	Fusion	Fusion	Fission
(Cost of Capital)		(15 %)	(20 %)	(25 %)	
Plant Cost	25.02	43.78	43.78	43.78	44.19
O&M	4.45	5.00	5.00	5.00	15.60
Fuel	17.40	4.49	5.60	6.76	6.95
Total Cost	48.87	53.27	54.38	55.54	66.74

4.1. Research and Development Expenditures

Estimating the R&D needed to solve the physics and technology problems of D-^{3}He fusion is an uncertain undertaking. Recently, the annual United States Department of Energy funding was over $345 million for R&D on fission, $311 million on coal and $331 million on magnetic fusion[1]. The procurement of lunar ^{3}He will require *additional* expenditures for space research including lunar mining, heavy lift vehicles, and Moon based operations. These ^{3}He related R&D activities are estimated at an additional cost of $100 million by the mid-1990s and a growth rate thereafter of 4%. The total investment over nearly 21 years until the first production of ^{3}He is assumed to be $3.2 billion.

There are many policy options for funding the *additional* R&D ranging from complete private financing by the LMCo to sharing of the funding with a government agency to complete government funding. The choice of policy has significant implications for pricing ^{3}He and hence its feasibility as a competing fuel.

---

[1]See *Physics Today*, June 1993; *Nuclear News*, May 1993; and *Federal R&D Expenditures...*, September 1992. The coal expenditures are for 1992. The expenditures for fission and fusion are for 1993.

To see the impact of the LMCo completely bearing the R&D costs, the assumed yearly R&D expenditures prior to 2015 have been accumulated to 2015 at the cost of capital. It is also assumed that the LMCo has other business which allows it to deduct R&D costs yearly for tax purposes. The accumulated investment at year 2015 and the required return on it, as well as the income tax effect, is then applied at a uniform amount to each gram of ^{3}He produced over the next 20 years.[2] Using the assumption that ^{3}He production starts at 0.08 tonnes in 2015 and grows to 64.1 tonnes in 2050 the required R&D component would be \$3,006/g of ^{3}He if the cost of capital was 15%. The cost per gram is nearly 10 times that amount when the cost of capital is 25%. To see why the costs are so large, Table 6, panel (a) shows the accumulated investment and the required cost per gram separated into the profit and tax components for costs of capital of 15%, 20% and 25%. The fact that the accumulated investment amount exceeds the \$3.2 of R&D expenditures is the result of the fact that no investor receives a cash payment during the twenty years of R&D investment. Rather the investor receives the required return in the form of a "promise" of a future return similar to a "payment-in-kind" security. It is this accumulated but unpaid *investor required return* that causes the very significant impact on the cost of producing ^{3}He.

If the LMCo finances the entire R&D cost its investors must wait over twenty years from the first expenditure until lunar mining activity begins. Furthermore, the payoffs will be low in the first years following 2015 because mining activity will be in small volumes. Thus the cash flows to investors will still fall far short of the required return in the years immediately following 2015. Only later does the volume of mining activity rise to the point where cash flows from mining activities are such that investors realize their required return.

The main culprit in increasing the cost of ^{3}He is the slow build up of the mining volumes subsequent to 2015. Comparing panels (a) and (b) of Table 6 shows how this slow build up of mining volume affects the cost of ^{3}He. In panel (a) mining volume starts at a very low level and then increases as more D-^{3}He fusion power plants are built. Because of the slow start, return on investment is delayed and the required profit and income taxes related to R&D are substantial. In panel (b) it is assumed that the mining volume starts at 64.1 tonnes and remains constant for the 20 years over which the R&D costs are repaid by an increment to the price of ^{3}He. It shows that the R&D recovery per gram of ^{3}He ranges from \$38 to \$200. The large difference in the cost impacts in panels (a) and (b) is solely a result of delayed cash flow *from lower volumes of mining in the early years following 2015.* R&D costs would have only a modest impact on the cost of ^{3}He if the scale of mining operations were at high volumes at initiation.

This long lead time and the lack of cash flow would have a dampening effect on incentives for private enterprise to embark on a lunar mining initiative. However if society as a whole, through the mechanism of a government agency, bears some or all of these costs, then the LMCo would incur its first costs nearer to the time when ^{3}He would be a marketable fuel and there would be a greater incentive for the LMCo to embark on mining.

---

[2]The selection of a 20 year period for return of the R&D investment is arbitrary.

Table 6. R&D Component of Cost of ^{3}He

(a)Production of ^{3}He Increases from 0.08 tonnes in 2015 to 64.0 tonnes in 2050

Cost of Capital	15 %	20 %	25 %
Accumulated Investment at 2015	$17.52B	$33.02B	$63.41B
Profit on R&D Investment $/g	$ 1,924	$ 6,150	$18,631
Inc Taxes $/g	$ 1,082	$ 3,460	$10,480
R&D Component of Cost $/g	$ 3,006	$ 9,610	$29,111

(b)Production of ^{3}He is Constant at 64.0 tonnes from 2015 to 2050

Cost of Capital	15 %	20 %	25 %
Profit on R&D Investment $/g	$24	$56	$128
Inc Taxes $/g	$14	$32	$ 72
R&D Component of Cost $/g	$38	$88	$200

There are incentives for public support of the R&D activity beyond providing citizens with a safe and economical fuel. They are related to the potential benefits of the ^{3}He mining activity which would accrue to scientific bases on the Moon or Mars. These potential benefits are obtained from the by-products of ^{3}He mining, which would be in the form of volatiles, which could be consumed by the bases. Transferring the volatiles from the lunar mining site to the governmental lunar base would reduce launch costs that would otherwise be necessary to supply the lunar base with consumables and thus these avoided costs represent an additional payoff for the R&D investment necessary to supply the scientific bases. The policy implications relating to the use of by-products will be discussed further in section 4.3.

4.2 Cost Offset from Sale of Volatiles

If a scientific base exists on the Moon and is close enough so that volatiles can be transported from the mining site to the scientific base an offset to the costs of producing ^{3}He may exist. In receiving volatiles from the LMCo, the scientific base can avoid transporting them from the earth. A number of parameters affect the offset: i) the mass of volatiles produced by the LMCo; ii) the fraction of the volatiles transferred to the scientific base; iii) the transfer price for the volatiles to the scientific base.

For each kg of ^{3}He produced there will be 18,200 kg of volatile by-products(Kulcinski, et. al. 1992). Assuming the LMCo completely financed the R&D, sales of volatiles could potentially offset some of the R&D cost shown in Table 6. Figure 1 shows

the offsets available per gram of ^{3}He given that a fraction of the volatiles are sold to the scientific bases at a fraction of what the bases would have to pay for launch costs if they were launched from earth. The contour lines in Figure 1 correspond to the R&D cost components of the cost of ^{3}He shown in Table 6(a) for costs of capital of 15% and 20%. For example, the lower line shows that if, say, 33% of the volatiles were sold at 50% of launch costs, the volatile sales would bring in revenue of $3,006 per gram of ^{3}He mined completely, offsetting the R&D cost under a 15% cost of capital. The upper line -- for a cost of capital of 20% -- shows that 75% of the volatiles would have to be sold at 70% of launch costs to offset the R&D costs when the cost of capital was 20%. It would not be possible to offset the R&D cost component if the cost of capital was 25% and the resulting R&D component of the cost of ^{3}He was $29,111.

In addition to the observation that the volatile sales would not be sufficient to offset the impact of a very high cost of capital on the price which the LMCo would have to charge for ^{3}He, obtaining these by-product profits clearly depends on the LMCo being a monopolist for producing volatiles on the Moon. If there was competition in the form of more than one mining company, there would be a tendency for the transfer price to fall thus reducing the offset. There may also be substantial costs to transport the volatiles from the mining site to the scientific base thus reducing the offset. In any case, the size of the offset could be large but is quite speculative and would add to the perceived risks which investors would face.

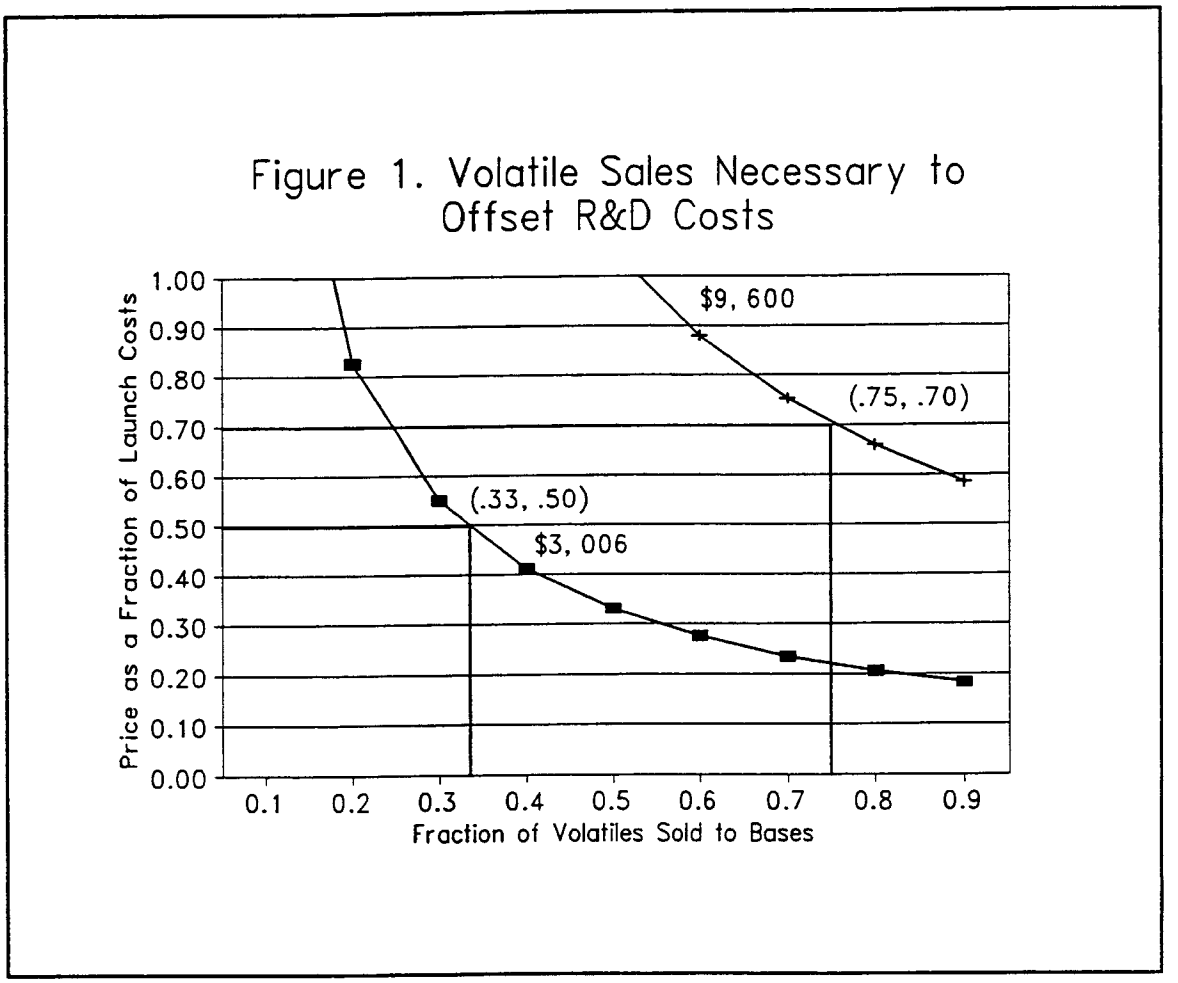
It appears that the LMCo will face very high "barriers to entry" into ^{3}He mining if it must bear the additional R&D expenditures necessary to develop the mining capability. The extent of the "barriers" to entry can be affected by the extent to which the government will subsidize the *additional* space R&D necessary to develop lunar mining capabilities. Furthermore the price at which the volatile by-products are sold to a lunar or Mars base will also affect the incentives for the LMCo to exploit the opportunity. There are many scenarios that could be developed regarding government funding and volatiles demand and price. The cost of ^{3}He depends quite importantly on the choice of scenario.

In the next section the role of complete government financing of R&D is discussed.

4.3 Government Funding of R&D and Ownership of Volatiles

One feasible policy approach suggests that government completely fund the *additional* Space R&D and in return assume ownership of all volatile by-products from the mining operation of the LMCo. The key question in analyzing this alternative is the benefit that accrues to the government from ownership of the volatiles.

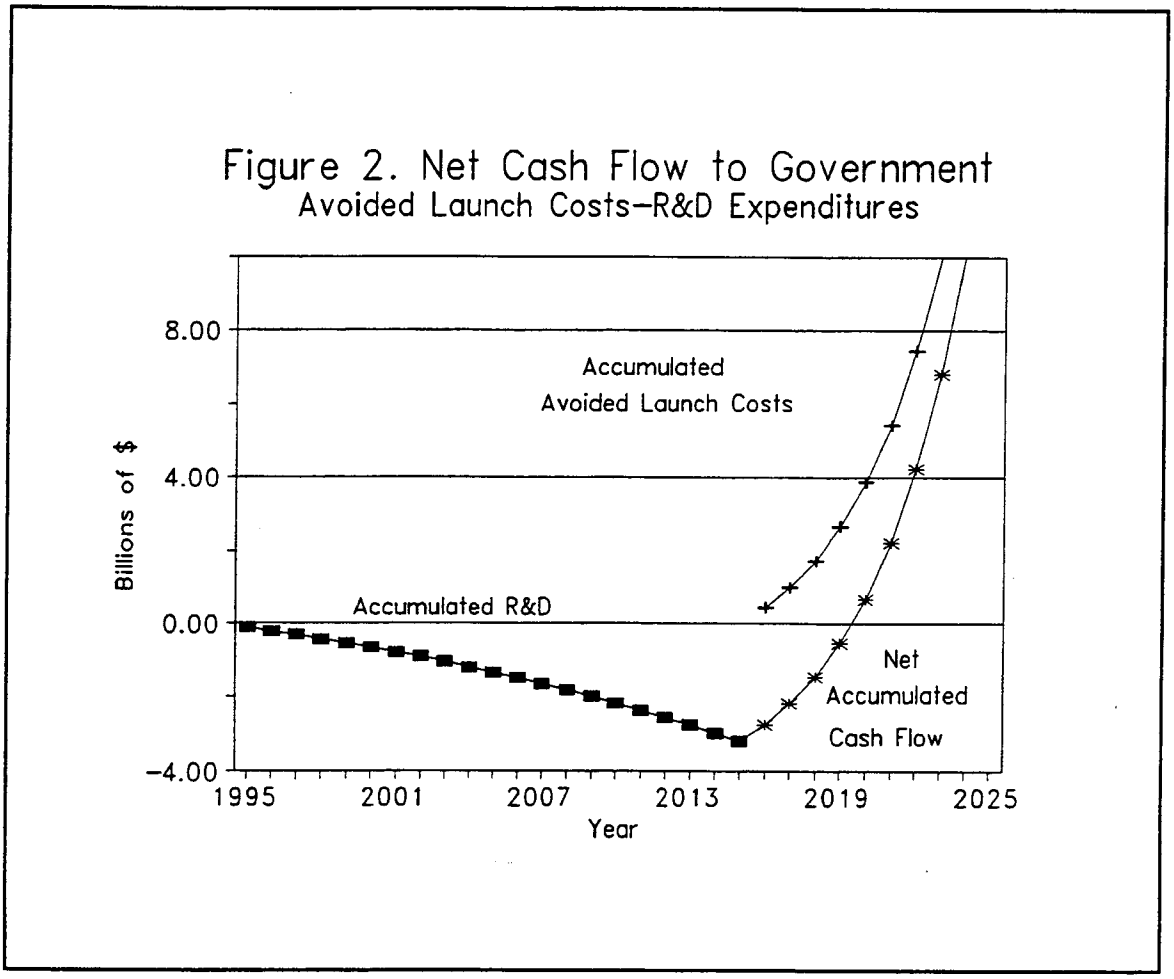
The benefit to the government of any volatiles used at the scientific bases would be the avoidance of launch costs which would otherwise be incurred if they were delivered from earth. If the government bases used, say, 30% of the volatiles generated in one year they would avoid launch costs of $5,460 for each gram of ^{3}He mined in that year. In addition the remaining 70% of the volatiles could be stored avoiding $12,740 of launch costs at some future date when they were needed.



The net benefit to the government then depends on the time profile of lunar ^{3}He production and the fraction of volatiles used immediately following production and the fraction of volatiles stored for future use by the scientific bases. Figure 2 shows net accumulated cash flows declining through the R&D period and then rising as payback in the form of launch cost avoidance occurs following 2015. If 30% of the volatiles are used by the base, the payoff period (when the accumulated inflows first exceed the accumulated outflows) occurs in 2019.

The rate of return earned by the government given the scenario shown in Figure 2 is 16.2%. Clearly, if a higher proportion of the volatiles are used in the year they are generated, the rate of return on the R&D investment will be greater than 16.2%. Also if the avoided costs from the volatiles stored or government sale of volatiles to third parties were included a further increase in the rate of return to the government would be realized.

The scenario of complete government funding of R&D along with ownership of volatiles appears to be a profitable investment without considering the benefits of D-^{3}He fusion. That it allows D-^{3}He fusion to be competitive is an added incentive for its selection as the policy alternative for R&D funding.



5. SUMMARY

The analysis of this paper suggests the following: i) the most significant costs to the LMCo are the capital related costs - required profit and taxes; ii) the price of ^{3}He depends importantly on the required rate of profit; iii) excluding R&D costs and assuming launch costs at \$1000/kg, ^{3}He will be an economic fuel - between \$500 and \$800/g.

If private enterprise must entirely bear the "up-front" *additional* Space R&D costs, ^{3}He mining may appear as a very high risk venture to potential LMCos. The most viable alternative is for the government to fund all *additional* Space R&D necessary to develop lunar mining technology and capability in return for ownership of all volatiles which are produced. This alternative suggests a return of R&D expenditures by 2020 and a rate of return of at least 16% which, while possibly somewhat low for high risk, long term privately financed projects, would be quite reasonable for a publicly financed project.

Acknowlegement

I would like to acknowledge the significant input received from S. E. Kratz, G. L. Kulcinski, H. H. Schmitt, and I. N. Sviatoslavsky.

APPENDIX

Formulas used in Calculations

The calculation of the price of ^{3}He excluding R&D and volatile by-product sales is found by first determining the revenue per year per miner necessary to yield a specified cost of capital. Given this revenue the price per gram of ^{3}He is found by dividing the revenue obtained by the grams produced by a miner during the year. The basic formula is

$$L_m+M=\sum_{i=1}^{n}[(R-3H-3L)-\tau(R-3H-3L-D)](1+\rho)^{-i}$$

The left hand side of the equation is the sum of the costs of the miner and its launch cost. The right hand side is the present value of the cash flows from the mining operation. The symbols are defined as:

R = yearly revenue per miner
$\mathbf{L_m}$ = miner launch cost
M = cost of the miner
n = economic life of the miner
H = habitat cost per person
L = salary and fringe benefits per person
τ = income tax rate
ρ = cost of capital.

Solving the equation for **R** yields

$$R=3H+3L+[\frac{L_m+M}{pvf}-D]+\frac{\tau}{1-\tau}[\frac{L_m+M}{pvf}-D]+D$$

where

$$pvf=\sum_{i=1}^{n}(1+\rho)^{-i}$$

and the terms on the right hand side are, from left to right, habitat cost, labor cost, after tax profit, income taxes and depreciation and amortization with

$$D=\frac{L_m+M}{n}$$

being the yearly depreciation of the miner plus the yearly amortization of the launch costs.

The price per gram of ^{3}He is then

$$P=\frac{R}{q}$$

where **q** is the grams of ^{3}He produced per miner per year.

The previous formulas are used to calculate tables 1,2,and 3.

The fuel costs for the fusion plants in table 5 are calculated from

$$\frac{P}{19 \cdot e \cdot 24 \cdot 365}$$

where **e** is the efficiency factor.

The additional cost component in the price of ^{3}He which would be necessary if the LMCo had to bear all of the R&D costs is determined by first accumulating all R&D expenditures to 2015 and then equating that amount to the present value, over the next 20 years, of a constant addition to the price of ^{3}He. The equation, which must be solved for the additional cost component, **ΔP**, is

$$(1-\tau)\sum_{i=0}^{20} E(1+g)^i(1+\rho)^{20-i}=\Delta P(1-\tau)\sum_{i=0}^{19}\theta(1+a)^i(1+\rho)^{-i}$$

where the left hand side is the accumulated R&D (at the cost of capital) at 2015 and the right hand side is the present value of the needed price component to cover the R&D. The equation is solved for ΔP which is shown in Table 6. The symbol **E** is the *additional* Space R&D to support lunar mining, **g** is the growth rate in these R&D expenditures, **ΔP** is the addition to the cost for each gram of ^{3}He to recover the R&D expenditures over a 20 year period, θ is the first year production of ^{3}He in grams, and **a** is the growth rate in the production of ^{3}He.

The contour lines in Figure 1 are found by plotting

$$f_L=\frac{K}{18200 f_s}$$

where **K** is the cost component necessary to cover the R&D expenditure and f_L is price as a fraction of launch costs, and f_s is the fraction of volatiles sold. There are 18.2 kilograms of volatiles for every gram of ^{3}He produced and launch costs are assumed to be $1000/kg.

REFERENCES

1. D. A. Bula, L. J. Wittenberg, T. W. Tibbitts and G. L. Kulcinski, "Potential of Derived Lunar Volatiles for Life Support," *Second Proceedings on Lunar Bases and Space Activities of the 21st Century*, Houston 1990, Lunar and Planetary Institute.

2. Department of Energy, "An Analysis of Nuclear Power Plant Construction Costs," U.S. Energy Information Administration, DOE/EIA-0485, March (1986).

3. Department of Energy, "Electric Plant Cost and Power Production Expenses 1991", U.S. Energy Information Administration, DOE/EIA-0455(91), May (1993)

4. H. Koelle, "Lunar Development, Past and Future," *Spaceflight*, 35,48 (1993).

5. G. L. Kulcinski, I. N. Sviatoslavsky, J. F. Santarius. L. J. Wittenberg, E. N. Cameron, T. M. Crabb, and M. K. Jacobs, "Energy Requirements for Helium-3 Mining Operations on the Moon," *Space Nuclear Power Systems 1988*, Orbit Book Company, Inc. Melborne, FL, (1989)

6. G. L. Kulcinski, E. N. Cameron, J. F. Santarius, I. N. Sviatoslavsky, l. J. Wittenberg, and H. H. Schmitt, "Fusion Energy from the Moon for the Twenty-first Century," *The Second Conference on Lunar Bases and Space Activities of the 21st Century*, Houston 1988, NASA Conference Publication 3166, Vol 2,479(1992).

7. G. L. Kulcinski, et. al.,"Apollo -- An Advanced Fuel Fusion Power Reactor for the 21st Century," *Fusion Technology*, **15**,1233(1989)

8. I. N. Sviatoslavsky and M. Jacobs, "Mobile Helium-3 Mining and Extraction System and its Benefits Toward Lunar Base Self Sufficiency," *Space 88. Engineering Construction and Operations in Space,* Houston 1988, American Society of Civil Engineers, 310 (1988).

9. "Clinton's Budget Boosts Technology, Making Research Scientists Jittery," *Physics Today*, 83 ,June 1993

10. "Nuclear R&D 49 Percent Lower than in FY 1993," *Nuclear News*, **36**,25 (May 1993)

11. "Federal R&D Expenditures for Nuclear Energy, Coal, Solar and Renewable Energy, 1950-1992," Management Information Service, Inc. 116 4th St SE, Washington, D.C. September 1992

Potential ^{3}He Resources for D-^{3}He Fusion Development

William R. Wilkes
W^2 Technical Services
810 W. Alex-Bell Rd.
Dayton, OH 45459

ABSTRACT

^{3}He will be required in large quantities for research on ^{3}He-D fusion during the next 20 years or more. These large quantities of ^{3}He may be recoverable from terrestrial resources, but only if decisions are made soon to put into place the necessary recovery equipment. Wittenberg et.al.[1]. have estimated the availability of ^{3}He from these sources. In this paper, I attempt to refine this estimate for the period from the present to approximately 2015 to provide a framework for making these decisions.

1. INTRODUCTION

With the exception of ^{3}He extracted from natural gas, the only accessible terrestrial source of ^{3}He is the decay of tritium, specifically, tritium in the weapons reserves of the United States and the Former Soviet Union (FSU); and tritium which accumulates in the moderators of heavy water power reactors. The maximum quantity of ^{3}He that might be recovered from these sources is determined by their current inventories of tritium and ^{3}He, plus additional tritium which may be added during the next 20-25 years. More than 300 tonnes of ^{3}He are estimated to exist in natural gas, diluted with ^{4}He and other gases. Although this source far exceeds the other three, only trace quantities of ^{3}He are currently recovered from natural gas. ^{3}He recovery requires equipment capable of extracting ^{3}He at an initial isotopic concentration of 0.2 ppm.

2. ^{3}He FROM WEAPONS TRITIUM STOCKPILES

The inventories of tritium in the United States and FSU stockpiles are, of course, classified. Nevertheless, these quantities have been estimated. I shall use the Natural Resources Defense Council estimate of the size of the US stockpile[2] as a basis for estimating future availability of ^{3}He. **It should be noted here that my use of this estimate should not be construed as suggesting that the NRDC numbers are accurate.** For the purposes of the present exercise, I further assume that the FSU tritium stockpile is between 100 and 150% of the U.S. stockpile. The latter value takes into account that Soviet weapons tended to be larger than those of the U.S. to compensate for lower accuracy.

As shown in Table 1, the **total** current DOE ^{3}He inventory is estimated to range from 37 to 42 Kg. The high and low values are derived from 1984 tritium inventories

presented by Cochran, et. al.[2] plus tritium production of 10.2 Kg/yr until 1987, after which no tritium was produced. The present unclassified DOE inventory of ^{3}He is approximately 14 Kg, the remainder of 28 Kg stored at Mound Laboratory, in Ohio, prior to 1979. Information about how much still remains of the net 41 to 48 Kg of ^{3}He estimated to have been generated since 1984 is not publicly available. It is assumed that lack of ^{3}He recovery facilities except at DOE's Savannah River Site, diversion of ^{3}He to other uses (e.g., atmospheric tracer experiments), and losses have reduced the classified inventory by 50%. Savannah River personnel believe that all ^{3}He generated in the future (including ^{3}He recently decayed, but not yet reclaimed) can be recovered, however.

Table 1. Estimated DOE Tritium and ^{3}He Inventories (Kg)

Year	Tritium	Helium-3
1978		28 (actual,unclassified)
1984	72 - 90	
1990	85 - 97	26 - 29
1993	72 - 82	37 - 42
1995	64 - 74	42 - 48
2000	48 - 56	51 - 59
2005	37 - 42	54 - 63
2010	28 - 32	52 - 63
2015	21 - 24	45 - 57
2020	16 - 18	39 - 45

1978 Savannah River ^{3}He inventory assumed to be 0.
^{3}He sales, 1978-1992, are 14 Kg, 1 Kg in 1993, with 5% annual growth
1984 tritium inventory and 1985-87 tritium production of 10.2 Kg/yr from Cochran et. al. [2]
Zero tritium production assumed after 1987

Assuming FSU tritium inventories at 150% of U.S inventories, 81 to 90 kg of ^{3}He may have been generated (before losses) since 1984. Minimum FSU inventories are at least equivalent to those in the U.S.; Russia sold ^{3}He at a rate on the order of 10,000 liters/yr during 1992-93. Assuming loss of half the amount generated since 1984 yields a range of 14 to 45 Kg. (This may be too conservative. [3]) Thus the current quantity of ^{3}He in the U.S. and FSU inventories is estimated to range from 28 to 87 Kg. By 2015, the inventory of ^{3}He from U.S. and FSU weapons stockpiles could reach 145 Kg.

2. Tritium from Heavy Water Reactors.

Most of the heavy water power reactor capacity in the world is provided by CANDU (CANada DeUterium) reactors. The amount of tritium generated in a CANDU reactor is approximately 190 grams per year per 1000 MW(e) (allowing for an 80% capacity factor). With a total installed capacity of 15.7 GW(e) in Canada (of which 14.2 GW(e) is owned by Ontario Hydro), the potential tritium generation rate is

currently 3.0 Kg per year. The installed CANDU capacity currently exceeds actual demand, however. In 1992, the average Ontario Hydro generation rate was only 7.6 GW(e). Reducing the national generation rate by the same factor, the Canadian production of tritium is 1.9 Kg/yr.

The tritium in a CANDU reactor accumulates in the moderator water at a rate of approximately 2-3 Ci/Kg-yr. The Ontario Hydro target extraction level is 12 Ci/Kg, but currently the level is 19 Ci/Kg as a backlog is worked off. The time the tritium remains in the moderator water before recovery is determined by the generation rate and the level at which extraction is begun. Currently, this time appears to be about 9-10 years, during which any ^{3}He which is generated will be lost (there is no mechanism in place for recovering ^{3}He which escapes from the moderator water during reactor operation). This latency period results in a loss of 20-25% of the ^{3}He. Although the ^{3}He recovery fraction might be increased by extracting the tritium sooner, this is limited by extraction plant capacity and operating budget.

Once the tritium has been extracted from the moderator water, it is stored as titanium hydride in sealed containers with a capacity of approximately 0.5 MCi. These containers are designed for a 100 year service life, and are equipped with valves to permit recovery of either the tritium or the ^{3}He. In 1992, 2.4 Kg of tritium was extracted and stored by Ontario Hydro. To date, Ontario Hydro has stored 66 MCi of tritium of which 52 MCi is calculated to remain. The difference yields an inventory of approximately 1.4 Kg of ^{3}He.

Assuming a fixed generation rate, the amount of ^{3}He which can potentially be recovered from CANDU reactors in t years is given by

$$T = 0.78 * G [t + (e^{-\alpha t} - 1)/\alpha],$$

where G is the annual rate of tritium generation, and α is 0.056/yr. The factor of 0.78 accounts for ^{3}He lost from the moderator. Thus, with the current power demand, Table 2 shows that 16 Kg of ^{3}He might be recovered from Canadian reactors by 2015. It seems reasonable in the light of the success of the CANDU program, increasing population and an assumed continuing increase in the per capita use of electrical power to assume a modest increase in demand over the next 20 years. If we assume an annual demand increase of as little as 3% per year beginning in the year 2000, the potential amount of recoverable ^{3}He increases to 25 Kg.

In addition to the CANDU reactors in Canada, several additional CANDU reactors have been or are being constructed in Argentina, Pakistan, Korea and India. The current installed capacity of these reactors is 3 GW(e), with planned increases to 9.7 GW(e) by 2002. The maximum quantity that might be recovered from non-Canadian CANDU reactors is approximately 6 Kg by 2015.

Table 2. Estimated CANDU Inventory of ^{3}He (Kg)

Year	Constant Production	3%/yr Growth
1994	1.4	1.4
1995	1.6	1.6
2000	3.3	3.3
2005	6.5	7.5
2010	10.8	14.4
2015	16	24.8
2020	21.8	39.4

3. Natural Gas Sources

Several private companies and the U. S. Bureau of Mines extract helium from natural gas with a starting helium concentration around 0.3% or greater. The helium plants recover only 2/3 of the gas processed, however. [4]. This helium typically contains an isotopic fraction of 0.2 ppm ^{3}He. The Bureau of Mines annual report for 1991 lists a U.S. helium recovery capacity of 105 million M^3 per year [5]. An additional 25 million M^3 capacity has since been added. At an assumed ^{3}He isotopic fraction of 0.2 ppm, approximately 3.5 Kg of ^{3}He could conceivably be recovered from this source. Actual recovery of enriched ^{3}He from natural gas sources will, however, require a far greater expenditure effort than is the case with radiogenic ^{3}He.

The Bureau of Mines has performed small scale separations of ^{3}He and ^{4}He, principally to support production of low-^{3}He grade ^{4}He, using both superfluid separation and cryogenic distillation. Kilogram scale separation and enrichment of the ^{3}He in natural helium can, in principle, be performed in facilities similar to the lunar helium isotope separation plant design described by Wilkes and Wittenberg [6]. The lunar plant design incorporates both superfluid separation and cryogenic distillation to achieve a flow of 100 Kg/yr of >99% ^{3}He product from a starting concentration of 400 ppm.

A plant (or several parallel plants) sufficient to enrich the ^{3}He in all the current U.S. helium production would require a total feed rate 70 times as large as that of the lunar plant to produce 1/28 as much product. Although the technology exists today to construct such a plant, it could only be effective when used in conjunction with a helium liquefaction plant or other source of liquid helium. Current helium liquefaction capacity is 94 million M^3 per year [4], in nine plants, including that of the Bureau of Mines. Thus up to 2.5 Kg per year of ^{3}He might be recovered by the addition of cryogenic separators to current liquefaction plants. Any extension beyond this value would require increased liquid He production. Adding isotopic separation capacity to new liquid helium plants during construction could greatly reduce the incremental cost of the ^{3}He separation facilities, but the liquefaction plants would have to be economically justified in their own right. For the purposes of this estimate, it is assumed that no ^{3}He recovery from natural

gas occurs until 2000, after which recovery capacity is incremented by 1Kg/yr in 2000, 2005 and 2010.

Helium is produced at a rate of 11 million M^3 per year outside the U.S., principally in Poland and the FSU. This could provide an additional .3 Kg/yr of ^3He. Achievement of this potential is dependent upon the installation of isotope separation facilities at new or existing helium liquefaction plants.

4. COMPETITION FOR ^3He RESOURCES

So far, I have principally discussed the amount of ^3He that might be recovered from each major source. The amount of ^3He that might actually be available for fusion development will probably be less as alternate uses divert ^3He from fusion research. A significant amount of ^3He (currently around 1.4-2 Kg/yr) is sold for cryogenic research and neutron detectors, and the world market for tritium is about 0.1-.2 Kg per year. These amounts have been considered in the current estimate. A much more significant diversion could come from possible ^3He use in atmospheric tracing, as has already done, or from the use of ^3He for the production of new tritium. The U. S. Department of Energy has shut down its only tritium producing reactor, with no plans to restart it. Even with continued progress toward world peace, it is quite conceivable that the U.S. could determine that it needs to replenish its diminishing supply of tritium within the next 20 years. Construction and operation of a new tritium production reactor would simply enhance the amount of ^3He that could be available. If, however, it is decided to produce tritium by converting ^3He back to tritium, the supply of ^3He from the DOE could easily be reduced or even cut off entirely.

Table 3. Estimated ^3He Resources to 2020 (Kg)

Year	Source				
	Weapons Tritium		CANDU Tritium	Natural Gas	Total
	U. S.	FSU			0
1993	42	45	1.4	0	88
1995	48	55	1.6	0	105
2000	59	76	3.3	0	138
2005	63	85	7.5	5	161
2010	63	89	14.4	15	181
2015	57	87	24.8	30	199
2020	45	78	39.4	45	207

4. SUMMARY

Table 3 summarizes the quantities of ^{3}He that might be available for D-^{3}He fusion research between 1993 and 2020. These are considered to be maximum values unless extraordinary efforts are made to improve recovery capacity. Even these numbers may be very optimistic if military or other needs cause ^{3}He to be diverted away from the fusion program, or if FSU supplies are not available.

REFERENCES

1. Wittenberg, L. J., Cameron, E.N., Kulcinski, G. L., Ott, S. H., Santarius, J. F., Sviatoslavsky, G. I., Sviatoslavsky, I. N., and Thompson, H. E., "A Review of ^{3}He Resources and Acquisition for Use as Fusion Fuel," Fusion Technology, (21) 2230, 1992.

2. Cochran, T. B., Arkin, W. M., Hoenig, M. M., and Norris, R. S., Nuclear Weapons Databook, Volume II, Ballinger Publishing, Cambridge, MA, 1987, App. C.

3. Golovin, I.N., Kurchatov Institute, Private communication, July, 1993, estimates that the FSU tritium inventory may be twice the estimated U.S. value, and that nearly all of the ^{3}He has been captured and saved.

4. Moore, Billy J., and Williamson, Michael, U. S. Bureau of Mines, Private Communication, July 1993.

5. Leachman, William D., Helium, U. S. Department of the Interior, Bureau of Mines, September 1992.

6. Wilkes, W. R. and Wittenberg, L. J., "Isotopic Separation of ^{3}He/^{4}He from Solar Wind Gases Evolved from the Lunar Regolith," Presented at Space 92, The Third International Conference on Engineering, Construction, and Operations in Space, 31 May-4 June 1992, Denver, CO. and University of Wisconsin Report WCSAR-TR-AR3-9201-4.

Non-Lunar ^{3}He Resources

Layton J. Wittenberg
University of Wisconsin-Madison
1500 Johnson Drive
Madison WI 53706

ABSTRACT

The earth's reservoirs and proposed nuclear reactions to produce significant quantities of ^{3}He were considered. No natural resources were identified which could produce ^{3}He in either the quantities required or with a net energy pay-back. Nuclear reactions for the production of ^{3}He did not appear viable because of the required storage of large quantities of radioactive products. These combined reservoirs, however, could provide sufficient ^{3}He for the research and demonstration phases of a D-^{3}He fusion reactor.

1. INTRODUCTION

The potential environmental and safety benefits from the use of the D-^{3}He fusion fuel cycle as compared to the D-T fusion system has been well documented [1]. Although the reaction conditions required are more strenuous to achieve for the D-^{3}He fuel versus the D-T system, several advanced confinement concepts are being developed which can lead to the development of economically attractive D-^{3}He fusion reactors [2]. As the reactor development projects progress, the search for ^{3}He resources to fuel these proposed reactors intensifies. An inventory of ~one million metric tons (tonnes) of ^{3}He deposited in the lunar regolith by the solar wind has been well-established and concepts for its production are being developed [3]. Conversely, an initial survey of ^{3}He reservoirs on earth indicated that no large recoverable reservoirs exist [4].

Because ^{3}He is scarce on earth, it is often used by geologists as a tracer for ancient gas reservoirs. Conversely, ^{3}He exists in the cosmos at a ^{3}He/^{4}He ratio of ~300 ppm (atomic) and ^{4}He is the second most plentiful element in the universe [5]; consequently, the ^{3}He inventory in the cosmos is very large-comparable to the abundance of sulfur. Unfortunately, the earth, being a terrestrial planet accreted more sulfur than He, while the gas-giant planets, Jupiter and Saturn, probably contain millions of tonnes of ^{3}He, but the utilization of such reservoirs may require centuries to develop. Entrapment of the solar wind is a possible mechanism by which the terrestrial planets could have enriched their ^{3}He content; however, Mercury, earth and Mars have sufficiently strong geomagnetic fields that their surfaces are protected from the solar wind by a magnetosphere. Some of the solar wind particles do reach the earth's atmosphere through the polar, auroral flux lines, yielding a small ^{3}He flux of ~3 kg/yr. Mercury, being closer to the sun, has a larger auroral flux providing ~5.4 kg/yr of ^{3}He. Dawson [6] suggested, therefore,that Mercury could provide a resource for ^{3}He. The atmosphere is very thin [7], however, with a vertical column density of only $2 \times 10^{14}/cm^2$. If this entire atmosphere were He, it would contain only 360 kg of ^{3}He. Venus does not have a magnetosphere, but it does have a thick carbon dioxide atmosphere, ~8 MPa, and a He pressure of 0.6 MPa. Dawson has suggested that the Venusian atmosphere could intercept the solar wind which would mix with the gases present to yield an atmosphere which would be isotopically similar to He in the solar wind. If this mechanism were demonstrated, the Venusian atmosphere may contain 2×10^9 tonnes of ^{3}He.

Of more immediate concern are the quantities of ^3He which will be available on earth during the research and development of the D-^3He fusion reactors and the start-up of a fusion power industry. This review provides an update of the earth's ^3He reservoirs and discusses nuclear reaction schemes proposed to produce significant quantities of ^3He.

The requirements for ^3He during the fusion development phase are modest, ~150 kg through the power demonstration reactor operation [3]. Much of the supply might come from the radioactive decay of ^3H which is stored in nuclear weapons' stockpile of several nations — if it were collected. Before a fusion industry could develop the assured availability of tonnes of ^3He per year would be required. For instance, the electrical power usage in the USA during 1992 was 3.15×10^5 MWe·yr. During the next 25 years, while fusion is being developed, this usage could increase to 5.16×10^5 MWe·yr [8]. If D-^3He fusion were to provide 25% of this power, the assured fuel supply of ^3He must be 13 metric tonnes/yr, for just the USA.

2. TERRESTRIAL HELIUM RESERVOIRS

Significant earthen ^3He reservoirs are considered and their ^3He inventories are estimated, Table 1. Each of these reservoirs has a distinct $^3He/^4He$ ratio, Fig. 1, which aids in its identification. Insignificant He-bearing reservoirs are excluded such as diamonds [9], because the host mineral is so rare, and Li/U-bearing rocks because the concentrations of ^3He per weight of rock is so small.

Table 1. Estimated Earth Inventory of ^3He

	^3He (tonne)			
	Proved	Probable	Possible	Speculative
Atmosphere	4000	---	---	---
Oceans	13	---	---	---
U.S. crustal natural gas	0.23	0.18	0.20	0.08
Subduction zone natural gas	0.03	---	1000	25,000
Mantle gas	---	---	---	10^6 to 10^7
	4×10^3	0.18	10^3	10^6 to 10^7

2.1. Mantle-Derived He

The earth is shielded from the solar wind because of its geomagnetic field and the amount of ^3He produced as spallation products from energetic cosmic rays reacting with the atmosphere and rocks is small. Consequently, the terrestrial ^3He is believed to have existed since the formation of the earth.

The earth is believed to have accreted ~4.5 billion years ago from asteroids which have compositions similar to the chondritic meteorites [10]. During the accretion phase, the temperature rise due to frictional heating was sufficient to evolve occluded gases, including He, due to diffusion and gaseous hydrodynamic flow. As a result the earth was depleted of volatile gases except for water which may have been borne by comets which accreted on the new earth. Some of the volatile gases were trapped, however, in the mantle of the earth and slowly trickle to the surface.

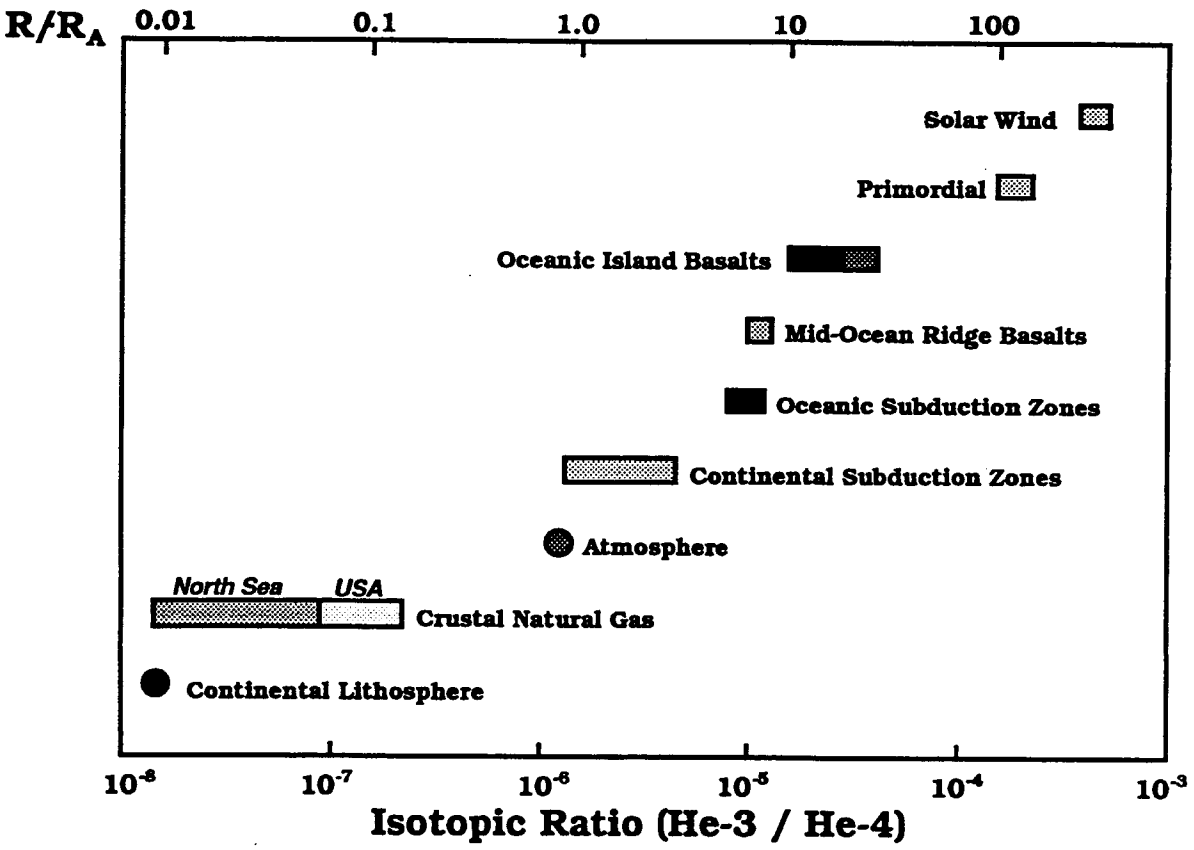


Fig. 1. Helium isotopic ratios for major natural reservoirs; R/R_A = isotopic ratio of a sample compared to the earth's atmospheric ratio.

The $^3He/^4He$ ratio of these primordial gases was 200-300 ppm; however, ^4He is continuously produced in the earth by the α-particle decay of U and Th ores so that the primordial ^4He accounts for only ~7% of the total He [11]. Some ^3He is formed in the earth as a result of neutrons produced by the α-bombardment of oxides. These neutrons are captured by ^6Li in the rocks to form tritium (^3H) which decays to ^3He. Based upon this reaction an assessment of U, Th, and Li in the primitive rocks predicts a He ratio of 1.5×10^{-8}. Gases with higher ratios are considered to have gaseous mantle constituents.

Gases emitted from Hawaiian volcanoes have the highest $^3He/^4He$ ratios (up to 30 at.ppm) and are believed to arise from the deepest mantle, which contains only a small amount of U and Th. These gases have been diluted with α-decay He during their passage through the upper mantle and crust. Gases, CO_2 and ^3He, emitted from such subaerial volcanoes have been estimated based upon the simulataneous emission of the radioactive tracer polonium -210. Marty and Le Cloarec [12] suggest that this total world-wide emission is only 100 mol/yr (300 g ^3He)/yr). Clearly, this is not a large, potential ^3He resource.

Additionally, Kurz has measured the He occluded in vesicles of the lava from the Hawaiian volcanoes [13]. This He is released when the lava is crushed in a vacuum system and analyses indicate the gas concentrations are in the range of 1.2×10^{-17} mole (^3He)/g of rock. The edifice of Mauna Loa, for instance, contains 4.25×10^5 km^3 of solidified lava at ~3 tonnes/m^3; consequently, the total ^3He available in all this rock would be only 47 kg, an insignificant amount compared to the energy required to mine such a resource.

The discovery of He and other gases venting from the mid-ocean ridges suggested another potential resource of He. Craig, et al. [14], estimated that these vents provided a ^4He flux of $\sim 3 \times 10^5$ atoms/cm^2·s to the atmosphere, with a $^3He/^4He$ ratio of 14 at.ppm. The calculated ^3He flux averaged over the entire surface of the earth is, therefore, only ~3 kg/yr.

Recognizing the dynamic nature of the evolution of He from the upper mantle of the earth to the atmosphere, Tolstikhin [11] in 1975 proposed a degassing model for the earth. This model assumed a primordial concentration of ^4He in the early earth of 5.5×10^{-6} cm^3/g with a $^3He/^4He$ ratio of 3×10^{-4}. The degassing of He was constraint by the fact that the other primordial rare gases ^{20}Ne and ^{36}Ar, which would be evolved with the He, have remained in the atmosphere while the He isotopes have escaped. Based upon this model, the present ^3He inventory in the upper mantle was calculated to be 10^6 - 10^7 tonnes. This value is very tentative because a subsequent article by Azel and Tolstikhin [15] indicates that the degassing process is more complex than originally assumed. For instance, the degassing rate was much higher during the early stages of the tectonic plate formation. Also, the subducting plates were found to become contaminated with atmospheric concentrations of ^{20}Ne and ^{36}Ar which were eventually recycled as fresh magma at the mid-ocean ridges [16].

2.2 Oceanic ^3He

Craig and Lupton [17] described in detail the He isotopic ratios determined by degassing of oceanic waters collected at numerous stations and a series of depths in the Atlantic and Pacific oceans. The waters with the highest $^3He/^4He$ ratios were collected at the undersea vents associated with sea-floor spreading zones. For instance, waters near the East Pacific Rise spreading-zone (104° W Longitude, 15° S) had an $R/R_A = 1.5$, where R is the $^3He/^4He$ ratio of the sample and R_A is the corresponding ratio for the $^3He/^4He$ in the atmosphere, $\sim 1.4 \times 10^{-6}$. As these waters flowed away from the vents, the He gases were diluted with gases derived from the atmosphere and ^4He derived from the out-gassing of U/Th ores; however, the enriched ^3He waters which peaked at a depth of 2.5-3 km below the surface could be traced for thousands of km westward of the vents. Based upon such measurements and using the Ne isotopes as an internal standard, the authors estimated the He inventory in the oceans to be 5.9×10^{13} liters (STP) and 9.5×10^7 liters (STP) ^3He (~13 tonnes of ^3He). The ^3He flux was estimated to be 24,000 liters/yr with a residence time of 4000 yr, resulting in very strong ^3He gradients both horizontally and vertically as confirmed by experiments. The total quantity of ^3He in oceanic waters and its rate of replacement are too small to be of interest as a major fusion fuel. Additionally, it is spread around the world.

Confirmation of the occurrence of primordial gases deep within the earth has initiated one attempt to search for it. For a deep gas reservoir to be present, it must be capped by an impermeable granite rock structure. The Siljan Lake District of Central Sweden was selected as a deep drilling site because it was the impact point for a large meteoroid 360 Myr ago which fractured the granite bedrock causing large fissures in the base rock [18]. The drilling project has proceeded to a record depth of 6 km in granite rock and fissures have been found; however, all the fissures have been infiltrated with carbonate deposits from surface waters [19]. Consequently, no mantle gases have been found, thus far.

2.3. Tectonic Plate Subduction Zones Gas Wells

The formation of new oceanic crust at the mid-ocean ridges previously described initiates tectonic plates which move several cm/yr until they encounter a continental plate of lower density. The oceanic plate of higher density subducts below the continental plate, returns to the mantle, dissolves into the mantle and eventually is recycled. These subduction zones are rich sources of ^3He because they serve as access probes into the ^3He enriched mantle. In addition, the sediments on the oceanic plates collect interplanetary dust particles [20] which contain ~0.1 cm^3 (STP) $^4He/g$ with an R/R_A ratio of 100-150. This source has provided ~200 tonnes of ^3He world-wide to these sediments during the 200 Myr of the present tectonic plate epoch. Anderson [21] has suggested that the recycle of these IDP particles within the mantle may be related to the high $^3He/^4He$ ratios found in gases emitted from intraplate (Hawaiian) volcanoes; however, the ability of the IDP's to retain He during subduction has not been demonstrated [22].

As the subducting plates recede into the mantle, the pelagic biotic residues decompose because of the thermal and hydraulic pressure, forming natural gas and petroleum reservoirs which entrap helium. These reservoirs which are abundant in the Western Pacific can be accessed by deep-drilling and supply natural gas for Japan, Taiwan and the Philippines [23]. The He content of these gases vary from 50-200 ppm with R/R_A ratios of 2-7. The calculated reservoir in this natural gas is based upon an estimate that 200 Mkm^3 of sediment has been subducted in 200 Myr.; containing approximately 1 wt% carbon compounds. If 0.1% of the carbon is converted to methane than these reservoirs would contain 10^{16} m^3 (STP) of methane; hence, the ^3He inventory is ~10^3 tonnes. The present geological epoch represents only ~4% of the total accumulated subduction zone sites which have been identified from past epochs. If previous subduction zone accumulates contain gas mixtures similar to the present zones, then these potential gas wells could have an inventory of up to 25,000 tonnes of ^3He.

2.4. Continental Gas Wells

During previous geological epochs, ancient flora and fuana were buried within the earth and subjected to heating and pressure forming our present fossil fuels, natural gas, petroleum and coal. In order for the methane to be retained, the gas had to be absorbed in a porous structure, such as sandstone, and capped with an impervious rock structure to form a reservoir. Such reservoirs are also capable of occluding He release from the radioactive decay of U and Th ores. This He should have a $^3He/^4He$ ratio of 10^{-2} R/R_A, in agreement with natural gas derived from fields in the North Sea.

In the USA during the early 1900's, the Hugoton gas field of Kansas and Texas were discovered to contain high He contents, up to 8%, with a $^3He/^4He$ ratio of ~10^{-1} R/R_A. The occurrence of this He has never been adequately explained; however, the high ^3He content indicates that some primordial He has seeped into this reservoir. For many years these fields were the only known source of He in the world and much of it was lost as the natural gas was burned as fuel. Because of the increasing uses of He and the apparent limited supply the U.S. Government implemented the Helium Acts of 1925 and 1960. These acts authorized the Bureau of Mines to purchase helium from private contractors and store it in the partially depleted Cliffside gas fields near Amarillo, Texas. This field presently contains 1.1×10^9 m^3 of He containing ~30 kg of ^3He. By 1967 the production of He by the private contractors greatly exceeded the anticipated demand. All purchasing contracts were terminated in 1973 and have not been reinitiated. In 1987, private producers [24] requested that federal agencies should not

be required to purchase He solely from the Bureau of Mines which has the effect of establishing a market price for this commodity. Because of the recent demand for liquid He at medical facilities for cryogenic purposes, two private suppliers have opened He separation facilities to supply ~5×10^7 m^3 (STP)/yr of He (containing ~1.7 kg of ^3He).

The Bureau of Mines estimates periodically the reserves of He contained in the natural gas wells of the USA [25]. These reserves increased nearly 230% from 1980-1982 as the newly discovered He-bearing wells of the Riley Ridge field in Wyoming was added. These gas wells are classified according to their He-content as: >0.3%, 0.29% to >0.1%, and <0.10%. In order to evaluate the proved and potential He reserves, the proved and potential resources of natural gas are surveyed and their He contents are estimated with the results noted in Table 1. Consequently, the calculated ^3He in all these categories is only ~0.7 tonnes, insignificant to supply a fusion industry.

2.5. Atmospheric He

The He concentration in the atmosphere has been measured [26] from samples collected at 12 locations in the USA, giving a value of 5.2204±0.0041 ppm(vol) and a $^3He/^3He$ ratio of 1.393×10^{-6}. Based upon these values and the weight of the atmosphere, the total quantity of ^3He is calculated to be 4000 tonnes, in good agreed with the value by Craig of 2.9×10^{10} liters (STP) ^3He (3900 tonnes).

A review of the He flux into and out-of the atmosphere indicates that the atmospheric inventory appears to have attained a steady-state [10]. The He escape flux is chiefly due to diffusive thermal escape; however, a non-thermal factor, such as a hydrodynamic flow has also been postulated. The influx from the mid-ocean ridges, through the oceans as previously discussed, is a large factor, while the degassing of the continental crust is much smaller. Cosmic ray spallation contributes a small influx by forming ^3He and ^3H which decays to ^3He. A significant influx is attributed to "auroral precipitation" when He in the solar wind leaks through the earth's magnetosphere at the magnetic poles.

3. POTENTIAL PRODUCTION OF ^3He FROM EARTH'S RESERVOIRS

This review of the earth's reservoirs of ^3He indicates that several of the sources would not be sufficient to supply a fusion power industry. For instance, the quantity of ^3He in the deep mantle appears to be very large; however, this estimated value has many assumptions which can not be verified. Also, no known technique is available to stimulate the release of this gas from the molten magma within chambers below island volcanoes or a mid-ocean ridges. Encouraging the degassing of such chambers could lead to large-scale natural disasters. The normal evolution from these sources contributes only ~5 kg of ^3He per year, an insignificant amount. These gases which are released under water form an inventory of only 13 tonnes which is spread throughout the world oceans and it is replenished at the rate of only 4 kg/yr.

Most of the world's He needs are supplied from natural gas wells in the USA, although a small amount ~6×10^6 m^3/yr is produced in Poland and Russia. The He content in the natural gas presently consumed as fuel is estimated to be 1.7×10^8 m^3 (STP)/yr, containing ~4.5 kg of ^3He. Past experience has shown that only 50% of this He can be profitable separated from the

methane. Consequently, if the ^3He were separated from this He, its rate of production would be only 2-3 kg (^3He)/yr.

The 4000 tonnes of ^3He in the atmosphere and the potential 25,000 tonnes of ^3He in subduction zone natural gas appear attractive; however, the energy expended to retrieve the ^3He from the resources must be considered. The operations of the most efficient helium production plant, the National Helium Corp. at Liberal, Kansas requires the liquefaction of all the methane, which aids in the removal of undesirable water, sulfur-bearing gases, CO_2, and some nitrogen. [27] The unliquefied gas, called "Crude Helium" contains 86% He with mostly nitrogen as the impurity. The operators of this plant have found that 242 kWH of energy is required to supply 5 kg (10^3 ft^3) of He. Another facility, the Greenwood Plant of Phillips Petroleum also removes He from natural gas but prepares "pure" liquefied He at an energy cost of 1520 kWH/5 kg of He. The $^3He/^4He$ isotopic separation would require very high purity for the He and is conducted in the liquid state at 1.6-2 K. Some of "waste" liquefied ^4He from this operation would be utilized to cool the incoming He stream; Consequently, the energy cost for obtaining pure ^3He were estimated by the following procedure. The energy expended in cooling the methane from 300 K to its condensation temperature of 111 K was assumed to be 242 kWH/(5 kg He) The remaining He was cooled and condensed at 4.2 K and a 60% recovery of this cryogen energy was assumed; therefore, the energy cost for He (mixed gas) at 330 K to liquid at 4.2 K was 750 kWH/5 kg ^4He (1.2×10^9 kWH/kg (^3He).

After the He isotopes were liquefied at 4.2 K, the energy required to isotopically separate the He isotopes was determined. First, the energy needed to cool the mixture to 1.6 K was determined based upon the Cp (2.25 kJ/kg·K) of liquid He and the assumption that 75% of the cryogenic energy would be recovered in a recuperator at 4 K. This sensible heat removal would require 2.7×10^3 kWH/kg (^3He). The isotopic separation techniques used a "superfluid/ superleak" to enrich the ^3He from 2×10^{-7} to 10^{-2} fraction of the ^4He. The enriched product was enriched further to 99.9% by a cryogenic distillation which operated at a boiler temperature of 2.4 K and a condense temperature of 1.6 K, as described by Wilkes [28]. The "superleak" apparatus required 1.1×10^3 kWH/kg (^3He) of heat and the distillation system boiler required an additional 3×10^4 kWH/kg (^3He). Because these separation energies would be rejected at nearly 300 K, each of the latter two values were multiplied by a factor of 10^3.

Based upon the above values the energy required to separate high purity ^3He from USA natural gas wells (>0.3 vol % He and $^3He/^4He$ ~0.2 ppm at.) was calculated. As noted in Table 2, the energy required to separate the methane from the He and provide liquid He at 4.2 K is 1.2×10^9 kWH/kg (^3He). The isotopic separation energy is small, 3×10^7 kWH/kg (^3He), making the total energy requirement at 1.23×10^9 kWH/kg (^3He). As noted, however, the energy produced by the fusion of D-^3He is only 1.7×10^8 kWH/kg (^3He); therefore, the energy multiplication for this process is negative. The only means by which this system could have a positive energy pay-back would be to separate the methane for other purposes, such as removal of undesirable impurities, and charge this separation cost to the sale of the methane. In such a case, however, the availability of ^3He would be determined by the production requirements for natural gas, which at present consumption would yield only 2-3 kg (^3He)/yr.

A similar calculation was performed for the ^3He recovery from subduction zone gas, taking into account that the ^4He content in this gas is 50 to 200 ppm (vol) with a $^3He/^4He$ isotopic ratio 2-10 ppm. The energy cost for separation of the He from the methane is in the range of 0.3 to 6 $\times 10^9$ kWH (^3He). The cost of isotopic separation using the "superleak" and liquid distillation is

very small by comparison, only 7×10^5 kWH/kg (^{3}He), Table 2; consequently, the ratio, ^{3}He fusion energy produced/energy cost of ^{3}He production, is marginally unfavorable for even the best case.

The possibility of extracting He from the atmosphere was considered. Several successful permeator systems have been designed recently which separate certain trace gases from air or other gases. Such systems have been successful because the permeating gas demonstrates some solubility in the separation membrane. Unfortunately, He is not soluble in any membrane and has a very low liquefaction temperature. Consequently, all the other gases are removed so that He remains as the non-condensable gas and the energy cost for He is related to the compressive work required in handling the other gases. The energy cost of producing He from air at the National Helium Corp. plant has been estimated to be 1.5×10^5 kWH/5 kg of He, approximately 10^3 times higher than for He production from natural gas; however, the plant would need to be redesigned to handle air instead of natural gas. This He would be only 86% pure, and as previously noted, the energy cost should be increased significantly in order to obtain high purity liquid ^{4}He, Table 2. The energy cost for production of liquid He from air is 9×10^{10} kWH/g(^{3}He) while the isotopic separation requires only 4×10^6 kWH/kg (^{3}He); hence, the energy cost for the production of ^{3}He is 450 times greater than the fusion yield. If these energy costs were borne by the sales of other gases, such as liquefied nitrogen, then the amount of ^{3}He recovered would be only 0.02 kg (^{3}He)/year in the USA.

Table 2. Energy Payback from Earth's ^{3}He Resources

	Energy Expended, kWh/kg (^{3}He)				
Source	Separate from Carrier Gas Cool to 4.2 K	Isotopic Separation	Toltal Energy	Fusion Energy Payback*	Potential Product (as a By-Product) kg (^{3}He)/yr
USA natural gas	1.2×10^9	3×10^7	1.23×10^9	Negative	2.5
Subduction zone gas	1×10^9	7×10^5	1×10^9	Negative	<0.1
Air	9×10^{10}	4×10^6	9×10^{10}	Negative	0.02

*Energy produced by D-^{3}He fusion = 1.7×10^8 kWH/kg (^{3}He).

4. ARTIFICIAL PRODUCTION OF ^{3}He

Recognizing the scarcity of ^{3}He on earth, several investigators have proposed nuclear reaction schemes to produce ^{3}He. These concepts include: (1) production of tritium followed by β-decay to ^{3}He; (2) fusion of D-D to produce ^{3}H, ^{3}He, p and neutrons; (3) fusion of ^{6}Li + p to give ^{3}He + ^{4}He. Each of these schemes will be reviewed briefly.

4.1. Production of ^{3}He by Tritium Decay

Any source of neutrons can be used to interact with Li and form ^{3}H. Both fission and fusion reactors have been designed to be net tritium breeders. A review [29] of such reactors which have been proposed in the USA for large-scale production of tritium reveals that there can be an order of magnitude difference in the cost of the tritium, depending upon the reactor facility.

For instance, the use of an accelerator to produce a high energy proton beam which bombards a Pb target forming neutrons by spallation was estimated to produce tritium at the highest cost, nearly \$160,000/g of ^3H. When a U fission pile was utilized with a low-temperature, heavy water (D_2O) moderator the cost was ~\$100,000/g(^3H). If a High Temperature Gas-Cooled reactor were utilized which sold excess electrical power the cost dropped by ~50% to \$55,000/g(^3H). Two types of magnetically confined, fusion reactors were designed using D/T fuel, one a tokamak and the other a tandem mirror. The devices operated at low temperature so that no fusion power was utilized and electrical power had to be purchased; consequently, the costs were \$36,000 and 49,000 \$/g of ^3H for the tandem mirror and tokamak, respectively. Another set of conceptual fusion reactor designs were based upon the Inertial Confinement Fusion concept, using laser beam irradiation of fuel targets. In each case liquid Li was used as the high temperature coolant so that sufficient thermal power could be recovered and used to generate all the electrical power needed in the facilities. In these ICF facilities, the costs decreased to between 10,000 to 12,000 \$/g of ^3H.

The cost and safety associated with storage of ^3H while it decays to ^3He must also be considered. A recent study of storage of ~45 kg of ^3H indicated [30] that if the ^3He were collected for 10 half-lifes (123 yr) the additional cost of ^3H storage was ~\$420/g of ^3He; consequently, the lowest total cost (production of ^3H plus storage) would be ~\$10, 500/g of ^3He. Consequently, the fuel cost from a 1000 MWe plant using the D-^3He fusion fuel cycle would be 130 mills/kWH(e). At such a high cost, the generation of electrical power by fusion on a large scale would probably never be competitive with alternative fuel systems.

In addition, the generation of 1000 MW(e) requires ~100 kg/yr of ^3He for a D-^3He fusion plant. If the ^3He were produced from ^3H, the ^3He would need to be continuously separated from 1.8 tonnes of ^3H. The storage of such a large quantity of a potentially gaseous, radioactive material would be difficult to license, probably impossible in the present political climate.

4.2. D-D Fusion Reactions

The D-D fusion produces ^3He via one of two reaction channels according to:

$$D + D = {}^3He + n$$

and

$$D+D = {}^3H + p\,,$$

where the channel probabilities are ~50:50 at >1 keV. The ^3He produced can be allowed to react with the excess D or it can be rapidly extracted and used in a D-^3He satellite fusion reactor, as reviewed by Miley [31]. If the latter option were utilized, in what is known as the semi-catalyzed mode, the D-D breeder operates at a temperature of <40 keV while the satellite power-producing reactor would operate at a higher temperature of 80-140 keV. A detailed study of a combined breeder-satellite system was reported by Shuy, et al. [32], basing both plants on a tandem mirror reactor. The optimum operating temperature for the breeder was found to be 28 KeV while the satellite operated at 75 keV. In addition, the ^3H was extracted from the recycled plasma fuel and stored along with ^3H generated by the neutron absorption in a Li blanket. These ^3H batches were stored and allowed to decay to form additional ^3He fuel. By such a method, they were able to supply 12,000 MW(e) satellite power reactors at a cost of 43.4 mills/kWH (1985) with 3000 MW of fusion power in the breeder.

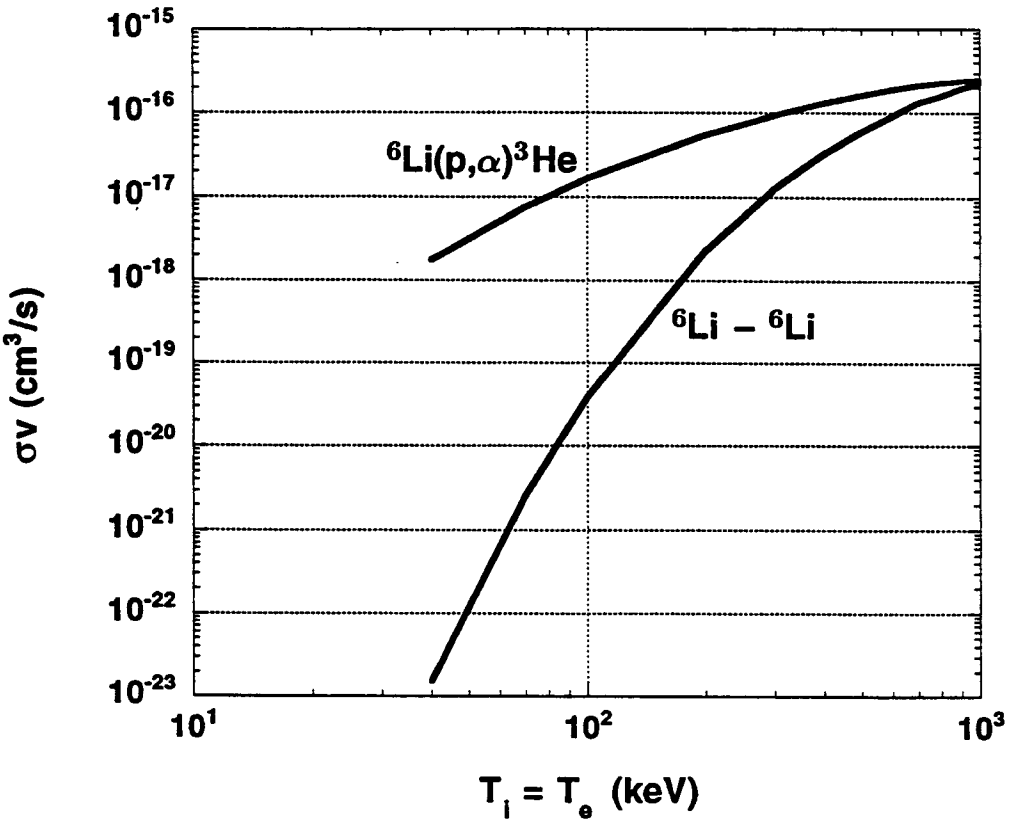


Fig. 2. Reaction parameters versus ion temperature.

The environmental impact of such a system must be considered. The breeder reactor would have the same safety and radioactive waste disposal ratings as a D/T reactor, and the breeding of tritium with its long-term storage in large amounts (~tonnes) would be an additional concern. In addition, two operational licenses would be required, the breeder and the satellite.

4.3. The p + 6Li Reactions for Breeding ^{3}He

The p - ^{6}Li fusion reaction, i.e. p(^{6}Li,α)^{3}He has been studied [31] as a potential supply route for ^{3}He, because no radioactive reactants or products are produced in the principal channel. Such a reaction, however, requires operational temperature of several 100's keV in order to obtain a reasonable reaction rate (Fig. 2). Because of the high electron density, in an equilibrium plasma where $T_i = T_e$,, the proton rapidly losses energy, decreasing the reaction probability. As a result, no viable steady-state burn prospects for p - ^{6}Li have been demonstrated. Consequently, supplementary power would be required for proton heating, which would decrease net power from any D-^{3}He satellite reactor which would use the ^{3}He which is produced. The viability of such a breeder-satellite reactor has not been investigated. The possible use of proton beams interacting with a Li plasma may deserve further study [33].

In addition to the principal reaction p(^{6}Li,α)^{3}He, ^{6}Li - ^{6}Li reactions have been calculated. For instance at ~300 keV, these ^{6}Li - ^{6}Li side reactions can be 10% of the principal reaction [34], Fig. 2. These ancillary reactions include a significant production of ^{7}Be + n, leading to high radioactivity in the confinement device. Such radioactive waste products would be no better than those from a D-T reactor and the development costs for the p - ^{6}Li system may be formidable.

5. SUMMARY

This study leads to the following conclusions:

1. No natural sources has been identified which can produce ^3He either in the quantities required for a fusion power industry or with a net energy pay-back.

2. The production of ^3He by the decay of tritium produced in a fission or fusion reactor is uneconomical and the tonnes of tritium which must be stored are environmentally unacceptable.

3. The production of ^3He via D-D fusion carries all the undesirable safety and environmental aspects of D-T fusion. A p - ^6Li fusion reactor has not been demonstrated to be viable and ancillary ^6Li - ^6Li reactions could lead to undesirable radioactive products.

The outlook for obtaining ^3He for research and demonstration D-^3He fusion reactors is much better. Commercial vendors who produce liquid helium could be given incentives to isotopically separate the helium isotopes. This ^3He separated at the rate of 4-8 kg/yr could be stored for several years and combined with the ^3He resulting from several tritium stockpiles. These combined stores could produce up to 100 kg of ^3He required for research and development projects.

REFERENCES

[1] G.L. Kulcinski, et al., "Safety and Environmental Characteristics of Recent D-^3He and D-T Tokamak Power Reactors," *Fusion Technology*, **21**, 1779 (1992).

[2] R.F. Post and J.F. Santarius, "Open Confinement Systems and the D-^3He Reaction," *Fusion Technology*, **22**, 13 (1992).

[3] L.J. Wittenberg, et al., "A Review of He-3 Resources and Acquisition for Use as Fusion Fuel," *Fusion Technology*, **21**, 2230 (1992).

[4] L.J. Wittenberg, "Terrestrial Sources of ^3He - A Trip to the Center of the Earth," *Fusion Technology*, **15**, 1108 (1989).

[5] B.A. Mamyrin and L.N. Tolstikhin, *Helium Isotopes in Nature*, Elsevier, Amsterdam (1984).

[6] J.W. Dawson and W. Livesy, "^3He on Venus and Mercury," *Bull. Amer. Phys. Soc.*, **31**, 1393 (1986).

[7] R.E. Hartle, S.A. Curtis and G.E. Thomas, "Mercury's Helium Exosphere," *J. Geophys. Res.*, **80**, 3689 (1975).

[8] Monthly Energy Review, DOE/EIA-0035 (93/03), March 1993.

[9] M.D. Kurz, J.J. Gurney, W.J. Jenkins and D. E. Lott III, "Helium Isotope Variability Within Single Diamonds from the Orapa Kimberlite Pipe," *Earth Plant. Sci. Letters*, **86**, 57 (1987).

[10] M. Ozima and F.A. Podosek, *Noble Gas Geochemistry,* Cambridge University Press, Cambridge (1983).

[11] I.N. Tolstikhin, "Helium Isotopes in the Earth's Interior and in the Atmosphere," *Earth Plant. Sci. Letters*, **26**, 88 (1975).

[12] B. Marty and M.F. Le Cloarec, "^{3}He and CO_2 Fluxes from Subaerial Volcanos Estimated from Polonium -210 Emissions," *J. Volcano. Geothermal Res.*, **53**, 67 (1992).

[13] M.D. Kurtz, M.O. Garcia, F.A. Frey and P.A. O'Brien, "Temporal Helium Isotope [13]Variations Within Hawaiian Volcanoes: Basalts From Mauna Loa and Haleckalei," *Geochem. Cosmochem. Acta*, **51**, 2903 (1987).

[14] H. Craig, W.B. Clarke and M.A. Beg, "Excess ^{3}He in Deep Water on the East Pacific Rise," *Earth Planet. Sci. Letters*, **26**. 125 (1975).

[15] I.Ya. Azel and I.N. Tolstikhin, "Geodynamics, Magnetism and Degassing of the Earth," *Geochimica Cosmochimica Acta*, **54**, 139 (1990).

[16] K.A. Farley and R.J. Poreda, "Mantle Neon and Atmospheric Contamination," *Earth Plan et. Sci. Lett.*, **114**, 325 (1993).

[17] H. Craig and J.E. Lupton, *Helium-3 and Mantle Volatiles in the Ocean and the Ocean* [17]*Crust*, in The Sea, Vol. 7, The Oceanic Lithosphere, C. Emiliani (Ed.), Wiley-Interscience, New York, 391-428 (1981).

[18] T. Gold and S. Sater, "The Deep-Earth Gas Hypothesis," *Scientific American*, June 1980, pp. 154-161.

[19] J.W. Valley, S.C. Komor, K. Baker, A.W.A. Jeffrey, I.R. Kaplan, *Calcite Crack Cement in* [19]*Granite from the Siljan Ring*, in Deep Drilling in Crystalline Bedrock, Vol. 2, Eds. B. Boden and K.G. Eriksson, Springer-Verlag, 156 (1988).

[20] M. Takayanagi and M. Ozima, "Temporal Variation of the ^{3}He/^{4}He Ratio Recorded in Deep-Sea Sediment Cores," *J. Geophysical Res.*, **92**, 12531 (1987).

[21] D.L. Anderson, "Helium-3 from the Mantle: Primordial Signal or Cosmic Dust," *Science*, **261**, 170 (1993).

[22] K.A. Farley, "Is Primordial Helium Really Extraterrestrial?" *Science*, **261**, 166 (1993).

[23] A.W.A. Jeffrey, "Detection/Differentiation System Development for Deep Source Gases, Completion of Phase I," DOE/MC 21131-2350 (Feb. 1987).

[24] M. Crawford, "Dismantling the Helium Empire," *Science*, **237**, 238 (1987).

[25] R.D. Miller and J.E. Hamak, "Helium Resources of the United States, 1989," Bureau of Mines Information Circular, IC-9267 (1990).

[26] P.W. Holland and D.E. Emerson, "A Determination of the ^{4}He Content in Near-Surface Atmospheric Air Within the Continental USA," *J. Geophysical Res.*, **92B**, 12557 (1987).

[27] R.C. Seamans, "The Energy Related Applications of Helium and Recommendations Concerning the Management of the Federal Helium Programs," ERDA-13 (April 11, 1975).

[28] W.R. Wilkes and L.J. Wittenberg, "Isotopic Separation of ^{3}He/^{4}He from Solar Wind Gas [28]Evolved from the Lunar Regolith," SPACE'92, *Proc. of the Conf. Engineering, Construction and Operation in Space*, Amer. Soc. Civil Eng., New York, 1992, p. 547-554.

[29] L.J. Wittenberg, "Comparison of Tritium Production Reactors," *Fusion Technology*, **19**, 1040 (1991).

[30] F. Najmabadi, R.W. Conn and the ARIES Team, "The ARIES-III D-^{3}He Tokamak-Reactor Study," UCLA 1993 (in press).

[31] G.H. Miley, "^{3}He Sources for D-^{3}He Fusion Power," *Nucl. Instr. Methods Phys. Res.*, **A271**, 197 (1988).

[32] G.W. Shuy, A.E. Dabiri and H. Gurol, "Conceptual Design of a D-^{3}He Fueled Tandem Mirror Reactor Satellite/Breeder System," *Fusion Technology*, **9**, 459 (1986).

[33] G.H. Miley, Personal Communication, July 20, 1993.

[34] L. Ruby and T.-P. Lung, "Effect of ^{6}Li + ^{6}Li Reactions in a Fusion Reactor Operating on ^{6}Li (p,α)^{3}He," *Nucl. Sci. Eng.*, **69**, 107 (1979).

6) D-^{3}He Near-Term and Commercial Tokamak Reactor Design 193
P. Komarek, Chair

6-1 Near-Term Experiments on D-He^3 Burning 195
B. Coppi

6-2 Potential for D-^{3}He Experiments in ITER 205
G.A. Emmert

6-3 ARIES-III: D/He-3, Second Stability, Tokamak 211
R.W. Conn

6-4 D-^{3}He, Second Stability Tokamak Reactor Study 213
V.I. Pistunovich and S.G. Bespoludennov

6-5 Overview of Apollo Studies and Economic Assessment of Several Proposed Variations 221
Laila A. El-Guebaly and Charles W. Maynard

Near-Term Experiments on D-He^3 Burning

B. Coppi
Massachusetts Institute of Technology
77 Massachusetts Avenue, 26-217
Cambridge, MA 02139-4307

ABSTRACT

The advanced design characteristics of the Ignitor-Ult experiment, where the plasma current can be raised up to 12 MA and D-T ignition conditions can be attained with peak densities $n_o \simeq 10^{15} cm^{-3}$, are suitable to investigate the physics of the fusion heating due to D-He^3 reactions in the near-term. The Ion Cyclotron Heating system that has been adopted can supply up to 18 MW to the plasma and focus this power on a small fraction of its total volume. This system can be used to bring a minority population of He^3 nuclei in a deuterium plasma up to energies of the order of 1 MeV. Under these conditions up to about 2 MW of D-He^3 fusion power can be produced while the peak plasma density is in the range 2 - 4 $\times 10^{14} cm^{-3}$ and the slowing down time of the fusion products can be shorter than the expected energy confinement time. An issue that is of special importance is whether the produced 14.7 MeV protons, whose single particle confinement is ensured by the high currents (>6 MA) of Ignitor, will lead to the excitation of new types of collective modes, due to the high velocity of these particles relatively to other plasma characteristic velocities.

The criteria that have been followed for the design and construction (by now near completion) of the key components of the Ignitor machine have also been used to identify the parameters and carry out the feasibility studies of a high field experiment that was proposed at first in 1980 with the intent to reach D-He^3 fusion burn conditions on the basis of existing technologies and knowledge of plasma physics. This is called Candor and is capable of producing plasma currents up to 25 MA with toroidal magnetic fields $B_T \gtrsim 13T$. Unlike Ignitor, Candor would operate with values of β_p around unity and the central part of the plasma column in the Second Stability Region.

1. INTRODUCTION

The discovery of the so-called Second Stability Region [1], in the relevant parameter space, made it possible to predict that known toroidal magnetic configurations could be suitable to confine plasmas where the particle pressure is a considerable fraction of the magnetic field pressure. From this followed the realization [2] that experiments on D-^{3}He burn and ignition conditions could be designed and constructed on the basis of existing technology and knowledge of plasma physics. The validity of the main ideas [3], on which the relevant machines (called Candor that in Latin means cleanliness) were based, have been confirmed by the subsequent progresses that have been made in the relevant physics and technologies. These were:

i) High density [4] plasmas (e.g. with peak electron temperature $n_{eo} \simeq 2 \times 10^{21} m^{-3}$) can be well confined in high magnetic field ($B_T \gtrsim 13$T) axisymmetric toroidal configurations.

ii) High plasma currents that correspond to high poloidal fields ($\bar{B}_p \sim 4T$) can be produced in tight aspect ratio configurations and can insure that values of the confinement parameter $n_o \tau_E$, as expected from the results of existing experiments, can be obtained in the range needed for D-He^3 ignition.

iii) D-^{3}He ignition conditions can be reached with values of the parameter $\beta_p = 8\pi < p > / \bar{B}_p^2$, where $< p >$ is the volume average plasma pressure, around unity and with only the central part of the plasma column entering the second stability region. Thus the macroscopic stability of the plasma column can be ensured as shown by recent experiments operating under similar conditions.

iv) The plasma heating to the high temperatures where substantial D-^{3}He burning is produced can be accomplished by the combined injection of waves at the Ion Cyclotron frequency and α-particle heating due to D-T burning that is used as a trigger.

v) Synchrotron emission, once evaluated properly taking into account both the effects of reabsorption and reflection from the walls, is not an unsurmountable obstacle and in fact the relevant power loss is only a fraction of bremsstrahlung emission.

vi) The technology of high field magnets with cryogenically cooled copper conductors is appropriate for this type of experiments. The need for extended current pulse lengths suggested [3] the development of an appropriate helium-gas cooling system ($T^{initial} \sim$ 30K), that by now has been incorporated in the design of the Ignitor [5] experiment.

While studies on the Candor type of machines have progressed, the design of the Ignitor experiment that has the purpose to achieve D-T ignition conditions has evolved to the point where many of the features envisioned for the Candor machines could be

incorporated in it. Thus, as we shall show in detail, meaningful initial experiments on D-^{3}He burning can be carried out by it. Ignitor is at the stage where the construction of full size prototypes of the key components of the machine [toroidal magnet, central solenoid, plasma chamber, main structural element so-called C-clamp] is being completed.

2. THE IGNITOR EXPERIMENT

The parameters of the Ignitor-Ult machine are listed in Table 1 and an illustration of its core with its main components is given in Fig. 1. This device is an updated version of the first experiment [5] proposed and designed in order to reach D-T ignition conditions has undergone on the basis of progresses made in understanding the physics of thermonuclear plasmas and of advancements in the technology of relevant machines.

Table 1. Reference design parameters of the Ignitor Ult experiment.

$R_o \simeq 1.32$ m	Major radius of the plasma column
$a \times b \simeq 0.47 \times 0.87 \mathrm{m}^2$	Minor radii of the plasma cross section
$R_o/a \simeq 2.8$	Aspect ratio of the plasma column
$\delta_G \simeq 0.4$	Triangularity of the plasma cross section
$I_p \lesssim 12$ MA	Plasma current in the toroidal direction
$I_\theta \lesssim 9$ MA	Plasma current in the poloidal direction
$B_T \lesssim 13$ T	Vacuum toroidal field at R_o
$\Delta B_T \lesssim 1.5$ T	Paramagnetic (additional) field produced by I_θ
$\langle J_\phi \rangle \lesssim 9.3$ MA/m^2	Volume-average toroidal current density
$\bar{B}_p \lesssim 3.75$ T	Mean poloidal field
$I_p \bar{B}_p \lesssim 45$ MN/m	Confinement strength parameter
$q_\psi \simeq 3.3$	Edge magnetic safety factor at $I_p = 12$MA
$V_o \simeq 10$ m^3	Plasma volume
$S_o \simeq 36$ m^2	Plasma surface area
$P_{RF} \lesssim 18$ MW	Injected heating power (ICRF with $100 \lesssim \nu \lesssim 210$ MHz)

With the present configuration Ignitor is designed to satisfy the conditions where the 14.7 MeV protons and the 3.6 MeV α-particles produced by the D-^{3}He reactions can supply thermal energy to a well confined plasma as it can:

- sustain a plasma current exceeding that required ($I_p \gtrsim 6$ MA) to confine the proton orbits at birth;
- have more than sufficiently high densities that the slowing down time of both the protons and the α-particles is shorter than the electron energy replacement time of the thermal plasma in which they are produced.

In order to boost the D-^{3}He fusion reactivity, ion-cyclotron heating of a D plasma with a ^{3}He minority can be used to create a tail in velocity space for the ^{3}He distribution function [6] with an optimal mean energy value. We note that the D-^{3} He fusion cross section has a maximum near E $\simeq$ 650 keV for a helium beam incident on a deuterium target.

A preliminary analysis of the fusion power P_F that may be produced in Ignitor by this method indicates that $P_F \simeq 2$ MW may be reached, thanks primarily to the high value of the RF power density that can be coupled to the helium nuclei. We recall that in previous experiments, fusion power levels of 1.5 kW and 140 kW have been obtained in PLT [7] and in JET [8], respectively. However, neither of these experiments had the particle densities and currents required for the confinement and the slowing-down of the 14.7 MeV protons.

Numerical simulations [9] for this scenario in Ignitor were performed using the FPPRF [10] code, that combines a ray tracing package with the solution of the Fokker-Planck equation for the minority species. Typical RF parameters were $P_{RF} = 18$ MW, $\upsilon = 132$ MHz, $< k_{||} > =$ 5-10 m^{-1}. The parallel wavelength $< k_{||} >$ is estimated on the basis of the size of the adopted ICRF antennas.

The helium distribution function is obtained, at several times during the simulation, and the relevant level lines, in the $(\upsilon_{||}, \upsilon_{\perp})$ plane, show the characteristic two-horn shape with values of the relevant pitch angle about 60-80 degrees. Analytically, f can be described by a combination of a core Maxwellian and an anisotropic tail with a characteristic mean energy [6] represented by

$$T_{eff} \simeq T_e[1 + \frac{3}{2}\xi_{RF}].$$

Here the $\xi_{RF} \simeq P_{RF}\tau_s/(3n_{He}T_e)$, τ_s is the slowing down time of the helium nuclei and P_{RF} is the local value of the RF power density coupled to them. Therefore

$$\xi_{RF} \simeq 8.2\frac{\hat{T}^{1/2}}{\hat{n}_e\hat{n}_{He}ln\Lambda}\left(\frac{P_{RF}}{MW/m^3}\right)$$

when written in practical units $(\hat{T} = T/10keV, \hat{n} = n/10^{20}m^{-3})$.

Figures 2 and 3 show the RF power deposited into the plasma and the helium mean energy as functions of the minor radius for the case of maximum fusion reactivity referring to a plasma with $n_{eo} = 3 \times 10^{20}m^{-3}, T_{eo} = 20keV, T_{io} = 15keV, n_{3Heo}/n_{eo} = 10\%$ and $n_{To}/n_{eo} = 5\%$. Generally, over 95% of the RF power is deposited (promptly) into the helium. A substantial fraction of this power (up to 50%) is then transferred to the electrons by collisional processes. The fusion power output is estimated with several simplifying assumptions (e.g. an isotropic velocity distribution function for the fast ions) and the quoted value $P_F \simeq 2$ MW should be considered as tentative at this time.

Alternatively, the D-^{3}He reactivity parameter $< \sigma v >_F$ has been evaluated [9] for a ^{3}He distribution function of the type given in [6]. The relevant two-dimensional velocity space integral is computed numerically. In Fig. 4, the parameter $< \sigma v >_F$ is given as a function of ξ_{RF} for different values of the thermal plasma temperatures, T_e and T_i. We note that for a given set of temperatures, there is an optimal value of ξ_{RF} for which $< \sigma v >_F$ is maximum, and this value can be lowered considerably by increasing T_e and T_i as shown in Fig. 4. Since ξ_{RF} is inversely proportional to the square of the electron density (for constant minority concentration), while $P_F \propto n_{He} n_D < \sigma v >_F$, an increase in the thermal plasma temperature allows a higher optimal density at constant values of ξ_{RF} and therefore of P_F.

A 0-dimensional estimate of the total fusion power can be obtained as follows. On the basis of the inferred value of P_{RF}, we can select, for given temperatures, an optimal density product $\hat{n}_e \hat{n}_{He}$, in such a way that ξ_{RF} corresponds to the relevant maximum of $< \sigma v >_F$, e.g. $< \sigma v >_F^{max} \simeq 2.0 \times 10^{-22} m^2/s$. Then assuming that these optimal conditions can be produced only in a small fraction V_{eff} of the total plasma volume (say $V_{eff} \simeq V_o/20$)

$$P_F \simeq 6(\hat{n}_D \hat{n}_{He})^{optimal} \times (V_{eff}/M^3) MW.$$

In the case where $T_e = 20keV, T_i = 15keV$ for example, and $< P_{RF} >= 95 MW/m^3$ over $V_{eff}, \hat{n}_e^{optimal} \simeq 3, \hat{n}_{He}^{optimal} \simeq 0.1$, and $P_F \simeq 2.4$ MW.

Fig. 1. Main components of the Ignitor-Ult machine.

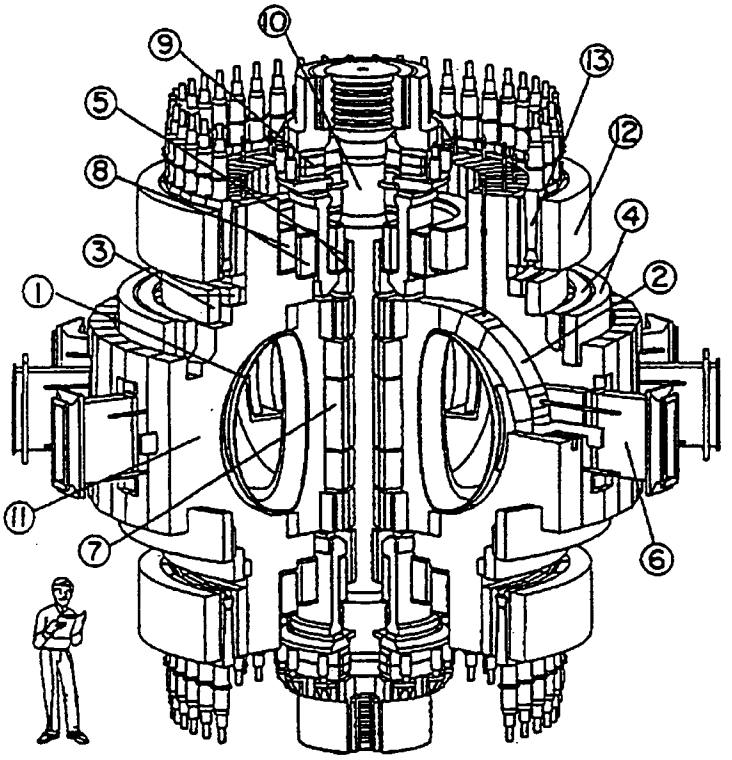


Fig. 2. RF power deposition profile for minority D-^{3}He acceleration. The RF power input is 18 MW. (courtesy of S. Migliuolo)

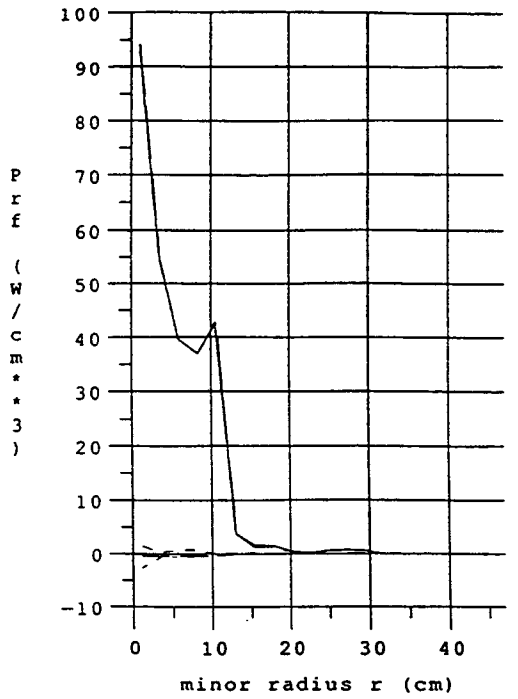


Fig. 3. Mean energy acquired by the RF minority (^{3}He) nuclei with a RF power input of 18 MW. (courtesy of S. Migliuolo)

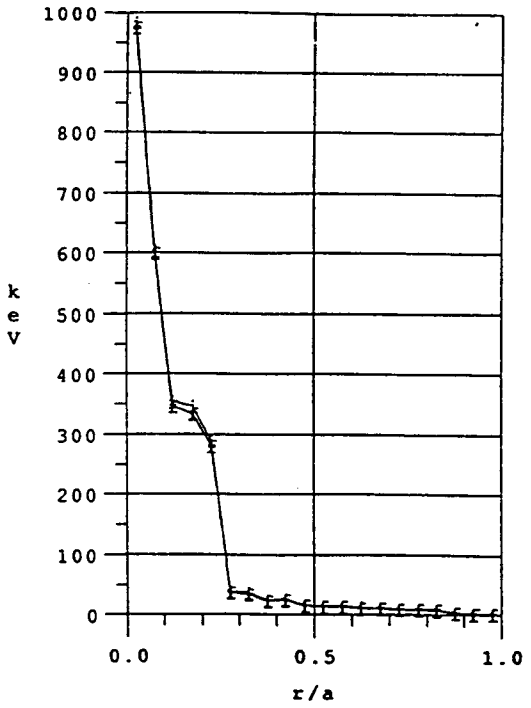
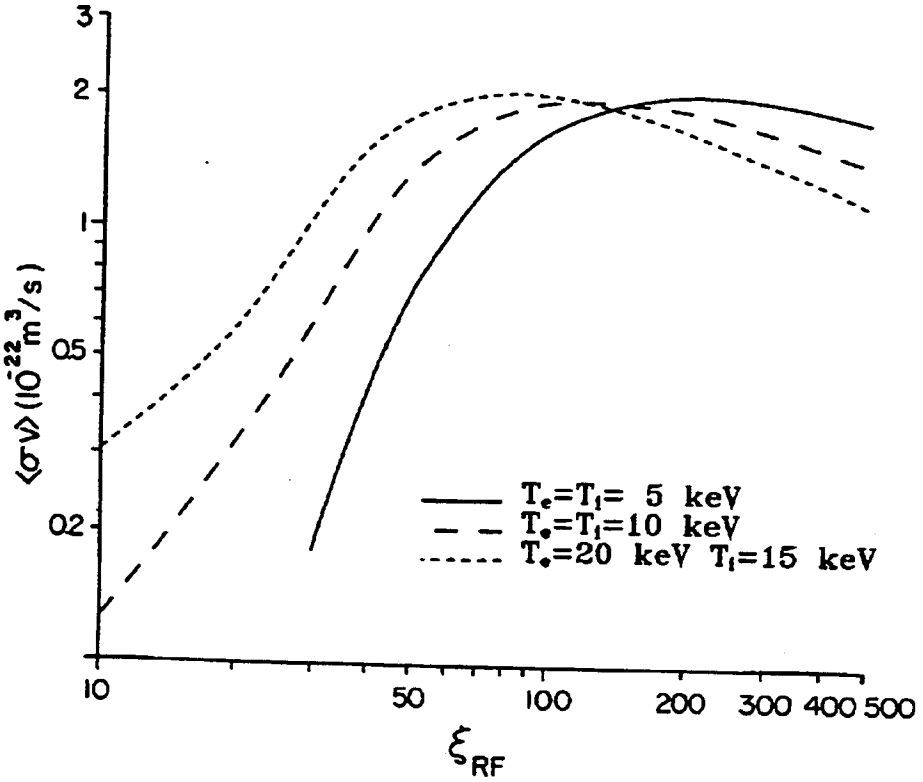


Fig. 4. Reactivity parameter $< \sigma v >_F$ as a function of the ξ_{RF} that characterizes the ^3He distribution function; different values for the thermal plasma temperatures T_e, T_i are considered. (courtesy of P. Detragiache)



3. The Candor Experiment

The Candor machine that is being studied at present is capable of producing plasma currents up to 25 MA with toroidal magnetic fields $B_T \approx 13T$. Unlike Ignitor, Candor would operate with values of β_p around unity and the central part of the plasma column in the Second Stability Region. D-^{3}He ignition in this case can be reached by a combination of ICRF heating and α-particle heating due to D-T fusion reactions that have the role of a trigger.

The reference plasma dimensions and parameters of Candor are reported in Table 2 and the reference plasma parameters in Table 3.

The machine's key elements are shown in Fig. 5. Note that the toroidal field coils are divided into two sets of coils and that the central solenoid (air core transformer) is placed between the two sets of toroidal field coils. Ignitor instead has the classical configuration involving only one set of toroidal field coils that surround the central solenoid. As indicated in Table 6, the poloidal magnetic flux variation Φ_T necessary to induce a current of 25 MA in Candor is large. The linked magnetic configuration adopted for the Candor design combined with the larger dimensions, when compared to Ignitor, makes it possible to produce the desired values of Φ_T with lower current densities (by more than a factor 2) in both the toroidal and poloidal field coils. Therefore assuming that the magnets operate in the same temperature range as those of Ignitor the characteristic times over which the plasma discharge can be sustained are longer by more than a factor 4. Among the drawbacks of the linked-magnet solutions we may single out the need of reliable joints for the external set of toroidal field coils.

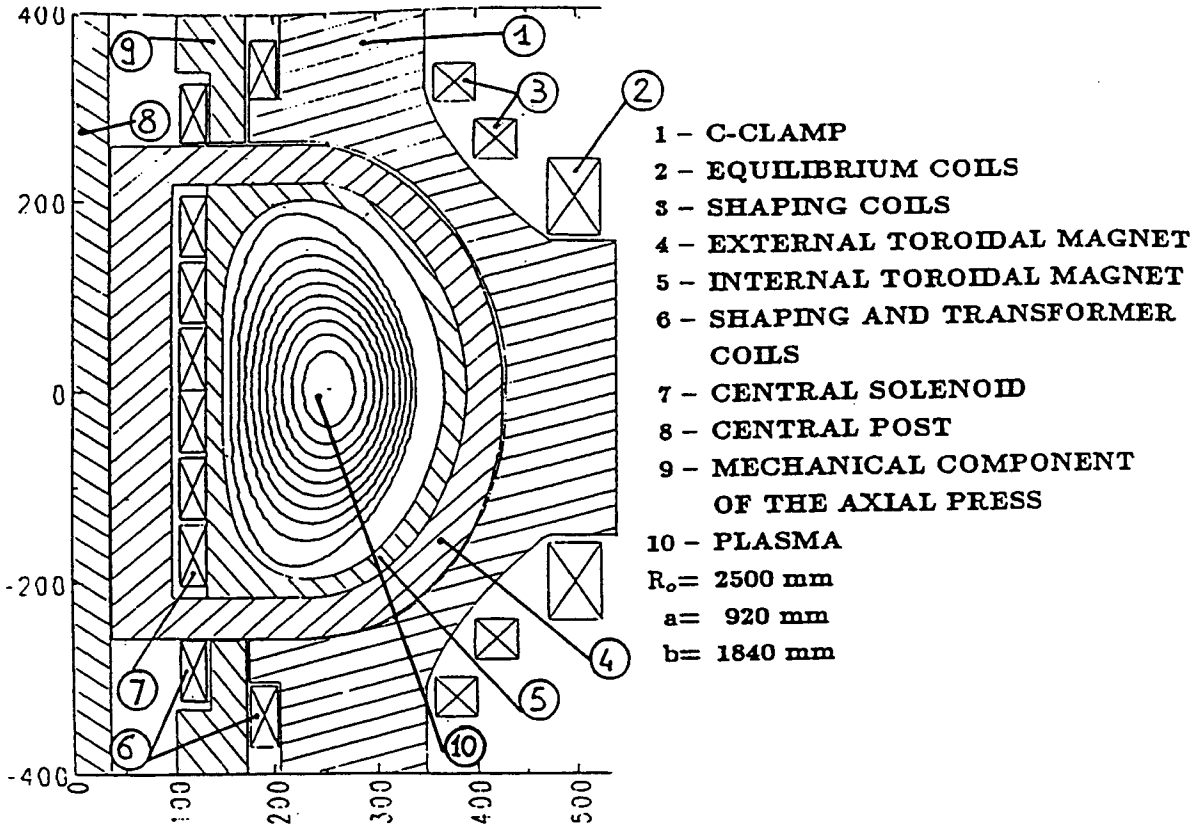
Table 2. Reference design parameters of the Candor machine.

$R_o \simeq 2.5$ m	Major radius of the plasma column
$a \times b \simeq 0.92 \times 1.84$ m^2	Minor radii of the plasma cross section
$\delta_G \simeq 0.31$	Triangularity of the plasma cross section
$I_p \lesssim 25$ MA	Plasma current in the toroidal direction
$B_T \simeq 13$ T	Vacuum toroidal field at R_o
$\langle J_\phi \rangle \lesssim 4.7$ MA/m^2	Volume-average toroidal current density
$\bar{B}_p \lesssim 3.8$ T	Mean poloidal field
$I_p \bar{B}_p \lesssim 96$ MN/m	Confinement strength parameter
$q_\psi \simeq 3.75$	Edge magnetic safety factor at $I_p = 25$ MA
$\Phi_T \simeq 160$ Vs	Total poloidal flux requirement
$V_o \simeq 84$ m^3	Plasma volume
$S_o \simeq 155$ m^2	Plasma surface area

Table 3. Reference plasma parameters for the Candor experiment.

$T_o \simeq 65$ keV	Peak plasma temperature
$n_{eo} \simeq 2 \times 10^{21} \mathrm{m}^{-3}$	Peak electron density
$p_o \simeq 400$ atm	Peak plasma pressure
$\beta_p \simeq 1.2$	Poloidal beta
$W \simeq 1.2$ GJ	Internal energy

Fig. 5. Main components of the Candor machine.



ACKNOWLEDGEMENTS

It is a pleasure to thank P. Detragiache, S. Migliuolo and M. Nassi for their contributions [9] to the subject of this paper. This work was sponsored in part by the U.S. Department of Energy.

REFERENCES

[1] B. Coppi, A. Ferreira, J.M.-W. Mark and J.J. Ramos, *Nucl. Fus.* **19**, 715 (1979); M.I.T. Report PRR (R.L.E.)-78/24 (1978).

[2] B. Coppi, Invited Paper at the 1980 International Conference on Plasma Physics, Nagoya University, Nagoya, Japan.

[3] B. Coppi, *Phys. Scripta* **T212**, 590 (1982).

[4] G.J. Boxman, B. Coppi, L.C. DeKock et al., *Proc. 7th Eur. Conf. on Plasma Physics 1975*, Ecole Polytechnique Fédérale de Lausanne, Switzerland, **2**, 14 (1976).

[5] B. Coppi, "High Current Density Tritium Burner", Report PRR (R.L.E.)-75/18, Massachusetts Institute of Technology, Cambridge, MA (1975) and *Comm. Plasma Phys. Cont. Fusion* **3**, 2 (1977).

[6] T.H. Stix, *Nucl. Fusion* **15**, 737 (1975).

[7] R.E. Chrien and J.D. Strachan, *Phys. Fluids* **26**, 1953 (1983).

[8] J. Jaquinot, G.J. Sadler, and the JET Team, *Fusion Tech.* **21**, 2254 (1992).

[9] B. Coppi, P. Detragiache, S. Migliuolo, M. Nassi and B. Rogers, "D-^{3}He Burning, Second Stability Region and the Ignitor Experiment", Massachusetts Institute of Technology Report PTP-93/5, R.L.E. (Cambridge, MA 1993), submitted to Fusion Technology.

[10] G.W. Hammett, "Fast Ion Studies of Ion Cyclotron Heating in the PLT Tokamak", PhD Thesis, Princeton University (1986).

Potential for D-^{3}He Experiments in ITER

G.A. Emmert
Fusion Technology Institute
Department of Nuclear Engineering and Engineering Physics
University of Wisconsin-Madison

ABSTRACT

The possibility of utilizing ITER to investigate relevant physics questions for D-^{3}He plasmas in tokamaks has been considered. Important physics questions such as plasma transport, synchrotron radiation transport, MHD stability, ash accumulation and impurity control, as well as plasma heating and current drive need investigation at the densities and temperatures expected in D-^{3}He plasmas before one can be confident that the technological advantages of D-^{3}He fusion can be realized in the tokamak configuration. Studying these issues in near-term facilities intended for the D-T program allows one to establish whether the present understanding of tokamak physics extrapolates to D-^{3}He conditions before a major investment is made in D-^{3}He specific facilities. The focus here is on ITER (EDA phase, major radius about 8 m) since it represents the most likely candidate for a near-term D-T facility.

Power balance calculations indicate that D-^{3}He breakeven in ITER can be obtained with a reduction of the major radius by 55 cm, an increase of the aspect ratio to 3.2 and an increase of the elongation to 2.0. The plasma still fits within the existing vacuum chamber. High Q operation can also be obtained by a small admixture of tritium into the plasma. Furthermore, the plasma will ignite at D-^{3}He temperatures using D-T fuel. Consequently, a range of operating conditions from breakeven to ignition can be investigated. The plasma physics questions listed above can be studied in these plasmas at conditions representative of D-^{3}He fusion.

1. INTRODUCTION

D-^{3}He fusion offers the possibility of fusion power with greatly reduced neutron production, associated radiation damage, and production of radioactivity in the structure, in comparison with the mainline approach of D-T fusion [1]. A D-^{3}He fusion fuel cycle also eliminates the need for periodic replacement of the first wall and the need for tritium breeding. The disadvantage of D-^{3}He fusion is that the fusion cross-section is much smaller and therefore more demanding of the plasma; it requires higher temperature operation and better confinement. In addition, the fusion power density in the plasma is smaller, but this disadvantage is offset by the elimination of the tritium-breeding blanket and the reduction in the required neutron shield thickness. Consequently, D-^{3}He fusion utilizes better the magnetic field generated by the toroidal field magnets. In addition, the environmental advantages of D-^{3}He are considerable and are more likely to lead to public acceptance of nuclear power.

Given the above advantages of D-^{3}He fusion, it is important to investigate plasma physics issues such as plasma transport, stability, current drive, heating, radiation losses, impurity control, ash accumulation, etc. at the densities and temperatures expected for D-^{3}He operation. Investigating these issues in a near-term D-T device will establish whether present-day physics extrapolates to D-^{3}He conditions without making a substantial investment in new facilities and without a significant delay in the D-T research program. Of the facilities currently in use or being planned, the obvious choice is ITER, since it has the greatest capability for producing

plasmas of interest for D-^{3}He. The optimum point in the operation schedule for investigating D-^{3}He is after initial operation of the plasma with deuterium and before the machine is activated by the use of tritium. An earlier investigation[2] of the potential for D-^{3}He experiments in ITER showed that, using currently fashionable physics assumptions, near-breakeven could be achieved in ITER without major changes in the facility. Achieving breakeven required an increase in the magnetic field at the magnet as well as a change in the plasma shape, although within the existing vacuum chamber. The parameters of ITER were those of the CDA phase of the ITER project. Since that time, ITER has grown from a major radius of 6 m to about 8 m and the magnetic field at the plasma has increased from 4.85 T to 6 T. In this study we revisit the question of whether meaningful D-^{3}He experiments can be done in the new, larger ITER.

2. CALCULATIONAL MODEL

The assessment of D-^{3}He operation has been done using a power balance code similar to the physics portion of the ITER systems code, but specialized for the peculiarities of D-^{3}He fuel. We refer the reader to Reference 2 and references therein for a discussion of the power balance code.

The figure of merit used to evaluate the performance of D-^{3}He fuel is the energy multiplication, Q, which is the ratio of the fusion power produced in the plasma to the injected power required to sustain the plasma. Note that Q=1 in D-^{3}He is equivalent to Q=5 in D-T from the point of view of the impact of fusion reactions on the plasma power balance. This is because essentially 100% of the fusion energy is in the form of charged particles for the D-^{3}He reaction, whereas it is only 20% for the D-T reaction. For the calculations presented in this paper, the fuel mixture is taken to be 60% D and 40% ^{3}He; this fuel mixture maximizes Q. Deuterium-rich operation reduces the electron density and thereby reduces the power losses and increases the fuel density for a given total charged particle density.

3. POWER BALANCE RESULTS

The parameters used for ITER for this study are:

Plasma current	25 MA
On-axis magnetic field	6.0 T
Major radius	7.75 m
Minor radius	2.80 m
Elongation	1.60

For an H-mode factor of 2.4 (relative to ITER-89P L-mode energy confinement scaling) and Troyon [3] coefficient of 3.1, this configuration produces a fusion power of about 3200 MW with D-T fuel at an average temperature of about 10 keV. These parameters represent the values in effect when this work was begun; the reference design for ITER has since evolved to a somewhat larger major radius.

Switching this machine to D-^{3}He fuel at an average temperature of 40 keV, with no further change in parameters, produces 127 MW of D-^{3}He fusion power, but requires an injection power of 360 MW to sustain the plasma; the plasma Q (ratio of fusion power to injected power) is thus 0.34. The performance can be changed by adopting less conservative assumptions concerning energy confinement and beta. Shown in Fig. 1 is the result of a set of calculations where the H-mode multiplier is varied from 2.0 (representing H-mode operation) to 4.0 (roughly equivalent

to VH-mode [4] operation) at a Troyon coefficient of 3.5%. A substantial improvement in the Q and reduction in the injected power is seen as the H-mode multiplier increases to 4.0. Figure 2 shows the effect of varying the Troyon coefficient at constant H-mode multiplier. Increasing the Troyon coefficient increases the Q, but also raises the required injected power. This is because the total energy content of the plasma is increasing and most of the power to sustain the plasma comes from the injected power.

In the results shown in Figs. 1 and 2 the maximum Q is 0.74 and the required injection power is 183 MW. Higher performance can be obtained by noting that the large injection power arises from the large plasma volume. While the injection power can be reduced by reducing the plasma size, it is important to maintain the plasma current since the energy confinement time depends strongly on the current. In addition, higher magnetic field at the plasma can be obtained by moving the plasma closer to the inboard leg of the toroidal field magnets. Figure 3 shows a sequence of shapes obtained when the plasma radius and minor radius are decreased by the same amount; the inner edge of the plasma is kept at a constant radius so the plasma is not interfering with the vacuum chamber in this variation. The plasma height is held constant so the elongation is increasing. Because of the combination of increased elongation and reduced minor radius, the plasma current is approximately constant in this variation. The Q-values and injection power resulting from this sequence are shown in Fig. 4. We see that breakeven (Q=1) is achieved when the major radius is reduced from the starting point of 7.75 m to about 7.2 m; the corresponding elongation is 2.0, the plasma current is 25.8 MA, and the injected power is 183 MW. Reducing the major radius to 6.75 m while holding the inner edge of the plasma constant increases the elongation to about 2.4 and increases Q to about 1.4.

Since the neutron power in these D-He plasmas is only about 10 MW while the D-T neutron power in ITER is about 2500 MW, the inboard blanket can be removed; the vacuum chamber provides enough shielding for the magnets in D-^{3}He operation. Limiting the elongation to 2.2 while further reducing the major radius to 6.5 m increases the Q to about 1.4 at an injected power of 204 MW; for this configuration the plasma current is 30.5 MA. and the aspect ratio is 3.17. Consequently, removing the blanket and further reducing the major radius does not greatly increase the Q while it adds to the complexity of converting the machine to D-^{3}He operation.

Higher Q operation can be obtained by seeding the plasma with a small amount of tritium. For R = 7.2 m, κ = 2.0, and A = 3.2, which gives Q = 1 for pure D-^{3}He, a plasma Q of 2.0 is obtained at an injection power of 120 MW when the tritium concentration is 11%. In this case about half the fusion power is due to D-^{3}He reactions and about half due to D-T reactions. The fast ions produced in the plasma are a mixture of energetic protons (14.7 MeV) and alpha particles (3.5-3.7 MeV). The power to the divertor is about 160 MW, the first wall surface heat flux is about 10 W/cm^2 and the neutron power is 423 MW. The extreme limit of tritium seeding is to use pure D-T plasmas; ignition is obtained (with an ignition margin of 1.2) using the same average ion temperature as for D-^{3}He plasmas; the fusion power is 1900 MW and the surface heat fluxes are less than those obtained in the ITER reference design. Consequently, a range of Q values from breakeven to ignition can be obtained with mixed D-^{3}He-T plasmas, all at an average ion temperature of 40 keV. Interesting and important physics questions can be studied in these plasmas even though a substantial fraction of the fusion power is due to D-T reactions. For example, the isotopic composition of the plasma does not play a strong role in plasma transport and microstability, synchrotron radiation transport, MHD stability, plasma heating, and other questions needing to be investigated at D-^{3}He relevant conditions. Isotopic composition may be important in ash accumulation, but this can be investigated by varying the fuel mixture.

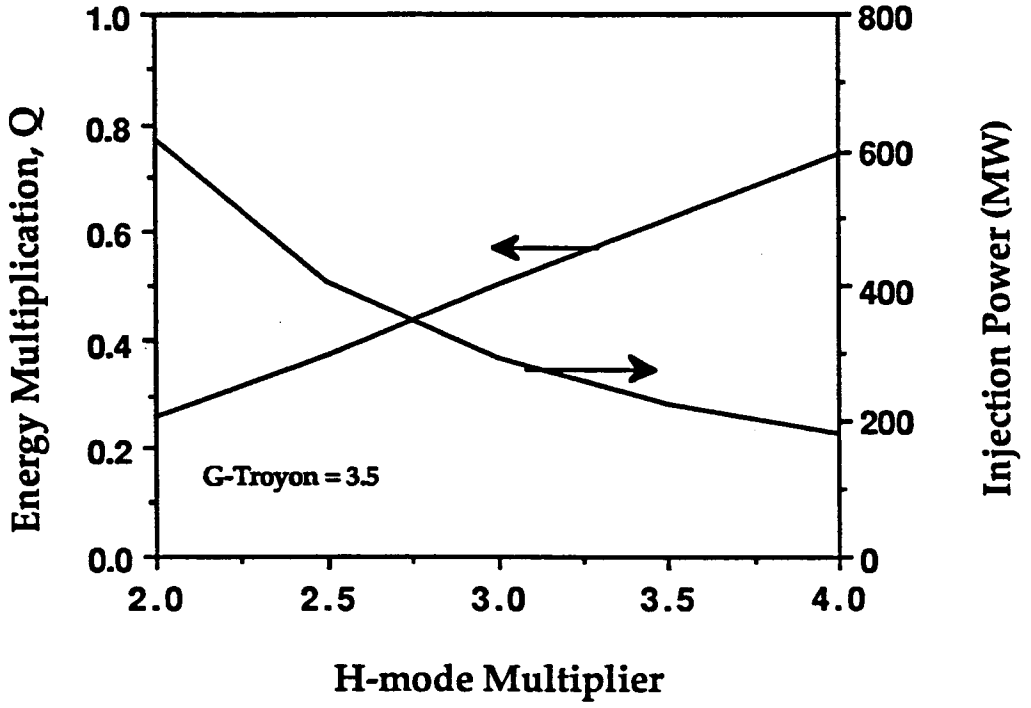


Fig. 1. Effect of the H-mode multiplier on the energy multiplication, Q, and the injected power. The Troyon coefficient is constant at 3.5%.

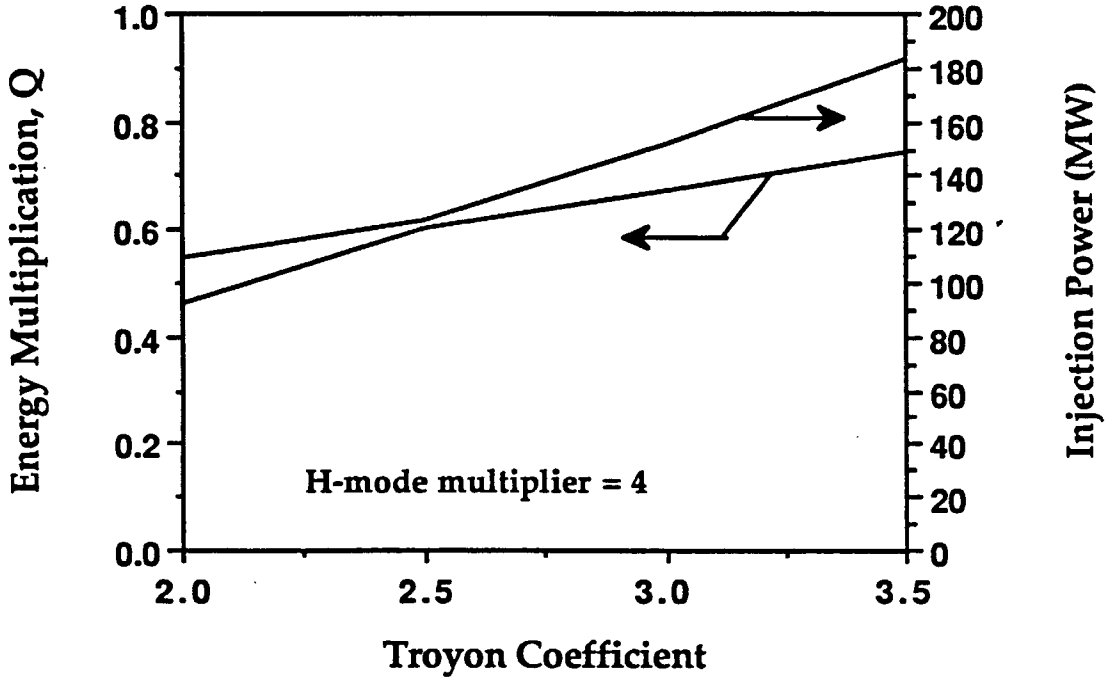


Fig. 2. Effect of beta on the energy multiplication, Q, and the injected power.

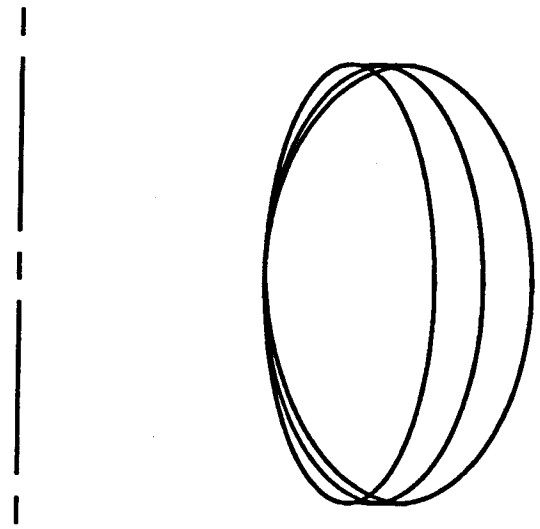


Fig. 3. Sequence of plasma shapes obtained by increasing the elongation while maintaining the plasma bore constant. This reduces the plasma volume and moves the plasma axis to higher magnetic field.

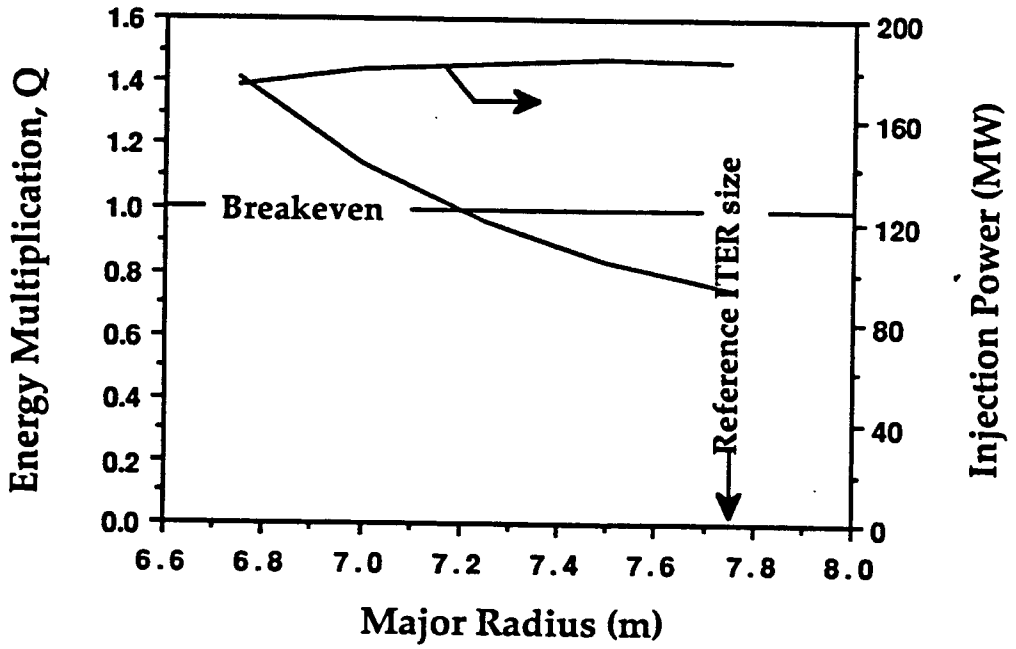


Fig. 4. Reducing the major radius while maintaining the inner bore of the plasma (see Fig. 3) improves the energy multiplication, Q. Breakeven is achieved when the major radius is reduced to 7.2 m. For this graph the H-mode multiplier is 4.0 and the Troyon coefficient is 3.5%.

4. SUMMARY

Using presently fashionable physics assumptions, breakeven (Q=1) with D-^{3}He can be obtained in ITER. Higher Q operation can be obtained at D-^{3}He relevant temperatures by seeding the plasma with a small amount of tritium. Ignition at D-^{3}He temperatures can be obtained with D-T fuel. This allows for the investigation of plasma physics questions important for D-^{3}He using a near-term D-T facility.

REFERENCES

[1] G.L. Kulcinski, G.A. Emmert, J.P. Blanchard, et al., *Fusion Tech.*, **15**, 1233 (1989).

[2] G.A. Emmert and R.R. Parker, *Fusion Tech.*, **21**, 2284 (1992).

[3] F. Troyon, R. Gruber, H. Saurenmann, S. Semenzato, S. Succi, *Plasma Physics & Controll. Fusion* , **26**, 209 (1984).

[4] G.L. Jackson, J. Winter, T.S. Taylor, et al., *Phys. Rev. Lett.*, **67**, 3098 (1991).

ARIES-III SECOND STABILITY, D-^{3}He TOKAMAK REACTOR DESIGN

Robert W. Conn
Institute of Plasma and Fusion Research
UCLA
44-139 Engineering IV
Los Angeles, CA 90024-1597

NO ABSTRACT OR PAPER RECEIVED

D-^{3}He, Second Stability Tokamak Reactor Study

V.I.Pistunovich, S.G.Bespoludennov
Nuclear Fusion Institute
Russian Research Center -
Kurchatov Institute, Moscow

ABSTRACT.

The optimization of the reactor parameters and analyses of the main critical issues of the modest magnetic field D-^{3}He reactor are presented in this paper. This includes plasma confinement, beta limit and the second stability regime, divertor problems, thermal- to- electric energy conversion and structural features of the design. The optimization of the plasma parameters at various plasma pressure profiles has allowed us to determine the set of the parameters, which is depended from the particle confinement time in the reactor plasma very strong. The control over the plasma pressure and current radial profiles can be one of the main tools for the transition from the low efficiency mode of operation to that with high efficiency.

1.INTRODUCTION.

The ignition of D-^{3}He reactions in tokamaks results in an increase in the reactor size in comparison with the D-T reactor. It is related with the necessity in a few times increase in the plasma confinement parameter, $n_e\tau_E$, in the attainment of a higher plasma temperature and a pressure limit. However, the ecological purity in the usage of D-^{3}He fuel can dominate over technical difficulties in the construction of a D-^{3}He reactor and make its industrial implementation economically - profitable.

The goal of the present study is the analysis of the main critical issues of the modest magnetic field D-^{3}He tokamak - reactor from the positions of modern knowledge in the plasma physics of large tokamaks and from the positions of the acceptable present day engineering solutions.

This includes plasma confinement, beta limit and the second stability regime, divertor problems, thermal-to-electric energy conversion and structural features of the design.

The approach to the solution of the first two problems is based on the experimental data obtained from tokamaks with a poloidal divertor. The energy confinement time in the experiments can exceed by 3.6 times the value obtained from the ITER scaling law for the L-mode. This value is used in the Study.

The maximal central beta of about 44% was obtained in DIII-D at a rather peaked radial plasma pressure profile. In the reactor study, the plasma density, temperature profiles and, hence, the pressure profile close to those obtained in the experiments on DIII-D are considered.

The divertor problems and the direct thermal-to-electric energy conversion are considered within the framework of conceptual proposals to be tested in the tokamak experiments. The solutions to these problems, in many respects, determine prospects for the fusion tokamak - reactor development.

2. PLASMA POWER BALANCE AND SECOND STABILITY REGIME

For determining optimal parameters of the D-^{3}He tokamak-reactor one dimensional stationary model of the power balance [1] has been used. The energy confinement time in the plasma has been determine with the ITER-89 scaling for the L-mode increased by 4 times on the basis of the experimental results from DIII-D [2] and from JET with a poloidal divertor. The reactor parameters have been optimized with respect to the major radius, aspect ratio, β-value, elongation factor K, toroidal magnetic field B_0 and with respect to the plasma density and temperature profiles,

$$n(r) = n_0[1-(r/a)^2]^{\alpha_n}, \quad T(r) = T_0[1-(r/a)^2]^{\alpha_T}.$$

The optimal helium-3/deuterium density ratio in the plasma is equal to $n_{He3}/n_D \cong 0.7$ (41% ^{3}He, 59%D). The optimal temperature at the maximum Q-value is equal to about 45keV ($Q = P_{Fus}/P_{Aux}$, where P_{Fus} is the fusion power and P_{Aux} is the power injected into the plasma).

The control over the plasma density and temperature profiles provides great opportunities for changes in the reactor parameters and its operation conditions.

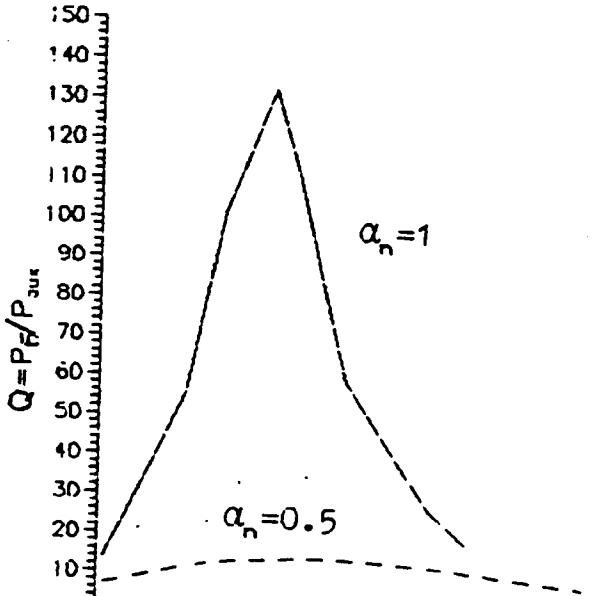


Fig.1. Q dependence on the temperature profile index α_T at α_n=1; 0,5 at τ_p/τ_E = 1.6.

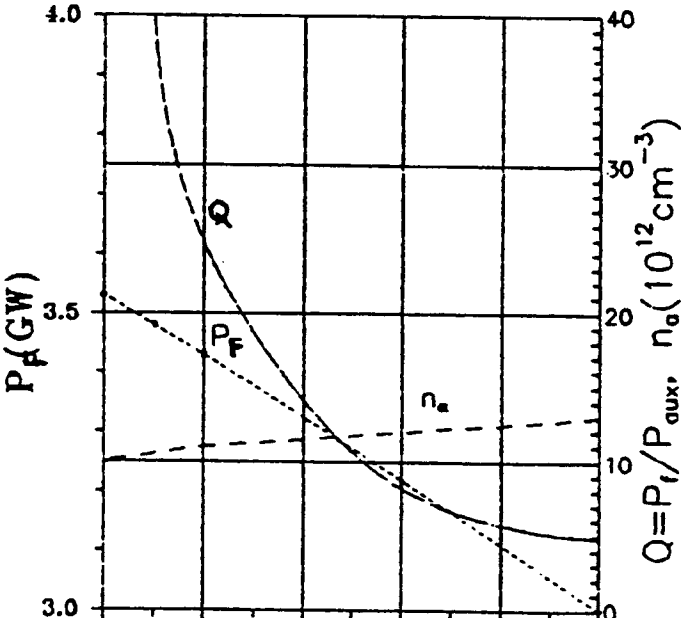


Fig.2. The dependence of α-particle n_α, fusion power P_F and Q on particle confinement time, α_n=1,α_T=1.5

The Q-dependencies on the temperature profile index, α_T, are given in Fig.1. One can see a maximum of Q dependence on α_T at α_T is equal about 0.7.

Such a dependence allows one to determine the most attractive Q-values of the reactor, since the experimental plasma pressure profiles are rather peaked [2]. The particle balance equation has been used for determining the stationary concentrations of D-^{3}He reaction products. The dependence of relative α-particle concentration, n_α, and that of fusion power and Q on the particle confinement time, for a one reactor modification, are given in Fig.2. A considerable effect of the particle confinement time growth on the fusion power magnitude and on the reactor parameters is observed. The calculations show that the reactor parameters can be attracted at ratio $\tau_p/\tau_E \leq 2$ only, Fig.2. Fusion power is reduced by about 30% at $\tau_p/\tau_E \cong 2$ in comparison with the case, when $\tau_p = 0$. The proton density is practically the same as that of α- particles. The relative concentration of tritium, n_T/n_D, is about 0.4%. At the temperature $T \cong 45$ keV it corresponds to the density $n_T \cong 3 10^{11} cm^{-3}$. The Q - value noticeably rises with increase in plasma pressure, $\beta \geq 15\%$. In this case a faster rise in the fusion power in comparison with the transport losses is observed.

Present theoretical analyses [3] indicate that high values of β can be achieved but it will require a D-shaped plasma with the central safety factor of $q_0 > 1$, and with finite values for both the pressure gradient and the plasma current density at the plasma edge. The data obtained from DIII-D tokamak, $\beta_0 = 44$ % and $<\beta> = 11\%$ [2], can be used as a basis for consideration such operating conditions in the reactor. A non-monotonous q-profile was a characteristic feature of such discharges in DIII-D. The stability analysis [3] has shown that the plasma core is in the second stable regime and the inner negative shear region allows one to have a large positive shear region near the boundary,even at low q. The recent studies [4-5] have shown that the production of non-monotonous q(r) profiles allows one to raise the critical β respective to the ideal ballooning modes for the q and p profiles close to the experimental ones from 6% up to 25% for the D-shaped tokamak cross section. A strong critical β sensitivity to the pressure profile is observed. However, the plasma is unstable to free-boundary kink modes which are stabilized by a combined system of passive and active control coils. In the experiments on DIII-D an increase in the energy confinement time and in the stability limit has been attained by modification of the current profile from the relatively broad shape obtained in a standard tokamak discharge to a more peaked one[6]. At the plasma elongation k=2.1, the energy confinement time was 1.8 -times longer than that in the H-mode at the internal inductance $l_i \cong 1.7$.At $l_i = 1.7$ the theoretical $\beta-$limit $\beta_N > 6$ ($\beta_N = \beta a B_0 / I$), with respect to ballooning modes, are attained. Given experimental results allow one to consider the tokamak reactor with the enhancement factor H=4 in confinement over the L-mode values and in the values of normalized toroidal beta β_N near 6% mT/MA. In this case the plasma elongation should be rather high, $k \geq 2$. The presence of high elongation means the usage of a double null divertor configuration.

The optimization of the plasma parameters at various plasma pressure profiles and particle confined time has allowed us to determine the sets of the reactor parameters, see Table I.

Table I. Key Parameters of FTR and ITER.

	FTR				ITER
Major radius, m	8.5				8.21
Aspect ratio	2.6				2.74
Magnetic field on axis,T	6.5				5.95
Maximum field at TF coils,T	13				
Plasma current, MA	55				25
Elongation, K	2.1				1.6
q_ψ / z_{eff}	3/1.58				2.85/1.6
β_0 / $<\beta_{th}>$, %	4 5/15				3.92
α_n / α_T	0.5/1	1/1.5		1/2	0.5/1
τ_p / τ_E	1.6	1.5	2	1.4	
$<n_e>$, $10^{20}m^{-3}$	2.25	2.13	2.24	2.22	2.0
$<n_D>$, $10^{20}m^{-3}$	0.86	0.79	0.8	0.82	
$<T_i>$, keV	44	46.6	44.3	44.7	
τ_E, s	10.1	10.6	10.8	11.1	3.0
Fusion power, MW	3220	3530	3000	3610	3000
Synchrotron power, MW	400	350	310	330	
Bremsstrahlung, MW	1670	1930	2050	2080	290
Transport power, MW	1360	1270	1260	1220	
$Q = P_F / P_{Aux}$	15.4	286	4.9	136	
DD-Neutron power, MW	62	68	59	68	
DT-Neutron power, MW	224	279	281	287	
Neutron wall load, MW/m^2	0.16	0.2	0.19	0.2	
Radiation wall load,MW/m^2	1.2	1.3	1.35	1.38	
Direct conversion efficiency, %	90	90	90	90	
Thermal conversion efficiency,%	40	40	40	40	
Net electric power, MW_e	1500	1900	1300	1800	
Net efficiency, %	46	54	43	50	

3. FTR PLASMA ENGINEERING.

The problem of a divertor allowing one to remove the heat from the plasma and to exhaust the reaction products is the most complicated tokamak reactor problem. The FTR (Future Tokamak Reactor) Study includes a double null (DN) divertor configuration at high plasma elongation. The main motivations for choosing the double null are the desire to operate with high elongation and triangularity, and DN is more favorable for advanced confinement conditions than single null(SN). Based on analysis of the division of power between inner and outer divertor plates in existing tokamaks, we have established requirements for the maximum power incident on the FTR divertor plates. For DN configuration the in/out power split is 1:4, 80% to the outer plates.

Because a D-^{3}He tokamak plasma is highly radiative, only a fraction, about 40% in FTR, passes the plasma separatrix as the transport power and appears on the divertor plates. However, the transport power is higher than for a DT reactor. For FTR this power is about 1300 MW.

In contrast to a DT reactor the main part of the thermonuclear energy released in the D-^{3}He reactor can be converted into the electric energy by means of the direct transformation with the efficiency higher than that of a thermal cycle. According to experimental data there are some currents between the divertor plates and the vacuum vessel in JET [7] and DIII-D [8].

The presence of the current between the divertor plates and the chamber walls on JET and on DIII-D confirms the opportunity to use direct energy conversion in the tokamak-reactor. The direct transformation of the plasma energy into the electric energy is based on transport properties of the scrape-off layer (SOL) of the tokamak with the poloidal divertor. The key point is a local non-ambipolarity of particle fluxes which results in appearance of electric currents. For example, the presence of neutrals, momentum carrying waves etc. results in appearance of effective friction, which permits ions going away to the wall while electrons stream along the magnetic field. Experimentally measured current [8] are the direct evidence of the reality of the considered mechanism [9]. The efficiency of transformation of ion energy into electric energy can be high. However, an amount of power carried by ions is determined by the mechanism of SOL transport across separatrix and achieves a half of power carried by particle flux across separatrix. Then the efficiency of the energy conversion can be written in the form

$$\eta = \eta_r \frac{P_{rad}}{P_{Fus}} + \eta_{ce} \frac{P^E_s}{P_{Fus}} + \eta_{ci} \frac{P^I_s}{P_{Fus}},$$

where $\eta_r, \eta_{ce}, \eta_{ci}$ are the energy conversion efficiencies for radiation, electron and ion fluxes.

At the fusion power P_{Fus} = 3530 MW the power of cyclotron and bremsstrahlung radiation was calculated as $P_c + P_B \cong$ 2280 MW. The efficiency of the transformation of the radiation energy we assume to be equal to the thermal transformation efficiency, i.e. $\eta_r = \eta_T = 0.4$. The power carried out by electrons and ions through the separatrix surface $P_s \cong P^E_s + P^I_s \cong$ 1270 MW. At a P^E_s/P^I_s ratio equal to 1/1 $P^E_s \cong P^I_s \cong$ 635 MW. In principal the ion power

fraction through the separatrix, P_s^I, can be converted to electricity with high efficiency, $\eta_{ci} \cong 0.9$, due to a locally non-ambipolar particle transport in the divertor layer across the magnetic field [9], as was observed in DIII-D [8].

The power $P_s^E \cong 635$ MW enter the divertor plates and is converted into electricity with η_{ce} =0.4. The pessimistic estimate for η will be $\eta \cong 0.55$. Thus, even in this case one can get 15% increase of η using ion energy conversion. Thus the power on the divertor plates is about $P_d \cong 0.1\ P_s^I + P_s^E \cong$ 700MW. This value is not exceeded strong the ITER divertor power, and decision the divertor problem can be fulfilled together the development of the ITER design. The most immediate manifestation of the divertor problem is the power loading at the divertor plates. The engineering difficulty of the divertor derives from the power-per-unit area P_d/A on the divertor structures. In operation with a gaseous divertor or/and impurity radiative divertor the power density on the divertor structure may not exceed 5 MW/m^2. This means that the area of a collecting surface should be $A=2\pi R\Delta_D$ where the effective poloidal length of divertor structure wetted by the power flow $\Delta_D \cong$ 0.9m, i.e. the height of the divertor chamber should be about 1m. Preliminary analyses indicate that average heat load on the outboard divertor wall is estimated to be $\cong$ 2.5 MW/m^2.

Plasma start-up is an important issue for second stability regime. A preliminary start-up scenario has been identified which uses the current drive system both for heating and current drive. The steady state heating power P_{aux} is about 100 MW, but additional high heating equipment may be needed for start-up. The current drive power, however, should be large and can be adequate for current profile tailoring.

The D-^{3}He fuel cycle have a clear advantage over DT cycle in terms of the neutron production and tritium hazards. Because the neutron yield is low a thin shield is required to protect the magnets from the reduced gamma and neutron heating and radiation damage. The shield thickness is about 60 cm. The neutron flux on the first wall is rather low ($\cong$0.2 MW/m^2), but the peak heat flux is rather high ($\cong$1.3 MW/m^2). Therefore removing this heat flux is a critical issue. Because the thermal stored energy in a D-^{3}He tokamak plasma is about 5 times larger than in the DT reactor ITER, response of the first wall to plasma disruption is another critical issue.

4. SUMMARY.

The D-^{3}He tokamak reactor study presented here is based on the existing data base in plasma physics. The required reactor parameters do not differ much from those which are adopted for the ITER-93 design. An essential effect of the plasma density and temperature profiles and the particle confined time on the reactor reactivity Q has been emphasized. The control over the plasma and current profiles can one of the main tools for the transition to the second stability regime.

The opportunity to use the divertor plasma flow and synchrotron radiation direct energy conversion allows one to increase the net efficiency of the reactor by (10-15)% in comparison with DT reactor.

REFERENCES.

[1] S.G.Bespoludennov, V.I.Pistunovich, V.I.Kripunov, D^3He Tokamak Reactor Parameters, paper 1A2, Proceeding of the. Workshop, Kurchatov Institute, Moscow, 25 Sept.-2 Oct. 1991.
S.G.Bespoludennov, V.I.Pistunovich, Optimization of D^3He Tokamak Reactor Parameters. Fisika plasmy v.18, N 12, 1524(1992).
S.G.Bespoludennov et.al., D^3He Tokamak Reactor, 14^{th}Intern. Conf., CN-56/G-1-1-2, Wursburg, Germany, 30 Sept.- 7 Oct. 1992.

[2] T.C.Simonen, ITER Phys./Design Work Session, San Diego, GA, July 10-18, 1991.

[3] E.A.Lazarus et.al. An optimization of Beta in the DIII-D Tokamak, GA-A20571, July 1991.

[4] M.V.Medvedev, A.I.Yurchenko, High β in tokamak at non-monotonic q profile. Fisika Plasmy (1993), to be published.

[5] F.Najmabadi, R.W.Conn, et,al. The ARIES-III D-^{3}He Tokamak Reactor Study-Final Report Univ. of California Los. Angeles report UCLA-PPG-1384 (1992).

[6] J.R.Ferron et.al. Improved confinement and stability in the DIII-D Tokamak obtained through modification of the current profile. GA-A21151, GA Project 3466, December 1992.

[7] P.J.Harbour et.al. J. Nucl. Mater. v.162-164, 236 (1989). JET Team, in Plasma Phys. and Contr. Fusion Research 1988, Proc. 12th Int. Conf., Nice 1989, Vol.1 IAEA Vienna, 159 (1989).

[8] M.J.Shaffer, B.J.Leikind, Nucl.Fusion, v.31,N 9, 1750 (1991).

[9] S.V.Bazenkov, S.G.Bespoludennov, M.V.Osipenko, V.I.Pistunovich, O.P.Pogutse, On the Energy Conversion in D-^{3}He Reactor Tokamak, Preprint IAE, Moscow 1992.

Overview of Apollo Studies and Economic Assessment of Several Proposed Variations

Laila A. El-Guebaly and Charles W. Maynard
University of Wisconsin-Madison
1500 Johnson Drive
Madison, WI 53706

ABSTRACT

Highlights of the Apollo series of D-^{3}He conceptual reactor studies are briefly summarized in this paper. The 1000 MWe designs operate in the first-stability regime and employ dual energy recovery systems: direct conversion for synchrotron radiation power and thermal conversion for neutron, bremsstrahlung, and transport powers. A key feature of all Apollo designs is the low neutron production that reduces the damage to the structure and eliminates the need for first wall replacements during the entire reactor lifetime. Considerable reduction in the required shielding space results from the low neutron production and the absence of the tritium breeding blanket. The impact of coolant choice and shield design on the overall machine parameters and cost of electricity was assessed. The consequences of utilizing recent concepts for high-efficiency current drive are explored. The safety and environmental features of the designs and the high system availability allowed the D-^{3}He tokamak reactors to compare favorably with recent D-T tokamak designs.

1. INTRODUCTION

The Apollo study, led by the University of Wisconsin, investigates the possibility of burning D-^{3}He fuel in tokamaks, the world's current leading concept. Besides tokamaks, the D-^{3}He fuel can be burned successfully in tandem mirror, FRC, dipole, electrostatic, and large orbit devices, as detailed in companion papers in these proceedings. The aim of the Apollo study is to illustrate the technological, economic, safety, and environmental features and identify the physics and other critical issues associated with the D-^{3}He fuel cycle. Over a period of 5 years, four Apollo conceptual designs have been completed assuming minimum extrapolation in technology and reasonable extrapolation in physics. The investigated areas during the course of the 5 years study were the D-^{3}He physics, current drive, disruption, direct conversion, fuel cycle, radiation damage, shielding, safety, system availability, ^{3}He resources/cost, and economics. Details can be found in several publications and other papers in this proceedings [1-16]. Ranges of major parameters considered in the various designs are listed in Table 1. General features include the operation in the first stability regime, low neutron wall loading, relatively high magnetic field and plasma current, low aspect ratio, direct conversion of synchrotron power using rectennas, permanent first wall/shield components, and inherently safe design with competitive cost of electricity (COE).

This paper briefly describes the Apollo design series and highlights the general features of the reactors. Variations in design parameters that enhance the attractiveness of the design were assessed for the most recent Apollo-L4 design. The impact of the coolant and shielding materials on the machine parameters and economics is examined. A comparison with D-T designs in the areas of radiation damage, system availability, and economics is presented.

Table 1. Highlights of Apollo Designs

First stability plasma regime	6-10% β
Net electric power	1000-1200 MWe
D : ^{3}He ratio	2 : 1
Low neutron wall loading	0.1 MW/m^2
Low aspect ratio	2-4
Major radius	6-8 m
Elongation	2.0
Triangularity	0.5
High field magnets	20 T at coil
Plasma current	40-80 MA
Current drive gamma	1-5 A/Wm^2
Direct conversion of synchrotron radiation	80% efficiency
Thermal conversion of other powers	35-50% efficiency
Low level waste	Class A
Inherently safe design	LSA=1
High system availability	>75%
Operation time	40 y
Competitive cost of electricity	60-90 mills/kWh

2. APOLLO DESIGNS

Detailed list of parameters is given in Table 2 for the four Apollo designs and a vertical cross section of the latest Apollo-L4 design is shown in Fig. 1. The recent designs are 1000 MW

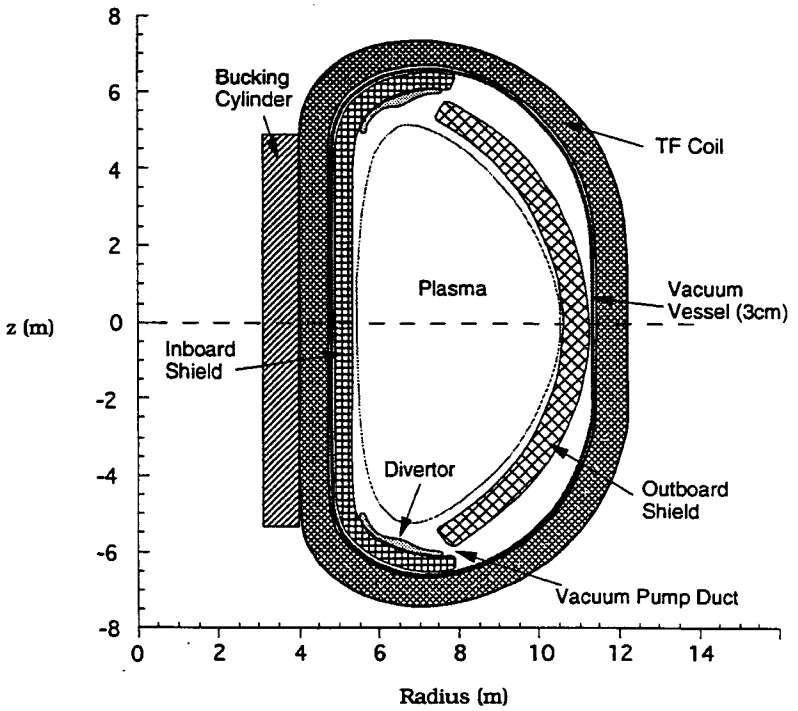


Fig. 1. Vertical cross section of Apollo-L4 design showing plasma, shield, and TF coil (courtesy of E. Mogahed, University of Wisconsin).

Table 2. Key Parameters for Apollo Series

Design Year of Study	Apollo-L 1988	Apollo-L2 1989	Apollo-L3 1991	Apollo-L4 1993
Energy conversion	synchrotron	synchrotron	mixed	mixed
Net power (MWe)	1200	1200	1000	1000
Shield type-thickness (cm)	SS/H_2O-57	SS/H_2O-59	SS/OC-65	SS/H_2O-57
Direct conversion efficiency	80%	80%	80%	80%
Thermal conversion efficiency	---	---	44%	35%
Net system efficiency	42%	41%	43%	37%
Fusion power (MW)	2872	2807	2144	2437
Synchrotron power (MW)	1626	1663	1027	1082
Bremsstrahlung power (MW)	959	790	652	756
Transport power (MW)	192	267	456	485
Neutron power (MW)	118	138	147	171
Injected power (MW)	23	40	138	57
Average Γ (MW/m^2)	0.1	0.1	0.1	0.1
Average first wall heat flux (W/cm^2)	91	67	84	98
Major radius (m)	8.0	7.1	7.9	8.06
Aspect ratio	4	2.5	3.15	3.12
Peak coil/on-axis field (T)	20/13	20/10	19/10.9	19/11.2
Plasma current (MA)	47	80	53	55
Beta	6.3%	9.3%	6.7%	6.7%
Troyon coefficient	3.5%	3.25%	3.5%	3.5%
H-mode coefficient	2	2.5	4	4
Density/temperature profile exponent	1/1.5	0.75/0.75	0.95/0.55	0.95/0.55
$n_e \tau_E$ (10^{20} m^{-3}s)	80	41	29	31
$\tau_P^{ash}/\tau_E^{bulk}$	1	0.55	1	1
Energy confinement time (s)	38	24	16	16
Average ion/elec. temperature (keV)	69/55	71/56	57/51	57/51
Average ion/elec. density (10^{20} m^{-3})	1.3/2.1	1.1/1.7	1.3/1.9	1.4/1.95

electric power reactors to be able to compare to recent DT tokamak designs. The Apollo studies favor first stability plasma regime with high magnetic field, peaked density and flat temperature profiles, and relatively high average temperatures. In order to lower the plasma current, and hence alleviate disruption concerns, the aspect ratio was reduced to ~3, considering ITER-89P energy confinement scaling law. A value for $\tau_P^{ash}/\tau_E^{bulk}$ of one was chosen and may require active means of ash removal from the plasma core. Overall, the physics parameters were chosen to produce a high level of synchrotron radiation in order to directly convert the synchrotron radiation to electricity and to use it for current drive. All other powers are converted via a Rankine cycle with η = 35-45%, depending on the coolant type.

Table 3. Impact of Shield Design on COE

Shield Type Coolant	SS Organic Coolant	SS Water	SiC/B_4C Helium	$SiC/SS/B_4C$ Helium
Structure-cost ($/kg) Filler-cost ($/kg)	SS-60 SS-25	SS-60 SS-25	SiC-200 SiC-57	SiC-200 SS-25
Shield thickness (cm)	63	57	86	73
Thermal efficiency	44%	35%	49%	49%
Pumping power (MW)	10	10	50	50
COE* (mills/kWh) LSA=1	84 (94,LSA=2)	89	93	89

*Costed in constant 1992 dollars for a conservative case: 75% availability, 1.35 CD gamma, and 1000 $/g of ^3He

In recent Apollo designs, about 20% of the plasma current is driven using external power. The synchrotron radiation drives 45% of the current while the bootstrap current comprises the balance. Highly efficient current drive system is needed to limit the external power and, thus, improve the economy of the design. Recent development in advanced concepts (e.g., compact toroid) looks promising considering the high operating temperature and the flat profile of the D-^3He plasma. An efficient current drive (CD) system, possessing high CD gamma, did indeed reduced the external CD power of Apollo-L4 by a factor of 2-3 compared to the previous design, and hence lowered the COE significantly.

The low level neutron wall loading offers several technological, safety, and environmental advantages. The first wall and shield qualify as Class A near surface burial waste [11,13]. The overall design is inherently safe and has a level of safety assurance (LSA) of 1 (a fission reactor has LSA of 4). The radiation damage is greatly reduced [10] allowing the first wall and shield to be reactor-lifetime components. This certainly has a positive impact on the availability of the system and, more importantly, eliminates the need to dispose of any radioactive waste during reactor operation.

The shield, protecting the superconducting magnets, is relatively thin (almost half of that required for DT reactors). This is mainly due to the reduced wall loading and the lack of the tritium breeding blanket. The preferred option for the latest Apollo-L4 design is the water cooled modified HT-9 ferritic steel shield as it leads to a more conservative design, has the best shielding performance, and meets the inherently safe criteria. Organic coolant (OC), having no major decomposition problems under the reduced neutron environment of D-^3He, possesses higher thermal efficiency and lower shielding performance relative to water. Other options include the use of advanced materials (such as SiC/SiC composites) with helium coolant. As evident from Table 3, there is no clear shielding or economical advantages for employing such highly developmental materials in D-^3He reactors.

3. ECONOMIC ANALYSIS

The economics of Apollo were performed using the WISCAF code: WIsconsin System Code for Advanced Fuel [17]. The code is written in C and runs on NeXT (UNIX) machines and is made up of two programs. The main program is called WISCAF and the second is WISCAF-e, the economic stand alone part of WISCAF where the physics parameters must be input. WISCAF itself is essentially a combination of two other codes: RAGE, an updated version of DHE3TOK [18], a point model plasma physics code to obtain details of the plasma and its requirements; and a tokamak engineering program called Generomak [19]. RAGE is built into the main program with no changes in the calculational parts and much borrowing from the input and output routines, while the Generomak part (which mainly does the engineering extrapolations and economic calculations) has been revised so much that one might be justified in failing to mention it in this discussion since language has been changed, physics and other sections were left out, and many of the calculational algorithms have been changed to include the latest costing scheme [20], LSA factors, and 1992 unit costs. The program as a whole accepts input data for a tokamak reactor, then allows online changes of any parameters, calculates the physics data, then calculates the direct and indirect costs of the power plant, and the cost of electricity. Benchmarking of the WISCAF-e code against the well developed ARIES system code [21] showed excellent agreement in costing.

4. PARAMETRIC VARIATIONS

The economic results presented so far are for a conservative case where 75% availability, 35% thermal efficiency, 1000 \$/g ^{3}He unit cost, 1.35 A/Wm^2 CD gamma, and 57 cm thick inboard shield were considered. Sensitivity of COE to variations in these parameters was assessed to determine their economical impact. The first variation shows the effect the system availability has on COE. Figure 2 indicates that a 1% increase in availability saves 0.8 mill/kWh. It is pertinent to mention that the first wall and shield of Apollo are permanent components and do not require frequent replacement during reactor operation like blankets of D-T systems. Hence, D-^{3}He designs should possess higher availability compared to DT by at least 10% [1-10].

The second variation considers more efficient thermal conversion cycles and Fig. 3 shows that a 1% increase in thermal efficiency saves 0.7 mill/kWh. The next variant considered was the cost of the ^{3}He fuel. A recent study [16] has revealed that the projected cost of ^{3}He from the moon is ~500 \$/g. As illustrated in Fig. 4, a decrease of 100 \$/g of ^{3}He reduces COE by 1.3 mills/kWh. The fourth variation considers the impact of the CD system on COE. Significant reduction in injected power and up to 15 mills/kWh could be saved (see Fig. 5) if highly efficient CD system is employed. For instance, a CD gamma of 5 A/Wm^2 would drop the injected power to 57 MW from 140 MW at 1.35 A/Wm^2.

The last variant considered was to quantify the impact of the inboard shield on the overall design. The 57 cm thick reference shield was varied in thickness from 40 to 75 cm. The lower and upper ends correspond to a factor of 10 increase and a factor of 10 decrease in the magnet radiation limits [9], respectively. The increase in COE with shield thickness shown in Fig. 6 is the result of the cost increase of having bigger reactor and moving all components radially outward. It was found that a centimeter increase in the inboard shield thickness costs 0.3 mill/kWh, or 20 M\$ in terms of total cost, and changes the major radius by 2 cm.

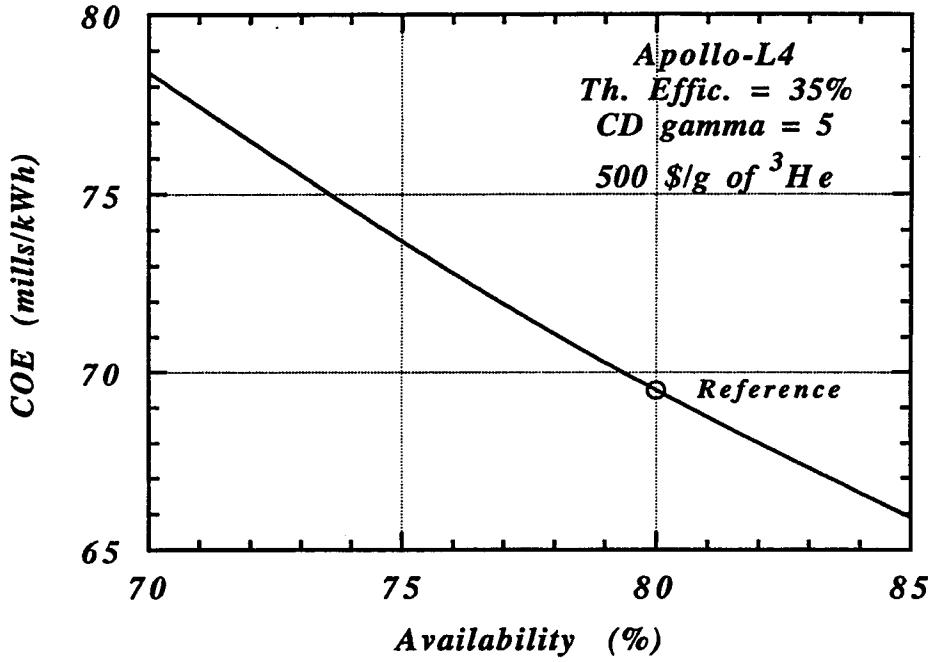


Fig. 2. Dependence of COE on availability.

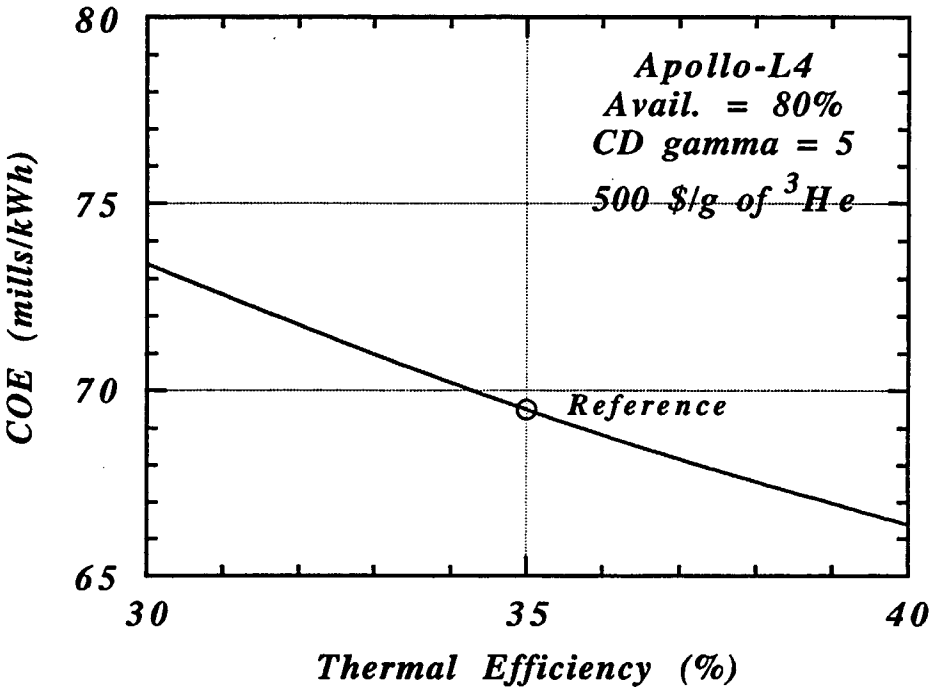


Fig. 3. COE as a function of thermal cycle efficiency.

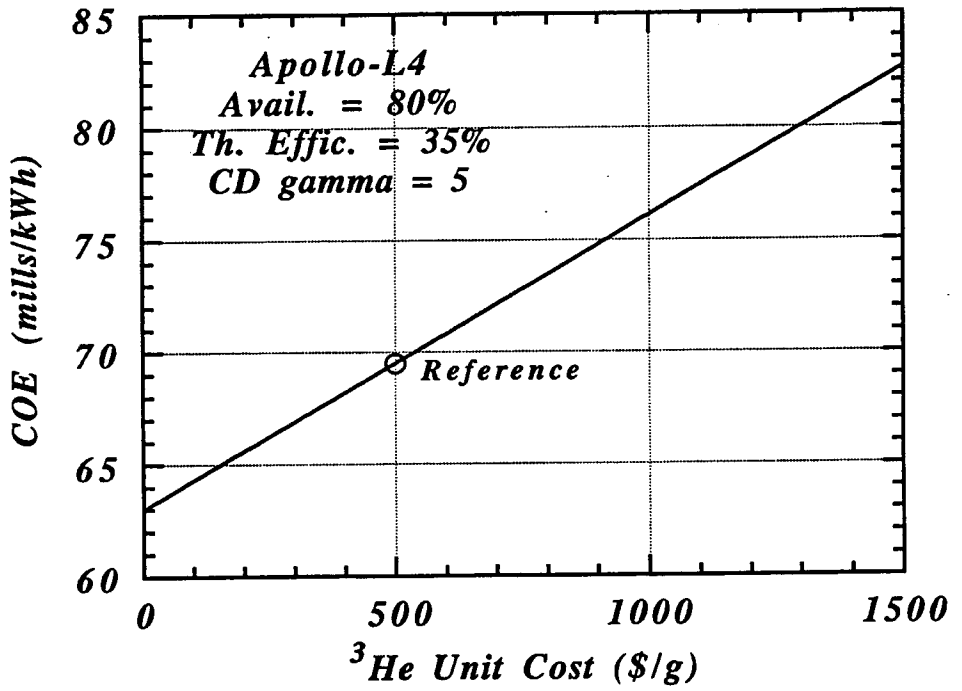


Fig. 4. Sensitivity of COE to ^{3}He cost.

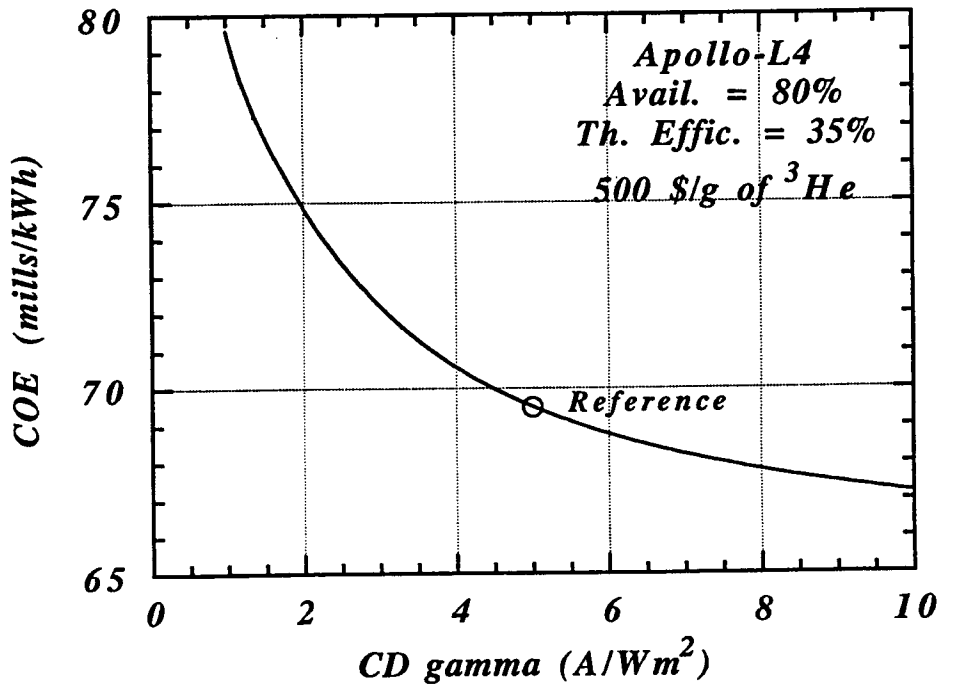


Fig. 5. Reduction in COE due to high efficiency current drive system.

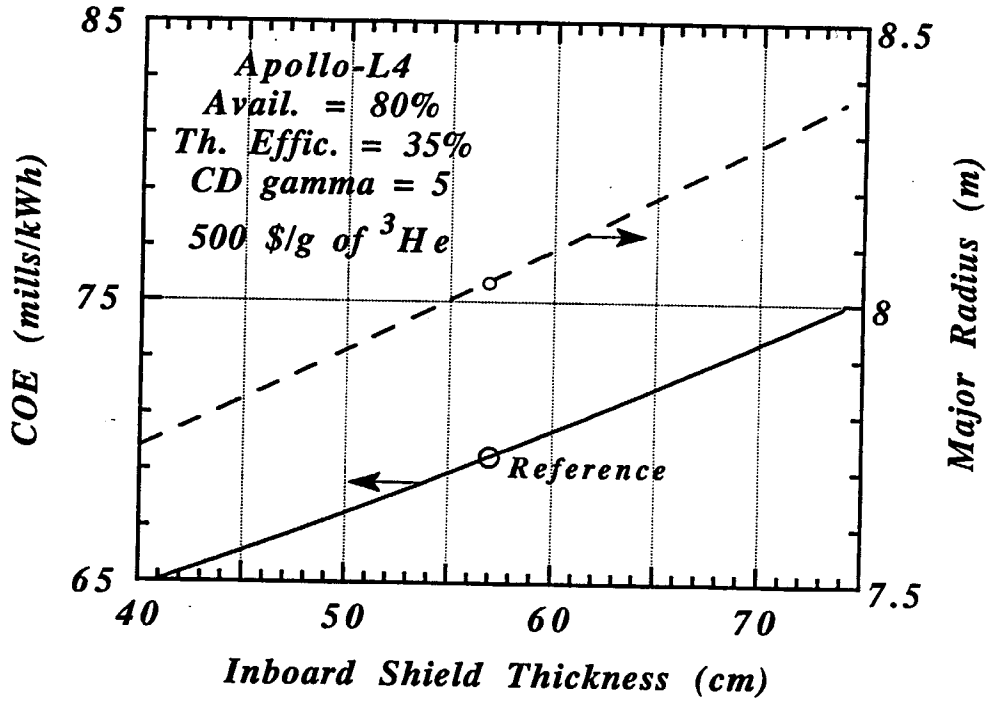


Fig. 6. Projected increase in COE and major radius as a function of inboard shield thickness.

The economic impact of the anticipated improvements in the Apollo-L4 design is presented in Table 4. The reference case calls for 80% availability, 500 $/g of ^{3}He, and 5 A/Wm^2 CD gamma. These improvements result in a 20% saving in COE and more optimistic values could reduce the cost even further. The direct cost breakdown is given in Fig. 7 for the reference case. As can be seen, the magnet accounts for most of the cost followed by the turbines and rectennas. It should be mentioned that the attractive safety features of Apollo-L4 allowed the design to achieve LSA of 1. The significance of the LSA rating is that many of the reactor components do not have to be nuclear grade and thereby result in a cost saving of ~22%, as illustrated in Fig. 8.

Table 4. Economic Impact of Anticipated Improvements in Apollo-L4 Design

Case	Reference	Conservative	Optimistic
Availability (%)	80	75	85
^{3}He unit cost ($/g)	500	1000	300
CD gamma (A/Wm^2)	5	1.35	10
COE (mills/kWh) (LSA=1)	70	89	60

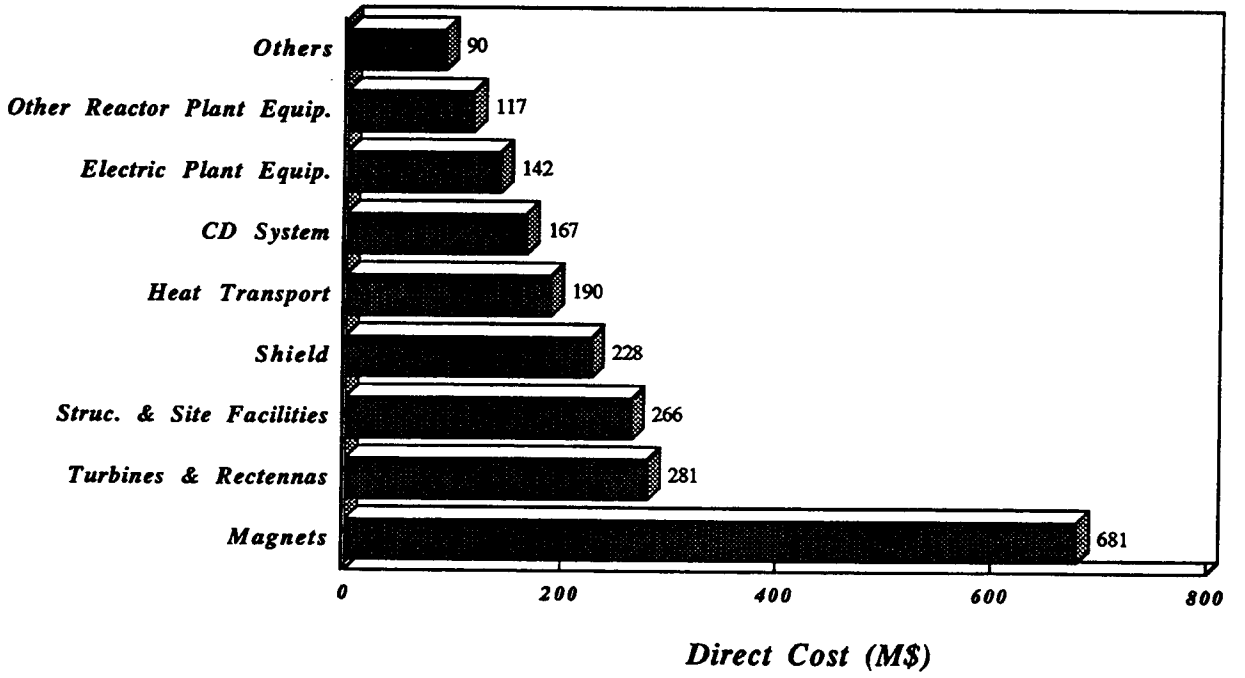


Fig. 7. Breakdown of the direct capital cost of the reference Apollo-L4 design.

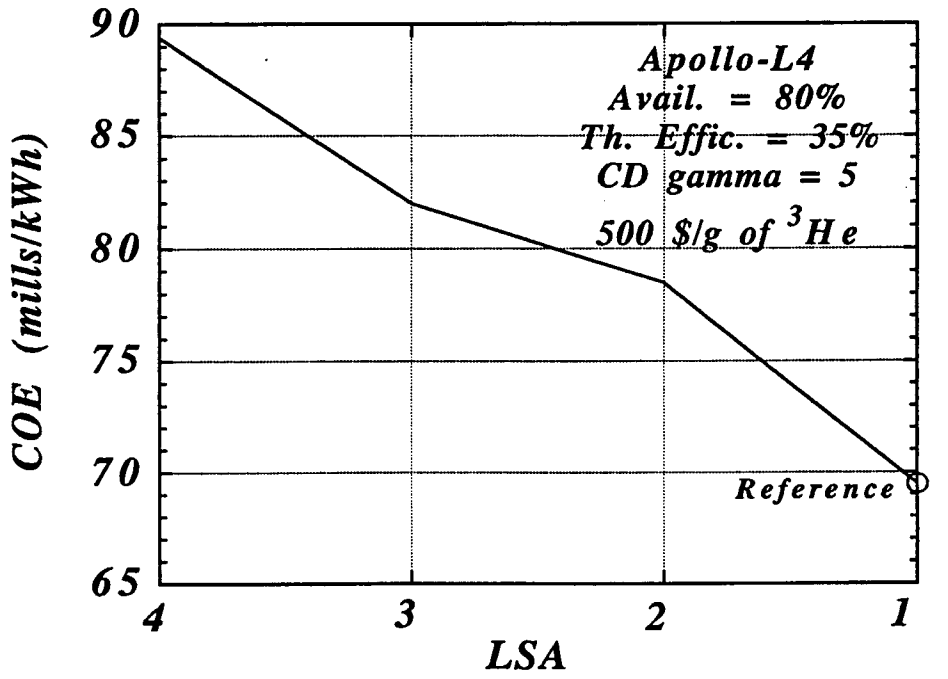


Fig. 8. Comparison of COEs evaluated at different LSA ratings.

Table 5. Economic Competitiveness of Apollo-L4 Reactor Design

Design	Fuel	Availability (%)	COE* (mills/kWh)	Self Consistent Comparison Availability (%)	Self Consistent Comparison COE (mills/kWh)
Apollo-L4	D-^{3}He	80	70	80	70
ARIES-III	D-^{3}He	76	89	80	85
ARIES-I	D-T	76	94	70	102
ARIES-II	D-T	76	72	70	78
ARIES-IV	D-T	76	63	70	68

*As of July 1993.

The Apollo-L4 design is compared to the most recent DT tokamak reactor designs [21-23] which are costed on the same economic basis in constant 1992 dollars. For a self-consistent comparison, the 10% difference in availability between the D-^{3}He and DT fueled reactors was maintained. This is reflected in the last two columns of Table 5 where the COEs were adjusted accordingly. It is clear from the table that Apollo-L4 compares favorably with recent advanced tokamak designs.

6. CONCLUSIONS

The study has concluded that the D-^{3}He fuel can produce economical electricity in a tokamak system given reasonable extrapolations in plasma physics. Recent concepts for high-efficiency current drive combined with high system availability and reduced ^{3}He fuel cost will allow the Apollo design to have a competitive cost of electricity. It became apparent from the study that D-^{3}He tokamaks have the best performance with direct conversion of synchrotron radiation, efficient current drive system, and high field (20 T) magnets. The physics requirements are more demanding, compared to DT. These include: factor of 5 increase in plasma current, factor of 4 increase in $n\tau_E$ for ignition, factor of 2-3 increase in operating temperature, and possible need for active ash removal.

The greatly reduced neutron production offers several environmental and technological advantages over DT such as factor of 30 reduction in neutron wall loading, factor of 30-50 lower radiation damage, reduced shielding and activation, permanent first wall and shield components, factor of 4 lower volume of radioactive materials, Class A low level waste, and inherently safe operation.

ACKNOWLEDGEMENTS

Partial support for this work was provided by the Grainger Foundation, Bechtel Corporation, Grumman Aerospace Corporation, Wisconsin Electric Utilities Research Foundation, Fusion Power Associates, Electric Power Research Institute, and McDonnell Douglas Corporation.

REFERENCES

[1] G.L. Kulcinski, G.A. Emmert, et al., "Apollo - An Advanced Fuel Fusion Power Reactor for the 21st Century," *Fusion Technology*, **15**, No. 2, Part 2B, 1233 (March 1989).

[2] G.A. Emmert, G.L. Kulcinski, et al., "Apollo-L2, An Advanced Fuel Tokamak Reactor Utilizing Direct Conversion," *Proceedings of IEEE 13th Symposium on Fusion Engineering*, Knoxville, Tennessee, Vol. 2, 1043 (Oct. 1989).

[3] G.L. Kulcinski, G.A. Emmert, et al., "Apollo-L3, An Advanced Fuel Fusion Power Reactor Utilizing Direct and Thermal Energy Conversion," *Fusion Technology*, **19**, No. 3, Part 2A, 791 (May 1991).

[4] G.A. Emmert, G.L. Kulcinski, et al., "An Improved First Stability Advanced Fuel Tokamak, Apollo-L3," *Procceedings of IEEE 14th Symposium on Fusion Engineering*, San Diego, CA, Vol. 2, 1106 (Sept. 1991).

[5] G.L. Kulcinski, J.P. Blanchard, et al., "Summary of Apollo, A D-^{3}He Tokamak Reactor Design," *Fusion Technology*, **21**, No. 4, 2292 (July 1992).

[6] G.L. Kulcinski, J.P. Blanchard et al., "Safety and Environmental Characteristics of Recent D-^{3}He and DT Tokamak Power Reactors," *Fusion Technology*, **21**, No. 3, Part 2B, 1779 (May 1992).

[7] G.A. Emmert and J.F. Santarius, "Physics Issues for the Apollo Advanced Fuel Tokamak," *Proceedings of IEEE 13th Symposium on Fusion Engineering*, Knoxville, Tennessee, Vol. 1, 655 (Oct. 1990).

[8] G.A. Emmert, J.F. Santarius et al., "The Physics of Apollo: A D-^{3}He, First-Stability, Tokamak Reactor," these proceedings.

[9] L.A. El-Guebaly, "Shielding Design Options and Impact on Reactor Size and Cost for the Advanced Fuel Reactor Apollo," *Proceedings of IEEE 13th Symposium on Fusion Engineering*, Knoxville, Tennessee, Vol. 1, 388 (Oct. 1989).

[10] M.E. Sawan and I.N. Sviatoslavsky, "Assessment of First Wall Lifetime in D-^{3}He and D-T Reactors with Impact on Reactor Availability," these proceedings.

[11] H.Y. Khater, "Safety Characteristics of D-^{3}He Fusion Reactors," this proceedings.

[12] H.Y. Khater, M.E. Sawan, et al., "Activation and Safety Analyses for the D-^{3}He Fueled Tokamak Reactor Apollo," *Proceedings of IEEE 13th Symposium on Fusion Engineering*, Knoxville, Tennessee, Vol. 1, 728 (Oct. 1989).

[13] H.Y. Khater and M.E. Sawan, "Safety and Environmental Aspects of the Apollo-L2 D-^{3}He Reactor," *Procceedings of IEEE 14th Symposium on Fusion Engineering*, San Diego, CA, Vol. 2, 704 (Sept. 1992).

[14] L.J. Wittenberg, E.N. Cameron, et al., "A Review of ^{3}He Resources and Acquisition for Use as a Fusion Fuel," *Fusion Technology*, **21**, No. 4, 2230 (July 1992).

[15] G.L. Kulcinski and H.H. Schmitt, "Fusion Power From Lunar Resources," *Fusion Technology*, **21**, No. 4, 2221 (July 1992).

[16] H.E. Thompson, "Cost of ^{3}He From the Moon," these proceedings.

[17] C.W. Maynard, L.A. El-Guebaly, and G.A. Emmert, "WISCAF Code: Wisconsin System Code for Advanced Fuel," Manual to be published.

[18] G.A. Emmert and R. Parker, "Potential for D-^{3}He Experiments in Next-Generation Tokamaks," *Fusion Technology*, **21**, No. 4, 2284 (July 1992).

[19] J.G. Delene, R.A. Krakowski, et al., "Generomak, Fusion Physics, Engineering and Costing Model," Oak Ridge National Laboratory Report, ORNL/TM-10728 (June 1988).

[20] J.G. Delene, "Updated Comparison of Economics of Fusion Reactors With Advanced Fission Reactors," *Fusion Technology*, **19**, No. 3, Part 2A, 807 (May 1991).

[21] F. Najmabadi et al., "The ARIES-III D-^{3}He Tokamak Reactor Study," University of California Los Angeles Report, UCLA-PPG-1384 (to be published).

[22] F. Najmabadi et al., "The ARIES-I Tokamak Reactor Study," University of California Los Angeles Report, UCLA-PPG-1323 (1991).

[23] F. Najmabadi et al., "The ARIES-II and -IV Second Stability Tokamak Reactors," University of California Los Angeles Report, UCLA-PPG-1461 (to be published).

7) Non-Maxwellian D-^{3}He Fusion Reactor Concepts 233
D.D. Ryutov, Chair

7-1 Physics Issues for Large Orbit Fusion Schemes 235
Nicholas A. Krall

7-2 Inertial-Electrostatic Fusion from D to ^{3}He: A Practical Strategy for Fusion Development 241
Robert W. Bussard and Lorin W. Jameson

7-3 Overview of IEC at Illinois 249
G.H. Miley

7-4 Self Colliders for D-He^3 Fusion 257
Norman Rostoker

Physics Issues for Large Orbit Fusion Schemes

Nicholas A. Krall
Krall Associates
1070 America Way
Del Mar, CA 92014

ABSTRACT

Progress is reported on some physics issues related to a fusion idea in which ions, confined by a spherical electrostatic potential well produced by an electron cloud, converge to a dense focus at the center of a sphere. The studies presented include a detailed analysis of the collisional effects which will eventually destroy ion convergence, and a study of the stability of counterstreaming ion beams. The stability study is nonlocal, carried out for a spherical plasma with density increasing inward as $1/r^2$. These issues are common to most large orbit fusion schemes.

1. INTRODUCTION

In the First Wisconsin Symposium on ^{3}He and Fusion Power, I described the Polywell™ concept, a device which was proposed by R. W. Bussard [1,2] as a significant variation of earlier work on electrostatic confinement [3]. This device proposes to inject high energy electrons into a quasi-spherical magnetic field; the electrons create a potential well of sufficient depth to accelerate ions from low energy at the periphery to fusion energies at the dense center of the sphere. Injection of electrons keeps the system electrically nonneutral, so that a potential well is maintained which confines the ions within the device and accelerates them inward, returning them again and again at high velocity to the central focus.

In my earlier presentation, I listed a number of physics issues which were essential to the success of that concept. Two of these issues, collisional relaxation of the ion distribution and stability of counterstreaming ion flows, are common to any scheme that relies on large orbit convergent ions. In the present paper, I will describe progress made since the last Symposium on understanding these two issues.

2. COLLISIONAL RELAXATION OF A CONVERGENT ION DISTRIBUTION

An essential feature of convergent ion fusion schemes is that the ions must maintain a nonthermal velocity distribution, with primarily radial flow, long enough to produce fusion in the dense focus at the center. Collisions and instabilities will both act to eventually cause the ions and electrons to be more or less uniformly distributed throughout the device. In order to calculate the rate of relaxation, it is necessary to take into account the very different parameters encountered by the ions during their transit, while recognizing that a 'collision' in the context of relaxation of ion convergence is not exactly the same as in other applications of collisional relaxation theory.

If the ion source is at the periphery and ions return to their birth point (turning points), then an isotropic source at R will clearly produce an anisotropic (non-Maxwellian) distribution at $r < R$, since v_r increases as $\sqrt{2e\phi(r)/m_i}$, while from conservation of angular momentum $v_\perp$ increases as $v_\perp = v_{\perp R}\, R/r$, with $2e\phi_{max}/m_i = v_{\perp R}^2\, R^2/r_c^2$ determining r_c, the closest approach of an ion to the center; $v_{\perp R}$ is the velocity perpendicular to $\hat{i}_r$ of an individual ion at $r = R$, and $\phi = 0$ at the location of the ion source [1,2]. There are two distinct effects that collisions have on ion convergence. First, as ions born at low energy pass through the dense core of the device, collisional processes will tend to thermalize their velocity distribution. An ion which is upscattered in energy will have a turning point outside the radius at which it was born, and will eventually escape from the device. Second, collisions in the lower density plasma outside the core will tend to isotropize the ion velocity. In this large region, even a small-angle ion-ion collision can transfer enough momentum from the primarily radial flow required for good convergence to azimuthal velocity, which clearly decreases the convergence of the ions to the core.

In addition to the core and the bulk plasma which surrounds it, there is a third region with distinctive collisional properties, namely the edge plasma, where the ions have their turning points. In this region ion velocities are low, and collisions much more frequent than in the interior. The ion distribution in this region changes both because of local collisions and because collisions in the interior change the distribution of the ions which enter the edge. Collisions in the interior drive the edge toward anisotropy, while collisions in the edge drive the edge toward isotropy. An isotropic distribution at the edge will produce exactly the strong radial convergence desired for convergence. **If edge collisions dominate, even though large angle scattering will eventually thermalize the entire system, small angle scattering (which competes with the fusion reacting time scale) will force the distribution to stay non-Maxwellian in the interior. The question is simply a matter of competitive rates of thermalization in the various regions.** Important progress in the understanding of large orbit fusion schemes was made by a recent calculation of the relevant rates for destroying or recovering ion convergence, and this section summarizes that work [4].

Collisions depend on energy and density, and these parameters characterize three distinct regions, namely: the **edge**, where the ion energy is of the order of a few eV and the density is $n = n_{edge}$, the **bulk**, where the potential increases so that the ions are of order keV's, and the density can be shown to be

$$n_B = \frac{3}{4}\left[\frac{E_o}{e\phi}\right]^{1/2}\left[\frac{R^2}{r^2}\right] n_{edge} \quad , \quad r_c < r < R \quad , \tag{1}$$

and the **core**, where again the energy is keV's, and the density is [1,2]

$$n_c \sim \left[\frac{E_o}{e\phi_{max}}\right]^{1/2}\left[\frac{R}{r_c}\right]^2 n_{edge} \quad , \quad r < r_c \quad , \tag{2}$$

$$r_c \simeq (m_i v_{\perp o}^2/2e\phi_{max})^{1/2}\, R \quad . \tag{3}$$

Table 1. Representative reactor parameters.

$e\phi_{max}$ (depth of the potential well)	100 keV
E_o (ion birth energy)	5 eV
n_c (ion core density)	10^{18} cm^{-3}
R (radius of device)	2 m
B (magnetic field at R, m = 3)	1 T

The parameters in Table 1 along with the spatial variation from Eqs. (1)-(3) allow us to calculate the classical collision time τ, weighted by the time an ion spends in each region, giving the number of collisions per ion per transit in each region as

$$(N_{coll})_c \sim \frac{2R}{\tau_{iic}} \left[\frac{E_o}{E\phi_{max}}\right]^{1/2} \left[\frac{m_i}{2e\phi_{max}}\right]^{1/2} \cong 3 \times 10^{-4} \quad , \tag{4}$$

$$\frac{(N_{coll})_{edge}}{(N_{coll})_c} = \frac{1}{3}\left[\frac{e\phi_{max}}{E_o}\right]\left[\frac{\ell n\Lambda_e}{\ell n\Lambda_c}\right] \cong 2 \times 10^{3} \quad , \tag{5}$$

$$\frac{(N_{coll})_B}{(N_{coll})_c} = \frac{2R}{r_c}\left[\frac{E_o}{e\phi_{max}}\right]\left[\frac{\ell n\Lambda_B}{\ell n\Lambda_c}\right] \cong 2 \times 10^{-2} \quad . \tag{6}$$

From the above, we see that the number of collisions per pass is by far the highest at the edge region, where the low energy ion distribution is originally isotropic. The result of small angle collisions will be to produce a steady state edge distribution which is slightly anisotropic, reflecting the competition between the (weak) bulk collisions driving toward isotropy in the bulk and anisotropy in the edge, and the (strong) edge collisions, driving toward isotropy in the edge and anisotropy in the bulk. This gives [4] $(T_\perp - T_r)_{edge} \sim T_{ro}(T_{ro}/e\phi_{max})^{1/2} << T_{ro}$. Thus the quasisteady solution to this nonlocal collision relaxation process is an ion distribution which is nearly Maxwellian at the edge, so that convergence persists. We emphasize again that this result follows because the edge collision frequency per transit is many orders of magnitude larger than that in the bulk. A similar healing effect might be expected for instabilities with quasilinear development times long compared with transit times. The remaining loss effects then are as follows.

2.1. Ion Loss by Large Angle Scattering

A single 90 ^{o} scattering collision will produce an effect which is impervious to edge healing. This rate is obtained by simply setting log Λ = 1 in the classical collision rates [5].

There are two large angle scattering effects. First there is upscatter in radial velocity in the core. For the reactor parameters in Table 1,

$$\tau_{loss} \sim \tau_{iic}\, \ell n\Lambda_c\, \frac{t_B}{t_c} \sim \tau_{iic}\, \ell n\Lambda_c\, (\frac{R}{r_c}) \sim 85 \text{ ms} \quad , \tag{7}$$

which is large compared to fusion reaction times of order 10 ms, from Refs. 1 and 2. The second effect is large angle scattering in the bulk, which destroys radial flow, given by

$$\tau_{loss,B} = \tau_{loss,core}\, (\frac{n_c}{n_B})\, (\frac{r_c}{R}) \simeq \tau_{loss,core}\, (\frac{e\phi}{E_o})^{1/2} \simeq 10s \quad . \tag{8}$$

This is also negligible compared with τ_{fusion}.

2.2. Loss Due to Residual Edge Anisotropy

The anisotropy mentioned above which develops at the edge due to small angle scattering in the rest of the device also produces some degradation of the core. Since the increase in $T_{\perp o}$ at r = R is of order $E_o(E_o/e\phi)^{1/2}$, and since the increase in core size is $\Delta r_c/r_c \simeq \Delta v_\perp/v_\perp$, it follows that

$$\frac{\Delta r_c}{r_c} \simeq \left[\frac{E_o}{e\phi}\right]^{1/4} < 10^{-1} \quad , \tag{9}$$

with this small Δr_c taking place on a time scale of a few ion transits. The conclusion then is that small angle scattering, when the Maxwellization of the plasma near the ion turning points is taken into account, is a very small contribution to core degradation.

3. NONLOCAL STABILITY OF COUNTERSTREAMING ION BEAMS

Although we have shown that the effect of collisions is relatively benign, instabilities might also reduce ion convergence. An obvious instability is that arising from counter-streaming ion beams in a hot electron background.

Since the last Symposium, a nonlocal theory for this instability in spherical geometry has been constructed [6], treating specifically the case of spatially constant streaming velocities, corresponding to density increasing inward as $1/r^2$. Despite the nonuniform density, the instability persisted with growth rate and eigenfunctions similar to the case of counterstreaming beams in a uniform density slab having the same boundary conditions used in the spherical calculation. This is seen in Figures 1 and 2, which show the eigenfunctions for the two cases. The only effect of the spherical geometry and nonuniform density is to produce the small wiggles seen in Figure 1. The growth rate and number of modes depends on the density (through the Debye length λ_e, and the core size b) as seen in Table 2.

The results are also insensitive to the spatial variation of the streaming velocity U_o. Figure 3 shows the eigenfunction for a case in which U_o decreased smoothly from the center to the boundary. Figure 4 shows a case in which U_o decreased primarily near the edge. Note that the results are similar to the U_o = const case, except for the absence of the short λ oscillations. We have identified the short λ wiggles as arising from stationary solutions to the wave equations, $d\phi/dt = 0$. Figure 5 shows the $d\phi/dt = 0$ solution for U_o = const. Figure 6 shows it for $U_o = 1 - r^4$. Notice that the U_o = const solution nearly satisfies the boundary conditions at r = a, while the $U_o(r)$ solution does not. We conclude that the U_o = const case superposes the $\gamma = 0$ solution on the $\gamma \neq 0$ solution. The $U_o(r)$ case is unable to do this and still satisfy the boundary conditions. The structure of the eigenfunction will influence the nonlinear behavior and macroscopic effects of the mode, especially if there is a strong coupling to that stationary solution. There is clearly room for more work.

Table 2. Growth rates (in units of U/a) of the first few modes.

Quasineutral theory	$(\lambda_e/b)^2 = 0.001$ b/a = 0.01	$(\lambda_e/b)^2 = 0.01$ b/a = 0.01	$(\lambda_e/b)^2 = 0.02$ b/a = 0.01
2.91	2.91	2.53	1.96
4.29	4.20	3.25	3.00
5.90	5.71	4.44	X
7.40	6.88	6.16	X
8.94	7.75	X	X
10.45	X	X	X

This work was supported in part by a subcontract to Energy/Matter Conversion Corporation, and in part by the U.S. Department of Energy. We thank Dr. R. W. Bussard for his assistance and collaboration, and Dr. Walter Sadowski for his continued support.

REFERENCES

[1] R. W. Bussard, "Some Physics Considerations of Magnetic Inertial-Electrostatic Confinement: A New Concept for Spherically Converging-Flow Fusion," *Fusion Tech.* **19**, 273 (1991).

[2] N. A. Krall, "The Polywell™: A Spherically Convergent Ion Focus Concept," *Fusion Tech.* **22**, 42 (1992).

[3] R. L. Hirsch, "Inertial-Electrostatic Confinement of Ionized Fusion Gases," *J. of Applied Phys.* **38**, 4522 (1967).

[4] M. Rosenberg and N. A. Krall, "The Effect of Collisions in Maintaining a Non-Maxwellian Plasma Distribution in a Spherically Convergent Ion Focus," *Phys. Fluids B*, **4**, 1788 (1992).

[5] D. L. Book, *NRL Plasma Formularly*, NRL Publication 0084-4040 (1987).

[6] S. K. Wong and N. A. Krall, "A Nonlocal Theory of Counterstreaming Ion Instability," *Phys. Fluids* B **5**, 1706 (1993).

Figure 1

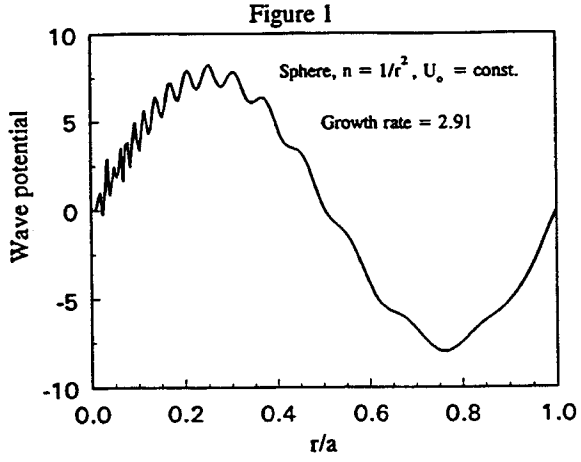


Figure 2

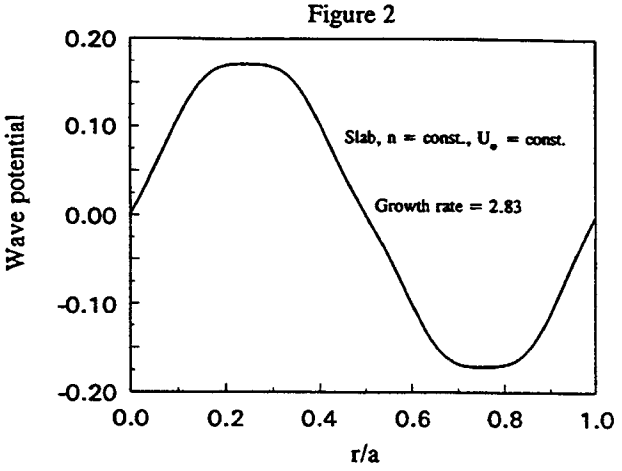


Figure 3

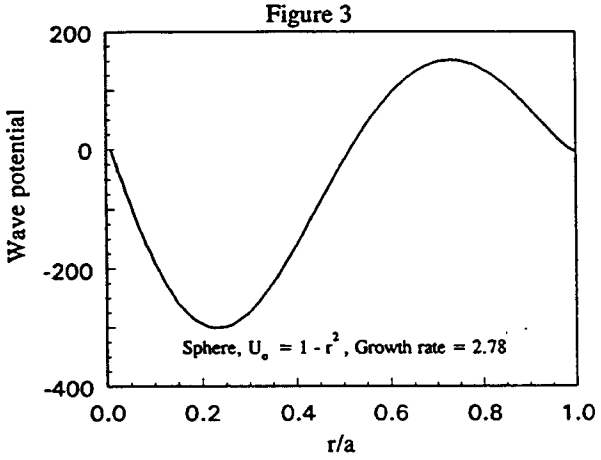


Figure 4

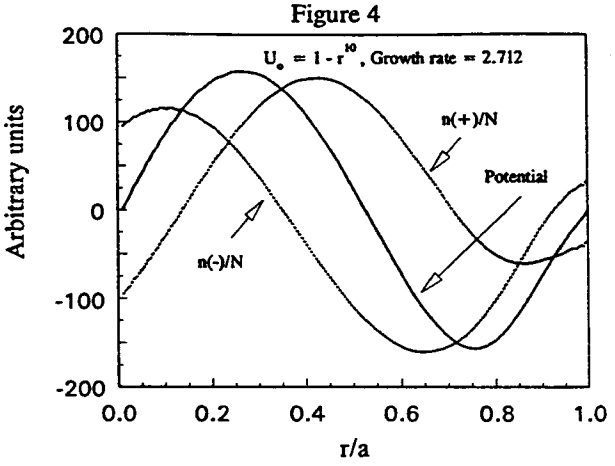


Figure 5

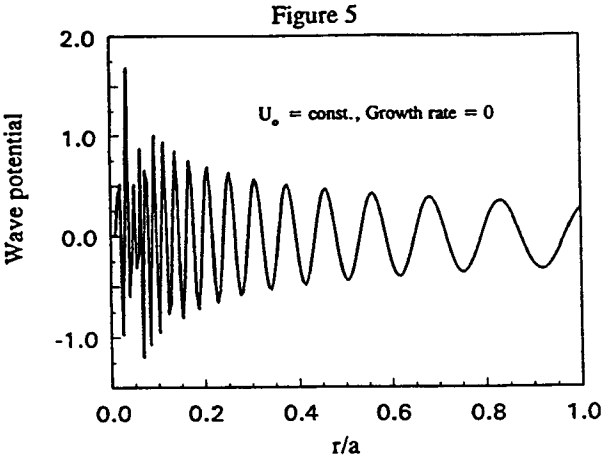
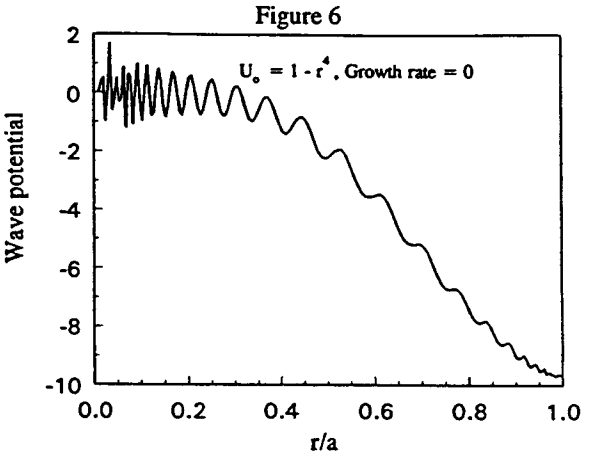


Figure 6



EMC2® ENERGY/MATTER CONVERSION CORPORATION
9100 A Center Street, Manassas, VA 22110, (703) 330-7990

Inertial-Electrostatic-Fusion From D to ^{3}He: A Practical Strategy for Fusion Development

Robert W. Bussard and Lorin W. Jameson
Energy/Matter Conversion Corp. (EMC2), Manassas, Virginia 22110

Since 1985, considerable study has been made of the unique Polywell™ concept[1] for inertial-electrostatic-fusion (IEF). This confines ions in a net negative plasma formed from by injection of energetic electrons into a special quasi-spherical, polyhedral B field configuration which traps the electrons; called the EXL (Electron ACCELeration) concept. Unlike earlier approaches that used grids to establish particle accelerating potentials, it has no grids and avoids the collisional losses that limited these. The ions and electrons in EXL systems are never in LTE and never Maxwellian. The device operates as a metastable, driven, non-neutral, spherically-focussing fusion reaction system in which the ion reaction energies are narrowly limited to their kinetic energy at the central core. And, the fusion products can not react with in-situ fuels; they will be exhausted into the external vacuum system, where they can be recovered, reinjected or stored for later application.

No significant physics or engineering obstacles have yet been found. First and second order critical physics issues have been identified and analyzed, and complex computer codes have been developed for particle and potential distributions (EIXL code) and for power balance (PBAL code) in EXL reactors. A host of power balance studies have been made with these codes, over a range of realistically-attainable physics conditions, and a wide variety of potential fusion fuels. These included DT, DD (alone), DD 1/2 and full-catalyzed by ^{3}He (called DDcatA and -catB cycles), D^{3}He (50:50 mix; exogenous ^{3}He), ^{3}He^{3}e, ^{6}Li^{6}Li (through p/^{8}He catalytic chain) and p^{11}B. All of these fuels were found able to run with net power in EXL systems with relatively low-technology engineering parameters. The studies showed that EXL devices of approximately 2.5-4.5 m radius can be made to yield net power on DD, with B fields of 10-15 kG or so, and electron drive voltages of 50-70 keV. Higher power or gain can be achieved by reinjection of the ^{3}He produced in one branch of the DD reaction (DDcatA). This increases the energy per DD reaction by about 2.8x, and reduces the neutron power fraction to about 9.4% of total system power. Storage of the T produced in the other branch yields another ^{3}He after T decay. This, too, can be reinjected to give 15.7 MeV/DD reaction (DDcatB), over 4.0x higher than from DD alone. These -catA/B cycles are the most promising of all combinations for near-term practical fusion power. EXL systems show gross gain over 10:1 (recirculating power < 10%) at net electric power 700-1000 MWe with thermal conversion efficiencies of only 35% in machines 3. -4.0 m in radius, for system operation with conventional materials (stainless steels) at well-proven steam conditions (e.g. 2000 psia, 600-650°F).

It is thus logical to consider fusion R&D along a DD path that starts at the same size and with the same or higher B field and electron drive voltage/current as required for a final reactor power unit. Initial experimentation can be done using H with trace D additives, and all electron power loss, ion upscattering, system ion/electron recirculation flow stability, control and fueling issues be determined without significant fusion reactions. First power production can use D, only, and small scale testing with stockpile ^{3}He can be done to verify stability, and operational control. The DDcatA cycle requires addition of an exhaust system T/^{3}He extraction and separation plant, and injection of the recovered ^{3}He into the EXL system. The final and experimental power devices here are the same relatively small size (ca. m radius), at modest power (ca. 100-200 MWe). Because of this, the operational cost and time scale for this development process can be kept below $250 M and within 7-9 years, if a vigorous effort is undertaken.

By this means, the DDcatA power economy can be started without recourse to problematic extraction of ^{3}He from sea floor vents, or development of the entire space flight infrastructure needed to obtain ^{3}He from the Moon. The eventual saturated DDcatB cycle will also be self-sustaining, with no exogenous ^{3}He requirement, and only 5.5% neutron power fraction. The cost of power from such systems/cycles is inherently significantly smaller than from any other power source. The balance-of-plant for thermal DDcatA/B cycles is the same as that for coal, oil, or nuclear fission plants, but the fusion power core is very much smaller and less expensive. By use of the EXL concept and the R&D approach from D to self-generated-^{3}He-catalyzed DD systems, economically practical fusion power could be developed and deployed within 10 years.

-12

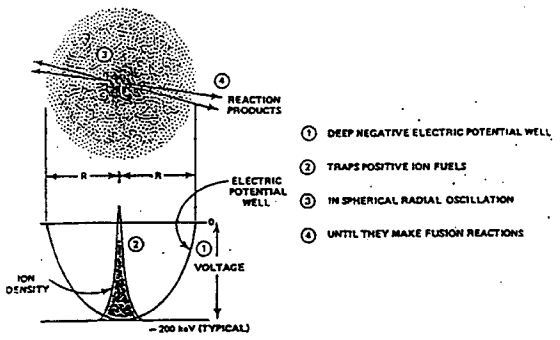
Inertial-Electrostatic-Fusion (IEF) from D to ^{3}He:

A Strategy for Practical Fusion Development

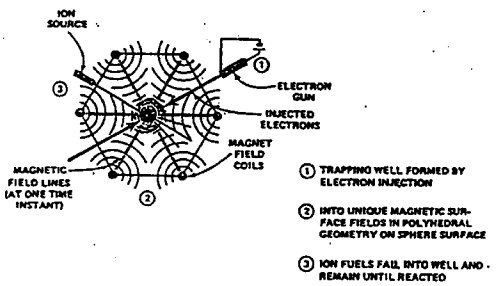
Robert W. Bussard and Lorin W. Jameson
Energy/Matter Conversion Corp. (EMC2)
Manassas, VA 22110

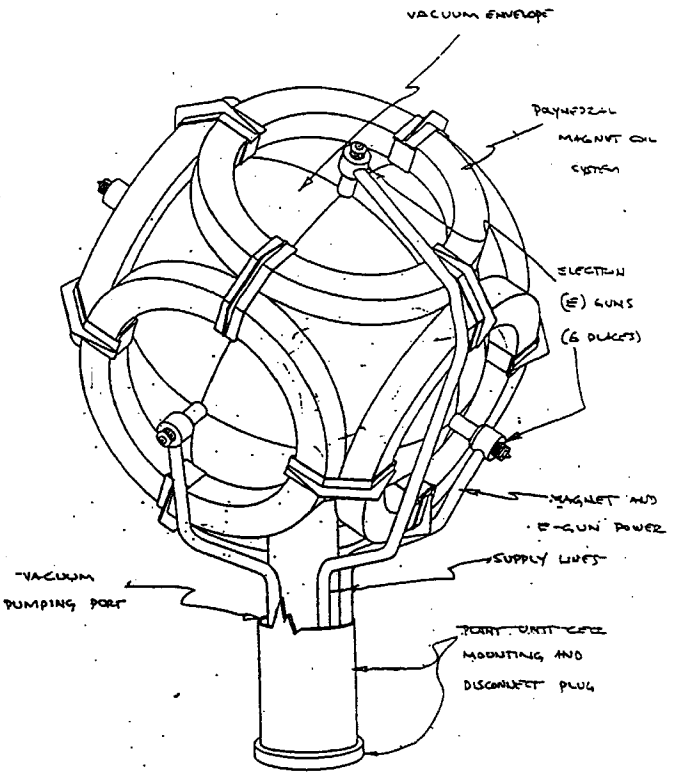
Second Wisconsin Symposium on Helium-3 and Fusion Power
Madison, Wisconsin
19-21 July 1993

PRINCIPLE OF OPERATION



APPROACH





FROM D TO ^{3}He

FUSION REACTION/CHAIN	MeV/Fusion	% Neuts.
D + D $\longrightarrow$ ^{3}He + n (DD, CAT A, CAT B)	3.65	33.6 %
D + D $\longrightarrow$ T + p (DD, CAT A, CAT B)		
D + ^{3}He $\longrightarrow$ ^{4}He + p (CAT A, CAT B)	10.24	9.6 %
D + ^{3}He $\longrightarrow$ ^{4}He + p (CAT A, CAT B)	14.4	5.7 %
^{3}He + ^{3}He $\longrightarrow$ ^{4}He + 2p	12.9	
D + T $\longrightarrow$ ^{4}He + n	17.6	80.1 %

EXL POWER BALANCE CALCULATION USING PBAL

- DESIGN POINT ANALYSIS OF FUSION POWER, INJECTION POWER, MAGNET POWER, AND BREMSSTRAHLUNG LOSSES
- PARAMETRIC VARIABILITY IN INJECTION ENERGY, B FIELD, DEVICE RADIUS, ANODE HEIGHT, FUEL MIXTURE, THERMAL AND DIRECT CONVERSION EFFICIENCY, ION CONVERGENCE RADIUS, MAGNET TYPE AND COOLING SYSTEM, AND BLANKET ENERGY
- REPORTING OPTIONS INCLUDE G_{gr} (E_o,B), G_{gr} (E_o,R), AND G_{gr} (B,R) AND THE COMPANION FUNCTIONS FOR P_{net} , P_{fus} , P_{brem} , AND P_{mag}

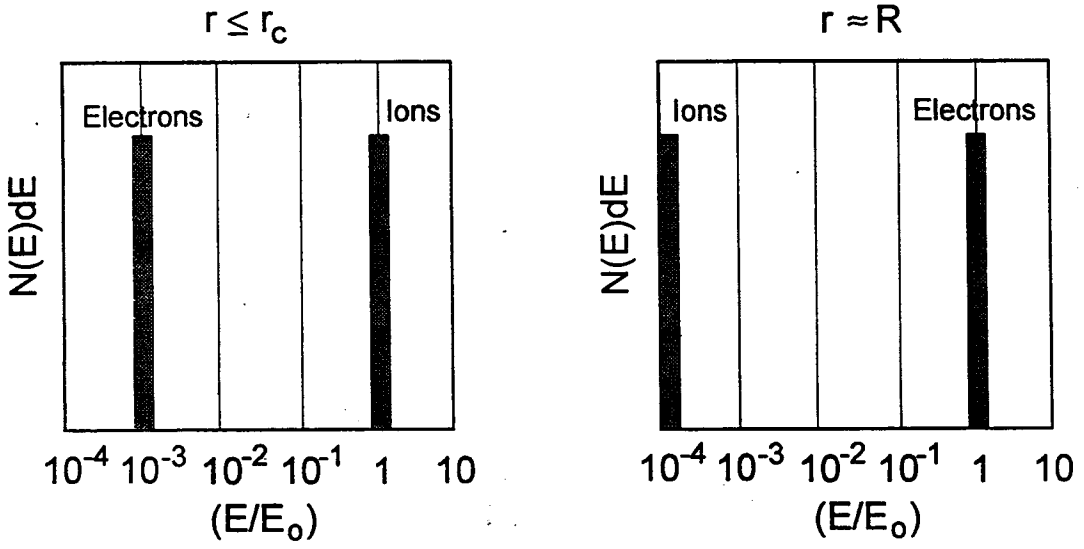
BREMSSTRAHLUNG RADIATION IN IEF SYSTEMS

$$\frac{\text{Bremsstrahlung}}{\text{Fusion}} = \frac{P_{brm}}{P_{fus}} \approx \frac{(n_e/n_i)^2}{\sigma_f(E_i)}\sqrt{\frac{E_e}{E_i}} \quad \text{IN CORE} = \frac{(f_2(Z-1)+1)^2}{f_2(1-f_2)}\frac{\sqrt{\eta/(1-\eta)}}{\sigma_f(E_i)}$$

WHERE $E_e = \eta\, E_o$; $E_i = (1 - \eta)\, E_o$; f_2 = HIGH Z FRACTION

- NON-EQUILIBRIUM EXL/IEF SYSTEMS CAN OPERATE WITH:
  $\eta << 1$; $E_e << E_i$ IN CORE
  COLLISIONAL EQUILIBRATION NOT SIGNIFICANT OVER ELECTRON LIFE IN MACHINE
  RADIATION COOLING AT HIGH DENSITY SUPPRESSES E_e

- TYPICALLY $E_e < 0.01\, E_i$ IN EXL (WITH SMALL η)
  $E_e > E_i$ IN IXL (WITH LARGE η)



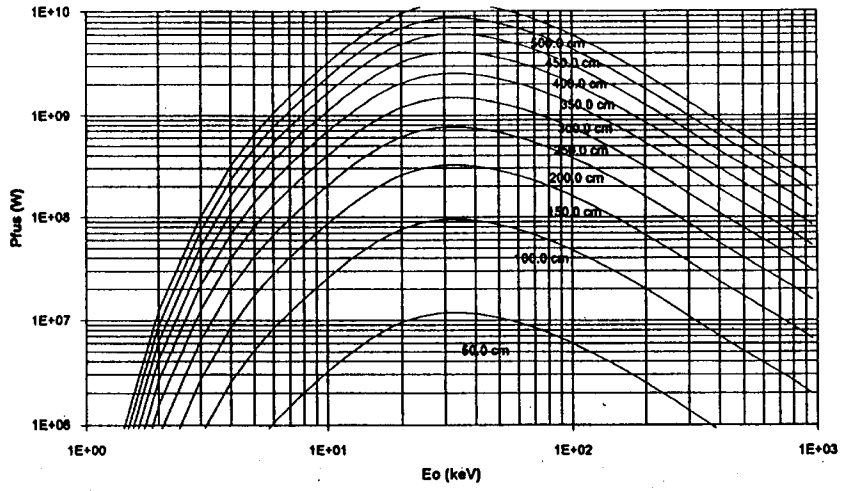
Particle Energy Distribution in EXL Machine

<rc> : 0.0100, Super Conducting Magnets

Etae : 1.00e-2, Etadc : 0.000, Etac : 1.000
f2 = 0.500

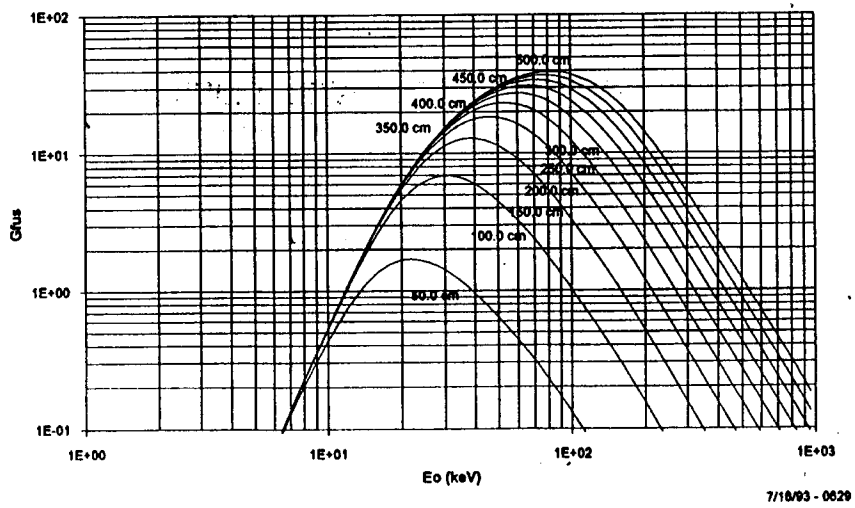
Pfus at Various Values of R(cm)

B (G) = 1.50e+4 Fuel : DD(catA)



Gfus for Various Values of R (cm)

B (G) = 1.50e+4 Fuel : DD(catA)



7/16/93 - 0629

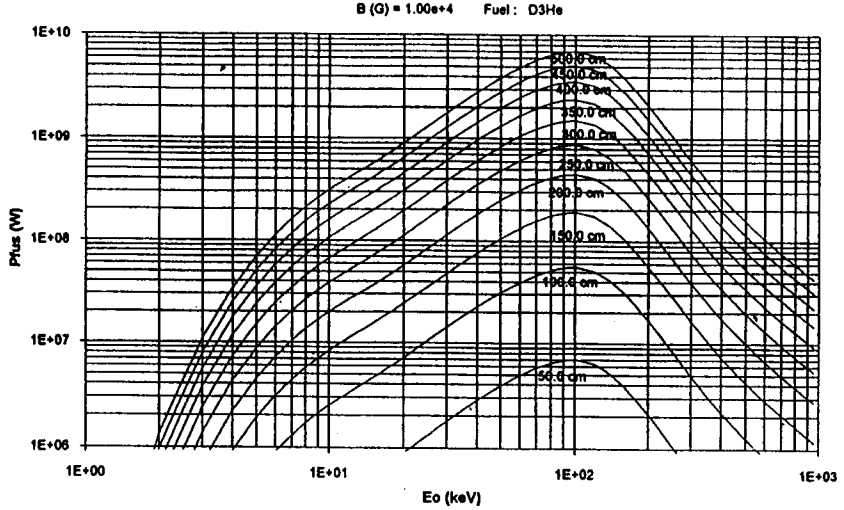
EMC2

<rc> : 0.0100, Super Conducting Magnets

Etae : 1.00e-2, Etadc : 0.000, Etac : 1.000
f2 = 0.261

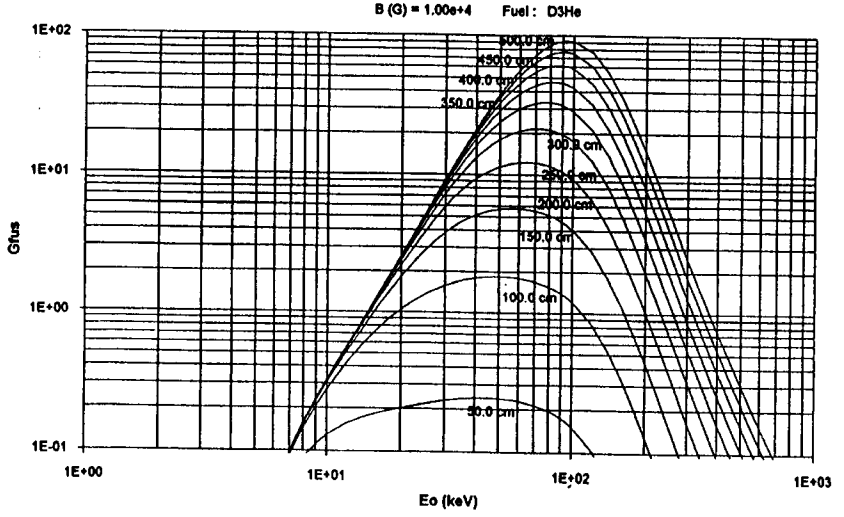
Pfus at Various Values of R(cm)

B (G) = 1.00e+4 Fuel : D3He



Gfus for Various Values of R (cm)

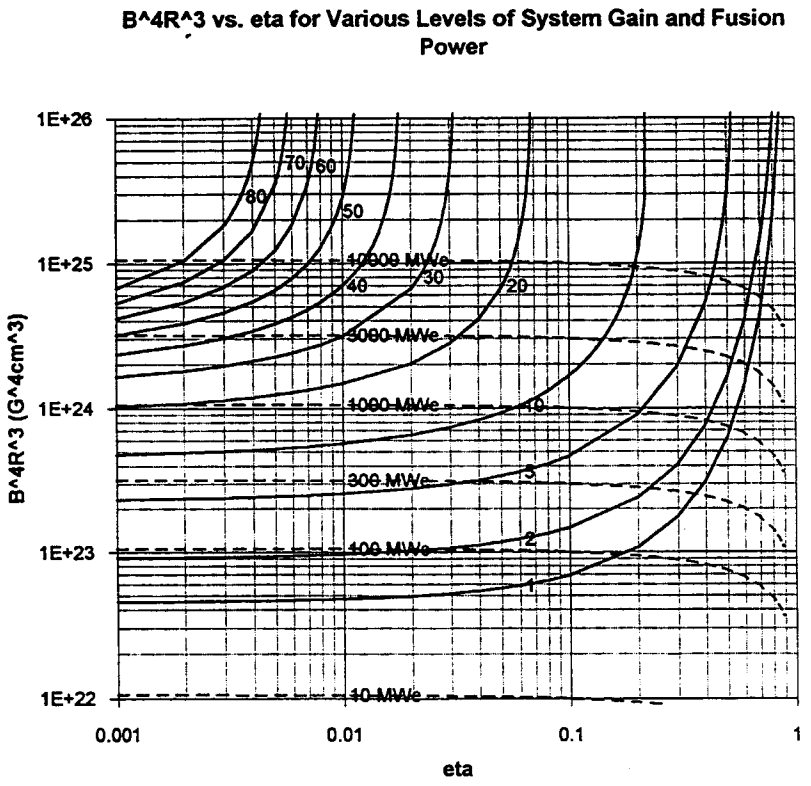
B (G) = 1.00e+4 Fuel : D3He



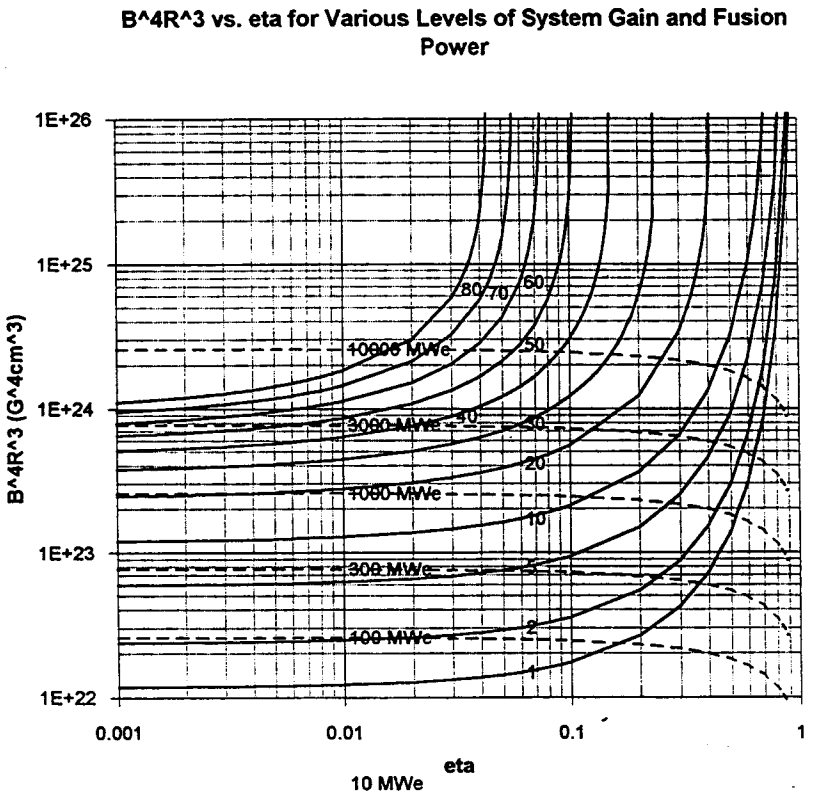
7/16/93 - 0632

ENERGY/MATTER CONVERSION CORPORATION

Fuel : DD(catA)
<rc> : 0.01
m: 9.94
kl: 2
f2: 0.5
alphar: 0
alphag: 0.9
GMG: 1
GICC: 1
fperp: 0.3
Eo: 100
etac: 1
etadc: 0
N: 8
Ng: 8



Fuel : D3He
<rc> : 0.01
m: 9.94
kl: 2
f2: 0.261
alphar: 0
alphag: 0.9
GMG: 1
GICC: 1
fperp: 0.3
Eo: 105
etac: 1
etadc: 0
N: 8
Ng: 8



IEF SYSTEM SCALING BOUNDS SIZE AND FIELD

$$\Delta(MEP) \sim 10\langle MEP\rangle_{mean}$$

$$\langle MEP\rangle \sim (\eta)^{1/4}; \sim \langle r_c\rangle$$

THUS

$$B(R^{3/4}) \sim (\eta)^{1/4}; \sim \langle r_c\rangle^{1/4}$$

SYSTEM INSENSITIVE TO ION FOCUS AND CORE

ANODE HEIGHT AROUND MEAN <MEP> RANGE

R & D TEST SYSTEM PARAMETER RANGE

CHOOSE R = 3 m, IN RANGE OF 2 < R < 4 m, THEN:

FUEL	DD	catA	catB	D^3He
<MEP> (G^4cm^3)	1.6E24	0.9E24	0.65E24	0.16E24
B_o (kG)	11.7/23	11.4/20	10.5/18.5	7.4/13.0

FOR $^3He^3He$, <MEP> = 3E26, with R = 5 m, B_o = 39.4 kG

FOR DT <MEP> = 2E21, with R = 2 m, B_o = 4.0 kG

PRACTICAL FUSION POWER DEVELOPMENT - I

FIXED, SMALL-SIZE IEF TEST DEVICE

CHOOSE TO FIT POWER PLANT APPLICATION

START WITH DD
- PROVE FUSION PHYSICS
- STABILITY UNDER BURN
- DEVELOP DEVICE/SYSTEM CONTROLS

SWITCH TO D + VARIABLE-^{3}He
- SIMULATE catA,catB CYCLES
- ^{3}He FROM STOCKPILE SOURCE
- SAME MACHINE AS FOR DD

PRACTICAL FUSION POWER DEVELOPMENT - II

USE DEVICE WITH R ~ 2.5-3.0 m, B_o ~ 12-15 kG

E_o ~ 100 keV, P_{drive} ~ 200 MWe @ I ~ 2000 A

YEAR	0	4	8	12	
DD	XXXXXXXXXXXxxxx				$ 250M
catA,catB		xxxxXXXXXXXXxxxx			$ 150M
DEMO POWER PLANT			xxxXXXXXXXXXXXX		$ 600M

PRACTICAL FUSION POWER IN < 12 YEARS AT < $ 1 B

OVERVIEW OF IEC AT ILLINOIS

G.H. Miley
Fusion Studies Laboratory
100 NEL, 103 South Goodwin Avenue
Urbana, IL 61801-2984 USA
217-333-3772 (voice)
217-333-2906 (fax)
miley@uiucvmd.bitnet

ABSTRACT

Recent experimental studies of a single-grid Inertial Electrostatic Confinement (IEC) device are described. Both near-term applications as a portable D-D neutron source and potential future applications as a D-^{3}He power plant are discussed.

1. INTRODUCTION

A small combined experimental/theoretical research project at the U. of Illinois involving inertial electrostatic confinement (IEC) fusion is described in this presentation. This research follows along the lines originally suggested over twenty years ago by Elmore, Tuck, and Watson,[1] Farnsworth,[2] and Hirsch.[3,4] A natural question to ask is: "Why undertake studies of this approach, which has lain dormant for so long?" One reason, most germane to this workshop, is that the characteristic non-Maxwellian energy plasma distribution and the absence of a magnetic field in the IEC make it ideally suited for burning D-^{3}He. An equally important reason is that preliminary analyses of eventual reactor designs are very favorable. Indeed an Electric Power Research Institute (EPRI) blue-ribbon commission, convened last February, concluded that "If the plasma physics question discussed earlier can be solved in a reactor configuration . . ., the IEF (inertial electrostatic fusion) concepts could meet the EPRI requirements for a desirable reactor better than any other concept proposed to date."[5] An equally compelling reason, from a university research program standpoint, is that meaningful IEC experiments can be carried out with relatively simple equipment and a modest budget.

This presentation will first very briefly review the basic IEC concept and then provide a brief overview of recent experimental results obtained from the project at the U. of Illinois. Tentative plans for a D-^{3}He "proof-of-principle" experiment will also be presented, as well as some comments about several recent conceptual reactor design studies and potential applications. A highlight of the present research is that the current device appears to offer a very attractive low-level neutron source for a variety of practical commercial applications. This development will be stressed here.

1. THE IEC CONCEPT

The basic IEC configuration used in the U. of Illinois experiments is illustrated in Fig. 1.* Ions produced by a glow discharge in the region between the vessel wall and cathode grid are subsequently accelerated toward the center of the spherical chamber by the grid. Some fusion is achieved directly by beam-beam reactions that occur in the central "core." The high ion density in the core creates a positive potential well, which subsequently accelerates electrons into the "core." This then produces a potential well structure, such as illustrated in Fig. 2. Farnsworth and Hirsch originally discussed multiple potential wells, which they called *poissors*. However, the work carried out at Illinois is mainly aimed at the development of a "double potential well," which can be maintained in a stable condition and which serves as a trap for ions, providing a strong recirculating ion flow within the core region. Indeed, results have been previously presented,[6] which used the emission of protons produced by D-D reactions in the central core region to deduce the potential well structure. Those results indicate that a shallow double well has been achieved in some of the present experiments. Consequently the fusion reactions (i.e. neutron emissions) discussed here come from a combination of beam-background gas reactions plus beam-beam reactions, including both primary beam self-interactions and interactions with ions trapped by both the grid and the double well. A primary goal of future experiments, which will use higher injected ion currents, is to demonstrate the creation of deeper double potential wells.

The IEC operation described here uses purely electrostatic fields. An alternate approach, termed the "Polywell," uses magnetic confinement of the electrons.[7,8] Issues related to core physics are the same for the two approaches, thus there is a close tie between work described here and the "Polywell."

The Illinois experiments represent the first extensive studies of this type, since the work reported by Hirsch in 1967. Figure 3 summarizes the most significant changes and new results since the early Hirsch work.[3] First, and most significantly, the Illinois IEC uses a single grid arrangement to both produce and accelerate ions. In contrast, most of the results reported by Hirsch involved separate ion injectors or multiple grids, although he did carry out some single grid experiments which were not reported. New results include the discovery of the Star and Halo discharge modes and the potential well measurements based on D-D proton detection.

The discovery of the two new discharge modes is important for device operation. The Star mode has ion channels which pass through the openings between the grid wires and converge in the central spot. (Thus the name "Star" follows from the visual appearance of light emission. See Fig. 4). Such operation is achieved through careful selection of experimental parameters, including operating pressure, voltage/current, and geometry. The ion microchannels are an important phenomena, since they allow a much higher effective transmission fraction through the grid than would be possible if a uniform ion beam passed through it.[9] That point is illustrated in Fig. 5, where data is compared to "normal" transmission fractions calculated from the grid geometric transparency. This increased effective transmission is exceedingly important to the success of the present neutron source experiments. The added recirculation of ions results in a much-needed increase in efficiency, i.e. an increased neutron emission rate per kW input power.

---

* Figures located at end of paper.

A photograph of the Halo mode is shown in Fig. 6. The transition to the Halo from the Star mode is achieved by providing additional electrons to the core region. (This is accomplished in present experiments with an electron jet created by enlarging one or more of the grid openings. However, future experiments will employ alternate electron injection techniques.) The significance of this mode is that it achieves a deeper double potential well than the Star mode, as is vividly illustrated by a two-fold jump in neutron emission production when the device enters the Halo mode.

2. RECENT NEUTRON SOURCE RESULTS

There are a number of practical applications for an isotropic MeV neutron source, with strength on the order of 10^{6-7} n/s. Consequently, an intermediate goal of this research is to develop the IEC as a small portable neutron source for commercial use.[10] Recent neutron measurements using the IEC operating in the Star mode are shown in Fig. 7. As expected, the neutron yield is a strong function of voltage and depends almost linearly on current. The goal of 10^6 n/s is achieved with operation at 70-kV applied voltage and 15-mA ion current. Indeed, a version of this device is currently under design for use in calibration of the neutron diagnostics on the Joint European Torus (JET). It can be moved around on a track inside the JET torus to calibrate the neutron tomography unit as a function of source position. Other applications, such as a portable source for activation analysis studies, are also contemplated.

Of special interest to the present audience may be the use of the IEC as a teaching experiment for student plasma physics laboratories. This offers a relatively low-cost means of providing a hot fusing plasma which enables students to perform diagnostic measurements of both neutrons and energetic fusion protons. In addition, a variety of diagnostic tools, such as probes, spectroscopic units, etc. can be employed to study the dense plasma itself. One advantage of the IEC unit, compared to a plasma focus device used in some labs to obtain a fusing plasma, is that the IEC is steady-state, considerably simplifying diagnostics requirements. Another advantage is the relative low cost of the basic unit; for example, the current experiment involves a total capital cost of $20-25,000. Additional diagnostics may be desired, depending upon the student experiments of interest, and this adds to cost. Still, in terms of maximum fusion reactions per dollar invested, the IEC holds an unique place among possible experimental apparati.

3. TENTATIVE D-^{3}He "PROOF-OF-PRINCIPLE" EXPERIMENT

Present experiments and the corresponding theoretical studies are focused on obtaining a reliable extrapolation of the fusion reaction rate as a function of ion current, i.e. an IEC "scaling law." Results from these studies show that the reaction rate should scale with the square or cube of the current, for levels above 50 mA. In the voltage range (70-100 kV) used in present experiments, the D-D and D-^{3}He fusion cross sections are quite comparable. Consequently, the present D-D neutron reaction data can be directly interpreted in terms of equivalent D-^{3}He reactions. An upgraded experimental unit ultimately capable of currents in the 1- to 10-A range is planned. To achieve this, a modified grid design and larger power supplies are required. This is viewed as a "proof-of-principle" experiment, in the sense that at these higher ion currents, the reaction-rate scaling with current should show enhanced confinement due to the formation of deep double potential wells and other effects, such a wave densification of the central core. Such scaling would lead to an attractive energy gain for a reactor. Consequently, experiments in this ion current range

can demonstrate that the core confinement is adequate to justify development of larger systems, thus representing a "proof-of-principle" experiment.

In addition to studying IEC scaling relations, this experiment would enter a region of current densities where the effect of possible instabilities on IEC performance could be examined. Such data would be an important check of the growing number of theoretical studies of IEC instabilities that may be encountered.[11,12,13]

Such experiments could be carried out without actually employing D-^{3}He; however, there are important reasons to utilize that mixture. Direct experimental data on the behavior of mixed species in the IEC potentials will be provided. Also the 14-MeV proton obtained from D-^{3}He reactions provides a unique and effective diagnostic for the study of the core dynamics and potential wells. Further, the ability to minimize the neutron flux at the high fusion rate levels predicted in the work avoids the need for excessive shielding to protect the operator and minimize induced radioactivity in the equipment.

4. REACTOR DESIGN STUDIES

Two preliminary conceptual design studies, based on a scaled-up D-^{3}He-fueled IEC, have been performed. One explores the applicability of the IEC concept to space propulsion, and the other its use for hydrogen and synfuel production.

A conceptual sketch of the IEC-driven spacecraft is shown in Fig. 8. The goal of this design is to achieve a manned mission to Mars with a 120-day one-way travel time. A "Venetian-blind" direct collector unit is included in the D-^{3}He design to directly convert energy carried by escaping alphas and protons to high-voltage direct current. The resulting high voltage is stepped down to the keV range to drive advanced design electric thruster. (Earlier design studies by R. W. Bussard used the alternate approach of driving an electron beam to vaporize propellant).[14] The resulting spacecraft was found to offer a very high power-to-weight ratio device, capable of meeting the 120-day mission goal. The study identifies a number of developmental issues including extension of IEC operation to high ion currents, protection of both IEC and direct collector grids, radiation effects on insulators, high voltage standoff under space conditions, and efficient dc voltage step-down. Still, no "showstoppers" were identified. Further details are presented in Ref. 15.

The second study adapted a D-^{3}He IEC unit to power a hydrogen production plant. This approach capitalizes on the large fraction of IEC fusion energy carried by 14-MeV protons. Efficient radiolysis is obtained using steam.[10] As illustrated conceptually in Fig. 9, protons pass through a thin wall that separates the IEC chamber and the radiolysis region. Further details, flow diagrams, energy balances, etc. are presented in Ref. 16. A projected overall plant efficiency (energy equivalent of output hydrogen divided by the input fusion energy) of ~48% is predicted. Some electricity and process steam is also obtained from the unit. Like the propulsion study, this design study identified a number of technology developments that are essential to achieve such a plant. However the results confirm that the D-^{3}He IEC could potentially provide a very attractive approach to synfuel production. Further details are presented in Ref. 16.

5. SUMMARY

Experiments described here have provided important new insight into IEC operation, including the use of Star and Halo mode operation to achieve enhanced fusion reaction rates. Neutron rates achieved in existing D-D devices are already in the range of interest for a variety of near-term applications. The long range goal, however, is to achieve a D-^{3}He IEC for applications such as space propulsion and synfuel production, illustrated by the design studies cited here.

6. ACKNOWLEDGEMENTS

This project is supported by DOE contract 9XG2-Y5958-1 and NASA NAS7-1235. A number of staff have contributed to the effort including H. Hora, J. Javedani, Y. Yamamoto, A. Satsangi, Y. Gu, and P.F. Heck. Important discussions with R. Hirsch, R.W. Bussard, R. Nebel, D.C. Barnes, N. Krall, R. Burton, and N. Schulze are gratefully acknowledged.

7. REFERENCES

1. W. Elmore, J. Tuck, and K. Watson, Phys. Fluids, 2, 239 (1959).
2. P. Farnsworth, U.S. Patent #3,258,402, June 28, 1966; U.S. Patent #3,386,883, June 4, 1968.
3. R. Hirsch, J. Appl. Phys., 38, 4522 (1967).
4. R. Hirsch, U.S. Patent #3,530,497, September 22, 1970; U.S. Patent #3.664,920, May 23, 1972.
5. R. Gross, S. Dean, R. Symons, D. Papadopolous, D. Meade, G. Kulcinski, R. Krakowski, "Panel Report to the EPRI," Washington, DC (2 November 1992) Palo Alto, CA: Electric Power Research Institute (1993).
6. J.H. Nadler, G.H. Miley, Y. Gu, and T.A. Hochberg, Fusion Technology, 21, 1639 (1992).
7. R. W. Bussard, Fusion Technology, 19, 273 (1991).
8. N. A. Krall, Fusion Technology, 22, 42 (1992).
9. T.A. Hochberg, "Characterization and Modeling of the Gas Discharge in a SFID Neutron Generator," M.Sci. Thesis, Dept of NucE, U. of Il., Urbana, IL (1992).
10. G.H. Miley, et al., "Inertial-Electrostatic Confinement Neutron/Proton Source," Proceedings, *The Third International Conference on Dense Z-pinches*, London (19-23 April 1993).
11. M. Rosenberg and N.A. Krall, Phys. Fluids B, 4, 1788 (1992).
12. S.K. Wong and N.A. Krall, Phys. Fluids B, 5, 1706 (1993).
13. N.A. Krall, "Physics Issues for Large Orbit Fusion Schemes," *Second Wisconsin Symposium on ^{3}He and Fusion Power*, Madison, WI (19-21 July 1993).
14. R.W. Bussard and L.W. Jameson, "The QED Engine Spectrum: Fusion-Electric Propulsion for Air-Breathing to Interstellar Flight," *AIAA/SAE/ASME/ASEE 29th Joint Propulsion Conference*, AIAA 93-2006, Monterey, CA (28-30 June 1993).
15. G.H. Miley, et. al, "Inertial Electrostatic Confinement as a Power Source for Electric Propulsion," Proceedings, *Vision 21 Conference*, Cleveland, OH (30-31 March 1993).
16. G.H. Miley, et al., "Hydrogen Generation with an Inertial Electrostatic Confinement Power Source," Proceedings, *First International Conference on New Energy Systems and Conversions*, Yokohama, Japan (27-30 June 1993).

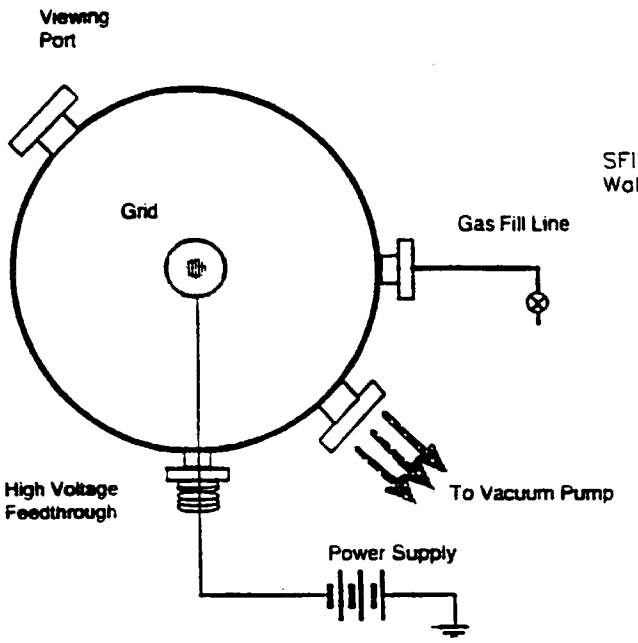


Figure 1. **Schematic of the Single-Grid IEC**

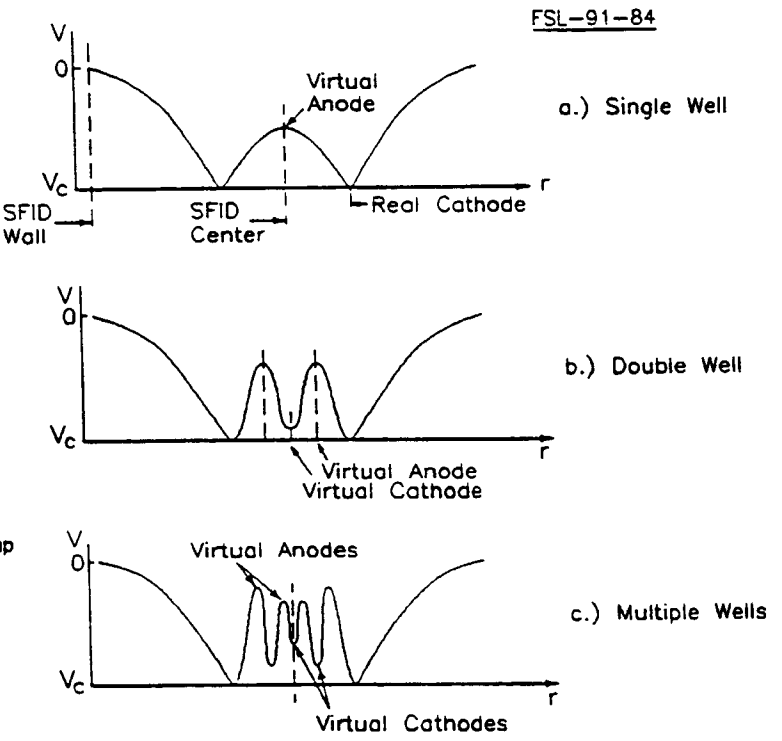


Figure 2. **Illustration of Various Potential Well Structures: a) Single Well, b) Double Well, and c) Multiple Wells ("Poissors")**

- Grid discharge ion production, simpler, less costly than ion guns
- Discovery of modes giving high "effective" transparency
  - Star (microchannels)
  - Halo (deeper well)

  → *Key to present n-Source*
- D-D proton measurement of double well → *Key to Future*
- Cylindrical/focussed neutron source

Figure 3. **Changes and New Results since Hirsch's Early Experiments**

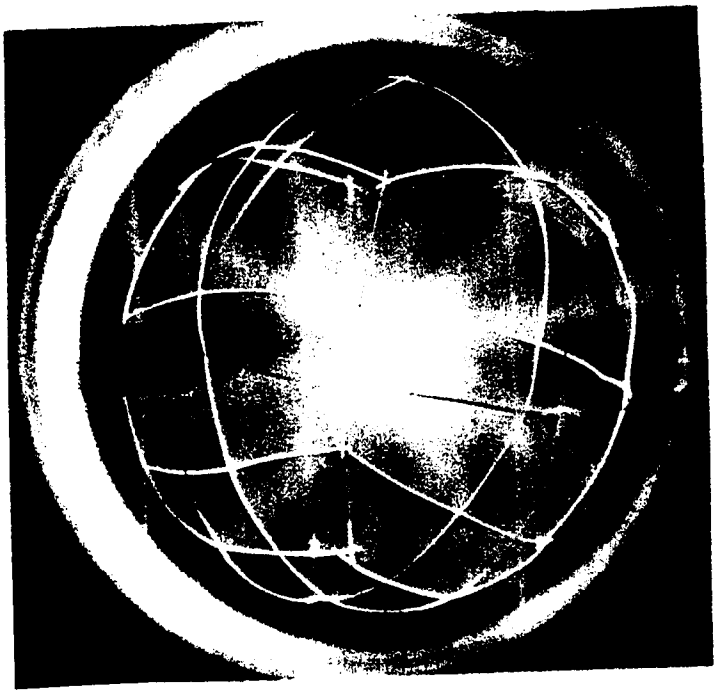


Figure 4. **Photograph of a Typical Star Mode Discharge. created in the center of the grid openings, significantly increasing the grid transparency and leading to efficient neutron production.**

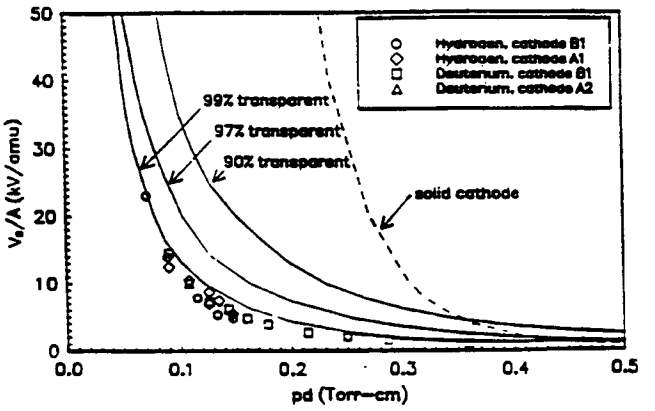


Figure 5. **Calculated Paschen curves (t = 90%, 97%, 99%; R = 25%) Streams of ions flow through the microchannels compared with IEC measurements.**

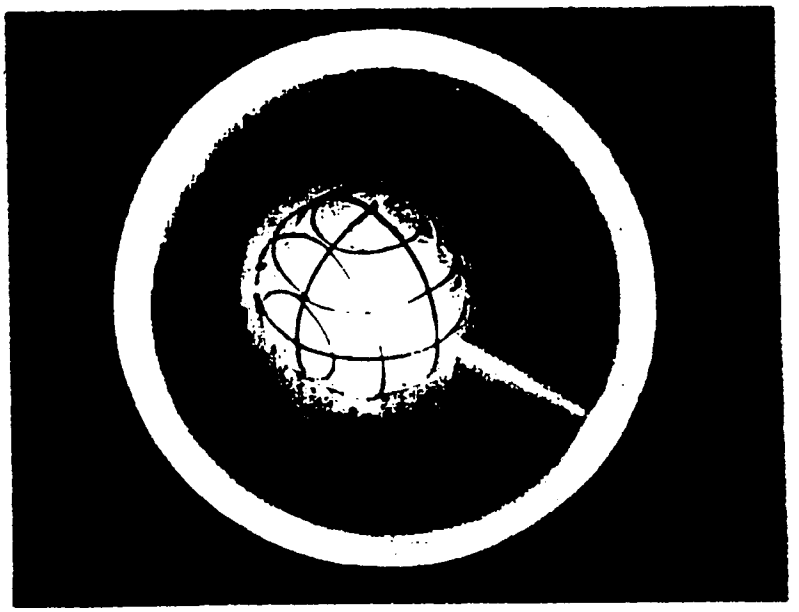


Figure 6. **Photograph of a Typical Halo Mode Discharge. The electron beam at the surface of the Halo is employed to balance charge flows.**

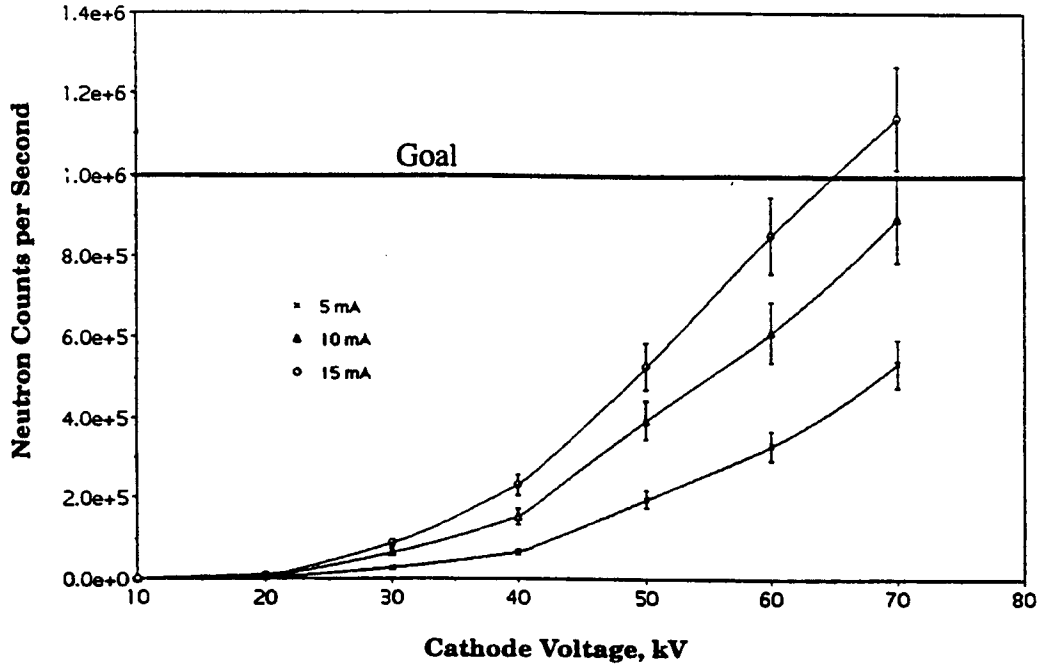


Figure 7. **D-D Neutron Yields vs. Applied Voltage for Various Ion Currents**

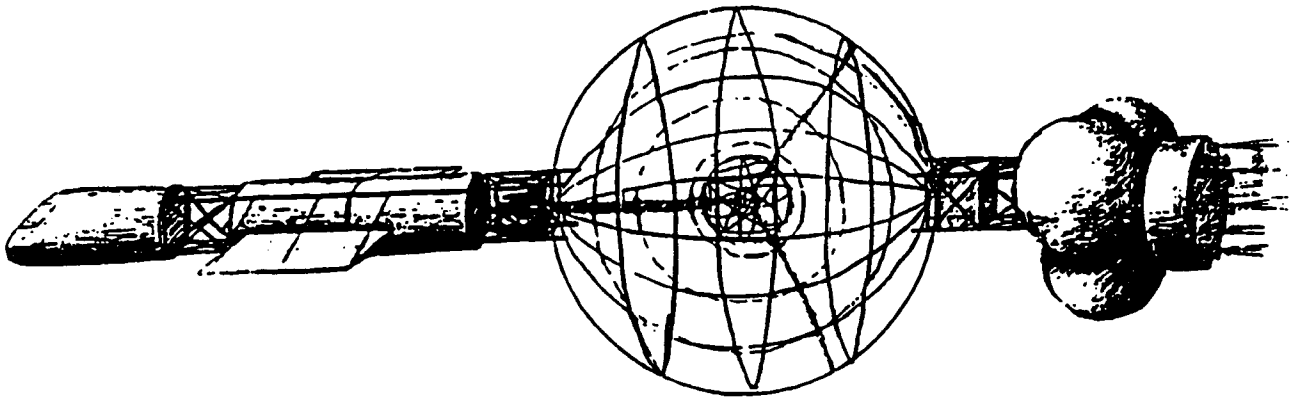


Figure 8. **Sketch of the D-^{3}He IEC-powered spacecraft for a manned Mars mission**

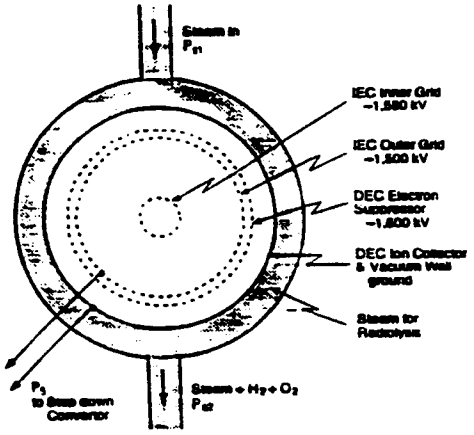


Figure 9. **Radiolysis Chamber Concept for D-^{3}He IEC-powered H_2 Plant**

Self Colliders for D-He^3 Fusion

Norman Rostoker
University of California
Irvine, California 92717-4575

ABSTRACT

High Beta self-consistent equilibria are described with the Vlasov/Maxwell equations. For these equilibria, almost all of the particle orbits are betatron orbits rather than the adiabatic orbits of conventional magnetic confinement systems usually considered for fusion. Conditions required for long wavelength/low frequency stability are considered. If they are satisfied classical confinement [1] would be expected. Classical estimates of slowing down and diffusion are made for D and He^3. These estimates are based on Coulomb collisions and test-particle models. The result is that the lifetimes of D and He^3 for slowing down and diffusion exceed the nuclear reaction time.

1. INTRODUCTION

Magnetically confined high energy ion beams were studied at the Oak Ridge National Laboratory (ORNL) from approximately 1958-1968. A similar series of experiments at about the same time were carried out at the Kurchatov Institute. A beam [2] of about 5 milliamperes of 600 keV D_2^+ ions was injected into a magnetic mirror. Ionization took place due to collisions with background atoms or ions, i.e. $D_2^+ \rightarrow D^+ + D$ and D^+ was trapped. An ion density of about 10^8 cm^{-3} was obtained that was limited by instability and charge exchange.

During the period 1972-1975 there was considerable interest in the wet-wood burner [3] that involved the trapping of high energy ion beams in a Tokamak with a background plasma of hot electrons and cold ions. The energy gain Q is the fusion energy divided by the investment in beam energy. The gain was < 4 because the cold ions slow down the fast beam ions too quickly. There is some improvement in the value of Q for counter streaming[4] beams but it is still limited by ion-ion collisions.

From 1975-1985, experiments were carried out [5] with MIGMA which was similar to the ORNL experiments (called DCX) except that a particular configuration was studied with the density maximum on the axis. The boundary conditions were changed by applying potentials to external screens. This stabilized the plasma and reduced the fluctuation level. The density increased to about 10^{10} cm^{-3} and was limited by charge exchange which also determined the confinement time of about 20 sec.

From 1988-1992, experiments were carried out with high energy large orbit ions in Tokamaks [6] (TFTR, D-III-D, and JET). These experiments proved that large orbit ions slow down and diffuse classically in the presence of anomalous fluctuation levels and anomalous transport of the plasma with keV temperatures. The explanation is that particles average [7] the fluctuations so that only wavelengths longer than the gyroradius are important; for small orbit particles this is not a significant restriction, but for large orbits

most of the spectrum of fluctuations is ineffective. These results apply only to low beam density; for larger beam density, Alfven waves grow and beam losses are enhanced if the beam speed exceeds the Alfven wave velocity. Alfven waves are long wavelength Magnetohydrodynamic waves which is not inconsistent with the explanation of the classical transport for low density beams.

For a plasma composed of mainly large orbit ions and small orbit neutralizing electrons, it should be possible to have classical transport provided that long wavelength modes are stable. In view of the fact that the classical Coulomb cross section for scattering is inversely proportional to the square of the particle energy, it should be possible to obtain adequate confinement with a small reactor. In this paper we discuss this possibility and determine the classical containment time.

2. SELF-CONSISTENT HIGH BETA EQUILIBRIA

The problem of ion-ion collisions in the wet-wood burner can be solved by eliminating the low energy ions. [8] If the ions have distributions of the form

$$f_j(\underset{\sim}{x},\underset{\sim}{v}) = \left(\frac{m_j}{2\pi T_j}\right)^{3/2} n_j(r,z)\exp-\frac{m_j}{2T_j}\left[\left(v_x+\omega_j y\right)^2+\left(v_y-\omega_j x\right)^2\right] \tag{1}$$

and ω_j, T_j are the same for all ions, then ion-ion collisions do not change the distribution functions. Only ion-electron collisions need to be considered, which change the distribution function very slowly. The Vlasov/Maxwell equations and the condition of charge neutrality determine [9] nj(r,z):

$$n_j = n_{oj}\exp\left[\frac{m_j\omega_j{}^2r^2}{2T_j}-\frac{q_j\Phi}{T_j}+q_j\frac{A_\theta\omega_j r}{cT_j}\right] \tag{2}$$

$$\nabla x\underset{\sim}{B} = 4\pi\ \underset{\sim}{j}/c\ \ = (4\pi/c)\sum_j n_j q_j r\omega_j\hat{\theta} \tag{3}$$

$$\sum_j n_j q_j = 0 \tag{4}$$

$\Phi, \underset{\sim}{A}$ are electric and magnetic potentials and are functions of (r, z); $\underset{\sim}{E} = -\nabla\Phi$, $\underset{\sim}{B} = \nabla x\underset{\sim}{A}$; $\underset{\sim}{A}$ has only a θ-component. Equations (2), (3), and (4) with suitable boundary conditions determine n_j, Φ and $\underset{\sim}{A}$.

In Fig. 1, various confinement systems for high energy ions are illustrated. The Migma is distinguished by the fact that the density maximum is on axis. The rings have the density maximum off axis. Field reversal on the axis is possible with a ring, but not with a Migma.

In Fig.2, specific calculations for a one-dimensional field-reversed model are plotted. The parameters assumed for D-He^3 are indicated. The orbits of almost all of the particles are betatron orbits that oscillate about the null field surface as illustrated in Fig. 1.

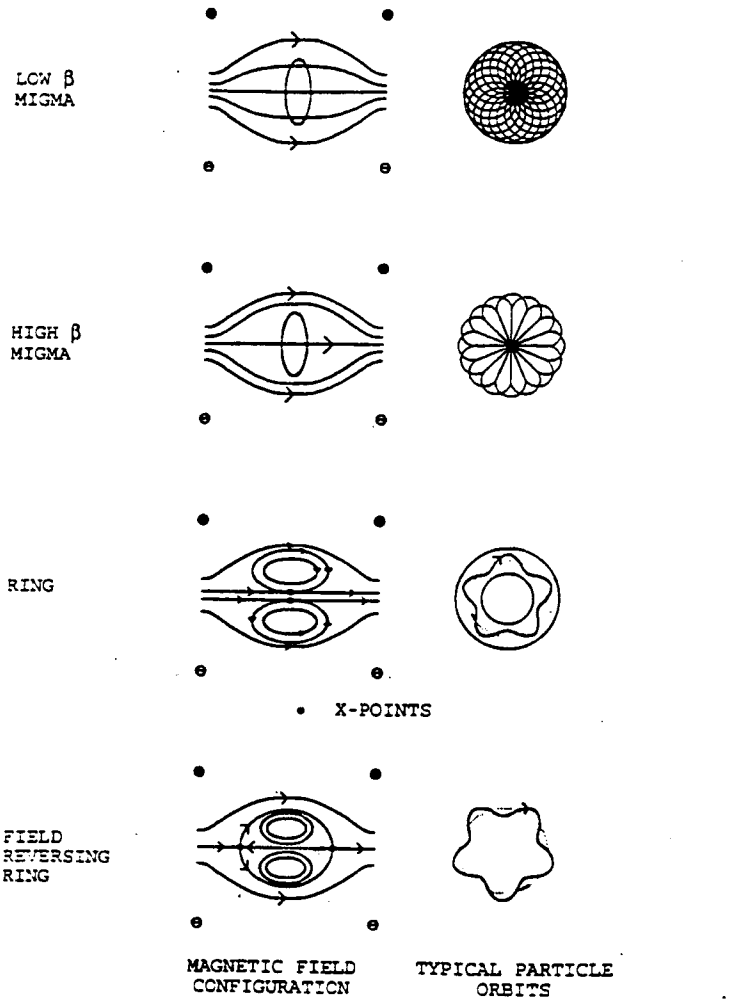


Figure 1. Self-Colliding Systems

The density maxima for D and He^3 do not coincide but are close enough for nearly complete overlap. The electric field indicates that the ring is positively charged so as to confine electrons. The potential well for electrons has a depth $e\Delta\Phi \cong kTe$. The case illustrated in Fig. 2 has a boundary condition only at $r = \infty$. If a boundary condition is applied at a finite radius - for example that $\Phi(r) = 0$; $r = R$, then for large R there will be no solution. For small R there will be two solutions and for a particular value of R there will be one solution. [1] This property is called bifurcation and it happens for any finite boundary condition. The solution still has the same shape as in Fig. 2, but one solution is broad and the other narrow. In two dimensions the two solutions illustrated in Fig. 3 have similar properties. For the shallow solution the density at the wall is not much smaller than the density maximum. For the deep solution it is generally smaller by many orders of magnitude. This is an important property for magnetic confinement fusion if one wishes to avoid thermal conduction and first wall problems.

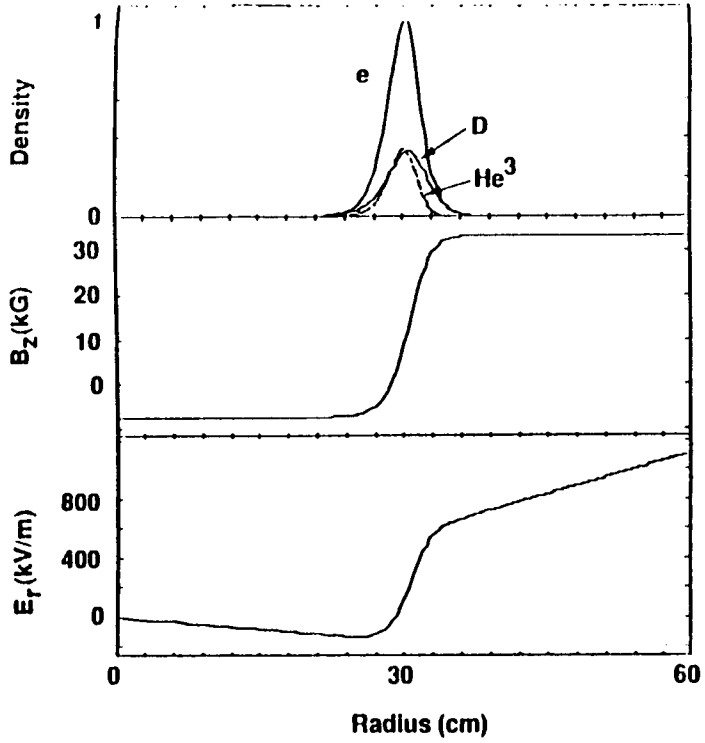
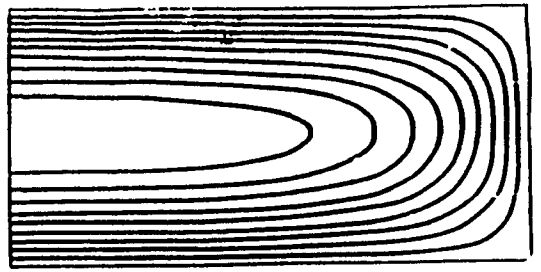


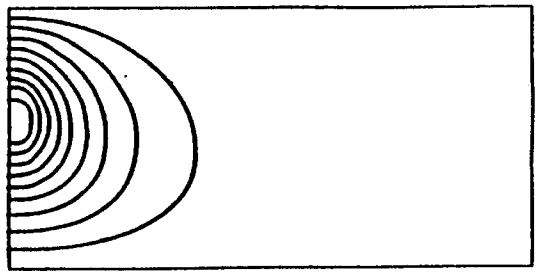
Figure 2. One-Dimensional Equilibrium for D-He^3.

r_o = 30 cm kE(D) = .8 MeV T = 100 keV

n_o = 10^{14} cm^{-3} kE(He^3) = 1.2 MeV T_e = 50 keV



Shallow Solution



Deep Solutions

Figure 3. Two-Dimensional Equilibrium-Density Contours or Equipotentials.

3. STABILITY

We assume that micro-instabilities, if they exist, can be neglected for large orbit particles. From the extensive research in FRC's (field reversed configurations) we know of two long wavelength instabilities - the rotational kink mode that has been eliminated with quadrupole windings and the tilt mode that is stabilized by finite gyroradius. It is possible that both modes will be stabilized by energetic particles. There has been an idealized model calculation of stability for a field reversed system with betatron orbits for all ions. [10] The model involves an infinitely long annular layer of zero thickness. The techniques of this paper are being applied to the ring and the high beta Migma.

4. CLASSICAL SCATTERING

Various lifetimes can be obtained from test particle formulae where all particles are in thermal equilibrium except for a small number of test particles in the form of a beam with a specific energy and propagating in a specific direction with no energy perpendicular to that direction initially. We assume the parameters of Fig. 2 for a ring of major radius r_o = 30 cm and minor radius a = 5 cm. Then the time required for a large angle deflection of the test particle [11] is

$$\tau_i = W_i / \left(\partial w_\perp / \partial t\right)_i$$

$$\left(\frac{\partial w_\perp}{\partial t}\right)_i = \frac{2\pi e^4 Z_i^2 \ln\Lambda}{m_i v} \sum_j n_j Z_j^2 \left[1 + \frac{\partial}{\partial v}\frac{v_j^2}{v}\right] erf\frac{v}{\sqrt{2}v_j} \qquad (5)$$

i refers to the test particle of charge Z_ie mass m_i and velocity v. j refers to the field particle Z_je, mass m_j and thermal velocity v_j such that $m_j v_j^2 = T_j$. It is possible to give separate expressions for like particle scattering and unlike particle scattering from Eq. (5). The ion velocity satisfies the inequality $v_i < v < v_e$

$$\tau_{ei} = \frac{\sqrt{m}T_e^{3/2}}{\pi e^4 \ln\Lambda} \frac{1}{n_e\langle Z^2\rangle} = .45x10^{-3}\,\text{sec.} \equiv \tau_{ee}$$

$$\langle Z^2\rangle = \sum_j \frac{n_j Z_j^2}{\sum_j n_j} = \frac{5}{2} \qquad \ln\Lambda = 20$$

$$\tau_{ie} \equiv \frac{3\sqrt{\pi}}{2}\frac{m_i}{m}\frac{W_i}{T_o}\frac{\langle Z^2\rangle}{Z_i^2}\tau_{ei} = 162\,\text{sec} \quad (D)$$

$$= 92\,\text{sec}\ (He^3)$$

$$\tau_{ii} \cong \sqrt{\frac{m_i}{m}}\tau_{ei} = .027 \text{ sec} \quad (D) \quad ; \; .033 \text{ sec } (He^3)$$

τ_{ei} is the time for a large angle scattering of electrons by ions, etc. The slowing down time is

$$\tau_i \cong \frac{m_i}{m}\tau_{ei} = 1.62 \text{ sec} \quad (D) \quad ; \; 2.43 \text{ sec } (He^3)$$

For the ring under consideration, the usual slowing down time does not apply. The current is carried by the ions and if the ions slow down an induced electric field LdI/dt will arise to oppose this. The slowing down time is therefore $\tau_S = L/R$ where

$$L = \left(4\pi r_o / c^2\right)\left[\ln\left(r_o / a\right) + .32\right]$$

is the ring inductance and $R = 2r_O/a^2\sigma$ is the resistance where

$$\sigma = \sum_i \frac{n_i (Z_i e)^2}{m_i}\tau_{ie} + \frac{n_e e^2}{m_c}\tau_{ei}$$

$$= 3.14x10^{21} + 2.15x10^{19} = 3.16x10^{21} \text{ sec}^{-1}$$

and $\tau_S = 1.17 \times 10^3$ sec. Inductances due to electron and ion inertia have been neglected in comparison with the macroscopic inductance of the ring.

In the time of a large angle scattering for ions the amplitude of the betatron oscillations will increase by

$$\frac{v}{\Omega_i} = \frac{vA_i}{10^7 Z_i B} = 5.8 \; cm(D) \; ; \; 4.35 \; cm(He^3)$$

This is the gyroradius in the magnetic field B ≅ 30 kG, v is the ion velocity and A_i the atomic mass number. The result is about the same as the minor radius a so that the time τ_{ie} is an estimate of the diffusion time. We note that the Maxwellization times τ_{ii} and τ_{ee} are short compared with times describing the interaction of ions and electrons which justifies the assumption of Maxwell distributions. The nuclear burn time for D-He^3 reactions is $\tau_B = \left[n_i \langle \sigma v \rangle\right]^{-1} \cong 50$ sec for $n_i = 10^{14} cm^{-3}$ and $T_i = 100 \; keV$. Thus $n\tau \cong 10^{16}$ and the confinement time τ is longer than the burn time. These estimates apply only to a break-even experiment or pulsed operation of a reactor. For steady-state operation the current would not decay and the conventional slowing down time τ_i would apply. However one must also consider the speeding up due to interaction with the reaction products He^4 and H. Steady state operation is presently being considered.

REFERENCES

[1] N. Rostoker, F. Wessel, H. Rahman, B. C. Maglich, B. Spivey, and A. Fisher, "Magnetic Fusion with High Energy Self-Colliding Ion Beams," *Phys. Rev. Lett.* **70**, 1818 (1993).

[2] S. Glasstone and R. H. Lovberg, *Controlled Thermonuclear Reactions*, D. Van Nostrand Co., N.Y. (1960), Chapter 9.

[3] J. M. Dawson, H. D. Furth, and F. H. Tenney, "Production of Thermonuclear Power by Non-Maxwellian Ions in a Closed Magnetic Field Configuration," *Phys. Rev. Lett.* **26**, 1156 (1971).

[4] D. L. Jassby, "Neutral Beam Driven Tokamak Fusion Reactors," *Nucl. Fusion* **17(2)**, 309 (1977).

[5] M. Salameh, et al., "Experiment with Stored .7 MeV Ions: Observation of Stability Properties of a Non-Thermal Plasma," *Phys. Rev. Lett.* **54**, 746 (1985).

[6] W. Heidbrink, "Measurement of Classical Deceleration of Beam Ions in the D-III-D Tokamak," *Phys. Fluids* **B-2**, 4 (1990); W. Heidbrink, et al., "The Diffusion of Fast Ions in Ohmic TFTR Discharges", *Phys. Fluids* **B-3**, 3167 (1991).

[7] H. Naitou, T. Kamimure and J. Dawson, "Kinetic Effects on the Convective Plasma Diffusion and Heat Transport," *J. Phys. Soc. Japan* **46**, 258 (1979).

[8] N. Rostoker and H. Rahman, "Nonthermal Reactors Based on Intense Neutralized Ion Beams," *Comments Plasma Phys., Controlled Fusion* **10**, 81 (1986).

[9] N. Rostoker and H. Rahman, "Large Orbit Confinement for Aneutronic Systems," *Nonlinear and Relativistic Effects in Plasmas*, Am. Inst. of Physics, ed. V. Stefan, p. 116, (1992).

[10] H. V. Wong, H. L. Berk, R. V. Lovelace and N. Rostoker, "Stability of Annular Equilibrium of Energetic Large Orbit Ion Beams," *Phys. Fluids* **B-3**, 2973 (1991).

[11] M. N. Rosenbluth and N. Rostoker, "Test Particles in a Completely Ionized Plasma," *Phys. Fluids* **3**, 1 (1960).

8) Advanced D-^{3}He Fusion Reactor Concepts and Applications-II 265
H. Momota, Chair

8-1 Next Step in FRC Development 267
Alan L. Hoffman and John T. Slough

8-2 Direct Energy Conversion System for D-^{3}He Fusion 273
Y. Tomita, L.Y. Shu, and H. Momota

8-3 Overview of the Mirror Fusion Propulsion System (MFPS):
An Optimized Open Magnetic Field Configuration Using D-^{3}He 279
Scott A. Carpenter and Marc E. Deveny

8-4 Prospects for Novel Thermonuclear and Non-Thermonuclear Fusion 285
L.J. Perkins

Next Step in FRC Development

Alan L. Hoffman & John T. Slough
University of Washington
Seattle, WA 98195

ABSTRACT

Field Reversed Configurations (FRC) are probably the most attractive option for burning advanced fuels due to their high β and unrestricted end-flow from a natural divertor. The Large s Experiment (LSX), which was operated for one year at STI Optronics, demonstrated that moderate s (ratio of minor radius to ion gyroradius) FRCs could be formed without experiencing a predicted tilt instability, and there are now both experimental and theoretical reasons to hope that this trend can be continued up to the large s values required in a reactor. The LSX facility has been transferred to the University of Washington where it is being modified to perform a Tokamak Fueling by Accelerated Plasmoid (TRAP) experiment. However, the modified facility may also be ideal for continuing basic FRC development by translating and trapping 5-10 mWb low density hot FRCs, and then augmenting or sustaining the flux through use of neutral beams or rotating magnetic fields (RMF). The latter scheme is favored due to its simplicity, and examples are given for RMF current drive on both FRCs which can be produced by the modified LSX device, and on a nominal D-^{3}He reactor.

1. INTRODUCTION

The only magnetic configurations which have exhibited reactor level confinement are toroidal, but toroidal magnet systems are complex and lead to difficult engineering. Compact toroids offer the singular attractiveness of being able to provide a toroidal magnetic field topology in a non-toroidal external system. Thus, the potential exists for both providing adequate plasma confinement and engineering simplifications. An often overlooked additional advantage is that a natural divertor is provided with unrestricted flow out the ends of a linear magnet/vacuum system. The field-reversed-configuration (FRC), which contains only poloidal magnetic fields, has the added attractiveness of being very high beta, thus maximizing the potential for compactness, and also providing perhaps the only toroidal confinement geometry with real possibilities for burning advanced fuels.

FRCs have generally been thought of as being ideal MHD unstable due to the unfavorable curvature at the ends, and previous experiments were thought to exhibit stability to a predicted internal tilt instability only due to kinetic effects present when the number of internal ion gyroradii, characterized by the parameter s, was less than 2. The Large s Experiment (LSX) was constructed at STI Optronics in the period between 1986 and 1990 to study FRC physics in the large s regime where the influence of stabilizing kinetic effects is diminished. Although the facility was only operated for one year, several substantial results were obtained. Tilt stable FRCs were produced with s up to 8 [1], and new calculations suggest that certain naturally occurring pressure profiles may even be MHD stable due to strong compressional effects present when flux surfaces are racetrack-like and current

profiles are hollow [2]. Good confinement, in agreement with previous low s empirical scaling, was also realized up to s = 4. For the first time, particle confinement times approached 1 msec, which is specially notable since this occurred at densities over 10^{15} cm^{-3} and flux levels under 10 mWb. Confinement times have been noted to scale approximately linearly with poloidal flux, and even sub-GW reactors will have multi-Wb poloidal fluxes.

s values beyond 4 and flux levels over 10 mWb could only be obtained on LSX by operating at such high densities and low plasma temperatures that the FRCs were highly collisional, and symmetric equilibria with good elliptical flux surfaces could not be produced, using the highly dynamic field reversed theta pinch (FRTP) method of formation employed on LSX. During the last days of LSX operation there was some indication that good equilibria could be produced at even higher s and higher flux by careful control of the formation process, but it is probably not technologically feasible (due to high required voltages and extreme formation uniformity requirements) to produce FRCs with more than 10s of mWb of flux using the FRTP formation method. Thus, some means of flux augmentation is necessary for continued development of the FRC concept. Neutral beams have been previously proposed and reactor formation sequences have been discussed by Momota [3]. However, a simpler technique, utilizing the rotating field current drive already demonstrated on low temperature rotomak devices [4], appears to have engineering advantages, and its use on a modified version of the LSX device is discussed here.

2. LSX EXPERIMENTAL RESULTS

LSX was a 4.5-m long, 90-cm diameter slow FRTP, which could operate over a wide range of fill pressures. A complete description is given in Ref. 1. Fairly low voltages ($E_\theta \approx$ 100 V/cm) were used so that significant shock heating only occurred for fill pressures below 1 mTorr D_2. FRCs could be formed at fill pressures as high as 15 mTorr, but due to the inability to produce uniform preionization, and the low temperatures and low axial viscosity, these FRCs never achieved the good equilibria (characterized by symmetric axial diamagnetism distributions and hollow radial density distributions) reached at lower fill pressures. Nevertheless, the high density FRCs did not exhibit any tilt instability despite s values as high as 8.

Good symmetric equilibria could be formed at fill pressures below 6 mTorr, and these FRCs exhibited good confinement scaling in agreement with results achieved at lower s [5]. A plot of particle confinement time versus a previously noted r_s^2/ρ_i parameter is shown on Fig. 1. (r_s is the separatrix radius, ρ_i the ion gyroradius in the external magnetic field, and $x_s \equiv r_s/r_c$, the ratio of separatrix to confining coil radius.) The LSX results, in combination with the results achieved on previous smaller machines, illuminate the basic flux dependent scaling since, at least for a rigid rotor profile, the poloidal flux is given by $\phi_p = 0.31 x_s \pi r_s^2 B_e$.

Stability measurements are typified by the B_θ probe [6] mode traces shown on Fig. 2 for an s = 3 FRC. At this fill pressure and formation flux level (ϕ_{lo} is the flux present when the radial implosion begins) the formation is very dynamic, as seen by the peak in cross tube emission measured by a tomography detector at the tube centerplane. The large n=1 signals measured during the formation phase can easily be mistaken for signs of a tilt instability, but

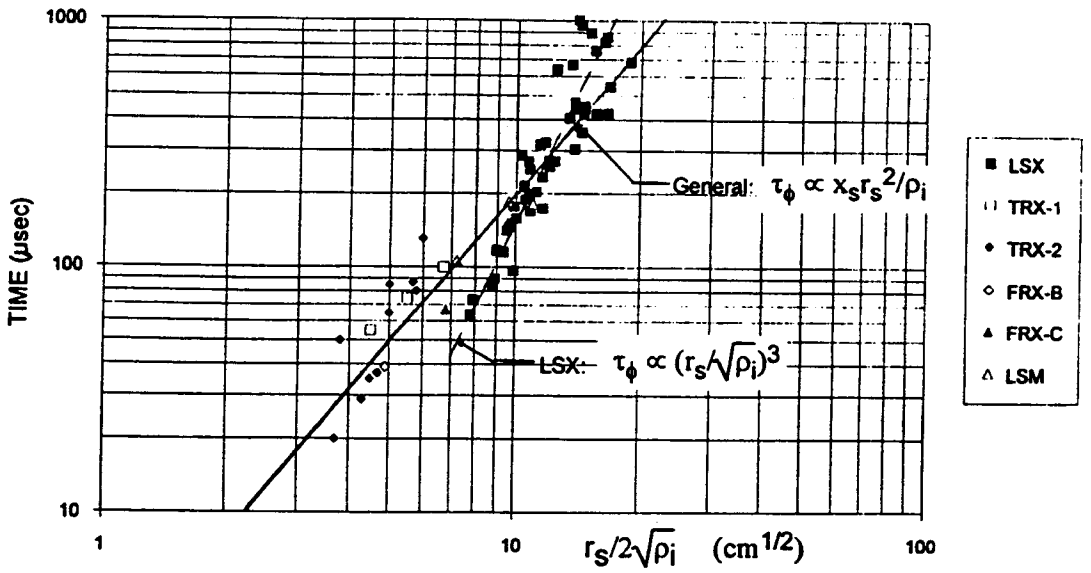


Fig. 1 FRC Particle Lifetime Scaling

as can be seen from the traces, they are formation related, and a stable FRC is formed which persists until the development of the rotating n=2 mode, which was not stabilized by multipole fields in these experiments.

The LSX facility is presently being moved to a University of Washington facility and the LSX magnet/plasma system is being modified (LSX/mod) to perform translation experiments to develop tokamak refueling methods. The TRAP (Tokamak Refueling by Accelerated Plasmoids) experiments will utilize the type of cold, high density FRCs produced on LSX at high fill pressures to penetrate strong transverse fields. However, a much more interesting regime for FRC development is the sub-mTorr fill pressure regime where up to 2 keV total temperatures were realized [1, 5].

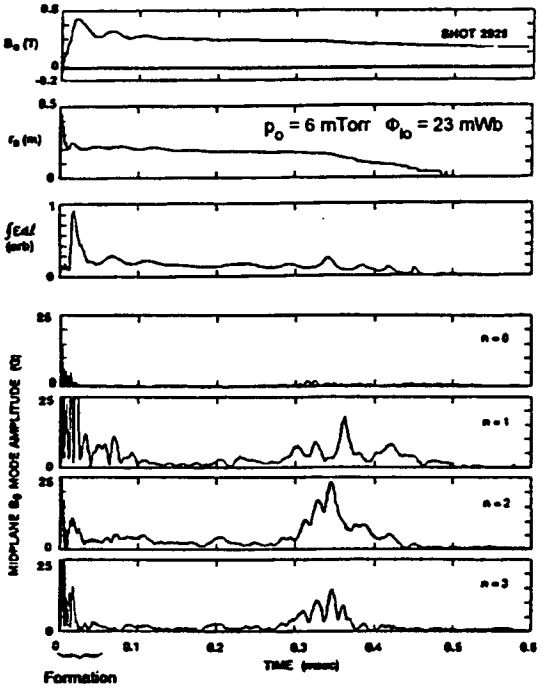


Fig. 1 B_θ Mode Amplitudes

3. LSX/MOD

LSX/mod uses the same power supplies as LSX to power a 2.5-m long, 46-cm diameter formation coil system, and a 2.0-m long, 30-cm diameter acceleration section. Although only one-half the size of LSX, LSX/mod should be able to form hot FRCs with the same 5-10 mWb flux levels as formed on LSX at sub-mTorr fill pressures. In the short time LSX was

operating it was only possible to utilize about one-fourth the bias field capability at low fill pressures due to difficulties in achieving uniform, strong preionization at sub-mTorr fill pressure levels. Due to higher forward fields which will be available on LSX/mod, high temperatures can be reached with higher fill pressures, and the plasma can then be translated and expanded to low densities. The TRAP acceleration coils can even be used to increase the final plasma energy content.

Assuming FRCs with 8 mWb of flux can be formed in LSX/mod, the conditions achievable at various stations are shown in Table 1. The calculated temperatures are based on standard heating scenarios, with half the ions present in an original 2-mTorr D_2 fill entrained in the FRC, and the translational energy produced upon ejection from the formation and acceleration sections reconverted into thermal energy upon trapping in the confinement section. The second set of conditions listed for the acceleration section are obtainable by activating the acceleration coils, but the confinement section conditions were calculated without utilizing this extra step.

Table 1. FRC Conditions at Various Sections (ϕ_p = 8 mWb)

Section	r_c	B_e	r_s	x_s	<n>	T_t	l_s	s
	(cm)	(kG)	(cm)		(cm^{-3})	(keV)	(cm)	
Formation	23	10	12.3	0.53	$1.1x10^{15}$	2.0	50	1.9
Acceleration	15	6.5	12.3	0.82	$0.5x10^{15}$	1.4	100	2.2
	15	10	10.7	0.71	$1.0x10^{15}$	2.0	75	2.2
Confinement	45	3	23	0.51	$1.0x10^{14}$	2.0	150	1.0

4. D-^{3}He REACTOR REQUIREMENTS AND LSX/MOD EXPERIMENTS

A steady state D-T reactor could not operate at much above 10^{20} m^{-3} densities due to the high neutron flux, but a steady state D-^{3}He reactor could take full advantage of the high β nature of the FRC and operate at 10^{21} m^{-3} densities. This considerably reduces the required energy confinement times. A list of nominal conditions for a D-^{3}He reactor and a scaled experiment on LSX/mod are given in Table 2. Both the classical and empirical (from Ref. 5) flux lifetimes are given. There are no experimental results available for current drive efficiencies in FRCs using

Table 2. LSX/mod and Reactor Conditions

	LSX	D-^{3}He Reactor
B_e (T)	0.3	10
n_e (m^{-3})	$2x10^{20}$	$2x10^{21}$
T_e (keV)	0.3	30
T_i (keV)	0.7	70
r_s (m)	0.23	1.0
r_c (m)	0.45	1.5
ϕ_p (Wb)	0.0075	6.8
s	1.4	26
τ_ϕ (classical)	20 msec	400 sec
τ_ϕ (empirical)	0.25 msec	0.025 sec
τ_ϕ (desired)	2.5 msec	25 sec

either neutral beams or RF fields, although high energy ion beam decay is expected to be classical based on tokamak experiments

In order for current drive schemes to be sufficiently efficient for good reactor power balance, about a 25 sec equivalent flux confinement time would be required. (At the density listed the energy confinement time need be only one-hundredth this value.) The desired equivalent τ_ϕ for RMF current drive to be efficient on LSX/mod is also listed.

5. RMF CURRENT DRIVE

If a cross cylinder rotating magnetic field (similar to the m=1 Alfvén mode) is applied with a rotational frequency ω greater than the ion cyclotron frequency ω_{ci} and much less than the electron cyclotron frequency ω_{ce} (both ω_{ci} and ω_{ce} based on the rotating field magnitude B_ω) then a simple two-fluid calculation [4] shows that the azimuthal and axial current densities are given by $j_\theta = -en_e\omega r/[1 + 2/(\omega_{ce}\tau_e)^2]$, $j_z = -e^{i\omega t}j_\theta/(\omega_{ce}\tau_e)$. These calculations assume that the rotating field penetrates into the plasma column, although the classical skin depth $\delta = \sqrt{2\eta/\mu_o\omega}$ is small. This penetration can occur due to the synchronous rotation of the electrons (and reduced j_z) at large $\omega_{ce}\tau_e$, with the penetration depth increasing by the factor $\delta^* = (\omega_{ce}\tau_e)\delta$. Since the resistivity $\eta = m_e\nu_e/n_ee^2$ and $\tau_e = 1/\nu_e$, the effective penetration depth is proportional to $\nu_e^{-1/2}$ rather than to $\nu_e^{1/2}$.

This field penetration due to synchronous electron motion has been measured on many rotomak experiments. Almost all of these experiments used the rotating field to both ionize the gas and reverse an initial axial field. The resultant plasmas were cold, and the electron collision frequency was relatively high, but most likely classical, with $\nu_e = \nu_{ei}$(classical). No experiments have been performed on hot, preformed FRCs, where the most important consideration is whether the effective electron collision cross section for diffusion in the θ direction (θ-z gyro-orbits) will remain nearly classical, or will be closer to the value for anomalous diffusion in the r direction (r-θ gyro-orbits). The relevant parameters for rotomak experiments, are listed in Table 3. Also listed are requirements for the LSX/mod experiment and for a steady-state D-^{3}He reactor. The synchronous line current density is defined as $I'_{sync} = en_e\omega r_s^2/2$, and the required RMF power input per meter is just $I'V_\phi$, where V_ϕ is defined as ϕ_p/τ_ϕ.

6. CONCLUSIONS

Continued development of the FRC concept requires some form of flux enhancement beyond that entrained in FRTP formation. LSX/mod is an ideal facility to carry out this continued development since it can produce FRCs with the required high temperatures and initial flux levels. Utility of the RMF current drive technique depends on the effective electron collision frequency with respect to diffusion across the rotating field lines. In order to generate the required line currents (shown in brackets on Table 3) this effective collision frequency must be much lower than the anomalous collision frequency for poloidal flux diffusion. If RMF current drive works at all for high temperature FRCs, it will also be highly efficient and require relatively low input powers. An experiment on LSX/mod will provide a good test of this concept.

Table 3. RMF Parameters for Various Experiments

	μsec Duration Rotomaks		msec Duration Rotomaks		LSX/mod Experiment	D-^{3}He Reactor
	Xe [4]	A [7]	H [8]	H [9]	D	D-^{3}He
r_s (cm)	1.5	1.8	10	11	23	100
B_e (kG)	0.7	0.3	0.5	0.04	3	100
n_e (10^{20} m^{-3})	5	2.5	1.0	0.06	2	20
T_e (eV)	15	5	(30)	6	300	30000
ν_{ei} (10^6 s^{-1})	250	670	18	12	1	0.01
ν^* (10^6 s^{-1})					9	0.2
ω (10^6 s^{-1})	7.9	4.2	6.3	6.3	1.0	0.2
B_ω (G)	500	200	(50)	20	50	20
ω_{ci} (10^6 s^{-1})	0.04	0.05	0.5	0.16	0.25	0.08
ω_{ce} (10^6 s^{-1})	9000	3600	900	300	900	360
δ^* (cm)	0.2	0.6	0.13	0.4	0.16	0.02
r_s/δ	8	3	80	28	140	6000
ω_{ce}/ν^*	36	5	(300)	25	100	2000
I'_{sync} (kA/m)	71	27	500	37	800	32000
I'_{exp} (kA/m)	77	24	70	7	[400]	[13000]
$d\phi_p/dt$ (V)					3	0.3
P'_{rmf} (MW/m)					1.2	3.5

REFERENCES

[1]. A.L. Hoffman et al., "The Large s Experiment (LSX)", *Fusion Technology*, **23**, 185 (1993).

[2]. R. KANNO, A. ISHIDA, L.C. STEINHAUER, "Ideal MHD Stability of the Tilting Mode in Field Reversed Configurations", in preparation. Also *Bull. Am. Phys. Soc.* **37**, 1609 (1992) paper 9S23.

[3]. H. Momota et al., "Conceptual Design of the D-^{3}He Reactor Artemis", *Fusion Technology*, **21**, 2307 (1992).

[4]. H.A Blevin and P.C. Thonemann, "Plasma Confinement Using An Alternating Magnetic Field", *Nuclear Fusion: 1962 Supplement, Part 1*, 55 (1962).

[5]. A.L. Hoffman and J.T. Slough, "Field Reversed Configuration Lifetime Scaling Based on Measurements from the Large s Experiment", *Nuclear Fusion*, **33**, 27 (1993).

[6]. M. Tuszewski, "Mirnov Loop Array for Field-Reversed Configurations", *Rev. Sci. Instrum.*, **61**, 2937 (1990).

[7]. W.N. Hugrass, I.R. Jones, M.G.R. Phillips, "An Experimental Investigation of Current Production by means of Rotating Magnetic Fields", *J. Plasma Physics*, **B26**, 465 (1981).

[8]. M. Frank et al., "Rotomak Research at Essen", *Advances in Compact Torus Research - Proceedings of IAEA 4-7 March, 1985 Meeting in Sydney, Australia (IAEA-TECDOC-369)*, 165 (1986).

[9]. G. Durance et al., "Studies of Equilibrium in the AAEC Rotomak", *Plasma Physics Contr. Fusion*, **29**, 227 (1987).

Direct Energy Conversion System for D-^{3}He Fusion

Y.Tomita, L.Y.Shu, and H.Momota

National Institute for Fusion Science
Nagoya 464-01, JAPAN

ABSTRACT

A novel and highly efficient direct energy conversion system is proposed for utilizing D-^{3}He fueled fusion such as D-^{3}He FRC reactor "ARTEMIS-L"[1]. The particles that escape directly out of burning plasma consist of thermal components with energy of few hundreds keV and fusion protons with high energy of 15 MeV. In order to convert kinetic energy of ions characterized by the above energy spectrum, we applied a pair of direct energy conversion systems each of which has a cusp-type DEC and a traveling wave DEC (TWDEC). In a cusp-type DEC, electrons are separated from the escaping ions at the first line-cusp and the energy of thermal ion components is converted to electricity at the second cusp DEC. Since the orbit of 15 MeV protons is hardly affected by the cusp-magnetic field because of their high energy, fusion protons go through the cusp-type DEC and arrive at the TWDEC, which principle is similar to "LINAC." The TWDEC consists of a modulator, which modulates velocities incident proton beams, and a decelerator, which decelerates the bunched beams. The energy of fusion protons is recovered to electricity with an efficiency of more than 70%. These DECs bring about the high efficient fusion plant.

1. INTRODUCTION

In D-^{3}He FRC fusion reactor such as "ARTEMIS-L," more than 70% of fusion energy is carried by charged particles which escape directly out of burning plasma. By introducing these particles to direct energy converters (DEC) along the magnetic lines of force, it is expected to obtain a fusion reactor with high plant efficiency. The D-^{3}He fueled fusion is characterized by the component of fusion protons with high energy of 15 MeV. These fusion protons are not allowable to use the traditional Venetian-Blind DEC [2] in view of a high applied voltage to recover the energy of fusion protons. In order to avoid the problem, a novel direct energy conversion system is proposed, which consists of a cusp-type DEC and a traveling wave DEC. In a cusp-type DEC, electrons are separated from escaping ions. Note that a cusp-type DEC avoids unnecessary bombardment losses of energetic protons which is inevitable to a Venetian-Blind DEC. The 15 MeV fusion protons pass through the cusp-type DEC without any bombardments and orbital change because of their high energy. These protons are guided to the TWDEC and recovered their energy. The applied electric voltage in the TWDEC is less than 1MV, which is much lower than that of flashover of the insulators. In this paper, the principles of a cusp-type DEC as well as a traveling wave DEC are presented.

2. CUSP-TYPE DIRECT ENERGY CONVERTER

In order to separate electrons from the escaping ions and to convert the energy of the thermal ions to electricity , a double-cusp magnetic field configuration is introduced. Because of the small Larmor radius of electrons, electrons go along the magnetic field lines and are introduced to the first line-cusp. The thermal ions ,which energy is characterized to be few hundreds keV, pass through the first line cusp. The higher magnetic field at the second line-cusp compared with the first line-cusp leads the thermal ions to the second line-cusp.On the other hand, the orbit of fusion protons with energy of 15 MeV is hardly affected by this cusp-magnetic field and they pass through these line-cusps. The characteristic Larmor radii of incident fusion protons and thermal ions are 2.6m and nearly 1m , respectively, in case of "ARTEMIS-L," From these Larmor radii, the coil radii of the inlet and outlet of the cusp-type DEC are determined to be 5.3 m and 4.2 m, respectively. The distances of line-cusp coils are 4.2 m and 6.4 m (Fig.1). The electrons diffuse out of the burning region with the mono-energetic distribution that is characterized to be 167 keV for "ARTEMIS - L " reactor. This energy corresponds to the floating potential of the plasma. This potential accelerates the escaping ions out of the burning plasma. We adopt the following form as the diffused energy distribution of thermal ions:

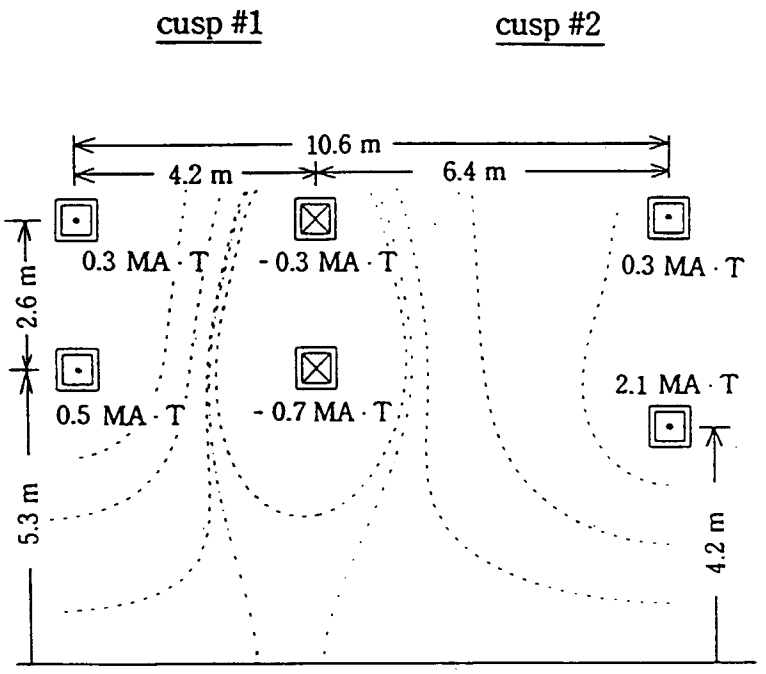


Fig.1 The arrangement of cusp type DEC ; the radii , distances and currents of cusp coils : The incident particles come from the left side. The magnetic field lines are also shown by dashed lines.

$$f_{ion} \propto e^{-(\varepsilon-\varepsilon_{min})/\beta} \quad : \varepsilon > \varepsilon_{min} \quad . \tag{1}$$

The minimum energies ε_{min} are 167 keV for proton , deuteron and triton, and 334 keV for ^{3}He and ^{4}He, respectively. The energy spread β is 167 keV for all ion species if $\tau_N / \tau_\varepsilon = 2$.
On the other hand, fusion protons have a shifted Maxwellian energy distribution :

$$f_p \propto e^{-(\sqrt{\varepsilon}-\sqrt{\varepsilon_0})^2/\beta_p} \quad : \varepsilon > \varepsilon_{min} \quad , \tag{2}$$

with the center energy ε_0 of 15 MeV and the minimum energy ε_{min} of 167 keV. The fusion reaction with a plasma temperature of about 100 keV spreads the energy distribution of fusion protons by 1 MeV (= β_p).

The particle orbit traces bring the classification of ions with respect to their energy and the incident radius. In case that the currents of the inlet and the outlet coil are 0.8 MA · T and 2.4 MA · T (Fig.1), which high current is needed to prevent the thermal ions from passing these cusps, the particle classification diagram in ion energy and incident radius space is shown in Fig.2, where as references the characteristic Larmor radii of ions are also indicated. The ions with lower energy are introduced to the first cusp and those with higher energy pass through these cusps. The particles with middle energy bounded by two lines in Fig.2 are introduced to the second line-cusp. For the thermal ions , whose minimum energy is 167 keV or 334 keV, lower energy parts are introduced to the second line - cusp , higher energy parts pass through cusps. For fusion protons with Larmor radius of 2.6 m, the protons with higher energy than 5MeV are pass through these line-cusps (Fig.2). For the electrons , the energy scale of Fig.2 is changed to be lower by its mass ratio to proton (= 1/1836). This indicates that electrons with energy of 167 keV are almost introduced to the first cusp. From the consideration of particle orbit traces included with the energy distributions , a classification fraction of incident particles is tabulated in Table 1. More than 99% of electrons are introduced to the first line - cusp. On the other hand, because of higher energy, majority of fusion protons are pass through these line-cusps. A part of thermal ions is introduced to the second line-cusp, but the rest passes through these cusps.

As a result, in the first line-cusp there are only electrons and in the second line-cusp there exist only thermal ions.

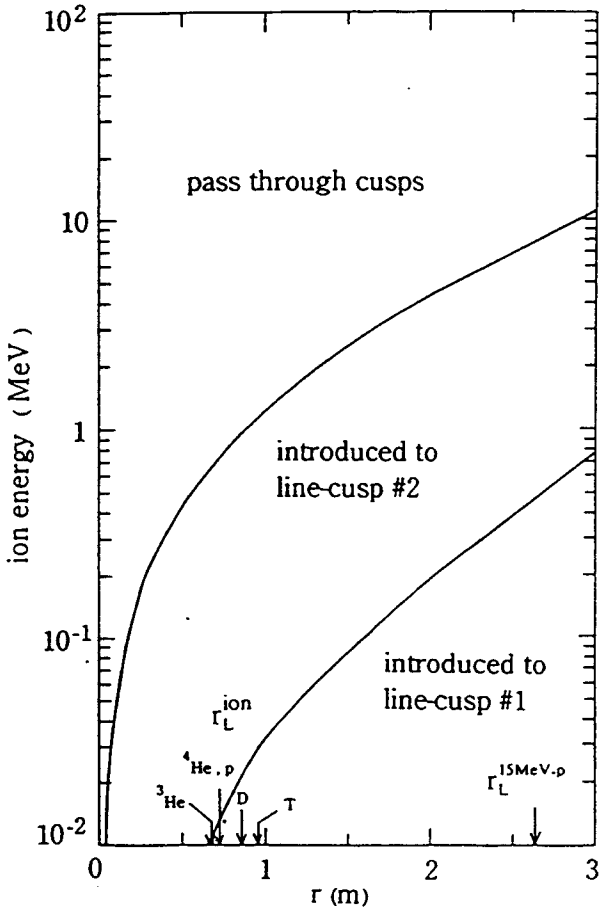


Fig.2 The particle classification diagram in ion energy and incident radius space , here as reference the characteristic Larmor radii of ions are also indicated.

	electrons	thermal ions					fusion protons
		D	^{3}He	^{4}He	p	T	
introduced to line-cusp #1	> 0.99	0	0	0	0	0	0
introduced to line-cusp #2	< 0.01	0.96	0.48	0.64	0.90	1.0	< 0.01
pass through cusps	< 0.01	0.04	0.52	0.36	0.10	0	> 0.99

Table 1 The classification fraction of incident particles to the cusp type DEC.

3. TRAVELING WAVE DIRECT ENERGY CONVERTER [3]

The 15 MeV fusion protons, which pass through cusp type DEC, are guided to the traveling wave direct energy converter , which consists of a modulator and a decelerator. At the modulator, a traveling electric field is excited by grid meshes installed in the proton beams. The velocities of incident proton beams are modulated to form a bunched protons at the down stream by this traveling electric field of 1 MV/m with a phase velocity that corresponds to the velocity of 15 MeV protons. At the down stream of the modulator, a length of 11 m is needed to bunch the fusion proton beams. The energy of the bunched beams is recovered by the decelerator, which utilizes a principle of a "LINAC" [4].

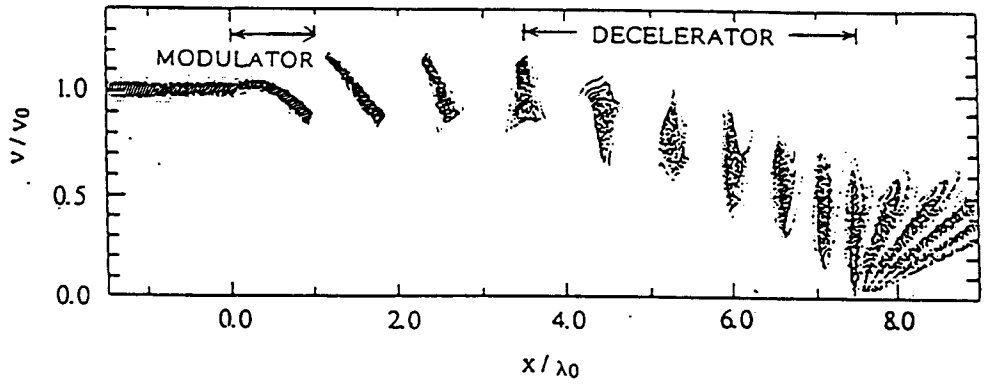


Fig.3 The phase trajectory of fusion protons in the traveling wave DEC. The velocity is normalized by that of 15 MeV proton (= 5.3 × 10^7 m/sec), and distance is measured by the wave length of 4.7 m.

By choosing the initial phase of traveling wave to be self-phasing and decelerating of incident bunched protons and controlling to match the phase velocity and the spacing of grids to the velocity of the decelerated proton beams, the energy of fusion protons is recovered to

electricity with high efficiency. The phase trajectory of fusion protons in the traveling wave DEC is exhibited in Fig.3, where the total length of the TWDEC is 31 m and 95 % of the energy of fusion protons is decelerated. The grid meshes at the modulator and the decelerator are installed with a spacing of 1.33 m. This grid pipe with 8 mm radius and 1 mm thickness is cooled by the water with a pressure gradient of 1.2 MPa/10m. This pressured water restrains the temperature increment at the outlet of a grid pipe to the value of 30 ℃. Taken into consideration of bombardment of fusion protons to the grids and the energy recovery at the end collector, the conversion efficiency of the traveling wave DEC is estimated as high as 0.76 (Fig.4).

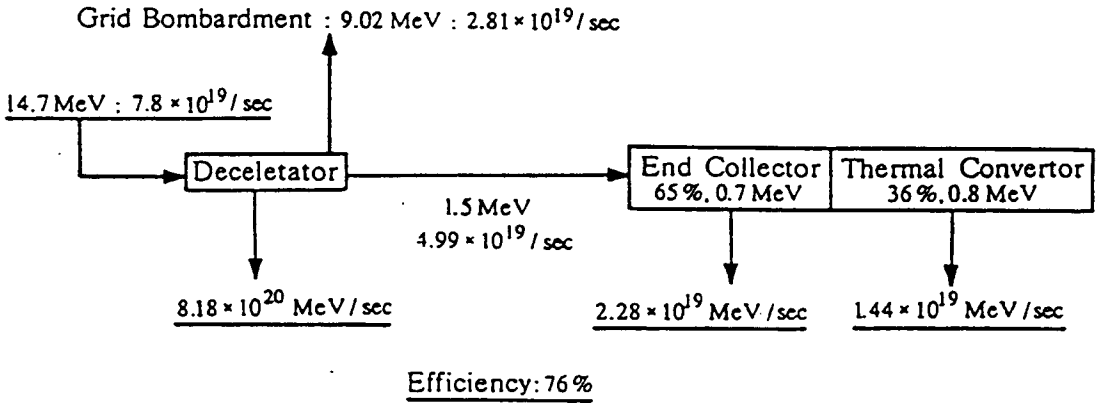


Fig. 4 The energy flow diagram of traveling wave DEC.

4. CONCLUSIONS AND DISCUSSIONS

A novel and highly efficient direct energy conversion system was proposed for utilizing D-^{3}He fueled fusion reactor. It consists of a cusp-type DEC and a traveling wave DEC. In a cusp-type DEC, electrons are introduced to the first line-cusp. Thermal ions with lower energy are introduced to the second line-cusp. Concerning a higher energy part of thermal ions that pass through this cusp-type DEC, they are able to be reflected into the cusp-type DEC by use of a reflector electrode with an applied voltage of less than 1 MV, which is installed outside the outlet of the cusp-type DEC. The 15 MeV fusion protons pass almost through the cusp-type DEC, because of their high energy. This cusp-type DEC avoids completely unnecessary bombardment losses of energetic fusion protons. Thus, we confirmed a principle of the cusp-type DEC. The energy recovery of classified thermal ions is still remained as one of the future issues. Fusion protons with 15 MeV, which pass through the cusp-type DEC, are guided to a traveling wave DEC and are converted their energy to electricity with a high efficiency of more than 70%. In this TWDEC, the applied electric voltage is controlled less than 1 MV which allows us to avoid flashover of the insulators. The cross-sectional drawing of "ARTEMIS-L" is shown in Fig.5, which includes the proposed DECs , i.e., the cusp-type DEC and the traveling wave DEC. By the use of these novel DECs, one is able to obtain a fusion reactor with high plant efficiency.

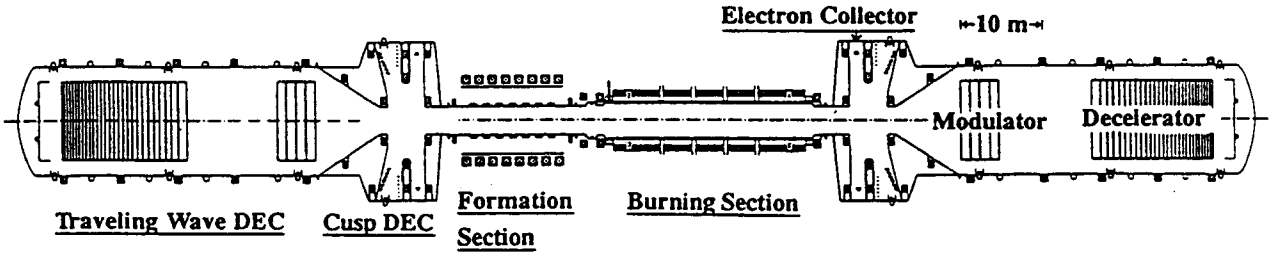


Fig.5 The cross-sectional drawing of "ARTEMIS-L."

REFERENCES

[1] H.Momota, Y.Tomita, A.Ishida, Y.Kohzaki, M.Ohnishi, S.Ohi, Y.Nakao and M.Nishikawa, "D-3He Fueled FRC Reactor "ARTEMIS-L"," *Proc. 14th Int. Conf. Plasma Physics and Controlled Nuclear Fusion Research*, Wurzburg, Germany , 1992 , IAEA, Vienna , IAEA-CN-56/G-1-13 (1992).

[2] R.W.Moir, et al., "Mirror Reactor Studies," *Proc. 6th Int. Conf. Plasma Physics and Controlled Nuclear Fusion Research*, Berchtesgaden, 1976, IAEA, Vienna, **3**, 223 (1977).

[3] H.Momota, "Direct Energy Conversion for 15 MeV Fusion Protons," LA-11808-C, Los Alamos National Laboratory , 8 (1990).

[4] D.W.Fry , R.B.R.-S.-Harvie , L.B.Mullett and W.Walkinshaw , "Travelling-Wave Linear Accelerator for Electrons," *Nature*, **160**, 351 (1947).

OVERVIEW OF THE MIRROR FUSION PROPULSION SYSTEM (MFPS): AN OPTIMIZED OPEN MAGNETIC FIELD CONFIGURATION USING D-^{3}He

Scott A. Carpenter
CDE Fission / Fusion Systems
721 Coventry Road, Suite A
Kensington, CA 94707
(510) 559-8071

Marc E. Deveny
CDE Spacecraft Systems
1925 Turnberry Lane
Corona, CA 91719
(714) 734-5395

Abstract

Successful application of fusion power to space propulsion requires rethinking the engineering solution to controlled fusion energy. Initial mass to low earth orbit (IMLEO), specific jet power (kW_{thrust}/kg_{engine}), and reusability drive the engineering solution for successful application of fusion power to space propulsion. These space-based design drivers led us to identify three design principles which we used to adapt, then optimize, a thermal-barrier-tandem-mirror (TBTM) fusion-reactor configuration for propulsion in space. These three design principles are: (1) provide maximum direct access to space for waste radiation to minimize component temperatures, (2) operate components as passive radiators to minimize cooling-system mass, and (3) optimize the plasma fuel, fuel mix, and temperature for best specific jet power. The resulting space-based solution is called the Mirror Fusion Propulsion System (MFPS) and has several intriguing features that include competitive IMLEO (1260 tonnes for a reference 90-90-90-day mission to Mars with continuous mission-abort capability), reusability, high specific jet power (4.1 kW_{thrust}/kg_{engine}), modularity, potential to magnetically shield the crew and for in-orbit characterization of the target body's surface composition using fusion x-rays and neutrons, and a post-human-rated "design-missions-plus-one" strategy for enabling of a low-cost non-stand-alone extra-solar-system mission.

INTRODUCTION

Contemporary utility-based-fusion-reactor configurations are inappropriate for space propulsion due to design-driver differences between terrestrial and space environments. However, through application of certain design principles, modifications to contemporary designs can result in appropriate space-fusion-propulsion configurations.

In Part 1, we apply three primary design principles [5] that help us to adapt, and then optimize, a candidate-fusion-reactor configuration for propulsion in space. In Part 2, we demonstrate the improved mission performance of the resulting Mirror Fusion Propulsion System (MFPS) over the nuclear thermal gas core fission reactor for a hypothetical human-piloted Mars-exploration mission of 90-90-90-day duration. IMLEO and mission window are compared. We also characterize MFPS' ability to complete an extra-solar-system mission called the solar-gravity-lens (SGL) mission.

1. APPLYING DESIGN PRINCIPLES (DPs) TO FUSION-REACTOR CONFIGURATIONS FOR PROPULSION IN SPACE

We describe application of three design principles to the thermal-barrier-tandem-mirror (TBTM) that adapts it for propulsion in space, minimizing its IMLEO and maximizing its reusability and specific jet power.

1.1 Thermal-Barrier-Tandem-Mirror (TBTM) Configuration

Magnetic-mirror machines for the purpose of controlling thermonuclear fusion reactions fall into three distinct evolutionary classes [1]. The earliest mirror machines were called simple mirrors (SM). A breakthrough came in 1976 with development of the tandem mirror (TM). And, in 1979, the electron thermal barrier (TB) concept was added to the tandem mirror. A new commercial reactor design study based on TBTM was completed in 1986 called MINIMARS for MINI-Mirror Advanced Reactor Study [2], Figure 1. The acronym chosen for this study is possibly prophetic, although at the time, MINIMARS had nothing to do with traveling to the planet Mars.

1.2 Application of Design Principles to the TBTM

All fusion-grade plasmas emit four primary plasma radiations: (1) neutron, (2) Bremsstrahlung, (3) synchrotron, and (4) plasma transport. In all cases, there will be a substantial amount of waste power radiated from the plasma. For a 4-GWt fusion power plant in space, as much as 50%, 2 GW, of waste radiation must be rejected to space, somehow. If we look at the MINIMARS design, Figure 1, we see that the plasma, at ~300 million kelvins, is surrounded by metallic superconducting coils at 4.2 kelvins. On earth, this represents a serious thermal management problem; in space, it represents an un-manageable problem. MINIMARS is a solution to the TBTM that is unsuitable for space propulsion.

DP-1: Provide maximum direct access to space for waste radiation to minimize component temperatures. We seek to apply the first design principle to find means to provide direct access to space for as much of the waste radiation as possible. In searching the literature, we found that at the end of the MINIMARS design study, a new, better method of central-cell plasma stabilization was identified and studied, consisting of a ripple-magnetic field and an electrically-conducting wall [2] (in contrast, MINIMARS relied on a smooth central-cell magnetic field for stability). In this new stabilization method, discrete circular coils are used rather than the pancake coils used in MINIMARS. These coils are placed along the length of the central cell, with inter-coil distances that form magnetic-field ripples of 10-15%. The spacing between the coils provide an exit path for waste radiation to escape directly to deep space.

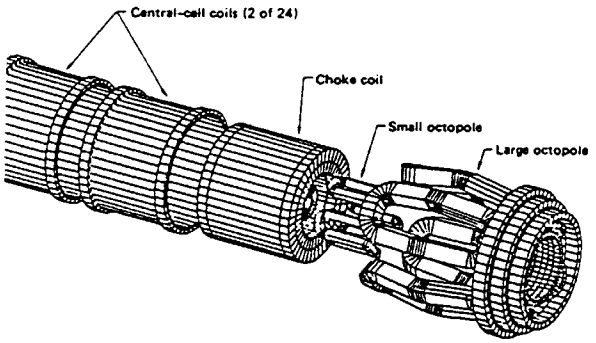


Figure 1. MINIMARS; the leading earth-based design.

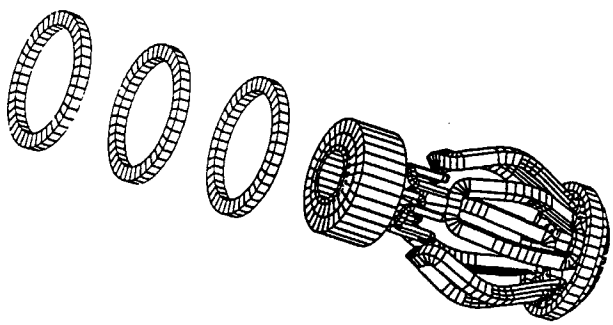
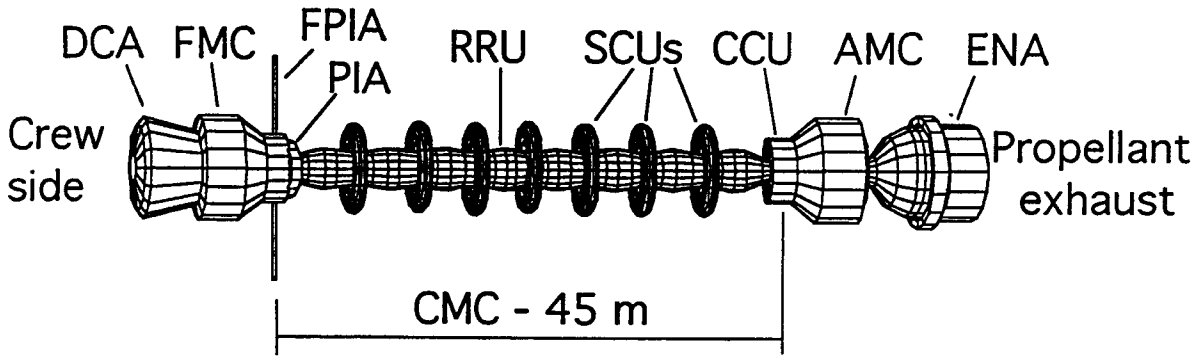


Figure 2. Widely spaced coils; an exit path for radiation.

There are other structures that surround the plasma in addition to the superconducting coils as shown in Figure 3, the most important being the electrically-conducting wall that completely encircles the plasma and required for plasma stability purposes. Applying again the first design principle (DP-1) to this structure leads us to seek materials that are semi-invisible to the plasma-generated neutron and x-ray radiation. We propose that it is possible to construct the electrically-conducting wall from three materials, molybdenum, graphite, and advanced carbon fiber, such that between 50-70% of the Bremsstrahlung and neutron radiation generated in the plasma pass through this structure.



ATCS	Active Thermal Control Subsystem (not shown)	RRU	Reflector-Radiator Unit
DCA	Direct Converter Assembly	SCU	Shield-Coil Unit
FMC	Forward Mirror Cell	CCU	Choke Coil Unit
CMC	Central Mirror Cell	AMC	Aft Mirror Cell
FPIA	Fuel Pellet Injection Assembly	ENA	Exhaust Neutralizer Assembly
PIA	Propellant Injection Assembly	HCS	High-Compression Structure (not shown)

Figure 3. The Mirror Fusion Propulsion System (MFPS) - drawn to scale.

The generic MFPS is about 79 m long and 8 m in diameter and produces 4-GWt of fusion power. The Central Mirror Cell (CMC) contains the plasma core in a stable, ignited mode and consists of six components or subassemblies: (1) the Reflector-Radiator Unit (RRU), (2) seven Shield-Coil Units (SCUs), (3) two Choke Coil Units (CCUs), (4) a Fuel Pellet Injection Assembly (FPIA), (5) a Propellant Injection Assembly (PIA), and (6) a High-Compression Structure (HCS). The Forward and Aft Mirror Cells (FMC and AMC) located forward (crew side) and aft (propellant-exhaust side) of the CMC, respectively, each consist of one large octopole magnet and several shaping magnets that aid central-cell plasma stability during startup and axial plasma confinement during all operations [2]. The Direct Converter Assembly (DCA), located forward of the FMC, directly converts charged-particle kinetic energy to electricity. The electrical power is used for space vehicle electrical loads and recirculation power for fusion reactor subsystems. The Power Conditioning Subsystem (PCS) consists of several subsystems responsible for the distribution of power from the DCA to the reactor and ship systems. It also provides the charging power for the Reactor Ignition Subsystem used to restart the fusion reactor and for pellet injection. The Propellant Delivery Subsystem (PDS) pumps liquid-hydrogen propellant through the superconducting coils to provide cooling. The PDS then injects the propellant into the central-cell plasma through its Propellant Injection Assembly (PIA) located on the CMC. The Exhaust Neutralizer Assembly (ENA) neutralizes the plasma/propellant mixture, thereby detaching the particles from the magnetic field lines to produce thrust. The ENA contains neutral gas-injection jets for charge exchange with the hot plasma/propellant exhaust. The Active Thermal Control Subsystem (ATCS) consists of radiator panels, pump assemblies, and pipes distributing the cooling fluids to all shield/magnet assemblies throughout the mirror cells.

In MFPS, the discrete superconducting coils are called Shield-Coil Units (SCUs) and the electrically-conducting wall is called the Radiator-Reflector Unit (RRU). The SCUs produce the magnetic field that contains the radial pressure of the reacting d-^{3}He and other fusion reaction particles in the Central-Mirror Cell (CMC). The RRU consists of a thin-walled rippled tube that surrounds the plasma. The RRU wall is composed of three layers: (1) the inner layer is a thin foil of molybdenum 10-50 μm thick, (2) the middle layer is graphite, about 1 cm thick, and (3) the third layer is carbon fiber, also about 1 cm thick. The RRU performs four functions: (1) the molybdenum foil reflects synchrotron radiation back into the plasma where it

is absorbed, thereby increasing the power available for thrust; (2) the graphite layer (in proximity to the plasma surface) aids stabilization of the plasma by acting as an electrically conducting wall, producing an image-current counter force to growing plasma instabilities; (3) the carbon fiber layer acts as a "blackbody" radiator, thereby minimizing external cooling-system mass and providing directional structural strength; and (4) the three layers together allow most of the neutrons and over half of the plasma x-rays (Bremsstrahlung) to pass directly through the RRU to deep space (Figure 4) thereby reducing the RRU temperature (Figure 5).

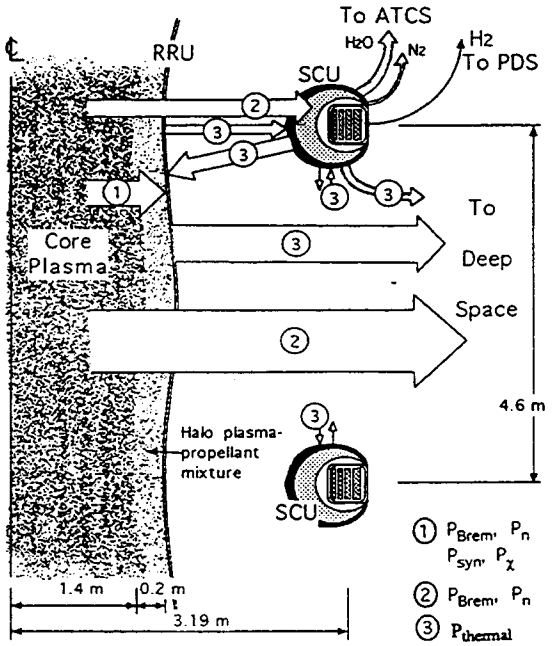


Figure 4. Waste power flow in MFPS.

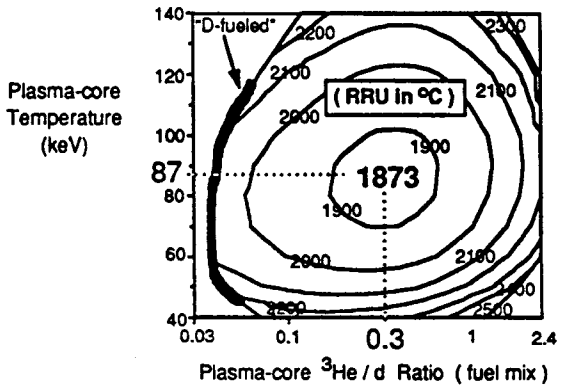


Figure 5. RRU temperature.

DP-2: Operate components as passive radiators to minimize cooling-system mass. In addition to neutron and x-ray radiation, the RRU also absorbs a small amount of plasma, synchrotron radiation, and radiated thermal heat from the Shield-Coil Units (SCUs). The single heat-sink term is provided by the carbon fiber RRU surface acting as a "blackbody" radiator, with most of the radiated heat going directly to space (Figure 4).

The strategy used to minimize heat absorption in the RRU (wall thinness and low cross-section for radiation) cannot be used with the SCUs, because they are inherently thick, and materials with large interaction cross-sections are desired. Consequently, the surfaces of the SCUs are also operated as "blackbody" radiators because they intercept a fraction (~24%) of the outgoing waste radiation (Figure 4).

DP-3: Optimize the plasma fuel, fuel mix, and temperature for best specific jet power. There is a plasma-operating window with relatively good percent-power-available for thrust (Figure 6). Where we desire to operate in this regime is determined by other, more subtle criteria that include component temperatures (Figure 5). There are numerous other factors that will determine the exact plasma-core fuel-mix and temperature optimization, and these include the fraction of ^{3}He burn up (acquisition and cost problem), the magnetic field strength and associated structural masses, the radiator masses, the shielding materials and masses, the specific jet power and overall IMLEO, and more. Of these, the specific jet power is one of the most important and Figure 7 shows that the desired fuel mix moves towards a one-to-one ^{3}He-to-d ratio. It is possible to understand the effects of plasma thermodynamics on subsystems of MFPS by studying the breakdown of the plasma radiations as a function of fuel mixture (Figure 8).

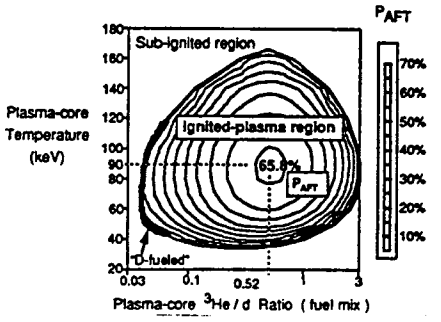


Figure 6. Power available for thrust.

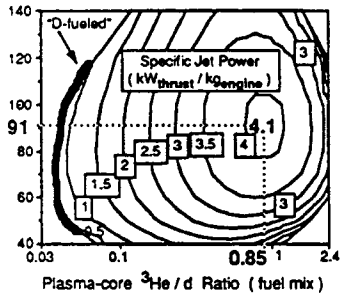


Figure 7. Specific jet power in a 4-GWt MFPS.

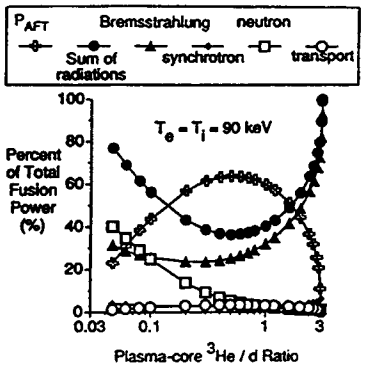


Figure 8. Primary plasma radiations.

2. Space Mission Performance

We define specific mission scenarios relevant to the fusion propulsion regime. These mission scenarios include (1) a 90-90-90-day human-piloted Mars-exploration mission with continuous mission-abort capability and (2) a post-design-life robot-piloted mission to the large gravitational focal zone of the Sun called the solar-gravity-lens (SGL) mission [3]. The trajectories are modeled similar to those of other studies [4]. These missions can be accomplished with less propellant mass and with shorter flight times using the Mirror Fusion Propulsion System (MFPS) than is possible with other proposed propulsion systems due to (1) MFPS' ability to provide steady, continuous acceleration at a magnitude of up to 2 cm/sec^2, and (2) MFPS' high specific impulse (Isp) that can be varied between 37,000 seconds (human-piloted Mars mission) and ~350,000 seconds (post-design-life robot-piloted-MFPS SGL mission).

2.1 Mars Human-Piloted Mission

Figure 9 shows the IMLEO of MFPS and NTR gas core propulsion systems versus mission window for constant 90-day travel times to and from Mars. Figure 10 shows the "carry-on" mass required by the vehicle to operate a 4-GWt MFPS for 180 days. If the fuel-mix is 0.85 and the plasma temperature is 90 keV, then the total ^{3}He load would be about 700 kg to complete the 90-90-90-day Mars mission. Figure 11 shows the ^{3}He-mass-rate inventory in the plasma as a function of fuel mixture at 90 keV.

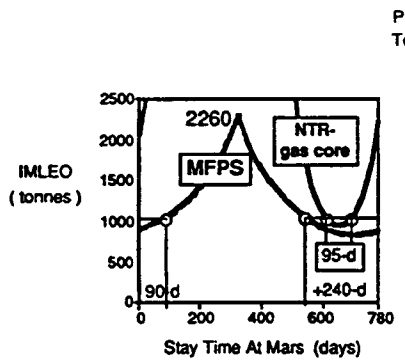


Figure 9. IMLEO of MFPS and NTR gas core.

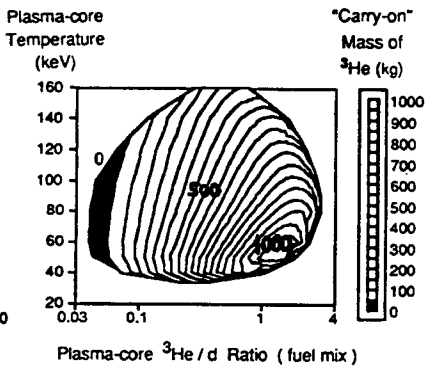


Figure 10. ^{3}He "carry-on" mass for 180 days at 4 GWt.

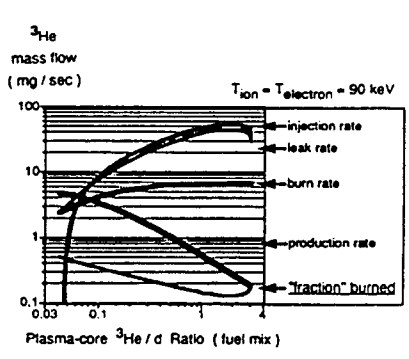


Figure 11. ^{3}He-mass-rate inventory.

2.2 Solar-Gravity-Lens (SGL) mission

In an effort to implement any extra-solar-system mission, we argue that time-relevant (within the lifetime of the society that initiates the project) and non-stand-alone missions would be required to gain approval from governments and the public. Consequently, we propose the "N-Missions-Plus-One" strategy for implementing extra-solar-system missions.

In this scenario, an MFPS would complete its design rated missions (N missions) which for the 4-GWt-generic MFPS is 8-90-90-90-day Mars missions with the limiting criteria being the neutron fluence to the superconducting magnets. Following completion of the 8-90-90-90-day missions, MFPS would be ready for disposal. MFPS would be robotized, with a gradual power-program reduction to extend component operating life, and sent on the extra-solar-system mission for final disposal. Figure 12 shows the mass break down of a post-human-rated 4-GWt MFPS that has been robotized for one final mission to the large gravitational focal zone of the Sun.

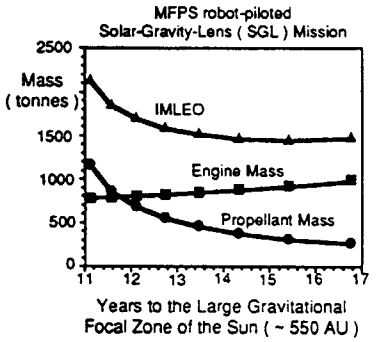


Figure 12. Years to the Large Gravitational Focal Zone of the Sun (~550 A.U.).

Finally, we note that MFPS is (1) conducive to modularity, (2) has the potential for using its magnetic energy to shield the crew from Van Allen radiation and solar particle events, and (3) by allowing fusion x-rays and specific-energy neutrons to escape the plasma core, it may be possible to perform an in-orbit characterization of the target body using these plasma radiations prior to human landing.

Acknowledgments

The authors wish to acknowledge the following people and their contributions to this paper. We thank Dr. Heino Nitsche (LBL) for his encouragement and usual selfless support. We thank Dr. Kathleen Brennan for performing many endless hours of computer-program optimization runs. We thank Dr. Daniel R. Dietderich (LBL) for his comments on application of high-Tc, high-field superconductors and Raymond C. Gatti (LBL) for his comments on fuel-pellet shelling. We thank Dr. Giovanni Vulpetti for discussions concerning the INTERFLIGHT [3] and the solar-gravity-lens mission. We thank Dr. Ken Fowler, Ralph Moir, Richard Post, and Lynda LoDestro of LLNL for discussions on various aspects of MFPS. We thank Dr. John Santarius (UW-Madison), Dr. C.R. Easton and Bill Haloulakos (McDonnell Douglas), and Norman R. Schulze for reviews and suggested new directions.

References

[1] Post, R.F.; Special Review, The Magnetic Mirror Approach to Fusion; Nucl. Fusion **27**, No. 10 (1987).

[2] MINIMARS Conceptual Design: Final Report; J.D. Lee Ed.; UCID-20773, Vol. 1, September 1986.

[4] Battin, R.H.; An Introduction to the Mathematics and Methods of Astrodynamics; New York, N.Y., American Institute of Aeronautics and Astronautics, 1987.

[3] Vulpetti, G.; Workshop for an Extra-Solar Mission: Identification, Feasibility & Planning; Technical Proposal, Rev. 1.0, November 1992.

[5] Carpenter, S.A. and Deveny, M.E.; Mirror Fusion Propulsion System (MFPS): An Option for the Space Exploration Initiative (SEI); Paper No. IAF-92-0613 presented at the 43rd Congress of the International Astronautical Federation, August 28-September 5, 1992, Washington, DC.

PROSPECTS FOR NOVEL THERMONUCLEAR AND NON-THERMONUCLEAR FUSION*

L. J. Perkins, J. H. Hammer, C. W. Hartman

Lawrence Livermore National Laboratory
PO Box 808 (L-637), Livermore, CA 94550, USA

There is growing conviction in the world fusion program that although the scientific goals may be realized at some future date, our present, conventional, approaches to DT thermonuclear fusion, both magnetic and inertial, will not lead to attractive reactor products able to compete in the energy market place of the 21st century. This is a result of the projected low power density, high complexity, large unit sizes, and very high development costs. It is our contention that any breakthrough leading to economically-viable fusion will lie in new, unexplored physics areas rather than in refined engineering concepts for the present approaches. Consequently, we have commenced studies of several novel advanced fusion concepts, with the object of identifying schemes with the potential for a step-change in our approach to fusion energy. These schemes fall into two distinct groups:

(a) Novel thermonuclear approaches: We suggest that if we are constrained by thermonuclear operation, then the most viable approach may lie in pulsed, medium to high density systems which side-step the complexity and expense of the plasma/vacuum/solid-wall/magnet interface of conventional, low-density, magnetically-confined fusion. We are investigating both magnetically-insulated schemes, and novel ignitor, high density schemes. However, we are also considering low-density fusion in a novel, coil-free configuration that may have potential for D-^{3}He operation.

(b) Non-thermonuclear approaches: We can directly trace the cost and complexity of conventional, thermonuclear fusion reactors to the constraints of a minimum required product of $n*\tau*T$ (magnetic confinement) or, equivalently, $\rho*R*T$ (inertial confinement). These requirements arise directly from the given value of the Maxwell-averaged reaction rate, $\langle\sigma v\rangle$. Therefore, we suggest that if we are to achieve a fundamental breakthrough in the physics of fusion, then the inherent limitations set by either the thermal averaging and/or by the cross-section itself must be circumvented. This is particularly true if we are ever to realize clear economic viability with the advanced fusion fuels such as D-^{3}He. Accordingly, we are studying some new, non-thermonuclear possibilities including non-thermal schemes, schemes which circumvent the Coulomb barrier, and shape-(not spin) polarized, advanced-fuel fusion. The latter may have potential for the higher-Z, deformed-nuclei fusion fuels such as p-^{11}B and p-^{7}Li.

For any such advanced physics schemes to be considered serious contenders, they must be coupled with engineering realizations in order to clearly identify the potential for a step-change in capital costs, complexity and development path relative to our present concepts.

* Work performed under the auspices of the US D.O.E by Lawrence Livermore National Laboratory under contract W-17405-ENG-48

NO PAPER RECEIVED

9) D-^{3}He Tokamak Reactor Design-I 287
R.W. Conn, Chair

9-1 Synchrotron Radiation from High-Temperature Plasmas 289
Winfried Kernbichler

9-2 Assessment of First Wall Lifetime in D-^{3}He and D-T Reactors with Impact on Reactor Availability 299
M.E. Sawan and I.N. Sviatoslavsky

9-3 Engineering Design of ARIES-III 309
D.K. Sze, C. Wong, E. Cheng, M.E. Sawan, I.N. Sviatoslavsky, J.P. Blanchard, L.A. El-Guebaly, H.Y. Khater, E.A. Mogahed, P. Gierszewski, R. Hollies, and the ARIES Team

Synchrotron Radiation from High-Temperature Plasmas

Winfried Kernbichler
Technische Universität Graż
Institut für Theoretische Physik
Petersgasse 16, A–8010 Graz, Austria

ABSTRACT

Synchrotron radiation is an important energy loss mechanism in fusion plasmas. This is especially true for either D-T or D-^{3}He plasmas under conditions relevant for future fusion devices. Many reactor studies (e.g. ARIES, APOLLO, ...) favour regimes with high average temperatures, peaked density and temperature profiles and high magnetic field strength on axis. In some cases also a low reflection coefficient at the first wall has to be used because of the choice of ceramics as first wall material. The choice of all these parameters strongly affects the role of synchrotron radiation in the overall power balance of a fusion plasma and its role in increasing the energy transport from the center to the plasma edge.

In addition to that, one in principal has the possibility to utilize synchrotron radiation for passive current drive in a tokamak. For that purpose, fish-scale like structures would be necessary at the first wall to convert the initially symmetric radiation into one with a strong asymmetric distribution to be able to drive a net current. Together with the bootstrap current this mechanism could generate an important contribution to the overall current.

The accurate computation of synchrotron radiation losses from fusion plasmas and of the pertinent energy transport mechanism from the center to the edge is thus very important for the calculation of the energy balance in reactor grade fusion plasmas.

The calculation of synchrotron radiation losses, of related transport phenomena and passive current generation includes a variety of problems: (1) Calculation of emission and absorption coefficients for a wide range of plasma parameters and frequencies; (2) calculation of current drive efficiencies; (3) solution of the radiation transport equation in non-homogeneous plasmas; (4) proper consideration of a given geometry and (5) correct inclusion of wall reflectivity and mode mixing at the first wall.

Here synchrotron radiation losses are numerically computed by solving the radiation transfer equation for different plasma configurations – cylinder, screw pinch, field-reversed configuration, tokamak.

1 SYNCHROTRON POWER LOSS FROM PLASMA SLAB OR CYLINDER

The power loss through synchrotron radiation from an inhomogeneous plasma per unit plasma volume is given as

$$P^{\pm}_{sl,cy} = \frac{8}{\ell} \int_{\omega=0}^{\infty} d\omega \int_{\theta=0}^{\pi/2} d\theta \, \sin^2\theta \int_{\phi=0}^{\pi/2} d\phi \, \cos\phi \, \left(I^{+}_{out} + I^{-}_{out}\right)_{sl,cy} , \qquad (1)$$

where $I^{\pm}_{out}$ denotes the outgoing intensity which leaves the plasma volume V (I^{+}_{out} corresponds to the intensity of the extraordinary wave and I^{-}_{out} to that of the ordinary wave).

Here, one considers two plasma geometries, an infinite (in z-direction) plane plasma slab (sl) with the thickness ℓ and infinite plasma cylinder (cy) with the radius ℓ. In general the outgoing intensity depends on the frequency, ω, the direction of the wave propagation relative to the z-direction, $\theta = \angle(\underline{k}, \underline{e}_z)$, the planar angle between the x-coordinate and the projection of the ray, $\phi = \angle(\underline{k}_\perp, \underline{e}_x)$, the magnetic field strength, $\underline{B}(r)$, the plasma temperature, $T_e(r)$, the density, $n_e(r)$, and the reflection conditions at the first wall.

The outgoing intensity can be specified as

$$
\begin{aligned}
I^{+}_{out} &= (1-\Gamma^{+}) \cdot \frac{\Gamma^{-+} d^{+} \hat{I}^{-} + (1-\Gamma^{--} d^{-}) \hat{I}^{+}}{(1-\Gamma^{++} d^{+}) \cdot (1-\Gamma^{--} d^{-}) - \Gamma^{+-} d^{-} \Gamma^{-+} d^{+}} \,, \\
I^{-}_{out} &= (1-\Gamma^{-}) \cdot \frac{\Gamma^{+-} d^{-} \hat{I}^{+} + (1-\Gamma^{++} d^{+}) \hat{I}^{-}}{(1-\Gamma^{++} d^{+}) \cdot (1-\Gamma^{--} d^{-}) - \Gamma^{+-} d^{-} \Gamma^{-+} d^{+}} \,,
\end{aligned}
\tag{2}
$$

where the indices sl and cy of $I^{\pm}_{out}$, $d^{\pm}$ and $\hat{I}^{\pm}$ are omitted for simplicity. In Eq. 2 the following definitions are used

$$
\begin{aligned}
d^{\pm}_{sl,cy} &= \exp\left(-\kappa^{\pm}_{sl,cy}(0,\ell)\right) \,, \\
\hat{I}^{\pm}_{sl,cy} &= g_{sl,cy} \int_0^{\ell} dx\, I_{bb}(x)\, \alpha^{\pm}(x) \exp\left(-\kappa^{\pm}_{sl,cy}(x,\ell)\right) \,, \\
\kappa^{\pm}_{sl,cy}(x_1,x_2) &= g_{sl,cy} \int_{x_1}^{x_2} dx\, \alpha^{\pm}(x) \,,
\end{aligned}
\tag{3}
$$

where $I_{bb}(x)$ is the black body intensity in the Rayleigh-Jeans approximation, $I_{bb}(x) \sim \omega^2 \cdot T_e(x)$, and $\alpha^{\pm}(x)$ is the absorption coefficient for synchrotron radiation. Here one can choose between different models for the absorption coefficient, e.g. (i) a model with a full description of the resonant behavior of the absorption coefficient in a sum-integral representation [1] or (ii) a model with a smooth approximation in ω [2] which is good for higher temperatures and higher wave numbers.

The geometry factors g_{sl} and g_{cy} for slab and cylinder geometry, resp., are given as

$$
g_{sl} = \frac{1}{\sin\theta \cos\phi} \,, \qquad g_{cy} = \frac{2\cos\phi}{\sin\theta} \,. \tag{4}
$$

For the reflection coefficient the following relations hold,

$$
\begin{aligned}
\Gamma^{++} &= \Gamma^{+} \cdot (1 - M^{+-}) \quad , \quad \Gamma^{+-} = \Gamma^{+} \cdot M^{+-} \,, \\
\Gamma^{--} &= \Gamma^{-} \cdot (1 - M^{-+}) \quad , \quad \Gamma^{-+} = \Gamma^{-} \cdot M^{-+} \,,
\end{aligned}
\tag{5}
$$

where Γ^{+} and Γ^{-} denote the reflection coefficient at the first wall for the extraordinary (+) and the ordinary (−) mode of propagation. M^{+-} and M^{-+} denote the mode changing factor at the first wall from the extraordinary to the ordinary mode and vice versa.

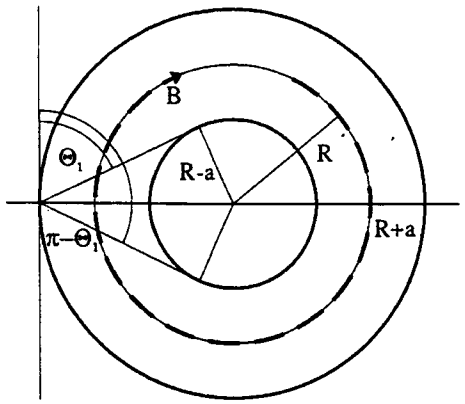


Figure 1: Tokamak model. Cut through an infinite tube.

2 POWER LOSS FROM PLASMAS WITH TOKAMAK GEOMETRY

A simple model of a toroidal plasma is given in Fig. 1. The figure shows a cut through an infinite tube consisting of an inner and an outer wall. This model has similar features as the cylindrical model, e.g. the ray balance equations can be solved analytically assuming angle conservation during the reflection at the first wall. In addition to that, this scheme of a tokamak also allows to model the 1/R dependency of the magnetic field strength. It also deals in a proper way with the fact that in a tokamak some rays pass twice through the center on their way from wall to wall. The power loss in that case is given as

$$
\begin{aligned}
P_{to}^{\pm} \;=\; & \frac{2(A+1)}{R} \int_{\omega=0}^{\infty} d\omega \int_{\phi=0}^{\pi/2} d\phi \, \cos\phi \left\{ \int_{\theta=0}^{\theta_1} d\theta \, \sin^2\theta \left(I_{ob,1}^{+} + I_{ob,1}^{-} \right)_{to} \;+ \right. \\
& + \int_{\theta=\theta_1}^{\pi/2} d\theta \, \sin^2\theta \left(I_{ob,2}^{+} + I_{ob,2}^{-} \right)_{to} \;+ \\
& \left. + \int_{\theta=0}^{\pi/2} d\theta \, \sin\theta \sqrt{1 - \left(\frac{A+1}{A-1} \right)^2 \cos^2\theta} \quad \left(I_{ib}^{+} + I_{ib}^{-} \right)_{to} \right\} .
\end{aligned}
\tag{6}
$$

Here $A = R/a$ is the aspect ratio of the tokamak, R is the major radius and $a = \ell$ is the minor radius. As shown in Figure 1, θ is the angle in the perpendicular cut of the tube, whereas ϕ gives the direction of the wave propagation relative to the z-direction, $\phi = \angle(\underline{k}, \underline{e}_z)$. The critical angle θ_1 is given as $\theta_1 = \arccos((A-1)/(A+1))$.

The difference between the tokamak model and e.g. the cylinder model of a plasma is that in the case of a tokamak you have also emission at the in-board side (denoted as I_{ib}^{-} and I_{ib}^{+}) and the emission at the out-board side has two components. For $\theta < \theta_1$ a typical ray starts and ends at the out-board side without hitting the inner wall. These intensities are denoted as $I_{ob,1}^{-} = I_{out}^{-}$ and $I_{ob,1}^{+} = I_{out}^{+}$ and can be calculated from equation 2. For $\theta \geq \theta_1$ a typical ray starts at the out-board side is reflected at the inner wall and ends at the outer wall. These intensities are denoted as $I_{ob,2}^{-}$ and $I_{ob,2}^{+}$.

The intensities I_{ib}^{+}, I_{ib}^{-}, $I_{ob,2}^{+}$ and $I_{ob,2}^{-}$ are given as

$$
\begin{aligned}
I_{ib}^{+} &= (1-\Gamma^{+})\cdot\Big\{\left(d_2^{-}d_1^{+}\Gamma^{--}\Gamma^{-+}+d_1^{+}d_2^{+}\Gamma^{-+}\Gamma^{++}\right)\hat{I}_1^{-} \\
&+ \left(1-d_1^{-}d_2^{-}\Gamma^{--^2}-d_1^{-}d_2^{+}\Gamma^{-+}\Gamma^{+-}\right)\hat{I}_1^{+} \\
&+ \left(d_1^{+}\Gamma^{-+}-d_1^{-}d_1^{+}d_2^{+}\Gamma^{-+^2}\Gamma^{+-}+d_1^{-}d_1^{+}d_2^{+}\Gamma^{--}\Gamma^{-+}\Gamma^{++}\right)\hat{I}_2^{-} \\
&+ \left(d_1^{-}d_2^{-}d_1^{+}\Gamma^{--}\Gamma^{-+}\Gamma^{+-}+d_1^{+}\Gamma^{++}-d_1^{-}d_2^{-}d_1^{+}\Gamma^{--^2}\Gamma^{++}\right)\hat{I}_2^{+}\Big\} \quad / \quad N_{to}\,, \\
I_{ib}^{-} &= (1-\Gamma^{-})\cdot\Big\{\left(1-d_2^{-}d_1^{+}\Gamma^{-+}\Gamma^{+-}-d_1^{+}d_2^{+}\Gamma^{++^2}\right)\hat{I}_1^{-} \\
&+ \left(d_1^{-}d_2^{-}\Gamma^{--}\Gamma^{+-}+d_1^{-}d_2^{+}\Gamma^{+-}\Gamma^{++}\right)\hat{I}_1^{+} \\
&+ \left(d_1^{-}\Gamma^{--}+d_1^{-}d_1^{+}d_2^{+}\Gamma^{-+}\Gamma^{+-}\Gamma^{++}-d_1^{-}d_1^{+}d_2^{+}\Gamma^{--}\Gamma^{++^2}\right)\hat{I}_2^{-} \\
&+ \left(d_1^{-}\Gamma^{+-}-d_1^{-}d_2^{-}d_1^{+}\Gamma^{-+}\Gamma^{+-^2}+d_1^{-}d_2^{-}d_1^{+}\Gamma^{--}\Gamma^{+-}\Gamma^{++}\right)\hat{I}_2^{+}\Big\} \quad / \quad N_{to}\,, \\
I_{ob,2}^{+} &= (1-\Gamma^{+})\cdot\Big\{\left(d_1^{-}d_2^{+}\Gamma^{--}\Gamma^{-+}+d_1^{+}d_2^{+}\Gamma^{-+}\Gamma^{++}\right)\hat{I}_2^{-} \\
&+ \left(1-d_1^{-}d_2^{-}\Gamma^{--^2}-d_2^{-}d_1^{+}\Gamma^{-+}\Gamma^{+-}\right)\hat{I}_2^{+} \\
&+ \left(d_2^{+}\Gamma^{-+}-d_2^{-}d_1^{+}d_2^{+}\Gamma^{-+^2}\Gamma^{+-}+d_2^{-}d_1^{+}d_2^{+}\Gamma^{--}\Gamma^{-+}\Gamma^{++}\right)\hat{I}_1^{-} \\
&+ \left(d_1^{-}d_2^{-}d_2^{+}\Gamma^{--}\Gamma^{-+}\Gamma^{+-}+d_2^{+}\Gamma^{++}-d_1^{-}d_2^{-}d_2^{+}\Gamma^{--^2}\Gamma^{++}\right)\hat{I}_1^{+}\Big\} \quad / \quad N_{to}\,, \\
I_{ob,2}^{-} &= (1-\Gamma^{-})\cdot\Big\{\left(1-d_1^{-}d_2^{+}\Gamma^{-+}\Gamma^{+-}-d_1^{+}d_2^{+}\Gamma^{++^2}\right)\hat{I}_2^{-} \\
&+ \left(d_1^{-}d_2^{-}\Gamma^{--}\Gamma^{+-}+d_2^{-}d_1^{+}\Gamma^{+-}\Gamma^{++}\right)\hat{I}_2^{+} \\
&+ \left(d_2^{-}\Gamma^{--}+d_2^{-}d_1^{+}d_2^{+}\Gamma^{-+}\Gamma^{+-}\Gamma^{++}-d_2^{-}d_1^{+}d_2^{+}\Gamma^{--}\Gamma^{++^2}\right)\hat{I}_1^{-} \\
&+ \left(d_2^{-}\Gamma^{+-}-d_1^{-}d_2^{-}d_2^{+}\Gamma^{-+}\Gamma^{+-^2}+d_1^{-}d_2^{-}d_2^{+}\Gamma^{--}\Gamma^{+-}\Gamma^{++}\right)\hat{I}_1^{+}\Big\} \quad / \quad N_{to}\,,
\end{aligned}
\tag{7}
$$

with the denominator

$$
\begin{aligned}
N_{to} &= 1-d_1^{-}d_2^{-}\Gamma^{--^2}-d_2^{-}d_1^{+}\Gamma^{-+}\Gamma^{+-}-d_1^{-}d_2^{+}\Gamma^{-+}\Gamma^{+-}+d_1^{-}d_2^{-}d_1^{+}d_2^{+}\Gamma^{-+^2}\Gamma^{+-^2} \\
&- 2d_1^{-}d_2^{-}d_1^{+}d_2^{+}\Gamma^{--}\Gamma^{-+}\Gamma^{+-}\Gamma^{++}-d_1^{+}d_2^{+}\Gamma^{++^2}+d_1^{-}d_2^{-}d_1^{+}d_2^{+}\Gamma^{--^2}\Gamma^{++^2}\,.
\end{aligned}
\tag{8}
$$

Without mode mixing at the first wall the relations for the intensities are simplified to

$$
I_{ib}^{+}=(1-\Gamma^{+})\cdot\frac{\hat{I}_1^{+}+d_1^{+}\Gamma^{++}\hat{I}_2^{+}}{1-d_1^{+}d_2^{+}\Gamma^{++^2}}\quad,\quad I_{ob,2}^{+}=(1-\Gamma^{+})\cdot\frac{d_2^{+}\Gamma^{++}\hat{I}_1^{+}+\hat{I}_2^{+}}{1-d_1^{+}d_2^{+}\Gamma^{++^2}}
$$

$$I_{ib}^{-} = (1-\Gamma^{-}) \cdot \frac{\hat{I}_1^{-} + d_1^{-}\Gamma^{--}\hat{I}_2^{-}}{1 - d_1^{-}d_2^{-}\Gamma^{--2}} \quad , \quad I_{ob,2}^{-} = (1-\Gamma^{-}) \cdot \frac{d_2^{-}\Gamma^{--}\hat{I}_1^{-} + \hat{I}_2^{-}}{1 - d_1^{-}d_2^{-}\Gamma^{--2}} \,. \tag{9}$$

The definitions given in Eq. 2 for $d^{\pm}$, $\hat{I}^{\pm}$ and $\kappa^{\pm}$ can be used by replacing the indices *sl* or *cy* with the index *to* using the following definition for the geometry factor

$$g_{to} = F \cdot \frac{\sin\theta}{\cos\phi} \,, \tag{10}$$

with

$$F = (A+1) \cdot \begin{cases} 2 & \text{for } \sin\theta \le \sin\theta_1 \\ 1 - \sqrt{1 - \frac{4A}{(A+1)^2 \sin^2\theta}} & \text{for } \sin\theta > \sin\theta_1 \end{cases} \tag{11}$$

The indices 1 and 2 in Eq. 7 and 9 stand for ray passes from the outer side to the inner side of the tube and vice versa.

3 PROFILES

The radius r as a function of the integration variable x has to be defined differently for slab and cylinder geometry

$$r_{cy}(x) = \sqrt{\ell^2 - 4x(l-x)\cdot\cos^2\phi} \,, \qquad r_{sl}(x) = 2 \cdot \left| \frac{\ell}{2} - x \right| . \tag{12}$$

In the case of the tokamak the radius ρ is counted from the center of the device and is given as a function of x as

$$\begin{aligned} \rho(x) &= \sqrt{(xF\sin\theta)^2 + (R+a)^2 - 2x(R+a)F\sin^2\theta} \\ r_{to}(x) &= |R - \rho(x)| \,. \end{aligned} \tag{13}$$

Parabolic Profiles: In this case parabolic profiles are used for the radial dependency of temperature and density. The magnetic field strength is varied along the radius according to the diamagnetic effect of the plasma pressure.

$$\begin{aligned} T_e(r) &= <T_e> (\alpha_T + 1) \cdot \frac{1 + (q_T - 1)\left[1 - (r/\ell)^2\right]^{\alpha_T}}{\alpha_T + q_T} \,, \\ n_e(r) &= <n_e> (\alpha_n + 1) \cdot \frac{1 + (q_n - 1)\left[1 - (r/\ell)^2\right]^{\alpha_n}}{\alpha_n + q_n} \,, \\ B_z(r) &= B_0 \cdot \sqrt{1 - f(r) <\beta>} \,, \end{aligned} \tag{14}$$

with

$$f(r) = \frac{\left\{1 + (q_n - 1)\cdot\left[1 - (r/\ell)^2\right]^{\alpha_n}\right\} \cdot \left\{1 + (q_T - 1)\cdot\left[1 - (r/\ell)^2\right]^{\alpha_T}\right\}}{1 + (q_n - 1)/(\alpha_n + 1) + (q_T - 1)/(\alpha_T + 1) + (q_n - 1)(q_T - 1)/(\alpha_n + \alpha_T + 1)} \,, \tag{15}$$

$$<\beta> \;\le\; \frac{1 + (q_n - 1)/(\alpha_n + 1) + (q_T - 1)/(\alpha_T + 1) + (q_n - 1)(q_T - 1)/(\alpha_n + \alpha_T + 1)}{q_n q_T} \,.$$

Here $< T_e >$ and $< n_e >$ are the mean electron temperature and the mean electron density, respectively, and B_0 is the external magnetic field strength. The parameters α_n and α_T define the steepness of the profiles, whereas the parameters q_n and q_T give the ratio of the maximum to the edge value of $n_e(r)$ and $T_e(r)$, respectively.

In the case of the tokamak the relation for the magnetic field must be rewritten as

$$B(\rho) = B_0 \cdot \frac{R}{\rho} \cdot \sqrt{1 - f(r) <\beta>} \,. \tag{16}$$

The angle $\hat{\theta}$ between the ray and the direction of the magnetic field lines is specified as

$$\hat{\theta} = \begin{cases} \theta - \alpha & \text{for } \theta \leq \pi/2 \\ \\ \pi - \theta - \alpha & \text{for } \theta > \pi/2 \end{cases} \tag{17}$$

with

$$\sin\alpha = \frac{s_\perp}{\rho} \cdot \cos\theta \quad , \quad s_\perp = xF \sin\theta \tag{18}$$

Screw Pinch: To simulate the poloidal field component, e.g. in a tokamak, the following relation is introduced for the poloidal field strength $B_p(r)$,

$$B_p(r) = B_z(r) \cdot g(r/\ell) \quad , \quad g(r/\ell) = \frac{1}{A} \cdot \frac{r/\ell}{1 + (q_{edge} - 1)(r/\ell)^2} \,, \tag{19}$$

where A is the Aspect Ratio and q_{edge} is the safety factor on edge.

With that, the total field strength is given as

$$B(r) = \sqrt{B_z^2(r) + B_p^2(r)} = B_z(r) \cdot \sqrt{1 + g(r/\ell)} \,, \tag{20}$$

and the angle $\hat{\theta}$ between the ray and the direction of the magnetic field lines is specified as

$$\cos\hat{\theta}(r) = \frac{\underline{k} \cdot \underline{B}(r)}{B(r)} = \frac{\cos\theta - g(r/\ell)\sin\phi\sin\theta}{\sqrt{1 + g(r/\ell)}} \,. \tag{21}$$

Field-Reversed Configuration: One can learn from experiments that in field-reversed configurations (FRCs) the radial dependency of $T_e(r)$, $n_e(r)$ and $B_z(r)$ is very well represented by

$$\begin{aligned} T_e(r) &= <T_e> \,, \\ n_e(r) &= <n_e> \,/\, <\beta> \cdot \frac{1}{\cosh^2\left[k_f \cdot \left((r/r_{maj})^2 - 1\right)\right]} \,, \\ B_z(r) &= B_0 \cdot \tanh\left[k_f \cdot \left((r/r_{maj})^2 - 1\right)\right] \,, \end{aligned} \tag{22}$$

Table 1: Basic parameter set

Symbol	Dimension	Value	Symbol	Dimension	Value
ℓ	$[m]$	1.0	α_n	$[-]$	1.0
B_0	$[Tesla]$	10.0	α_T	$[-]$	1.0
$<\beta>$	$[-]$	0.05	q_n	$[-]$	100.
$1/A$	$[-]$	0.2	q_T	$[-]$	100.
q_{edge}	$[-]$	3.0	Γ^-	$[-]$	0.95
k_f	$[-]$	1.0	Γ^+	$[-]$	0.95
$<n_e>$	$[10^{20}m^{-3}]$	1.0	M^{-+}	$[-]$	0.0
$<T_e>$	$[keV]$	20.0	M^{+-}	$[-]$	0.0

with the following definitions for the major radius r_{maj}, the reversal factor k_f, the average β, the maximum field strength within the separatrix B_{max}, the maximum electron density $n_{e,max}$ and the radius of the wall r_w

$$\begin{aligned} r_{maj} = r_{sep}/\sqrt{2} \quad &, \quad |B_{max}| = B_0 \cdot \tanh k_f \,, \\ k_f = \operatorname{artanh}\left[|B_{max}|\,/B_0\right] \quad &, \quad n_{e,max} = <n_e> \,/\, <\beta> \,, \\ <\beta> = (\tanh k_f)/k_f \quad &, \quad r_w = r_{sep}/\sqrt{2(1-<\beta>)}\,. \end{aligned} \tag{23}$$

Here r_{sep} is the separatrix radius which is to be associated with the parameter ℓ and B_0 is the value of the external field strength.

4 RESULTS

In the following some results for the spectrum and the power loss are given. For each plot one or two parameters are varied whereas the others are kept constant at their basic value specified in Table 1. If not specified otherwise calculations are done for cylinder geometry and magnetic field strength corrections according to the diamagnetic effect, Eq. 14 and 15.

Parabolic Profiles: In Figure 2 results are given for the outgoing intensity (sum of ordinary and extraordinary mode of propagation) as a function of the wave number $\overline{\omega}$. Figure 3 shows the synchrotron power loss as a function of $<\beta>$ and the profile parameters. It is shown how the outgoing intensity and the power loss are decreased for increasing values of the magnetic field utilization factor $<\beta>$ which is due to the fact that the diamagnetic effect reduces the magnetic field strength in the center where $n_e(r)$ and $T_e(r)$ are high. Numerical results also show the approximate $B^{5/2}$-dependency and that the spectrum is shifted to higher frequencies for increasing values of the magnetic field strengths.

Figures 2 and 3 show the influence of the profile parameters on the spectrum and the power loss. The influence of α_n is more moderate and the maximum of the spectrum is kept at approximately the same location. The influence of α_T is much more pronounced, shifting the maximum of the spectrum to higher wave numbers for increasing α_T and increasing the overall loss power.

The approximate $n_e^{1/2}$-dependency and the approximate $T_e^{5/2}$-dependency is also numerically confirmed for non-homogeneous plasmas. The overall $(1-\Gamma)^{1/2}$-dependency of the power loss

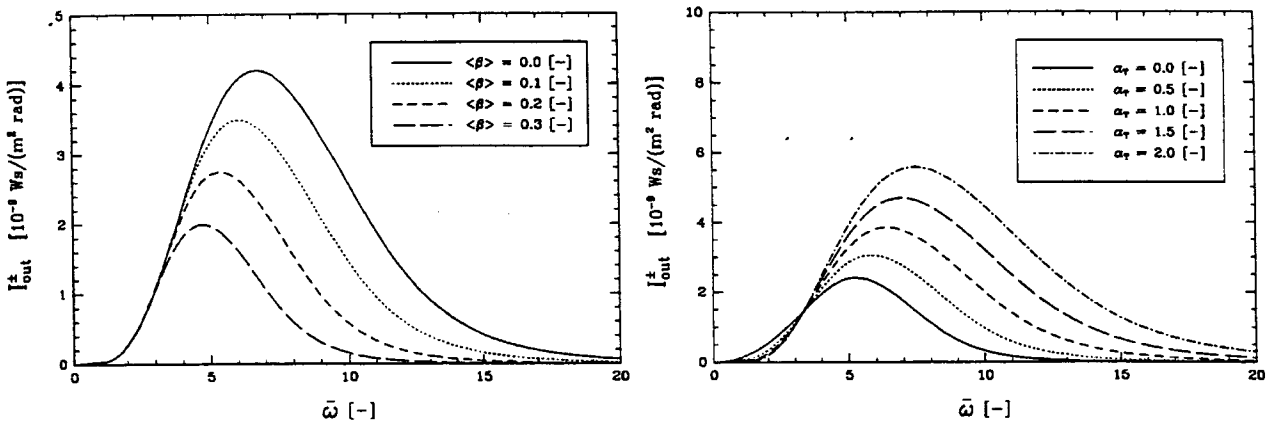


Figure 2: Intensity of synchrotron radiation versus wave number for a non-homogeneous cylindrical plasma with parabolic profiles.

is also reproduced numerically. The values of the mode changing parameters clearly change the contributions of the ordinary and extraordinary mode to the overall loss but only in the case of $M^{+-} > 0$ the sum of both modes is affected more than a few percent.

Tokamak: The left picture in Fig. 4 shows the power loss from three different geometries as a function of the profile parameters, whereas the right picture shows the influence of the inverse aspect ratio on the power loss. In general, it must be noted that the power loss per unit volume increases with decreasing aspect ratio A. This effect is less pronounced for steep temperature profiles.

Screw-pinch: The influence of the inverse aspect ratio $1/A$ and the safety factor on edge q_{edge} on the results is only very small. This is due to the fact that for the chosen parameter range the poloidal field component is much less than the field component in z-direction. This would change only for much higher values of the poloidal field strength.

Field-reversed configuration: Figure 5 shows the influence of the reversal factor k_f on the spectrum and on the power loss. It should be noted here (i) that the maximum of the spectrum is shifted very little with changing k_f, (ii) that the power loss is increased monotonically with increasing values of k_f for all values of interest, and (iii) that the power loss is much less compared to cases with parabolic profiles because of the high $<\beta>$-values of FRCs.

ACKNOWLEDGEMENT

The research work was supported by the Austrian Academy of Sciences, the Department of Science and Research of Austria under Grant No. GZ. 77.781/2-25/91, the Styrian Government and the International Atomic Energy Agency. The author takes pleasure in acknowledging informative discussions with Sergei Kasilov and Gerolf Heinrichs.

REFERENCES

[1] A. Nassri and M. Heindler, Phys. Fluids **29**, 3275 (1986).

[2] J.D. Gordon, et al., Fusion Reactor Engineering – Evaluation of Proton-Based Fuels for Fusion Power Plants, TRW-FRE-007 (1981).

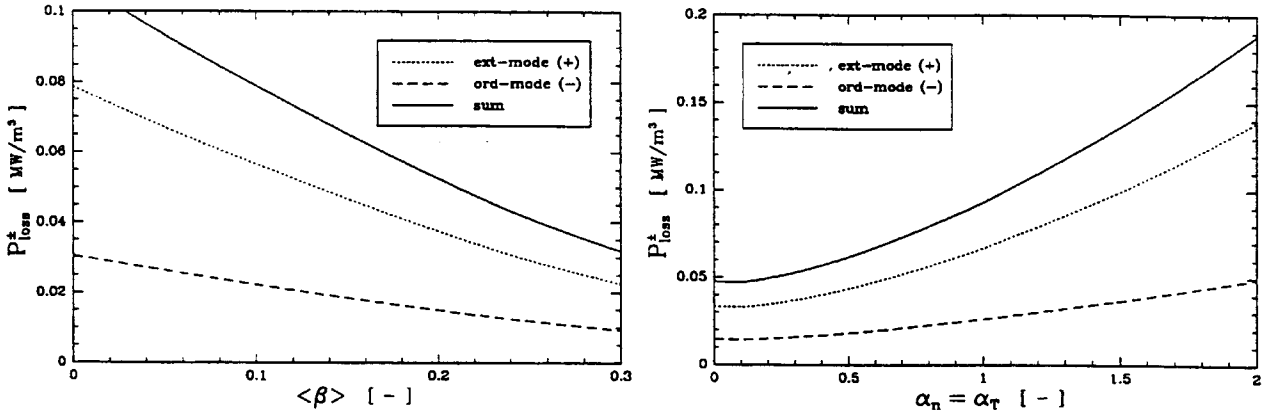


Figure 3: Synchrotron power loss versus $<\beta>$ and versus $\alpha_T = \alpha_n$, resp., for a non-homogeneous plasma with parabolic profiles.

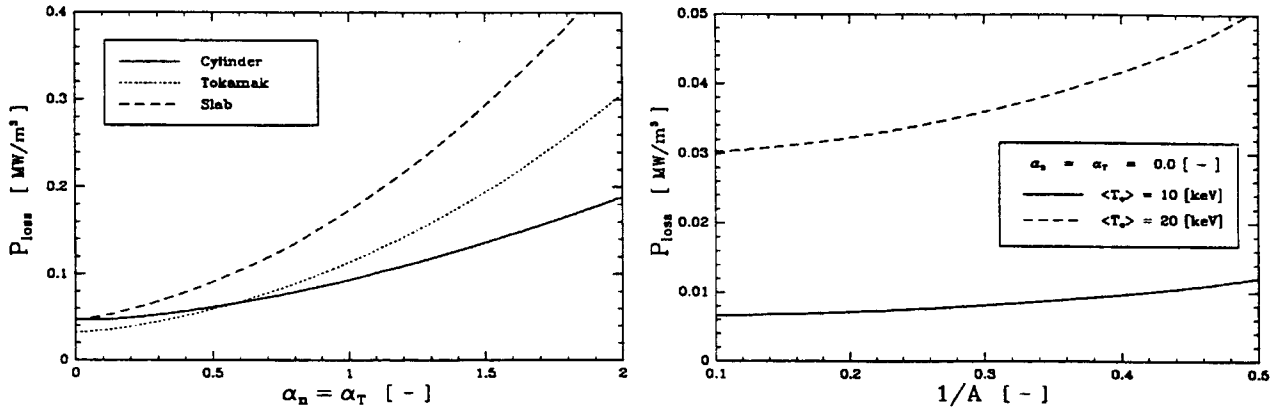


Figure 4: Comparison between cylinder, tokamak and slab results (left). Power loss as a function of 1/A for a homogeneous plasma (right).

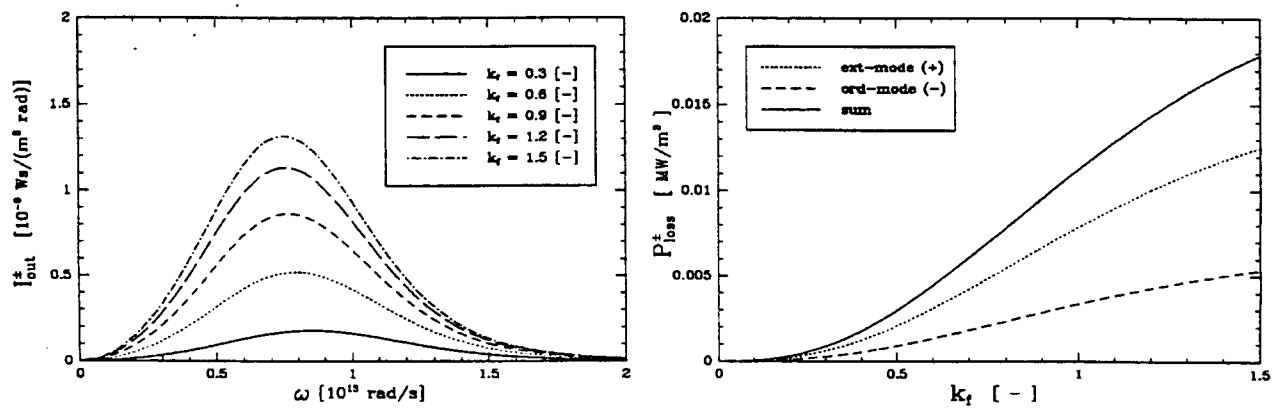


Figure 5: Intensity of synchrotron radiation versus wave number and synchrotron power loss versus k_f for a non-homogeneous plasma with FRC profiles.

Assessment of First Wall Lifetime in D-^{3}He and D-T Reactors With Impact on Reactor Availability

M. E. Sawan and I. N. Sviatoslavsky
Fusion Technology Institute
The University of Wisconsin
Madison, Wisconsin 53706

ABSTRACT

The neutron yield in a D-^{3}He reactor is much lower than that in a D-T reactor of equivalent power. As a result, the rate of neutron damage and gas production in the first wall of D-^{3}He reactors is lower than that in a D-T reactor by more than an order of magnitude. The different candidate structural materials proposed for use in commercial fusion reactors will last the whole reactor lifetime of 30 FPY in a D-^{3}He reactor. On the other hand, frequent replacement of the first wall and blanket is required during the lifetime of a D-T power reactor. The blanket modules might require up to 30 replacements depending on the structural material used and the maximum allowable damage level. The down time required for replacement of first wall and blanket in a D-T reactor will impact the reactor availability and consequently the cost of electricity. It appears that a D-^{3}He reactor should have a 10% advantage in availability over a D-T reactor.

1. INTRODUCTION

In a tokamak fusion power reactor utilizing the D-^{3}He fuel cycle, only a small fraction of the fusion power (~5%) is carried by neutrons. About 65% of these neutrons are 2.45 MeV neutrons produced from DD reactions and the rest are 14.1 MeV DT neutrons. This compares to the case of DT fusion reactors where 80% of the fusion power is carried by 14.1 MeV neutrons. Hence, the neutron wall loading at the first wall of a D-^{3}He reactor is much lower than that in a D-T reactor of equivalent power. On the other hand, the peak surface heat flux in the first wall of a D-^{3}He reactor is relatively high (~2 MW/m^2). This places a premium on the design of the first wall which should be capable of removing the high surface heat without exceeding temperature and stress limits. As a result of the lower neutron wall loading, the rate of neutron damage and gas production in the first wall of D-^{3}He reactors is lower than that in a D-T reactor by more than an order of magnitude. The first wall lifetime is determined primarily by neutron damage and gas production rates. In this paper, peak damage and gas production rates are determined for different structural materials exposed to the nuclear environment of both D-T and D-^{3}He commercial power reactors [1,2,3]. The structural materials considered include the austenitic steel alloy 316 SS, the ferritic steel alloy HT-9, the vanadium alloy V5Cr5Ti and the SiC composite. The need for first wall and blanket replacement during the commercial reactor lifetime of about 30 Full Power Years (FPY) will be assessed. The down time required for replacement of first wall and blanket in a D-T reactor will impact the reactor availability and consequently the cost of electricity. An attempt to quantify the impact on availability will be made for reactors using the four structural materials.

2. CALCULATIONAL PROCEDURE

Neutronics calculations have been performed to determine the peak damage and gas production rates in the first wall for fusion power reactors utilizing the D-T and D-^{3}He fuel cycles.

The one-dimensional discrete ordinates code ONEDANT [4] was used with nuclear data based on the ENDF/B-V evaluation. The model used for D-T reactors included a first wall made of a 4-mm-thick coolant layer sandwiched between two 3-mm-thick structural plates. The first wall is backed by a 50-cm-thick blanket zone. The blanket composition affects neutron reflection and, hence, impacts the damage parameters in the first wall. Different blanket concepts are used for the four structural materials considered. For 316 SS, a $Li_2O/Be/H_2O/SS$ blanket concept is used. For HT-9 structure, a self-cooled LiPb blanket is considered. A self-cooled Li/V blanket is used for the case with V5Cr5Ti first wall. In the case where SiC structure is used, a $Li_2O/Be/He/SiC$ blanket concept is used. In D-^{3}He reactors a high synchrotron radiation power is produced and a reflective first wall coating is needed to reflect most of this energy back into the plasma. The model used in this analysis utilizes a 1.5-mm-thick Be coating. The first wall configuration is similar to that used in the model for D-T reactors. Since tritium breeding is not needed in D-^{3}He reactors, the blanket used behind the first wall in the model for D-T reactors is replaced by a shield made of the first wall structural material with 20% coolant. Helium gas is used as coolant in the SiC case and water is utilized in the other cases.

The toroidal effect and neutron source profile in a tokamak result in the peak neutron wall loading occurring in the outboard region at midplane. To first order, the first wall damage scales with the neutron wall loading. Commercial D-T fusion reactors are expected to have average and peak neutron wall loadings around 3 and 5 MW/m^2, respectively [1]. The neutronics results obtained for D-T reactors are scaled to a neutron wall loading of 5 MW/m^2 to determine the expected peak first wall damage and gas production rates. The fraction of fusion power carried by neutrons in a D-^{3}He reactor depends on temperature and D-^{3}He mix ratio. The average and peak neutron wall loadings in commercial D-^{3}He fusion reactors, with equivalent net electric power, are expected to be around 0.1 and 0.15 MW/m^2, respectively [2,3]. About 75% of the neutron power is carried by 14.1 MeV DT neutrons with the rest being carried by 2.45 MeV DD neutrons. The energy spectrum of the neutron source used in the calculations reflects this mix of DT and DD neutrons. The results are normalized to a neutron wall loading of 0.15 MW/m^2 to determine the expected peak first wall damage and gas production rates.

The impact of blanket replacement on a fusion reactor availability is very design dependent and extremely complex. Since there are no fusion reactors on which we can base the experience, we must rely on data available from fission reactors and make a qualitative assessment to determine the penalty of blanket replacement on reactor availability. A 1976 study by McDonnell Douglas [5] was the first to signal that blanket replacements in fusion reactors will be very difficult and time consuming. For example, they estimated the time to replace a single blanket sector in UWMAK-I [6] at 115 days, UWMAK-III [7] at 48 days and the CULHAM MARK II [8] reactor at 35 days. A more recent study at AEA Fusion (Culham Laboratory) [9] estimated the replacement time required for 16 blanket sectors in a single null fusion reactor design of the ITER type. The lifetime of the divertor plates was 2 calendar years. The reactor unavailability due to blanket replacement was 20% and that of divertor plate replacement was 9%. Since some of the work for both goes in parallel, the overall impact on availability was 25%. The conventional and auxiliary plant unavailability of 13% also goes in parallel with the 25% and thus is not additive. However, the unplanned unavailability of 7% is additive and brings the total to 32%, resulting in an overall availability of 68%. It should be pointed out that the irreducible unavailability, even with no blanket replacement is 20% which is made up of auxiliary plant maintenance of 13% with parallel divertor replacement and the unplanned unavailability of 7%. We are using this study as the basis for determining the impact of blanket replacement on reactor availability.

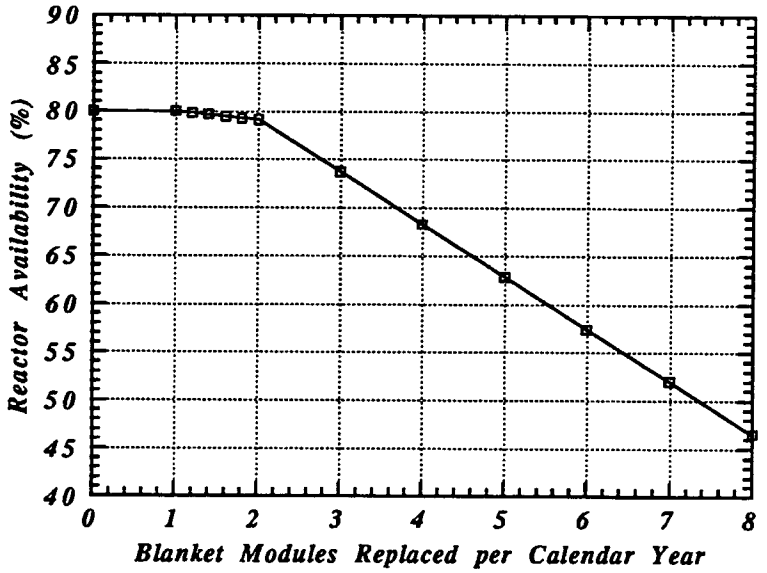


Fig. 1. Reactor availability as a function of number of blanket modules replaced per year.

The planned unavailability of 25% for replacing four blanket sectors and one half of the divertor plates per year is equal to 91 days. Of these, 12 days are needed for pre and post replacement preparation which is the same regardless of how many sectors are replaced. This involves reactor shutdown, cool down, draining of coolants, bringing up the reactor to normal pressure, moving in needed maintenance equipment, opening up the vacuum chamber, and the reverse of these functions upon completion of blanket/divertor replacement. From this we obtain the time needed for replacement of a single blanket sector at 474 hours or 19.75 days. Notice that this replacement time is much shorter than estimated by the early McDonnell Douglas study [5]. Figure 1 shows the overall reactor availability as a function of the number of blanket sectors replaced per calendar year. It is assumed that the replacement frequency for the divertor is proportional to that for the blanket. Note that replacement of a single blanket sector per year draws no penalty, since the time needed to accomplish this (~9%) is within the 13% allocated for auxiliary plant maintenance. The impact is minimal at 2 sectors (79.1%) and decreases linearly to 46% for 8 sector replacements per year. Note that the 4 replacements gives the 68% availability arrived at by the study [9]. This methodology will be used to determine the impact on reactor availability for the aforementioned 4 reactor designs.

3. FIRST WALL LIFETIME

The useful lifetime of the structural material in a fusion reactor is determined by the requirement that its structural integrity be preserved. Different indicators influence the lifetime of different structural materials. For metallic structural materials, the key indicators are swelling and embrittlement. The main concerns for SiC are the effects of irradiation on dimensional changes and fracture toughness as well as the burnup of the SiC molecules. The two parameters that have the most impact on the lifetime indicators are the dpa level and amount of helium generated. In addition hydrogen production affects structural material burnup.

Table 1. Peak Damage and Gas Production Rates in D-T or the D-^{3}He reactors for the Different Structural Materials

	dpa/FPY		He appm/FPY		H appm/FPY	
	D-T	D-^{3}He	D-T	D-^{3}He	D-T	D-^{3}He
316 SS	51	2.20	882	19.6	3435	80.8
HT-9	90	2.16	750	16.6	2419	54.6
V5Cr5Ti	51	2.36	320	7.1	1533	33.5
SiC	49	3.45	7070	149.1	2626	57.1

The peak dpa, helium production and hydrogen production rates have been determined for the 316 SS, HT-9, V5Cr5Ti and SiC structural materials when used in commercial power reactors utilizing either the D-T or the D-^{3}He fuel cycles. The results are given in Table 1. The relatively high dpa rate for HT-9 in the D-T reactor is attributed to the neutron multiplication and reflection from the lead used in the LiPb self-cooled blanket. The very large helium production rate in SiC results from the (n,3α) reactions in C. It is clear from the results that the lower yield and softer spectrum of neutrons emanating from the D-^{3}He plasma result in significant reduction in damage and gas production rates in the structural materials. Larger reduction is obtained in the gas production rates which result from high energy threshold reactions. This is demonstrated by comparing the contributions from the high energy DT neutron components to the damage and gas production rates in the D-^{3}He reactor as shown in Figure 2. While the DT source neutrons represent only 35% of the source neutrons, they are responsible for almost all of the gas production. The contribution of DT source neutrons to the dpa rate is less than their contribution to the neutron wall loading (75%). This is due to the larger number of low energy DD neutrons that can still produce atomic displacements. The helium to dpa ratio is given in Figure 3 for the candidate structural materials in D-T and D-^{3}He reactors. The ratio is lower in D-^{3}He reactors due to the softer neutron energy spectrum.

Unfortunately, there is relatively little information on effects of neutron irradiation on the structural materials at levels expected in commercial fusion reactors. Hence, no well defined damage parameter limits are available for useful lifetime determination. For this reason, the expected lifetimes for the candidate structural materials are given in Figure 4 as a function of the dpa limit. It is clear that even at the lower dpa limit of 100 dpa, all structural materials are expected to survive for the whole D-^{3}He reactor lifetime of 30 FPY. On the other hand, frequent first wall and blanket change outs will be required in a D-T reactor. Each blanket module has to be replaced about 15 times over the reactor lifetime if the dpa limit is 100 dpa with 12 more replacements needed for a self-cooled LiPb/HT-9 blanket. For SiC structural material, the parameter that limits the useful lifetime is expected to be the burnup of SiC molecules. The burnup rate is determined for SiC in both D-T and D-^{3}He reactors. The expected first wall lifetime is given in Figure 5 as a function of maximum allowed burnup fraction. It is clear that significant enhancement of SiC lifetime is achieved in a D-^{3}He reactor. The lifetime enhancement is more pronounced here compared to cases where atomic displacement is the lifetime limiting parameter. Even for the low burnup limit of 1%, SiC first walls are lifetime components in D-^{3}He reactors. Several replacements will be required in D-T reactors with the blanket change out frequency depending on the burnup limit.

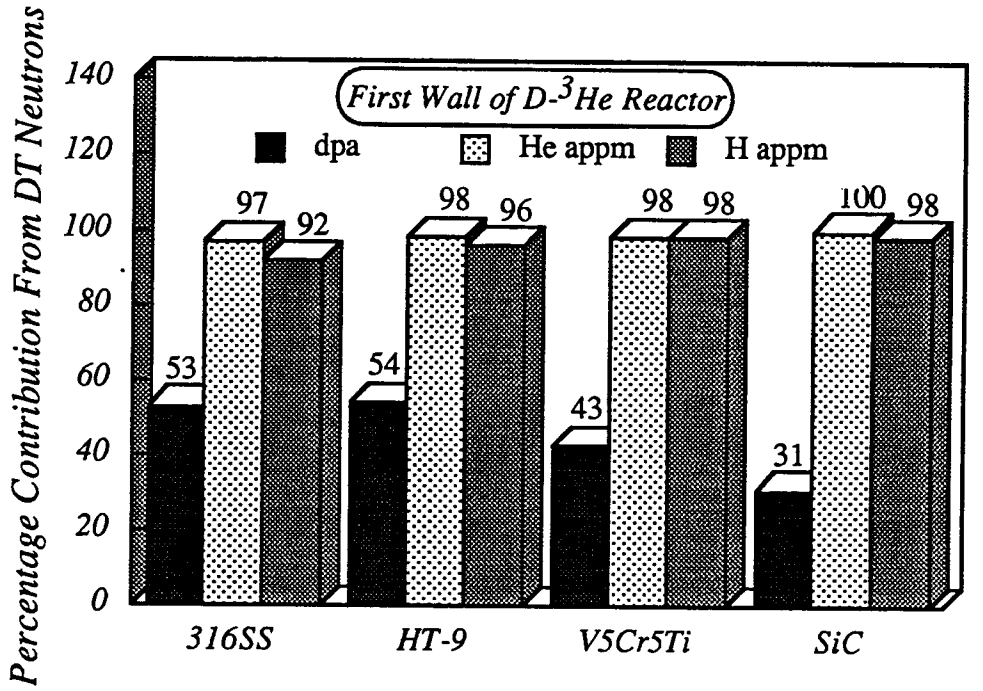


Fig. 2. DT neutron contribution to the damage and gas production rates.

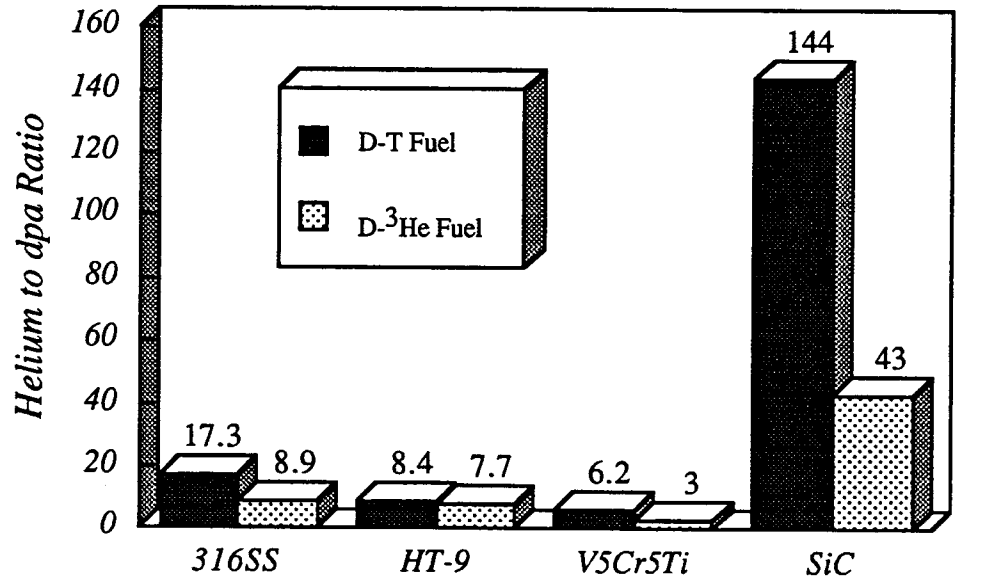


Fig. 3. Helium to dpa ratio for the candidate structural materials in D-T and D-^{3}He reactors.

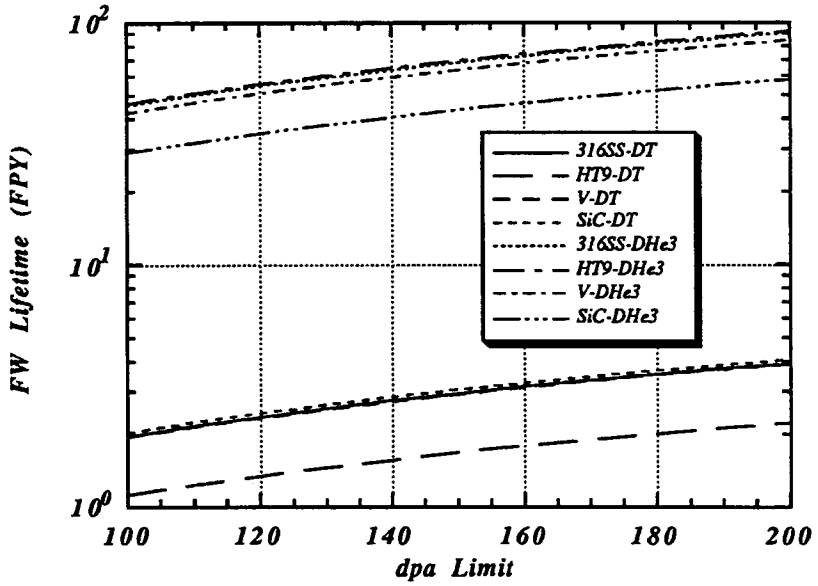


Fig. 4. Expected lifetime for the candidate structural materials as a function of the dpa limit.

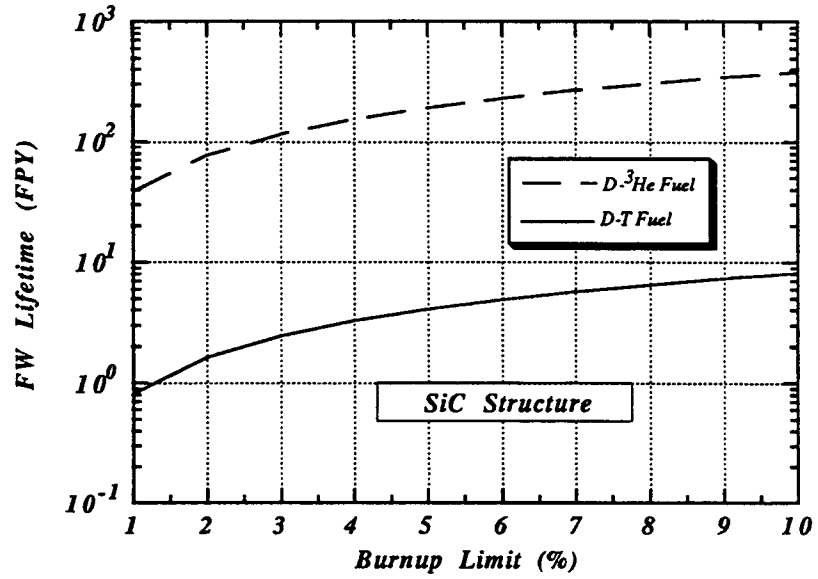


Fig. 5. Expected SiC first wall lifetime as a function of maximum allowed burnup fraction.

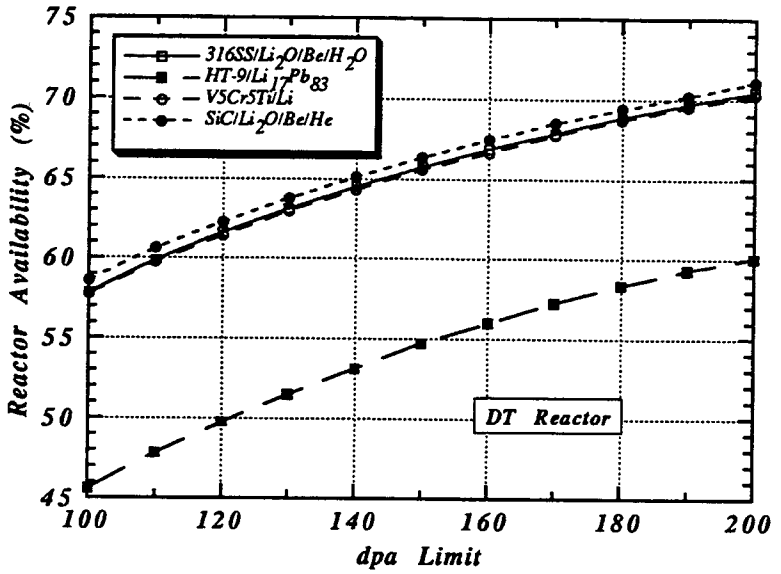


Fig. 6. Availability as a function of dpa limit for the four reactor designs.

4. IMPACT ON REACTOR AVAILABILITY

The methodology described in Section 2 has been applied to determine the impact on availability for the four candidate designs, SiC He-cooled solid breeder (ARIES-I), 316 SS water-cooled solid breeder, Vanadium alloy self-cooled Li, and HT-9 self-cooled LiPb. Because the dpa limit for these materials is still not well known, the availability is determined as a function of dpa limit from 100 to 200. Since the dpa rate is given per FPY, the problem is solved iteratively until a convergence occurs with the number of sectors to be replaced per calendar year consistent with the availability. Fig. 6 shows the availability as a function of dpa limit for the four reactor designs. The common assumptions in this exercise is that the reactors have 20 blanket sectors and all have the same level of difficulty for replacement. Figure 6 demonstrates the structural/breeder/coolant materials effect on the dpa and directly on availability. The reactors utilizing SiC, 316 SS and V are bunched together, ranging in availability from 58% to 71%, while the ferritic steel (FS) reactor is somewhat lower at 45% to 60%. This appears to penalize FS, but in matter of fact has nothing to do with the structural materials, and is due to neutron multiplication in the LiPb. Figure 7 shows the availability of a SiC structure/He cooling/solid breeder and a generic metallic structure in a Li self-cooled configuration as a function of dpa limit. The SiC is better than the metallic structure by only one percentage point along the whole curve. At 200 dpa limit, the SiC blanket achieves an availability of 71%, whereas the ARIES I reactor design assumed 76%.

In Figure 8, the reactor availability is shown as a function of the SiC burnup fraction limit from 0 to 10%. For a fractional burnup limit of 5% the availability is 71%. It is ludicrous to imagine that any material could maintain reasonable structural integrity with 5% of its atoms destroyed. A more likely value would be 2-3% making the availability in the range of 54%-63%.

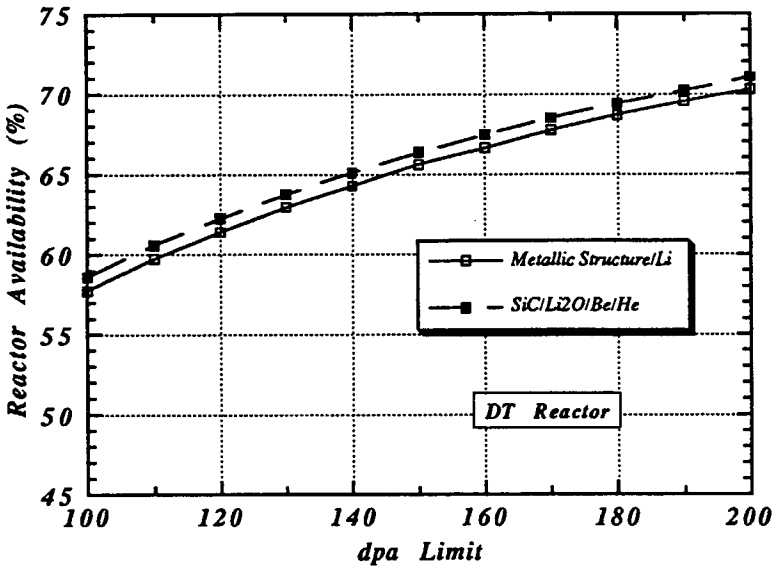


Fig. 7. Availability of a SiC structure and a generic metallic structure in a Li self-cooled configuration as a function of dpa limit.

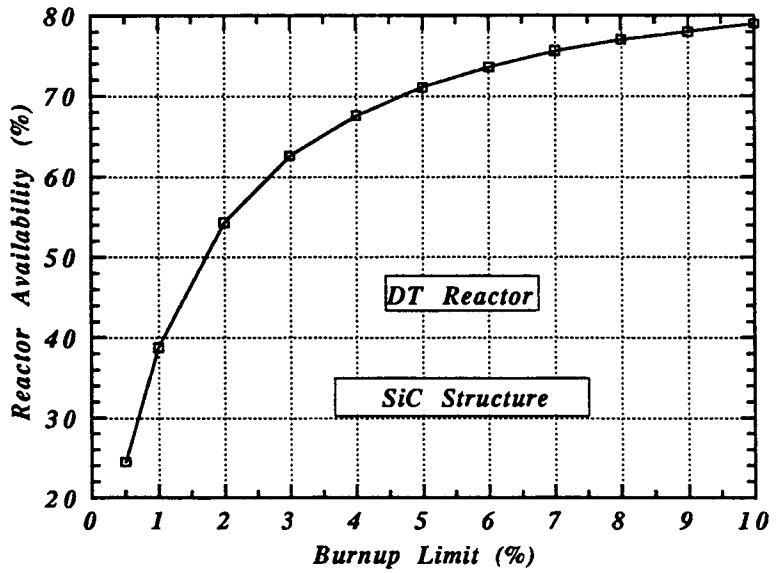


Fig. 8. Reactor availability as a function of the SiC burnup fraction limit.

Here the value of D-^{3}He becomes obvious. Figure 4 shows that even at a dpa limit of 100, all the reactor designs achieve a lifetime of 30 FPY, which is 37.5 calendar years at 80% availability. This means that no blanket sectors need to be replaced due to radiation effects for the entire lifetime of the reactor. Statements have been made that disruptions in the higher current carrying D-^{3}He reactors will have serious consequences for the reactor first wall and may consequently necessitate shield sector replacement. However, it should be recalled that since no tritium breeding is needed in a D-^{3}He reactor, the first wall and shield could be made structurally massive to be capable of withstanding very high electro-mechanical forces. Furthermore, recent Russian experiments [10] have shown that vapor shielding has an effect of more than an order of magnitude higher than had been originally assumed, reducing the consequences of high surface heat loads due to the thermal dump of a disruption. In situ recoating with Be of first wall elements can also be envisaged.

Finally, it can be seen from Fig. 1, that up to two blanket sectors can be replaced per calendar year while maintaining a 79-80% availability. From this we can infer that a D-^{3}He reactor can achieve an availability on the order of 80% even if all the divertor plates are replaced every two years and up to two shield sectors are replaced per year. It is important that this fact be recognized and factored into the COE (cost of electricity).

5. CONCLUSIONS

The reduced neutron yield and softer neutron energy spectrum results in neutron wall loadings at the first wall of a D-^{3}He reactor that are much lower than those in a D-T reactor of equivalent power. As a result, the rate of neutron damage and gas production in the first wall of D-^{3}He reactors is lower than that in a D-T reactor by more than an order of magnitude. Damage and gas production calculations for the different candidate structural materials proposed for use in commercial fusion reactors predict that the first wall and shield in a D-^{3}He reactor will last the whole reactor lifetime of 30 FPY. On the other hand, frequent replacement of the first wall and blanket is required during the lifetime of a D-T power reactor. Each module may require up to 30 replacements depending on the structural material used and the maximum allowable damage level. This is a major advantage for a D-^{3}He reactor compared to a D-T reactor, where the difficult task of remotely replacing highly radioactive reactor-core components must be performed. Qualitatively, it appears that a D-^{3}He reactor under pessimistic assumptions should have a 10% advantage in availability over a DT reactor using the most optimistic assumptions. An irreducible value of 20% unavailability is needed due to balance of plant maintenance and unscheduled outages. This implies an availability of 80% for D-^{3}He reactors and 70% for D-T reactors. A 3% fractional burnup limit in a SiC material dictates an availability of only 63%.

REFERENCES

[1] R. O'Dell et al., "Users Manual for ONEDANT: A Code Package for One-Dimensional, Diffusion-Accelerated, Neutral Particle Transport," Los Alamos National Laboratory, LA-9184-M (1982).

[2] F. Najmabadi et al., "The ARIES-II and ARIES-IV Second Stability Tokamak Reactors," Fusion Technology, **21**, 1721 (1992)

[3] F. Najmabadi et al., "The ARIES-III D-^{3}He Tokamak Reactor Study - Final Report," University of California, Los Angeles, UCLA-PPG-1384 (1992).

[4] G.L. Kulcinski et al., "Summary of Apollo, A D-^{3}He Tokamak Reactor Design, *Fusion Technology*, **21**, 2292 (1992).

[5] H.S. Zahn, "Developing Maintainability for Tokamak Fusion Power Systems," McDonnell Douglas Astronautics Co., St. Louis, COO-4184-4 (1977).

[6] B. Badger et al., "UWMAK-I, A Wisconsin Toroidal Fusion Reactor Design," University of Wisconsin, Madison, UWFDM-68 (1973).

[7] B. Badger et al., "UWMAK-III, A Noncircular Tokamak Power Reactor Design," University of Wisconsin, Madison, UWFDM-150 (1976).

[8] J. Mitchell, "A Tokamak Reactor with Servicing Capability," *Proc. 9th Symposium on Fusion Technology*, Garmisch-Partenkirchen, 1976.

[9] D.V. Sherwood, R.W. Seddon, R. Hancox and J-Ch Sublet, "Evaluation of a Fusion Power Reactor Maintenance Concept," AEA Technology Report AEA FUS 204, September 1992. Also "Evaluation of Maintenance Concepts Suitable for Fusion Power Reactors," to be published in *Fusion Engineering & Design* (1993).

[10] J.M. Gahl, J.M. McDonald, A. Zakharov et al., "Heat Load Material Studies: Simulated Tokamak Disruptions," *J. Nuclear Materials* **191-194**, 454 (1992).

ENGINEERING DESIGN OF ARIES-III*

D.K. Sze, Argonne National Laboratory, Argonne, IL 60439

C. Wong, General Atomics, San Diego, CA 92138

E. Cheng, TSI Research, Solana Beach, CA 92075

M.E. Sawan, I.N. Sviatoslavsky, J.P. Blanchard, L.A. El-Guebaly, H.Y. Khater, E.A. Mogahed

University of Wisconsin, Madison, WI 53706

P. Gierszewski, Canadian Fusion Fuels Tech. Project., Mississauga, ON, Canada, L5J 1K3

R. Hollies, Hollies Fluids Consulting, Pinawa, MB, Canada ROE 1 L0

and the ARIES Team

Abstract

An efficient organic cooled low activation ferritic steel first wall and shield has been designed for the D-^{3}He power reactor ARIES-III. The design allows removal of the large surface heat load without exceeding temperature and stress design limits. The structure is expected to last for the whole reactor life. The major concerns regarding using the organic coolant in fusion reactors have been greatly alleviated.

1. Introduction

ARIES-III is a conceptual design for a D-^{3}He tokamak fusion power reactor. The 1000 MWe reactor operates in the second stability regime. The plasma major radius is 7.5 m and the aspect ratio is 3. The plasma current is 30 MA and the toroidal field on axis is 7.5 T. Only 4% of the fusion power is carried by neutrons with the rest being carried by charged particles that deposit energy as surface heat on the first wall (FW) and divertor. The average neutron wall loading is only 0.08 MW/m^2 with the peak value at midplane being 0.114 MW/m^2. Since no tritium breeding blanket is required in a D-^{3}He reactor, only a simple relatively thin shield is needed for magnet radiation protection. On the other hand, the peak surface heat flux on the FW is 1.86 MW/m^2. This has placed a premium on the design of the FW which should be capable of removing the high surface heat without exceeding temperature and stress limits. In addition, the FW should be capable of withstanding a plasma disruption.

Organic coolants have been used in fission reactor [1] and useful experience of operating an organic cooled system was generated. Organic coolants can be used at a higher temperature than water (450°C vs. 350°C) with

* Work supported by the U.S. Department of Energy, Office of Fusion Energy under Contract No. W-31-109-Eng-38. We also acknowledge the support from CFFTP and AECL.

The submitted manuscript has been authored by a contractor of the U. S. Government under contract No. W-31-109-ENG-38. Accordingly, the U. S. Government retains a nonexclusive, royalty-free license to publish or reproduce the published form of this contribution, or allow others to do so, for U. S. Government purposes.

a much lower pressure (1 MPa vs. 20 MPa). The key disadvantage of organic coolant for D-T fusion reactors is the high radiolytic decomposition rate [2]. However, in a D-^{3}He reactor, the neutron power is only about 4% of the fusion power. Therefore, the concern regarding radiolysis is much alleviated. The high surface heat flux in ARIES-III requires a coolant with good heat removal capability. In addition, the high capital cost and recirculation power require good thermal conversion efficiency. Furthermore, the first wall synchrotron reflectivity is required to be 0.99. Be coating was identified as the only choice of material with sufficient electrical conductivity to provide such reflectivity. To limit the evaporation of Be, a maximum Be temperature of 750°C was selected. This puts severe limitations on the FW and coolant temperature. These requirements resulted in the selection of the organic coolant for the ARIES-III FW and shield. Since the organic coolant is limited to about 450°C, advanced structural materials are not required. The low activation ferritic steel (modified HT-9) was, therefore, selected as the structural material. The overall features of the ARIES-III FW and shield design are described in this paper.

2. Unique Feature of D-^{3}He Reactor

There are three unique features of D-^{3}He reactor which have major impact on the first wall and shield design.

2.1 First wall heating load

For a D-T reactor, 80% of the fusion energy is in the neutrons. Thus, only 20% of the fusion energy will be deposited on the first wall and the divertor surface. For a D-^{3}He reactor, 96% of the fusion power will be deposited on the surface. To keep the reactor in reasonable size, the heat flux to the first wall and divertor will be large. Therefore, a coolant with good heat transfer capability is required.

2.2 First wall reflectivity

A highly conducting first wall is required for synchrotron radiation reflection. High synchrotron reflection is needed for plasma power balance. For the ARIES-III design, the first wall synchrotron reflectivity required is 0.99. To achieve this reflectivity, Be was selected as the first wall coating. (W could also be used, but only at a temperature of a few hundred degree C.) To limit the evaporation of the Be, a maximum Be temperature of 750°C was selected. This maximum allowable Be temperature put severe limitations on the temperature of the first wall and coolant.

2.3 Plasma recirculation power

The ARIES-III reactor operates in the second stability plasma region. A large power is required for plasma current profile control. This large power requirement results in engineering Q at only 4.1. Therefore, an efficient power conversion system is required.

Organic coolant is thus selected for the ARIES-III design due to its high heat transfer capability and its potential to achieve high thermal converting efficiency at a modest coolant temperature.

3. Comparison with a D-T Reactor

The key advantage of a D-^{3}He reactor over a D-T reactor is the factor of 20 reduction of neutron production. Also, the design of the blanket can be simpler because there is not breeding requirement. Table 1 summarizes the comparison between a D-T (ARIES-II) and a D-^{3}He (ARIES-III) reactor.

Table 1. Comparison Between a D-T and D-^{3}He Reactor

Fuel Cycle	D-^{3}He	D-T
Peak neutron wall loading	0.11 MW/m^2	5.1 MW/m^2
Peak DPA/FPY	2	63
First wall life (based on DPA only)	100 FPY	3.17 FPY
Total FW/B/S/VV thickness	70 cm	115 cm
Structural material	MHT-9	V5Cr5Ti
Coolant/Breeder	Organic coolant	Li/Li
Total activity (MCi)		
@ shutdown	1549	3848
@ 1 day	863	396
@ 1 year	254	59
Total decay heat (MW)		
@ shutdown	5	53
@ 1 day	1.4	3.2
@ 1 year	0.2	0.3
Integrated decay heat after 1 week, GJ	635	1846
Radwaste class	A	C

The following points can be made from this comparison.

a. First wall life. Based on the dpa limit of the first wall, a D-^{3}He reactor's first wall/blanket can be lifetime components. This is a key advantage over a D-T reactor, whose first wall/blanket life is about 3 FPY. How important this advantage is depends on the first wall/blanket replacement time for a D-T reactor.

b. Radwaste. This is an important advantage over a D-T reactor. Not only the radwaste is classified as class A, but also the volume

is much smaller (due to the lifetime components of the first wall/blanket).

c. Decay heat. There is about a factor of three of integrated decay heat in favor of a D-^{3}He reactor. This difference in decay heat does not seem to be critical because, based on LOFA and LOCA calculations, decay heat is not a major safety concern for either D-T or D-^{3}He reactor.

d. Total FW/B/S thickness. Due to lower neutron flux and no breeding requirement, the total FW/B/S thickness of a D-^{3}He reactor is only 60% of a D-T reactor. However, the benefit of thinner FW/B/S is offset by the larger surface area, so that the total volume of the FW/B/S are about the same.

e. Total activity. The comparison of the total activities of the two reactors is difficult due to the different structural materials used. Also, using lithium in the D-T reactor reduces the activity due to the fact that lithium is a good neutron absorber.

4. Organic Coolant Issues

The unique design feature of the ARIES-III FW and shield is using organic coolant. The organic compounds of interest for fusion are the terphenyl isomers. These compounds have good irradiation stability, good thermal stability up to around 400°C, soluble decomposition products, and reasonable availability at relatively low cost. Organic coolants are low pressure coolants with good heat removal capability which leads to simpler, more reliable mechanical designs. This allows operation at higher temperatures leading to higher thermal efficiency. They have low corrosion rates with a wide variety of structural alloys leading to low activity in the primary heat transport system. There have been some major concerns about organic coolants. However, the operating experience of the WR-1 [1] reactor helps resolve most of these concerns. These specific issues are briefly summarized here.

At high temperatures and in radiation fields, organic coolant decompose leading to potential surface fouling or channel plugging. These were significant problems in early fission reactor, but were successfully resolved in the WR-1 reactor. Coking is the formation of carbonaceous deposites in low-flow regions due to precipitation and growth of decomposition products. Coking is controlled by reducing the total decomposition rate and by maintaining high coolant velocity. The coolant velocity in ARIES-III is maintained above 10 m/s to prevent coking. Fouling is the formation of films on high temperature heat transfer surfaces, normally dependent on the nature and concentration of the coolant impurities. Fouling is prevented through coolant chemistry control, particularly minimizing chlorine and oxygen.

The flammability of organic coolants is a serious concern. However, experience with the organic coolant in twenty years of operation of the WR-1

reactor has shown that this hazard is readily managed. The combustion temperature is estimated to be about 1000°C and the combustion process is slow. In addition, if the building atmosphere is maintained with <12% oxygen, the organic coolant cannot be ignited.

The organic coolant decomposes due to both radiation and temperature. The decomposition rates can be predicted [3]. The decomposition product actually makes the organic coolant more stable. About 90% of the decomposition products can be recovered by the hydro-cracking process [4]. Decomposition will cause only a minor economic penalty.

The first wall is the most important part of the shield. It is designed to be capable of absorbing the incident high surface heat in the coolant while maintaining the thermal stresses at acceptable levels. The FW is composed of segments divided in the toroidal direction with poloidal coolant flow. The FW skin is composed primarily of MHT-9, 1.0 mm thick and is coated on the surface facing the plasma with tungsten and Be. The function of the W, which is 100 μm thick, is as a diffusion barrier between the Be and the steel. A coating of Be, 1.5 mm thick, is deposited on the W. Its function is to provide a high electrical conductivity at the surface to reflect synchrotron radiation and also as a sacrificial coating to mitigate against energy deposited by a plasma disruption. The FW skin is attached by a continuous spot welding process to a machined MHT-9 steel plate, and the two together constitute the FW segments. Immediately behind the FW skin there is a continuous series of rectangular channels 6 mm wide and 8 mm deep. These channels run in the poloidal direction in a continuous fashion from the bottom to the top. At the interface between the FW segments and the front shield zone, the FW segments are relieved such that they only make contact on the ends where the bolts which attach the segments to the front shield are located. This is done to thermally isolate the FW segments from the shield behind it.

Figure 1 is a midplane cross section of an OB module. The front part of the shield on which the FW segments are attached is an MHT-9 steel forging 20 cm thick and has a 5% coolant fraction. In the OB shield this piece is curved to conform to the plasma contour and is tapered from the midplane to the extremities. This front shield has the primary function of supporting the FW segments by means of bolts inserted from the back side. A single coolant channel is machined behind each FW segment. This coolant channel cools the front shield segment and also ducts coolant to the FW segments.

The rear shield is made of MHT-9 steel plates separated by rather large coolant channels. The large amount of coolant (30%) is needed for neutronic purposes and not from thermal hydraulic requirements. Both IB and OB rear shields have four coolant passages extending the full length of the modules. On the OB side, the rear shield is 50 cm thick and each channel is 3.75 cm deep. The IB side is only 35 cm thick, and the channels are 2.6 cm deep. The channels are connected in series, such that all the coolant flows through them. Coolant enters the rear shield at the top through a tube which feeds into the last channel. It flows down the full length of the module then crosses over to the next to last

channel at the bottom of the module and travels up. After making four traversals of the module vertical heights, the coolant is ducted into the front shield zone through coolant transition tubes at the top of the modules. The coolant then travels down through the front shield zone, then crosses over to the FW segments and finally travels up through the FW coolant channels.

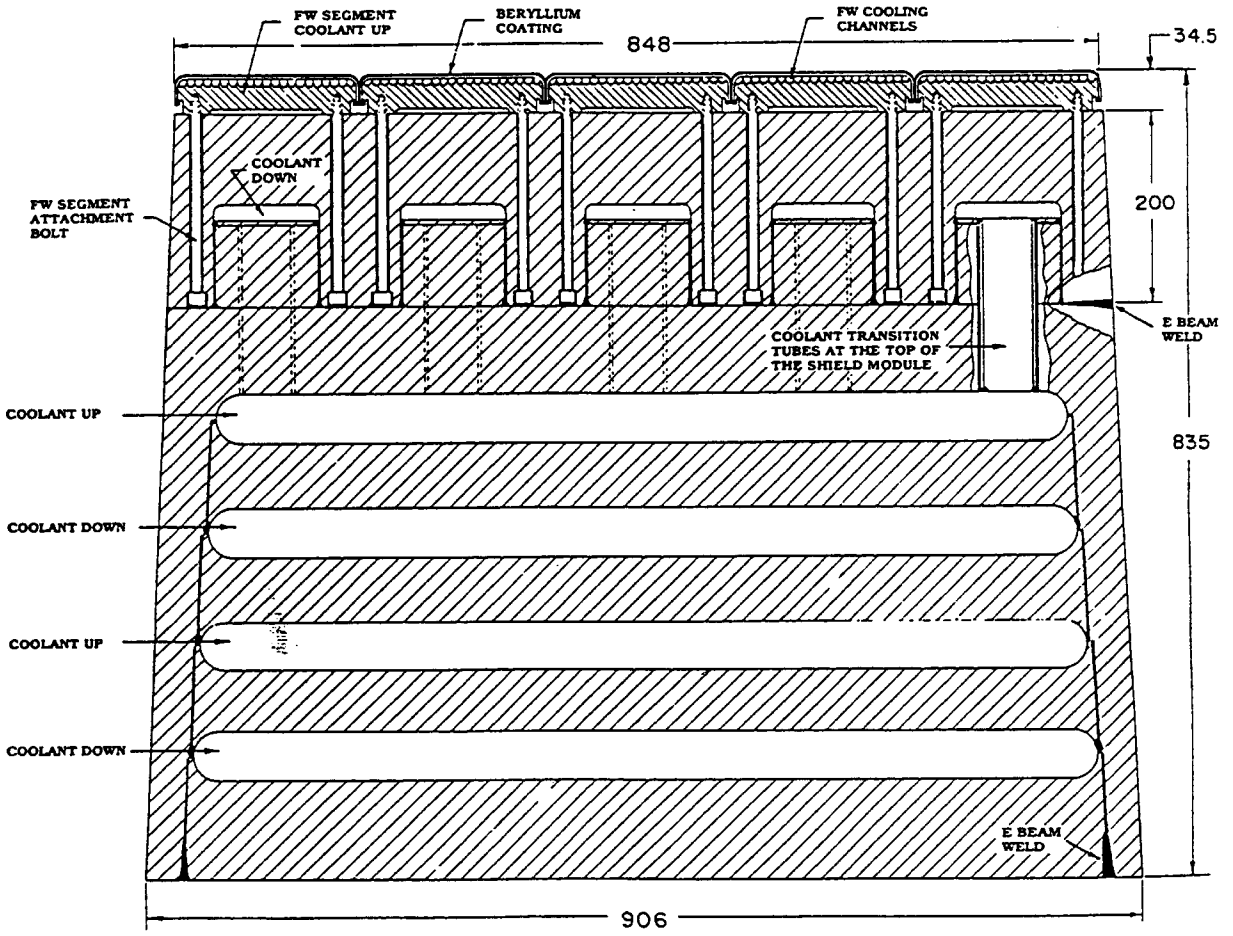


Figure 1. Midplane cross section of outboard shield module.

5. Thermal Hydraulics

The high capital cost and the high recirculation power requirement of a D-^{3}He reactor dominate the selection of the thermal design point of the ARIES-III reactor. The thermal efficiency of the power conversion system has to be maximized. Thus, both the maximum coolant temperature and the average coolant temperature have been pushed as high as possible. Based on organic cooled fission reactor experience, 425°C is selected as the coolant outlet temperature. To reduce the size of the steam generator, a coolant inlet

temperature of 350°C is selected for the ARIES-III study. The pinch point ΔT will be 15°C. The steam temperature is 399°C, and the steam pressure is 17.3 MPa. The anticipated cycle efficiency is 44%.

The heat transfer coefficient of the organic coolant is less than that of water, primarily due to the much lower thermal conductivity. To improve heat transfer, fission reactor applications used high coolant velocity and small coolant channels. The size of the ARIES-III first wall coolant channel is selected to be 0.8×0.6 cm. This size is selected from the tradeoff between pressure drop and heat transfer. With the energy deposited along the coolant tube, and the selected coolant inlet and outlet temperatures, the coolant velocity is calculated to be 16 m/s.

The ARIES-III reactor has a very high surface heat load. In addition, the second stability plasma pushes the plasma axis toward the outboard FW. Therefore, there is a very high peaked surface heat load at the middle point of the outboard FW. To reduce this peak heat load, the outboard scrape-off zone thickness at midplane is increased to 90 cm. This reduces the maximum heat flux from 2.8 MW/m^2 to 1.86 MW/m^2. This heat load can be handled by the organic coolant with the conditions described here. Two-dimensional finite element analysis of the FW and shield has been carried out using ANSYS and utilizing the nuclear heating profiles. At the midplane where the surface heating peaks, the combined primary and secondary stresses are 353 MPa at a bulk steel temperature of 497°C. The peak Be coating temperature is 571°C and the interface between W and Be is at 531°C. These values satisfy the thermal stress and peak temperature requirements for these materials. The thermal-hydraulics parameters are summarized in Table 2.

Table 2. Thermal Hydraulics Parameters

First wall configuration	poloidal flow, once through
Coolant path length	8 m
Maximum first wall heat load	1.86 MW/m^2
Coolant tube dimensions	0.6×0.8 cm
Inlet temperature	350°C
Exit temperature	425°C
Maximum Be temperature	571°C
Maximum steel temperature in FW	531°C
Thermal energy per tube	126 kW
Coolant velocity	16 m/s
Re number	1.63×10^5
Maximum heat transfer coefficient	2.19 W/cm^2-°C
Maximum coolant film ΔT	128°C
Coolant pressure drop	1.6 MPa
Coolant pressure	2.6 MPa
Pumping power	9 MW

6. Power Conversion

Due to the large recirculation power required by the D-^{3}He plasma, an efficient power conversion system is desirable. However, the coolant temperature is severely limited by the first wall conducting requirement. It is a major challenge to achieve an efficient power conversion with a limited temperature. Lewis [5] proposed that if organic coolant could be heated up to 425°C, a power conversion system can be designed with a gross efficiency of 44%. It uses two reheat and 10 feed water heaters. It was judged that this power conversion is possible, but may be expensive due to the large number of heat exchangers required. Due to the high capital cost of the fusion power, and the high recirculation power of tlie D-^{3}He plasma, it is decided that the high efficiency can off-set the cost of the power cycle.

The power balance of the ARIES-III reactor is shown in Table 3 together with the power balance of a water cooled version of the same reactor. Even with 44% gross efficiency, the net efficiency of the ARIES-III reactor is only 33%. If water is used as the coolant, the net efficiency would be only about 25%, which is clearly not acceptable.

Table 3. Comparison with Water Cooled Reactor

	Organic Coolant	Water
Net electrical power	1000 MWe	1000 MWe
Recirculating power	341 MWe	341 MWe*
Gross electrical power	1341 MWe	1341 MWe
Gross thermal power	44%	35%
Reactor thermal power	3087 MW	3831 MW
Net thermal efficiency	33%	26%

* The recirculating power for water cooled system will be larger due to the high fusion power. If the recirculating power is proportional to fusion power, the net efficiency will be ~24%.

7. Summary

The engineering design of the ARIES-III D-^{3}He reactor is presented. A D-^{3}He reactor has many advantages over a D-T reactor. The most important one is that the first wall/blanket is life time components if dpa is the life limiting factor. It also has major advantages on waste disposal, both on the classification and on the mass. However, there are also many technical difficulties. The most important one is the first wall design. Also, to take full advantage of a D-^{3}He reactor, a direct conversion system is required. It is difficult to design a direct

convert power conversion system for a tokamak. Therefore, tokamak may not be the best reactor configuration for a D-^{3}He reactor.

References

1. D.R. Tegart, "Operating of the WR-1 Organic Cooled Research Reactor," Atomic Energy of Canada Limited Report, AECL-3523, 1970.

2. P.J. Gierszewski and R.E. Hollies, "Organic Coolants and Their Applications to Fusion Reactors," Canadian Fusion Fuels Technology Project Report, CFFTP-G-86004, 1986.

3. J.J. Smee et al., "Organic Coolant Summary Report," Atomic Energy of Canada Limited Report, AECL-4922, 1975.

4. D.A. Scola and R. Kafesijian, "Catalytic Hydro-cracking of Polyphenyl Systems for Use in Reclamation of Organic Nuclear Reactor Coolant," Atomic Energy of Canada Limited Report, IDO-11056, 1963.

5. W.B. Lewis, Prospect for 44% Cycle Efficiency from 400°C (750°F) Steam in Large Electric Generating Stations, Atomic Energy of Canada Limited Report, AECL-3221 (1968).

10) D-^{3}He Tokamak Reactor Design-II 319
S.O. Dean, Chair

10-1 Parametric Analysis of the ARIES-III D-^{3}He Tokamak Reactor 321
C.G. Bathke, K.A. Werley, R.L. Miller, R.A. Krakowski,
J.F. Santarius, and the ARIES Team

10-2 The Physics of Apollo: A D-^{3}He, First Stability, Tokamak Reactor 329
G.A. Emmert, J.F. Santarius, and J.P. Castro

10-3 Safety Characteristics of D-^{3}He Fusion Reactors 337
Hesham Y. Khater

10-4 Safety Analysis of the ARIES-III D-^{3}He Tokamak Reactor Design 349
J. Stephen Herring and Thomas J. Dolan

PARAMETRIC ANALYSIS OF THE ARIES-III D-^{3}He TOKAMAK REACTOR

C. G. Bathke, K. A. Werley, R. L. Miller, and R. A. Krakowski
Los Alamos National Laboratory, P.O. Box 1663, Los Alamos, NM 87545

J. F. Santarius
University of Wisconsin, 1500 Johnson Dr., Madison, WI 53706

and the ARIES Team

ABSTRACT

The multi-institutional ARIES study has completed a series of conceptual designs of tokamak fusion reactors that varies the assumed advances in technology and physics. The ARIES-III design uses a D-^{3}He fuel cycle and requires significant advances in physics to enhance economic attractiveness. The optimal design was characterized through systems analysis for eventual conceptual engineering design. Results from the systems analysis are summarized, and a comparison with the other ARIES designs is included.

1. INTRODUCTION

The Advanced Reactor Innovation and Evaluation Study (ARIES) [1] is a four-year, multi-institutional exploration of several tokamak-reactor visions emphasizing economic, safety, and environmental features. The first design completed, ARIES-I [2], is a D-T fueled reactor that uses near-term physics and advanced technology. The recently completed ARIES-II/IV designs [3] are also D-T fueled reactors, but are based on advanced physics and near-term technology. The ARIES-II/IV designs are differentiated only by the blankets: V structure with liquid-lithium coolant and SiC structure with He coolant, respectively. The ARIES-III design [4], reported herein, uses D-^{3}He fuel and requires the most advanced physics of the ARIES designs and near-term technology. The technological advances invoked for ARIES-III include: high-efficiency ($\eta_{CD} = 0.68$), energetic (3-6 MeV) neutral beams for current drive; and advanced, high current-density (40 MA/m^2, averaged over TF coil) but moderate peak-field (< 14 T) superconducting coils. A low activation HT-9 shield (a tritium breeding blanket is unnecessary) with an organic coolant recovers the thermal neutron energy. Economics dictates physics operation in a high-beta ($\beta = 0.24$), high-safety-factor ($q_0 = 1.95$, $q_{edge} = 6.85$), second-stability regime (SSR) to achieve acceptable power density at moderate magnetic field ($B_{\phi 0} = 7.6$ T) and approximately ITER-level plasma current ($I_\phi = 30$ MA). The plasma density profile is optimized to minimize bootstrap-current "overdrive" (a characteristic of the high $\epsilon\beta_\theta$ SSR) to 25%; the

†Work supported by US DOE, Office of Fusion Energy.

externally driven current is 7.5 MA. Furthermore, a large energy-confinement-time enhancement factor of $H = 7.4$ over the ITER-89P scaling [5] is required. The ARIES-III design point was increased in size (major radius $R_T = 7.5$ m and minor radius $a_p = 2.5$ m) relative to the cost-of-electricity (COE) minimum at a 2% penalty in COE to ensure a peak neutron (DD, DT) wall loading of $I_w = 0.1$ MW/m^2. Sensitivity studies about the COE optimum indicate that the design window available to D-^{3}He tokamak reactors is severely limited. A common-basis comparison of all the ARIES designs [3] is made.

2. MODEL

The ARIES-III design was parametrically analyzed with the ARIES systems code (ASC) [3]. The models used in the ASC are described in Ref. 3, with essential features and notation summarized below. At the core of the ASC are plasma and plant power balances. Standard radial profiles are assumed for density and temperature: $n(r) = n_0[1 - (r/r_p)^2]^{\alpha_n} + n_E$ and $T(r) = T_0[1 - (r/r_p)^2]^{\alpha_T}$, respectively; where r_p is the circularized plasma radius. The plasma toroidal beta is constrained by a Troyon-type relation: $\beta \equiv 2\mu_0\langle p\rangle/B_{\phi 0}^2 = C_T I_\phi/aB_{\phi 0}$; where $\langle p\rangle$ is the volume averaged plasma pressure, $B_{\phi 0}$ is the vacuum toroidal magnetic field on axis ($R \simeq R_T$), and C_T is determined by stability considerations for each ARIES case. In the first stability region (FSR), C_T is a constant. In the second stability region (SSR), C_T is proportional to $\epsilon\beta_\theta$; where $\epsilon \equiv A^{-1} = a/R_T$ and β_θ is the poloidal beta.

The design requirements of the ARIES-III blanket and shield are relaxed because the D-^{3}He fuel cycle reduces neutron activation and material damage by a factor of 10-20 relative to the D-T fuel cycle and eliminates the need for a tritium breeding blanket (^{3}He is assumed to be available from lunar sources at 1 M$/kg [6]). An HT-9 shield that is 0.65 and 0.80 m thick inboard and outboard, respectively, captures the neutrons from D-T and D-D reactions for the thermal cycle and protects the advanced superconducting TF coils. An organic coolant is used in the reduced neutron environment to obtain a high thermal efficiency, $\eta_{TH} = 0.44$.

Because the fusion reactivity of the D-^{3}He fuel cycle is low compared to that of the D-T fuel cycle, high beta that leads to high plasma current is needed to produce a net electric power of $P_E = 1$ GWe in a reasonably sized power plant. The fraction, f_{BC}, of the plasma current driven internally by the pressure-gradient-driven bootstrap effect must approach unity to maximize economic attractiveness. Even if the global bootstrap current-drive fraction is unity, some externally driven current is required to match the (externally and internally) driven radial current-density profile with the equilibrium current-density profile; a seed current must be driven on axis, and the overdrive in the plasma edge must be canceled. As a result of these current-density profile effects the fraction of the plasma current driven externally cannot vanish and is constrained to $| 1 - f_{BC} | \geq 0.25$. The high temperature required to maximize the D-^{3}He fusion power requires neutral beam injection (NBI) for current drive, because ICRF waves cannot penetrate to all plasma regions.

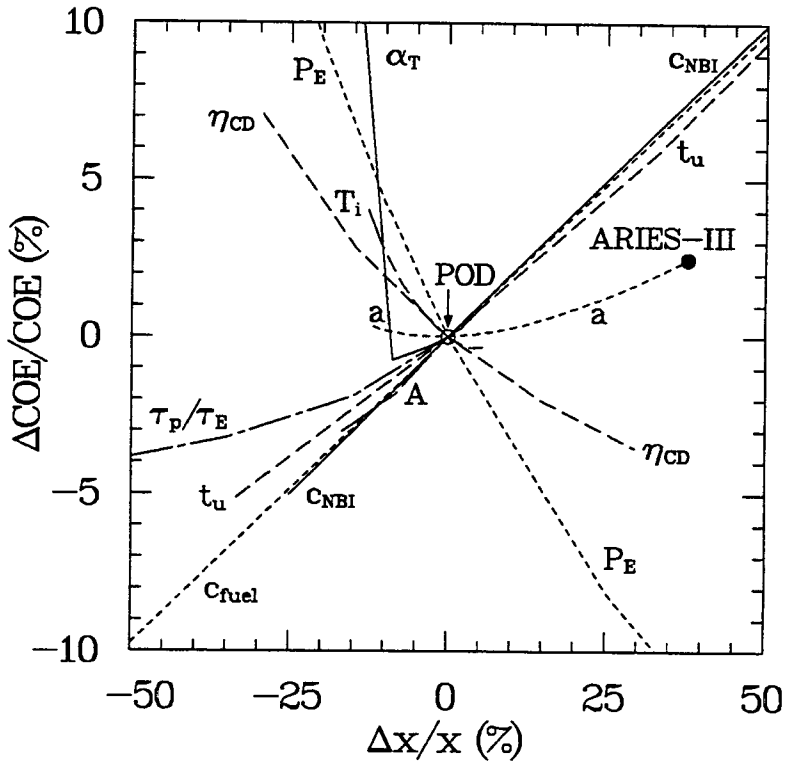


Fig. 1. Per cent change in the cost of electricity resulting from per cent changes about the POD in aspect ratio, A, ion temperature, T_i; ratio of particle-to-energy confinement time, τ_p/τ_E; temperature-profile exponent, α_T; net electric power, P_E; current-drive efficiency, η_{CD}; unscheduled maintenance time, t_u; unit cost of the NBI system, c_{NBI}; plasma minor radius, a; and unit cost of the fuel, c_{fuel}.

3. RESULTS

Two options were considered initially for ARIES-III: FSR and SSR. The high plasma currents (I_ϕ = 67.3 MA) and the low bootstrap current (f_{BC} = 0.43) characteristic of the FSR required a supplemental synchrotron current drive (f_{SC} = 0.35). To open an operating window in which the D-^{3}He plasma is maintained in power balance, $\tau_p/\tau_E \leq 1$ must be assumed. A low edge safety factor (q = 2.75) that produces high beta (β = 0.1) in the FSR is also required. Even with these optimistic assumptions and highly efficient (η_{DC} = 0.8), solid-state direct conversion of synchrotron power, the FSR option has a significantly higher COE than the SSR option by ~ 20 mill/kWeh and was abandoned in favor of the SSR option.

An operating window exists for SSR without auxiliary heating only at high β and low A and τ_p/τ_E. To maximize physics credibility and ease the engineering design, the minimum C_T = 0.15 and maximum τ_p/τ_E = 2 and A = 3 permitted by power balance are assumed. An ion temperature of T_i = 55 keV, which is near the fusion-power reactivity peak for D-^{3}He, is also assumed. As is shown in Fig. 1, a shallow minimum in COE with respect to a occurs because magnetic field, current, and, hence, recirculating power increase with decreasing a; and

mass ($\propto MPD^{-1}$; MPD is the ratio of the net electric power to the mass of the fusion power core) increases with increasing a. The COE minimum in a then serves as a point of departure (POD) for parametric analysis of the ARIES-III option. In the aspect-ratio variation shown in Fig. 1, as A is increased β decreases, which in turn requires larger, more massive (lower MPD) reactors with higher magnetic field and COE. The higher field increases synchrotron losses that must be offset by improved energy confinement (higher $n_i\tau_E$). The improved confinement increases the impurity fraction, which further degrades reactor performance. For $A = 3.05$, $n_i\tau_E$ increases to a value beyond which plasma-power-balance solutions cannot be achieved without inordinate amounts of auxiliary heating power. In the temperature variation shown in Fig. 1, increased $T_i(\sim T_e)$ increases both bremsstrahlung and synchrotron radiation that in turn require higher $n_i\tau_E$. The increased T_i also increases the NBI current-drive efficiency (i.e., lowers the current-drive power P_{CD}) and subsequently lowers COE. At lower T_i the fusion reactivity decreases, which requires higher $n_i\tau_E$. In the τ_p/τ_E variation shown in Fig. 1, increased τ_p/τ_E leads to better confined fusion products, which raise the impurity fraction, f_{IMP}. Higher f_{IMP} produces two effects: a) fuel dilution, which requires a more massive (lower MPD) reactor with higher plasma current that in turn results in higher COE, and b) higher required $n_i\tau_E$, which compensates for fuel dilution. The off-optimum ARIES-III design choice is indicated in Fig. 1, and the associated design parameters are given in Table I. The ARIES-III design was selected by increasing a from the POD until the peak neutron wall loading decreased to $0.1\,\mathrm{MW/m^2}$ to reduce neutron activation. For the ARIES-III design the peak neutron wall loading is 1.25 times the average wall loading reported in Table I. Nevertheless, a level-of-safety-assurance [7] $LSA = 2$ rating was given to ARIES-III, because of the significant chemical ($\sim 6,000$ GJ) stored energy available to release the radioactive inventory during an accident. All of the cases in power balance are stable to ballooning modes, but require feedback stabilization of the kink modes.

A comparison of the ARIES parameters given in Table I reveals that the lower power density of the D-^{3}He fuel compared to D-T fuel requires ARIES-III to have three times the plasma current of ARIES-I and nearly five times the plasma current of ARIES-II/IV. The ARIES-III higher beta results in an on-axis field that is two-thirds that used in ARIES-I, but is comparable to that used in ARIES-II/IV. Consequently, the magnets are a large cost for ARIES-I, whereas the current-drive system is the dominant cost for ARIES-III. Thus, the development of advanced, high-efficiency current-drive methods would have significant impact on ARIES-III. The lower first-wall, blanket, and shield costs and higher beta of ARIES-III relative to ARIES-I, which used an expensive breeder compared to ARIES-IV, ultimately result in a lower COE for ARIES-III. If ARIES-I used the ARIES-IV blanket, then the ARIES-I COE would be lower than the ARIES-III COE by $\sim 6\,\mathrm{mill/kWeh}$. Because of the $LSA = 1$ rating and high β and f_{BC}, the ARIES-IV design has the lowest COE. The ARIES COEs should be compared to advanced fissile power plants that are projected to produce electricity at $\sim 45\,\mathrm{mill/kWeh}$ in 1992 $ [8]. The sensitivity of COE to perturbations in major design variables that is shown in Fig. 1 indicates that the ten variables examined weakly affect COE. An $\sim 100\%$ change in several variables is required to produces the $\sim 50\%$ decrease in COE required to make ARIES-III economically competitive with advanced fissile power

TABLE 1. Reactor Parameters for 1-GWe ARIES-I, -II, -III, and -IV.

ARIES	I	II	III	IV
Stability regime	FSR	SSR	SSR	SSR
D/T/^{3}He mix, (%)	50/50/0	50/50/0	50/0/50	50/50/0
Plasma major toroidal radius, R_T(m)	7.02	5.60	7.5	6.04
Plasma minor radius, a(m)	1.56	1.40	2.5	1.51
Plasma aspect ratio, $A = R_T/a$	4.5	4.0	3.0	4.0
Edge safety factor, q	4.5	12.2	6.85	12.2
Peak-to-average density ratio, n_0/n	1.30	1.12	1.06	1.12
Peak-to-average temperature ratio, T_0/T	1.90	2.65	1.75	2.65
Troyon coefficient, C_T	0.032	0.059	0.151	0.059
Plasma beta, β	0.019	0.034	0.24	0.034
Stability parameter, $\epsilon\beta_\theta$	0.62	1.35	1.80	1.35
Ion temperature, T_i(keV)	20	10	55	10
Ion density, $n_i(10^{20}/\mathrm{m}^3)$	1.20	2.15	2.02	1.98
Particle-to-energy confinement time ratio, τ_p/τ_E	4	9.8	2	9.2
Lawson parameter, $n_i\tau_E(10^{20}\mathrm{s/m}^3)$	3.72	2.72	23.5	2.92
Confinement multiplier, H	2.9	3.1	7.4	3.2
On-axis toroidal field, $B_{\phi 0}$(T)	11.3	7.97	7.61	7.62
Peak Field at TF coil, $B_{\phi c}$(T)	20.9	15.9	14.0	15.9
Radiation fraction, f_{RAD}	0.56	0.18	0.68	0.23
Plasma toroidal current, I_ϕ(MA)	10.6	6.43	30.0	6.63
Bootstrap-current fraction, f_{BC}	0.68	0.87	0.75	0.87
Current-drive power to plasma, P_{CD}(MW)	104	66	164	68
Neutron wall loading, $I_w(\mathrm{MW/m}^2)$	2.1	2.9	0.08	2.66
Thermal conversion efficiency, η_{TH}	0.49	0.46	0.44	0.49
Recirculating power fraction, $1/Q_E$	0.20	0.15	0.24	0.19
Mass power density, MPD(kWe/tonne)	91.4	92.1	87.4	110.1
Level of safety assurance [7], LSA	2	2	2	1
Systems costs (1992 M$):				
magnets	422	206	300	222
current drive	160	257	534	232
first wall, blanket,and shield	621	320	204	335
Cost of electricity, COE(1992 mill/kWeh):				
capital return	69	59	63	50
O& M	9	9	9	8
blanket replacement	15	2	0	4
decommissioning	1	1	1	0
fuel	0		18	0
total[†]	94(107)	72(82)	90(101)	63(85)

[†] The COE without safety cost credits ($LSA = 4$) is also reported in parenthesis.

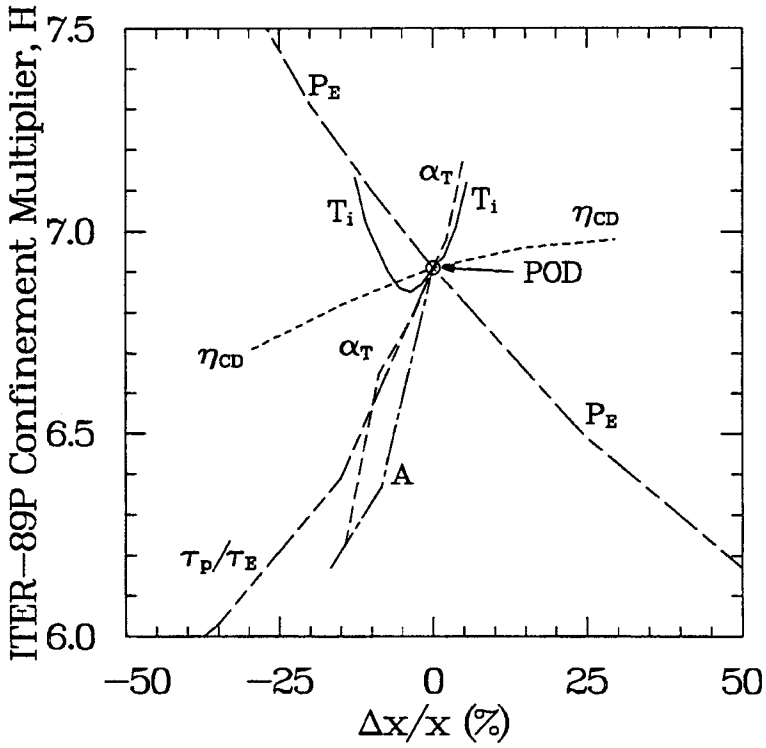


Fig. 2. Change in the required ITER-89P confinement multiplier, H, produced by per cent changes about the POD in aspect ratio, A; ion temperature, T_i; ratio of particle-to-energy confinement time, τ_p/τ_E; temperature-profile exponent, α_T; net electric power, P_E; current-drive efficiency, η_{CD}; unscheduled maintenance time, t_u; and unit cost of the NBI system, c_{NBI}.

plants. Also of interest is the affect the design variables have on the ITER-89P confinement multiplier, H, presented in Fig. 2. Only three variables can be changed to decrease COE and H simultaneously: τ_p/τ_E, A, and P_E. However, τ_p/τ_E is at the design limit, A is already small, and P_E is already near present-day utility limits.

SUMMARY

The ARIES team has completed the design of a tokamak reactor based on the D-^{3}He fuel cycle to examine the consequences of a neutron-lean fuel cycle. A D-^{3}He fuel cycle eliminates the need for a tritium breeding blanket that accounts for $\sim$ 30% of the reactor equipment cost for the expensive ARIES-I SiC blanket and shield; the reduced neutron generation also allows the use of an organic coolant to obtain a high thermal efficiency $\eta_{TH} = 0.44$. The second-stability design, based on limited experimental results, outperformed the first-stability design by a wide margin. Even exchanging the organic coolant for water to attain $LSA = 1$ does not change the COE because the economic benefit of $LSA = 1$ is canceled by decreased thermal efficiency (η_{TH} decreases from 0.44 to 0.35). None of the ARIES designs are competitive with advanced fission power plants [8]. Generally, significant

extrapolations beyond the present physics data base are required to burn D-^{3}He fuel in tokamaks as presently understood or envisioned.

REFERENCES

1. R. W. Conn and F. Najmabadi, "Visions of the Future, A Program in Tokamak Reactor Studies," University of California Los Angles report UCLA-PPG-1201 (December 1987).
2. F. Najmabadi, "The ARIES-I Tokamak Reactor Study," University of California Los Angles report UCLA-PPG-1323 (1991).
3. F. Najmabadi, "The ARIES-II and -IV Second Stability Tokamak Reactors," University of California Los Angles report UCLA-PPG-1461 (to be published).
4. F. Najmabadi, "The ARIES-III D-^{3}He Tokamak Reactor Study," University of California Los Angles report UCLA-PPG-1384 (to be published).
5. D. E. Post, et al., "ITER Physics," International Thermonuclear Experimental Reactor documentation series, No. 21, International Atomic Energy Agency, Vienna (1991).
6. H. E. Thompson, "Cost of ^{3}He from the Moon," The Second Wisconsin Symposium on ^{3}He and Fusion Power, Madision WI (July 19-21, 1993).
7. J. P. Holdren, et al., "Report of the Senior Committee on Environmental, Safety, and Economic Prospects of Fusion Reactors," Lawrence Livermore National Laboratory report UCRL-53766 (June 1989).
8. J. G. Delene, "Updated Comparison of Economics of Fusion Reactors with Advanced Fission Reactors," *Fus. Technol.* **19**, 807 (1991).

The Physics of Apollo: A D-^{3}He, First Stability, Tokamak Reactor

G.A. Emmert, J.F. Santarius, J. P. Castro
Fusion Technology Institute
Department of Nuclear Engineering & Engineering Physics
University of Wisconsin-Madison

ABSTRACT

The Apollo D-^{3}He reactor design continues to evolve as various problems are analyzed and newer data becomes available. Current thinking on ash accumulation, synchrotron radiation transport, direct conversion of synchrotron radiation to electricity, and advanced current drive options is summarized.

1. INTRODUCTION

The Apollo reactor study represents the evolving design [1-3] of a first-stability, D-^{3}He advanced-fuel tokamak utilizing synchrotron current drive and direct conversion of synchrotron radiation to electricity. The latest in this series is Apollo L-4; an overview of this design is presented in an other paper [4] in this meeting. The various designs differ primarily in choices made for energy conversion systems, shield materials and coolant and other engineering concerns. The physics concepts in the Apollo study are relatively constant, although the numerical values change as the design point evolves with continued optimization. In this paper we focus on some of the critical physics issues for Apollo; the issues we consider here are ash accumulation, synchrotron radiation transport, direct energy conversion, and current drive.

2. ASH ACCUMULATION

First stability D-^{3}He tokamaks are more sensitive to ash (protons and ^{4}He), accumulation than either second stability D-^{3}He tokamaks or D-T tokamaks. This is because a larger fraction of the power loss is due to radiation (synchrotron and bremsstrahlung) and hence plasma transport losses must be kept small. To the extent that good confinement of the plasma energy means good particle confinement of the ash, the accumulation of the ash will be more severe. High ash concentration depletes the fuel density, decreases the fusion power output, increases the synchrotron and bremsstrahlung losses from the plasma, and thereby causes the plasma to lose power balance. To compensate for this, the plasma has to be made larger and the fraction of wall area devoted to waveguides transporting the synchrotron power to the rectennas has to be made smaller. This reduces the synchrotron contribution to current drive and the fraction of the electrical power output due to the rectennas and increases the amount of power needed for the auxiliary current drive system. Shown in Fig. 1 is the effect of increasing the ratio of the particle confinement time of the ash to the energy confinement time of the background plasma. In this calculation the electrical power output is held constant at 1000 MW_e and the plasma power and current balance is maintained, but at the expense of increasing the major radius and the injection power. We see that a severe penalty is exacted if we are forced to operate with higher values of τ_p^{ash}/τ_E.

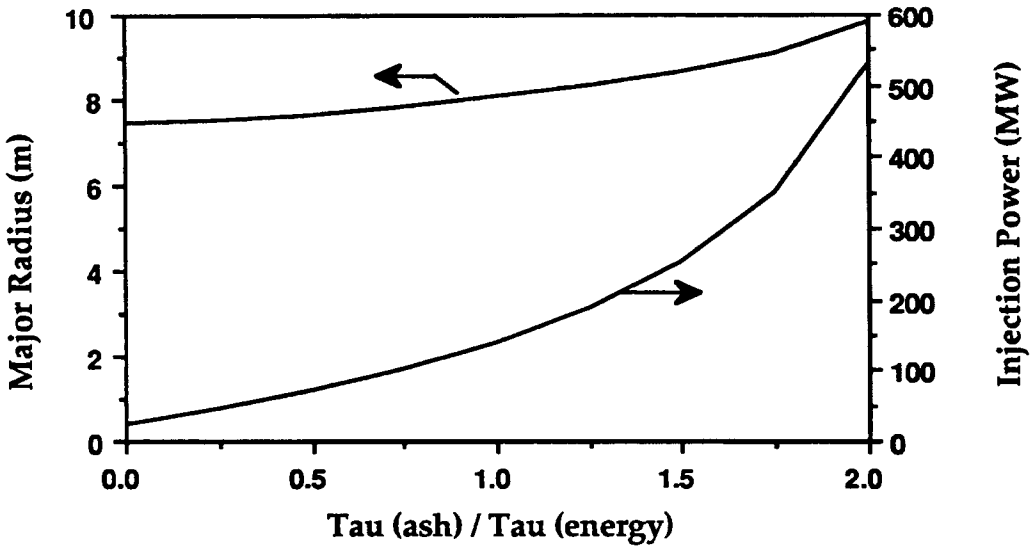


Fig. 1. A sequence of design points for increasing ash confinement time. The net electrical power produced is kept constant, requiring that the plasma size and injection power increase for larger concentrations of ash.

The database on τ_p^{ash}/τ_E in experiments is meager since measurements on particle transport are difficult. Some of the most detailed data is from TFTR for L-mode and supershot plasmas and indicates that $D_{He}/\chi_{eff} \cong 1$ [5]. This implies that $\tau_p^{ash}/\tau_E \cong 1$, except that this is without recycling. Recycling of ash back to the plasma core will increase the effective τ_p^{ash}/τ_E. Recycling is difficult to assess because it is heavily design dependent and depends on the cross-sections for ionization and charge exchange with the background plasma, which will be different for the ash from D-^{3}He fusion as compared with the ash from D-T fusion.

If it turns out that the ratio of τ_p^{ash}/τ_E in D-^{3}He plasmas is too large from normal transport processes, then active means will be necessary to reduce the accumulation of ash. Proposals have been made for enhancing the transport of the ^{4}He ash in D-T plasmas; one idea due to Chang [6] is to use RF waves resonating with alpha particles to enhance their radial transport. These same ideas can also apply to enhancing the radial transport of the ash in D-^{3}He plasmas.

3. SYNCHROTRON RADIATION TRANSPORT

Synchrotron power loss accounts for about 50% of the power loss from the plasma; bremsstrahlung is second at 30% and plasma transport is third at 20%. Shown in Fig. 2 is the radial profile of the synchrotron power density. In the center of the plasma the synchrotron power is negative implying a net emission of radiation. Near the edge the synchrotron power is positive implying a net absorption of radiation. About 25 % of the radiation leaving the core is re-absorbed in the edge before reaching the plasma edge. The effect of this is to cause a flow of energy from the center to the outer portions of the plasma and produce a flattening of the electron temperature profile. To study this effect we have coupled the SNECTR radiation transport code to the WHIST plasma transport code, so that radiation transport is self-consistent with the temperature profile obtained from WHIST. Shown in Fig. 3 is the flattening of the electron temperature profile due to radiation transport. Flattening the electron temperature profile will

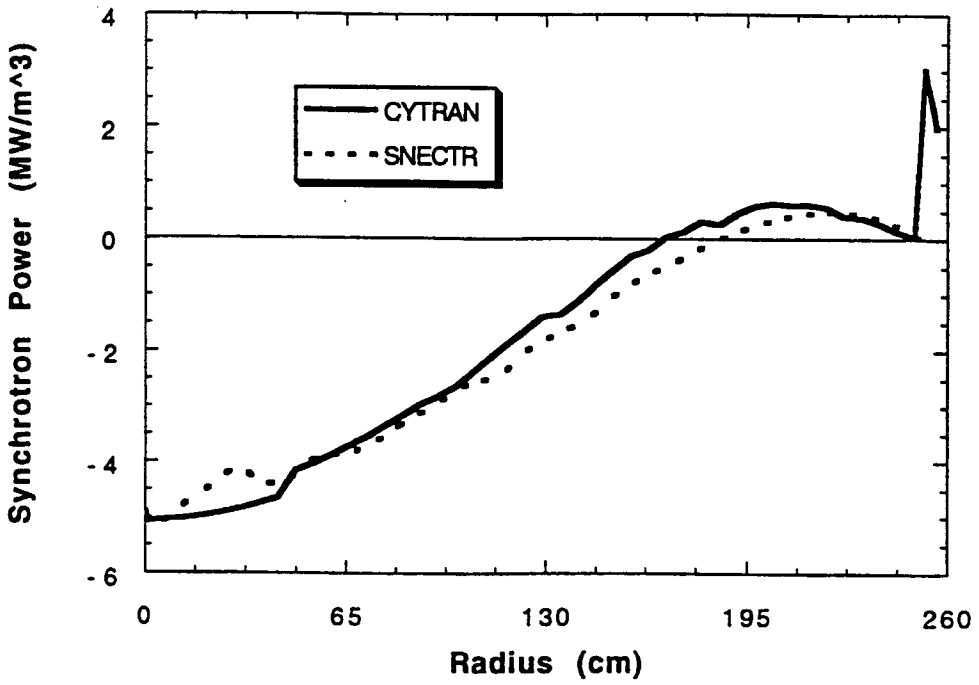


Fig. 2. Net synchrotron radiation profile versus radius using the CYTRAN and SNECTR codes for the Apollo parameters. Near the edge of the plasma there is net absorption of synchrotron radiation, while there is net emission near the center.

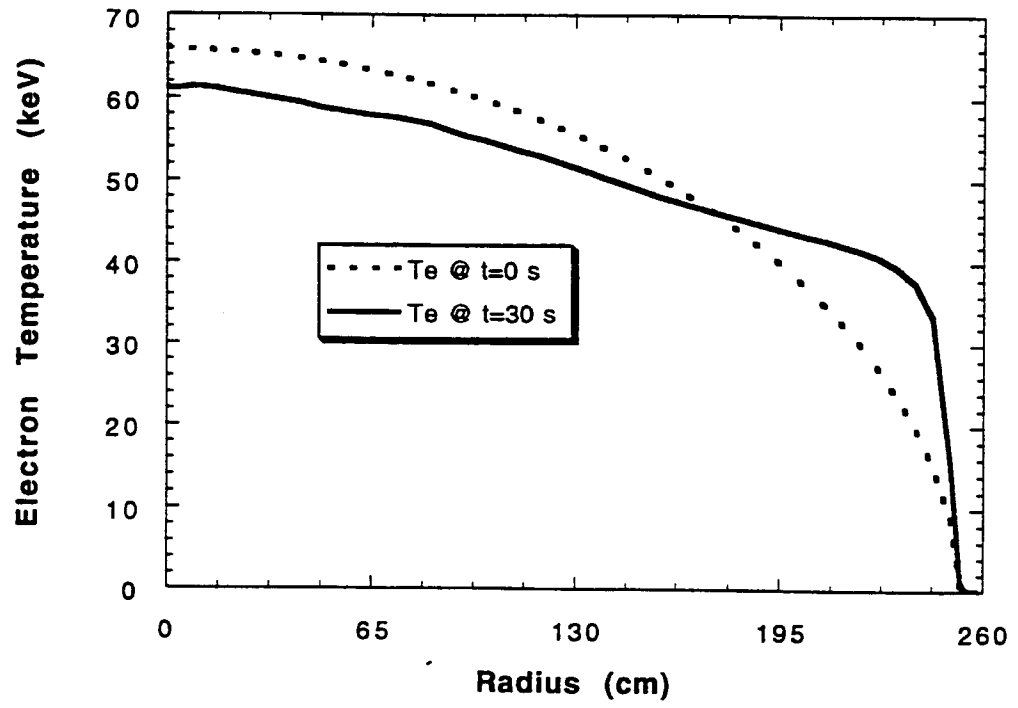


Fig. 3. Evolution of the electron temperature calculated self-consistently with the synchrotron radiation profile. Flattening of the electron temperature profile arises from the synchrotron radiation transport from the center to the edge.

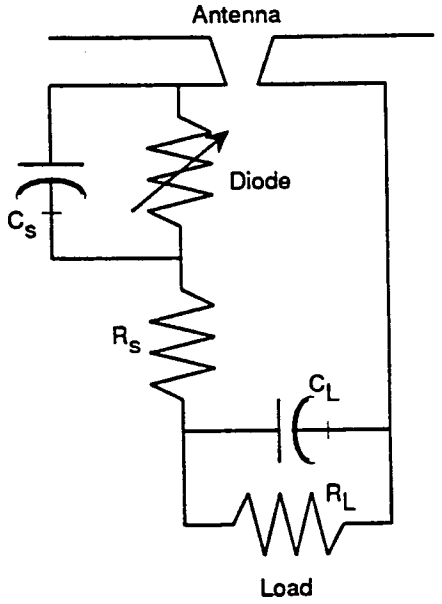


Fig. 4. Equivalent circuit for the rectennas.

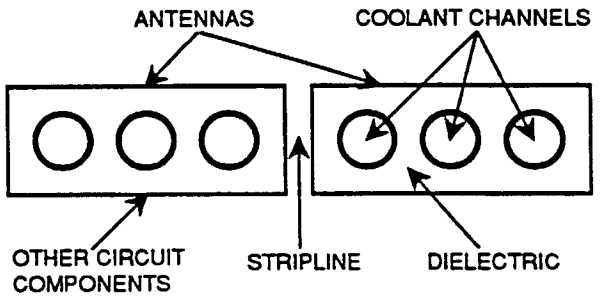


Fig. 5. Schematic of the rectennas showing the antenna elements on the upper surface, coolant tubes in the middle, and other components on the lower surface.

indirectly flatten the ion temperature profile (through rethermalization) and reduce the power output of the plasma. This effect has not yet been included in the systems code.

4. SYNCHROTRON DIRECT ENERGY CONVERSION

The concept of directly converting synchrotron radiation to electricity using rectennas was originated by Grant Logan [7]. The idea is to channel synchrotron radiation out of the tokamak using overmoded waveguides and convert it in a separate chamber. Rectennas (rectifying antennas) were developed in the 1970's. The present state of the art is that thin-film rectennas have been demonstrated at 2.45 GHz with 85% RF-to-DC conversion efficiency [8], but the technology requires demonstration at frequencies of interest for fusion---about three orders of magnitude higher. Nevertheless, the rectenna option appears feasible, as it would use integrated circuit technology well within the state-of-the-art, and high frequency diodes are developing at a rapid pace. The circuit can be simple, consisting of an antenna, one or a few diodes, and a few resistors and capacitors. Rectenna costs are uncertain, but they appear reasonable based on extrapolating costs for large production runs of large-scale integrated circuits.

The spectrum of synchrotron radiation will be spread from about 1 - 20 THz and peaked at about 5 - 10 THz. Since reflections from the tokamak chamber walls will tend to depolarize the spectrum, the calculations discussed below assume a random polarization. About half of the synchrotron power will be transported out the waveguides to the rectennas. The waveguide losses will be less than 5% of the total power entering the waveguide for a ratio of waveguide length to diameter of 30. Depending on shield design considerations, the waveguide diameter would be 10 - 20 cm for 3 - 6 m of length and then would widen to reduce losses until the conversion cavity was reached. The waveguide would be evacuated to approximately the tokamak chamber pressure, so no microwave transmission window is required.

The state of the art in integrated circuit technology is 100 times smaller than the 0.1 mm range required for the synchrotron radiation conversion antennas. A possible circuit option [7] is shown in Fig. 4. The key circuit component that is not presently available at the frequencies of interest is the diode. However, the field of vacuum microelectronics (for field-effect diodes) has been progressing rapidly in frequency. Monolithic microwave integrated circuits have been constructed which have achieved a cutoff frequency of 1.25 THz [9]. In the relevant time frame, the availability of suitable diodes appears likely. The efficiency of full-wave rectifying circuits has been calculated to approach 100% with log-spiral antenna geometries that give a frequency range of 2 - 10 times the nominal resonant frequency [10]. If such geometries are compatible with the integrated circuit design, broad-band coverage of this amount would suffice to keep the number of differently tuned rectennas small. The cavity could then be covered with a variety of differently resonant rectennas, since the reflectance off a non-resonant rectenna should approach 100% efficiency.

Present thinking about rectenna design is that the basic geometry would be a dielectric slab with the antennas facing the synchrotron radiation, with coolant channels through the dielectric, and with the remaining circuit components on the opposite side of the slab, as shown in Fig. 5. Connecting the antennas to the other components appears to be feasible using stripline techniques. The key difficulty in designing circuits at the very high frequencies of interest is capacitive coupling. The design goal of 1 MW/m^2 heat dissipated appears to be feasible, although detailed thermal hydraulics calculations remain to be done. Experimental programs [11] exist in two regimes that bracket the range of interest for D-^{3}He tokamak reactors.

5. ADVANCED CURRENT DRIVE OPTIONS

A major problem in designing D-^{3}He tokamak reactors is the high plasma current required. In Apollo, synchrotron radiation [12] drives 35% of the total current, the bootstrap current accounts for 43%, and an auxiliary current drive is needed for the remaining 22%. Because the presently leading current-drive schemes, ICRF and neutral beams, have very low current-drive efficiency, methods that could increase this efficiency would provide a large leverage. Several advanced candidates for the auxiliary current drive exist; these include helicity injection [13], compact-toroid injection [14], and alpha-particle-driven lower-hybrid waves [15].

Current drive using synchrotron radiation was first proposed by Dawson and Kaw [12]. The original concept used a fish-scale wall that would preferentially absorb synchrotron radiation propagating in one direction and thereby react back on the electrons to drive a current in the plasma. For Apollo, the waveguides used to transport synchrotron radiation to the direct energy conversion chamber are angled in the toroidal direction to accomplish preferential absorption.

Both helicity injection [13] and compact-toroid injection [14] would greatly increase the current-drive efficiency, perhaps by as much as a factor of ten. These techniques do not allow good control of the current density profile. Precise profile control should not be necessary, however, for the relatively broad current profiles of a first-stability tokamak such as Apollo.

An interesting new idea [15] is to tap the free energy of expansion present in alpha particles. The basic concept is that the alpha particles would resonate with lower-hybrid waves and amplify them. The lower-hybrid waves would subsequently damp on electrons, providing a current. The latter mechanism is the basis of the well-demonstrated technique of lower-hybrid wave current drive. Theoretically, this tapping of the alpha-particle energy consumes very little power, although there may be problems with wave penetration in some parameter regimes.

REFERENCES

[1] G.L. Kulcinski, G.A. Emmert, et al., *Fusion Tech.* **15**, 1233 (1989).

[2] G.A. Emmert, G.L. Kulcinski, et al., *Proc. 13th Symp. Fusion Eng.*, Knoxville TN, Vol. 2, p. 1043 (1990).

[3] G.L. Kulcinski, G.A. Emmert, et al., *Fusion Tech.* **19**, 791 (1991).

[4] L.A. El-Guebaly and C.W. Maynard, "Overview of Apollo Studies and Economic Assessment of Several Proposed Variations", this conference.

[5] E.J. Synakowski, P.C. Efthimion, et al., *Phys. Fluids B*, **5**, 2215 (1993).

[6] C.S. Chang, J.Y. Lee, and H. Weitzner, *Phys. Fluids B*, **3**, 3429 (1991).

[7] B.G. Logan, "Economical D-^{3}He Fusion Using Direct Conversion of Microwave Synchrotron Radiation," *Fusion Power Associates Annual Meeting*, April 24, 1986, Washington, DC.

[8] W.C. Brown, "Rectenna Technology Program: Ultra Light 2.45 GHz Rectenna and 20 GHz Rectenna," Report prepared for NASA Lewis Research Center.

[9] W-J. Ho, et al., "Monolithic Integration of HEMTs and Schottky Diodes for Millimeter Wave Circuits," *IEEE GaAs IC Symposium*, p. 301 (1988).

[10] M.J. Schaffer, private communication (1989).

[11] J.L. Christian, Jr. and R.J. Acosta, "Candidate Technologies for Beamed Space Power Application," NASA Lewis Report (1989).

[12] J.M. Dawson and P.K. Kaw, *Phys. Rev. Lett.*, **48**, 1730 (1982).

[13] A.H. Boozer, *Phys. Fluids*, **29**, 4123 (1986).

[14] C.W. Hartman and J.H. Hammer, *Phys. Rev. Lett.*, **48**, 929 (1982).

[15] N.J. Fisch and J-M. Rax, Phys. *Rev. Lett.*, **69**, 612 (1992).

Safety Characteristics of D-^{3}He Fusion Reactors

Hesham Y. Khater
Fusion Technology Institute
University of Wisconsin-Madison
1500 Johnson Drive
Madison, Wisconsin 53706-1687

ABSTRACT

A D-^{3}He reactor has the potential to be an inherently safer fusion reactor because most of the energy released in the plasma would be in the form of protons rather than neutrons. Only 1-5% of the fusion power is carried by fusion neutrons which are produced from the deuterium-deuterium (D-D) and deuterium-tritium (D-T) secondary reactions. A detailed activation and safety analysis, where activation due to both protons and neutrons is considered, has been performed for a selected reactor design (APOLLO-L2) to identify the possible safety and environmental advantages of using the D-^{3}He fuel cycle. Results of the activation analysis showed that proton-induced activity represents a small fraction of the total radioactivity generated in the steel structure. A decay heat comparison showed that there is two to three orders of magnitude difference in the level of decay heat generated by fusion neutrons and protons at any time after shutdown. At the end of the reactor lifetime, its structure would easily qualify for shallow land burial as low level waste. Finally, The thermal response of the reactor shield following a loss of coolant accident (LOCA) has been determined up to two weeks after an unscheduled shutdown of the reactor. The maximum temperature the first wall reaches is 500 °C. The low temperature of the structure during a LOCA results in the release of a very small fraction of the radioactive inventory at the onset of an accident.

1. INTRODUCTION

One of the main goals in the design of fusion reactors is to achieve as clean an environment as possible. A D-^{3}He reactor has the potential to be an inherently safer fusion reactor due to the fact that most of the energy released in the plasma would be in the form of charged particles (protons) rather than neutrons. Even though most protons thermalize on the background plasma, a small fraction would follow orbits that strike the reactor structure, producing radioactive isotopes or more neutrons as a result of (p,n) reactions. Proton interaction with structural materials presents a potential source of induced radioactivity that has been ignored due to the general lack of cross section data for proton interactions with different target elements and the expectation that it would be significantly smaller than the radioactivity induced by neutrons.

The appearance of D-^{3}He fusion reactors as a possible alternative to the D-D and D-T reactors brought up several questions not only about what level of radioactivity would be induced in such reactors by proton interactions with the different structural materials, but also what kind of previously unconsidered radioisotopes may be produced and what sort of problems they would present as potential sources for radiological hazard for both the reactor safety and the long-term storage of fusion waste.The two main sources of radioactivity production in D-^{3}He fusion reactors can be categorized as:

- Proton-induced radioactivity, which in turn can be divided into the radioactivities resulting from:
    1. The decay of the radioactive isotopes formed by interactions of proton with the structural materials.
    2. Neutrons produced by proton interactions with the structural materials. In this paper, these neutrons are refer to as (p,n) neutrons.
- Neutron-induced radioactivity from both the D-D and D-T secondary reactions. In this paper, these neutrons are refer to as fusion neutrons.

A library that contains thick-target activation yields for nuclides produced by protons activation of several stable nuclides has been compiled. In its present form, the library contains thick-target yield data for 164 radioactive isotopes. In addition, a computer program that produces the neutron flux of the (p,n) neutrons has been developed. The developed library and computer program were used in this paper to examine the level of importance of proton-induced radioactivity compared to fusion neutron-induced radioactivity in D-^{3}He fusion reactors. Finally a Safety analysis has been performed for a D-^{3}He reactor (APOLLO-L2) to identify the possible safety and environmental advantages of using the D-^{3}He fuel cycle.

2. CALCULATION OF PROTON-INDUCED RADIOACTIVITY

The main difficulty in the application of protons for activation analysis is the need to use nuclear cross sections. The nuclear cross section is not a convenient quantity to use for this purpose because it is strongly dependent on proton energy, such that it continually varies as protons slow down in the irradiated material. One alternative quantity to cross section that is widely used is the thick-target yield, which is usually expressed in the units of μCi/μA.hr.

Experimental cross section data, for (p,γ), (p,2n), (p,α) and (p,pn), were collected from several publications [1,2,3] for protons, with E $\leq$ 14.7 MeV, interacting with 109 naturally occurring isotopes of 58 target elements. Proton stopping powers were taken from the most complete data sets compiled by Anderson and Ziegler [4]. The proton stopping data were used with the measured cross sections to calculate the thick-target activation yields for the 164 radionuclides included in the library.

The neutron-induced radioactivity in D-^{3}He fusion reactors is mainly dominated by neutrons produced from the D-D and D-T secondary reactions (fusion neutrons). The energies of such neutrons are quite high being ~ 2.45 and 14.1 MeV, and are nearly monoenergetic for D-D and D-T secondary reactions, respectively. Another source of neutrons that needs to be considered is the neutrons produced by the proton interactions with the different structural materials in the reactor. Although contributions from such neutrons to the total level of radioactivity in the reactor is expected to be minimal, an evaluation of their effect is needed to have a comprehensive analysis of the radioactivity induced in D-^{3}He fusion reactors.

A computer program was developed to evaluate the energy spectrum of the (p,n) neutrons by using the multigroup transfer matrices method [5,6]. The program is linked to a cross section data library. In the library, experimental cross section data for protons, with E = 14.7 MeV, interacting with 65 naturally occurring isotopes of 36 target elements are found. The program gives the energy spectrum of the produced neutrons in a 46-neutron-energy-group structure. This neutron spectrum can be used to generate the neutron flux in the different reactor zones for activation calculations by using a neutron transport code.

3. COMPARISON BETWEEN PROTON AND NEUTRON INDUCED RADIOACTIVITY

An activation analysis for the APOLLO-L2 reactor has been performed in order to compare the radioactivity induced in its structure by both protons and neutrons. APOLLO-L2 is a D-^{3}He fueled tokamak reactor design that utilizes direct conversion. The reactor has a major radius of 7.43 m and an aspect ratio of 4 [7]. The design considers operation for 30 full power years and would produce a net electric power of 1200 MW_e; the peak neutron wall loadings on the inboard and outboard sides of the midplane are 0.1 and 0.14 MW/m^2, respectively. Only 5% of the 14.7 MeV protons produced in the plasma are assumed to strike the reactor first wall.

A comparison between the proton-induced and fusion neutron-induced radioactivity was conducted for a first wall made of the low activation austenitic steel Tenelon. The calculations showed that while proton-induced activity (a result of proton direct interactions with the first wall) might add a very small contribution to the fusion neutron-induced activity for short-term (< 5 years) and mid-term (< 10 years) activities after shutdown, its contribution to long-term activity is negligible when compared to the activity induced by fusion neutrons in the reactor first wall. The short-term induced activity is dominated by ^{56}Mn ($T_{1/2}$ = 2.6 hr), ^{54}Mn ($T_{1/2}$ = 313 day), ^{55}Fe ($T_{1/2}$ = 2.7 yr), and ^{51}Cr ($T_{1/2}$ = 27.7 day) in case of fusion neutrons. In the case of proton-induced activity the major contributors are ^{56}Co ($T_{1/2}$ = 78.5 day) produced from ^{56}Fe, ^{57}Co ($T_{1/2}$ = 271 day) produced from ^{57}Fe and ^{60}Ni, ^{52}Mn ($T_{1/2}$ = 5.63 day) and ^{52m}Mn ($T_{1/2}$ = 21.4 min) produced from ^{52}Cr , ^{54}Mn produced from ^{54}Cr, and ^{55}Fe produced from ^{55}Mn. While ^{57}Co is produced through (p,n) and (p,α) reactions, other contributors to the proton-induced activity are mainly produced through (p,n) reactions. In the period between 5 years and 10 years after shutdown, ^{55}Fe, ^{54}Mn, ^{63}Ni ($T_{1/2}$ = 100 yr) and ^{60}Co ($T_{1/2}$ = 5.7 yr) represent the major contributors to the fusion neutron-induced activity. For the same period of time, proton-induced activity is dominated by ^{55}Fe, ^{57}Co and ^{54}Mn. The long-term activity is due only to radionuclides produced from fusion neutron interactions with the reactor first wall such as ^{14}C ($T_{1/2}$ = 5730 yr), ^{59}Ni ($T_{1/2}$ = 80,000 yr), and ^{53}Mn ($T_{1/2} = 3.8 \times 10^6$ yr).

A Comparison between proton and fusion neutron induced specific activity as a function of time following shutdown is shown in Figure 1. Similar conclusions can be drawn out of a biological hazard potential (BHP) comparison because BHP is dominated by the same radionuclides that dominate the induced activity. Proton-induced decay heat is mostly produced by ^{52}Mn and ^{52m}Mn. Figure 2 shows a comparison for the specific decay heat generated following shutdown. A high fusion neutron-induced decay heat is generated in the first wall within the first eight hours following shutdown due to the high content of manganese in Tenelon. In the meanwhile, one can notice that proton-induced decay heat generated following shutdown can be neglected if compared to the fusion neutron-induced one. Results of the analysis also showed that the (p,n) neutron flux is more than two orders of magnitude less than the fusion neutron flux. Figure 3 shows a comparison for the total activity induced in all zones of APOLLO-L2 (with Tenelon structure) per cm height at the reactor's midplane. Similar to the differences in the two neutron fluxes, there is a two to three orders of magnitude difference in the level of induced-radioactivity. The calculations showed that even within the reactor first wall itself, the level of activity induced by the (p,n) neutrons is somewhat less than that induced by proton interactions with the wall structure at all times following shutdown.

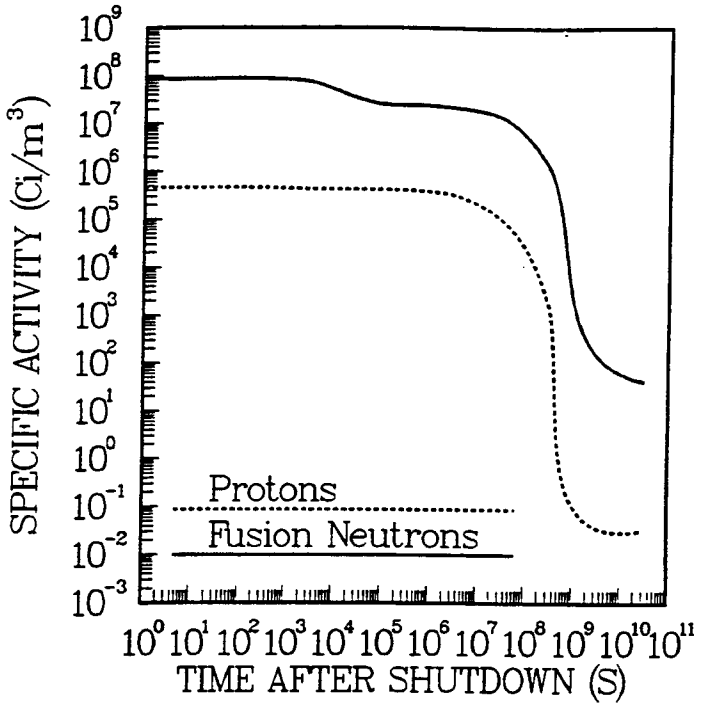


Fig. 1. Comparison between proton and fusion neutron induced specific activity in the first wall of APOLLO-L2.

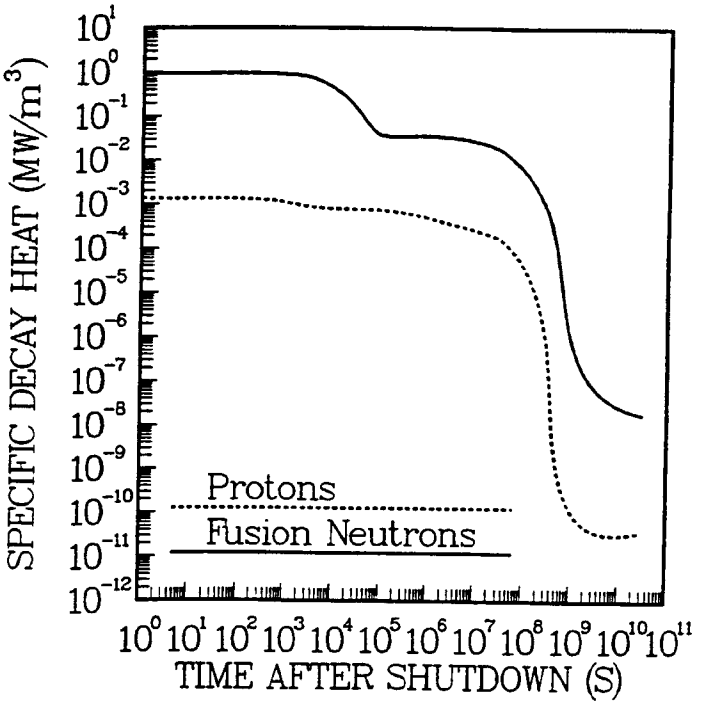


Fig. 2. Comparison between the specific decay heat generated by protons and fusion neutrons in the first wall of APOLLO-L2.

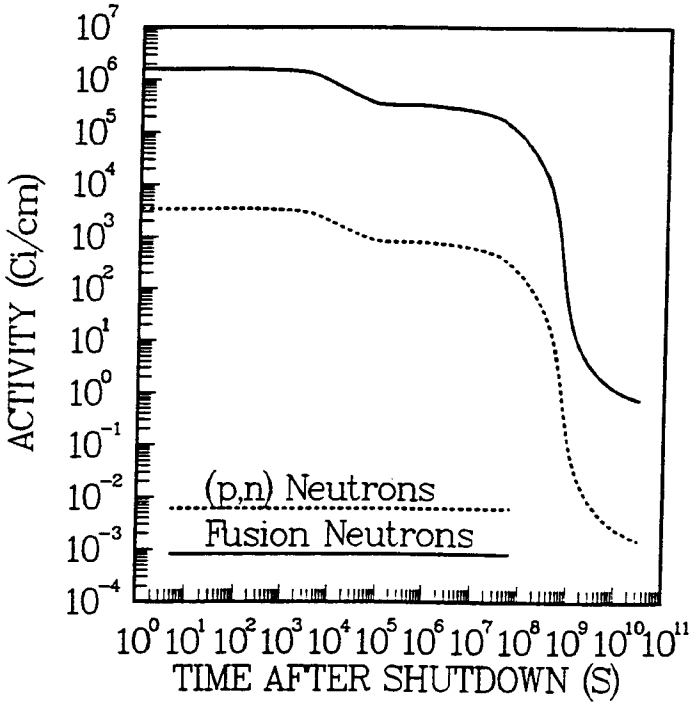


Fig. 3. Comparison between the (p,n) and fusion neutron-induced activity in APOLLO-L2.

4. SAFETY ANALYSIS OF APOLLO-L2

Safety analysis has been performed for APOLLO-L2 to identify the possible safety and environmental advantages of using the D-^{3}He fuel cycle. APOLLO-L2 has an austenitic steel water cooled shield. The options of using the nickel-stabilized (316 SS), and the manganese-stabilized (Tenelon) austenitic steel have been assessed. The lower nickel content in Tenelon reduces the inventory of the cobalt isotopes, improves waste management and reduces the accidental off-site dose. In the meanwhile, the higher manganese content results in a higher decay heat and hence higher temperature increase in case of a loss of coolant accident (LOCA). The radioactive inventories generated by the two steel alloys were used to calculate the waste disposal ratings (WDR) at the end of the reactor life-time (30 years). For each alloy, the decay heat generated was utilized to calculate the temperature rise in the first wall and shield during the first 2 weeks following the LOCA. The off-site doses have been calculated for the total radioactive inventory generated in the reactor and as a function of its structure temperature following the loss of coolant.

A one-dimensional toroidal cylindrical geometry model which includes both the inboard and outboard first wall, shield and magnets has been used in the neutronics and activation calculations. The one-dimensional discrete ordinates neutron-transport code ONEDANT [8] along with the ENDF/B-V cross section data files were used to generate the neutron flux in the different reactor zones. The neutron flux was then used in a several activation calculations performed using the DKR-ICF [9] code with activation cross sections taken from the ACTL [10] library. The reactor was assumed to operate for 30 full power years (FPY) which corresponds to 40 years of operation at 75% availability. The activation results were utilized in the radwaste classification and the off-site dose calculations performed according to the worst case weather conditions used in the FUSCRAC3 code [11]. The decay heat results were used to determine the thermal response of the shield following a loss of coolant accident using the ATHENA [12] code.

4.1. Waste Disposal Rating (WDR)

The specific activities calculated for the different radioactive nuclides have been used with the 10CFR61 waste disposal concentration limits (WDL) [13] to evaluate the radwaste of the structure of APOLLO-L2. Since radiation damage effects will greatly be reduced in a D-^{3}He environment, the calculations were made considering the first wall and shield and magnet will last for the full life of the reactor (30 FPY). The use of one first wall and shield assembly for the full life of the reactor has the advantage of reducing the total amount of radioactive waste to be disposed. The waste disposal ratings for Class A and Class C low level waste (LLW) are shown in Table 1. The Class A WDR are given after waiting period of 15 years if the first wall and shield are disposed together. The waiting period is required to allow for the specific activity of the short-lived nuclides ($T_{1/2} \leq 5$ years) to drops below 7000 Ci/m^3. In the same time, the Class C values were calculated after only one year cooling period. Only a Tenelon structure would qualify as Class A LLW. If Class C limits are used then 316 SS would still not qualify for shallow land burial. ^{63}Ni ($T_{1/2}$ = 100 yr) produced from ^{63}Cu, and ^{94}Nb ($T_{1/2}$ = 20,000 yr) produced from ^{93}Nb and ^{94}Mo are the major contributors for the waste disposal ratings if the 316 SS is used. In the meanwhile, a Tenelon structure WDR is dominated by ^{94}Nb, and ^{14}C ($T_{1/2}$ = 5730 yr) produced from ^{14}N and ^{17}O depending on the class of waste.

Table 1. Waste Disposal Rating (WDR) for APOLLO-L2 Structure

WDR	316 SS	Tenelon
Class A	206 (192 ^{63}Ni, 9 ^{94}Nb)	0.4 (0.17 ^{94}Nb, 0.09 ^{14}C)
Class C	2.47 (1.06 ^{63}Ni, 0.91 ^{94}Nb)	0.027 (0.017 ^{94}Nb, 0.01 ^{14}C)

Finally, it is important to notice that the major contributors to the proton-induced activity in APOLLO-L2 had no noticeable effect on the waste classification. The reason is that proton-induced activity is mainly dominated by radioactive nuclides with half-lives less than five years. 10CFR61 only gives waste disposal limits to radioactive nuclides with half-lives more than five years. Added contribution from long-lived radioactive nuclides produced by proton interactions with the reactor structure is negligible if compared to the contribution given by the radionuclides produced as a result of fusion neutron interactions.

4.2. Tritium Inventory

A small amount of tritium is produced in D-^{3}He reactors due to the D-D reaction. In APOLLO-L2 only 50% of the tritium produced is assumed to be burned in the plasma. The amount of tritium exhausted from the plasma chamber is 20.7 gram per full power day of operation. The tritium is removed from the exhaust fuel system through the vacuum pumps and resides for only few hours in the reactor tritium processing system at any time during operation. The tritium can be stored in uranium getter beds and let to decay to ^{3}He. In this case the steady state inventory of the stored tritium is estimated to be 134 kg. To avoid the safety implications of tritium handling one might consider the option of burning 100% of the tritium produced in the plasma chamber. Burning all the tritium in the plasma results in doubling the number of 14.1 MeV neutrons and hence allowing more high energy threshold reactions which

consequently produce more intermediate and long-lived nuclides. Since intermediate and long term activities in the APOLLO-L2 shield are dominated by radionuclides produced by (n,2n) and (n,p) reactions, such activities will approximately double as a result of burning all the tritium in the plasma. However this increase in activity should not change the conclusions reached regarding the waste disposal rating of the reactor structure as most of the radionuclides that dominate the WDR are produced by (n,γ) reactions. Similarly the thermal response of the shield following a LOCA is not expected to change significantly as most of the decay heat generated in the first few hours following LOCA is dominated by short-lived nuclides as ^{56}Mn.

4.3. LOCA Analysis

The first wall and shield of the inboard and outboard regions have been analyzed with respect to loss of coolant accidents (LOCA). The plasma was assumed to stay on for 10 seconds following the loss of cooling in the reactor shield. The code ATHENA (a version of RELAP5) was used in the analysis. The inboard and outboard sides are solved interactively assuming that all of the coolant channels are filled with air at the atmospheric pressure. The inner legs of the superconducting TF coils are assumed to have an initial temperature of 4.2 K allowing the coils to act as a heat sink. Figure 4 gives the temperature histories in the inboard and outboard sides of the reactor for the first wall and shield. As shown in the figure, a structure made of Tenelon will have the highest thermal response following a LOCA within the first 8 hours. That initial increase in the temperature is caused by the large amount of decay heat generated by ^{56}Mn which has a half-life of 2.578 hours. After two weeks, a 316 SS structure produces the highest temperature. This analysis showed that the highest temperature an APOLLO-L2 structure, which is made of austenitic steel, would reach as a result of a loss of coolant is about 500°C.

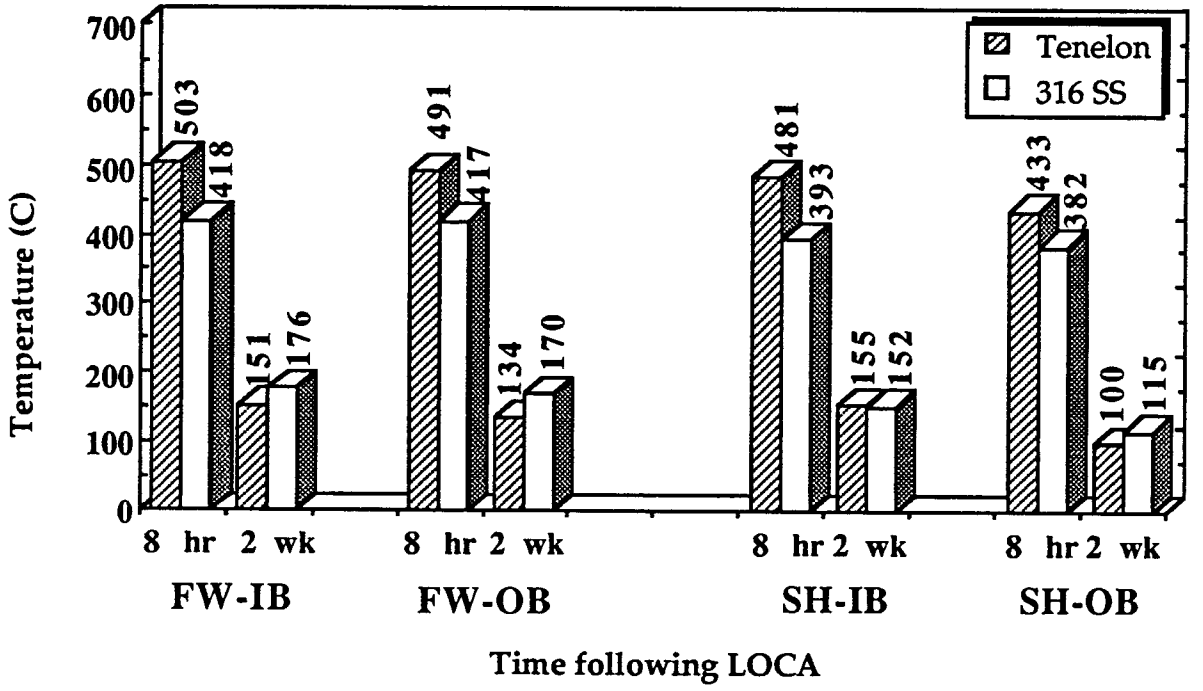


Fig. 4. Temperature of APOLLO-L2 structure following a LOCA.

4.4. Activation Product Mobilization

The maximum temperature reached by the activation products generated in the reactor structure is determined by the amount of energy available at the onset of an accident. In the meanwhile the highest temperature the structure would reach determines the release fractions of these radioactive products. Since an APOLLO-L2 water cooled steel structure concept has no important chemical reaction concerns, the decay heat generated in the structure during a loss of coolant accident has been identified as the major source of energy available to mobilize the radioactive inventory. The low temperature of the shield following a LOCA indicates that only a small fraction of the inventory can be released following such an accident.

The release characteristics used in calculating the off-site doses following the accidental release of the activation products represent the worst case conditions. Based on these conditions it is possible to calculate the potential off-site doses produced by the release of 100% of the radioactive inventory for each of the two steel alloys. As shown in Figure 5, the nickel-stabilized austenitic steel alloy 316 SS has higher potential for off-site doses if its radioactive inventory was released than the manganese-stabilized austenitic steel alloy Tenelon. The key element for 316 SS is cobalt. ^{58}Co and ^{60}Co produced from nickel and cobalt in the steel contribute about 60% of the potential off-site-dose. The 316 SS composition used in this paper contains 13.2 w% of nickel. The rest of the dose is dominated by the manganese isotopes. The key element for Tenelon is manganese. ^{54}Mn and ^{56}Mn produced from iron and manganese in Tenelon produce about 85% of the potential dose. The Tenelon composition used in this analysis contains 15 w% manganese.

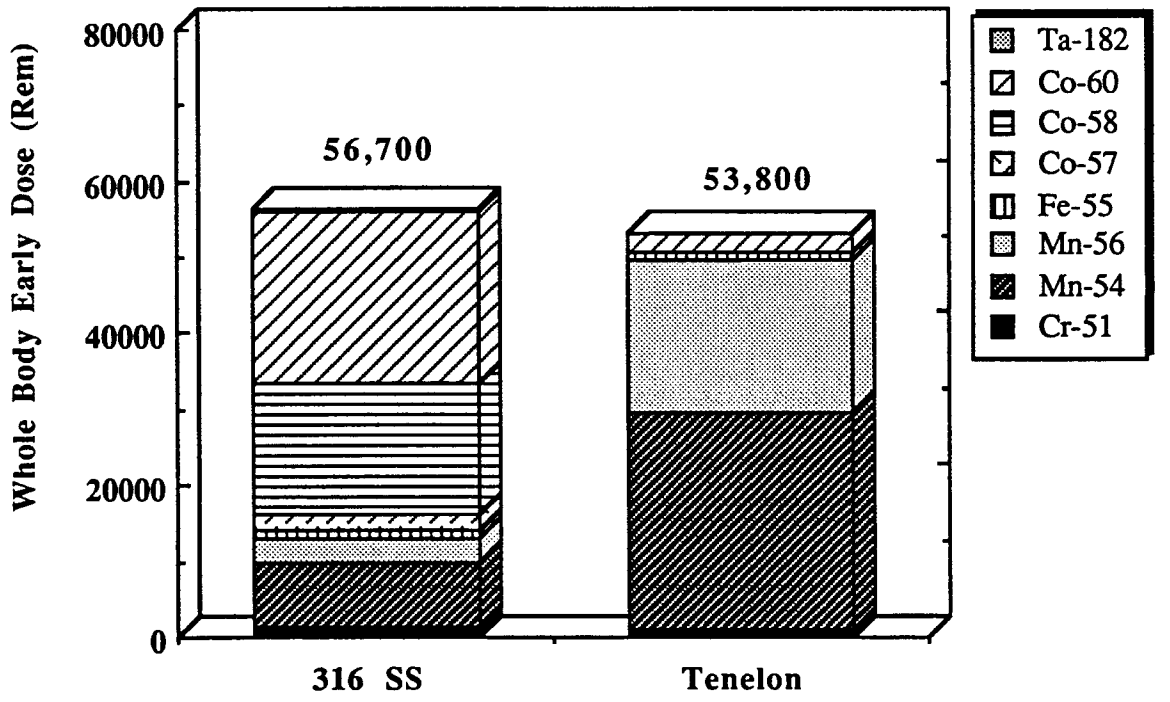


Fig. 5. Potential whole body early off-site dose from 100% release.

Since mobilizing all of the radioactive products is quite unlikely, off-site dose calculations were done based on the experimental volatility rates [14] of the different radioactive nuclides in the structure as a function of the shield temperature during a LOCA. A summary of the results is shown in Figure 6. Even though the highest temperature the structure would reach is less than 500°C the volatility rates used in this paper were those given at 600°C and 800°C for the nickel-stabilized and manganese-stabilized austenitic steel alloys in dry air, respectively. To estimate the release fractions for each radioisotope, a 10 hours LOCA in which the 1 hour release rates are used for the full 10 hours to account for any possible loss of oxide protection. Since no cobalt was detected in the PCA (nickel-stabilized austenitic steel alloy) volatility test, cobalt volatility was included in the dose calculations by using its volatility rate detected from a ferritic steel HT-9 test in dry air.

As shown in the figure, a structure made of 316 SS would results in highest off-site dose. However neither of the two steel alloys used produce a whole body early dose, at the reactor site boundary (1 km), greater than 12 rem which is far below the 200 rem prompt dose limit adopted by the ESECOM [15] committee as a threshold for avoidance of early fatalities in case of accidental release of the radioactive inventory. The elimination of the nickel element in Tenelon resulted in the elimination of the accident hazard of the cobalt isotopes. The 316 SS off-site doses are dominated by ^{58}Co and ^{60}Co. If one will not include the cobalt volatility in the analysis, 316 SS would only produce an off-site dose which is in the same order of that produced by Tenelon (~ 30 mrem). In such case, the off-site dose in each of the two alloys is dominated by ^{54}Mn and ^{56}Mn.

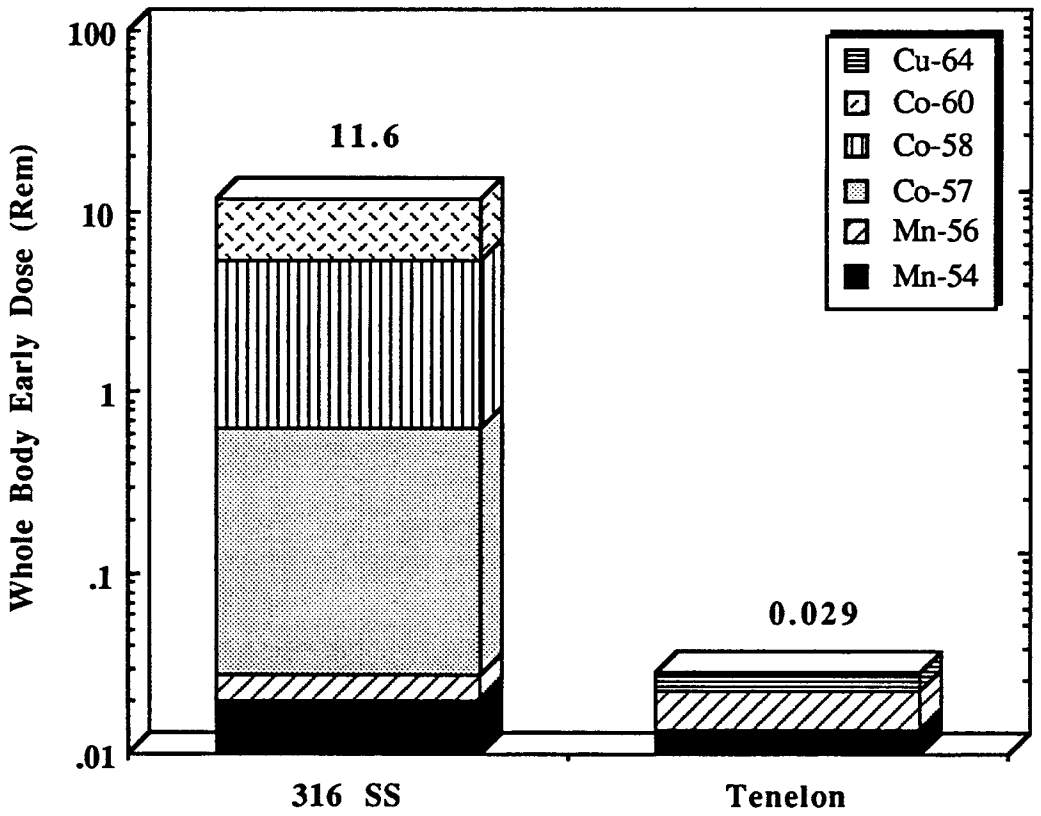


Fig. 6. Whole body early off-site dose using experimental volatility data at 600 °C.

5. SUMMARY

A library that contains thick-target activation yields for radionuclides produced by proton interactions with several stable target elements has been developed. Proton energy-dependent cross sections were used along with proton stopping data to produce the library. A safety analysis for a D-^{3}He tokamak fusion power reactor design (APOLLO-L2) has been carried out. 316 SS and Tenelon were considered for use as structural materials. Results of the activation analysis showed that proton-induced activity represents a small fraction of the total radioactivity generated in the Tenelon structure. A decay heat comparison showed that there is two to three orders of magnitude difference in the level of decay heat generated by neutrons and protons at any time after shutdown. Fusion neutrons remain the main concern in any safety analysis in case of loss of coolant accident (LOCA). The APOLLO-L2 Tenelon structure would qualify for Class A low level waste (LLW) and hence meet the U.S. requirements for shallow land burial. Assuming heat conductions to the magnets, the highest temperature an austenitic steel structure would reach following a loss of coolant accident (LOCA) is less than 500°C. During a LOCA, 316 SS would result in a whole-body early off-site dose which less than 12 rem. The dose released from the Tenelon structure is about 30 mrem requiring no public evacuation plans.

ACKNOWLEDGMENTS

This work was supported by the Wisconsin Electric Utilities Research Foundation, the Grainger Corporation, Fusion Power Associates, the Electric Power Research Institute, McDonnell Douglas Corporation and the Grumman Aerospace Corporation.

REFERENCES

[1] B. V. Robuch and A. Gentilini, "Proton-Nuclide Reaction Cross Sections a Collection of Data from Literature," Comitato Nazionale Per La Ricerca E Per Lo Sviluppo Dell'Energia Nucleare E Delle Energie Alternative, **RT/FUS/87/31** (1987).

[2] H. Münzel et al., "Karlsruhe Charged Particle Reaction Data Compilation," Fachinformationszentrum Karlsruhe, **Physics Data, No. 15** (1982).

[3] National Nuclear Data Center, *On-Line Data Bases*, Brookhaven National Laboratory (1990).

[4] H. H. Anderson and J. F. Ziegler,*HYDROGEN Stopping Powers and Ranges in All Elements*, Pergamon Powers, New York (1977).

[5] S. T. Perkins, "Multigroup Transfer Matrices for Charged-Particle and Neutron-Induced Reactions. Part I: The General Two-Body Interaction," *Nuclear Science and Engineering*, **80**, 130 (1982).

[6] S. T. Perkins, "Multigroup Transfer Matrices for Charged-Particle and Neutron-Induced Reactions. Part II: An Analytic Integration of the Inner Integral," *Nuclear Science and Engineering*, **80**, 579 (1982).

[7] G. L. Kulcinski et al., "Apollo - L2 An Advanced Fuel Tokamak Reactor Utilizing Direct Conversion," *Proceedings of the IEEE 13 th Symposium on Fusion Engineering*, 2-6 October 1989, Knoxville, TN., pp. 1043-1046 (1989).

[8] R. O'Dell et al., "User's Manual for ONEDANT: A Code Package for One-Dimensional, Diffusion-Accelerated, Neutral Particle Transport," Los Alamos National Laboratory, **LA-9184-M** (1982).

[9] D. L. Henderson and O. Yasar "DKR-ICF: A Radioactivity and Dose Rate Calculation Code Package," University of Wisconsin, Madison, **UWFDM-714, Vol. 1** (1987).

[10] M. A. Gardner and R. J. Howerton, "ACTL: Evaluated Neutron Activation Cross Section Library - Evaluation Techniques and Reaction Index," Lawerence Livermore National Laboratory, **UCRL-50400, Vol. 14** (1976).

[11] Lisa J. Porter, "Upgrade of a Fusion Accident Analysis Code and Its Application to a Comparative Study of Seven Fusion Reactor Designs," Massachusetts Institute of Technology, **PFC/RR-89-10** (1989).

[12] H. Chow et al., "ATHENA Code Manual," EG&G Idaho Report, **RST7034, Vol. 1 Draft** (1985).

[13] Nuclear Regulatory Commission, 10CFR part 61, "Licensing Requirements for Land Disposal of Radioactive Waste," Federal Register, **FR 47**, 57446 (1982).

[14] S. J. Piet et al., "Initial Experimental Investigation of the Elemental Volatility from Steel Alloys for Fusion Safety Applications," Idaho National Engineering Laboratory, **EGG-FSP-8459** (1989).

[15] J. P. Holdren et al., "Report of the Senior Committee on Environmental, Safety, and Economic Aspects of Magnetic Fusion Energy," Lawrence Livermore National Laboratory, **UCRL-53766** (1989).

Safety Analysis of the ARIES-III D-^{3}He Tokamak Reactor Design[a]

J. Stephen Herring, Thomas J. Dolan
Idaho National Engineering Laboratory
EG&G Idaho, Inc.
P. O. Box 1625, MS 3880
Idaho Falls, Idaho 83415-3880

ABSTRACT

The ARIES-III reactor study is an extensive examination of the viability of a D-^{3}He-fueled commercial tokamak power reactor. Because neutrons are produced only through side reactions (D+D→^{3}He+n; and D+D→T+p followed by D+T→^{4}He+n), the reactor has reduced activation and low afterheat.

The ARIES-III reactor uses an organic coolant to cool the first wall, shield and divertor. Radiation damage requires processing the coolant to remove and crack radiolytic products that would otherwise foul cooling surfaces. Waste from the cracking process must be buried or incinerated. We estimated the offsite doses due to incineration at five candidate locations.

The demands on the divertor are more severe for D-^{3}He than for D-T, particularly during a disruption. We explored isotopically tailoring the 4-mm tungsten layer on the divertor in order to reduce the off-site doses due to a tungsten aerosol.

We modeled a loss-of-cooling accident (LOCA) and organic coolant fire. Because the maximum temperature is less than 600 °C, release fractions are small. These results re-emphasize the need for low activation materials and advanced divertor designs, even in reactors using advanced fuels.

1. INTRODUCTION AND DESIGN SUMMARY

The safety analysis of the ARIES-III commercial tokamak design has considered several of the important implications in the use of ^{3}He as a fusion fuel. The reaction ^{3}He(d,p)^{4}He + 18.3 MeV produces no neutrons and releases all its energy via charged particles. Neutrons are produced by the side reactions D(d,n)^{3}He + 3.1 MeV and D(d,p)T → T(d,n)^{4}He + 17.6 MeV. As a result, the neutron activation in a D-^{3}He reactor is one to two orders of magnitudes lower than in a similar D-T-fueled reactor.

The D-^{3}He reaction rate is about 12-17 times smaller than the D-T reaction rate, thus requiring a higher plasma current and more thermal energy resident in the plasma, resulting in more divertor damage in a disruption.

---

[a] This work was supported by U.S. Department of Energy, Director of Energy Research, Office of Fusion Energy, under Contract No. DE-AC07-76IDO1570.

About 50 percent of the tritium produced in the D-T and D-D reactions will be burned in the plasma before reaching the divertor or first wall. The remaining half of the tritium produced can either be returned to the plasma or recovered for storage or use in D-T reactors. The ARIES team felt that the additional activation of the first wall and shield posed a smaller danger than the 10 grams per day of tritium that would have to be stored and/or transported.

In addition, small amounts of tritium are produced in the first wall, shield and coolant. About 78 Ci/day of tritium is produced via (n,2n) reactions with the 1-mm layer of beryllium used for impurity control on the first wall. We assume that 26 Ci of the tritium in the beryllium diffuses into the organic coolant and the remainder diffuses back into the plasma and is burned. In addition, 3.6 Ci/day of tritium is produced via other reactions, all of which diffuses into coolant. Finally about 8 Ci/day of tritium is produced in the steel of the shield itself, which also diffuses into the coolant. Thus, about 37 Ci/day would be eventually incinerated with the degraded coolant.

The first wall and shield in ARIES-III are low-activation ferritic steel. Since there is no need to breed tritium, the primary roles of the first wall and shield are to remove the radiant heat from the plasma and to shield the superconducting magnets from the neutron and gamma heating. Ferritic steel was chosen because of its established database and industrial sources.

2. DOSE DEFINITIONS FOR ACCIDENTAL RELEASES

We have considered both accidental and routine releases of radionuclides for the ARIES-III reactor. For accidental releases, the early whole body doses were computed. The early whole body dose is to the most exposed individual (MEI), who remains the entire seven days following an accident at a fixed location, 1 km from the radioactivity release point. We do not assume any short-term evacuation in calculating the dose. The atmospheric stability is Class F, the windspeed is 1 m/s, the inversion layer is 250 m, the release is at groundlevel and the release duration is 0.05 hour. The deposition velocity for tritium was 0.001 m/s, for the noble gases zero, and for all other nuclides 0.01 m/s. The dose coefficients are those calculated by Porter [1].

2.1 Levels of Safety Assurance Definitions

In this safety analysis we have adopted the levels of safety assurance (LSA) as defined in the ESECOM study [2]. Those definitions give a reactor a safety rating ranging from LSA=1 (the most desirable level) to LSA=4, a reactor requiring active safety systems. The level 1 and 2 definitions, quoted from the ESECOM Report are:

- In a level 1 reactor, safety is assured by passive mechanisms of release limitation no matter what the accident sequence. The radioactive inventories and material properties in such a reactor preclude a fatal release regardless of the reactor's condition.

- In a level 2 reactor, safety is assured by passive mechanisms of release limitation, as long as severe reconfiguration of large-scale geometry is avoided, and escalation to fatality-producing reconfigurations from less severe initiating events can plausibly be precluded by passive design features. In such a reactor, natural heat-transfer mechanisms suffice to keep temperatures below those needed - its radioactivity inventories and materials properties - to produce a fatal release unless large-scale geometry is badly distorted.

2.2 Logic in Determining the LSA Rating

The analysis of a reactor's LSA rating follows the logic used in the ESECOM study and begins by calculating the fractional release of a reactor radioactive inventory that would result in a dose of 200 rem to the most exposed individual (MEI). If the entire inventory of the plant could be released without causing a dose of 200 rem, then the reactor clearly has an LSA=1. If the amount of radioactivity in the plant is sufficient to cause a 200 rem early dose, then one proceeds to the analysis of the stored energies and material properties. Using the possible mobilization fractions for the materials involved at the temperatures that could be reached through release of the stored energy (plasma, chemical, magnetic, etc.) one then calculates whether the early dose to the MEI is >200 rem. If it can clearly be shown that there is insufficient energy available to cause a dose >200 rem, then the reactor has LSA=1 on the basis of energy. Mobilization fractions include volatilization as well as transport of particles out of the failed reactor. According to the definition of LSA=1, no credit can be taken in this analysis for the reactor or its building retaining its geometry, including filter systems and the integrity of the vacuum vessel or containment building.

If the mobilization fractions still indicate that an early dose >200 rem could result, then we proceed to the analysis of conceivable accident scenarios. If early doses >200 rem result only if the large-scale geometry of the reactor and its building fail and if this failure can be prevented by passive means, then the reactor has LSA=2.

2.3 Radioactive Inventory

The early whole body dose at 1 km due to the release of 52 percent of the 6000 kg of tungsten would be 200 rem, if either isotopically tailored tungsten mixture in Table 1 were used. If natural tungsten is used in the divertor, release of 6.5 percent of the tungsten of the divertor would result in a dose of 200 rem.

The ferritic steel shield weighs about 7000 t. If 0.5 percent of the radioactive inventory in the shield is released, the early dose at 1 km is 200 rem. Thus the ARIES-III design cannot be designated LSA=1 on the basis of radioactive inventory alone.

2.4 Stored Energy

The reactor contains 187 m^3 of organic coolant with a density of 0.8 kg/l and heat of combustion of 40 MJ/kg for a stored energy of 6000 GJ. The magnetic fields contain

about 165 GJ and the plasma thermal energy is about 8 GJ. The decay heat for one week is about 600 GJ. This energy is sufficient to raise the temperature of the first wall, shield, and divertor by 850° C, *if the energy is uniformly distributed over the entire shield.* However, we cannot make such an assumption in a LSA=1 analysis. A fire within the plasma chamber could release the 0.5 percent of the shield which would result in an early dose of 200 rem. About one GJ will melt one tonne of steel and about five GJ will vaporize a tonne of steel. While the radioactivity in the shield is distributed throughout its 7000 t mass, the organic coolant contains enough energy to mobilize more than 0.5 percent of the steel, especially considering the potential for producing volatile oxides.

Experiments [6] have shown that, at 1000°C to 1200° C, the tungsten would be completely oxidized in about 12-42 hours. Thus we cannot clearly show that ARIES-III has LSA=1 on the basis of inventory and stored energy. We then proceed to a set of conceivable accidents to show LSA=2.

3. CONCEIVABLE ACCIDENTS

We considered several accidents in analyzing the safety of the ARIES-III design: a disruption during which part of the divertor tungsten is vaporized, a LOCA in the divertor, a LOCA in the shield and a LOCA in the shield combined with a fire outside the reactor. We assume that the large-scale geometry of the reactor and its building remains intact, although we take no credit for the vacuum vessel, reactor building or filters retaining radionuclides once they are released from the parent steel or tungsten.

3.1 Divertor Accidents

The most probable accident is a disruption in which 7.7 GJ of the plasma thermal energy is deposited on the plates of the bottom divertor only and is proportionally divided between the inner and outer plates. The maximum depth of evaporation, including allowance for vapor shielding, is 3.9 mm, which results in a triangular trough in the divertor 300 mm wide and 3.9 mm deep, evaporating 720 kg, i.e. 14 percent of the tungsten on the divertor. The evaporated material has the same elemental composition as the base material.

Two isotopically tailored forms of tungsten and natural tungsten were analyzed for the dose calculations. The early whole body doses at the 1-km site boundary were 423 rem for natural tungsten and 56 rem and 53 rem for the two isotopic tailorings. We have assumed no redeposition of the tungsten vapor or aerosol within the reactor or the reactor building, consistent with the ESECOM methodology.

A second divertor accident is a fire fed by the organic coolant within the plasma chamber. We assume that the plasma chamber has been breached at two locations, allowing air to sustain the fire. The tungsten mass on the divertors is about 6000 kg and the thermal energy available from the organic coolant inventory is about 6000 GJ.

We considered a simple LOCA in which the temperature of the divertor reached 800° C, as estimated by Grotz and Khater. We found that the early dose at 1 km was 8.1 rem for the natural tungsten and 2.0 and 2.5 rem for the two isotopically tailored alloys. We have used the volatilization data in air [3], which results in a release of 0.003 percent of the tungsten and 12 percent of the rhenium, which is a transmutation product of the original tungsten.

We should note that these volatilization experiments show the amount of material that is evaporated from the surface of the alloy. Additional radionuclides could be transported out of the reactor as aerosols or small dust particles if the oxide layer on the surface is continually broken up by vibrations or turbulence in the gas stream. Although the flame temperature of the organic coolant fire is above 1000° C, recent experiments with tungsten in air [3] and steam [4] show the formation of loosely attached oxides.

3.2 Shield LOCA and Fire

Steve Grotz [5] calculated the maximum temperature in the first wall/shield due to a LOCA and due to a LOCA plus an external organic coolant fire. For the LOCA with no fire, he found that the maximum temperature in the first wall/shield was 504°C and that temperature peak occurred 3.7 days after the onset of the LOCA.

For the LOCA with organic coolant fire he assumed that the coolant burns with a flame temperature of 1000°C in a pool beneath the reactor for 10 hours. The flame was exposed to the back of the shield, which could also radiate to the surrounding containment walls. Two temperature peaks occurred: 598°C 10 hours after the LOCA, at the end of the coolant burn, and 515°C 3.5 days after the LOCA.

To assess the release of radionuclides from the first wall and shield resulting from the LOCA and fire we used data from ferritic steel activation product volatility experiments at the INEL [6]. The doses for various maximum temperatures are shown in Figure 1.

Thus, after considering these four conceivable accidents we can state that the ARIES-III design is clearly large-scale passively safe (i.e. LSA=2), since none of the accidents result in early doses >200 rem.

3.4 Offsite Doses due to Routine Effluent Releases

The ARIES-III design uses a diphenyl organic coolant in the first wall and shield because of its low vapor pressure at the 450° C operating temperature. Because of neutron and gamma irradiation, the coolant is degraded, forming a high-boiling point fraction which would plug the 4-mm diameter cooling tubes. About 85 percent of the 'high boiler' can be reclaimed through catalytic cracking, but the remaining 15 percent is a chemically and radioactively hazardous waste. We analyzed the off-site doses due to incineration of the non-reclaimable coolant, releasing 47 Ci of tritium per day. We

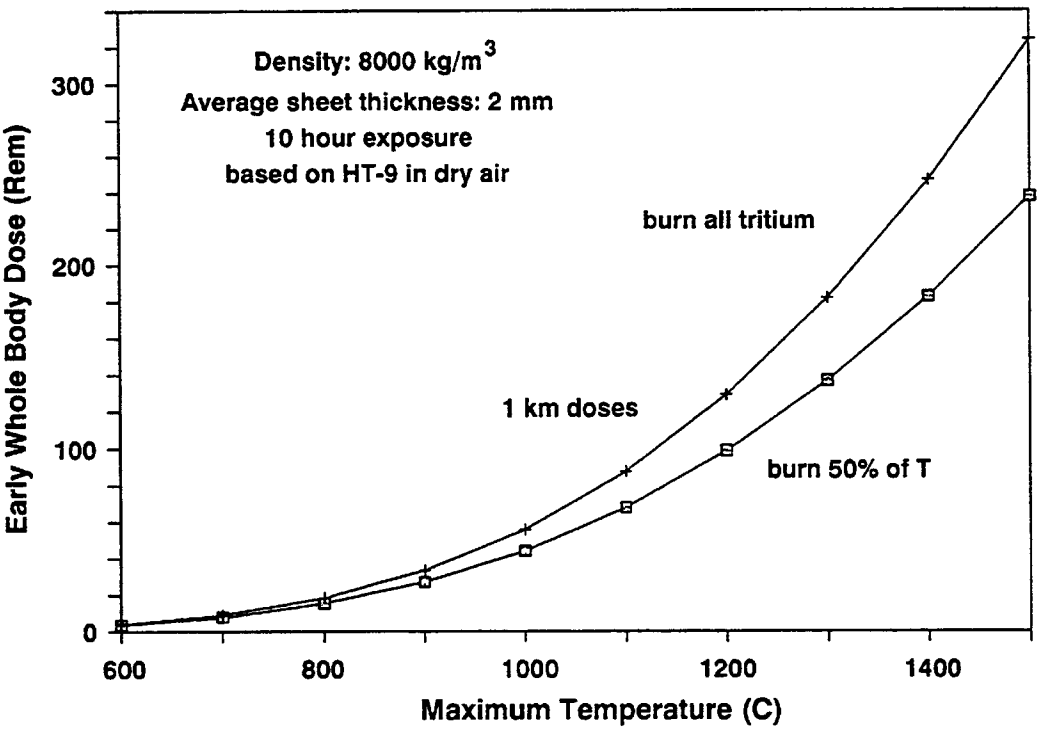


Figure 1 Off-site doses due to release of radionuclides from ferritic steel shield

also included 1.2 Ci/yr of ^{14}C, produced by $^{14}N(n,p)^{14}C$ reactions assuming that the organic coolant is saturated with air. Finally we included 18.9 mCi/yr of ^{60}Co, due to activation of natural ^{59}Co, which is used on valve facings, based on Canadian experience.

We used the EPA code AIRDOS-PC [7], which determines compliance with the Clean Air Act per 40 CFR 61.93 and 61.94, to calculate the annual dose, 300 and 1000 m from the release point, due to routine release of the above radionuclides from typical locations near Chicago, Albuquerque, Boston, Butte, Montana and Los Angeles. The worst doses were in the Los Angeles area, but were only 1.3 mrem/yr, primarily due to the tritium, much less than the 10 mrem/yr EPA effluent limit.

4. CONCLUSIONS

We found that the radioactive inventory in the divertor and shield were too large to declare LSA=1 on the basis of inventory alone. We determined the amount of energy available to melt and mobilize the shield and divertor, about 6000 GJ. We found that the combustion energy in the organic coolant, if not uniformly distributed through the shield, was sufficient to mobilize enough of the shield and divertor to produce an early dose at 1 km >200 rem.

We looked at four conceivable accidents which the large-scale geometry of the reactor was maintained. All of the conceivable accidents which have been analyzed result in early doses at 1 km of less than 200 rem, if isotopically tailored tungsten is used on the divertor. Therefore, we conclude that the ARIES-III reactor design is clearly passively safe (LSA=2).

The routine releases due to incineration of the degraded organic coolant are manageable and less than the 5 mrem/year limit imposed on present nuclear facilities. The burning of all the D-D produced tritium in the plasma increases the 1 km early dose by about 30 percent.

We should note that this analysis has been limited to the operation of the reactor alone and did not consider the environmental and safety impacts of recovering and transporting the ^{3}He from lunar or planetary sources. A more detailed analysis of the D-^{3}He fuel cycle should consider those risks.

5. REFERENCES

[1] Lisa J. Porter, "Upgrade of a Fusion Accident Analysis Code and its Application to a Comparative Study of Seven Fusion Reactor Designs," PFC/RR-89-10, Massachusetts Institute of Technology, June 1989.

[2] John P. Holdren, D. H. Berwald, R. J. Budnitz, J. G. Crocker, J. G. Delene, R. D. Endicott, M. S. Kazimi, R. A. Krakowski, B. G. Logan and K. R. Schultz, *Report of the Senior Committee on Environmental, Safety, and Economic Aspects of Magnetic Fusion Energy,* UCRL-53766, September 25, 1989, p. 69.

[3] G. R. Smolik, R. M. Neilson, Jr. and S. J. Piet, "Oxidation-Driven Volatility from Copper and Tungsten Alloys for Fusion Reactor Applications," Conf-981007-35, IEEE 13th Symposium on Fusion Energy, Knoxville, TN, October 2-6, 1989.

[4] G. R. Smolik, S. J. Piet and R. M. Neilson, Jr., "Predictions of Radioactive Tungsten Release from Hypothetical ITER Accidents," *Fusion Technology*, 19, (3,part B), May 1991, pp. 1342-1348.

[5] Steven P. Grotz, private communication, March 19, 1991.

[6] S. J. Piet, et.al., *Initial Experimental Investigation of the Elemental Volatility from Steel Alloys for Fusion Safety Applications*, EGG-FSP-8459, April 1989.

[7] User's Guide for AIRDOS-PC, Version 3.0, EPA 520/6-89-035, U. S. Environmental Protection Agency, Office of Radiation Programs, Las Vegas, NV, December 1989.

Appendix: Post-Conference Contributed Paper 357

Implications of the Results from the CTX Experiment Towards the Development of a D-^{3}He Dipole Fusion Reactor 359
Michael E. Mauel and Harry P. Warren

Implications of the Results from the CTX Experiment Towards the Development of a D-^{3}He Dipole Fusion Reactor

Michael E. Mauel and Harry P. Warren
Department of Applied Physics
Columbia University
New York, NY 10027

ABSTRACT

A levitated dipole magnet may well be suitable to confine a high pressure, $\beta > 1$, high temperature plasma for the production of D-^{3}He fusion power. [See *Comments Plasma Phys. Contr. Fusion*, **11** (1987) 147, *Nuclear Fusion*, **31** (1991) 2405, and *Fus. Tech.*, **22** (1992) 27.] In this report, we present the first observations of wave-induced plasma transport of hot plasma confined by a dipole magnetic field. The experiment was built and operated in order to better understand the dynamics of plasma confinement within planetary magnetospheres, and, for this reason, the dipole magnet is not levitated and can not be used for global confinement studies. However, a fundamental premise of the dipole fusion concept is the tendency for dipole-confined plasmas to evolve to a state of marginal-stability with respect to low-frequency instabilities. In a dipole plasma, this occurs when the distribution function, $F(\mu, J, \psi)$, satisfies $\partial F/\partial \psi \approx 0$, where μ, J, and ψ are the three adiabatic invariants of charged-particle motion. In our experiment, we have identified drift-resonant instabilities which may indeed lead to such a plasma profile.

1. INTRODUCTION

The dipole fusion concept was first proposed by Hasegawa [1]. A dipole fusion reactor would consist of a single levitated circular magnet within a large vacuum chamber. A relatively low pressure plasma would be created at the outer region of the vacuum chamber, and applied low-frequency fluctuations would adiabatically drive the plasma inward to a state of vanishing net particle flux. This occurs when the plasma distribution function satisfies the condition $\partial F/\partial \psi \approx 0$, where ψ is the magnetic flux and the third adiabatic invariant of magnetized particle motion. The induced radial transport would be accompanied by adiabatic heating since the low-frequency fluctuations preserve the first two adiabatic invariants, μ and J. Since the radial particle flux is proportional to $\Gamma_\psi = -(\pi/2) \sum_\omega \delta(\omega - \omega_d) |\dot{\psi}(\omega)|^2 \partial F/\partial \psi$, once the distribution evolved to a profile with $\partial F/\partial \psi \approx 0$, low-frequency fluctuations no longer induce transport. "Anomalous" transport and convective cells which may deteriorate confinement in other magnetic configurations do not lead to transport in dipolar magnetic fields. Unlike these other magnetic topologies, the volume of a flux tube surrounding a dipole, $V(L) = \psi \int dl/B$, varies strongly as a function of radius, L, and the condition $\partial F/\partial \psi \approx 0$ corresponds to a relatively steep pressure profile,

scaling as $L^{-20/3}$. In contrast, consider a long-thin magnetic mirror such as a tandem mirror. In this device, $V(L)$ is approximately constant. The condition $\partial F/\partial \psi \approx 0$ corresponds to a constant pressure profile, and low frequency fluctuations induce radial transport for fusion-relevant profiles.

Conceptual designs for D-^{3}He dipole reactors were presented by Hasegawa, *et al.* [2] and Hasegawa, *et al.* [3]. These designs differed from Hasegawa's original reactor concept since they used central heating and fueling (*e.g.* neutral beam injection) which evolved to a profile having $\partial F/\partial \psi \approx 0$ through the "natural excitation" of low-frequency fluctuations, outward radial diffusion, and adiabatic cooling. These studies presented requirements for the superconducting dipole, the magnet heating rates and equilibrium surface temperatures, and self-consistent operating points both at low field (20 MA) and low fusion power (70 MW) and at high field (40 MA) and high fusion power (1.1 GW). The theory for MHD ballooning stability for high pressure plasmas having $\beta > 1$ was also presented for both anisotropic and isotropic pitch-angle distributions.

The dipole reactor concept has been extended in important ways. Teller, *et al.* [4] has shown that the dipole reactor is attractive for space propulsion for distant missions. Pastukhov and Sokolov, [5] have shown that, for sufficiently large dipole reactors, the plasma heat flux to the levitated dipole can be transformed completely to bremsstrahlung radiation, and Morozov, *et al.* [6] have described a 23 MA, 1 GW dipole reactor satisfying these requirements.

Although the dipole reactor concept has attracted considerable attention as a possible alternate fusion concept, our primary source of information of dipole-confined plasma are satellite observations made within planetary magnetospheres. Measurements of energetic ring-current protons in the earth's magnetosphere made with the Explorer XII, XIV, XV satellites show that the average equatorial pressure profile scales approximately as L^{-6} between 3 and 7 earth radii [7], and this corresponds approximately to the profile produced when $\partial F/\partial \psi \approx 0$. Measurements from the Voyager 1 and 2 spacecraft show the trapped energetic particle pressure throughout most of the Jovian magnetosphere exceeds the dipole magnetic field pressure, $\beta \geq 1$, Krimigis, *et al.* [8], and this observation supports the possibility of high pressure plasmas needed for a dipole fusion reactor. Finally, our modern understanding of the radial transport process within a dipole magnetic field was advanced in large part to explain the observed high-energy proton distribution of the Van Allen radiation belt undergoing transport induced by random $m = 1$ fluctuations of the global magnetosphere caused by the solar wind, Farley, *et al.* [9].

In the interest of better understanding the fundamental properties of collisionless transport in a dipole magnetic field, a new experiment has been built at Columbia University called the Collisionless Terrella Experiment, CTX. The experiment consists of a high-field electromagnet suspended within a large nearly spherical vacuum chamber. A microwave plasma source is capable of generating localized population of trapped, energetic electrons forming an "artificial radiation belt". The design and goals of CTX have been described by Mauel and Hasegawa [10].

Although the CTX experiment does not have a levitated dipole, some of the basic properties of collisionless radial transport in a dipole magnetic field can be observed. Ongoing experiments should lead to (1) the observation of the wave spectrum required for the onset of chaotic diffusion, and (2) the evolution of the pressure profile caused by intense low-frequency fluctuations.

This report describes the first results from the CTX experiment and their relationship to the basic plasma physics needed to establish the dipole fusion reactor concept. In Section 2,

we briefly describe CTX and present a typical discharge illustrating the production of an energetic electron belt. In Section 3, we present the measurements of multi-mode drift-resonant electrostatic hot electron interchange instabilities (HEI) which induce rapid radial transport of the energetic electrons. Finally, in Section 4, we discuss the implications of these experimental results on the prospects for further advancement of the dipole reactor concept.

2. THE CTX EXPERIMENT

The "Collisionless Terrella Experiment", or CTX, is a relatively new laboratory experiment built at Columbia University in order to directly observe the unique and fundamental properties of collisionless radial transport of plasma trapped within planetary magnetospheres. Collisionless radial transport in a dipole-confined plasma occurs only when wave-particle interactions are sufficiently intense and broad-banded and when the particle motion satisfies well-defined conditions for chaos. In spite of the importance of radial transport to determine the global properties of magnetospheric plasmas, it is noteworthy that (1) CTX is the first collisionless dipole laboratory experiment capable of observing collisionless radial transport, (2) plasma waves exist which break only the third adiabatic invariant making radial transport relatively simple to characterize fully, and (3) the impact of collisionless transport on a plasma's global profile is predicted to have an unique signature that should be readily identified. In many respects, understanding how localized wave-particle interactions result in global modifications of the plasma profile is illustrative of many problems in plasma physics: a strong connection exists between the microscopic (in this case, chaotic wave-particle interactions) and the macroscopic (*e.g.* evolution of plasma profiles).

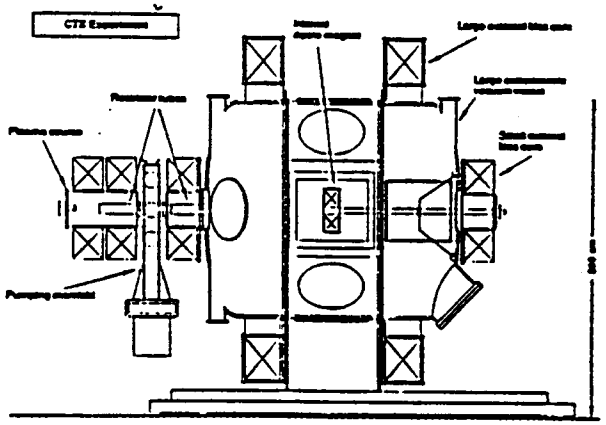


Figure 1. A cross-sectional schematic of the CTX experiment showing the support for the internal, high-field dipole magnet, the large vacuum chamber, and the microwave plasma source.

The CTX experiment was built in two years with the support of the National Science Foundation and an extensive use of "surplus" laboratory equipment once used in DOE's magnetic fusion energy program. Figure 1 shows a schematic of the experiment. CTX consists of (1) a large nearly spherical vacuum chamber approximately 1.6 m in diameter, (2) an internal dipole magnetic suspended along the axis of one magnetic pole by a stainless-steel tube carrying electrical power and water cooling, and (3) a microwave plasma source which can be used to make either a "plasma stream" or a source of microwaves for direct heating of electrons, magnetically trapped by the dipole. For our first experiments, we have operated the microwave source to maximize the intensity of an "artificial radiation belt" consisting of trapped electrons with energies between 10 and 30 keV. These electrons have a collisional mean-free-path longer than 1,000 drift orbits about the equator, and they provide

the ideal laboratory medium with which to study radial transport in dipole geometry. By inserting "skimmer" probes, we have determined that the energetic electron belt is highly localized at the fundamental electron cyclotron resonance, and the belt intensity can be controlled by adjusting the neutral hydrogen gas pressure.

Figure 2 shows the time history of a typical CTX discharge and the production of an energetic electron belt. The discharge duration was arbitrarily programmed to last approximately 0.5 sec, and the several signals represent the time history of the ion-saturation current to a Langmuir probe, the hydrogen gas pressure, the forward and reflected microwave power, and the x-ray spectra as recorded by a krypton proportional counter. The experiment is fully computer controlled, and the gas pressure, pulse length, and heating power can be programmed independently for each discharge. For discharges similar to that shown in Figure 2, intense fluctuations are observed both during the microwave heating and during the "afterglow" when the heating power has been switched-off. These fluctuations only occur in the presence of the energetic electron belt, and we have characterized them as a complex and nonlinear development of drift-resonant hot electron interchange instabilities (HEI) first described by Krall [11]. The HEI is the electrostatic "analog" of the electromagnetic kinetic Alfvén instabilities occurring in planetary magnetospheres.

3. OBSERVATION OF RADIAL TRANSPORT INDUCED BY DRIFT-RESONANT INSTABILITIES

Figure 3 shows the probe fluctuations on a faster, 10 msec, time-scale. During the microwave heating, quasi-periodic "bursts" are observed; whereas, during the afterglow, the probe signals are seen to evolve more gradually. As shown, in Figure 4, the quasi-periodic bursts correspond to rapid radial transport of electrons from the belt region. This is observed directly with a gridded electron detector and indirectly by large and negative decrease in the probe's floating potential.

By using very high-speed data recorders, we have identified the drift-resonant instabilities inducing this rapid electron transport. Figure 5 shows a frequency spectrogram of the instabilities occurring both during the microwave heating and during the afterglow. During the heating, the quasi-periodic pulsations consist of relatively wide-band signals ranging from 0.1 MHz $\leq f <$ 2 MHz. In contrast, the instabilities observed during the afterglow consist of a multi-mode collection of relatively coherent rising tones. Closer examination of the quasi-periodic bursts during heating also show a collection of rising tones. The difference in the frequency spectra can be linked to the energy

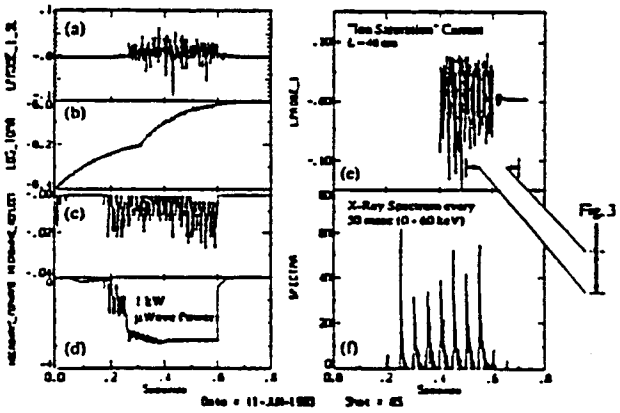


Figure 2. A typical CTX discharge when the hydrogen gas puff has been adjusted to produce an energetic electron belt. (a) Ion saturation current, (b) H_2 gas pressure, (c) reflected microwave power, (d) forward power, (e) Ion saturation current, and (f) several x-ray spectra averaged over 50 msec intervals.

of the electron belt as measured with the x-ray proportional counter. When the average belt energy is relatively low, $\langle E \rangle$ – 10 keV, (such as found during the heating), the wave frequency is also relatively low. During the afterglow, when the cooler electrons scattering into the terrella's polar regions, $\langle E \rangle$ gradually increases to more than 30 keV, and the frequencies of drift-resonant instabilities also increase. The rate of rise of the frequency is also linked to the average energy of the trapped electron belt.

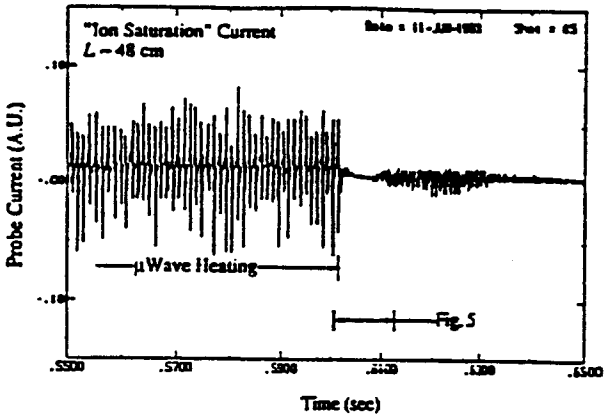


Figure 3. Fluctuations induced by the energetic electron belt during the heating and during the after glow.

Multiple probes are used to determine the azimuthal and radial structure of the drift-resonant waves. Figure 6 shows the magnitude and phase of the correlation of two probes located on the same flux-surface. The two probes indicate that the waves propagate in the electron drift direction, and the wave spectrum consists of multiple azimuthal mode numbers, m, as well as multiple frequencies. When the probes are positioned on different flux surfaces, we observe a broad radial mode structure and "twisting" of the instability wave fronts. The later effect may be due to the strong radial variation of the electron drift frequency.

4. DISCUSSION

Although the CTX experiment has been operating for less than one year, our early results already have important implications for understanding the basic process of collisionless radial transport in a dipole magnetic field. First, transport in a dipole magnetic field seems to require multiple modes. This is a unique property of the dipole magnetic geometry resulting from the strong radial dependence of a particle's azimuthal drift frequency, $\omega_d \propto 1/L^2$, where L is the equatorial radius of a flux surface. Global transport can only occur with multiple modes since a particle does not remain correlated with a single wave

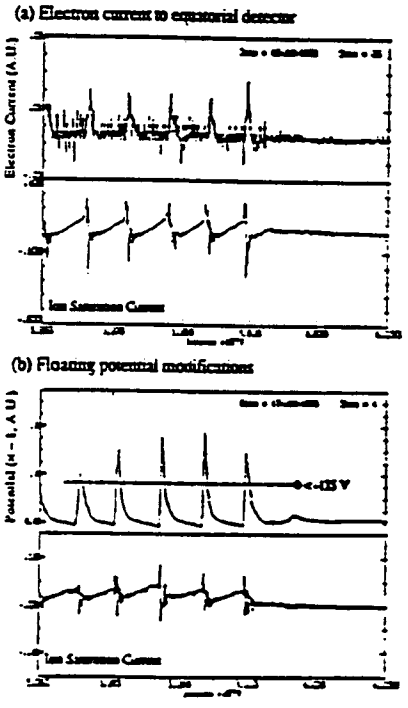


Figure 4. Observations of energetic electron transport: (a) from an equatorial gridded particle detector, and (b) from large, negative floating potential modifications.

as it diffuses radially. Secondly, the radial transport rate is fast. In CTX, large electron bursts lasting only 10's of drift periods are observed to cause significant transport. Finally, drift-resonant instabilities lead to transport causing self-stabilization and continuous, quasi-periodic bursting. This is observation is important. It implies that the transport-inducing waves also decrease the radial pressure gradient of the electron belt—but do not destroy electron confinement altogether. For a dipole magnetic field, the marginally stable pressure profile scales like $p \propto L^{-20/3}$. The observation of the profile evolution during radial transport is one of the major goals of our on-going CTX experiments.

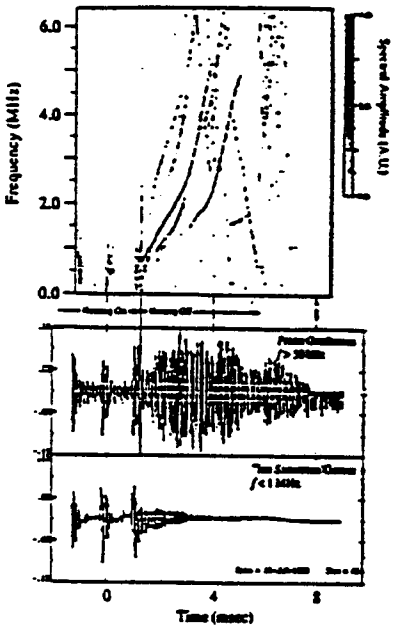


Figure 5. Frequency spectrograms of rising-tone, multi-mode drift-resonant instabilities.

Do the CTX results support the dipole fusion concept? The answer is definitely yes, but it is clear that much more experimentation is required. Perhaps the most encouraging result is simply that an intense energetic electron ring has been successfully created within the dipole. Secondly, the most recent concept of core heating of the dipole reactor appears plausible in light of CTX results, although the details differ. In CTX, quasi-periodic bursts of drift-resonant fluctuations drive the energetic electrons towards the marginally stable $\partial F/\partial \psi = 0$ profile. These appear to "over flatten" the pressure profile causing stabilization and damping of the fluctuations. A truly stationary $\partial F/\partial \psi = 0$ may not be possible in a dipole reactor, but the magnitude of the profile oscillations has not yet been measured.

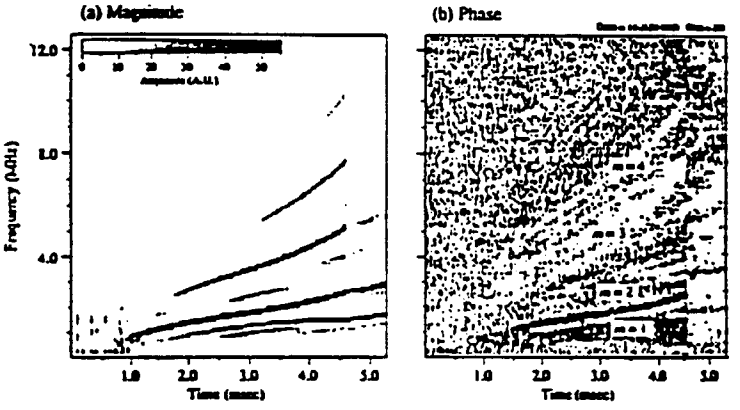


Figure 6. Spectrograms of the (a) magnitude and (b) phase of the two-position correlation of the instabilities. Multiple azimuthal mode numbers as well as multiple modes are observed.

The most important test of the dipole fusion concept requires a levitated coil, and several design possibilities exist. Even for a device as small as CTX, a liquid-nitrogen cooled copper dipole or a more sophisticated superconducting dipole could be used as a first step in the investigation of global confinement of dipole-confined plasma.

ACKNOWLEDGMENTS

The authors would like to gratefully acknowledge the many suggestions and comments of A. Hasegawa whose inspiration lead to the construction of the CTX experiment. The CTX experiment was built and operated using support from NSF Grant ATM-88-20369 and AFOSR Grant F49620-93-I-0071.

REFERENCES

[1] A. Hasegawa, *Comments Plasma Physics Control. Fusion* **11** (1987) 147.

[2] A. Hasegawa, L. Chen, and M. E. Mauel, *Nuc. Fusion* **30** (1990) 2405.

[3] A. Hasegawa, *et al*, *Fus. Tech.* **22** (1992) 27.

[4] E. Teller, *et al.*, *Fus. Tech.* **22** (1992) 82.

[5] V. P. Pastukhov and A. Yu. Sokolov, "On Anomalous Transport Processes near a Levitated Coil Immersed into the Plasma," Report Presented at the Workshop on D-^{3}He Based Reactor Studies," Kurchatov AEI, Moscow, (September 25 – October 2, 1991).

[6] A. I. Morozov, V. P. Pastukhov, A. Yu. Sokolov, "High β Axisymmetric D-^{3}He Reactor with Internal Levitated Coil," Report Presented at the Workshop on D-^{3}He Based Reactor Studies," Kurchatov AEI, Moscow, (September 25 – October 2, 1991).

[7] L. R. Davis, *Proc. Plasma Space Science Symposium*, Washington, D.C. (1963).

[8] S. M. Krimigis, *et al.*, *J. Geophys. Res.* **86** (1981) 8227.

[9] T. A. Farley, A. D. Tomassian, M. Walt, *Phys. Rev. Lett.* **25** (1970) 47.

[10] M. E. Mauel and A. Hasegawa, "Measurement of Nonadiabatic and Chaotic Charged-Particle Motion in a Collisionless Laboratory Terrella," in *Physics of Space Plasmas (1990), SPI Conference Proceedings and Reprint Series, No. 10*, T. Chang, G. B. Crew, and J. R. Jasperse, eds. (Scientific Publishers, Cambridge, MA, 1991).

[11] N. A. Krall, *Phys. Fluids* **9** (1966) 820.